

**ENVIRONMENTAL STUDIES
AT THE FLOWER GARDENS AND SELECTED BANKS:
NORTHWESTERN GULF OF MEXICO, 1979-1981**

FINAL REPORT

Northern Gulf of Mexico Topographic Features Study
Contract No. AA851-CT0-25

Submitted to the
U.S. Department of the Interior
Minerals Management Service
Outer Continental Shelf Office
New Orleans, Louisiana

Technical Report No. 82-7-T

Research Conducted Through
the Texas A&M Research Foundation

1982

ENVIRONMENTAL STUDIES AT THE FLOWER GARDENS AND SELECTED BANKS:

NORTHWESTERN GULF OF MEXICO, 1979-1981

FINAL REPORT

**Northern Gulf of Mexico Topographic Features Study
Contract No. AA851-CTO-25**

**Submitted to the
U.S. Department of the Interior
Minerals Management Service
Outer Continental Shelf Office
New Orleans, Louisiana**

**Department of Oceanography
Texas A&M University
College Station, Texas**

Technical Report No. 82-7-T

**Research Conducted Through
the Texas A&M Research Foundation**

1982

This volume has been reviewed by the Minerals Management Service and approved for publication. Approval does not signify that the contents necessarily reflect the views and policies of the Service, nor does mention of trade names or commercial products constitute endorsement or recommendation for use.

CONTRIBUTORS

Technical Director
Richard Rezak

Program Manager
David W. McGrail

Assistant Program Manager
Sylvia C. Herrig

Principal Investigators
Texas A&M University
Department of Oceanography

David W. McGrail
Geological

Richard Rezak
Geological

Thomas J. Bright
Biological

Research Staff

Michael Carnes
Thomas Cecil
Lawrence Goldberg
Fern Halper
Jeffrey Hawkins
Doyle Horne
James Stasny

Research Staff

Jeffrey Payne
David Risch
John Stafford
Kyung Woo

Research Staff

Christopher Combs
George Kraemer
Greg Minnery
Richard Titgen

University of Texas Marine Science Institute
Port Aransas Marine Laboratory

Patrick L. Parker
R.S. Scalan
Richard K. Anderson

Texas A&M University
Department of Chemistry

C.S. Giam
Lee E. Ray
H.E. Murray
D. Allen

Editor

Rose Norman

ACKNOWLEDGEMENTS

This report reflects the work of dedicated support staff and the valuable services of Texas A&M personnel and others. The authors wish to extend their thanks to the following people.

1. For final drafting of maps and preparation of the West Flower Garden side-scan sonar mosaic, Christopher Mueller-Wille, head, Cartographic Services Unit, and drafting personnel: Kathy Roemer, Sally Kirk, Denise Hoyt, and Dorie Slane, Texas A&M University.
2. For preparation of the MacNeil Bank side-scan sonar mosaic, James Coleman and David Prior, Coastal Studies Institute, Louisiana State University, Baton Rouge, LA.
3. For original drafting of structure and roughness maps, Jeff Payne, David Risch, Kyung-Sik Woo, and Dale Harber.
4. For laboratory analyses, Milton P. Looney, Dale Harber, John Stafford, and Gregory Minnery.
5. For proofreading and numerous copy preparation duties, Monica Arndt, Roxanne Bogucki, Beth O'Brien, and Cathy Knebel.
6. For word processing, Karen Dorman and Lori Lingbeck.

TABLE OF CONTENTS

	Page
CONTRIBUTORS.....	iii
ACKNOWLEDGEMENTS.....	iv
LIST OF FIGURES.....	vii
LIST OF APPENDIX FIGURES.....	xviii
LIST OF TABLES.....	xix
LIST OF APPENDIX TABLES.....	xxiii
Chapter	
I. INTRODUCTION AND PROJECT MANAGEMENT	
BACKGROUND ON PREVIOUS STUDIES.....	1
GOALS OF THE PRESENT STUDY.....	6
PROJECT MANAGEMENT.....	8
DATA MANAGEMENT.....	12
II. GEOLOGY OF THE FLOWER GARDEN BANKS	
INTRODUCTION.....	19
GENERAL DESCRIPTION.....	19
PHYSIOGRAPHY AND STRUCTURE.....	20
SEDIMENTOLOGY.....	21
CONCLUSIONS AND RECOMMENDATIONS.....	24
APPENDIX A: FLOWER GARDENS SEDIMENT ANALYSES.....	A-1
III. BIOLOGICAL MONITORING AT THE FLOWER GARDEN BANKS	
BIOTIC ZONATION.....	39
CORAL AND CORALLINE ALGAE POPULATIONS.....	52
CORAL GROWTH AND MORTALITY.....	66
RECRUITMENT AND EARLY GROWTH OF CORALS.....	88
APPENDIX B: CORAL POPULATION TABLES.....	B-1
IV. WATER AND SEDIMENT DYNAMICS AT THE FLOWER GARDEN BANKS	
INTRODUCTION.....	103
LONG TERM CURRENT MEASUREMENTS.....	103
TRANSMISSIVITY TIME SERIES DATA.....	160
LARGE SCALE BEDFORMS.....	168
CLIMATOLOGICAL WIND TIME SERIES MEASUREMENTS.....	169
PHISH DATA.....	172
BOUNDARY LAYER DYNAMICS.....	209
SUMMARY AND CONCLUSIONS.....	224

TABLE OF CONTENTS (Continued)

Chapter	Page
V. CHEMICAL ANALYSES	
HIGH MOLECULAR WEIGHT HYDROCARBONS IN <u>SPONDYLUS</u> <u>AMERICANUS</u>	227
HIGH MOLECULAR WEIGHT HYDROCARBONS, TOTAL ORGANIC CARBON, AND DELTA C-13 IN SEDIMENTS.....	234
VI. GEOLOGY OF SELECTED BANKS	
INTRODUCTION.....	253
EWING BANK.....	253
PARKER BANK.....	254
BOUMA BANK.....	256
18 FATHOM BANK.....	257
BRIGHT BANK.....	257
STETSON BANK.....	259
MACNEIL BANK.....	260
APPENDIX C: SEDIMENT ANALYSES.....	C-1
SELECTED BIBLIOGRAPHY.....	301

LIST OF FIGURES

CHAPTER II		
Figure		Page
II-1	Flower Garden Banks location map.....	20
II-2	West Flower Garden Bank bathymetry showing locations of seismic lines on Figures II-7 and 9, and sediment grab stations.....	26
II-3	West Flower Garden perspective views.....	27
II-4	East Flower Garden bathymetry showing location of 3.5 kHz profile on Figure II-10.....	28
II-5	East Flower Garden perspective views.....	29
II-6	West Flower Garden structure-isopach map.....	30
II-7	West Flower Garden 3.5 kHz sub-bottom profile.....	31
II-8	West Flower Garden 3.5 kHz sub-bottom profile.....	32
II-9	West Flower Garden 3.5 kHz sub-bottom profile.....	33
II-10	East Flower Garden 3.5 kHz sub-bottom profile.....	34
II-11	Sediment distribution in the Flower Garden Banks area..	35
II-12	East Flower Garden structure/isopach map.....	36
II-13	East Flower Garden seafloor roughness map.....	37
Plate 1	West Flower Garden side-scan sonar mosaic.....	Pocket
CHAPTER III		
III-1	Depth ranges of recognizable biotic zones and sedimentary facies (other than hard bottoms).....	42
III-2	Biotic zonation, East Flower Garden Bank.....	44
III-3	Biotic zonation, West Flower Garden Bank.....	45
III-4	Species-Transect length curve based on pooled data from 18 East Flower Garden transects and 18 West Flower Garden transects.....	54
III-5	X-radiographs of sectioned <u>Montastrea annularis</u> cores and a <u>Diploria strigosa</u> core from the East and West Flower Garden coral reefs.....	67

LIST OF FIGURES (Continued)

Figure		Page
CHAPTER III (Continued)		
III-6	Vertical growth rates of <u>Montastrea annularis</u> and <u>Diploria strigosa</u>	69
III-7	Coral recruitment at Flower Garden reefs, short-term control samples.....	95
III-8	Coral recruitment at Flower Garden reefs, long-term control samples.....	96
CHAPTER IV		
IV-1	Mooring positions for all six current meter array deployments from January 1979 to July 1981.....	107
IV-2	Data inventory for current meter arrays: January 1979 through December 1979.....	109
IV-3	Data inventory for current meter arrays: April 1980 through October 1980.....	110
IV-4	Data inventory for current meter arrays: October 1980 through July 1981.....	111
IV-5	One-month averages of speed and direction for current meters in the range: (a) from 32 m to 64 m depth; (b) from 11 m to 18 m from the bottom; and (c) from 4 m to 8 m from the bottom.....	119
IV-6	Monthly mean current vectors for all deployments and all moorings.....	120
IV-7	Ratio of the variance along the major axis to the variance along the minor axis, plotted in the direction of the major axis for (a) all meters on mooring 2 deployed before March 1981, and (b) all meters on mooring 2 for the March to July 1981 deployment.....	126
IV-8	Ratio of the variance along the major axis to the variance along the minor axis, plotted in the direction of the major axis for all meters on mooring 1.....	127
IV-9	Ratio of the variance along the major axis to the variance along the minor axis, plotted in the direction of the major axis for all meters on mooring 3.....	127

LIST OF FIGURES (Continued)

Figure	CHAPTER IV (Continued)	Page
IV-10	Ratio of the variance along the major axis to the variance along the minor axis, plotted in the direction of the major axis for all meters on mooring 4.....	127
IV-11	Shaded region in each circle shows the range of directions of the major axis of velocity variances for most one-month velocity segments at each mooring.....	128
IV-12	Sum, K, of the variances along the major and minor axis directions, plotted in the direction of the major axis for all meters on mooring 1.....	129
IV-13	Sum, K, of the variances along the major and minor axis directions, plotted in the direction of the major axis for all meters on mooring 2 deployed before March 1981.....	129
IV-14	Sum, K, of the variances along the major and minor axis directions, plotted in the direction of the major axis for all meters on mooring 2 for the March to July 1981 deployment.....	129
IV-15	Sum, K, of the variances along the major and minor axis directions, plotted in the direction of the major axis for all meters on mooring 3.....	130
IV-16	Sum, K, of the variances along the major and minor axis directions, plotted in the direction of the major axis for all meters on mooring 4.....	130
IV-17	Low-pass filtered time series of temperature and horizontal velocity at the moorings and meters indicated.....	132
IV-18	Time series of temperature and horizontal velocity from meter 2 of mooring 2.....	134
IV-19	Time series of horizontal currents at the upper and lower meters of moorings 1, 2, and 3.....	136
IV-20	Time series of temperature at the upper and lower meters of moorings 1, 2, and 3.....	137
IV-21	Autospectrum of u-component (east-west) of velocity for meter 1 of mooring 3, recovered July 1981.....	143

LIST OF FIGURES (Continued)

Figure	CHAPTER IV (Continued)	Page
IV-22	Autospectrum of v-component (north-south) of velocity for meter 1 of mooring 3, recovered July 1981.....	143
IV-23	Frequency response and phase between the u and v components of velocity for meter 1 of mooring 3, recovered July 1981.....	143
IV-24	Coherence squared between the u and v components of velocity for meter 1 of mooring 3, recovered July 1981.....	144
IV-25	Rotary spectrum of the u-v velocity vector for meter 1 of mooring 3, recovered July 1981.....	144
IV-26	Autospectrum of u-component (east-west) of velocity for meter 2 of mooring 3, recovered July 1981.....	145
IV-27	Autospectrum of v-component (north-south) of velocity for meter 2 of mooring 3, recovered July 1981.....	145
IV-28	Frequency response and phase between the u and v components of velocity for meter 2 of mooring 3, recovered July 1981.....	145
IV-29	Coherence squared between the u and v components of velocity for meter 2 of mooring 3, recovered July 1981.....	146
IV-30	Rotary spectra of the u-v velocity vector for meter 2 of mooring 3, recovered July 1981.....	146
IV-31	Autospectrum of u-component (east-west) of velocity for meter 3 of mooring 3, recovered July 1981.....	147
IV-32	Autospectrum of v-component (north-south) of velocity for meter 3 of mooring 3, recovered July 1981.....	147

LIST OF FIGURES (Continued)

Figure	CHAPTER IV (Continued)	Page
IV-33	Frequency response and phase between the u and v components of velocity for meter 3 of mooring 3, recovered July 1981.....	147
IV-34	Coherence squared between the u and v components of velocity for meter 3 of mooring 3, recovered July 1981.....	148
IV-35	Rotary spectra of the u-v velocity vector for meter 3 of mooring 3, recovered July 1981.....	148
IV-36	Autospectrum of u-component (east-west) of velocity for meter 4 of mooring 3, recovered July 1981.....	149
IV-37	Autospectrum of v-component (north-south) of velocity for meter 4 of mooring 3, recovered July 1981.....	149
IV-38	Frequency response and phase between the u and v components of velocity for meter 4 of mooring 3, recovered July 1981.....	149
IV-39	Coherence squared between the u and v components of velocity for meter 4 of mooring 3, recovered July 1981.....	150
IV-40	Rotary spectra of the u-v velocity vector for meter 4 of mooring 3, recovered July 1981.....	150
IV-41	Autospectrum of temperature for meter 1 of mooring 3, recovered July 1981.....	156
IV-42	Frequency response and phase between temperature and the v (north-south) component of velocity for meter 1 of mooring 3, recovered July 1981.....	156
IV-43	Coherence squared between temperature and the v (north-south) component of velocity for meter 1 of mooring 3, recovered July 1981.....	156
IV-44	Autospectrum of temperature for meter 2 of mooring 3, recovered July 1981.....	157

LIST OF FIGURES (Continued)

Figure	CHAPTER IV (Continued)	Page
IV-45	Frequency response and phase between temperature and the v (north-south) component of velocity for meter 2 of mooring 3, recovered July 1981.....	157
IV-46	Coherence squared between temperature and the v (north-south) component of velocity for meter 2 of mooring 3, recovered July 1981.....	157
IV-47	Autospectrum of temperature for meter 3 of mooring 3, recovered July 1981.....	158
IV-48	Frequency response and phase between temperature and the v (north-south) component of velocity for meter 3 of mooring 3, recovered July 1981.....	158
IV-49	Coherence squared between temperature and the v (north-south) component of velocity for meter 3 of mooring 3, recovered July 1981.....	158
IV-50	Autospectrum of temperature for meter 4 of mooring 3, recovered July 1981.....	159
IV-51	Frequency response and phase between temperature and the v (north-south) component of velocity for meter 4 of mooring 3, recovered July 1981.....	159
IV-52	Coherence squared between temperature and the v (north-south) component of velocity for meter 4 of mooring 3, recovered July 1981.....	159
IV-53	Raw velocity and transmissivity time series records for April-June 1980 from (a) mooring 1 meter 2, and (b) mooring 3 meter 2.....	162
IV-54	Lowpass filtered records of velocity and transmissivity time series records for April-June 1980 from (a) mooring 1 meter 2, and (b) mooring 3 meter 2... ..	163
IV-55	Bandpass velocity and transmissivity time series records for April-June 1980 from mooring 1 meter 2.....	164

LIST OF FIGURES (Continued)

Figure	CHAPTER IV (Continued)	Page
IV-56	Bandpass velocity and transmissivity time series records for April-June 1980 from mooring 3 meter 2.....	165
IV-57	Large scale bedforms on the West Flower Garden Bank as determined from a digital side-scan sonar mosaic.....	166
IV-58	Large scale bedforms on the East Flower Garden Bank as determined from side-scan sonar records.....	167
IV-59	Monthly averaged wind vectors at the High Island weather station near the East and West Flower Garden Banks for 1979 and for the last half of 1980.....	171
IV-60	Composite plots of temperature and salinity profiles taken near the East and West Flower Garden Banks on three cruises.....	177
IV-61	Vertical section of temperature from northwest to southeast across the East Flower Garden Bank.....	179
IV-62	Map of the East Flower Garden Bank showing locations of stations taken on the BALTIC SEAL cruise of October 1980.....	179
IV-63	Temperature at meter 1 of mooring 1 (54 m depth) during the period when PHISH stations were taken around the East and West Flower Garden Banks on the October 1980 BALTIC SEAL cruise.....	180
IV-64	Horizontal velocity vectors at a depth of 70 m determined from PHISH stations taken on the October 1980 BALTIC SEAL cruise.....	182
IV-65	Plot of temperature, salinity, transmissivity, and sigma-t at EFG station 5E, October 1980.....	183
IV-66	Plot of temperature, salinity, transmissivity, and sigma-t at EFG station 6E, October 1980.....	183
IV-67	Depth in metres of the 19.6°C isotherm at stations taken around the East and West Flower Garden Banks in March 1981 on the GYRE cruise.....	184

LIST OF FIGURES (Continued)

Figure	CHAPTER IV (Continued)	Page
IV-68	Horizontal velocity vectors at 1 m from bottom determined from PHISH stations taken on the March 1981 GYRE cruise.....	185
IV-69	Transmissivity versus SPM concentration determined from samples taken at the bottom of PHISH cast from stations near the East and West Flower Garden Banks.....	188
IV-70	Hydrographic station location map for the BALTIC SEAL cruise, October 10-20, 1980.....	190
IV-71	Hydrographic station location map for the GYRE cruise, March 3-8, 1981.....	191
IV-72	Hydrographic station location map for the NORTH SEAL cruise, July 13-17, 1981.....	192
IV-73	Hydrographic stations at the East Flower Garden Bank for the NORTH SEAL cruise, July 13-17, 1981.....	193
IV-74	Plots of temperature, salinity, transmissivity, and sigma-t from WFG stations 13S and 17S, March 1981.....	194
IV-75	Plots of temperature, salinity, transmissivity, and sigma-t from WFG station 2W and EFG station 4E, March 1981.....	195
IV-76	Vertical extent of BNL from bottom during the BALTIC SEAL cruise, October 1980.....	197
IV-77	Vertical extent of BNL from bottom during the GYRE cruise, March 1981.....	198
IV-78	Vertical extent of BNL from bottom during the NORTH SEAL cruise, July 1981.....	199
IV-79	Vertical extent of BNL from bottom of EFG during the NORTH SEAL cruise, July 1981.....	200
IV-80	Minimum XMS of BNL during the BALTIC SEAL cruise, October 1980.....	201

LIST OF FIGURES (Continued)

Figure	CHAPTER IV (Continued)	Page
IV-81	Minimum XMS of BNL during the GYRE cruise, March 1981.....	202
IV-82	Minimum XMS of BNL during the NORTH SEAL cruise, July 1981.....	203
IV-83	Minimum XMS of BNL at EFG during the NORTH SEAL cruise, July 1981.....	204
IV-84	Plots of temperature, salinity, transmissivity, and sigma-t at WFG stations 1W and 3W, October 1980, showing minimum and maximum vertical extent of BNL in October.....	205
IV-85	Plots of temperature, salinity, transmissivity, and sigma-t from EFG station 10E (October 1980) and WFG station 25 (July 1981) illustrating an advected turbid layer.....	207
IV-86	Plot of temperature, salinity, transmissivity, and sigma-t from EFG station 1E (March 1981) showing an advected BNL overlaying a thin bottom layer of cold clean water containing a sharp temperature decrease which inhibits bottom mixing.....	208
IV-87	Plot of temperature, salinity, transmissivity, and sigma-t from WFG station 26 (July 1981) showing a bottom mixed layer formation with no associated BNL.....	208
IV-88	Diagrammatic representation of dye emitter apparatus used in October 1980 boundary layer experiments at the Flower Garden Banks.....	215
IV-89	Diagrammatic representation of tautline mooring on which vanes and dye emitters were assembled for 1979 and 1980 boundary layer experiments at the Flower Garden Banks.....	216
IV-90	Location of October 1979 submersible dive stations where dye emission experiments were made.....	219
IV-91	Location of October 1980 submersible dive stations where dye emission experiments were made.....	222

LIST OF FIGURES

Figure		Page
CHAPTER V		
V-1	Gas chromatogram of EFG-2G hexane eluate.....	239
V-2	Gas chromatogram of EFG-2G benzene eluate.....	240
V-3	Mass spectrum of fluoranthene from sample EFG-2G.....	241
V-4	Mass spectrum of pyrene from sample EFG-2G.....	242
V-5	Mass spectrum of chrysene from sample EFG-2G.....	243
V-6	Mass spectrum of benz[a]anthracene from sample EFG-2G...	244
CHAPTER VI		
VI-1	Location map for the banks discussed in Chapter VI.....	263
VI-2	Bathymetric map of Ewing Bank showing locations of seismic lines illustrated in Figures VI-4 and 5.....	264
VI-3	Perspective views of Ewing Bank.....	265
VI-4	Boomer profiles on Ewing Bank.....	266
VI-5	A 7 kHz high resolution sub-bottom profile and side-scan sonar record on Ewing Bank.....	267
VI-6	Structure-Isopach map of Ewing Bank.....	268
VI-7	Seafloor roughness map of Ewing Bank.....	269
VI-8	Bathymetric map of Parker Bank showing sediment sample locations and seismic lines illustrated in Figures VI-11 and 12.....	270
VI-9	Perspective views of Parker Bank.....	271
VI-10	Structure-Isopach map of Parker Bank.....	272
VI-11	Boomer profile across Parker Bank.....	273
VI-12	A 7 kHz high resolution sub-bottom profile across Parker Bank.....	274

LIST OF FIGURES (Continued)

Figure	CHAPTER VI (Continued)	Page
VI-13	Seafloor roughness map of Parker Bank.....	275
VI-14	Bathymetric map of Bouma Bank showing location of seismic line and side-scan sonar record illustrated in Figure VI-18.....	276
VI-15	Perspective views of Bouma Bank.....	277
VI-16	Structure-Isopach map of Bouma Bank.....	278
VI-17	Seafloor roughness map of Bouma Bank.....	279
VI-18	A 7 kHz high resolution sub-bottom profile and side-scan sonar record across Bouma Bank.....	280
VI-19	Bathymetric map of 18 Fathom Bank showing location of the seismic line illustrated in Figure VI-21.....	281
VI-20	Perspective views of 18 Fathom Bank.....	282
VI-21	Boomer profile across 18 Fathom Bank.....	283
VI-22	Structure-Isopach map of 18 Fathom Bank.....	284
VI-23	Seafloor roughness map of 18 Fathom Bank.....	285
VI-24	Bathymetric map of Bright Bank showing the location of the seismic line and side-scan sonar record illustrated in Figure VI-26 and locations of sediment sample stations.....	286
VI-25	Perspective views of Bright Bank.....	287
VI-26	A 7 kHz high resolution sub-bottom profile and side-scan sonar record across Bright Bank.....	288
VI-27	Seafloor roughness map of Bright Bank.....	289
VI-28	Bathymetric map of Stetson Bank showing locations of bathymetric and sub-bottom profiles shown on Figures VI-31 and 32.....	290
VI-29	Sediment station locations at Stetson Bank.....	291
VI-30	Perspective views of Stetson Bank.....	292

LIST OF FIGURES (Continued)

Figure		Page
	CHAPTER VI (Continued)	
VI-31	A 3.5 kHz high resolution sub-bottom profile across Stetson Bank.....	293
VI-32	A 12 kHz bathymetric profile across Stetson Bank.....	293
VI-33	Distribution of sediment types at Stetson Bank.....	294
VI-34	Structure-Isopach map of Stetson Bank.....	295
VI-35	Seafloor roughness map of Stetson Bank.....	296
VI-36	Bathymetric map of MacNeil Bank showing locations of seismic profiles illustrated in Figure VI-39.....	297
VI-37	Perspective views of MacNeil Bank.....	298
VI-38	Structure-Isopach map of MacNeil Bank.....	299
VI-39	Boomer profiles on MacNeil Bank.....	300

LIST OF APPENDIX FIGURES

Figure		Page
A-1	Sediment grab sample locations for September 5, 1979, on the East Flower Garden Bank.....	A-5
A-2	Sediment grab sample locations for October 1979 and October 1980 at the West Flower Garden Bank.....	A-6

LIST OF TABLES

Table		Page
CHAPTER I		
I-1	Summary of Data Gathered in Previous TAMRF-BLM Topographic Features Studies, 1974-80.....	2
I-2	Key Personnel and Associates.....	9
I-3	Modification Breakdown.....	11
I-4	Summary of Cruises.....	14
I-5	Data Carry-over from Previous Contracts.....	17
CHAPTER II		
II-1	Relationship Between Sediment Facies and Biological Zones at the East Flower Garden Bank.....	23
CHAPTER III		
III-1	Population Levels of Corals at the West Flower Garden Listed in Decreasing Order of Importance.....	58
III-2	Population Levels of Corals at the East Flower Garden Listed in Decreasing Order of Importance.....	59
III-3	Population Levels of Corals at the EFG Sites Listed in Decreasing Order of Importance.....	60
III-4	Vertical Growth of <u>D. strigosa</u> and <u>M. annularis</u>	70
III-5	Lateral Encrusting Growth of <u>Montastrea</u> <u>annularis</u> at Each Station.....	72
III-6	Lateral Encrusting Growth of <u>Agaricia</u> <u>agaricites</u> at Each Station.....	73
III-7	Lateral Encrusting Growth for the Hydrozoan Coral <u>Millepora alcicornis</u> at Each Station.....	73
III-8	Lateral Encrusting Growth for <u>Diplora strigosa</u>	74
III-9	Lateral Encrusting Growth for <u>Porites</u> <u>astreoides</u>	74
III-10	Lateral Encrusting Growth for <u>Montastrea</u> <u>cavernosa</u>	74
III-11	Mortality (Lateral Retreat) for Coral Species.....	75

LIST OF TABLES (Continued)

Table		Page
CHAPTER III (Continued)		
III-12	Lateral Encrusting Growth Rates for the Various Corals During Two Time Periods.....	76
III-13	Lateral Encrusting Growth Rates for the Various Corals During Both Periods Combined.....	77
III-14	Lateral Encrusting Growth Rates for Various Corals During All Periods Measured.....	77
III-15	Coral Mortality Rates During the Two Time Periods Combined (Sep 79 - Jun 80).....	78
III-16	Coral Mortality Rates During All Periods Measured....	78
CHAPTER IV		
IV-1	HydroProducts Current Meter and Associated Time Series Data Inventory, East and West Flower Garden Banks.....	112
IV-2	Quality Assessment of HydroProducts Current Meter and Associated Time Series Data, East and West Flower Garden Banks.....	114
IV-3	Marsh-McBirney Electromagnetic Current Meter Data Inventory.....	117
IV-4	Data Inventory for Conductivity-Temperature Probe Deployed on Mooring Line Adjacent to the Marsh-McBirney Electromagnetic Current Meter.....	118
IV-5	Average Direction of Major Axis of Variance Compared to Local Isobath Direction.....	124
IV-6	Theoretical Frequency and Period of Major Tidal Constituents and of Inertial Currents.....	151
IV-7	Tidal Current Amplitudes in cm/sec at Mooring 3 for 6 Mar to 16 Jul 81.....	152

LIST OF TABLES (Continued)

Table		Page
CHAPTER V		
V-1	Concentration of Alkanes in <u>Spondylus americanus</u> (October 1980).....	230
V-2	Percent Distribution of <u>n</u> -Paraffins; Concentrations of <u>n</u> -Paraffins, Pristane, Phytane, and Total Alkanes; and Calculated Ratios Found in <u>Spondylus</u> (October 1980).....	231
V-3	Comparison of Selected Parameters for <u>Spondylus</u> <u>americanus</u> from the East Flower Garden and Other Sites for 1976-1980.....	233
V-4	GC-MS Standard Operating Conditions.....	236
V-5	Normal Hydrocarbon Concentrations (Sample: EFG-1Ga)...	245
V-6	Normal Hydrocarbon Concentrations (Sample: EFG-2G)....	245
V-7	Normal Hydrocarbon Concentrations (Sample: EFG-3Ga)...	246
V-8	Normal Hydrocarbon Concentrations (Sample: EFG-4Ga)...	246
V-9	Normal Hydrocarbon Concentrations (Sample: WFG-1Ga)...	247
V-10	Normal Hydrocarbon Concentrations (Sample: WFG-2Ga)...	247
V-11	Normal Hydrocarbon Concentrations (Sample: WFG-3Ga)...	248
V-12	Normal Hydrocarbon Concentrations (Sample: WFG-4Ga)...	248
V-13	Concentration and Retention Time of Aromatic Hydrocarbons in Sediments (Sample: EFG-1Ga).....	249
V-14	Concentration and Retention Time of Aromatic Hydrocarbons in Sediments (Sample: EFG-2G).....	249
V-15	Concentration and Retention Time of Aromatic Hydrocarbons in Sediments (Sample: EFG-3Ga).....	249
V-16	Concentration and Retention Time of Aromatic Hydrocarbons in Sediments (Sample: EFG-4Ga).....	249
V-17	Concentration and Retention Time of Aromatic Hydrocarbons in Sediments (Sample: WFG-1Ga).....	250

xxii
LIST OF TABLES (Continued)

Table		Page
CHAPTER V (Continued)		
V-18	Concentration and Retention Time of Aromatic Hydrocarbons in Sediments (Sample: WFG-2Ga).....	250
V-19	Concentration and Retention Time of Aromatic Hydrocarbons in Sediments (Sample: WFG-3Ga).....	251
V-20	Concentration and Retention Time of Aromatic Hydrocarbons in Sediments (Sample: WFG-4Ga).....	251
V-21	TOC and Delta C-13 Values in Sediments.....	252
V-22	Peak Identifications in Benzene Eluates.....	252
CHAPTER VI		
VI-1	Summary of Survey Data on Selected Banks.....	253

LIST OF APPENDIX TABLES

Table		Page
APPENDIX A		
A-1	Flower Gardens Sediment Texture.....	A-3
A-2	Flower Gardens X-ray Diffraction Analyses.....	A-3
A-3	Sediment Particle Types: Flower Garden Banks.....	A-4
APPENDIX B		
B-1	Coral Population Level Parameters (Site - BLM, Species - <u>Montastrea annularis</u>).....	B-2
B-2	Coral Population Level Parameters (Site - BLM, Species - <u>Diploria strigosa</u>).....	B-3
B-3	Coral Population Level Parameters (Site - BLM, Species - <u>Montastrea cavernosa</u>).....	B-4
B-4	Coral Population Level Parameters (Site - BLM, Species - <u>Colpophyllia</u> spp.).....	B-5
B-5	Coral Population Level Parameters (Site - BLM, Species - <u>Millepora</u> spp.).....	B-6
B-6	Coral Population Level Parameters (Site - BLM, Species - <u>Porites astreoides</u>).....	B-7
B-7	Coral Population Level Parameters (Site - BLM, Species - <u>Agaricia</u> spp.).....	B-8
B-8	Coral Population Level Parameters (Site - BLM, Species - <u>Madracis decactis</u>).....	B-9
B-9	Coral Population Level Parameters (Site - BLM, Species - <u>Stephanocoenia michelini</u>).....	B-10
B-10	Coral Population Level Parameters (Site - BLM, Species - <u>Siderastrea siderea</u>).....	B-11
B-11	Coral Population Level Parameters (Site - BLM, Species - <u>Scolymia cubensis</u>).....	B-12
B-12	Coral Population Level Parameters (Site - BLM, Species - <u>Mussa angulosa</u>).....	B-13
B-13	Population Level Parameters: Filamentous Algae and Total Live Coral (Site - BLM).....	B-14

LIST OF APPENDIX TABLES (Continued)

Table	APPENDIX B (Continued)	Page
B-14	Coral Population Level Parameters (Site - CSA, Species - <u>Montastrea annularis</u>).....	B-15
B-15	Coral Population Level Parameters (Site - CSA, Species - <u>Diploria strigosa</u>).....	B-16
B-16	Coral Population Level Parameters (Site - CSA, Species - <u>Montastrea cavernosa</u>).....	B-17
B-17	Coral Population Level Parameters (Site - CSA, Species - <u>Colpophyllia</u> spp.).....	B-18
B-18	Coral Population Level Parameters (Site - CSA, Species - <u>Millepora</u> spp.).....	B-19
B-19	Coral Population Level Parameters (Site - CSA, Species - <u>Porites astreoides</u>).....	B-20
B-20	Coral Population Level Parameters (Site - CSA, Species - <u>Agaricia</u> spp.).....	B-21
B-21	Coral Population Level Parameters (Site - CSA, Species - <u>Madracis decactis</u>).....	B-22
B-22	Coral Population Level Parameters (Site - CSA, Species - <u>Stephanocoenia michelini</u>).....	B-23
B-23	Coral Population Level Parameters (Site - CSA, Species - <u>Siderastrea siderea</u>).....	B-24
B-24	Coral Population Level Parameters (Site - CSA, Species - <u>Scolymia cubensis</u>).....	B-25
B-25	Coral Population Level Parameters (Site - CSA, Species - <u>Mussa angulosa</u>).....	B-26
B-26	Population Level Parameters: Filamentous Algae and Total Live Coral (Site - CSA).....	B-27
B-27	Coral Population Level Parameters at the Flower Garden Banks (Species - <u>Montastrea annularis</u>).....	B-28
B-28	Coral Population Level Parameters at the Flower Garden Banks (Species - <u>Diploria strigosa</u>).....	B-29
B-29	Coral Population Level Parameters at the Flower Garden Banks (Species - <u>Montastrea cavernosa</u>).....	B-30

LIST OF APPENDIX TABLES (Continued)

Table		Page
	APPENDIX B (Continued)	
B-30	Coral Population Level Parameters at the Flower Garden Banks (Species - <u>Colpophyllia</u> spp.).....	B-31
B-31	Coral Population Level Parameters at the Flower Garden Banks (Species - <u>Millepora</u> spp.).....	B-32
B-32	Coral Population Level Parameters at the Flower Garden Banks (Species - <u>Porites astreoides</u>).....	B-33
B-33	Coral Population Level Parameters at the Flower Garden Banks (Species - <u>Agaricia</u> spp.).....	B-34
B-34	Coral Population Level Parameters at the Flower Garden Banks (Species - <u>Madracis decactis</u>).....	B-35
B-35	Coral Population Level Parameters at the Flower Garden Banks (Species - <u>Stephanocoenia michelini</u>).....	B-36
B-36	Coral Population Level Parameters at the Flower Garden Banks (Species - <u>Siderastrea siderea</u>).....	B-37
B-37	Coral Population Level Parameters at the Flower Garden Banks (Species - <u>Scolymia cubensis</u>).....	B-38
B-38	Coral Population Level Parameters at the Flower Garden Banks (Species - <u>Mussa angulosa</u>).....	B-39
B-39	Population Level Parameters at the Flower Garden Banks: Filamentous Algae and Total Live Coral.....	B-40
B-40	Coral Diversity, Evenness, Richness (Site - BLM).....	B-41
B-41	Coral Diversity, Evenness, Richness (Site - CSA).....	B-42
B-42	Coral Diversity, Evenness, Richness: EFG/WFG.....	B-43
	APPENDIX C	
C-1	Parker Bank Sediment Texture Data (1977).....	C-2
C-2	Parker Bank Grain Type Data (1977).....	C-2
C-3	Stetson Bank Sediment Texture Data (1958 and 1974)....	C-3
C-4	Stetson Bank Sediment Texture Data (1976).....	C-4
C-5	Stetson Bank Grain Type Data (1974).....	C-5
C-6	Stetson Bank Grain Type Data (1976).....	C-6

CHAPTER I

INTRODUCTION

D. McGrail, Program Manager
S. Herrig, Assistant Program Manager

This report concerns Gulf of Mexico studies performed in 1979-1981 by Texas A&M oceanographers for the U.S. Department of the Interior, Minerals Management Service (MMS).^{*} Formerly known as the New Orleans Outer Continental Shelf Office of the Bureau of Land Management (BLM), MMS is the new title of the government agency which has funded continuing Gulf of Mexico studies directed by Richard Rezak and Thomas J. Bright since 1975 and by Drs. Bright, Rezak, and David W. McGrail since 1977 (Bright and Rezak, 1976; Bright and Rezak, 1978a,b; Rezak and Bright, 1981a). These studies built upon previous investigations and were motivated by concerns about the environmental effects of oil and gas lease sales on the Outer Continental Shelf (OCS) of the Gulf of Mexico.

BACKGROUND ON PREVIOUS STUDIES

The U.S. Department of the Interior, Bureau of Land Management, held public hearings in 1973, 1974, and 1975, prior to Texas OCS oil and gas lease sales. The hearings were held because of concerns about the possible environmental impact of oil and gas drilling and production operations on coral reefs and fishing banks in or adjacent to lease blocks to be sold. Concerns were articulated by government agencies, such as the National Marine Fisheries Service, by university scientists, and by private citizens. As a result of these hearings, certain restrictive regulations were established for drilling operations in the vicinity of the well documented coral reefs at the East and West Flower Garden Banks.

At that time, very little was known about the geology and biology of the South Texas OCS banks lying in or near lease blocks to be offered for sale in 1975. To fill this information gap, BLM contracted with Texas A&M oceanographers for what became a series of Gulf of Mexico studies. Dates and types of data obtained since the original 1975 study are summarized in Table I-1.

^{*}The division of the Department of the Interior Bureau of Land Management (BLM) dealing with offshore minerals leasing was reorganized to become the Minerals Management Service (MMS), effective May 10, 1982. It should be borne in mind that all references in the present report to leasing and resource management by BLM are presently administered by the newly created MMS.

TABLE 1-1
SUMMARY OF DATA GATHERED IN PREVIOUS
TAMRF-BLM TOPOGRAPHIC FEATURES STUDIES, 1974-80

BANK NAME (abbrev.)	CONTRACT YEAR(s) STUDIED	MAPPING CRUISE	§SUB. OBS. (geo/bio/ hydro)	ROCK SAMP- LES	SEDIMENT SAMPLING	SIDE- SCAN SONAR	SUB-BOTTOM SEISMIC PROFILES	HYDRO- GRAPHIC MEASURE- MENTS	SPECIAL STUDIES
Adam:									
Big Adam (BAD)	CT-5	Jun 75	Jun 75 (geo)	X	X	X			
Small Adam (SAD)	CT-5	Nov 74	none	X		X			
Little Adam (LAD)	CT-5	Nov 74	(no topographic expression)						
Alderdice (ALD)	CT-8	Sep 78 (geo/bio)	Oct 78	X	X	X**	X**(S/I;R)	X	
Applebaum (APL)	CT-5	May 75	none	X	X	X			
(Little Sister)	CT-8		none			**			
Aransas (ARA)	CT-5 CT-6	Nov 74	Sep 76 (bio)			X			
Baker (BAK)	CT-5	Oct 74	May 75	X	X	X			
South Baker (SBA)	CT-5 CT-6	Oct 74	May 75 Sep 76	X	X	X			††PDE
Blackfish (BLA)	CT-5 CT-6	Nov 74	TV only			X			
Bouma (BOU)	CT-7 CT-0	May 77	Sep 77 (bio)	X		X **	X **(S/I;R)		
Bright (BRI)	CT-7 CT-0	May 77	Sep 77 (bio)		X	X **	X **(R)	X	
Claypile (CLA)	CT-6 CT-7	Jun 77	Sep 76 (bio)	X		X	X		
Coffee Lump (COF)	CT-8	Sep 78	Sep/Oct 78	X	X	X**	X**(S/I;R)	X	
Diaphus (DIA)	CT-8	Sep 78	Oct 78	X	X	X**	X**(S/I;R)	X	
Dream (DRE)	CT-5	Nov 74	Jun 75	X	X	X			

† : Chart prepared in 1969 by Southwest Research Institute; revised by TAMU in 1974.

* : Sediment distribution map constructed.

** : Interpreted; S/I = structure/isopach map; R = seafloor roughness map; M = side-scan sonar mosaic.

†† : PDE = post-drilling environmental assessment.

Eco = quantitative ecological study of relationship of nepheloid layer to epibenthic community distribution and abundance.

X : Studies conducted, as indicated in column heading.

§ : Unless otherwise indicated, geological, biological, and hydrographic observations were made from the submersible.

TABLE I-1 (Continued)

BANK NAME (abbrev.)	CONTRACT YEAR(s) STUDIED	MAPPING CRUISE	§SUB. OBS. (geo/bio/ hydro)	ROCK SAMP- LES	SEDIMENT SAMPLING	SIDE- SCAN SONAR	SUB-BOTTOM SEISMIC PROFILES	HYDRO- GRAPHIC MEASURE- MENTS	SPECIAL STUDIES
East (EAS)	CT-5	Nov 74	(no topographic expression)						
East Flower Garden Garden (EFG)	CT-5		Jun 75	X	X				††PDE
	CT-6	Jul 76	Sep 76	X	X	X	X	X	††Mon
	CT-7		Sep 77	X	X			X	††Mon
	CT-8		Oct 78	X	X*	**	**	X	††Mon
	CT-0		Sep 79 & Oct 80	X	X*	**	** (S/I;R)	X	††Mon
Elvers (ELV)	CT-8	Sep 78	Oct 78 (bio)			X**	X** (S/I;R)		
Ewing (EWI)	CT-7	May 77	Sep 77			X	X		
	CT-0					**	** (S/I;R)		
Fishnet (FIS)	CT-8	Sep 78	Oct 78	X	X	X**	X** (S/I;R)	X	
Four Rocks (4RO)	CT-5	May 75	(no topographic expression)						
Geyer (GEY)	CT-8	Sep 78	Oct 78 (bio)	X		X**	X** (S/I;R)		
Hospital (HOS) North Hospital (NHO)	CT-5	†	TV only						
	CT-6		Sep 76		X	X		X	††Eco
	CT-5	Nov 74	Jun 75			X			
Jakkula (JAK)	CT-8	Sep 78	Oct 78 (bio)	X	X	X**	X** (S/I;R)	X	
MacNeil (MAC)	CT-0	Aug/Sep 80	none			X* (M)	X** (S/I)		
Mysterious (MYS)	CT-5	Nov 74	TV only			X			
Parker (PAR)	CT-7	May 77	Sep 77 (geo)		X	X	X	X	
	CT-0					**	** (S/I;R)		
Rezak-Sidner (RSI)	CT-8	Oct 78	Oct 78	X	X	X**	X** (S/I;R)		
Sackett (SAC)	CT-7	May 77	Sep 77 (bio)		X	X	X	X	
Sonnler (SON) (Three Hickey Rock)	CT-7	May 77	Sep 77	X	X	X	X	X	

† : Chart prepared in 1969 by Southwest Research Institute - revised by TAMU 1974.

* : Sediment distribution map constructed.

** : Interpreted; S/I = structure/isopach map; R = seafloor roughness map; M = side-scan sonar mosaic.

†† : PDE = post-drilling environmental assessment.

Eco = quantitative ecological study of relationship of nepheloid layer to epibenthic community distribution and abundance.

Mon = monitoring study conducted.

X : Studies conducted, as indicated in column heading.

§ : Unless otherwise indicated, geological, biological, and hydrographic observations were made from the submersible.

1975 Studies

The initial Texas A&M investigation for BLM provided baseline biological and geological information required to facilitate judgements as to the need for and nature of protective regulations to be imposed on drilling operations near these banks. During the latter part of 1974 and early 1975, Texas A&M contracted to map 17 banks using precision navigation, precision depth recorder, and side-scan sonar. It was found that three of the areas mapped exhibited no topographic expression and were not studied further. Six of the seventeen banks were examined and sampled using the Texas A&M submersible DRV DIAPHUS. All seafloor observations were documented using 35 mm color still photography and black and white video recordings. Surface samples (grabs and cores) were taken at five of the banks. Results of this field work were reported in January 1976 (Bright and Rezak, 1976).

An important discovery made in 1975 was the presence of a layer of turbid water that blanketed the continental shelf surrounding all of the banks examined on the South Texas OCS. This layer of turbid water is associated with increased sedimentation and limited light, both of which have a profound influence on the biota of the banks and the sediments on and around them. The phenomenon is similar to the turbid layer identified by Ewing and Thorndike (1965) in the North Atlantic, for which they coined the term "nepheloid layer." Subsequent Texas A&M studies for BLM have investigated the origin and effects of the nepheloid layer.

1976 Studies

A second investigation initiated for BLM in 1976 (Bright and Rezak, 1978a) extended the mapping program to three more banks and included additional submersible observations of four banks. At four of the seven banks investigated, studies included post-drilling environmental assessments and at two banks scientists examined the quantitative ecological relationship between the nepheloid layer and epibenthic community population dynamics.

An important discovery during the course of this investigation was the existence of a high salinity brine lake at the East Flower Garden Bank. Through subsequent submersible observations (1977-1980), the brine lake has provided a unique opportunity for the study of effects of natural brine discharges. These data should prove useful in assessing the effect of brines which may be discharged from an offshore oil or gas platform over years of production. The presence of the brine lake also provided information on the nature of salt tectonism at the East Flower Garden Bank.

1977 Studies

Studies of the nepheloid layer at various banks and studies of the brine lake at the East Flower Garden Bank were continued in 1977 (Bright and Rezak, 1978b). Additional mapping studies in 1977 provided physiographic and sub-bottom data on eight more banks, seven of which

were observed from the submersible. A biological monitoring study was also initiated for the first time within the living coral portion of the East Flower Garden Bank.

1978-1980 Studies

Biological monitoring of the East Flower Garden coral reef was continued in 1978 (Rezak and Bright, 1981), as were studies of the nepheloid layer at selected banks. Both mapping and submersible studies were also undertaken at nine banks not previously observed. Among these was the West Flower Garden Bank, where monitoring studies identical to those at the East Flower Garden Bank were initiated in 1980.

During the 1978-1980 study, several technological changes were made. Provision for seismic and side-scan sonar equipment on mapping cruises made possible the preparation of a series of seafloor roughness and structure/isopach maps for several of the banks. Color video recordings were made of the submersible observations, and the biological monitoring study at the Flower Garden Banks instituted several experimental techniques that permitted quantitative statistical analyses.

Significant advances were made during 1978-1980 in the instrumentation used for hydrographic studies of the nepheloid layer. The deployment of current meter moorings and the development of a sophisticated new system for simultaneous hydrographic measurements have created a very large data base from measurements of turbidity, current velocities, temperature, and salinity in the region of the Flower Garden Banks.

GOALS OF THE PRESENT STUDY

The present study focused on biological and hydrographic monitoring of the East and West Flower Garden Banks, as well as geological analysis and interpretation of sub-bottom, side-scan, and sedimentological data from these two banks. Sub-bottom and side-scan data for seven selected banks were also analyzed and interpreted; with one exception, these data had been acquired in previous studies (see Table I-1). Specific goals for the various types of studies are given below.

Flower Garden Banks Region

Geology (Chapter II)

Geological studies at the Flower Garden Banks produced a sediment distribution map for the Flower Gardens region and examined the relationship of sediment facies to biotic zones. Analysis of side-scan and sub-bottom data, as well as submersible observations, permitted construction of maps identifying faults on the two banks and interpreting

the structure of the banks. For purposes of display, a side-scan sonar mosaic was prepared for the West Flower Garden Bank, and a seafloor roughness map for the East Flower Garden Bank.

Biology (Chapter III)

Biological investigations at the Flower Garden Banks continued to be directed toward assessment of the health of biotic communities at the two banks. Biotic zonation maps were developed from direct observations and data gathered in the course of the continuing monitoring program. Identical coral ecology studies were carried out at the East and West Flower Garden coral reefs, and the results were compared.

Water and Sediment Dynamics (Chapter IV)

Investigations of water and sediment dynamics at the Flower Garden Banks had three goals: 1) to study the hydrographic climate (salinity, temperature, turbidity, and currents) in which the banks exist; 2) to develop an understanding of the dynamics of the nepheloid layer, particularly as it impinges on these shelf-edge banks; and 3) to ascertain the nature of the shelf-edge flow, including the driving mechanisms.

Chemical Analyses (Chapter V)

Chemical analyses of organisms and sediment samples from the Flower Garden Banks were performed to determine the significance of petroleum-derived hydrocarbons in the samples. These analyses were interpreted in part by comparison with baseline data from previous studies (1975-1978).

Studies of Selected Banks (Chapter VI)

The six banks selected for analysis and interpretation of existing sub-bottom and side-scan records were: Bouma, Bright, 18 Fathom, Ewing, Parker, and Stetson. Existing data are summarized in Table I-1. Similar investigations were carried out at MacNeil Bank, which was mapped for the first time in 1980. The purpose of these studies was to characterize the banks and identify possible geohazards.

New maps prepared in this study include the following:

East Flower Garden - seafloor roughness; structure/isopach; sediment distribution.

West Flower Garden - side-scan sonar mosaic; structure/isopach; sediment distribution.

MacNeil - bathymetry; side-scan sonar mosaic; and structure/isopach.

Ewing - seafloor roughness; structure/isopach.

Parker - seafloor roughness; structure/isopach.

Bouma - seafloor roughness; structure/isopach.

18 Fathom - seafloor roughness; structure/isopach.

Bright - seafloor roughness only (no sub-bottom data acquired).

Stetson - seafloor roughness only (no sub-bottom data acquired).

PROJECT MANAGEMENT

Introduction

The requirements in the Statement of Work were specified in order to obtain information that could be used by BLM and others in making policy and management decisions, in developing Environmental Impact Statements, lease stipulations, etc., and in supporting other mandated requirements. PI's have discussed and shared findings and implications at professional and technical conferences and meetings.

The Contractor was obligated to provide all necessary labor, material, supplies, equipment, facilities, and services to accomplish the specified work items. These work items were as follows:

1. Develop and operate from a Program Management Plan.
2. Plan and conduct a field sampling program in the northern Gulf of Mexico at the East and West Flower Garden Banks.
3. Plan and conduct submersible and monitoring studies and mapping.
4. Reduce, analyze, and synthesize data for the above tasks.
5. Manage and archive scientific data.
6. Prepare and submit plans, maps, and reports.

The Program Management Plan was updated as needed and used as a check and control measure for assessing the progress of contractual requirements and the status of work efforts. The Logistics Plan provided a framework for planning and assessing the field sampling program, submersible studies, mapping, and logistics. Quarterly summary reports, cruise reports, and other intermediate summary records were prepared throughout the period of performance and served as a basis for the integration of work results contained in this final report.

Personnel and Logistics

Table I-2 provides a list of key personnel and associates. Seven modifications were made to the original Statement of Work. These modi-

TABLE I-2
KEY PERSONNEL AND ASSOCIATES

PROGRAM MANAGER

David W. McGrail, Ph.D.

Program Management Staff

Sylvia Herrig; Assistant Program Manager
Rose Norman, Ph.D.; Project Editor

TECHNICAL DIRECTOR

Richard Rezak, Ph.D.

PRINCIPAL INVESTIGATORS

- a.) Thomas J. Bright, Ph.D.; Biological Studies
- b.) David W. McGrail, Ph.D.; Hydrographic Studies
Michael Carnes, Ph.D.; Associate
Doyle Horne; Associate
- c.) Richard Rezak, Ph.D.; Geological Studies and Mapping
C.S. Giam, Ph.D.; Chemical Analyses
Patrick L. Parker, Ph.D.; Chemical Analyses
University of Texas Marine Science Institute, Port Aransas,
Texas

fications, and the costs associated with each, are summarized in Table I-3. Briefly, the requirements in the modifications were as follows:

Modification #1

The Contractor and TAMU were provided funding for the purchase of two additional transmissometers. The TAMU Department of Oceanography purchased one transmissometer as a cost sharing measure. Title to the additional transmissometers was vested with the TAMRF. The three additional transmissometers were integrated with each of the three current meter arrays located in the vicinity of the Flower Garden Banks. This installation provided for a measure of the vertical extent of sediment suspension events.

Modification #2

The Contractor and TAMU were provided overrun funding to cover additional expenses caused by equipment failure and force majeure. These problems impaired the mapping, recovery, and testing efforts. Tropical Storm Danielle in early September 1980 and Hurricane Allen in August 1980 impacted schedules, requiring additional days of ship and crew time.

Modification #3

Additional funds were provided to the Contractor and TAMU to cover expenses for an additional current monitoring cruise at the Flower Garden Banks. A ternary meeting was also added. The additional meeting served as an information exchange between other state, federal, and private organizations. Proceedings have been published (Rezak, 1981).

Modification #4

Additional funds were provided to the Contractor and TAMU to cover expenses for presentation of biological data at the Estuarine Research Federation Conference held in Oregon.

Modification #5

BLM extended the scope of work to include a deployment cruise in the vicinity of the East Flower Garden Bank. Because the negotiations for Contract #AA851-CT1-55 terminated subsequent field work, this deployment cruise was cancelled.

Modification #6

The Contractor and TAMU were provided overrun funding. Equipment problems, manpower limitations, and the cancellation of field work necessitated a time extension to June 1, 1982.

TABLE 1-3
 MODIFICATION BREAKDOWN
 Contract #AA851-CTO-25 (RF 4260)

MOD #	EFFECTIVE DATE	ADDITIONAL AWARD	NEW TOTAL	PURPOSE
1	5/1/80	\$4,700	\$799,700	1) Purchase 1 additional transmissometer to be integrated with each of the 3 current meter arrays in the Flower Garden Banks area (total of 3 new transmissometers).
2	1/12/81	\$200,106	\$999,806	1) Add funds to cover cost overrun. 2) Extend period of performance to August 31, 1981.
3	5/1/81	\$278,172	\$1,277,978	1) Add a current monitoring cruise. 2) Add a progress meeting. 3) Extend period of performance to November 1, 1981. 4) Permission to purchase various equipment parts (to be used with Profiling Hardwired Instrumented Sensor for Hydrography (PHISH)).
4	9/9/81	\$ 1,734	\$1,279,712	1) Add travel funds for presentation of biological data at an oceanography conference.
5	8/3/81	\$ 29,000	\$1,308,712	1) Add funds to cover cost of cancelled cruise. 2) Permission to purchase equipment with existing funds.
6	9/1/81	\$ 89,978	\$1,398,690	1) Add funds to cover cost overrun. 2) Extend period of performance to June 1, 1982.
7	3/24/82*	no cost	\$1,398,690	1) Extended period of performance to July 31, 1982.

*Date of verbal approval

Modification #7

The period of performance was extended to July 31, 1982, in order to provide the necessary time frame within which to complete the final report.

Time, Funds, Space

The period of performance for all work tasks was originally 14 months, ending June 30, 1981. As indicated above, force majeure, changes in the scope of work, and other proposed changes extended the period of performance to July 1982. The final contract award was \$1,398,690.

The BLM Program Office was established in the Oceanography and Meteorology building at Texas A&M University (TAMU). Space was allocated for professional, technical, administrative, and support personnel. Data, records, and samples were stored and processed in the various laboratories on the TAMU campus. Analytical processes leading to the integration and synthesis of data into meaningful information were also performed in these laboratories. The facilities include the following:

Atomic Absorption Laboratory	Geophysical Laboratory
Cartographic Services Unit	Hydrocarbon Chemical Analytical
Center for Trace Characterization	Laboratories
Data Processing Center with Amdahl	Hydrology Laboratory
470V-6 System	R/V GYRE
DRV DIAPHUS	Machine Shop
Electron Microscopy Laboratory	Marine Operations Center
Electronic Technician Shop	Nuclear Science Center
Gas Chromatography-Mass	Photographic Laboratory
Spectronomy Laboratory	Sedimentology Laboratory
	X-Ray Diffraction Laboratory

DATA MANAGEMENTIntroduction

Data and information collected through research activities carried out on this contract were coordinated through data management activities. A data inventory system was used to monitor and control information processing requirements. First- and second-level inventory reports were supplied to the sponsor as contractually required. Data and sample collection, synthesis, and integration were accomplished to supply relevant and timely information for this report.

Data/Sample Collection

Sampling and data collection were carried out at the East and West Flower Garden Banks. The field program consisted of submersible and

monitoring activities. Also, mapping activities were carried out at MacNeil Bank. Table I-4 summarizes cruises conducted on this contract.

Submersible Tasks

Submersible tasks undertaken at the East and West Flower Garden Banks included both observational and sampling activities. Samples were taken for the purposes of clarifying observations and for sediment analyses.

Observational Tasks

Reconnaissance observations and associated sampling activities were carried out on one submersible cruise in three legs. Areas of past exploratory drilling, potential exploratory drilling, and other areas were inspected to assess the overall health of the East and West Flower Garden Banks.

Sampling Tasks

Seafloor sampling for geologic analysis and faunal identification was undertaken to facilitate interpretation of visual, photographic, and video tape observations and for site characterization. Spondylus americanus were collected at the East and West Flower Garden Banks for hydrocarbon analysis. Bottom grab samples were taken at West Flower Garden stations for sediment texture analysis. Sediment samples taken at both East and West Flower Garden stations were for mineralogy, total carbonate, total organic carbon, high molecular weight hydrocarbon, and Delta C-13 analyses.

Monitoring Tasks

Monitoring activities included both studies of currents and biological monitoring.

Current Monitoring and Hydrographic Data Collection

Time series current meter data were obtained for four deployment periods. Additionally, data on currents and other hydrographic measurements were collected on four cruises to the Flower Garden Banks, using XBT's, a dye emission study, and a Profiling Hardwired Instrumented Sensor for Hydrography (PHISH).

Biological Monitoring

Observational activities and inwater sampling were performed using SCUBA diving gear. Population levels of corals and other relevant information were studied through the use of plotless line transects. Coral recruitment settling plates were retrieved and replacements were emplaced for future retrieval.

TABLE I-4
SUMMARY OF CRUISES
(TAMRF-BLM CONTRACT AA851-CT0-25)

CRUISE	DATES	SHIP	SITE	CHIEF SCIENTIST
1st Mapping	19 Jun - 20 Jun 80 (aborted)	JUNE BOLLINGER	MacNeil	Rezak
1st Combined				
a) Mapping	29 Aug - 5 Sep 80	JUNE BOLLINGER	MacNeil	Rezak
b) Hydrography (PHISH & Current Meters)		JUNE BOLLINGER	EFG/WFG	McGrail
1st Monitoring (LGL)	10 Jun - 18 Jun 80	PETE & SUE	EFG/WFG	Viada
2nd Monitoring (LGL)	24 Sep - 1 Oct 80	JEFF & TINA	EFG/WFG	Viada
1st Sub Cruise	[22 Sep - 27 Oct 80]	BALTIC SEAL	EFG/WFG	
Leg 1 (Bright)	3 Oct - 11 Oct 80	BALTIC SEAL	EFG/WFG	Bright
Leg 2 (Rezak)	12 Oct - 16 Oct 80	BALTIC SEAL	EFG/WFG	Rezak
Leg 3 (McGrail)	19 Oct - 27 Oct 80	BALTIC SEAL	EFG/WFG	McGrail
2nd Combined			EFG/WFG	
Leg 1 Recover cm arrays PHISH/XBT Recover biological data collection facilities	8 Feb - 10 Feb 81	M/V EL PASO	EFG/WFG EFG/WFG	Horne
Leg 2 Redeploy arrays	3 Mar - 8 Mar 81	R/V GYRE	EFG/WFG EFG/WFG	McGrail & Merrell
3rd Combined				
Leg 1 Recovery/Sampling	13 Jul - 17 Jul 81	M/V NORTH SEAL	EFG/WFG	Carnes
Leg 2 Redeployment/Sampling	Cancelled		EFG/WFG	McGrail

Mapping Activities

Mapping activities were carried out at MacNeil Bank. The bank was mapped using precision depth recorder, 3.5 kHz sub-bottom profiler, Uniboom seismic system, and side-scan sonar.

Sample Analysis

Samples were transferred to the appropriate laboratories for analysis. Samples included bottom grabs for sedimentological analyses (texture, mineralogy, total carbonate, HMWH, Delta C-13, and total organic carbon), shipboard sampling for contaminants, and Spondylus americanus for hydrocarbon analysis. Bottom sampling was also undertaken for geological analysis and faunal identification in conjunction with photographs and visual observations. The analytical data and results are included in the appropriate sections of this report.

Data Analysis

Data analysis was performed by PI's on the basis of their individual areas of expertise. Analysis of existing data was also performed. Table I-5 lists data carried forward from previous contracts for analysis on Contract #AA851-CT0-25.

Where feasible, computerized techniques were applied for the efficient analysis and handling of large data volumes. Some of the computerized techniques include:

Cartographic Projection/Grid Programs	Report Generator Program
Current Meter Data Analysis	Rotary Spectral Analysis
Gaussian and Cascading Butterworth Filter Analysis	Spectral Analysis
Grain Size Analysis	Standard Fourier Fast Transform
Graphics and Plotting Programs	Standard Statistical Analysis
	Time Series Analysis
	Variance Tensor Analysis

The methods and procedures for these techniques are outlined in the appropriate chapters of this report.

Data Synthesis, Integration, and Archiving

Interpretation of biological, chemical, and geological data resulting from field activities, and from information gathered under previous contracts, was undertaken for data synthesis. Data synthesis resulted in area and bank characterization of the East and West Flower Garden Banks. Bathymetric and sub-bottom data from MacNeil Bank were used in preparing a side-scan mosaic and a structure/isopach map. Seafloor roughness maps were prepared for Ewing, Parker, Bouma, 18 Fathom, Bright, and Stetson Banks, using existing data. Existing sub-bottom data were used to prepare structure/isopach maps of Ewing, Parker, Bouma, and 18 Fathom Banks.

Once digitized and analyzed, the data were placed on magnetic tape and/or microfilmed and mailed to the National Oceanic and Atmospheric Administration (Environmental Data and Information Service) in an appropriate format. Analog records were microfilmed to enhance the life of mapping data.

TABLE I-5
DATA CARRY-OVER FROM PREVIOUS CONTRACTS

PI	CONTRACT #	DESCRIPTION OF DATA
Bright	AA551-CT8-35	Station data from plotless line transects and benthic algal biomass data gathered in Sep 79 and Dec/Jan 80.
Bright	AA551-CT8-35	Thirty-two coral recruitment settling plates emplaced on East and West Flower Garden Banks in Sep 79.
McGrail	AA551-CT8-35	Dye diffusion data gathered during the 1979 fall submersible cruise.
McGrail	AA551-CT8-35	Data from current meter array deployed at the West Flower Garden in Dec 79.
Rezak	AA550-CT6-18 AA550-CT7-15	Sea-bottom and near sub-bottom data.
All	AA551-CT8-35	Data gathered during the 1979 fall submersible cruise (samples, photographs, videotapes, etc.).

CHAPTER II

GEOLOGY OF THE FLOWER GARDEN BANKS

R. Rezak

INTRODUCTION

The Flower Garden Banks are similar in origin, general structure, and sediment distribution, but differ in the details of structure, physiography, and sedimentology. This chapter focuses on the specific differences in the geology of the two banks.

Our work on the geology of the Flower Garden Banks began in 1961. As a result of research cruises to the banks during 1961, 1968, 1969, and 1970, a Ph.D. dissertation directed by Richard Rezak was published (Edwards, 1971) as a Texas A&M Sea Grant Publication, describing the hydrology, biology, and geology of the West Flower Garden Bank. Much of the descriptive material on the West Flower Garden Bank (WFG) presented here is based to a large extent on the work conducted by Edwards, with details added from subsequent cruises to the bank funded by BLM. The geology of the East Flower Garden Bank (EFG) presented here is based upon work performed for BLM under BLM-TAMRF Contracts AA550-CT6-18 and AA851-CT0-25.

GENERAL DESCRIPTIONWest Flower Garden Bank

The West Flower Garden Bank is located 107 n.m. due south of Sabine Pass at latitude $27^{\circ}52'27''\text{N}$, longitude $93^{\circ}48'47''\text{W}$ (Figure II-1) in Lease Blocks A-383-85, A-397-99, and A-401 of the High Island Area, South Addition, and Lease Block GB-134 of the Garden Banks Area (Figure II-2). It is a large bank covering about 137 km^2 . The bank is oval-shaped and oriented in a northeast-southwest direction (Figure II-3). The crest of the bank lies at a depth of approximately 20 m. Surrounding depths vary from 100 m to the north, to 150 m to the south. Total relief on the bank is approximately 130 m.

East Flower Garden Bank

The East Flower Garden Bank is located at $27^{\circ}54'32''\text{N}$ latitude and $93^{\circ}36'\text{W}$ longitude in Lease Blocks A-366, A-367, A-374, A-375, A-388, and A-389 of the High Island Area (Figure II-1). The bank is pear-shaped and covers an area of about 67 km^2 (Figure II-4). Steep slopes occur on the east and south sides of the bank with gentle slopes on the west and north sides (Figure II-5). The shallowest depth on the bank is about 20 m in the northeastern part of Lease Block A-388. The surrounding water depths are about 100 m to the west and north and about 120 m on the east and south sides. An elongate depression in the north-central part of Lease Block A-389 has a depth of 136 m.

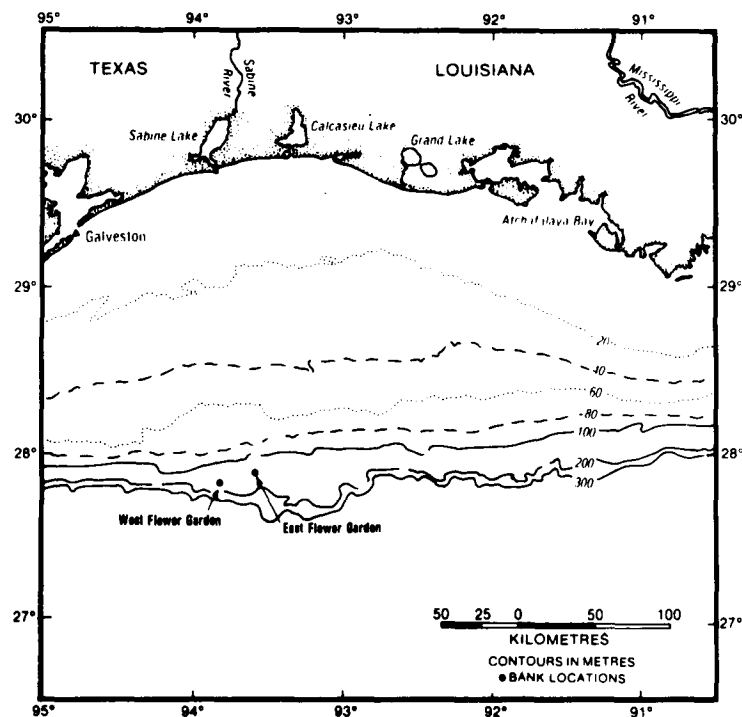


Figure II-1. Flower Garden Banks location map.

PHYSIOGRAPHY AND STRUCTURE

General

Both banks are the surface expression of salt diapirs capped by living coral reefs at their crests. The West Flower Garden is classified as a mature salt dome and the East Flower Garden is a rejuvenated salt dome. A discussion of the development and classification of salt diapirs is presented in Rezak and Bright (1981a, Vol. 1, pp. 23-31).

West Flower Garden Bank

The structure of the West Flower Garden Bank is typical of a mature salt diapir in which crestral faulting has occurred. The trough running from the southeast corner of Lease Block A-399 to the southeast corner of Lease Block A-384 (Figures II-2 and 3) is a crestral graben as displayed by the bathymetry. Figure II-6 is a structure/isopach map including faults delineated by Henry Berryhill (USGS) and those observed on our 3.5 kHz records. Because of the poor reflectivity in the area of the graben on our records, it is difficult to display the borders of the crestral graben on this map. The large east-west fault on the southeastern margin of the bank is illustrated in Figure II-7. This fault displaces the seafloor and appears to be the result of recent movement. Figures II-8 and 9 illustrate the abundance of normal faults on this bank. Edwards (1971, Figure 20) illustrates a one cubic inch air gun profile across the bank showing the crestral graben and numerous normal faults to the southeast of the bank. The numerous

bathymetric prominences on the bank represent horsts that stand above the surrounding grabens (Figure II-2).)

The living reef lies in the north-central portion of Lease Block A-398. It rises from depths of 40 to 50 m to a crest at about 20 m. Extending from near the base of the reef towards the northeast and the south is a broad terrace that extends to depths of about 60 to 70 m (Figure II-3 and Plate 1, pocket). The surface of this terrace is characterized by large waves of sediment consisting primarily of the gravels of the Gypsina-Lithothamnium Facies (Figure II-9). The gravel waves are oriented normal to the isobaths. Below these depths are numerous lineations (faults and outcrops of Tertiary bedrock covered by drowned reefs) and patch reefs scattered to depths as great as 170 m. Most of the patch reefs above 90 m appear to have formed during the last rise of sea level.

East Flower Garden Bank

The structure of the East Flower Garden Bank is typical of either a young or a rejuvenated salt dome. A comparison of Figures II-4 and 10 show that there is little evidence for faulting on the gentle western slope of the bank. The major faults are the peripheral faults on the southern and eastern margins of the bank. The numerous depressions on the bank (Figure II-4) probably represent the early stages of crestal collapse. The large depression between the living reef and the southeastern margin of the bank (Figures II-4 and 10c) has been identified as a young graben with a total relief of 10 m. Evidence for recent collapse of this structure has been presented by Rezak and Bright (1981a,b). It is expected that continued removal of salt from the crest of the East Flower Garden Bank diapir will result in continued deepening of this depression. A large part of the living reef lies within this fault block, and continued crestal collapse could eventually displace the living reef into water depths that are unfavorable for reef growth.

Side-scan sonar records show an abundance of drowned patch reefs up to 3 m in height below a depth of approximately 50 m (Figure II-13). The spatial frequency of these patch reefs is indicated on Figures II-13 and III-2 (Chapter III).

SEDIMENTOLOGY

The carbonate facies at the two Flower Garden Banks are identical in their composition and bathymetric distribution. The facies at the West Flower Garden Bank, delineated on Figure II-11, are based upon grab samples from 43 stations taken by Edwards (1971) and 12 additional samples taken during the present study. (Analyses of the additional samples indicate that Edwards' sediment facies map was an accurate portrayal of the sediment distribution at the West Flower Garden Bank, Edwards' facies were based solely upon sediment particle type identification as his goal was to delineate only the carbonate sediment facies. The analyses (both textural and particle type) of the 12 additional

samples are included in Appendix A. (The sediment facies at the West Flower Garden Bank are described in detail by Edwards,) and the facies at the East Flower Garden Bank are described by Rezak and Bright (1981a, Vol. 3). The Molluscan Hash Facies shown at the East Flower Garden Bank was not recognized by Edwards because only one of his samples was taken from this facies. Edwards' sample number 21 is the most southern sample on his station location map (his Figure 41). If he had taken more samples to the south and west of station 21, he probably would have recognized the facies in that area. Additional sediment samples were taken in that area during the March 1982 Student Cruise. However, the analyses of the new samples are not complete at the time of writing this report. That data will be included in a subsequent report (BLM-TAMRF Contract AA851-CT1-55).

The sediments of the two banks differ completely from the sediments of the open shelf surrounding the banks (Figure II-11). (Bank sediments are all derived from the skeletons of organisms that are living on the banks. On the other hand, the open shelf sediments in the area of the banks are sands and muds that have been eroded from the North American continent and mechanically transported to the Gulf of Mexico by streams such as the Mississippi, Trinity, Sabine, and Brazos Rivers. These sands and muds do not occur at depths shallower than 85 m at the Flower Garden Banks. The sediments above the 85 m level are all coarse sands and gravels and the rocky, limestone structure built by the corals and other reef-dwelling organisms. The loose sediments around the reef reflect the depth zonation of the biological communities that are present on the two banks. Table II-1 illustrates the relationship between the biological zones and the sediment facies.)

As may be seen in Table II-1, the sediment facies are intimately related to the biological zonation and hydrological conditions at each bank. However, the sediment boundaries do not coincide with the biotic boundaries. This is partly due to the downslope movement of loose sediment by the force of gravity and partly due to the use of soft-bodied organisms in delineating the biotic zonation. In Table II-1, for example, the lower boundary of the Algal-Sponge biotic zone is based upon the lower depth limit of Neofibularia, a colonial, soft-bodied sponge which also grows in the upper part of the Amphistegina Sand Facies.

Knowing the distribution of living, lime-secreting, skeletal organisms, we can demonstrate that the direction of sediment transport on the banks is downslope. The Coral Debris Facies accumulates between coral heads and in a narrow band around the base of the living reef. The Gypsina-Lithothamnium Facies consists of coarse gravel and massive limestone that are forming in situ due to the growth of calcareous algae and encrusting calcareous protozoans. However, the Amphistegina Sand Facies is composed of the recently dead skeletons of a small protozoan that lives and grows abundantly in the Gypsina-Lithothamnium Facies. Upon dying, the sand size skeletons of these protozoans are moved downslope by gravity to form the Amphistegina Sand. (At depths less than 85 m, the sediments of the banks are medium to coarse, calcareous sands and gravels. The living reef and the Gypsina-Lithothamnium Facies are natural sediment traps due to their highly

TABLE II-1
 RELATIONSHIP BETWEEN SEDIMENT FACIES AND BIOLOGICAL ZONES
 AT THE EAST FLOWER GARDEN BANK

SEDIMENT FACIES	DEPTH (m)	BIOLOGICAL ZONE	DEPTH (m)
1. Coral Reef	15-50	1. <u>Montastrea-Diploria-Porites</u>	15-36
a. Living Reef (massive limestone)	15-45		
b. Coral Debris (coarse sand and gravel)	25-50		
2. <u>Gypsina-Lithothamnium</u> (coarse gravel and massive limestone)	50-75	2. <u>Madracis</u>	28-46
3. <u>Amphistegina</u> Sand (medium to coarse sand, muddy at depths greater than 85 m)	75-90	3. <u>Stephanocoenia</u>	36-52
		4. Algal-Sponge	46-88
		5. Transition	88-89
4. Quartz-Planktonic Foraminifers (sandy mud)	90 +	6. Nepheloid	89
5. Molluscan Hash (muddy sand)	90 +		

irregular surfaces. Any fine sediments, such as occur below the 85 m depth, would be trapped in the irregular topography of these facies if they were ever carried to the top of the reef by either physical or biological processes. The surface irregularities would act as baffles that retard the velocity of the currents and cause deposition of the fine sediment in nooks and crannies on the reef and in the Gypsina-Lithothamnium zone. This process is analogous to a snow fence that traps snow away from highways and railroad tracks.

As indicated above, there is no land-derived mud in the bottom sediments above a depth of 85 m. This fact substantiates the conclusion from water and sediment dynamics studies that the nepheloid layer rarely rises to depths of 85 m (see below, Chapter IV). If the nepheloid layer were able to cover more of the bank, then we would find land-derived muds mixed with coarser sediments at shallower depths. Moreover, the 80 m isobath is a major boundary in the biological zonation. That depth separates the turbid water faunas below from the clear water faunas and floras above. If the nepheloid layer were able to rise to shallower depths, the lower limits of the clear water assemblages would also be raised by the same number of metres. (Bright and Rezak, 1978b; Rezak and Bright 1981a, Vol. 3.)

The sedimentary facies map (Figure II-9) is based upon a total of 139 samples taken from various sources. Forty-three samples were used by Edwards (1971) to delineate the facies distribution at the West Flower Garden Bank. Thirty-five samples were taken at the East Flower Garden Bank during 1979 in order to determine the sediment distribution on that bank. Fifty-one samples from a large collection donated by Tenneco were selected for the area away from the banks, and ten additional samples were taken in December 1979 in order to fill in the gaps in the off-bank areas.

The boundary between the areas of carbonate and terrigenous sedimentation is an artifact caused by the use of two different classification systems, carbonate (genetic) and terrigenous (textural). A discussion of the problems created by the use of these two classification systems is presented in Rezak and Bright (1981, Vol. 1, p. 32). A study of the percent of quartz sand, silt and clay, and heavy mineral composition is presently underway and will be reported under BLM-TAMRF Contract AA851-CT1-55.

CONCLUSIONS AND RECOMMENDATIONS

1. The conclusion from water and sediment dynamics studies indicating that it is impossible for suspended sediments in the bottom boundary layer to be transported to the top of the reef is corroborated by three findings from geological studies as follows:
 - a. (There are no land-derived muds in the bottom sediments above a depth of 85 m.) If the nepheloid layer ever reached the top of the reef, even only occasionally, there would be evidence of its presence in the bottom sediments.

- b. (The distribution of sediments around the reef indicates a down-slope movement due to gravity. There is absolutely no evidence for upslope transport of bottom sediments.)
- c. (The vigorous growth of corals on the living reef and the growth of other reef-building organisms such as coralline algae at depths shallower than 75 m attest to the fact that the nepheloid layer never envelops the reef. If it did, these organisms could not possibly survive (Rezak and Bright, 1981a; Rezak, 1977; Bright and Rezak, 1978b).)

Therefore, the established restrictions on drilling appear to be sufficient to protect the reefs from damage due to drilling activities.)

2. The danger of catastrophic collapse of the seafloor both on the hard bottoms of the banks and on the soft bottoms immediately surrounding the banks is very real. Pre-drilling hazard surveys should be undertaken prior to emplacement of seafloor structures. Areas of faulting should be avoided even though there is no evidence for recent displacement of the seafloor.

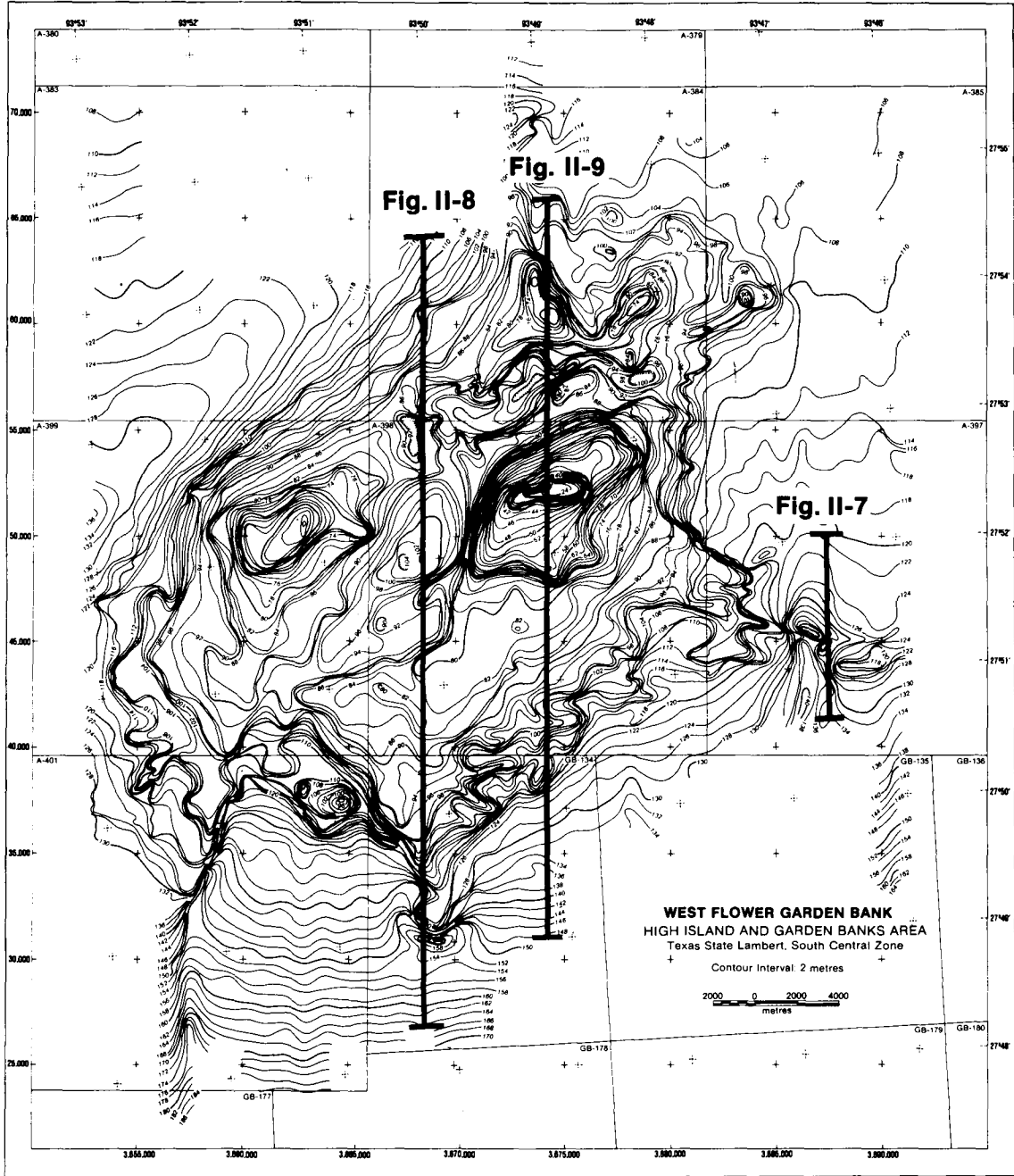
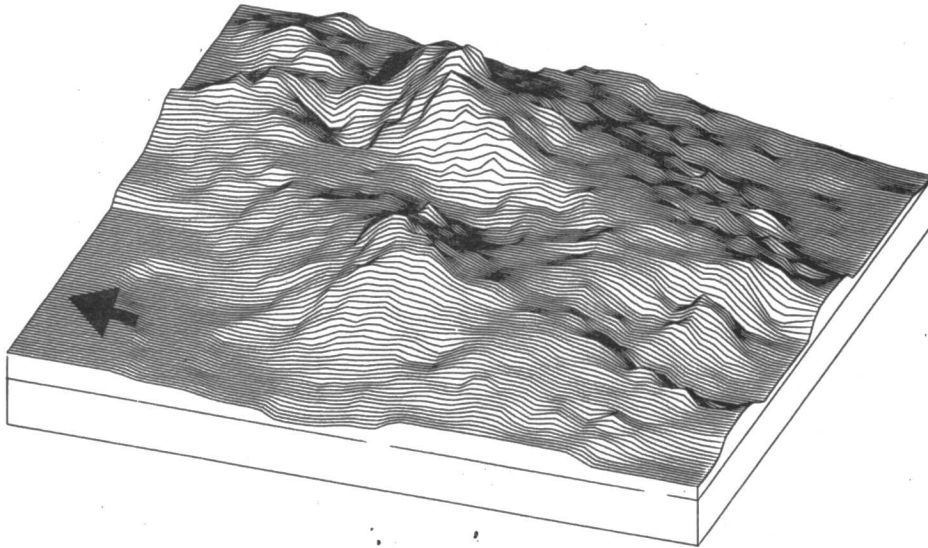
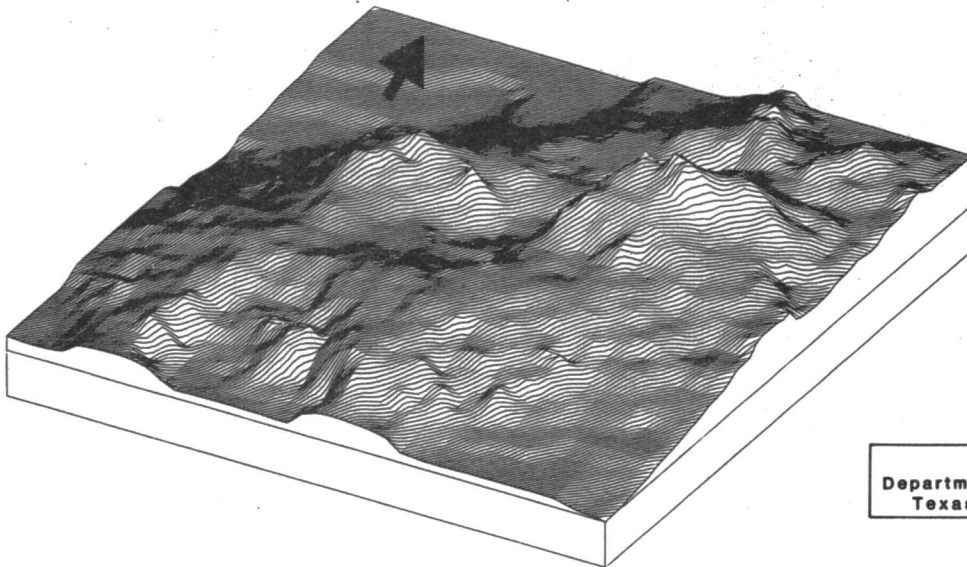


Figure II-2. West Flower Garden Bank bathymetry, showing locations of seismic lines on Figures II-7, 8, and 9.

WEST FLOWER GARDEN BANK



AZIMUTH = 70 ALTITUDE = 30
 *WIDTH = 6.50 *HEIGHT = 1.50
 *BEFORE FORESHORTENING



1.30 -24.21
 1.00 -51.51
 0.50 -97.16
 0.00 -142.81

Prepared by
 Department of Oceanography
 Texas A&M University

AZIMUTH = 330 ALTITUDE = 30
 *WIDTH = 6.50 *HEIGHT = 1.50
 *BEFORE FORESHORTENING

Figure II-3. West Flower Garden perspective views. Arrows point toward north. Graphic vertical scale relates the total range of water depths (right) to the arbitrary computer units after foreshortening (left).

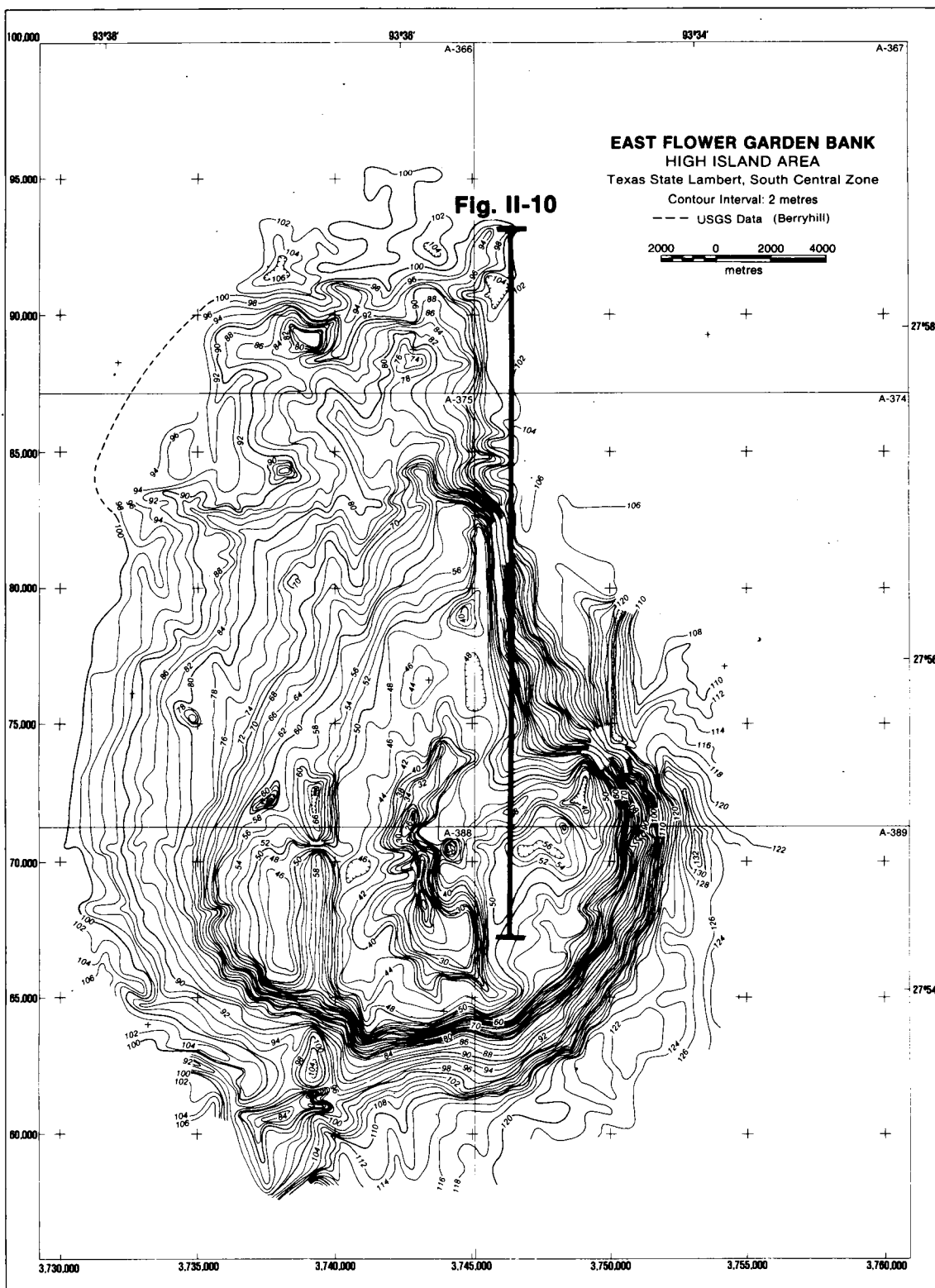
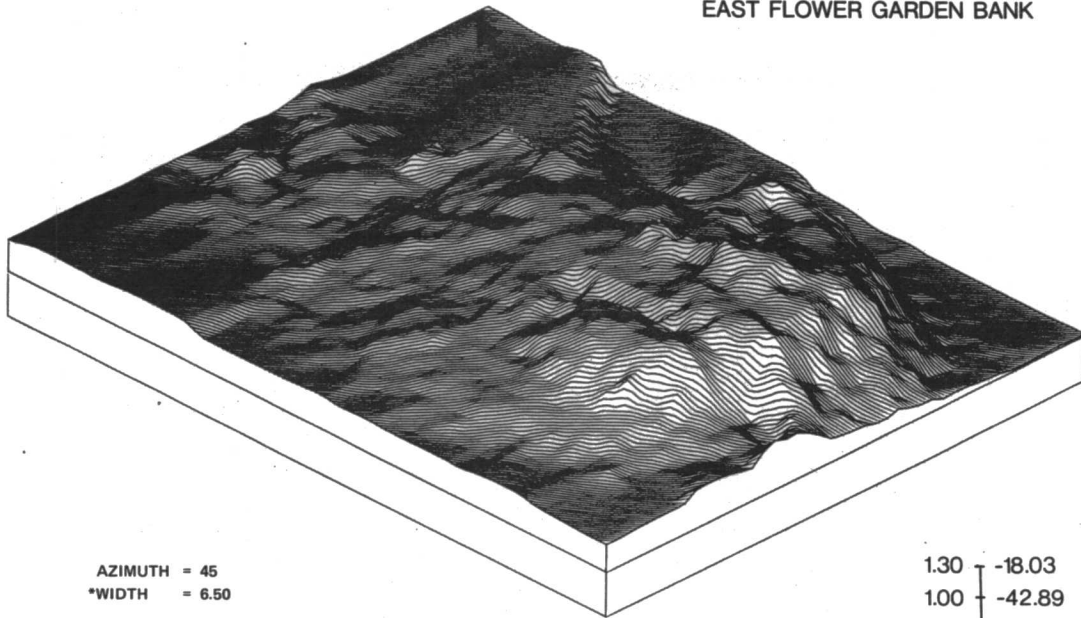


Figure II-4. East Flower Garden bathymetry showing location of 3.5 kHz profile on Figure II-10.

EAST FLOWER GARDEN BANK

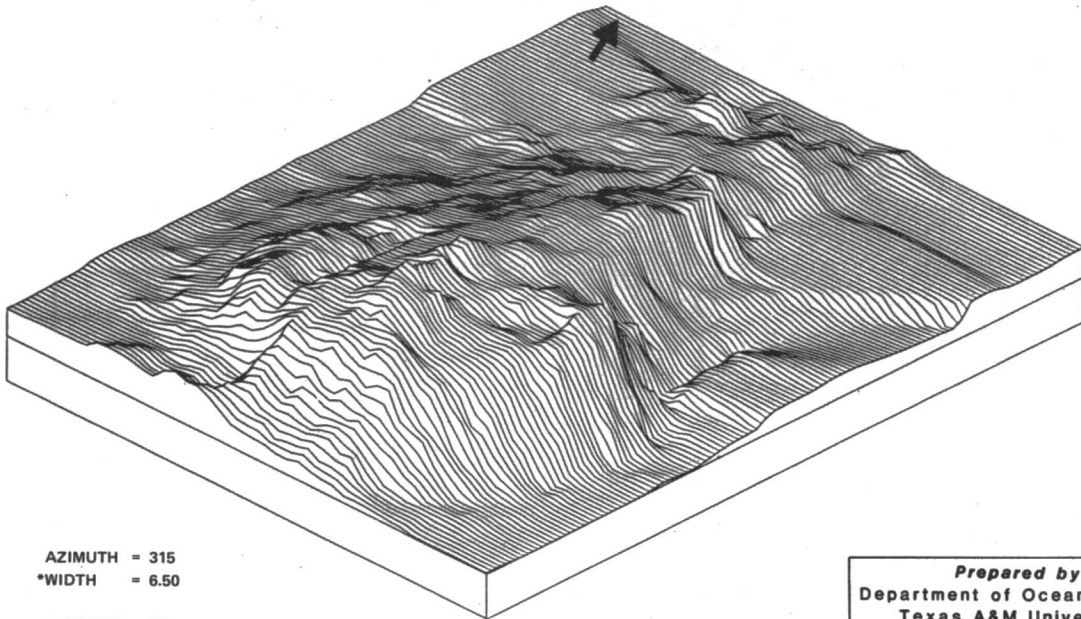


AZIMUTH = 45
 *WIDTH = 6.50

 ALTITUDE = 30
 *HEIGHT = 1.50

 *BEFORE FORESHORTENING

1.30	-18.03
1.00	-42.89
0.50	-84.44
0.00	-126.00



AZIMUTH = 315
 *WIDTH = 6.50

 ALTITUDE = 30
 *HEIGHT = 1.50

 *BEFORE FORESHORTENING

Prepared by
 Department of Oceanography
 Texas A&M University

Figure II-5. East Flower Garden perspective views. Arrows point toward north. Graphic vertical scale relates the total range of water depths (right) to the arbitrary computer units after foreshortening (left).

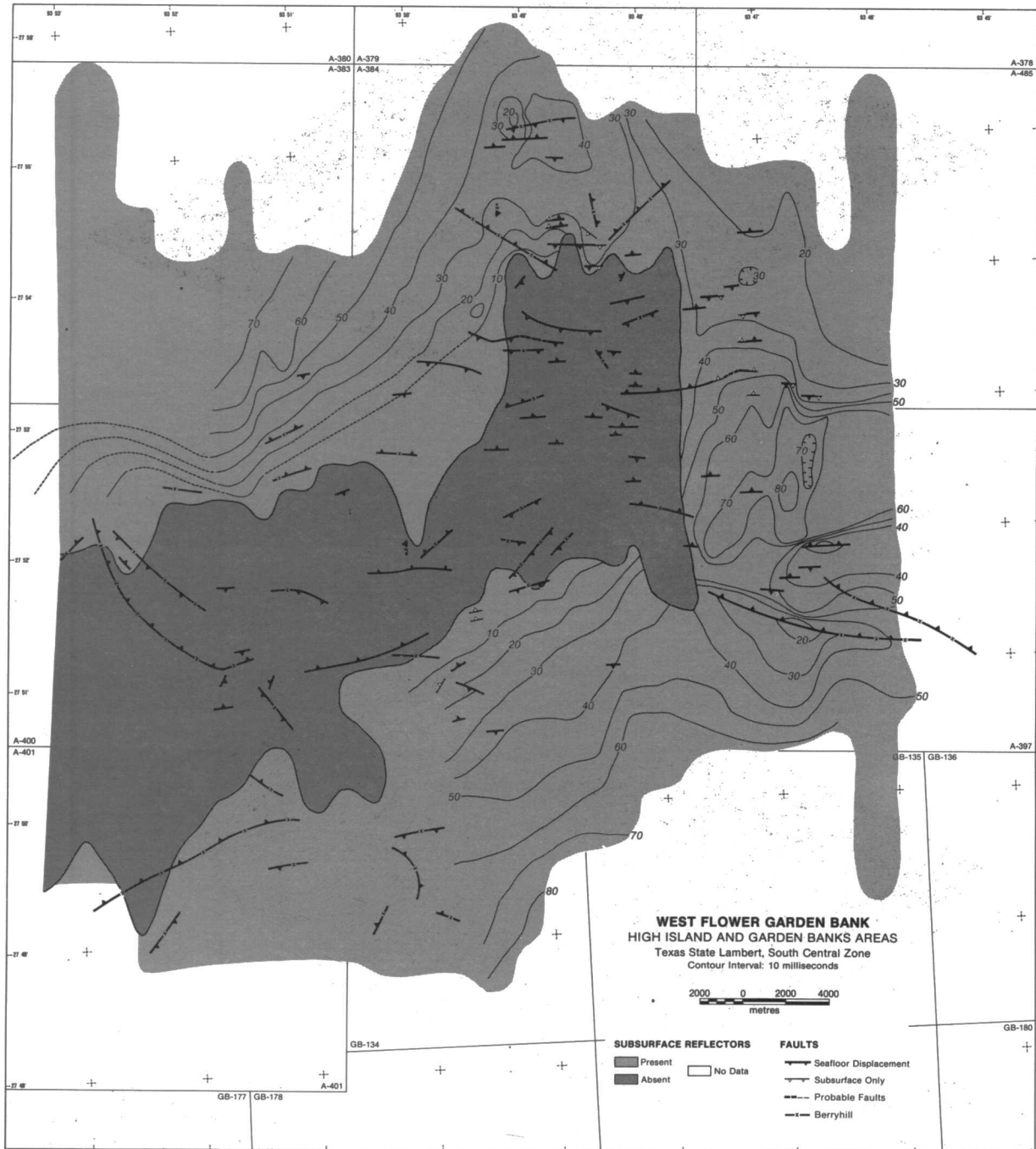


Figure II-6. West Flower Garden structure/isopach map. Isopach interval indicated on Figure II-9.

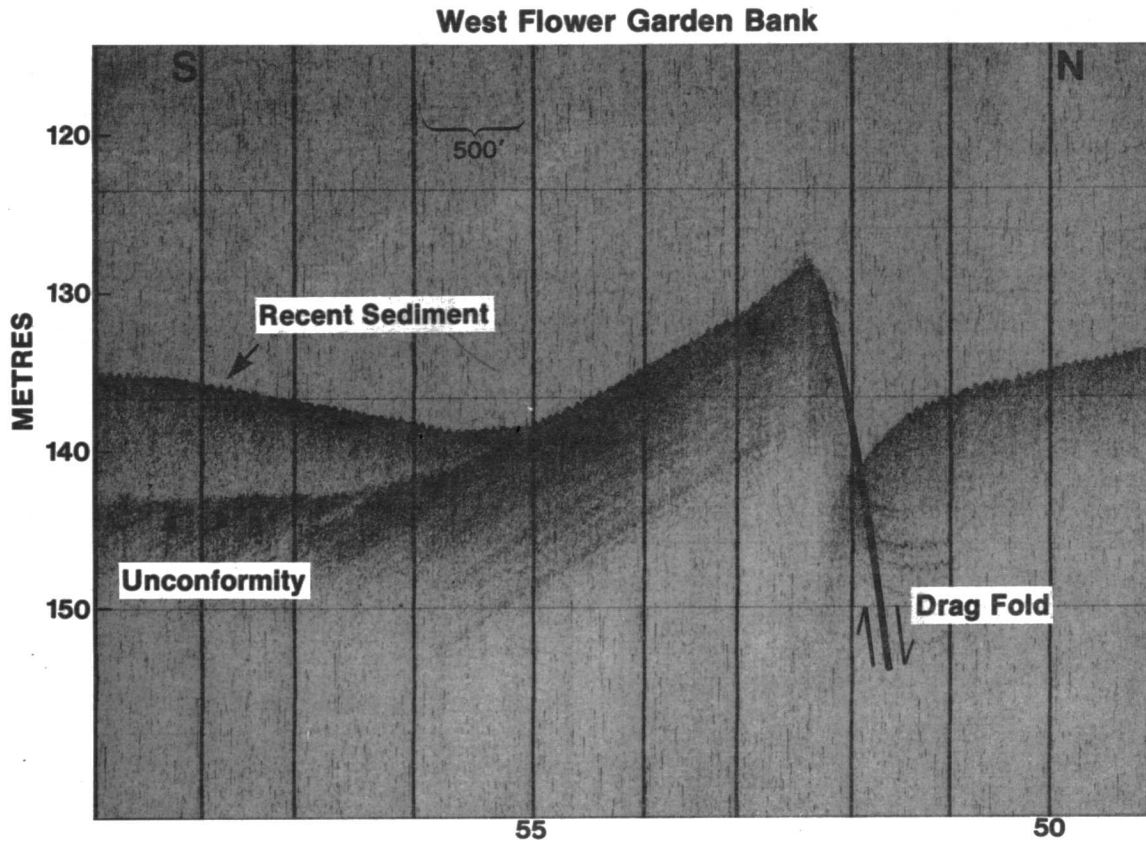


Figure II-7. West Flower Garden 3.5 kHz sub-bottom profile.

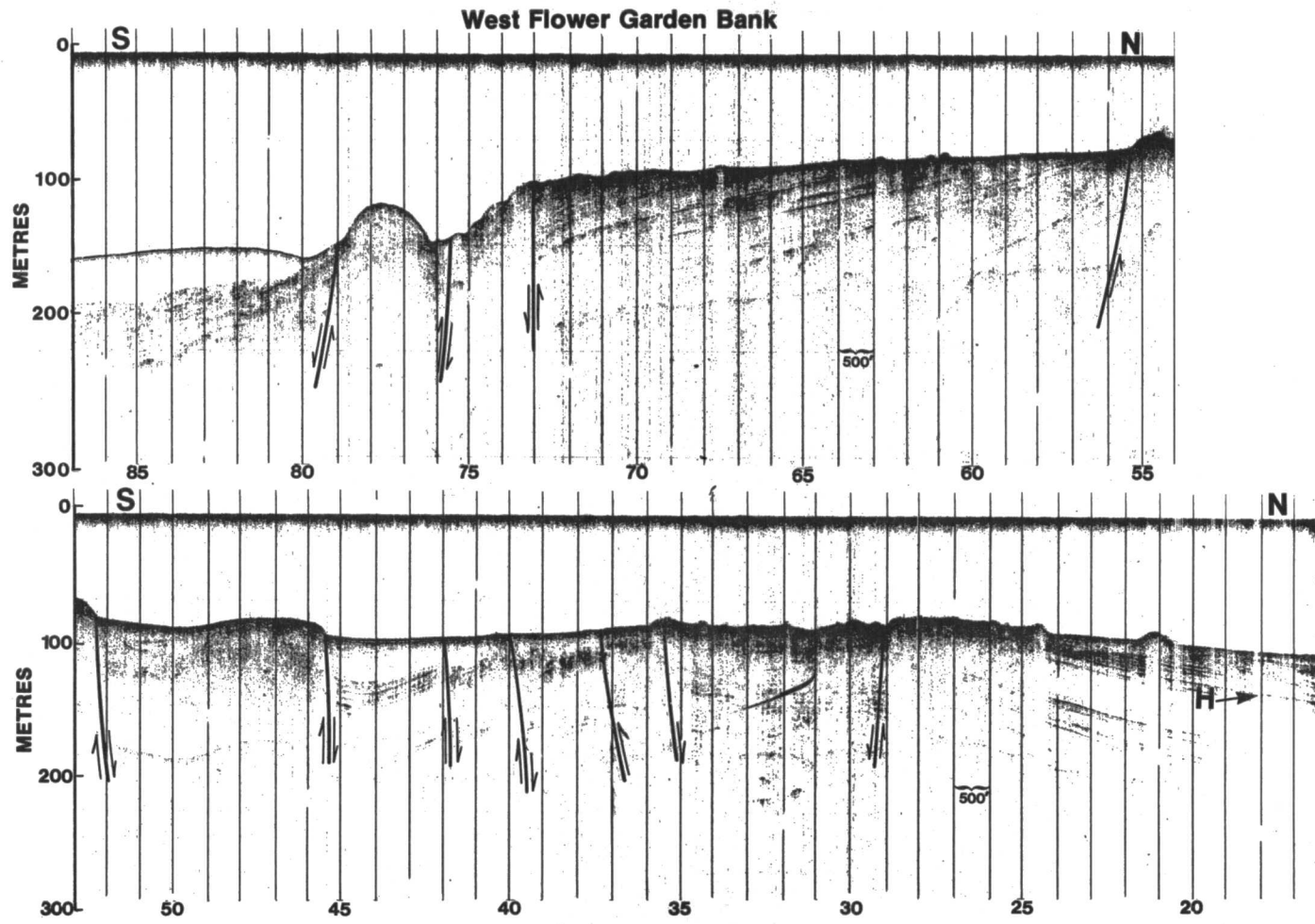


Figure II-8. West Flower Garden 3.5 kHz sub-bottom profile.
 H = horizon.

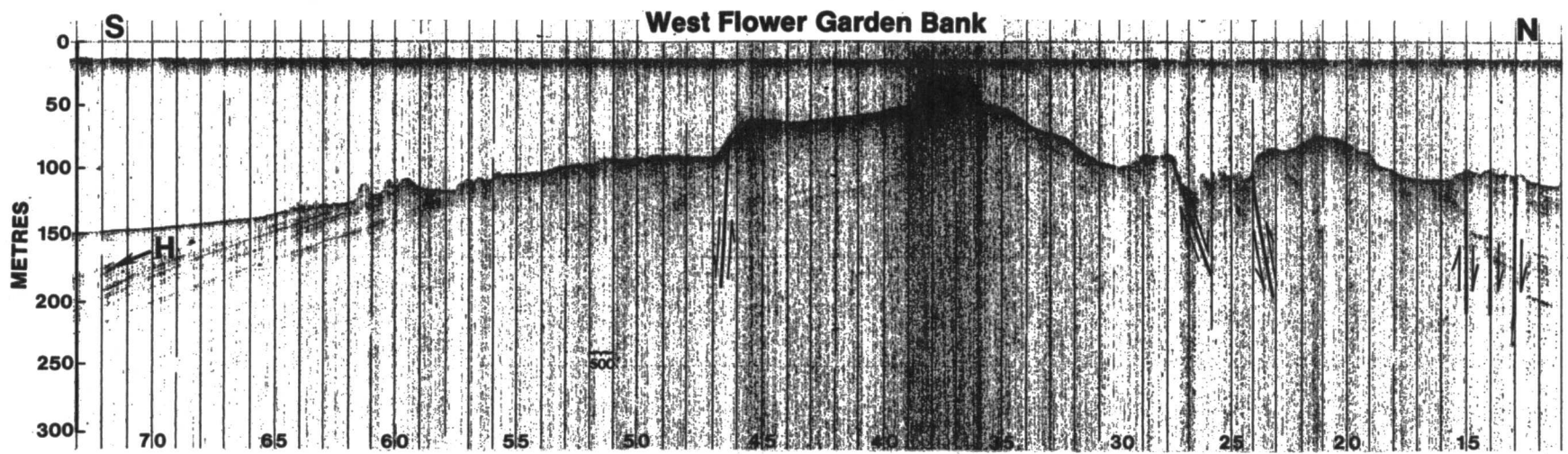


Figure II-9. West Flower Garden 3.5 kHz sub-bottom profile. H = horizon.

East Flower Garden Bank

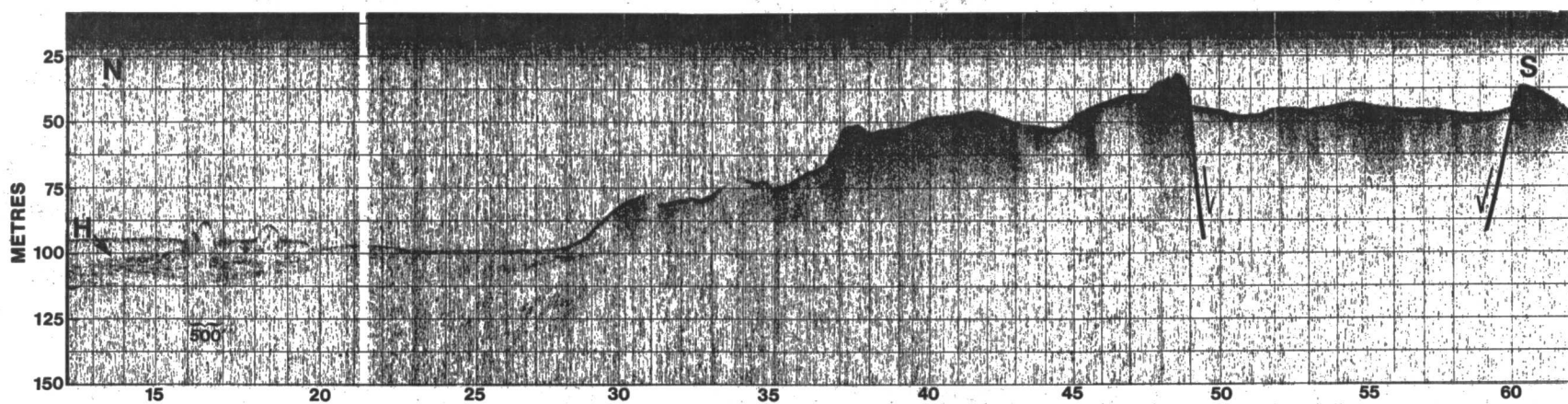


Figure II-10. East Flower Garden 3.5 kHz sub-bottom profile. H = horizon.

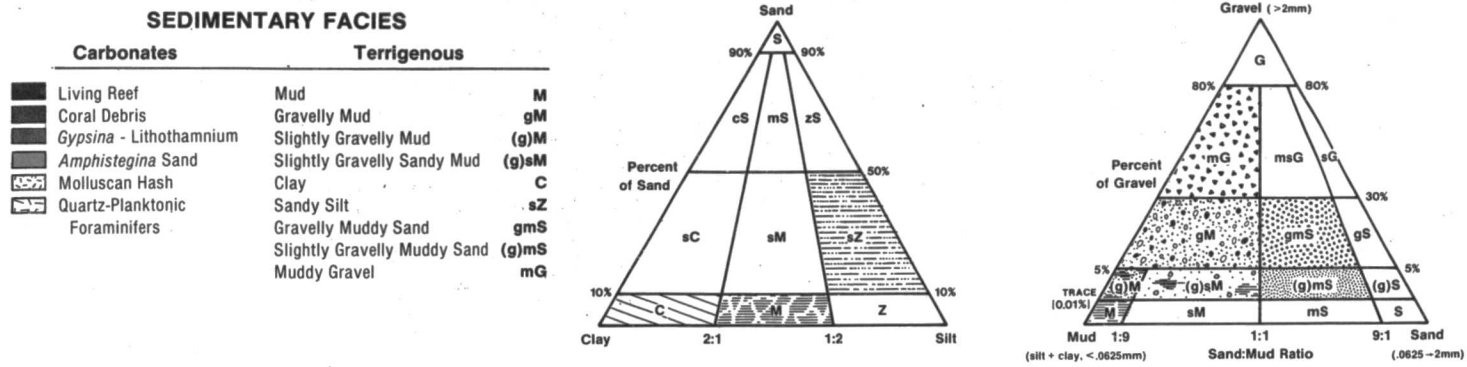
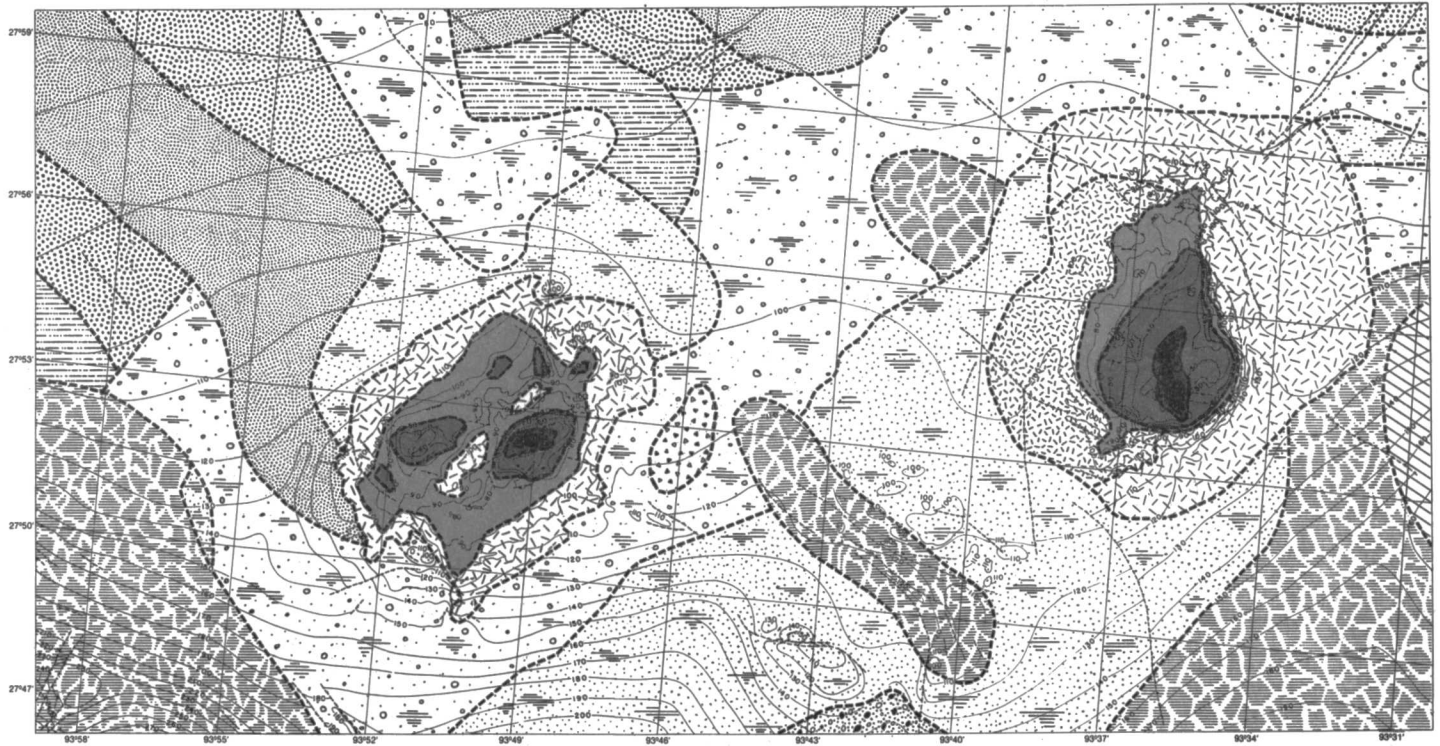


Figure II-11. Sediment distribution in the Flower Garden Banks area.



Figure II-12. East Flower Garden structure/isopach map. Base of isopach interval indicated by arrow on Figure II-10.

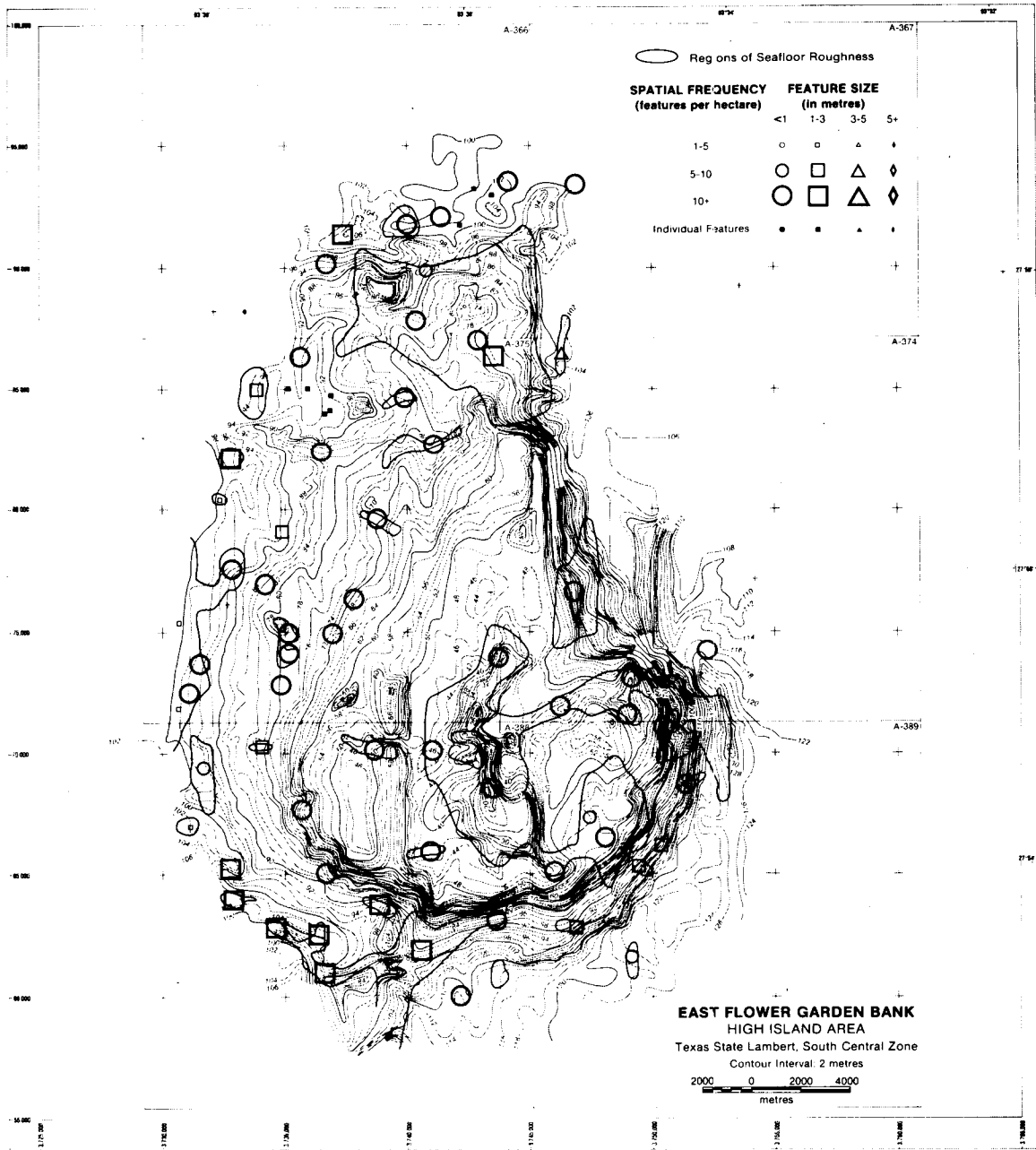


Figure II-13. East Flower Garden seafloor roughness map.

**APPENDIX A:
FLOWER GARDENS
SEDIMENT ANALYSES**

TABLE A-1
FLOWER GARDENS SEDIMENT TEXTURE

SAMPLE	GRAVEL	SAND	SILT	CLAY	MEAN	MEDIAN	STD DEV	SKEWNESS	KURTOSIS
EFG-1GB	0.0	1.24	46.96	51.81	8.02	8.07	1.58	-0.70	0.97
EFG-2GB	0.0	1.56	53.94	44.50	7.61	7.76	1.78	-0.43	-0.36
EFG-3GB	3.90	74.30	9.03	12.77	2.85	1.84	3.08	1.20	0.44
EFG-4GB	0.08	82.51	5.97	11.44	3.19	2.24	2.60	1.56	1.24
WFG-1GB	0.0	28.05	31.32	40.03	6.32	7.32	3.13	-0.46	-1.23
WFG-2GB	1.28	48.96	23.78	25.99	4.63	3.98	3.51	0.16	-1.26
WFG-3GB	0.20	26.84	28.25	44.72	6.51	7.62	3.18	-0.62	-0.96
WFG-4GB	0.0	13.28	44.24	42.48	7.03	7.54	2.49	-0.71	-0.24
WFG-5G	0.0	52.05	27.85	20.11	5.10	3.95	2.51	0.75	-0.72
WFG-6GA	4.88	55.35	18.41	21.36	3.38	1.48	3.99	0.45	-1.40
WFG-9G	0.0	6.22	36.53	57.25	7.86	8.35	2.11	-1.20	1.24
WFG-10G	7.52	77.90	5.81	8.76	1.53	0.53	3.04	1.64	1.76
WFG-10GB	7.97	73.12	6.89	12.01	1.97	1.02	3.35	1.30	0.52
WFG-11G	0.24	79.03	10.39	10.34	3.38	2.55	2.46	1.46	1.18
WFG-12G	0.16	30.79	38.48	30.57	6.05	5.62	2.62	0.07	-1.14
WFG-8G	14.57	83.19	0.62	1.62	-0.06	-0.54	1.66	3.57	17.00
WFG-1C	0.11	59.79	21.30	18.80	4.40	2.99	2.91	0.83	-0.60
WFG-2C	0.06	35.09	47.46	17.39	5.22	4.47	2.36	0.65	-0.17
WFG-3C	7.98	55.19	14.07	22.76	3.71	2.71	4.02	0.49	-1.10
EFG-33	2.31	70.24	17.27	10.19	3.56	3.13	2.59	0.88	0.67
EFG-34	7.47	52.31	22.82	17.40	3.62	2.62	3.62	0.35	-1.08
EFG-35	4.80	52.80	19.98	22.43	3.84	2.42	3.80	0.32	-1.37
82-G1-19	0.0	31.38	40.84	27.78	5.80	5.30	2.70	0.10	-1.03
82-G1-43	0.0	7.77	50.39	41.84	7.29	7.47	2.06	-0.41	-0.56

TABLE A-2
FLOWER GARDENS X-RAY DIFFRACTION ANALYSES

	FINE FRACTION					COARSE FRACTION
	Smectite	Illite	Kaolinite	Chlorite		
EFG-1	53.9	13.7	32.4	TR		low-Mg \approx qtz >> feld
EFG-2	66.5	21.5	12.0	--		low-Mg > qtz > high Mg > feld \approx arag
EFG-3	63.2	23.1	13.7	--		qtz > high-Mg > low-Mg \approx arag
EFG-4	71.2	13.1	15.7	TR		qtz > low-Mg \approx high-Mg > arag > feld
WFG-1	58.6	20.4	21.0	--		low-Mg > qtz > arag
WFG-2	59.0	28.3	12.7	--		low-Mg \approx high-Mg \approx qtz > arag
WFG-3	62.0	14.7	23.3	--		low-Mg > high-Mg > qtz > arag > feld
WFG-4	56.9	17.6	23.5	--		qtz > low-Mg > feld \approx arag \approx high-Mg
WFG-5	62.6	22.3	15.1	TR		qtz > feld > low-Mg
WFG-6	62.9	22.6	14.4	TR		high-Mg > low-Mg > arag > qtz
WFG-9	61.7	16.8	21.5	TR		low-Mg > qtz > arag
WFG-10	67.2	19.4	13.4	TR		high-Mg > low-Mg > arag > qtz
WFG-11	64.1	11.0	24.9	TR		high-Mg > low-Mg > arag > qtz
WFG-12	62.5	14.8	22.7	TR		qtz > low-Mg > feld >> high-Mg

TABLE A-3
SEDIMENT PARTICLE TYPES: FLOWER GARDEN BANKS

PARTICLE TYPES	WEST FLOWER GARDEN											EAST FLOWER GARDEN	
	1Gb	2Gb	3Gb	4Gb	5G	6Ga	8G	10G	10Gb	11G	12G	3Gb	4Gb
Mollusc frags.	12	50	16	6	3	54	48	44	53	57	1	73	56
Bryozoa		12	1	2		23	32	8	12	9		33	9
Worm tube		2				6	8	10	4	6		1	5
Pl. forams.	98	53	96	93	26	60		21	43	35	51	39	36
Benth. forams.	20	7	20	17	3	17	41	41	26	22	5	44	9
Coral		8	8			13	30	18	8	2		4	1
Coralline algae		4	1	2		2	24	2	11	16		15	3
Echinoid	9	4	7	24	1	4	6	16	8	10	1	12	22
Brachiopods							5	4	10				
Scaphopod			1			2							
Homotrena							1	1	2				
Problematica		1									4	1	
Lithoclasts	3	14	3				10	11	13		2	2	
Quartz	3	45	16	42	167					1	122	23	67
Peloids	4		35	16		11	17	30	29	36	14		14

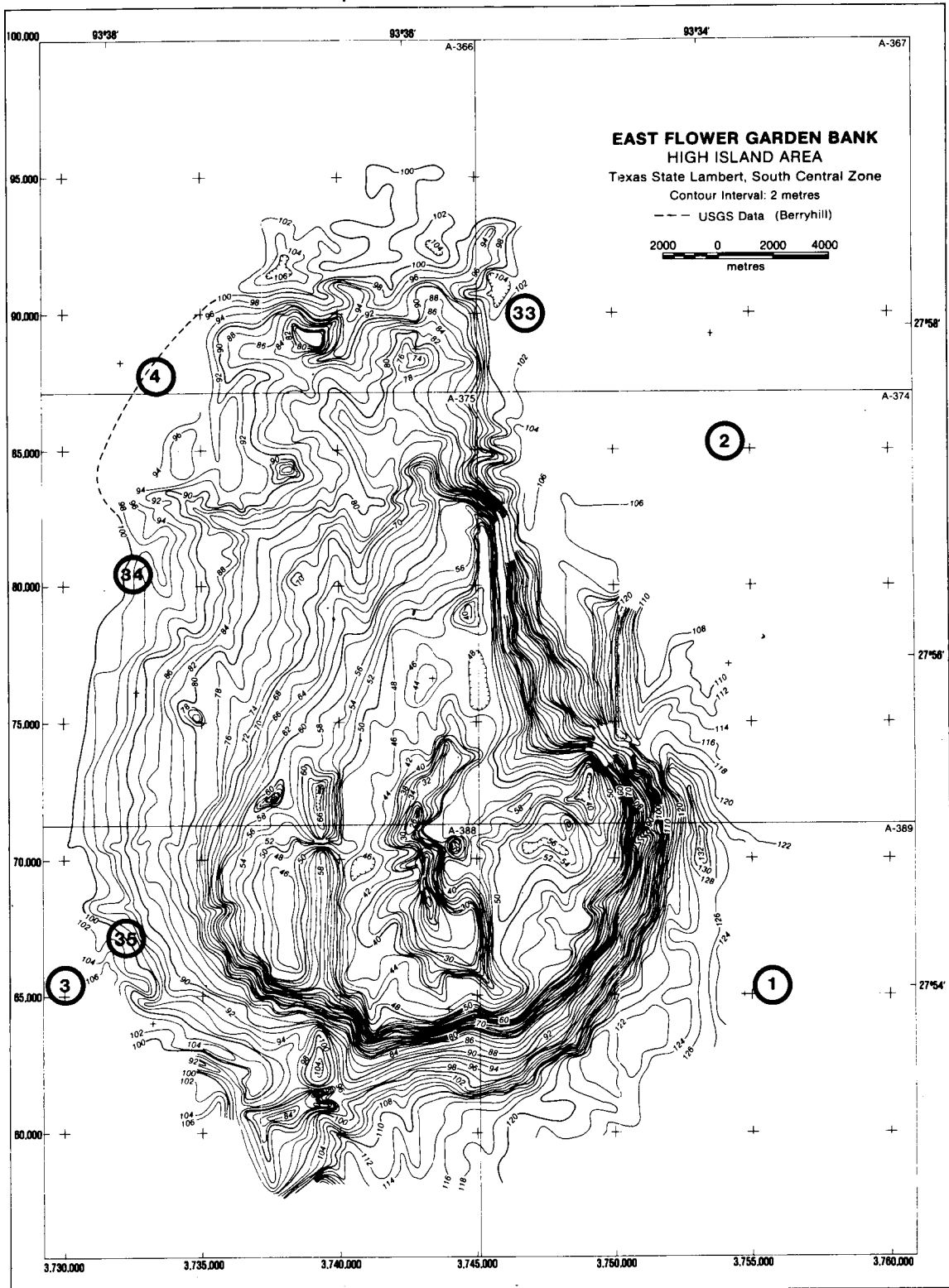


Figure A-1. Sediment grab sample locations for September 5, 1979, on the East Flower Garden Bank.

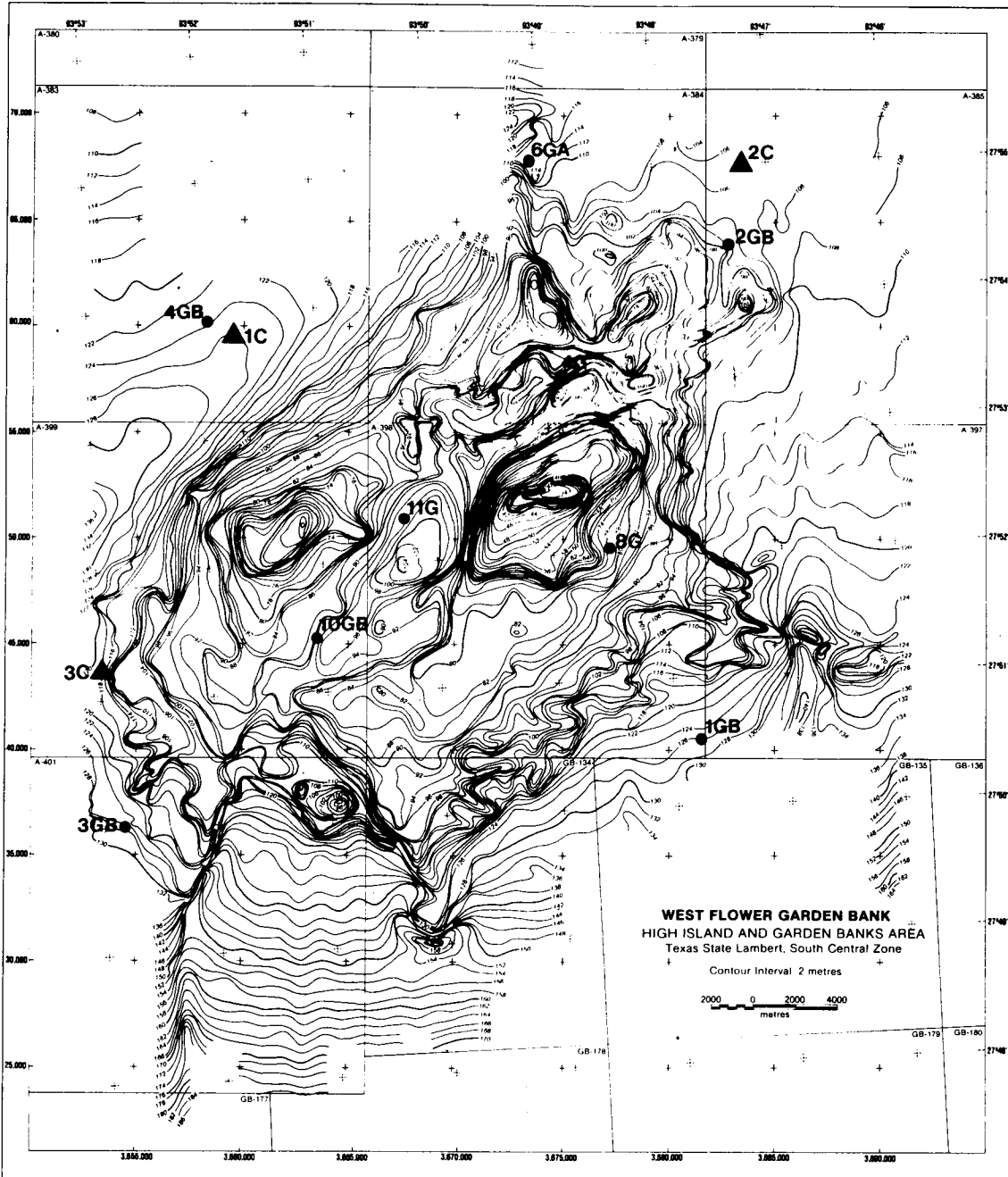


Figure A-2. Sediment grab sample locations for October 1979 (▲) and October 1980 (●) at the West Flower Garden Bank. Stations outside the map area are WFG-5G (27°59'22.8"N, 93°49'30.10"W), WFG-9G (27°48'28.93"N, 93°54'15.96"W), and WFG-12G (27°57'33.17"N, 93°44'49.12"W).

CHAPTER III

BIOLOGICAL MONITORING AT THE FLOWER GARDEN BANKS

T. Bright, C. Combs, G. Kraemer, G. Minnery

BIOTIC ZONATIONIntroduction

The East and West Flower Garden Banks are located approximately 110 n.m. south-southeast of Galveston, Texas at 27°55'N, 93°36'W and 27°52'N, 93°49'W, respectively. Both banks are capped by what are currently considered to be the northernmost thriving tropical, shallow water coral reefs on the eastern coast of North America. The northern limit of Bahamian reefs is some twenty miles south of the Flower Gardens latitude. Reefs of the Bermuda Islands are nearly 300 miles north of the Flower Gardens latitude, but they are situated 570 miles offshore from Cape Hatteras, North Carolina. The ecology of both the Bermudan and Bahamian island systems is influenced greatly by the warm Gulf Stream waters which surround them, and, like the Flower Gardens, they harbor elements of the typical Caribbean reef biota.

Within the Gulf of Mexico, the Flower Gardens appear to be elements of a discontinuous arc of reefal structures occurring on the continental shelf. The coral reefs closest to the Flower Gardens are off Cabo Rojo, about 60 miles south of Tampico, Mexico (Villalobos, 1971). Moore (1958) listed forty-three species of Caribbean reef invertebrates from there; many of them are also common at the Flower Gardens. However, certain abundant corals, such as Acropora palmata (Elkhorn coral) and A. cervicornis (Staghorn coral), do not occur at the Flower Gardens. Shallow water octocorals (seafans and seawhips), which are surprisingly absent from the Flower Gardens, are present but scarce at the Cabo Rojo reefs and reefs several miles south near Isla de Lobos (Chamberlain, 1966; Rigby and McIntire, 1966). Reportedly, octocorals are somewhat more abundant on Alacran reef (Kornicker et al., 1959) and other reefs on the Yucatan Continental Shelf. Coral reefs off the city of Veracruz were reported by Heilprin (1890). Logan (1969) described the physiography of all reefs and hard-banks on the Yucatan Shelf in some detail.

In the Eastern Gulf of Mexico, coral reefs occur in the Tortugas and Florida keys. Jordan (1952) described aspects of biota from the Florida Middle Ground, approximately 300 square miles of reef formations off Appalachicola Bay, Florida. Grimm and Hopkins (1977) indicate octocoral predominance at the Florida Middle Ground above 28 m (Muricea-Dichocoenia-Porites Zone) with dominance shifting to the hermatypic corals Dichocoenia and Madracis between 28 and 30 m. Millepora (fire coral) dominates from 30 to 31 m and becomes co-dominant with Madracis from 31 to 36 m. Zonation at the Florida Middle Ground therefore differs considerably from that of the aforementioned coral reefs, even though the dominant organisms are components of the

Caribbean biota. Elements of the Caribbean reef biota occupy hard-bottoms and "patch reefs" from Tampa Bay to Sanibel Island on the West Florida shelf (Joyce and Williams, 1969; Smith, 1976).

The Gulf of Mexico is, therefore, ringed by a combination of thriving coral reefs and scattered hard-banks and patches bearing elements of the Caribbean reef biota. To what extent the Caribbean biota are represented at the Flower Gardens with respect to all taxonomic groups is not yet known. Bright and Pequegnat (1974) reported 253 invertebrate species and 103 fishes from the West Flower Garden. Bright et al. (1981) listed over 30 species of benthic algae from the East Flower Garden. The list of species is expanding through ongoing research sponsored by the U.S. Bureau of Land Management (Bright and Rezak, 1976, 1978a,b).

It is not surprising that thriving reefs occur at the locality of the Flower Gardens. Though not well understood at present, the environmental conditions there do not seem inconsistent with the existence of coral reefs (see Stoddart, 1969, for discussion of reef ecology). (The oceanic water bathing the reef is clear, with visibility usually over 30 m. Salinity varies very little from 35 ‰, although we have detected surface salinities as low as 32 ‰ and bottom salinity on the coral reefs of 34 ‰. The depth is sufficiently shallow at the bases of reefs (40-46 m) to allow penetration of the sunlight necessary for massive coral growth. We have never observed significant suspended sediment in the water on the reefs, and there is no evidence of siltation. Stoddart (1969) indicates that coral reefs grow best at temperatures of 25°-29°C but can thrive in areas with an annual minimum of 18°C. He adds that "the resistance of corals to high and low temperatures varies with species and at their latitudinal limits reefs become gradually depauperate rather than suddenly extinguished." This may have some significance with regard to the Flower Gardens, but evidence indicates that surface temperatures there, which often extend isothermally to depths below the bases of the reefs, rarely drop below about 20°C and may go as high as 30°C or more during the summer.)

The most puzzling aspect of Flower Garden benthic community structure is the absence of shallow water octocorals and stony corals of the genus Acropora. Both groups are typically very abundant on Caribbean reefs and reefs in other parts of the Gulf of Mexico. One might account for the absence of Acropora palmata on the basis of its depth distribution. It is a shallow water form and does not occur in any abundance below 10 m (Logan, 1969), whereas the crests of the East and West Flower Garden reefs lie at about 16 and 20 m, respectively. However, the authors have observed sizeable Acropora cervicornis thickets at depths exceeding 30 m in the Bahamas and the Virgin Islands, and one might expect this species to occur at the Flower Gardens, though it has not been found. Shallow water octocorals occur abundantly elsewhere in the Gulf of Mexico, Caribbean, Bahamas, and Bermuda at Flower Gardens' depths. Their absence from the Flower Gardens is unexplained.

Biotic zonation at the Flower Gardens is distinct. Though most zones overlap or grade into one another to some extent, they are

never-the-less very recognizable and their depth ranges correlate consistently with those of known sedimentological facies (Figure III-1). The following is a general descriptive account of biotic zonation and biotopes at the East and West Flower Garden Banks.)

Coral Reefs

(Submerged coral reefs comprise the shallowest and largest reefal structures on the East and West Flower Garden Banks, occupying the crests of the banks down to 46 m, and in places 52 m, depth (Figures III-1, 2, and 3).) The main reeftops generally vary from 18 to 28 m, but 15 m depths are common and an 11 m depth has been encountered at the East Flower Garden. The reefs are made up of closely spaced or crowded coral heads up to 3 m in diameter and height. "Patches" of sand or carbonate gravel occur here and there among the coral heads. The heads are frequently very cavernous, showing evidences of substantial internal and surficial bioerosion.

(Two biotic zones are recognizable on the coral reefs: a high diversity assemblage (18 hermatypic coral species) limited to depths less than 36 m (Diploria-Montastrea-Porites Zone); and a comparatively low diversity assemblage (approximately 8 hermatypic coral species) between 36 and 46 to 52 m (Stephanocoenia-Millepora Zone).)

More is known of the Diploria-Montastrea-Porites community than of any other at the Flower Gardens because most of it is accessible to research divers using SCUBA. Edwards (1971) considered all coral reefs at the West Flower Garden to belong to this zone, thereby implying a hierarchy of coral dominance (percent cover) similar to that described by Logan (1969) for submerged reefs on the Yucatan Shelf, southwestern Gulf of Mexico. However, subsequent studies by Bright *et al.* (1974), Tresslar (1974), and Bright and Viada (unpublished) show conclusively that Montastrea annularis is the dominant coral, followed by Diploria strigosa, Montastrea cavernosa, Colpophyllia spp., and Porites astreoides. Convention should therefore dictate a change in zonal designation for high diversity reefs at the Flower Gardens to Montastrea-Diploria Zone to reflect the true order of coral dominance above 36 m. For convenience and to avoid confusion, however, the older designation is retained.

Transect measurements within the zone indicate that approximately 60% of the hard substratum is occupied by living coral (excluding sand and gravel patches). Montastrea annularis comprises about half of the living coral population and is, therefore, overwhelmingly dominant. Accretionary growth of this species is estimated at 6 to 8 mm/yr based on sclerochronological analyses (Hudson and Robbin, 1980; also see Bright *et al.*, this report p.68). This is comparable to accretionary growth rates for the same species in very shallow water (3-5 m) in the Florida Keys (Shinn, personal communication). Over the short-term, the balance between lateral encrusting growth of corals vs. coral mortality may be as important as accretionary growth in maintaining a stable cover of living scleractinian corals on the reefs.

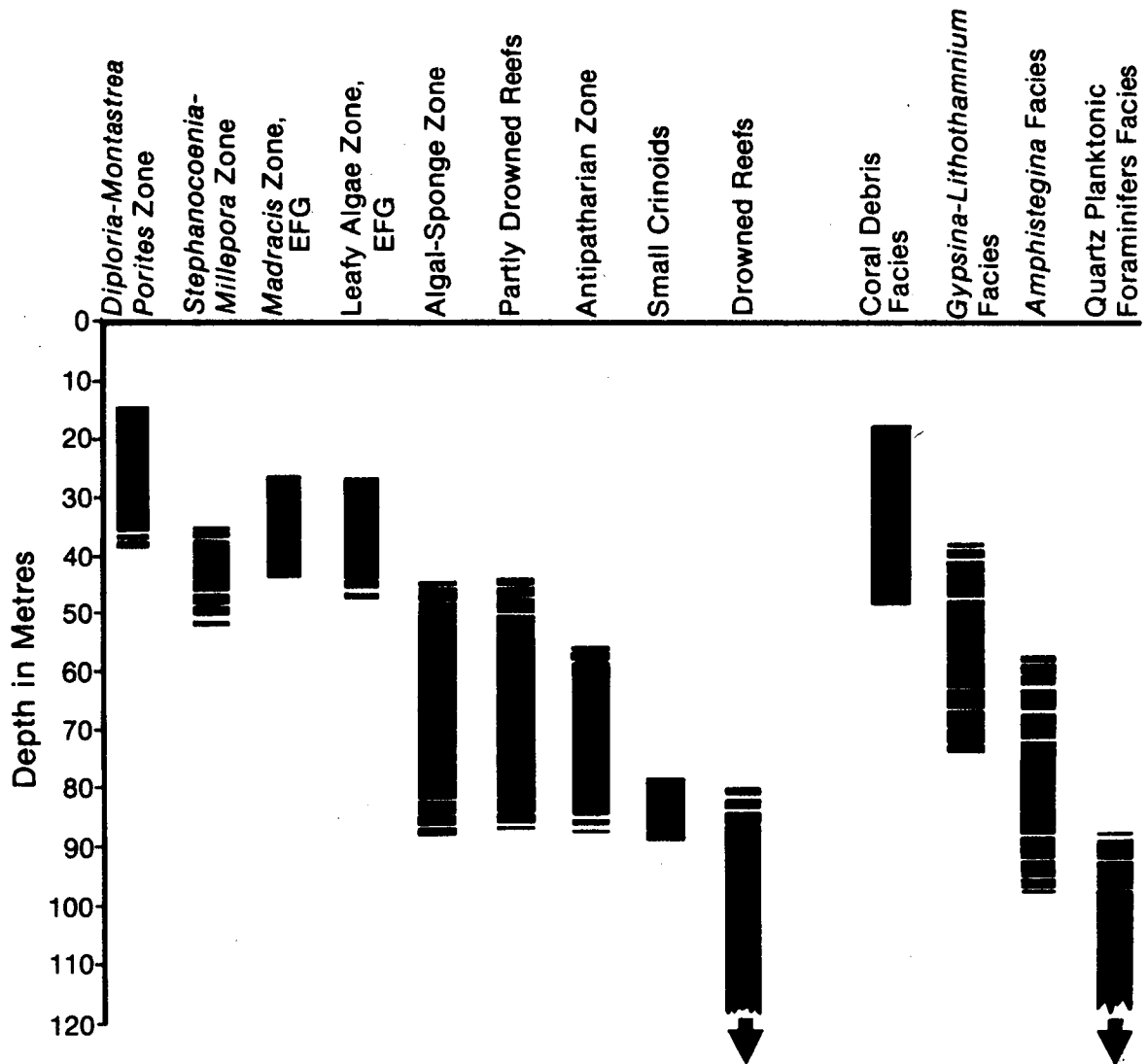


Figure III-1. Depth ranges of recognizable biotic zones and sedimentary facies (other than hard bottoms). Broken bars indicate varying upper and lower depth extremities for zones, depending on locations.

Crustose coralline algae are abundant on the high diversity reefs, and they add substantial amounts of calcium carbonate to the reef substratum. Intuitively it is felt that the contribution to frame building by the coralline algae on the high diversity reefs is minor compared to that of the hydrozoan and scleractinian hermatypic corals. Standing crops of leafy algae on the high diversity reefs are consistently low, possibly kept so by the grazing activities of mobile invertebrates and fishes.

The 253 species of reef invertebrates and 103 reef fishes reported in Bright and Pequegnat (1974) were almost all taken from the Diploria-Montastrea-Porites Zone at the West Flower Garden. Studies in progress imply a nearly identical community structure and diversity for the Diploria-Montastrea-Porites Zone at the East Flower Garden.

Among the typically caught sport and commercial fishes frequenting the high diversity coral reefs are several species of groupers and hinds (Mycteroperca spp. and Epinephelus spp.), amberjacks (Seriola spp.), Great barracuda (Sphyraena barracuda), Red snapper (Lutjanus campechanus), Vermilion snapper (Rhomboplites aurorubens), Cottonwick (Haemulon melanurum), Porgys (Calamus spp.), and Creolefish (Paranthias furcifer).

(Spiny lobsters, Panulirus argus, are known to occur on the high diversity reefs at both Flower Garden banks and have been seen by the author on several other banks (Sonnier Banks, 18 Fathom Bank, Bright Bank). Panulirus guttatus has been seen on the shallow coral reefs (26 m) at the East Flower Garden and probably occurs also at the West Flower Garden. (The Shovel-nosed lobster (Scyllarides aequinoctialis) is reported from the high diversity reef at the West Flower Garden and probably occurs also at the East Flower Garden. All of these species of lobsters are probably widely distributed on the Outer Continental Shelf banks in the northwestern Gulf of Mexico, but nothing is known of the magnitude and dynamics of the regional populations, or whether they could support a commercial lobster fishery.

(Between 36 and 38 m depth at both banks a transition is apparent from the Diploria-Montastrea-Porites assemblage to a reef zone of lower diversity which extends generally down to 46 m, with components to 52 m in places. Only approximately eight species of hermatypic corals are conspicuous in the zone: Stephanocoenia michelini, Millepora sp., Colpophyllia sp., Diploria sp., Mussa angulosa, and Scolymia sp., probably in that relative order of abundance.) The designation Stephanocoenia-Millepora Zone is, therefore, appropriate (see Figures III-1, 2, and 3).

Population levels of these corals have not been quantitatively determined, but visual observations indicate considerably lower total live coral cover than in the Diploria-Montastrea-Porites Zone and a great deal of variation in percent cover and relative abundance from place to place. Crustose coralline algae are substantially more conspicuous in the Stephanocoenia-Millepora Zone and are apparently the predominant encrusting forms occupying dead coral reef rock.

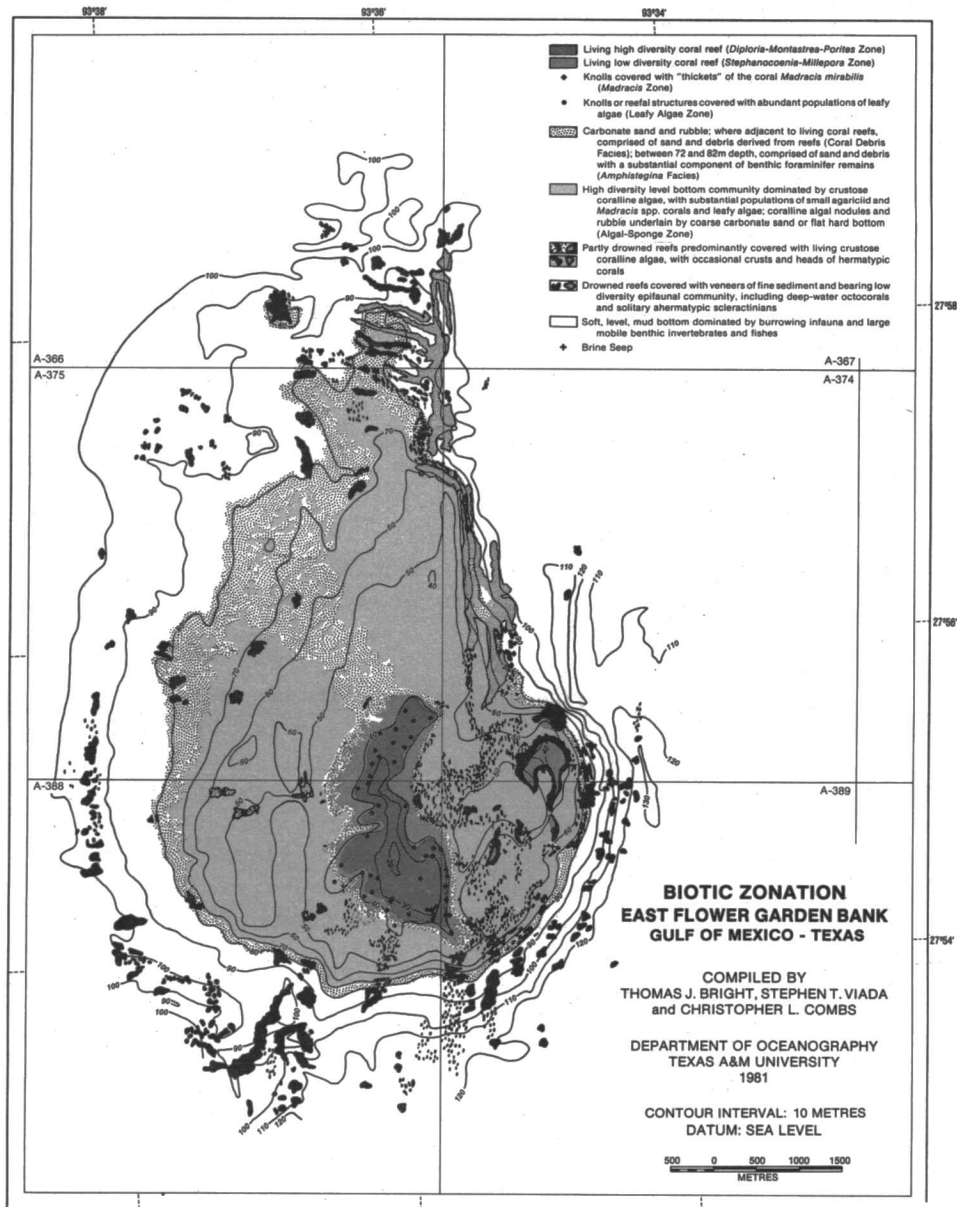


Figure III-2. Biotic zonation, East Flower Garden Bank. Note: the northwestern rim of the bank, between about 60 m and 90 m depth, is largely covered by crusts of coralline algae on hard, steeply inclined substratum. This extensive area is biologically similar to the partly-drowned reefs. It is depicted on the map by stippling somewhat finer than that for carbonate sand, but coarser than that for the other shaded zones. It is not represented or defined in the map's legend.

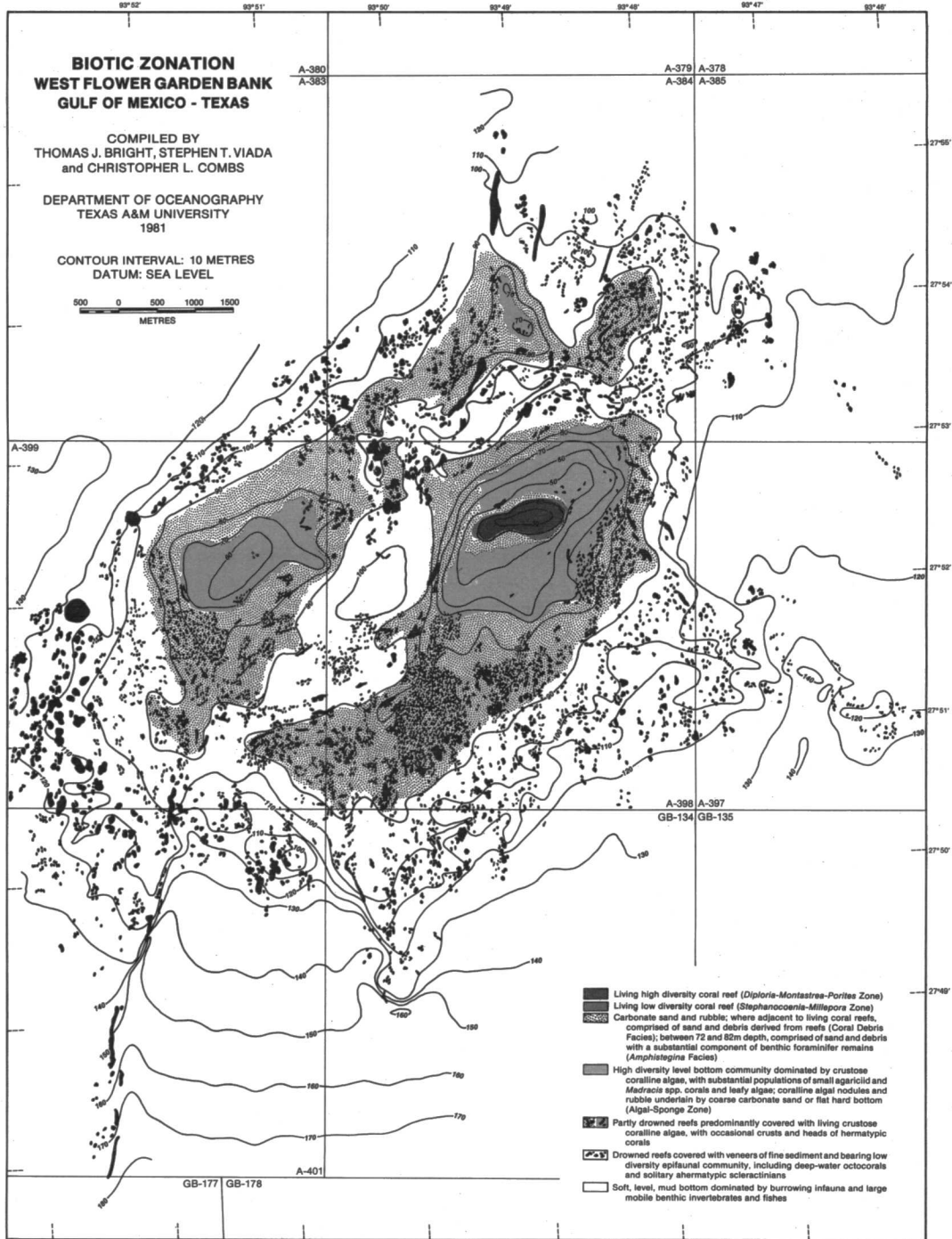


Figure III-3. Biotic zonation, West Flower Garden Bank.

Sclerochronologic interpretation of a specimen of Stephanocoenia michelini from 39 m depth at the East Flower Garden indicates an accretionary growth rate of approximately 6 mm/yr (assuming the "growth" bands examined are annual) (Bright et al., 1981).

Little is known of the assemblage of organisms inhabiting the Stephanocoenia-Millepora Zone. The reef fish populations appear less diverse than in the Diploria-Montastrea-Porites Zone. Population density of the black urchin, Diadema antillarum, which is a significant bioeroder, may be similar in both zones. Exceptional numbers of the American thorny oyster, Spondylus americanus, have been seen in the Stephanocoenia-Millepora Zone.

Successional relationships between the shallower, high diversity Diploria-Montastrea-Porites reefs and the deeper, low diversity, Stephanocoenia-Millepora reefs at the Flower Gardens cannot be determined from existing information. Presumably, the low diversity reefs could represent depauperate remnants of high diversity reefs which have been forced to a habitat too deep to support a majority of the contemporary coral species. In this case, much of the dead reef rock upon which the corals of the low diversity reefs now grow would be composed of the remains of corals species now living on the high diversity reefs. Conversely, contemporary high diversity reefs may have developed on the tops of low diversity reefs or other local topographical mounds (possibly accumulations of the coral Madracis mirabilis) whose crests achieved a depth above which high coral diversity and rapid coral growth are possible. More information is needed concerning the nature of the reef rock in both zones, rates of deposition of carbonate rock and sediment, and vertical movements of the substratum and sea level relative to one another in the past several thousand years.

Leafy Algae and Madracis Zones

On peripheral parts of the main reefal structure between 28 and 44 m depth at the East Flower Garden, large knolls occur which are generally devoid of coral reefs. Certain of these knolls are overwhelmingly dominated by living Madracis mirabilis (Madracis Zone). Some are covered by lush assemblages of leafy algae (Leafy Algae Zone), including species of Styopodium, Caulerpa, Dictyota, Chaetomorpha, Pocockiella, Rhodymenia, Valonia, Codium, and others. Other knolls are intermediate mixtures of the above. None of these assemblages resemble the adjacent coral reef community in structure although it is likely that most or all of the species found on the knolls also occur on the reefs.

The surficial substratum on these knolls is primarily composed of skeletal remains of Madracis mirabilis. Madracis gravel is also the predominant unconsolidated sediment in depressions between coral heads on peripheral parts of the main reef structure below approximately 28 m depth. Similar depressions in the central part of the main reef contain coarse carbonate sand. Presence of Madracis gravel among coral heads on the deepest parts of the high diversity coral reef, where large populations of living Madracis mirabilis do not occur, may imply

that the high diversity coral reef is encroaching upon the Madracis knolls at the reef edge. These knolls may, therefore, be one of the sequential steps in development of high diversity coral reefs at the East Flower Garden. Comparable knolls composed of Madracis gravel have been encountered at the West Flower Garden, interfingering with the high diversity coral reef on its eastern extremity.

Algal-Sponge Zone

The Algal-Sponge Zone includes a number of biotope types occurring between 46 m and 82 m at the East Flower Garden and between 46 m and 88 m at the West Flower Garden. Coarse carbonate sand and rubble surrounding the living coral reefs (Coral Debris Facies) mark a geo-biological transition between the coral reefs and the surrounding Algal-Sponge platform, which is largely covered with carbonate sand, gravel, nodules, and partly drowned reefal structures.

Large areas on both banks where nodules predominate comprise the Gypsina-Lithothamnium sedimentological facies. The most important contemporary producers of carbonate nodules and crusts on rubble and reefal structures are the coralline algae, mostly Lithophyllum and Lithoporella. These nodules are typically referred to as algal nodules.

The algal nodules, which range in size from less than 1 cm to 10 cm or more, and in most places cover 50 to 80% of the bottom, create a biotope which may support an infaunal and epifaunal community comparable in diversity to the living coral reefs. In addition to coralline algae and the encrusting foraminifer Gypsina, the nodules themselves house an abundance of boring and attached epibenthos. Numerous mobile invertebrates and small fishes find shelter under, between, and within the nodules. Beneath the nodules, coarse carbonate sand contains active soft-bottom infaunal populations, as evidenced by the presence of numerous burrows, often patterned in a fashion similar to burrows produced by certain decapod crustaceans in near-shore environments.

Most of the (leafy algae) occurring at both banks occurs among the algal nodules) and on reefal structures within the Algal-Sponge Zone (the aforementioned algae-covered knolls in shallower water at the East Flower Garden are comparatively small in area). Leafy algae are pervasive among the nodules and on hard surfaces within the Algal-Sponge Zone but are neither uniformly distributed nor uniformly abundant from place to place. At certain locations lush growths of Styopodium sp. and Pocockiella sp. may obscure all else on the bottom. The highly productive and renewable benthic algae populations must contribute substantial amounts of food to the surrounding communities.

Calcareous green algae, Halimeda spp. and Udotea sp., contribute to sediment production within the Algal-Sponge Zone. Patches in excess of 10 m diameter, composed almost exclusively of Halimeda sp., have been seen at both banks within the algal nodule zone. These patches are apparently long-lived, semi-permanent features because the plate-like remains of dead Halimeda sp. plants extend at least several

centimetres deep into the substratum. Halimeda spp. occur also as individual plants here and there among the nodules and on reefal structures.

Several species of hermatypic corals are abundant enough among the algal nodules to be considered major contributors to sediment production within the Algal-Sponge Zone. Saucer-like colonies of Helioseris cucullata and Agaricia sp. are pervasive but unevenly distributed, with populations varying from less than one to over ten colonies per square metre. Several small species of Madracis likewise occur with varying abundance among the algal nodules.

Of the numerous species of sponges which are conspicuous and abundant within the Algal-Sponge Zone, Neofibularia nolitangere is most distinctive. Subcircular crusts of this sponge a metre or so in diameter occur on nodules, sand, or rock within the zone at frequent intervals. Fishes and mobile invertebrates are attracted to the sponge, swimming or crawling among its chimney-like spires.

Populations of echinoderms within the Algal-Sponge Zone must add significantly to the carbonate substratum. Sizeable comatulid crinoids and a number of asteroid species are found everywhere on the banks except on the living coral reefs. A particularly large population of the asteroid starfish Linckia nodosa and great numbers of the urchins Pseudoboletia maculata and Arbacia punctulata were seen on the algal nodules and reefal structures of the platform west of the main reef at the East Flower Garden. Interestingly, similar concentrations of these particular asteroids and echinoids have not been seen on other parts of either bank. This may imply a small-scale environmental control on their distribution which would be reflected in carbonate sediment composition.

Small gastropods and pelecypods are abundant on and among the nodules, and gastropod shells are known to be nuclei around which some of the nodules are formed. The largest abundant pelecypod in the Algal-Sponge Zone is the American thorny oyster, Spondylus americanus, which occurs attached to nodules as well as reefs. Its distribution, as with many of the conspicuous organisms in the zone, appears irregular and locally contagious, resulting in a high degree of lateral variation in population levels. Small clumps (one-half metre or so in diameter) of vermicularian gastropod tubes occur infrequently among the nodules and on sand bottoms within the Algal-Sponge Zone. Their contribution to the carbonate sediment is probably minor.

There are obviously many species of plants and animals associated with algal nodules within the Algal-Sponge Zone which are involved to varied extents in the frame-building process. Their successful effort in this respect is probably the dynamic factor on which the stability of benthic community structure within the Algal-Sponge Zone depends.

Small Yellowtail reeffishes, Chromis enchrysurus, are the most abundant of the conspicuous fishes which congregate around irregularities in the Algal-Sponge Zone. Conical burrows a metre across and

one-half metre deep produced by the Sand tilefish, Malacanthus plumieri, are scattered about the zone from the base of the main coral reef down to at least 70 m. Other particularly characteristic fishes among the algal nodules are the small Cherubfish, Centropyge argi, and Orangeback bass, Serranus annularis.

Partly Drowned Reefs and Drowned Reefs

The nature of both types of living coral reefs (high diversity and low diversity) has been discussed. As indicated, uncertainty exists concerning the successional relationship, if there is one, between the high diversity and low diversity coral reefs. The developmental history of the deeper, and presumably older, partly drowned and drowned reefs may be even more complex, possibly involving subaerial exposure of the reef rock (see above, Chapter II).

The surficial biota now occupying partly drowned and drowned reefs at the Flower Garden Banks probably do not reflect the history of the reefs so much as they reflect contemporary environmental limitations on depth distributions of the organisms. Accordingly, partly drowned reefs are here defined as those reefal structures which exist now at depths below which hermatypic corals are capable of building sizeable heads or large crustose colonies, but within a depth range favoring the predominance of crustose coralline algae (46 to 82 m at the East Flower Garden; 46 to 88 m at the West Flower Garden). Drowned reefs are those reefal structures now existing at depths below which hermatypic corals commonly exist and below which crustose coralline algal populations are significant (below 82 m at the East Flower Garden; below 88 m at the West Flower Garden).

Not unexpectedly, partly drowned reefs are generally restricted to the Algal-Sponge Zone, of which they comprise a major biotope component. They bear crusts dominated by coralline algae, accompanied by other sessile organisms which are also typical of the algal nodules. In addition, they house large anemones such as Condylactis gigantea and Lebrunia danae, an abundance of large comatulid crinoids, occasional basket stars, limited crusts of the hydrozoan coral Millepora sp., and, infrequently, small colonies of the hermatypic corals Agaricia spp., Helioseris cucullata, Montastrea cavernosa, and Stephanocoenia michelini.

The partly drowned reefs attract a number of fish species which also occur on the living coral reefs. Most of these "expatriate" reef fishes occur consistently on similar structures at other banks in the northwestern Gulf which do not possess living coral reefs and, therefore, these reef fishes may not necessarily be recruited from the shallower coral reef fish assemblage at the Flower Gardens. The most abundant fish frequenting the partly drowned reefs is the small Yellowtail reeffish, Chromis enchrysurus, which is not often seen on the high diversity coral reefs.

Drowned reefs occur below approximately 82 m at the East Flower Garden and 88 m at the West Flower Garden, where coralline algae do not

thrive and hermatypic corals are generally absent. Comatulid crinoids, small deep-water octocoral whips and fans, antipatharians, encrusting sponges, and solitary ahermatypic corals are the most conspicuous attached organisms.

The assemblage of fishes frequenting drowned reefs include Red snappers (Lutjanus campechanus), Spanish flag (Gonioplectrus hispanus), Snowy grouper (Epinephelus niveatus), Bank butterflyfish (Chaetodon aya), Scorpionfishes (Scorpaenidae), and most characteristically, the Roughtongue bass (Holanthias martinicensis). The snappers are highly mobile schooling fish which congregate around reefal structures at all depths on the banks but seem to prefer the deeper "drop-offs" and bank-edge features, while showing little affinity for the high diversity reef tops. The other fishes listed are commonly found only on the drowned reefs and the deepest partly drowned reefs. Therefore, in basic species composition the drowned reef ichthyofauna is substantially different from, and of much lower diversity than, the ichthyofauna of the partly drowned reefs or the coral reefs.

Drowned reefs at the Flower Gardens exist in comparatively turbid water and are generally covered with veneers of fine sediment, the veneers being thicker on the deeper reefs. Light penetration, water turbidity, sedimentation, and temperature are probably the most important factors controlling the present distribution of hermatypic corals and coralline algae on the banks. It is suspected that were it not for the chronically turbid bottom water and sedimentation around the peripheries of the two banks, the living algal nodules, partly drowned reefs and other elements of the Algal-Sponge Zones would extend to slightly greater depths, as they do on certain other banks farther offshore, where soft bottoms surrounding the banks are deeper.

Transition Zones

White, bedspring-shaped antipatharian whips, Cirrhopathes spp., occur between 52 and 90+ m and, where they are most abundant (generally around 60 to 85 m), mark a transition between biotic assemblages which exhibit distinct shallow-water affinities (leafy algae, abundant coralline algae, hermatypic corals, sizeable shallow water reef fish populations) and assemblages which are deep-water oriented. The upper parts of this supposed "Antipatharian Zone" blend with the Algal-Sponge Zone, and it is impossible to find any sharp demarcation between the two. One might just as well speak of a lower Algal-Sponge Zone which has a sizeable antipatharian population.

Deeper parts of the "Antipatharian Zone" (over 80 m) are recognizably less diverse and characterized by antipatharians, comatulid crinoids, few if any leafy algae, thin to sparse populations of coralline algae, and a distinctly limited fish fauna including Holanthias martinicensis, Bodianus pulchellus, Chromis enchrysurus, Chaetodon sedentarius, Holacanthus bermudensis, and a few others.

Between 73 and 76 m the nature of the bottom changes, usually rather abruptly, from algal nodules and crusts to a soft level-bottom of

mixed coarse calcareous sand with an abundance of Amphistegina tests and fine silt- and clay-sized particles which are easily stirred up and remain in suspension for a long while. The foraminifer Amphistegina is known to live on the algal nodules at both banks. Non-living tests of this protozoan account for a large portion of the Amphistegina Facies sands occurring on both banks. Presumably, remains of spent Amphistegina from the algal nodule biotope are transported downslope to become incorporated into the Amphistegina Sand Facies.

The Amphistegina Sand Facies is characterized by the presence of a conspicuous population of echinoderms, particularly the urchin Clypeaster ravenelii and the asteroids Chaetaster sp., Narcissia trigonaria, and others. Also, patterned burrows (6 to 12 burrows in circular arrangements of diameters up to one-half metre or so) are overwhelmingly numerous. In places between 80 and 90 m a tremendous population of small comatulid crinoids occurs, clinging to carbonate gravel on the Amphistegina sand. These crinoids do not occur in such numbers elsewhere on the banks, and their distribution does not appear to be related to the distribution of larger crinoid species which occur in the lower Algal-Sponge Zone and on rocks and drowned reefs to depths exceeding 120 m. The presence of the small crinoids indicates a final transition from shallower, higher diversity, clear-water communities dominated by frame-building corals and coralline algae to subdued, deep-water communities subjected to turbidity, sedimentation, and chronically low light levels. With increasing depth, the coarser sediments of the Amphistegina Sand Facies are replaced by mud in the Quartz-Planktonic Foraminifer Facies.

The deep-water populations, whether on hard or soft bottom, represent an assemblage of species which differ substantially from the clear-water assemblages. Few conspicuous species of fish and invertebrates occur in both the clear, shallow-water and turbid deep-water environments on the banks.

Summary

(Benthic organisms inhabiting the Flower Garden Banks are stratified into distinct biotic zones, the limits of which seem to be related to substratum type, light penetration, turbidity, sedimentation, and depth. High diversity living coral reefs (the Diploria-Montastrea-Porites Zone) occur between 16 and 36 m depth, and lower diversity coral reefs (the Stephanocoenia-Millepora Zone) between 36 and 46 m. Crustose coralline algae are dominant on nodules and partly drowned reefs within the Algal-Sponge Zone between 46 and 82 m depth at the East Flower Garden and between 46 and 88 m depth at the West Flower Garden. Drowned reefs below these depths lack significant populations of hermatypic corals and coralline algae, are typically sediment covered, and are generally surrounded by finer sediments and soft-bottom biological assemblages.)

Over 30 species of algae, 250 invertebrates, and 100 fishes are known from the Flower Garden Banks. Most are representatives of the Caribbean reef biota, of which the Flower Garden assemblage is part.

CORAL AND CORALLINE ALGAE POPULATION LEVELS
AT THE EAST AND WEST FLOWER GARDEN BANKS

Introduction

The East and West Flower Garden Banks, separated by 22.2 km, are two of many diapiric structures rising from the continental shelf off the coasts of Texas and Louisiana. Such inorganic banks underlying organic buildups of reefal nature have been classified by Logan et al. (1969) as "submerged reef banks."

Biological and geological evidence published by Bright and Rezak (1977) indicates that both the East and West Flower Garden Banks are capped by healthy coral reefs to depths of 45-49 m. The current study of coral and coralline algae focuses on the high-diversity zone, occupied by what Logan et al. (1969) have termed a Diploria-Montastrea-Porites community. At the Flower Garden Banks, this zone occurs at depths of 19-37 m and is inhabited by at least 18 species of scleractinian corals. Previous work by Texas A&M University researchers compared two sites at the East Flower Garden Bank (Bright et al., 1981). The current study continues this comparison and extends the analysis to include a West Flower Garden site.

The invertebrate communities examined at the Flower Garden Banks are benthic and sessile in nature. These attributes permitted the use of concepts and methods developed originally by Canfield (1941) for terrestrial vegetation studies. Loya (1972) later adapted the methods for use in coral reef studies.

This study had two primary goals:

(1) quantitative assessment of the population levels of scleractinian corals and coralline algae from the Diploria-Montastrea-Porites Zone of the East and West Flower Garden Banks using stratified random line transect analysis; and

(2) determination of the species of scleractinian corals inhabiting both banks within this zone.

Methods

Field Procedure

Data were collected during three cruises:

- (1) 14 February - 22 February 1980
- (2) 13 June - 20 June 1980
- (3) 22 September - 29 September 1980.

Two sites located at the East Flower Garden had been established previously: the BLM site (27°54'15.69"N, 93°35'55.90"W), chosen during the 1977 Texas A&M University monitoring study, and the CSA site (27°54'37.37"N, 93°35'55.79"W), set up during a 1978 study by Continen-

tal Shelf Associates (Tequesta, FL). Texas A&M University established a site at the West Flower Garden (27°52'31.51"N, 93°48'52.53"W) on September 22, 1979. This site is known as the WFG site. All sites are located within the Diploria-Montastrea-Porites Zone.

At the East Flower Garden, the CSA site is situated on the "reef top" at a depth of about 25 m, and the BLM site is located on the "reef edge" at a depth of about 29 m. The BLM site is positioned about 400 m to the south of the CSA site and is adjacent to the transition zone between the Diploria-Montastrea-Porites Zone and the Madracis Zone. The West Flower Garden site is on the reef top at a depth of 26 m.

Sampling was accomplished by taking a series of 18 underwater stratified random line transects at each reef. The 18 East Flower Garden transects were evenly divided, 9 at each of the BLM and CSA sites. A camera jig apparatus was used to obtain a uniform series of photographs along each transect. A fiberglass metric measuring tape was stretched over the transect, providing a size scale for the photographs as well as establishing the transect boundaries. Photographs were taken along the length of the tape, allowing for a certain amount of overlap. This made it possible to construct a photographic mosaic of the transect from the developed prints. Six transects per cruise were taken at each East Flower Garden site, and at the single West Flower Garden site. In an effort to randomize the location of each transect within each zone, the diver-photographer descended to the bottom in the vicinity of the underwater site buoy and swam an unpre-scribed distance. The measuring tape was then stretched out in a direction randomly chosen by the diver-photographer. The equipment and procedures are described in detail in Volume Two, Chapter VII of Rezak and Bright (1981).

Loya (1972) determined that a minimum transect length of 10 m was required for accurate sampling of the coral reef community in his Red Sea study. This length was arbitrarily adopted for use in the 1980 Texas A&M University study. However, several of the photo-mosaics used in the present study resulted in only 8 to 8.5 m of data. Consequently, all transects were reduced in size to 8 m. To examine the effects of this reduction on the sampling accuracy, a species-transect length curve was constructed using data from 18 transects (Figure III-4). This curve is analogous to the species-area curve commonly used by terrestrial ecologists. The loss of information in reducing the sampling distance is minimal.

Representatives of the hermatypic corals found within the Diploria-Montastrea-Porites Zone were collected to ensure accurate identification of the coral species encountered in the transect photographs. Prior to collection, specimens were photographed in situ.

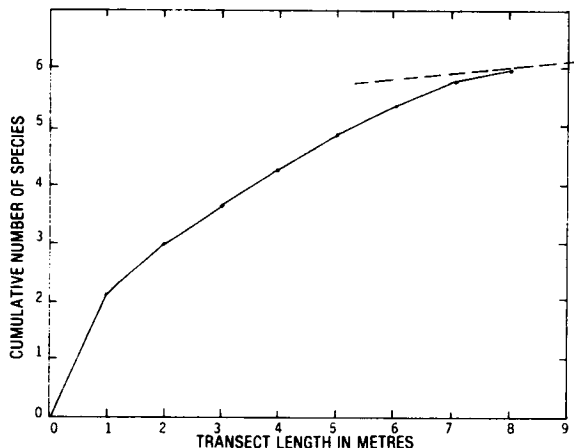


Figure III-4. Species-Transsect length curve based on pooled data from 18 East Flower Garden transects and 18 West Flower Garden transects. The point at which the dashed line is tangent to the curve represents the approximate point beyond which an increase in transect length may only result in a 10% increase in number of species sampled.

Statistical Methods for Transect Analysis

Line transect data were analyzed with a statistical program originally designed for analysis of range vegetation distributions determined by using the same line intercept method. A review of the literature concerned with this method may be found in Bright *et al.* (1981, Chapter VII).

The analysis compares line transect data from two study areas (i.e., BLM and CSA sites, on the EFG and WFG reefs) to discern similarities and differences between species compositional patterns and overall population indices. The program determined the total number of individuals of each species, the total of the transect intercept lengths for each species, and the total number of transects on which each coral species occurred. From these, eight parameters were calculated: 1) dominance (percent cover); 2) relative dominance; 3) relative density; 4) frequency of occurrence; 5) relative frequency of occurrence; 6) species diversity; 7) species evenness; and 8) species richness. Sample means were calculated for each taxon at each location for the first five parameters (Appendix B, Tables B-1 through B-39). Taxon diversity, evenness, and richness were calculated for each transect at each location (Appendix B, Tables B-40 through B-42). The species diversity, evenness, and richness values were calculated using only coral category data. For both relative dominance and relative density parameters, additional calculations were made which included coralline algae data to suggest relative proportions of the major carbonate producers on the reef.

Dominance

Dominance, or percent cover, is a measure of size, based on the percent cover along the entire length of a transect. The formula for dominance is as follows:

$$\text{DOMINANCE} = \frac{\text{Total of Intercept Lengths for Taxon "A"}}{\text{Total Transect Length}} \times 100$$

Relative Dominance

Relative dominance is a measure of the substrate cover of individual taxa in relation to the total cover of all taxa under consideration. The formula for calculating relative dominance is as follows:

$$\text{RELATIVE DOMINANCE} = \frac{\text{Total of Intercept Lengths for Taxon "A"}}{\text{Total of Intercept Lengths for All Taxa}} \times 100$$

Relative Density

Relative density (abundance) describes the number of individual colonies of a taxon within transect bounds, relative to the total number of such colonies within that transect. The formula is as follows:

$$\text{RELATIVE DENSITY} = \frac{\text{Total Number of Colonies of Taxon "A"}}{\text{Total Number of Colonies of All Taxa}} \times 100$$

Frequency

The frequency calculation relates the number of transects on which an individual coral species or category is found at least once to the total number of transects. The formula is as follows:

$$\text{FREQUENCY} = \frac{\text{Number of Transects on Which Taxon "A" Occurs}}{\text{Total Number of Transects}} \times 100$$

Species Diversity

The Shannon-Weaver Index of Diversity (H'') is used to measure the diversity of the coral assemblages. The formula is as follows:

$$H'' = - \sum_{i=1}^s \left(\frac{n_i}{N} \right) \ln \frac{n_i}{N}$$

where

H'' = taxonomic diversity

n_i = number of individuals (segments) in the i th taxon

N = total number of individuals (segments) in the sample

s = number of taxa.

When used in this fashion, the index does not take into account the amount of substratum covered by various species but considers only the numbers of colonies enumerated, regardless of size.

Taxon Evenness

Species evenness is a numerical representation of the distribution of individuals among the taxa in the transect. Pielou's evenness index, J , is simply the ratio of the observed diversity to the maximum diversity possible for the same number of taxa. The formula is as follows:

$$\text{TAXON EVENNESS} = H''/H_{\max} = H''/\ln(S)$$

where

H'' = taxon diversity for the sample

$$H_{\max} = -\frac{1}{S} \ln\left(-\frac{1}{S}\right) = \ln(S)$$

S = number of taxa identified in the transect.

Taxon Richness

Common richness indices compare the number of taxa present in a sample with an expected number. Margalef's index, D , was chosen. It is based on the presumed linear relationship between the number of taxa and the natural logarithm of the number of individuals present in the sample. The formula is as follows:

$$D = \frac{S-1}{\ln(N)}$$

where

D = taxon richness

S = number of taxa present in the sample

N = number of individuals present in the sample.

Other Statistical Analyses

Coefficients of variation (CV's) were calculated for all sample means to enable comparisons of the variability of parameters with widely disparate means. The formula for the CV of a sample is as follows:

$$CV = \frac{S^2}{\bar{X}}$$

where

s^2 = the variance of the sample

and

\bar{X} = the mean of a sample.

The F-test was employed to test sample variances for homogeneity. The null hypothesis (H_0) was the statement of equal variances. Depending on the F-test results, sample means were compared for statistical similarity using either Student's t-test (if H_0 accepted) or Satterwaithe's t'-test (if H_0 was not accepted). The null hypothesis for the t-test or t'-test was the statement of equal means. For the F-test, t-test, and t'-tests, a standard alpha level of 0.05 was used (i.e., 95% confidence level).

To evaluate the strength of the acceptance or rejection of H_0 , the significance probability (SP) was determined. The SP of a sample is the probability of obtaining a sample that is more contradictory than the observed sample, assuming H_0 to be true. The larger the probability of this is, the closer the two values under consideration are, and, hence, the more faith we can put in the conclusion that the two values are equal. So, in comparing the SP to the alpha level, we accept the null hypothesis when the SP is greater than the alpha level, and vice versa. The proximity of the SP to the alpha level is a measure of the strength of the decision (Gibbons and Pratt, 1975).

Results and Discussion

BLM-CSA Site Analysis

With a few exceptions, the results of the BLM-CSA site analysis for the East Flower Garden generally support the conclusions of Bright et al. (1981). It must be emphasized, however, that 17 transects per site were used in the previous study, while only 9 transects per site were analyzed in the current study.

The values of species diversity, evenness, and richness are statistically similar at both sites (SP = 0.06, 0.06, 0.50, respectively). The sizes of the coefficients of variation (CV) for these indices are orders of magnitude smaller than most population parameters of individual biotic categories in this study. Therefore, although inter-site differences in the population levels of many individual coral species do exist (Tables III-1 through 3), the overall assemblage varies little in terms of diversity, evenness, or richness.

The data indicate that Montastrea annularis is the most dominant and abundant coral species at the East Flower Garden reef. However, for corals only, and for corals and coralline algae, the data show statistical differences in numerical values for dominance, relative dominance, and relative density between the two sites. Although

TABLE III-1
 POPULATION LEVELS OF CORALS AT THE WEST FLOWER GARDEN
 LISTED IN DECREASING ORDER OF IMPORTANCE

DOMINANCE	RELATIVE DOMINANCE
1. <u>Montastrea annularis</u> 2. <u>Diploria strigosa</u> 3. <u>Montastrea cavernosa</u> 4. <u>Millepora</u> spp. 5. <u>Porites astreoides</u> 6. <u>Madracis decactis</u> 7. <u>Siderastrea siderea</u> 8. <u>Colpophyllia</u> spp. 9. <u>Agaricia</u> spp. 10. <u>Stephanocoenia michelini</u> 11. <u>Mussa angulosa</u> 12. <u>Scolymia cubensis</u>	1. <u>Montastrea annularis</u> 2. <u>Diploria strigosa</u> 3. <u>Montastrea cavernosa</u> 4. <u>Millepora</u> spp. 5. <u>Porites astreoides</u> 6. <u>Madracis decactis</u> 7. <u>Siderastrea siderea</u> 8. <u>Colpophyllia</u> spp. 9. <u>Stephanocoenia michelini</u> 10. <u>Agaricia</u> spp. 11. <u>Mussa angulosa</u> 12. <u>Scolymia cubensis</u>
RELATIVE DENSITY	FREQUENCY
1. <u>Montastrea annularis</u> 2. <u>Porites astreoides</u> 3. <u>Montastrea cavernosa</u> 4. <u>Millepora</u> spp. 5. <u>Diploria strigosa</u> 6. <u>Madracis decactis</u> 7. <u>Agaricia</u> spp. 8. <u>Colpophyllia</u> spp. 9. <u>Mussa angulosa</u> 10. <u>Siderastrea siderea</u> 11. <u>Stephanocoenia michelini</u> 12. <u>Scolymia cubensis</u>	1. <u>Montastrea annularis</u> 2. <u>Porites astreoides</u> 3. <u>Millepora</u> spp. 4. <u>Montastrea cavernosa</u> = <u>Diploria strigosa</u> = <u>Agaricia</u> spp. 5. <u>Madracis decactis</u> 6. <u>Colpophyllia</u> spp. 7. <u>Mussa angulosa</u> 8. <u>Siderastrea siderea</u> = <u>Stephanocoenia michelini</u> 9. <u>Scolymia cubensis</u>

TABLE III-2
 POPULATION LEVELS OF CORALS AT THE EAST FLOWER GARDEN
 LISTED IN DECREASING ORDER OF IMPORTANCE

DOMINANCE	RELATIVE DOMINANCE
1. <u>Montastrea annularis</u>	1. <u>Montastrea annularis</u>
2. <u>Diploria strigosa</u>	2. <u>Diploria strigosa</u>
3. <u>Colpophyllia</u> spp.	3. <u>Colpophyllia</u> spp.
4. <u>Millepora</u> spp.	4. <u>Montastrea cavernosa</u>
5. <u>Montastrea cavernosa</u>	5. <u>Millepora</u> spp.
6. <u>Madracis decactis</u>	6. <u>Madracis decactis</u>
7. <u>Porites astreoides</u>	7. <u>Porites astreoides</u>
8. <u>Agaricia</u> spp.	8. <u>Agaricia</u> spp.
9. <u>Stephanocoenia michelini</u>	9. <u>Stephanocoenia michelini</u>
10. <u>Mussa angulosa</u>	10. <u>Mussa angulosa</u>
11. <u>Siderastrea siderea</u>	11. <u>Siderastrea siderea</u>
12. <u>Scolymia cubensis</u>	12. <u>Scolymia cubensis</u>

RELATIVE DENSITY	FREQUENCY
1. <u>Montastrea annularis</u>	1. <u>Montastrea annularis</u> =
2. <u>Diploria strigosa</u>	<u>Diploria strigosa</u>
3. <u>Porites astreoides</u>	2. <u>Millepora</u> spp.
4. <u>Millepora</u> spp.	3. <u>Porites astreoides</u>
5. <u>Agaricia</u> spp.	4. <u>Agaricia</u> spp. = <u>Colpophyllia</u> spp.
6. <u>Montastrea cavernosa</u>	5. <u>Montastrea cavernosa</u>
7. <u>Colpophyllia</u> spp.	6. <u>Madracis decactis</u>
8. <u>Madracis decactis</u>	7. <u>Mussa angulosa</u>
9. <u>Mussa angulosa</u>	8. <u>Stephanocoenia michelini</u>
10. <u>Stephanocoenia michelini</u>	9. <u>Siderastrea siderea</u>
11. <u>Siderastrea siderea</u>	10. <u>Scolymia cubensis</u>
12. <u>Scolymia cubensis</u>	

TABLE III-3
POPULATION LEVELS OF CORALS AT THE EFG SITES
LISTED IN DECREASING ORDER OF IMPORTANCE

DOMINANCE		RELATIVE DOMINANCE	
BLM SITE	CSA SITE	BLM SITE	CSA SITE
<ol style="list-style-type: none"> 1. <u>Montastrea annularis</u> 2. <u>Colpophyllia</u> spp. 3. <u>Madracis decactis</u> 4. <u>Diploria strigosa</u> 5. <u>Millepora</u> spp. 6. <u>Montastrea cavernosa</u> 7. <u>Porites astreoides</u> 8. <u>Agaricia</u> spp. 9. <u>Mussa angulosa</u> 10. <u>Scolymia cubensis</u> 11. <u>Stephanocoenia michelini</u> 12. <u>Siderastrea siderea</u> 	<ol style="list-style-type: none"> 1. <u>Montastrea annularis</u> 2. <u>Diploria strigosa</u> 3. <u>Montastrea cavernosa</u> 4. <u>Millepora</u> spp. 5. <u>Colpophyllia</u> spp. 6. <u>Porites astreoides</u> 7. <u>Agaricia</u> spp. 8. <u>Madracis decactis</u> 9. <u>Stephanocoenia michelini</u> = <u>Siderastrea siderea</u> = <u>Scolymia cubensis</u> = <u>Mussa angulosa</u> 	<ol style="list-style-type: none"> 1. <u>Montastrea annularis</u> 2. <u>Colpophyllia</u> spp. 3. <u>Madracis decactis</u> 4. <u>Diploria strigosa</u> 5. <u>Millepora</u> spp. 6. <u>Montastrea cavernosa</u> 7. <u>Porites astreoides</u> 8. <u>Agaricia</u> spp. 9. <u>Mussa angulosa</u> 10. <u>Stephanocoenia michelini</u> 11. <u>Scolymia cubensis</u> 12. <u>Siderastrea siderea</u> 	<ol style="list-style-type: none"> 1. <u>Montastrea annularis</u> 2. <u>Diploria strigosa</u> 3. <u>Montastrea cavernosa</u> 4. <u>Colpophyllia</u> spp. 5. <u>Millepora</u> spp. 6. <u>Porites astreoides</u> 7. <u>Agaricia</u> spp. 8. <u>Madracis decactis</u> 9. <u>Stephanocoenia michelini</u> = <u>Siderastrea siderea</u> = <u>Scolymia cubensis</u> = <u>Mussa angulosa</u>
RELATIVE DENSITY		FREQUENCY	
BLM SITE	CSA SITE	BLM SITE	CSA SITE
<ol style="list-style-type: none"> 1. <u>Montastrea annularis</u> 2. <u>Porites astreoides</u> 3. <u>Diploria strigosa</u> 4. <u>Colpophyllia</u> spp. 5. <u>Millepora</u> spp. 6. <u>Madracis decactis</u> 7. <u>Agaricia</u> spp. 8. <u>Montastrea cavernosa</u> 9. <u>Mussa angulosa</u> 10. <u>Stephanocoenia michelini</u> 11. <u>Scolymia cubensis</u> 12. <u>Siderastrea siderea</u> 	<ol style="list-style-type: none"> 1. <u>Montastrea annularis</u> 2. <u>Diploria strigosa</u> 3. <u>Millepora</u> spp. 4. <u>Porites astreoides</u> 5. <u>Agaricia</u> spp. 6. <u>Montastrea cavernosa</u> 7. <u>Colpophyllia</u> spp. 8. <u>Madracis decactis</u> 9. <u>Stephanocoenia michelini</u> = <u>Siderastrea siderea</u> = <u>Scolymia cubensis</u> = <u>Mussa angulosa</u> 	<ol style="list-style-type: none"> 1. <u>Montastrea annularis</u> = <u>Millepora</u> spp. = <u>Diploria strigosa</u> 2. <u>Porites astreoides</u> 3. <u>Agaricia</u> = <u>Colpophyllia</u> spp. = <u>Montastrea cavernosa</u> 4. <u>Madracis decactis</u> = <u>Stephanocoenia michelini</u> 5. <u>Siderastrea siderea</u> 6. <u>Mussa angulosa</u> = <u>Scolymia cubensis</u> 	<ol style="list-style-type: none"> 1. <u>Montastrea annularis</u> = <u>Diploria strigosa</u> 2. <u>Millepora</u> spp. = <u>Porites astreoides</u> 3. <u>Agaricia</u> spp. = <u>Colpophyllia</u> spp. 4. <u>Madracis decactis</u> = <u>Montastrea cavernosa</u> 5. <u>Mussa angulosa</u> 6. <u>Siderastrea siderea</u> = <u>Stephanocoenia michelini</u> = <u>Scolymia cubensis</u>

M. annularis occurred on all transects at both sites, population level estimates are higher at the BLM site than at the CSA site. The degree to which the means are statistically dissimilar is substantial; the SP's for the three parameters noted above are 0.001, 0.002, and 0.002, respectively.

The brain coral, Diploria strigosa, ranks second overall in terms of population levels. Its relative coral dominance level for the CSA site is statistically greater than that of the BLM site, supporting last year's results (Bright et al., 1981). The mean dominance values for D. strigosa at the two sites are only weakly accepted as being equal (SP = 0.06). Relative coral density levels for D. strigosa at the two sites are not statistically different (SP = 0.31). The previous study, however, found strong differences in the relative density between the BLM and CSA sites, there being significantly more colonies at the CSA site (SP = 0.02). The variances for relative densities calculated for the previous study and for the present study were found to be statistically equal. The difference in the means may be due to the reduced number of transects taken during the present study. It seems doubtful that physical and/or biological forces could have produced such a large change in the relative density over a short period of time. A further discrepancy concerns the frequency of occurrence. The previous study found the frequency to be much greater at the CSA site (71%) than at the BLM site (47%). The current study produced frequencies of 100% at both sites. D. strigosa probably occurs in equal abundance at both sites. Mean colony size appears to be greater at the CSA site.

Since Colpophyllia natans and C. amaranthus were indistinguishable in the transect photographs, they were grouped together in the analysis. Population levels are statistically indistinct at both sites. The previous study results showed a higher frequency at the BLM station, 88% compared to 71% at the CSA site. Present data do not show

the prior suggestion that Millepora spp. colonies are more numerous at the reef top site than at the reef edge site.

Porites astreoides exhibits distributional patterns analogous to those of Millepora spp. The means of all population parameters are strongly similar (SP's for all parameters were > 0.46). The data support previous indications that P. astreoides occur as small, abundant colonies common at both stations.

As with the Colpophyllia spp. group, Agaricia fragilis and A. agaricites were combined. The population parameters are statistically similar at both sites. The distributional patterns of Agaricia spp. are similar to those of P. astreoides and Millepora spp., commonly forming small but abundant colonies. They are frequently found under ledges and outcrops. Consequently, Agaricia spp. often are not detected in the transect photographs. This probably results in underestimates of the true population levels.

Abundance and dominance values for Madracis decactis are relatively low. Since the BLM station is adjacent to the Madracis-Algae Zone, we might expect population levels to be greater at the BLM station than at the CSA station. Generally, this is the case. Madracis decactis occurred on the BLM transects at a frequency of 44%, and at a frequency of only 22% on the CSA transects. All values of the population level parameters are greater at the BLM station. However, because the data are quite variable, no statistical differences may be inferred.

The current data suggest that Stephanocoenia michelini and Siderastrea siderea also occur in similar distributional patterns at the BLM and CSA sites. Both species occur at low frequencies on the CSA station transects and do not occur on any BLM station transects. Earlier data question this grouping; S. siderea occurred as suggested, but no occurrences of S. michelini were recorded at the CSA site, and there was a 24% frequency at the BLM site. The rarity with which S. michelini occurs does not allow us to decide which data are more accurate. We may speculate that both S. siderea and S. michelini occur at fairly low, though equal, levels at both stations.

Scolymia cubensis is a rare solitary polyp form. Neither the CSA nor the BLM site transects included this species. Like Agaricia spp., S. cubensis tends to be found underneath larger forms. This similarity, coupled with the rarity of S. cubensis, probably accounts for its absence from the transect photo-mosaics. It is likely that S. cubensis occurs as small, widely scattered units at both sites.

Mussa angulosa contributed little substrate cover and was low in abundance. Current frequency data support the previous observation that M. angulosa is found predominantly at the BLM site. However, all population levels are statistically indistinguishable. M. angulosa appears in small colonies at the reef edge site. Population levels at the CSA site are probably quite low, hence its absence from all transects taken at this site.

Neither Madracis mirabilis nor Porites furcata were encountered in any transect. M. mirabilis colonies are generally found in abundance at depths greater than 30 m, and this species is the dominant coral of the Madracis-Algae Zone. Porites furcata is an uncommon species at the Flower Garden Banks. Both species have been observed during previous diving operations.

Coralline and filamentous algae comprise a significant portion of all transects. These opportunistic groups establish themselves in areas of coral mortality. Both algal types are found on all transects at both sites. The CSA site displays statistically higher levels (SP = 0.01) of filamentous algae than does the BLM site. Levels of coralline algae are not significantly different at the two sites.

The carbonate sand and rubble portions of the transects are statistically larger at the CSA site. This difference reflects the presence of small "sand flats" scattered throughout the reef top.

The percent live coral cover averaged 73% at the BLM site and 54% at the CSA site. The difference is statistically significant (SP = 0.02).

Site Analysis Summary

1. Species diversity, evenness, and richness values for the East Flower Garden reef edge (BLM) site and for the reef top (CSA) site are statistically similar.

2. Montastrea annularis exhibits the highest levels of dominance, relative dominance, and relative density of all coral species. M. annularis occurred on all transects at both stations.

3. Levels of all parameters for Montastrea annularis are higher at the reef edge (BLM) site. Filamentous algae dominance is higher at the reef top than at the reef edge. Diploria strigosa exhibits higher levels of relative dominance at the reef top.

4. All other parameter values occurred at statistically similar levels at both sites for any particular coral.

5. The average live coral cover was 73% at the BLM site and 54% at the CSA site. This difference is statistically significant.

EFG-WFG Reef Analysis

The data obtained from the 9 BLM and 9 CSA site transects from the East Flower Garden (EFG) were combined and compared with the 18 transects taken at the West Flower Garden reef (WFG).

There are few notable differences in the species composition patterns at the two banks. Evidently, the differences exert little effect on the species diversity, evenness, and richness indices, since they are statistically similar.

Montastrea annularis demonstrated the highest levels of abundance, dominance, and relative dominance at both locations. There is strong agreement between the EFG and WFG parameters (SP's all > 0.50). Current data estimate the percent of hard-bottom covered by M. annularis to be approximately 33% at both reefs. M. annularis averages approximately 53% of the total live coral cover for both locations. This species also occurred on all transects taken during the study. M. annularis occurs as large colonies and is very abundant at both reefs.

Population levels of Diploria strigosa at both reefs are statistically indistinguishable (SP's all > 0.20). Mean population levels are greater at the EFG reef, but the variances are consistently high. The frequencies with which D. strigosa occurred on the two sets of transects are strikingly dissimilar. Values of 56% and 100% of the WFG and EFG transects, respectively, were recorded. The data suggest that D. strigosa may occur more frequently and as larger colonies at the EFG reef. The degree of variability of the parameters disallows any conclusive statement.

The population levels of Colpophyllia spp. show strong between-reef differences in dominance and relative dominance means (SP's = 0.001, 0.01, respectively). The EFG levels are statistically greater than the WFG levels. The relative density levels are not significantly different (SP = 0.09). The frequency of occurrence is greater at the EFG reef (61%) than at the WFG reef (39%). Apparently, Colpophyllia spp. colonies at the EFG are larger than, but about equal in density to, colonies found at the WFG.

Montastrea cavernosa population levels are very similar at both locations (SP's all > 0.36). M. cavernosa appeared on an average of 56% of the transects at both reef locations. The transect data imply that M. cavernosa is equally common at the EFG and WFG reefs, occurring as colonies of equal average size. M. cavernosa, however, does not contribute greatly to substrate cover.

This study suggests that Agaricia spp., Porites astreoides, and Millepora spp. exhibit similar distributional patterns. Levels of dominance, relative dominance, and relative density are statistically similar at both reefs. Transect frequency values for these corals are similar at both locations. P. astreoides and Millepora spp. were identified on an average of 83% of all transects. Agaricia spp. occurred on approximately 58% of all transects. The relative dominance and density values of Agaricia spp. are also somewhat lower than P. astreoides and Millepora values. Since the photographic transect method tends to underestimate the true population levels of Agaricia spp., the Agarioids have been included in this group. At both locations, Agaricia spp., P. astreoides, and Millepora spp. are abundant but contribute little to substrate cover.

Population levels of Madracis decactis are statistically very similar on both reefs (SP's all > 0.50). Frequency values are also quite

similar. M. decactis colonies are characteristically small in size and low in abundance at both reefs.

Distributional patterns of Mussa angulosa are similar to those of M. decactis. Population level estimates are quite similar (SP's all > 0.50). The mean colony size and abundance of M. angulosa are similar to those of M. decactis at the EFG reef. Transects taken at the WFG reef indicate that although colony density levels of M. decactis and M. angulosa are statistically similar, M. decactis colony size is greater (SP = 0.04). Differences also exist between M. decactis and M. angulosa WFG frequency levels. Mussa angulosa inhabit both reefs as small, scattered units. M. decactis is also found as scattered, though somewhat larger, colonies.

The present data also suggest that Stephanocoenia intersepta and Siderastrea siderea are distributed in similar patterns at both reefs. There are no significant differences in the parameters tested for either species. The population level means indicate that the two species are neither abundant nor do they occur as large units. Viada (1980) states, however, that S. siderea are commonly found as hemispherical mounds often of large size. Only one WFG transect (HPLT-A1) supports this description. Without further surveying, the evidence remains inconclusive.

Scolymia cubensis was absent from all EFG transects and occurred on only two WFG transects. The comparative rarity of S. cubensis may be responsible for its absence from the EFG reef transects. None of the population level estimates demonstrate significant differences between the two reefs. This species is commonly found growing under larger forms, and the population estimates obtained in this study are probably low. S. cubensis occur as small, widely scattered units, possibly at both locations.

The percent live coral cover of all species combined is approximately 64% at the EFG reef and 55% at the WFG reef. The difference is not statistically significant.

Coralline algal dominance and abundance are statistically greater at the WFG reef. All parameters show strong dissimilarity (SP's all < 0.004). Since coralline algae are commonly found under coral growths and in crevices, the levels of abundance and dominance are likely to be underestimates. Coralline algae were found on all transects taken during the study.

Filamentous algae show no significant differences in dominance levels between reefs. The filamentous algae are quite abundant and, on the average, exceed all other categories except M. annularis in substrate cover at both reefs. For reasons similar to those given for coralline algae, population levels given here are probably underestimates. Filamentous algae were found on 100% of all transects taken during the study.

Carbonate sand and rubble is a fairly uncommon category in the transects at both locations. Statistical differences in dominance levels were not observed. Sandy areas were avoided during transect placement, so nothing can be concluded concerning sand and rubble occurrence on the reefs.

Summary: Population Levels

1. Coral species diversity, evenness, and richness values at the EFG and WFG reefs are statistically similar.

2. Montastrea annularis demonstrates the highest levels of dominance, relative dominance, and relative density among coralline algae and corals. M. annularis was identified on all transects at both reefs.

3. Colpophyllia spp. occurs at higher levels of dominance and relative dominance at the EFG reef.

4. All other corals occur at statistically similar levels of dominance, relative dominance, and relative density at both reefs. The similarity is generally quite strong.

5. Coralline algal dominance and abundance levels are statistically greater at the WFG reef. No differences in levels of filamentous algae were observed.

6. The percent live coral cover averages 64% at the EFG reef and 55% at the WFG reef. The difference is statistically insignificant.

CORAL GROWTH AND MORTALITY

Accretionary Coral Growth, East and West Flower Garden Banks

Seasonal variations in accretionary growth are reflected within coral skeletons in the form of alternating low and high density "bands," which become evident when sections of the coral skeleton are X-rayed. Study of the annual banding patterns of corals is termed "sclerochronology," similar to its terrestrial analogue, dendrochronology, which concerns the study of tree rings.

In order to obtain sclerochronological data from corals on the East and West Flower Garden Banks, a total of nine skeletal cores were removed from the two most abundant species of massive hermatypic corals: Montastrea annularis (7 cores) and Diploria strigosa (4 cores). Cores were obtained by using a 2.2 cm x 25 cm diamond-studded hollow corer tube driven by a small 3/8" hand-held pneumatic drill, powered by high pressure air from a scuba tank. The cylindrical cores were cut into 4 mm thick slabs, and X-rayed for 2 1/2 minutes at 5 mA and 50 Kv (Figure III-5).

Only six of the nine cores examined proved to be informative, as the remaining three cores were not well aligned parallel to the direc-

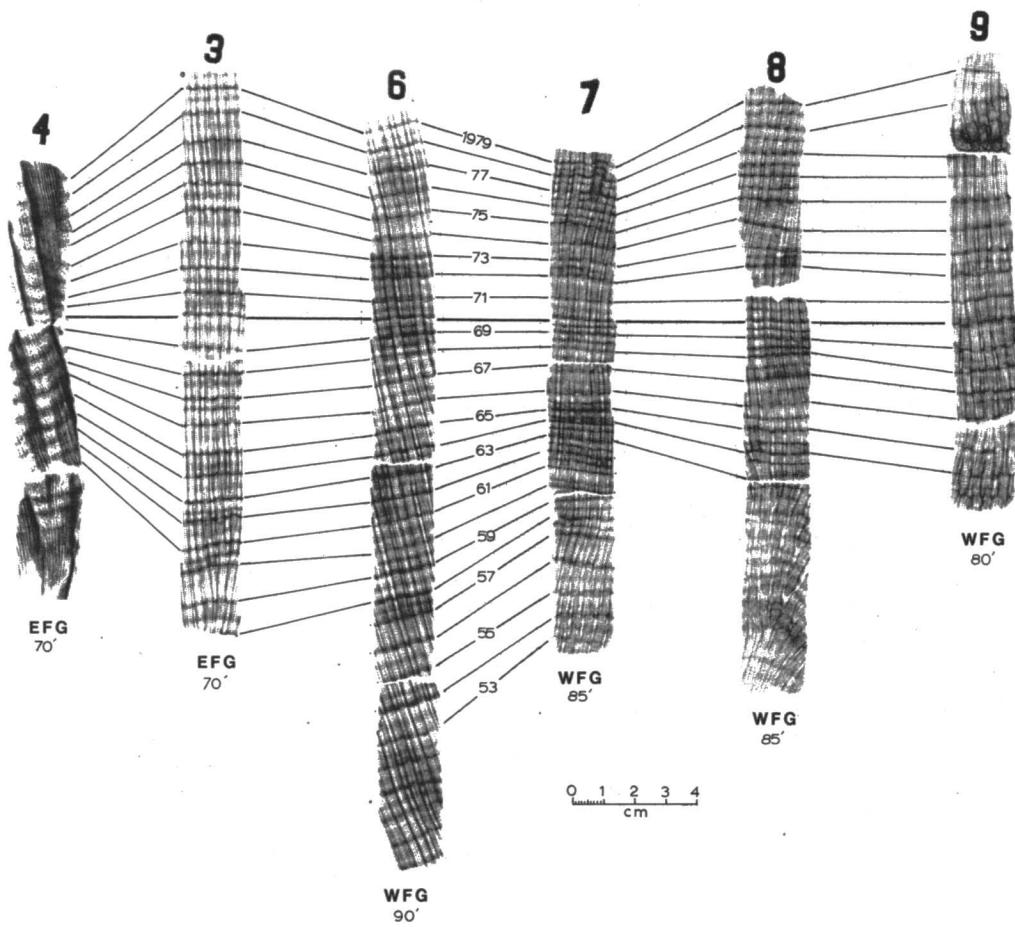


Figure III-5. X-radiographs of sectioned Montastrea annularis cores (3,6,7,8,9) and a Diploria strigosa core (4) from the East and West Flower Garden reefs.

tion of corallite growth on the corallum. All four of the M. annularis colonies have a faster vertical growth rate (average of 7.5 mm/yr) than the one D. strigosa colony (5.1 mm/yr) (see Table III-4). Two of the cores were taken from the same M. annularis colony, one from the top of the corallum and one from the side. The mean annual growth rate at the top of the corallum was 20% higher than the growth rate at the side of the colony (7.1 mm/yr vs. 5.9 mm/yr, Table III-4). Although a larger sample size would be more conclusive, it is suggested that such a differential growth rate within the same colony may account for the typical "gum drop" shape of the M. annularis corallum on the Flower Gardens.

An attempt was made to match the band width variations between the cores to determine if there were any inter-colony correlations in growth rates over the past 15-20 years. The results were inconclusive and appeared only to demonstrate that the "between colony" growth rates are highly variable. Figure III-6 plots the average growth rates of the four M. annularis colonies and the one D. strigosa colony, as determined in the present study. Data from Hudson and Robbin's (1980) measurements on Montastrea annularis are also plotted in Figure III-6 and appear to be in substantial agreement with those of the present study.

Encrusting Coral Growth and Mortality, West Flower Garden Bank

The short-term, seasonal monitoring of encrusting coral growth rates (lateral expansion of colony over bare reef rock) and mortality rates (loss of living coral tissue) provides a reliable and continuous biological indicator of coral health on the East and West Flower Garden Banks. Results of lateral encrusting coral growth studies at the East Flower Garden have been reported for the period Sep 78 - Aug 79 (Bright et al., 1981). The present study adopted identical techniques for the study of lateral encrusting growth at the West Flower Garden, covering the period Sep 79 to Jun 80.

Lateral coral growth and mortality rates were measured from seasonal repetitive photographs taken at specific sites on twenty different coral colonies on the West Flower Garden. Photographs were made at each station on the reef during the September 1979, February 1980, and June 1980 BLM cruises (at three stations photos were also available from September 1980). Four individual corallites that could be readily identified in all seasonal photos were selected as "designated corallites" for each station. The distances from each of the four designated corallites to the corallum edge were measured in all photographs from each station. Changes in the distances from these corallites to the colony border as the seasons progress reflect the lateral growth or mortality of the coral. For example, if the average distance from the four designated corallites to the colony edge was 3.0 mm in Sep 79, and 4.5 mm in Feb 80, then the lateral advancement of this coral from Sep 79 to Feb 80 was 1.5 mm.

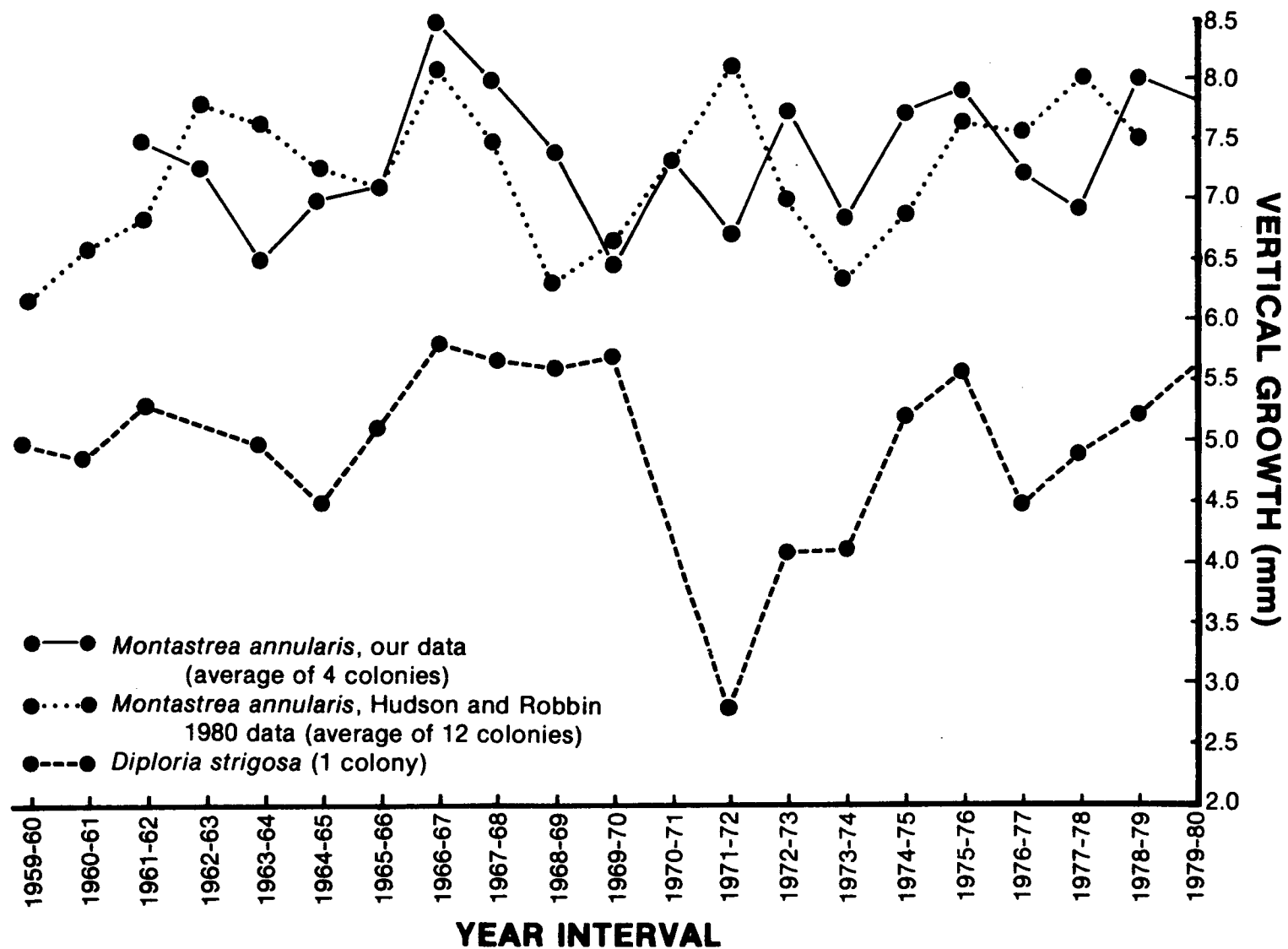


Figure III-6. Vertical growth rates of Montastrea annularis (average of four colonies and average of twelve colonies) and Diploria strigosa (one colony) from the East and West Flower Garden reefs.

TABLE III-4
 VERTICAL GROWTH OF D. strigosa AND M. annularis (mm) OBTAINED BY MEASURING THE WIDTHS BETWEEN
 HIGH DENSITY SEASONAL BANDING, VISIBLE IN CORAL CORE X-RADIOGRAPHS

CORAL	LOCATION	DEPTH (m)	NO. OF BANDS MEASURED	VERTICAL GROWTH DATA (mm)		
				Mean Thickness	Range	Standard Deviation
<u>Diploria strigosa</u>	EFG	23	20	5.1	2.8 - 6.3	0.82
<u>Montastrea annularis</u>	EFG	23	21	8.1	5.9 - 11.0	1.32
<u>Montastrea annularis</u>	WFG	30	31	7.2	5.2 - 9.9	1.06
<u>M. annularis</u> (top)*	WFG	28	15	7.1	5.1 - 8.7	0.97
<u>M. annularis</u> (side)*	WFG	28	23	5.9	4.2 - 9.9	1.33
<u>Montastrea annularis</u>	WFG	27	15	7.7	6.2 - 9.8	1.17

* M. annularis marked "top" and "side" indicate cores taken from the same coral colony, one from the top of the corallum, and one from the side.

Tables III-5 through 16 present the lateral growth and mortality data for five massive hermatypic corals and one hydrozoan coral (Millepora) in two ways. Tables III-5 through 11 show the net growth or mortality of each species from each station during each growth period (e.g., Sep 79 - Feb 80, or Feb 80 - Jun 80). Tables III-12 through 16 divide these data into millimetre/month increments for easier "between season" comparisons. In the following section, qualitative observations and quantitative information are summarized for each of the 20 stations monitored on the West Flower Garden Bank.

Growth and Mortality Photographic Observations by Station

Station 1

Montastrea annularis is growing laterally over a dead Diploria strigosa corallum. Boring barnacles are evident in the M. annularis colony at an approximate density of 70 barnacles per 370 cm² of surface area (1 individual per 5.3 cm²). The density of the barnacle infestation does not noticeably change over the observed Sep 79 - Jun 80 growth periods.

Growth period 1 (27 Sep 79 - 20 Feb 80): Average lateral growth of 2.9 mm (4 measurements).

Growth period 2 (20 Feb 80 - 17 Jun 80): Average lateral growth of 1.1 mm (4 measurements).

Average growth from Sep 79 - Jun 80 is 4.0 mm (4 measurements).

Other organisms beginning to settle on the dead Diploria corallum include coralline algae (growing only along the skeletal ridges) and green filamentous algae.

Station 2

Regression of Montastrea annularis is occurring due to the lateral encroachment of Millepora alcicornis.

Growth of M. alcicornis, Period 1 (27 Sep 79 - 20 Feb 80): Average lateral growth of 5.0 mm (3 measurements).

Growth of M. alcicornis, Period 2 (20 Feb - 17 Jun 80): Average lateral growth of 3.7 mm (3 measurements).

Average growth of M. alcicornis from Sep 79 - Jun 80 is 8.7 mm (3 measurements).

Regression of M. annularis, Period 1 (Sep 79 - Feb 80): Average regression of 11.1 mm (4 measurements).

Regression of M. annularis, Period 2 (Feb - Jun 80): No further regression has occurred, and there appears to be evidence of

TABLE III-5
 LATERAL ENCRUSTING GROWTH (mm) OF *Montastrea annularis* AT EACH STATION
 AT THE WEST FLOWER GARDEN BANK

SEASON	GROWTH (mm)									Summary Statistics (Growth Only)		
	Station									N	\bar{X}	S
	1	2	3	5	8	13	17	18	20			
Period 1 Sep 79 - Feb 80	2.9 f	NA	2.5 f	1.8 f	4.2 f	1.7 f	5.1 c	3.1 c	1.9 f	8	2.90	1.20
Period 2 Feb 80 - Jun 80	1.1 f	0.0 c	2.1 f	1.1 f	1.6 f	1.0 f	1.6 c	2.0 c	1.2 f	9	1.30	0.63

\bar{X} = mean

S = sample standard deviation

f = free growing border

c = border in interspecific competition with another coral

N = number of growth measurements made

NA = not applicable

TABLE III-6
LATERAL ENCRUSTING GROWTH (mm) OF *Agaricia agaricites* AT EACH STATION
AT THE WEST FLOWER GARDEN BANK

SEASON	GROWTH (mm)					
	Station			Summary Statistics		
	6	14		N	\bar{X}	S
Period 1 Sep 79 - Feb 80	5.5 f	3.3 f		2	4.40	1.56
Period 2 Feb 80 - Jun 80	2.0 f	1.6 f		2	1.80	0.28
Period 3 Jun 80 - Sep 80	1.0 f	NA		1	1.0	*

TABLE III-7
LATERAL ENCRUSTING GROWTH (mm) FOR THE HYDROZOAN CORAL
Millepora alcicornis AT EACH STATION
AT THE WEST FLOWER GARDEN BANK

SEASON	GROWTH (mm)					
	Station			Summary Statistics		
	2	4	9	N	\bar{X}	S
Period 1 Sep 79 - Feb 80	5.0 c	16.5 f	25.0 f	3	15.50	10.0
Period 2 Feb 80 - Jun 80	3.7 c	NA	7.0 f	2	5.35	2.33

\bar{X} = mean

S = sample standard deviation

f = free growing border

c = border in interspecific competition with another coral

N = number of growth measurements made

NA = not applicable

* = not valid

TABLE III-8
LATERAL ENCRUSTING GROWTH (mm) FOR *Diploria striigosa*
AT THE WEST FLOWER GARDEN BANK

SEASON	GROWTH (mm)
	Station 19
Period 1 Sep 79 - Feb 80	3.2 f
Period 2 Feb 80 - Jun 80	1.4 f

TABLE III-9
LATERAL ENCRUSTING GROWTH (mm) FOR *Porites astreoides*
AT THE WEST FLOWER GARDEN BANK

SEASON	GROWTH (mm)
	Station 11
Period 1 Sep 79 - Feb 80	5.1 f
Period 2 Feb 80 - Jun 80	1.4 f

TABLE III-10
LATERAL ENCRUSTING GROWTH (mm) FOR *Montastrea cavernosa*
AT THE WEST FLOWER GARDEN BANK

SEASON	GROWTH (mm)
	Station 18
Period 1 Sep 79 - Feb 80	3.1 c
Period 2 Feb 80 - Jun 80	2.0 c

c = border in interspecific competition with another coral
f = free growing border

TABLE III-11
 MORTALITY (LATERAL RETREAT) (mm) FOR CORAL SPECIES
 AT THE WEST FLOWER GARDEN BANK

SEASON	CORAL SPECIES			
	M. annularis	D. strigosa		P. astreoides
	Station 2	Station 10	Station 17	Station 16
Period 1 Sep 79 - Feb 80	11.1 c	125.0 rm	1.1 c	5.2 z
Period 2 Feb 80 - Jun 80	NA	30.0 rm	1.3 c	NA

c = border in interspecific competition with another coral
 rm = ridge mortality
 z = zooxanthellae loss
 NA = not applicable

TABLE III-12
 LATERAL ENCRUSTING GROWTH RATES (mm/mo) FOR THE VARIOUS CORALS
 AT THE WEST FLOWER GARDEN BANK
 DURING THE TWO TIME PERIODS:
 SEP 79 - FEB 80 AND FEB 80 - JUN 80

PERIOD I, 5 MONTHS (Sep 79 - Feb 80)			
CORAL	GROWTH (mm/mo)		
	\bar{X}	SE	N
<u>Montastrea annularis</u>	0.57	0.08	8
<u>Diploria strigosa</u>	0.63		1
<u>Montastrea cavernosa</u>	0.61		1
<u>Porites astreoides</u>	1.01		1
<u>Agarcia agaricites</u>	0.87	0.22	2
<u>Millepora alcicornis</u>	3.07	1.15	3

PERIOD II, 4 MONTHS (Feb 80 - Jun 80)			
CORAL	GROWTH (mm/mo)		
	\bar{X}	SE	N
<u>Montastrea annularis</u>	0.34	0.006	9
<u>Diploria strigosa</u>	0.37		1
<u>Montastrea cavernosa</u>	0.53		1
<u>Porites astreoides</u>	0.37		1
<u>Agarcia agaricites</u>	0.48	0.06	2
<u>Millepora alcicornis</u>	1.42	0.44	2

\bar{X} = mean
 SE = standard error
 N = number of observations

TABLE III-13
LATERAL ENCRUSTING GROWTH RATES (mm/mo) FOR THE VARIOUS CORALS
AT THE WEST FLOWER GARDEN BANK
DURING BOTH PERIODS, COMBINED:
(SEP 79 - JUN 80)

PERIODS I AND II, 9 MONTHS (Sep 79 - Jun 80)			
CORAL	GROWTH (mm/mo)		
	\bar{X}	SE	N
<u>Montastrea annularis</u>	0.45	0.06	17
<u>Diploria strigosa</u>	0.50	0.13	2
<u>Montastrea cavernosa</u>	0.57	0.04	2
<u>Porites astreoides</u>	0.69	0.32	2
<u>Agaricia agaricites</u>	0.60	0.14	5
<u>Millepora alcicornis</u>	2.41	0.76	5

TABLE III-14
LATERAL ENCRUSTING GROWTH RATES (mm/mo) FOR VARIOUS CORALS
DURING ALL PERIODS MEASURED:
EAST FLOWER GARDEN (SEP 78 - AUG 79)
WEST FLOWER GARDEN (SEP 79 - JUN 80)

ALL PERIODS, 21 MONTHS (Sep 78 - Jun 80)			
CORAL	GROWTH (mm/mo)		
	\bar{X}	SE	N
<u>Montastrea annularis</u>	0.45	0.11	26
<u>Diploria strigosa</u>	0.16	0.07	14
<u>Montastrea cavernosa</u>	0.34	0.13	15
<u>Porites astreoides</u>	0.35	0.24	4
<u>Millepora alcicornis</u>	1.97	0.64	8
<u>Agaricia agaricites</u>	0.60	0.14	5

\bar{X} = mean
SE = standard error
N = number of observations

TABLE III-15
 CORAL MORTALITY RATES (mm/mo)
 AT THE WEST FLOWER GARDEN BANK
 DURING THE TWO TIME PERIODS, COMBINED:
 SEP 79 - JUN 80

PERIODS I & II, 9 MONTHS (Sep 79 - Jun 80)			
SPECIES	AVERAGE MORTALITY RATES (mm/mo)		
	\bar{X}	SE	N
<u>Montastrea annularis</u>	2.20		1
<u>Diploria strigosa</u>	8.31	5.76	2
<u>Porites astreoides</u>	1.03		1

TABLE III-16
 CORAL MORTALITY RATES (mm/mo)
 DURING ALL PERIODS MEASURED:
 EAST FLOWER GARDEN (SEP 78 - AUG 79)
 WEST FLOWER GARDEN (SEP 79 - JUN 80)

ALL PERIODS, 21 MONTHS (Sep 78 - Jun 80)			
SPECIES	MORTALITY (mm/mo)		
	\bar{X}	SE	N
<u>Montastrea annularis</u>	1.15	0.50	4
<u>Diploria strigosa</u>	6.05	2.59	10
<u>Montastrea cavernosa</u>	0.27	0.09	2
<u>Porites astreoides</u>	2.21	1.18	2

\bar{X} = mean
 SE = standard error
 N = number of observations

some re-growth in the form of new corallites along the border. Subsequent to this re-growth, however, Millepora alcicornis grew closer to the M. annularis border, and zooxanthellae expulsion from M. annularis occurred.

The three seasonal photographs from this station suggest that the border/recession of M. annularis occurs in a series of rapid die-offs separated by periods of stable, or even accreting, border position. When Millepora alcicornis encroached to within 2-4 mm of the M. annularis border, M. annularis rapidly retreated an average of 11.1 mm in five months. During the next four months, the gap left by the retreat of M. annularis was colonized by coralline and green filamentous algae. As mentioned above, M. annularis has apparently begun re-growth in this area. The final photograph, taken in June 1980, shows that M. alcicornis has closed the gap between it and M. annularis (to about 2-4 mm) resulting in the expulsion of zooxanthellae along the border of M. annularis, indicating the beginning of another rapid die-off.

Station 3

Montastrea annularis is growing freely over a coralline algae-encrusted dead Diploria corallum.

Growth period 1 (Sep 79 - Feb 80): Average lateral growth of 2.5 mm (4 measurements).

Growth period 2 (Feb 80 - Jun 80): Average lateral growth of 2.1 mm (4 measurements).

Average growth from Sep 79 - Jun 80 is 4.6 mm (4 measurements).

Boring barnacles appear in the Montastrea annularis corallum at an approximate density of 19 individuals per 85 cm² surface area (or 1 per 4.5 cm²). Although the number of barnacles does not apparently change during the Sep 79 - Jun 80 growth periods, the height of their protuberances (openings of the borings) above the coral surface has increased over the 9-month period. As a result, the rather smooth corallum depicted in the September 1979 photo appears quite "knobby" by June 1980. Most likely this is due to growth of the barnacle within its boring.

Station 4

Millepora alcicornis is growing freely over a dead Diploria skeleton. Lateral growth of these hydrozoans is difficult to measure as there are no "reference corallites." Furthermore, the growth on this specimen appears sporadic, accreting rapidly in one area while displaying no growth in another. Apparently the phases of lateral growth are followed by periods of vertical thickening of skeleton. As vertical thickening occurs, lateral growth diminishes.

Growth period 1 (Sep 79 - Feb 80): Average lateral growth of 16.5 mm (2 measurements).

Growth period 2 (Feb 80 - Jun 80): Poor photo angle, but no noticeable growth has occurred.

Station 5

Montastrea annularis is growing freely over an unidentified dead coral substrate. Corallum of M. annularis appears very healthy and free from boring barnacles.

Growth period 1 (Sep 79 - Feb 80): Average lateral growth of 1.8 mm (4 measurements).

Growth period 2 (Feb 80 - Jun 80): Average lateral growth of 1.1 mm (4 measurements).

Growth period 3 (Jun 80 - 25 Sep 80): No measureable lateral growth; however, the addition of new corallites on the inter-polyary surface can be seen.

Average growth from Sep 79 - Jun 80 is 2.9 mm (4 measurements).

An interesting successional trend appears to be occurring on the dead coral substrate. In September 1979 the perhaps recently exposed substrate has been colonized by green filamentous algae. By February 1980 most of the green algal coverage has been lost to the red coralline algae and an orange laterally encrusting sponge. Presumably, the sponge will overgrow the entire exposed substrate before it is in turn overgrown by the M. annularis colony.

Station 6

Small plate of Agaricia agaricites (11 cm diameter) is growing freely over a coralline algae-encrusted dead Diploria skeleton.

Growth period 1 (Sep 79 - Jun 80): Average lateral growth of 5.5 mm (7 measurements).

Growth period 2 (Feb 80 - Jun 80): Average lateral growth of 2.0 mm (4 measurements).

Growth period 3 (Jun 80 - Sep 80): Average lateral growth of 1.0 mm (3 measurements).

Average growth from Sep 79 to Sep 80 is 8.5 mm (3 measurements).

The September 1979 and September 1980 photographs of this Agaricia colony depict extensive zooxanthellae expulsion around the perimeter of the corallum, making the edge of the colony appear a bleached white. This coral has the healthiest appearance (i.e., more of the greenish-

brown tissue) in the February 1980 picture. This seems to correlate well with the rapid winter season growth.

Station 7

Colpophyllia sp. is growing freely over an unidentified brain coral corallum. Photographs for only one growth period are available.

Growth period 1 (Sep 79 - Feb 80): Average lateral growth of 5.1 mm (4 measurements).

The growth of Colpophyllia occurred by a lateral flattening and extension of the ridge on the edge of the colony. It is likely that this ridge will continue to extend outward until a new polyp mouth develops. The subsequent upward folding of the ridge will cause the polyp to be situated in a typical valley-like depression.

Station 8

Montastrea annularis is approaching a small (7 cm diameter) colony of Agaricia agaricites. No photograph is available from June 1980.

Growth period 1 of M. annularis (Sep 79 - Feb 80): Average lateral growth of 4.2 mm (3 measurements).

From February 1980 to September 1980 part of the M. annularis colony approached to within about 4 mm of the Agaricia border. In this region, zero growth was recorded from February to September 1980. The area of the M. annularis not proximal to the Agaricia yielded an average of 1.6 mm growth for this 7-month period. Growth or regression at the competition border of these two corals is not evident.

Average growth of M. annularis along its free border from Sep 79 to Sep 80 is 5.1 mm (2 measurements).

Station 9

This series of seasonal photographs depicts Millepora alcicornis encircling and laterally encroaching into an irregularly-shaped area (approx. 28 cm²) of coralline algae, green algae, and exposed substratum. Poor scale placement and varying angles of the photographs make accurate lateral growth measurements impossible. One region of Millepora is growing laterally at a much faster rate than at other localities. A single measurement showed approximately 36 mm of growth between September 1979 and February 1980. This same area grew only an additional 7 mm from February 1980 to June 1980. An interesting color variation is also apparent in that the region of active growth ranges from a light tan to nearly white (at the border). The rest of the hydrozoan, where little or no growth is evident, assumes the more typical mustard-color aspect. This is likely related to the paucity of zooxanthellae in the rapidly accreting areas (similar to the white branch tips in rapidly growing ramose corals such as Acropora).

Parrotfish (Scaridae) bite marks that appear as a series of 10-15 mm long parallel scratches on the hydrozoan surface in the September 1979 photograph had completely healed by February 1980.

Station 10

At this station Diploria strigosa is undergoing very rapid ridge mortality. The September 1980 photo shows an apparently healthy Diploria colony. By February 1980, however, more than half of the colony (spreading up one side of the corallum, covering an area in excess of 344 cm²) had been affected by ridge death. Within this area approximately 5.5 cm² of skeletal surface had already been completely exposed, indicating that polyp death in the "valleys" had also occurred.

By June 1980 only an additional 10 cm² of ridge mortality was measured, suggesting that this phenomenon may be ceasing and will not spread over the entire corallum. Between February 1980 and June 1980, 156 cm² of skeletal surface had been completely exposed (i.e., ridge and valley death) within the infected region.

A red sponge that first appeared along the corallum periphery in February 1980 had encrusted over part of the exposed corallum by June 1980. The sponge had apparently spread over the dead Diploria surface by initially moving up the valleys, then thickening and spreading laterally over the ridges.

Other colonizers on the recently exposed substrate typically include coralline algae along the ridges, and green filamentous algae.

Station 11

This series of seasonal photos shows a small Porites astreoides colony (approx. 10 cm diameter) growing freely over a dead Diploria skeleton.

Growth period 1 (Sep 79 - Feb 80): Average lateral growth of 5.1 mm (4 measurements).

Growth period 2 (Feb 80 - Jun 80): Average lateral growth of 1.4 mm (4 measurements).

Average growth from Sep 79 - Jun 80 is 6.4 mm (4 measurements).

Station 12

Colpophyllia sp. is growing freely over a dead Diploria skeleton. Photo from February 1980 is missing.

Growth from Sep 79 to Jun 80 is 6.3 mm (4 measurements).

As previously mentioned, lateral growth occurs by a flattening and lateral extension of the border ridge. By flattening and extending

this ridge, growth would then proceed in a direction parallel to the valley orientation.

Station 13

Montastrea annularis is growing freely over a dead Diploria corallum.

Growth period 1 (Sep 79 - Feb 80): Average lateral growth of 1.7 mm (5 measurements).

Growth period 2 (Feb 80 - Jun 80): Average lateral growth of 1.0 mm (4 measurements).

Average growth from Sep 79 to Jun 80 is 2.9 mm (4 measurements).

Lateral accretion of M. annularis varied during growth period 1 from 4.0 mm in one region to 0.0 growth at another. Perhaps the irregular substrate of alternating Diploria valleys and ridges may be a factor in the varying rates of lateral growth of Montastrea.

Station 14

Agaricia agaricites is growing freely over a dead Diploria skeleton.

Growth period 1 (Sep 79 - Feb 80): Average lateral growth of 3.3 mm (5 measurements).

Growth period 2 (Feb 80 - Jun 80): Average lateral growth of 1.6 mm (4 measurements).

Average growth from Sep 79 to Jun 80 is 4.9 mm (4 measurements).

Similar to the Agaricia colony at Station 6, the Agaricia colony at this station displays fairly extensive zooxanthellae expulsion around the colony perimeter in the September 1979 photograph. The colony appears to be healthiest (more brown coloration) in February 1980, when the most rapid growth occurs. The light color of the corallum in the June 1980 photo may be the result of zooxanthellae expulsion or photograph over-exposure.

Station 15

Diploria strigosa is growing freely over a dead Diploria skeleton. Photos are available only for growth period 1, and the angle of the February 1980 picture prevents accurate measurement of border growth. Although it is apparent that slight lateral growth occurred during period 1, this observation cannot be supported quantitatively.

Station 16

At this station Porites astreoides is recolonizing, or recovering from, a badly damaged corallum. The September 1979 photo depicts two

small (10-15 cm) colonies of P. astreoides where approximately 70% of the tissue, or zooxanthellae within the tissue, has been lost. The reason for this mass zooxanthellae expulsion is unknown. Interestingly, part of a third P. astreoides colony in close proximity to the two damaged colonies has also been affected, possibly suggesting the spread of a bacterial or viral infection. A grazing attack by triggerfish (Balistidae) or parrotfish (Scaridae) can be ruled out, because the distinctive parallel bite marks are not evident.

The February 1980 photo shows rapid tissue recovery of about 50% of the damaged area. At best estimate, this represents a recovery of nearly 90 cm² of polypary surface in five months. The tissue recovery seems to spread from areas of still healthy polyps and progresses laterally over the corallum. Damaged tissue farthest away from the healthy (undamaged) polyps did not recover. This indicates that the closer the damaged tissue is to healthy tissue, the greater are its chances of recovery.

Peripheral areas of the corallum that did not recover show overgrowths by sponge, coralline algae, and green filamentous algae.

Station 17

This station depicts a competitive situation whereby Montastrea annularis is encroaching over Diploria strigosa. The presence of dead D. strigosa in the competition zone indicates that the transgression by M. annularis over D. strigosa has been occurring for a long time.

M. annularis growth period 1 (Sep 79 - Feb 80): Average lateral growth of 5.1 mm (3 measurements).

M. annularis growth period 2 (Feb 80 - Jun 80): Average lateral growth of 1.6 mm (3 measurements).

Average growth for M. annularis from Sep 79 to Jun 80 is 6.7 mm (3 measurements).

Although it is obvious that D. strigosa is regressing, no discoloration is apparent on the leading edge of the corallum that would indicate zooxanthellae expulsion.

Regression of D. strigosa, growth period 1 (Sep 79 - Feb 80): Average lateral regression of 1.1 mm (4 measurements).

Regression of D. strigosa, growth period 2 (Feb 80 - Jun 80): Average lateral regression of 1.3 mm (4 measurements).

Average regression from Sep 79 to Jun 80 is 2.3 mm (4 measurements).

Of interest are (a) the lack of zooxanthellae expulsion from the Diploria border and (b) the fact that the growth rate of M. annularis is nearly three times the regression rates of D. strigosa. Perhaps the

method of retreat of Diploria at this station is similar to the retreat of M. annularis from Millepora at Station 2. Instead of a continual retreat by Diploria, regression may occur by a series of rapid die-offs initiated by the approach of M. annularis to within a "critical distance" of the Diploria border. After the rapid retreat of Diploria to a "safe" distance, the border stabilizes.

Because the series of photos at this station shows an apparently healthy Diploria border (or one that is very slowly regressing) with a full complement of zooxanthellae, it is likely that the photos were taken during the recovery phase which follows the rapid regression.

Presumably, as M. annularis advances to within several millimetres of the D. strigosa border, zooxanthellae will be expelled and another rapid retreat of Diploria will ensue.

Station 18

This station is comprised of competitive borders between M. cavernosa and M. annularis. The very regular spacing between the corals over the entire border length in the photos indicates that a transgression/regression of one or the other corals is occurring. The 4 cm gap between the two species and the positive growth rates (net accretion) of both corals again suggest that the regressing species retreated very rapidly at some time in the recent past and is now in the "recovery phase."

Growth of M. annularis, period 1 (Sep 79 - Feb 80): Average lateral growth of 1.3 mm (4 measurements).

Growth of M. annularis, period 2 (Feb 80 - Jun 80): Average lateral growth of 1.6 mm (4 measurements).

Average growth from Sep 79 to Jun 80 is 2.9 mm (4 measurements).

Growth of M. cavernosa, period 1 (Sep 79 - Feb 80): Average lateral growth of 3.1 mm (4 measurements).

Growth of M. cavernosa, period 2 (Feb 80 - Jun 80): Average lateral growth of 2.0 mm (4 measurements).

Average growth from Sep 79 to Jun 80 is 5.1 mm (4 measurements).

The interspecific aggressive hierarchy of Lang (1973) rates M. annularis as a dominant over M. cavernosa (i.e., M. annularis should be able to out-compete and kill M. cavernosa in the competition for space). Two factors observed in the seasonal photographs suggest that M. cavernosa may, at least in this case, be the dominant over M. annularis. First, the faster growth rate of M. cavernosa, together with the below average growth rate of M. annularis, indicates that M. cavernosa may be the aggressor. Second, the dead corallites in the gap or "combat zone" between the two corals appear to be remnants of M. annularis that have been recently killed, presumably by M. cavernosa.

Because M. annularis is showing slow growth, it is likely that this coral has undergone a recent rapid regression and is now recovering some of its lost territory. Once again, as the gap between the two corals narrows to within a few millimetres, it is speculated that M. annularis will stage another rapid retreat.

Station 19

Diploria strigosa is growing freely over a dead Diploria skeleton.

Growth period 1 (Sep 79 - Feb 80): Average lateral growth of 3.2 mm (4 measurements).

Growth period 2 (Feb 80 - Jun 80): Average lateral growth of 1.4 mm (4 measurements).

Average growth from Sep 79 to Jun 80 is 4.6 mm (4 measurements).

Station 20

Montastrea annularis is growing freely over an unidentified skeletal substrate.

Growth period 1 (Sep 79 - Feb 80): Average lateral growth of 1.9 mm (4 measurements).

Growth period 2 (Feb 80 - Jun 80): Average lateral growth of 1.4 mm (4 measurements).

Average growth from Sep 79 to Jun 80 is 4.6 mm (4 measurements).

Discussion of Lateral Growth/Mortality

In addition to the quantitative information presented on coral growth rates, the seasonal monitoring of specific areas along the corallum borders provides numerous qualitative insights to coral "behavior" within the reef ecosystem. Subjective observations concerning, 1) interspecific coral interactions, 2) sporadic and localized advance and regression, 3) periodic massive zooxanthellae expulsions from the coral tissue, and 4) the succession of colonizers on bare reef rock may yield not only growth rates but supporting information relating to the general health of the reef tract.

Coral mortality was observed in only 4 of the 20 stations examined on the West Flower Garden Bank, and two of these were the result of interspecific coral aggression (thus, there was no net loss of living coral tissue coverage from the reef). It should be noted that these stations were not selected at random, but for the healthy appearance of their borders (to maximize growth data) or for examination of competitive interactions. Consequently, the ratio of accreting to regressing borders is biased. An important point to consider is the much greater rate at which tissue death can occur relative to its growth rate. A comparison of pooled results from the East and West Flower Garden Banks

illustrates this point (Tables III-14 and 16). Averaged Porites astreoides mortality occurred at more than six times its growth rate; averaged Montastrea annularis mortality rates were more than twice the average growth rate; and the not-uncommon ridge death of Diploria strigosa occurred at nearly forty times the average growth rate for this species.

These data demonstrate the sensitivity of corals to their environment, and the potential for rapid demise of coral reefs under adverse conditions. Localized massive zooxanthellae expulsion observed in Porites astreoides and Agaricia agaricites may be a method of purging the coral tissue of detrimental substances, parasites, or infectious bacteria and viruses. As observed in Station 16 for P. astreoides, the ability of the damaged tissue to recover may be related to its proximity to healthy tissue. The damaged tissue farthest away from the healthy polyps did not recover from its loss of zooxanthellae. Similarly, the ridge mortality commonly observed in D. strigosa rapidly spreads from a localized area on the corallum. The corals may have some yet unknown physiological defense to such "diseases." In support of this, the rapid ridge mortality of D. strigosa from both the East and West Flower Garden Banks subsided (or at least greatly slowed down) before the entire colony was affected.

This response to invasion is also evident along competitive borders between coral species. The lateral regression of a competitively subordinate species to the growth of a competitively dominant species (e.g., M. annularis encroaching over D. strigosa) is not a continual regression but a series of rapid retreats alternating with periods of border stabilization. As previously mentioned, the retreat of the regressing coral is apparently initiated when the aggressor grows to within a critical distance of the subordinate species. Once the regressing coral has rapidly retreated to a "safe distance" from the encroaching species, the border of the subordinate stabilizes, perhaps even resuming some lateral growth (as observed in Station 2). The cycle begins again when the dominant coral transgresses the critical distance between it and the subordinate species.

The interspecific competition for space between M. annularis and D. strigosa follows the digestive dominance hierarchy of Lang (1973). In addition, the hydrozoan Millepora appears dominant over M. annularis. An exception to Lang's hierarchy is evident from Station 18 where Montastrea cavernosa (a subordinate) is encroaching over M. annularis (a digestive dominant to M. cavernosa). As these two species are closely ranked in the coral dominance hierarchy, such exceptions might be related to variations in the health of different coral colonies of the same species.

Similar to the vertical growth data obtained from the sclerochronology study, the lateral growth rates of corals appear highest during the cooler months of late fall through winter. Variation in lateral growth along the coral borders also appears greatest during the winter months. One area of Millepora border (Station 9) accreted 36 mm between September 1979 and February 1980, while other areas along the

border showed little or no measurable growth. Such growth variability may be related to small topographic variations on the substrate over which the coral is growing, or perhaps alternating phases of lateral accretion along some areas of the border, and vertical thickening in others.

Summary: Coral Growth and Mortality

Sclerochronological analysis of cores taken from heads of the coral Montastrea annularis at the East and West Flower Garden Banks indicates an average accretionary growth rate for this species of 7.5 mm/year over the past 15 to 20 years. Similar analysis of one core of Diploria strigosa from the East Flower Garden indicates a growth rate of 5.1 mm/year.

Short-term seasonal measurements of encrusting growth (lateral advance of living tissue) and mortality (lateral retreat of living tissue) were made for selected species at both banks (Tables III-14 and 16). Our most reliable data are for the dominant corals Montastrea annularis and Diploria strigosa. The data suggest that, where mortality occurs in either of these species, it progresses at rates considerably greater than the measured rates of growth for the same species. The ratio of mortality to growth is approximately 2.5 for M. annularis and 10 for D. strigosa.

The fire coral, Millepora alcicornis, is almost certainly the fastest growing coral on the high diversity reefs at the Flower Gardens.

RECRUITMENT AND EARLY GROWTH OF CORALS

Introduction

Previous studies on coral recruitment and/or early growth include those in laboratory aquaria, and field studies in the nearshore environment. The present study was designed to examine recruitment and growth of corals at an offshore reef, and to provide baseline data from an environment which might soon become stressed by activities associated with oil exploration and drilling.

In the laboratory, coral settlement behavior, aggregation patterns, spatial orientation, and survival have been examined in several studies, such as those by Atoda (1947, 1951), Lewis (1971a,b), and Goreau, et al. (1981).

Birkland (1977) used cement blocks, plexiglass plates, and terracotta tile in coral recruitment studies off Panama in the Caribbean and the Pacific. Substrate preferences of corals were found to be associated with location, and spatial orientation preferences were found to be associated with light/depth. In a later study (Birkland and Rowley, 1981), recruitment differences in vertical and horizontal plexiglass surfaces were further examined.

Sammarco (1978, 1980) examined the relationships between abundance of the spiny urchin, Diadema, and benthic algal cover, and how this interaction affected coral spat mortality. Potts (1977) had similarly studied the interaction between algal population densities and coral growth and mortality, as affected by aggressive territorial behavior of a damselfish species. The control of algae population densities by other organisms or by environmental conditions is seen to be an important factor regulating the success or failure of coral recruitment and growth.

In a nearshore field study, Bak and Engel (1979) used a quadrat system to examine juvenile corals in the Netherlands Antilles at depths ranging between 3 and 37 m. They found that Agaricia agaricites dominated (60.6%) the juvenile community, while other genera (such as Montastrea, Madracis, and Acropora) dominated the adult community. They also found differences in spatial orientation of coral settlement with differences in depth and associated available light. Factors affecting juvenile survival were found to vary with depth.

In a later study, Bak and Steward-Van Es (1980) found species-specific differences in tissue regeneration success following artificial inducement of lesions simulating natural predation. Their results might easily be extended in considering the potential of coral (and other) community changes caused by man-induced environmental modifications.

Results reported here are exploratory, so specific comparisons with results from previously cited studies are not yet appropriate, although numerous such comparisons will be made in subsequent reports. Substantial adjustments for error in data analyses are available and will be applied to future data sets.

Methods

Construction of Sampling Plates

Because plates used in the prototype sampling system during the summer of 1979 had recruited corals successfully, the design was not altered for the new sampling system. Construction details are reported in Bright et al. (1981). Plates measured 10 cm x 10 cm square, and averaged 1.9 cm in thickness in a randomly selected group of 22 plates.

The wooden framework previously used to mold plates for the prototype system was permanently divided into two functional halves: one half was to be used to mold control (cement) sampling plates and the other half to mold barite/cement plates. Contamination of control plates by barite was thus avoided.

Construction of Sampling Racks

For each of four sampling sites, sampling racks were constructed from polyvinylchloride (PVC) pipe. At each study site, one rack consisted of only control samplers, and the other rack of only barite/cement samplers. The prototype rack design had proven functional, so no major design changes were made in the new racks.

Weight was added to the racks by embedding the legs in concrete in one-gallon plastic milk-jugs. Paper and plastic labels were removed from the jugs in order to avoid the possibility of such labels later becoming detached and drifting onto the surface of a nearby sampling plate. Legs were constructed to permit adjusting the height of the racks so that they might be installed at or near a horizontal plane. Legs were secured to the substrate using 600 lb.-test braided nylon line attached between each leg, and appropriately placed steel spikes driven into nearby limestone substrate.

Rods supporting sampling plates were reduced in length from 120 cm (as was used in the prototype system) to 91 cm, because the number of plates per rod was reduced from six (in the prototype) to four. Plates were spaced center to center: 16.6 cm apart within rods, and 22.5 cm apart between rods.

Early results from the prototype system indicated that most coral recruitment occurred on the undersides of sampling plates. It was decided to invert the plates in the new racks, so that the primary sampling surface would be oriented downwards. Plates were arranged in five rows per rack (20 plates/rack). Identifying letters for rows were burned into the cross-beams of each rack; control racks were assigned rows A-E (left to right, observed from rear of rack), and barite racks similarly were assigned rows F-J.

Fiberglass 1/4" rod-stock (bicycle flag-pole) was used to construct pins to be used to secure adjustable legs to the racks, and to lock rods in place within each rack. Such pins were necessary due to the experimental requirement that the positions of the rods be changed within each rack during each sampling trip, and they had worked well in the prototype system as designed.

Description of Study Sites

In order to examine possible seasonal and longer-term differences in recruitment rates and early growth rates of corals at the Flower Garden reefs, two study sites were selected at the East Flower Garden reef (Stations 1 and 2), and two at the West Flower Garden reef (Stations 3 and 4).

Station selection was non-random. At each reef, sites were chosen according to 1) availability of level or near-level bottom, 2) availability of nearby hard substratum to which racks could be secured with tie-down lines, and 3) locally maximal or minimal depth. The deepest

and shallowest serviceable stations at each reef were chosen as study sites.

Because racks were designed to permit removal and replacement of sampling rods, sufficient working-room was also required at each study site. No racks were installed atop living coral substrata, and no tie-down spikes were driven into living tissue of coral heads.

Locations and depths of selected stations were as follows:

<u>Station</u>	<u>Location</u>	<u>Latitude/Longitude</u>	<u>Depth(m)</u>
1	EFG	27°54'16"N, 93°35'54"W	28.3
2	EFG	27°54'37"N, 93°35'56"W	22.3
3	WFG	27°52'32"N, 93°48'53"W	26.8
4	WFG	(Same as Station 3)	25.3

Station 1 at the East Flower Garden reef was located approximately 20 m east of the prototype station, previously established at the "BLM site." The two racks were placed in a shallow canyon located between large coral heads, primarily Montastrea spp. and Diploria spp., rising 2-3 m above the base of the canyon. The solid limestone substrate was covered with a layer of sand measuring 2-10 cm in thickness. The racks were placed adjacent to one another, approximately a half-metre apart.

Station 2 was located in a shallower environment, at the "CSA site," more than 1 km north of Station 1. The racks were placed within an oval sand flat, approximately 5 m x 6 m in dimension, surrounded by coral heads rising 2-3 m above the flat. Several other sand flats, both smaller and larger, were located in the near vicinity. Coral heads were predominantly Montastrea spp. and Diploria spp. The sand substrate was deep, so spikes used to secure lines to the racks were driven into non-living basal portions of nearby coral heads.

Station 3, at the West Flower Garden reef, was located adjacent to the south rim of a large sand flat, estimated to measure 20 m in diameter north to south, and 50 m east to west. The station was established slightly west of center of the south rim; the bank rising above was dominated by Montastrea annularis. Racks were secured to the non-living bases of adjacent coral heads, and to portions of hard-bottom protruding through the sand.

Station 4 was located in a sandless, circular pit, approximately 5 m in diameter, with near-vertical walls, on the south bank above and about 20 m southeast of Station 3. The floor of the pit sloped upwards toward the southwest, but the adjustable legs of the racks permitted nearly horizontal installation. The walls stood 2-3 m high to the west, north, and east of the pit, but because of the upward-sloping floor, the south wall was only half as high as the others. The upper rim of the pit was at a uniform depth, and consisted mostly of Montastrea annularis heads.

Sampling Methods

Sampling was randomized wherever possible at all levels of the experiment. Numbered plates were randomly selected using random-number tables (Steel and Torrie, 1960), and assigned in groups of four to numbered rods. Placement of plates within each rod was randomly chosen. Plates were glued into rods (plate numbers facing upward) and oriented to the left side of the rack (viewing the rack from its back side). The front of each rod was identifiable by the presence of a 45° notch cut into that end of the rod. This system assured proper placement of rods within racks so that plate-orientation records could be kept.

To minimize the possibility of a positional effect of plates within a rack, positions of rods not being collected and replaced during a given sampling trip were changed within each rack according to a randomized schedule.

Short-term "seasonal" samples and longer-term samples were collected and replaced with new samplers within each rack during each of five cruises. A short-term sample was one which had been installed during the most recent previous cruise. A long-term sample was one which had been on site since the beginning of the experiment, or no longer than one year. Thus, sampling occurred over the following time schedule:

<u>Sample Number</u>	<u>Short-Term Sampling Periods</u>	<u>Sample Number</u>	<u>Long-Term Sampling Periods</u>
1	9/23-24/79 - 2/17-20/80	5	9/23-24/79 - 2/17-20/80
2	2/17-20/80 - 6/12-15/80	6	9/23-24/79 - 6/12-15/80
3	6/12-15/80 - 9/25-29/80	7	9/23-24/79 - 9/25-29/80
4	9/25-29/80 - 2/20-21/81	8	2/17-20/80 - 2/20-21/81

During each cruise, a short-term and long-term sample was collected from each rack, the remaining rods were re-positioned within the rack according to a predetermined randomized schedule, and replacement rods were installed.

Preservation, transport, and storage of sampling plates has been described elsewhere (Bright *et al.*, 1981).

Analysis of Samples

An overview of analysis procedures is included in Bright *et al.* (1981). Several analytical techniques not previously reported are described below.

An optical measuring grid was constructed for the microscope eyepiece by photographing through the microscope the surface of a haemocytometer (blood-cell counting chamber), and developing the film as a transparency. Two different series of fine black lines resulted on the film, which permitted linear measurement of corals to the

nearest 0.05 mm. From the developed film a disc was cut of a size sufficient to fit inside the microscope eyepiece. The eyepiece grid (reticle) was calibrated by overlaying its image on the observed haemocytometer grids of known size, and recording a series of known and observed linear measurements. Using linear regression, a corrected factor for measurements of coral basal diameters was derived, as follows:

$$\text{Corrected Diameter} = (-0.0120000001) + (1.04454546 \times \text{Observed Diameter}),$$

where the negative value is the Y-intercept, and the second constant is the slope of the regression line, with $r^2 = 0.9999689$.

Basal areas of corals were then calculated using the formula,

$$\text{Basal Area} = (3.1415927) \times ((\text{Corrected Diameter}/2)^2).$$

Both formulas were incorporated into a SAS program (Statistical Analysis System) designed to calibrate, correct, and compile raw data into several different new sets of data for later analysis.

Coral coverage for each plate-surface was expressed both as absolute and relative values rather than as percentages, which in most cases would have been quite small.

Dimensions of plate-surfaces are as follows:

- 1) lower (primary) surface = 10 cm x 10 cm = 100 cm² = 10,000 mm²;
- 2) upper (secondary) surface = (10 cm x 10 cm) - (3.5968 cm² area of stem in center of upper surface = 96.40 cm² = 9,640 mm²;
- 3) each side = 10 cm long x average 1.92 cm thick = 19.2 cm² average area = 1,920 mm² average area.

Plate tops are 96% as large as plate bottoms, and plate sides are less than 20% individually, or about 75% when four sides of the area of plate bottoms are combined.

Relative values of coral coverage were calculated by dividing coral basal area by function of a "standard" 100 cm² sampling surface. For corals located on the primary (lower) surface, basal areas were divided by 1.0000 (or by 100 to obtain percentage cover); basal areas for corals on the secondary (upper) surface were divided by 0.9640; and basal areas of coral from plate sides were divided by 0.1922.

An analysis of variance (ANOVA) was run comparing the average sums (between replicate plates within a sample and station) of relative coverage of corals occurring on lower, upper, and combined side surfaces of plates. Results suggested a need for more exact calculation of areas of side surfaces of plates.

At present, corals are categorized as one of three "types." Type 1 is probably Agaricia spp.; Type 2 is probably Porites spp.; and Type 3 is presently identified as any other coral morphologically similar to Type 1 (perhaps another 3-6 species). Until species can be positively identified, all coral basal areas have been combined to yield an areal coverage value per surface, sample, and station. These values, for short-term samples and for long-term samples, were plotted as block diagrams of sums, using the SAS-Graph package available through the Texas A&M University Data Processing Center (see Figures III-7 and 8). These diagrams graphically represent the combined total coverage (mm^2) of all corals found on each surface of two replicates (plates) per station and sample.

Results and Discussion

Figures III-7 and 8 illustrate total areal coverage of corals (mm^2) per two replicates (plates) per sample, for each of the four stations. In most cases, another two control plates per sample and station are being analyzed. Cement/barite plates which were collected concurrently are also being analyzed, and in some cases will provide data where it is missing in the control samples.

As noted in the footnotes to Figures III-7 and 8, damages presumably caused by rough seas associated with Hurricane Allen (9 August 1980) were extensive. Sample 3 (6/80-9/80) was destroyed at Stations 2 and 3, and samples 7 (9/79-9/80) and 8 (2/80-2/81) were destroyed at Station 2. Cement/barite samples 3, 7, and 8 were collected at Station 2, and may later provide useful information now missing. Samples 7 and 8, Station 1, are only partially analyzed, and therefore are not included in Figure III-8.

Damages Presumed Associated With Hurricane Allen

Hurricane Allen moved ashore at Corpus Christi, Texas, on 9 August 1980. It had come from the southeast, had stalled for several hours, and had developed winds in excess of 200 knots. Gale-force winds extended to the north to the vicinity of the Flower Gardens and beyond. It is not known what actual conditions occurred at the study sites, but hearsay information indicates 10 m waves at oil-rigs within a few kilometres of the Flower Gardens.

In September 1980, significant damage was found at all recruitment study-sites, as follows:

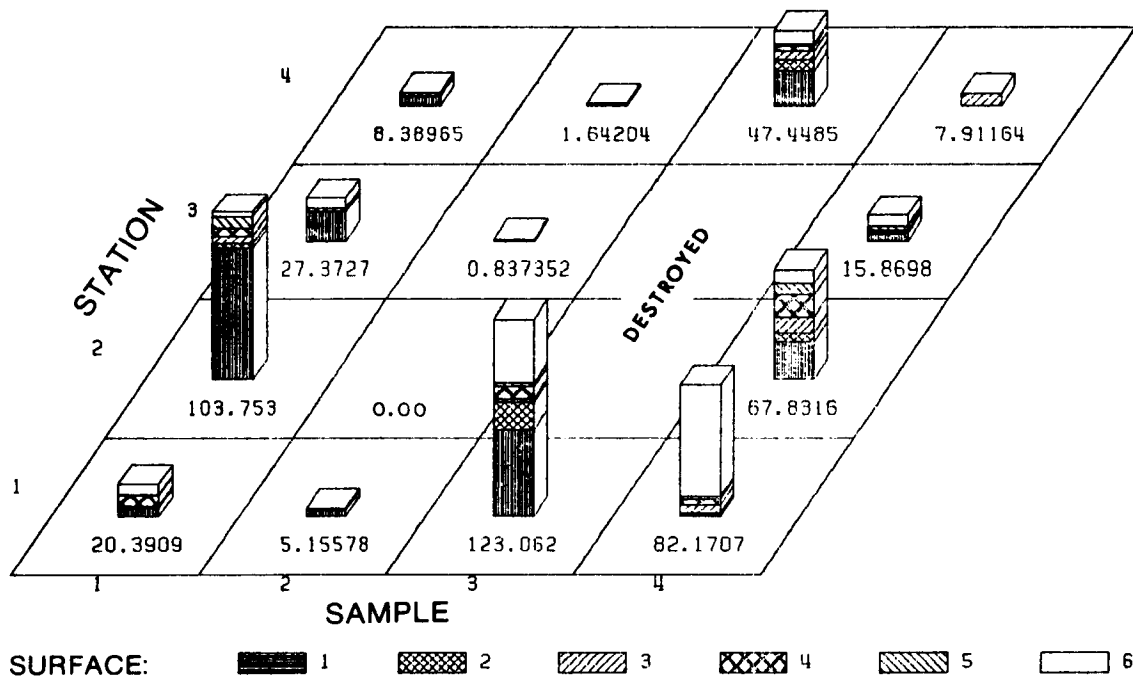
Station 1 (EFG/BLM): control rack partially damaged, barite rack partially destroyed;

Station 2 (EFG/CSA): control rack destroyed, barite rack partially destroyed;

Station 3 (WFG/sand-flat): both racks destroyed; two undamaged plates recovered, several badly scoured plates recovered from vicinity;

CORAL RECRUITMENT AT FLOWER GARDEN REEFS SHORT-TERM CONTROL SAMPLES

Coral Coverage (sq.mm) by Plate-Surface Orientation
Subsample 1 — Two Plates/Sample/Station shown



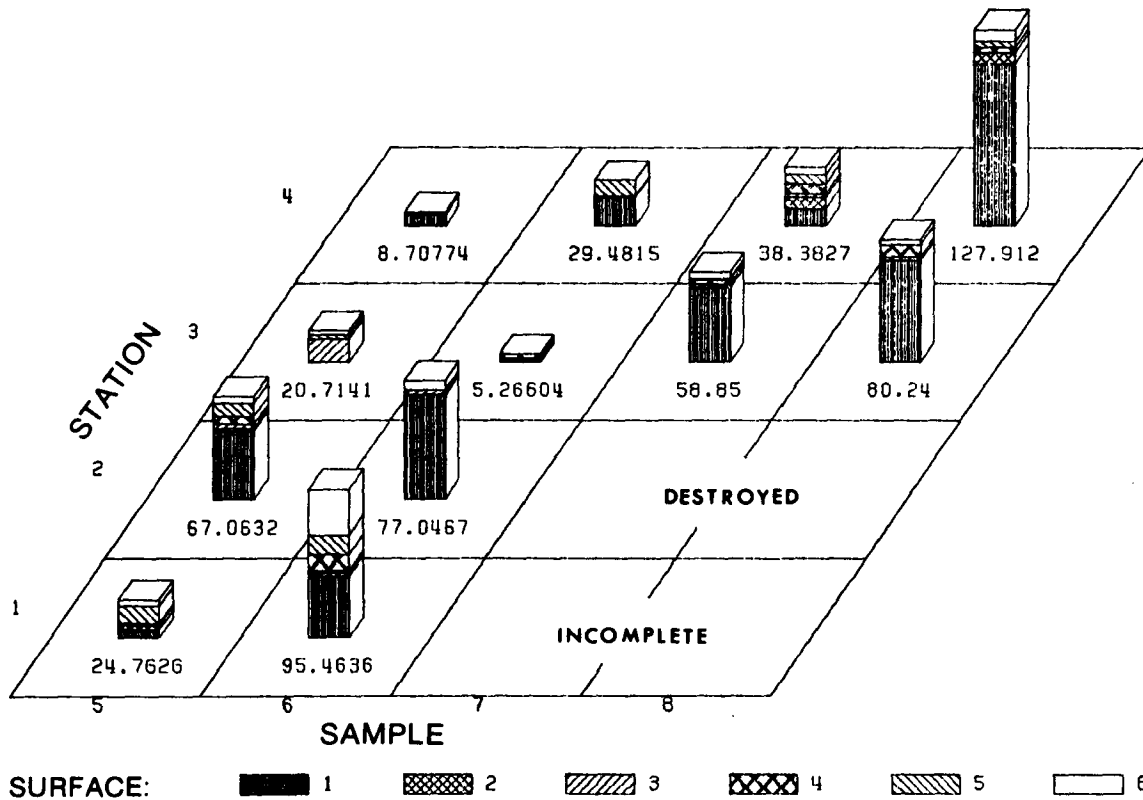
SURFACE: 1=BOTTOM,2=NORTH,3=EAST,4=SOUTH,5=WEST,6=TOP

STATIONS (DEPTH): 1=EFG/BLM (28.3 M), 2=EFG/CSA-A (22.3 M),
3=WFG/SAND-FLAT (26.8 M), 4=WFG/SOUTH BANK (25.3 M)
SAMPLES: 1=9/79-2/80, 2=2/80-6/80, 3=6/80-9/80, 4=9/80-2/81
**SAMPLES 3 FROM BOTH STATIONS 2 & 3 WERE
DESTROYED BY HURRICANE ALLEN, 8/9/80**

Figure III-7. Coral recruitment at Flower Garden reefs, short-term control samples.

CORAL RECRUITMENT AT FLOWER GARDEN REEFS LONG-TERM CONTROL SAMPLES

Coral Coverage (sq.mm) by Plate-Surface Orientation
Subsample 1 — Two Plates/Sample/Station shown



SURFACE: 1=BLACK, 2=CROSS-HATCH, 3=DIAGONAL, 4=CROSS-HATCH, 5=DIAGONAL, 6=WHITE

SURFACE: 1=BOTTOM, 2=NORTH, 3=EAST, 4=SOUTH, 5=WEST, 6=TOP

STATIONS (DEPTH): 1=EFG/BLM (28.3 M), 2=EFG/CSA-R (22.3 M), 3=WFG/SAND-FLAT (26.8 M), WFG/SOUTH BANK (25.3 M)

SAMPLES: 5=9/79-2/80, 6=9/79-6/80, 7=9/79-9/80, 8=2/80-2/81

SAMPLES 7 & 8, STATION 1, ONE PLATE EACH - NOT SHOWN

SAMPLES 7 & 8, STATION 2, WERE DESTROYED BY HURRICANE ALLEN, 8/9/80

Figure III-8. Coral recruitment at Flower Garden reefs, long-term control samples.

Station 4 (WFG/south bank): both racks partially damaged, but repairable.

All stations were rebuilt to the extent possible using all spare parts brought on cruise, plus salvageable parts recovered from wrecked stations. Stations 1 and 4 were nearly totally refurbished, but Stations 2 and 3 were only partially salvageable.

Analysis of Variance Procedures

The effects of location (STA), time (SAMP), and spatial orientation (SURF) on coral size (basal DIAMETER), and mean seasonal growth (SEASGRTH) were examined using factorial analysis of variance (ANOVA) procedures on samples 1 (9/79-2/80), 4 (9/80-2/81), and 5 (9/79-2/80). Short-term sample 1 and long-term sample 5 were emplaced, sampled, and removed concurrently. Sample 4 was collected during the same months as samples 1 and 5, but one year later.

It was necessary to approximate mean seasonal growth of corals because samples were not collected over equal time spans; sample durations ranged from three to five months. Daily growth was estimated by dividing the basal area of each coral by the number of days sampled (for the sampling plate containing that coral). The resulting mean daily "growth" values were multiplied individually by 91 days to yield mean "seasonal" growth values; these were then analyzed using ANOVA procedures.

Present results are based on a subsample of the data base, so are considered exploratory and subject to revision with the later addition of more data.

Null hypotheses used were:

- 1) no differences in effect of location (STA) on coral diameter, nor on seasonal growth;
- 2) no differences in effect of time (SAMP) on coral diameter, nor on seasonal growth;
- 3) no differences in effect of spatial orientation (SURF) on coral diameter, nor on seasonal growth;
- 4-7) no differences in effect of (STA)x(SAMP), (STA)x(SURF), (SAMP)x(SURF), nor (STA)x(SAMP)x(SURF) interactions on coral diameter, nor on seasonal growth.

For the dependent variable, DIAMETER, and independent variables, station (STA), sample (SAMP), and surface (SURF), results are given in the following ANOVA table:

Source	df	SS	MS	F-value	Pr>F	Result
Model	71	130.912	1.84	43.65	0.0001	Reject Ho
STA	3	41.563		27.40	0.0001	Reject Ho
SAMP	2	1.880		1.86	0.1588	No Reject
SURF	5	39.215		15.51	0.0001	Reject Ho
STA*SAMP	6	6.676		2.20	0.0450	Reject Ho
STA*SURF	15	6.644		0.88	0.05926	No reject
SAMP*SURF	10	14.020		2.77	0.0033	Reject Ho
STA*SAMP*SURF	30	20.913		1.38	0.1043	No reject
Error	179	90.509	0.506			
Total	250	221.421				

We conclude that for samples 1, 4, and 5, ANOVA indicates that the interactions between stations/samples/plate-surfaces, and between stations/surfaces are not demonstrated to significantly affect mean basal diameter of corals among those samples. Station location, surface orientation, station/sample interactions, and sample/surface interactions do significantly affect mean coral basal diameters in samples 1, 4, and 5.

A Duncan's multiple range test applied (at alpha = 0.05) to these data yielded the following results:

<u>Mean Diameter</u>	<u>Number of Corals</u>	<u>Station (Site,Depth)</u>
1.563774	100	2 (EFG/CSA, 22.3 m)
1.290506	66	1 (EFG/BLM, 28.3 m)
0.921948	44	3 (WFG/sand-flat, 26.8 m)
0.428610	41	4 (WFG/south bank, 25.3 m)

Means at all stations were significantly different from one another. These results agree with those from the ANOVA table, and indicate that these samples, collected at the same stations during the same or similar seasons, were statistically indistinguishable at a 95% level of confidence.

Differences between sampling surfaces were:

<u>Mean Diameter</u>	<u>Number of Corals</u>	<u>Surface (Orientation)</u>
1.669573	69	1 (Bottom)
1.494888	47	6 (Top)
0.965458	36	5 (West)
0.932679	34	3 (East)
0.864552	37	4 (South)
0.563334	28	2 (North)

Mean diameters from surfaces 1 and 6 were not significantly different, but were different from all other sides of plates. Means from surfaces 5, 3, and 4 were not significantly different but differed from surfaces 1 and 6, and from 2. Means from surfaces 3, 4, and 2 did

not differ significantly from one another, but differed from all others. The mean diameter of corals was largest on bottoms of plates as were the absolute numbers of corals. It should be recalled that the summed total sampling area of the combined four sides (76.88 cm^2) of plates is less than the total sampling area of either plate bottoms (100.00 cm^2) or tops (96.40 cm^2). On a relative scale, apparently greater numbers of corals were recruited to plate sides than to bottoms or tops in these samples.

The latter conclusion was supported by results of an ANOVA which was run on mean seasonal growth (SEASGRTH) differences of corals in samples 1, 4, and 5. This analysis resulted in rejection of all hypotheses concerning the absence of effects of station, sample, surface, and all main-effects interactions on seasonal coral growth rates. That is, stations, samples, surfaces, and all main-effects interactions could not be shown not to have a significant effect on mean seasonal growth of corals in samples.

A Duncan's multiple range test was run on the means of seasonal coral growth (mm^2) by station, sample, and surface, for samples 1, 4, and 5, in order to further examine the results of the ANOVA. Location (STA) effects were apparent, but with overlap between stations:

<u>Mean Seasonal Growth</u> (mm^2)	<u>Number of Corals</u>	<u>Station (Site, Depth)</u>
3.416259	100	2 (EFG/CSA, 22.3 m)
2.593921	66	1 (EFG/BLM, 28.3 m)
2.289153	44	3 (WFG/Flat, 26.8 m)
1.043186	41	4 (WFG/Bank, 25.3 m)

Mean growth of corals was greatest at EFG Station 2, and least at WFG Station 4. Station 4 was dissimilar to other stations in growth effects, while WFG deep station 3 and EFG deep station 1 were not statistically dissimilar. At the East Flower Garden sites, shallow station 2 and deep station 1 were not dissimilar in effects on growth although greater numbers of corals were recruited to Station 1.

The effects of sample (SAMP) dates on mean growth were minimal:

<u>Mean Seasonal Growth</u> (mm^2)	<u>Number of Corals</u>	<u>Sample (Dates)</u>
3.203375	83	4 (9/80-2/81)
2.631047	79	5 (9/79-2/80)
2.051518	89	1 (9/79-2/80)

Samples 4 and 5, collected during the same seasons in different years, were not statistically significantly different ($\alpha = 0.05$). Samples 5 and 1, collected at the same time, were likewise not different, although a difference between samples 4 and 1 was seen. Numbers of corals were similar in all samples, although a larger number of

smaller corals was collected in sample 1 than in sample 4; the latter was comprised of fewer but larger corals.

Plate orientation (SURF) differed in effect on seasonal growth (a relative value per unit surface area):

<u>Mean Seasonal Growth</u> (mm ²)	<u>Number of Corals</u>	<u>Surface (Orientation)</u>
4.292965	34	3 (East)
3.768687	36	5 (West)
3.293413	37	4 (South)
2.044266	28	2 (North)
1.749807	69	1 (Bottom)
1.592597	47	6 (Top)

These results, when compared to effects of surface (SURF) on coral mean diameters, show some interesting differences and similarities. Mean seasonal adjusted growth (coverage) is greatest on three of the plate sides, and least on the plate tops and bottoms. Mean coral diameters were least on the plate north sides, and greatest on plate bottoms and tops. On plate sides, mean seasonal growth was greatest on east sides, followed by west sides; mean basal diameters were greatest on west sides, followed by east sides. Figures III-7 and 8 show that west and east sides of plates were extensively utilized by corals; south sides were also important, whereas north sides were relatively important only in sample 3 at Stations 1 and 4.

In exploratory ANOVA and Duncan's tests on other available data sets, similar findings were made. An apparent tendency has been noted for corals to settle in larger numbers and to average larger sizes on west sides of plates, followed in order by east sides, then south and north sides.

For coral recruitment and early growth, these results suggest a probable effect of currents moving primarily from west to east, but possibly oscillating in both directions. On average, corals appeared to favor west sides of plates as settling sites in samples examined thus far. Most recruitment, in terms of both numbers of individuals and absolute coral coverage (mm²), occurs on plate bottoms, as seen in Figures III-7 and 8, but this is due in part to the larger available surface compared to other surfaces on each plate. A large percentage of coral cover on plate tops is seen in short-term samples 3 and 4. Long-term samples 7 and 8, from Stations 3 and 4 (Figure III-8), are dominated by coral coverage on plate bottoms. Figure III-7, sample 2, illustrates the reduced recruitment and growth of corals during winter and early spring. Sample 6, Figure III-8, appears to reflect growth of corals which probably settled before the winter season, since sample 2 indicates little to no new growth between February and June. Upper surface growth of corals may occur primarily in winter or spring, when light levels are insufficient for robust growth on undersides of plates (or natural surfaces), and when competition with filamentous algae is reduced, also due to low light levels.

The importance of plate sides as recruiting surfaces was recognized during analysis of samples, and has been designed into a new sampling system now being used in a separate experiment.

Summary

Two recruitment sampling stations were established at the East Flower Garden reef, and two at the West Flower Garden reef. Sampling was begun 22 September 1979, and terminated 21 February 1981.

Two types of sampling plates were installed in separate sampling racks at each of the four stations so that possible differences in recruitment and growth of corals caused by differences in substrate type might be examined. This report concerns only one of the two types, the "control" plates, constructed of portland type I cement.

Short-term and long-term samples were collected from each station during each sampling trip. Four collecting trips were made during the study; these ranged from three to five months apart.

The sampling scheme was severely disturbed by a loss of samples resulting from heavy seas presumed associated with Hurricane Allen, 9 August 1980. Because of this storm and its associated damage, samples collected after August 1980 were often incomplete. The sampling design was based on the availability of four sampling plates/sample/station/substrate-type. Samples not totally destroyed were in many cases damaged to a greater or lesser degree. For this report, samples composed of at least two control plates were used.

Corals were classified according to one of three generalized types, and were optically measured in diameter to the nearest 0.05 mm. Recruitment and growth were examined in terms of 1) numbers of corals per sampling surface over time, and 2) summed or averaged coverage (mm^2) of coral per sampling surface or combination of surfaces (e.g., all four sides of a plate combined).

Samples 1, 4, and 5 were directly compared using analysis of variance procedures (ANOVA) to examine effects of location (station), time (sample), and spatial orientation (surface) on recruitment and growth of young corals.

Because different samples were in some cases collected over unevenly distributed time-frames, ranging from three to five months, growth was roughly "normalized" by first calculating daily growth rates per individual coral specimen, and then multiplying this value by 91 days to obtain a "seasonal" growth value. These data were used in ANOVA procedures to compare (as an exploratory exercise) "seasonal" growth in different samples. Selected results are reported here.

Significant effects on growth in samples 1, 4, and 5 were found associated with different stations (locations and depths) and different plate surfaces. When these samples were compared to samples taken at other times, a time (sample) effect on growth was introduced.

The shallow station at the East Flower Garden reef (Station 2, 22.3 m) produced the largest corals (greatest growth) and the greatest number of corals over time (recruitment). At the West Flower Garden, the shallower station (Station 4, 25.3 m) produced the smallest and fewest corals of those observed so far.

In terms of absolute coverage, plate bottoms collected greater numbers of corals, and corals of larger sizes than other surfaces of plates. This may be in some measure due to the greater surface area of plate bottoms in comparison to tops and sides.

In terms of relative coverage, west and east sides of plates were, in general, apparently favored surfaces. These sides produced the largest mean seasonal growth values, suggesting the possibility of environmental influences on recruitment success, and on growth rates, such as possible west-east current oscillations.

Recruitment and growth were least during winter and early spring, and greatest during summer and early fall. Reduced light levels in winter may influence coral settlement on plate topsides. Older samples tend to have more corals on undersides than on other surfaces.

**APPENDIX B:
CORAL POPULATION TABLES**

TABLE B-1
CORAL POPULATION LEVEL PARAMETERS BY SITE, TAXON, AND TRANSECT
SITE - BLM SPECIES - Montastrea annularis

TRANSECT	DOMINANCE (% COVER)	RELATIVE DOMINANCE (C)	RELATIVE DOMINANCE (C&CA)	RELATIVE DENSITY (C)	RELATIVE DENSITY (C&CA)
HPLT-A1	51.37	68.84	65.76	50.00	40.00
HPLT-A2	41.87	55.19	51.15	44.44	26.67
HPLT-A3	39.50	47.45	45.73	32.14	24.32
HPLT-B1	36.37	43.30	43.05	36.36	34.78
HPLT-B2	69.75	91.03	85.98	53.85	35.00
HPLT-B3	39.37	67.16	59.21	47.06	34.04
HPLT-C1	49.12	73.32	65.28	66.67	45.16
HPLT-C2	47.37	59.03	54.38	33.33	26.09
HPLT-C3	47.37	84.22	72.19	44.00	25.58
MEAN VALUES	46.90	65.50	60.30	45.32	32.40
C.V.	2.12	3.90		2.63	

FREQUENCY: 100%

STATISTICAL VALUES	DOMINANCE (% COVER)	RELATIVE DOMINANCE (C)	RELATIVE DOMINANCE (C&CA)	RELATIVE DENSITY (C)	RELATIVE DENSITY (C&CA)
S ²	99.40	255.36	185.50	119.25	52.56
S	9.97	15.98	13.62	10.92	7.25
F-test	3.84; Acc H ₀	1.72; Acc H ₀	2.28; Acc H ₀	1.01; Acc H ₀	1.05; Acc H ₀
t-test	6.99; Rej H ₀	3.75; Rej H ₀	4.68; Rej H ₀	3.07; Rej H ₀	3.63; Rej H ₀
95% C.I.	39.24-54.56	53.22-77.78	49.83-70.77	36.93-53.71	26.83-37.97

C = corals only

CA = corals and coralline algae

S², S = variance and standard deviation, respectively.

C.I. = confidence interval around the sample mean.

C.V. = S^2 / \bar{X} (coefficient of variation).

F- and t-tests compare the variances and means, respectively, of M. annularis population parameters at the CSA and BLM sites. H₀ = equal sample variances, or equal sample means.

FREQUENCY = percentage of all transects at the BLM site on which M. annularis occurred at least once.

TABLE B-2
CORAL POPULATION LEVEL PARAMETERS BY SITE, TAXON, AND TRANSECT
SITE - BLM SPECIES - Diploria strigosa

TRANSECT	DOMINANCE (% COVER)	RELATIVE DOMINANCE (C)	RELATIVE DOMINANCE (C&CA)	RELATIVE DENSITY (C)	RELATIVE DENSITY (C&CA)
HPLT-A1	4.87	6.53	6.24	18.75	15.00
HPLT-A2	3.87	5.11	4.73	11.11	6.67
HPLT-A3	7.12	8.56	8.25	3.57	2.70
HPLT-B1	1.62	1.93	1.92	4.55	4.35
HPLT-B2	4.87	6.36	6.01	15.38	10.00
HPLT-B3	1.50	2.56	2.26	8.82	6.38
HPLT-C1	3.87	5.78	5.15	4.76	3.23
HPLT-C2	1.87	2.34	2.15	2.78	2.17
HPLT-C3	4.00	7.11	6.10	20.00	11.63
MEAN VALUES	3.73	5.14	4.76	9.97	6.90
C. V.	0.91	1.07		4.50	

FREQUENCY: 100%

STATISTICAL VALUES	DOMINANCE (% COVER)	RELATIVE DOMINANCE (C)	RELATIVE DOMINANCE (C&CA)	RELATIVE DENSITY (C)	RELATIVE DENSITY (C&CA)
S ²	3.39	5.52	4.48	44.89	19.71
S	1.84	2.35	2.21	6.70	4.44
F-test	54.71; Rej H ₀	76.54; Rej H ₀	72.91; Rej H ₀	3.92; Acc H ₀	4.07; Acc H ₀
t-test	2.28; Acc H ₀	2.64; Rej H ₀	2.57; Rej H ₀	1.05; Acc H ₀	1.05; Rej H ₀
95% C.I.	2.32 - 5.14	3.33 - 6.95	3.06 - 6.46	4.82 - 5.12	3.49 - 10.31

C = corals only

CA = corals and coralline algae

S², S = variance and standard deviation, respectively.

C.I. = confidence interval around the sample mean.

C.V. = S^2 / \bar{X} (coefficient of variation).

F- and t-tests compare the variances and means, respectively, of D. strigosa population parameters at the CSA and BLM sites. H₀ = equal sample variances, or equal sample means.

FREQUENCY = percentage of all transects at the BLM site on which D. strigosa occurred at least once.

TABLE B-3
CORAL POPULATION LEVEL PARAMETERS BY SITE, TAXON, AND TRANSECT
SITE - BLM SPECIES - Montastrea cavernosa

TRANSECT	DOMINANCE (% COVER)	RELATIVE DOMINANCE (C)	RELATIVE DOMINANCE (C&CA)	RELATIVE DENSITY (C)	RELATIVE DENSITY (C&CA)
HPLT-A1	0.00	0.00	0.00	0.00	0.00
HPLT-A2	13.62	17.96	16.64	11.11	6.67
HPLT-A3	6.62	7.96	7.67	14.29	10.81
HPLT-B1	0.00	0.00	0.00	0.00	0.00
HPLT-B2	0.00	0.00	0.00	0.00	0.00
HPLT-B3	0.00	0.00	0.00	0.00	0.00
HPLT-C1	6.00	8.96	7.97	9.52	6.45
HPLT-C2	4.75	5.92	5.45	2.78	2.17
HPLT-C3	0.00	0.00	0.00	0.00	0.00
MEAN VALUES	3.44	4.53	4.19	4.19	2.90
C.V.	6.59	8.73		8.00	

FREQUENCY: 44.44%

STATISTICAL VALUES	DOMINANCE (% COVER)	RELATIVE DOMINANCE (C)	RELATIVE DOMINANCE (C&CA)	RELATIVE DENSITY (C)	RELATIVE DENSITY (C&CA)
s^2	22.66	39.56	33.87	33.52	16.48
S	4.76	6.29	5.82	5.79	4.06
F-test	1.49; Acc H_0	2.71; Acc H_0	2.52; Acc H_0	4.06; Acc H_0	3.98; Acc H_0
t-test	0.77; Acc H_0	1.45; Acc H_0	1.38; Acc H_0	1.25; Acc H_0	1.24; Acc H_0
95% C.I.	0 - 7.10	0 - 9.36	0 - 8.66	0 - 8.64	0 - 6.02

C = corals only

CA = corals and coralline algae

s^2 , S = variance and standard deviation, respectively.

C.I. = confidence interval around the sample mean.

C.V. = s^2 / \bar{X} (coefficient of variation).

F- and t-tests compare the variances and means, respectively, of M. cavernosa population parameters at the CSA and BLM sites. H_0 = equal sample variances, or equal sample means.

FREQUENCY = percentage of all transects at the BLM site on which M. cavernosa occurred at least once.

TABLE B-4
CORAL POPULATION LEVEL PARAMETERS BY SITE, TAXON, AND TRANSECT
SITE - BLM SPECIES - Colpophyllia spp.

TRANSECT	DOMINANCE (% COVER)	RELATIVE DOMINANCE (C)	RELATIVE DOMINANCE (C&CA)	RELATIVE DENSITY (C)	RELATIVE DENSITY (C&CA)
HPLT-A1	7.00	9.38	8.96	12.50	10.00
HPLT-A2	11.37	14.99	13.89	22.22	13.33
HPLT-A3	0.00	0.00	0.00	0.00	0.00
HPLT-B1	23.12	27.38	27.22	13.64	13.04
HPLT-B2	0.00	0.00	0.00	0.00	0.00
HPLT-B3	11.50	19.62	17.29	8.82	6.38
HPLT-C1	0.00	0.00	0.00	0.00	0.00
HPLT-C2	12.50	15.58	14.35	16.67	13.04
HPLT-C3	0.00	0.00	0.00	0.00	0.00
MEAN VALUES	7.28	9.66	9.08	8.21	6.20
C.V.	9.01	11.00		8.92	

FREQUENCY: 55.56%

STATISTICAL VALUES	DOMINANCE (% COVER)	RELATIVE DOMINANCE (C)	RELATIVE DOMINANCE (C&CA)	RELATIVE DENSITY (C)	RELATIVE DENSITY (C&CA)
S ²	65.60	106.30	97.22	73.27	39.06
S	8.10	10.31	9.86	8.56	6.25
F-test	2.66; Acc H ₀	1.35; Acc H ₀	1.13; Acc H ₀	3.19; Acc H ₀	3.72; Acc H ₀
t-test	0.69; Acc H ₀	0.13; Acc H ₀	0.34; Acc H ₀	0.99; Acc H ₀	1.15; Acc H ₀
95% C.I.	1.06 -13.46	1.74 -17.58	1.50 -16.66	1.63 -14.79	1.40 -11.00

C = corals only

CA = corals and coralline algae

S², S = variance and standard deviation, respectively.

C.I. = confidence interval around the sample mean.

C.V. = s^2 / \bar{x} (coefficient of variation).

F- and t-tests compare the variances and means, respectively, of Colpophyllia spp. population parameters at the CSA and BLM sites. H₀ = equal sample variances, or equal sample means.

FREQUENCY = percentage of all transects at the BLM site on which Colpophyllia spp. occurred at least once.

TABLE B-5
CORAL POPULATION LEVEL PARAMETERS BY SITE, TAXON, AND TRANSECT
SITE - BLM SPECIES - Millepora spp.

TRANSECT	DOMINANCE (% COVER)	RELATIVE DOMINANCE (C)	RELATIVE DOMINANCE (C&CA)	RELATIVE DENSITY (C)	RELATIVE DENSITY (C&CA)
HPLT-A1	8.25	11.06	10.56	12.50	10.00
HPLT-A2	5.12	6.75	6.26	11.11	6.67
HPLT-A3	1.87	2.25	2.17	7.14	5.41
HPLT-B1	8.25	9.82	9.76	13.64	13.04
HPLT-B2	0.00	0.00	0.00	0.00	0.00
HPLT-B3	0.00	0.00	0.00	0.00	0.00
HPLT-C1	6.50	9.70	8.64	9.52	6.45
HPLT-C2	2.12	2.65	2.44	8.33	6.52
HPLT-C3	0.25	0.44	0.38	4.00	2.33
MEAN VALUES	3.60	4.74	4.47	7.36	5.60
C.V.	3.34	4.44		3.48	

FREQUENCY: 77.78%

STATISTICAL VALUES	DOMINANCE (% COVER)	RELATIVE DOMINANCE (C)	RELATIVE DOMINANCE (C&CA)	RELATIVE DENSITY (C)	RELATIVE DENSITY (C&CA)
s ²	12.04	21.07	19.01	25.60	18.84
S	3.47	4.59	4.36	5.06	4.34
F-test	3.10; Acc H ₀	2.62; Acc H ₀	2.48; Acc H ₀	1.52; Acc H ₀	1.23; Acc H ₀
t-test	0.74; Acc H ₀	0.82; Acc H ₀	0.73; Acc H ₀	1.74; Acc H ₀	1.31; Acc H ₀
95% C.I.	0.93 - 6.27	1.21 - 8.27	1.12 - 7.82	3.47 - 11.25	2.26 - 8.94

C = corals only

CA = corals and coralline algae

s², S = variance and standard deviation, respectively.

C.I. = confidence interval around the sample mean.

C.V. = s^2 / \bar{X} (coefficient of variation).

F- and t-tests compare the variances and means, respectively, of Millepora spp. population parameters at the CSA and BLM sites. H₀ = equal sample variances, or equal sample means.

FREQUENCY = percentage of all transects at the BLM site on which Millepora spp. occurred at least once.

TABLE B-6
CORAL POPULATION LEVEL PARAMETERS BY SITE, TAXON, AND TRANSECT
SITE - BLM SPECIES - Porites astreoides

TRANSECT	DOMINANCE (% COVER)	RELATIVE DOMINANCE (C)	RELATIVE DOMINANCE (C&CA)	RELATIVE DENSITY (C)	RELATIVE DENSITY (C&CA)
HPLT-A1	3.13	4.19	4.00	6.25	5.00
HPLT-A2	0.00	0.00	0.00	0.00	0.00
HPLT-A3	0.25	0.30	0.29	3.57	2.70
HPLT-B1	3.75	4.46	4.44	22.73	21.74
HPLT-B2	1.00	1.31	1.23	15.38	10.00
HPLT-B3	1.25	2.13	1.88	8.82	6.38
HPLT-C1	0.00	0.00	0.00	0.00	0.00
HPLT-C2	7.87	9.81	9.04	25.00	19.57
HPLT-C3	3.50	6.22	5.33	20.00	11.63
MEAN VALUES	2.31	3.16	2.91	11.31	8.56
C.V.	2.86	3.51		8.37	

FREQUENCY: 77.78%

STATISTICAL VALUES	DOMINANCE (% COVER)	RELATIVE DOMINANCE (C)	RELATIVE DOMINANCE (C&CA)	RELATIVE DENSITY (C)	RELATIVE DENSITY (C&CA)
s ²	6.61	11.09	9.30	94.67	63.04
S	2.57	3.33	3.05	9.73	7.94
F-test	4.16; Acc H ₀	1.27; Acc H ₀	1.55; Acc H ₀	1.21; Acc H ₀	1.76; Acc H ₀
t-test	0.77; Acc H ₀	0.07; Acc H ₀	0.12; Acc H ₀	0.11; Acc H ₀	0.15; Acc H ₀
95% C.I.	0.33 - 4.29	0.60 - 5.72	0.57 - 5.25	3.83 - 18.79	2.46 - 14.66

C = corals only

CA = corals and coralline algae

s², S = variance and standard deviation, respectively.

C.I. = confidence interval around the sample mean.

C.V. = s^2 / \bar{X} (coefficient of variation);

F- and t-tests compare the variances and means, respectively, of P. astreoides population parameters at the CSA and BLM sites. H₀ = equal sample variances, or equal sample means.

FREQUENCY = percentage of all transects at the BLM site on which P. astreoides occurred at least once.

TABLE B-7
CORAL POPULATION LEVEL PARAMETERS BY SITE, TAXON, AND TRANSECT
SITE - BLM SPECIES - Agaricia spp.

TRANSECT	DOMINANCE (% COVER)	RELATIVE DOMINANCE (C)	RELATIVE DOMINANCE (C&CA)	RELATIVE DENSITY (C)	RELATIVE DENSITY (C&CA)
HPLT-A1	0.00	0.00	0.00	0.00	0.00
HPLT-A2	0.00	0.00	0.00	0.00	0.00
HPLT-A3	0.00	0.00	0.00	0.00	0.00
HPLT-B1	0.00	0.00	0.00	0.00	0.00
HPLT-B2	0.50	0.65	0.62	7.69	5.00
HPLT-B3	3.25	5.54	4.89	17.65	12.77
HPLT-C1	0.37	0.56	0.50	4.76	3.23
HPLT-C2	1.75	2.18	2.01	8.33	6.52
HPLT-C3	1.12	2.00	1.71	12.00	6.98
MEAN VALUES	0.77	1.21	1.08	5.60	3.83
C.V.	1.60	2.77		7.25	

FREQUENCY: 55.56%

STATISTICAL VALUES	DOMINANCE (% COVER)	RELATIVE DOMINANCE (C)	RELATIVE DOMINANCE (C&CA)	RELATIVE DENSITY (C)	RELATIVE DENSITY (C&CA)
S ²	1.23	3.35	2.62	40.58	19.71
S	1.11	1.83	1.62	6.37	4.44
F-test	1.04; Acc H ₀	1.24; Acc H ₀	1.23; Acc H ₀	2.10; Acc H ₀	1.66; Acc H ₀
t-test	0.77; Acc H ₀	1.28; Acc H ₀	1.20; Acc H ₀	1.39; Acc H ₀	1.36; Acc H ₀
95% C.I.	0 - 1.62	0 - 2.62	0 - 2.33	0.70 - 10.50	0.42 - 7.24

C = corals only

CA = corals and coralline algae

S², S = variance and standard deviation, respectively.

C.I. = confidence interval around the sample mean.

C.V. = S^2 / \bar{X} (coefficient of variation).

F- and t-tests compare the variances and means, respectively, of Agaricia spp. population parameters at the CSA and BLM sites. H₀ = equal sample variances, or equal sample means.

FREQUENCY = percentage of all transects at the BLM site on which Agaricia spp. occurred at least once.

TABLE B-8
CORAL POPULATION LEVEL PARAMETERS BY SITE, TAXON, AND TRANSECT
SITE - BLM SPECIES - Madracis decactis

TRANSECT	DOMINANCE (% COVER)	RELATIVE DOMINANCE (C)	RELATIVE DOMINANCE (C&CA)	RELATIVE DENSITY (C)	RELATIVE DENSITY (C&CA)
HPLT-A1	0.00	0.00	0.00	0.00	0.00
HPLT-A2	0.00	0.00	0.00	0.00	0.00
HPLT-A3	26.00	31.23	30.10	28.57	21.62
HPLT-B1	11.00	13.10	13.02	9.09	8.70
HPLT-B2	0.00	0.00	0.00	0.00	0.00
HPLT-B3	1.75	2.99	2.63	8.82	6.38
HPLT-C1	1.12	1.68	1.50	4.76	3.23
HPLT-C2	0.00	0.00	0.00	0.00	0.00
HPLT-C3	0.00	0.00	0.00	0.00	0.00
MEAN VALUES	4.43	5.44	5.25	5.69	4.44
C.V.	17.64	20.50		15.53	

FREQUENCY: 44.44%

STATISTICAL VALUES	DOMINANCE (% COVER)	RELATIVE DOMINANCE (C)	RELATIVE DOMINANCE (C&CA)	RELATIVE DENSITY (C)	RELATIVE DENSITY (C&CA)
s^2	78.15	111.51	104.65	88.36	17.81
S	8.84	10.56	10.23	9.40	7.22
F-test	18.09; Rej H_0	10.47; Rej H_0	11.19; Rej H_0	1.17; Acc H_0	2.42; Acc H_0
t-test	1.13; Acc H_0	1.04; Acc H_0	1.05; Acc H_0	0.33; Acc H_0	0.37; Acc H_0
95% C.I.	0 - 11.23	0 - 13.56	0 - 13.11	0 - 12.92	0 - 9.99

C = corals only

CA = corals and coralline algae

s^2 , S = variance and standard deviation, respectively.

C.I. = confidence interval around the sample mean.

C.V. = s^2 / \bar{X} (coefficient of variation).

F- and t-tests compare the variances and means, respectively, of M. decactis population parameters at the CSA and BLM sites. H_0 = equal sample variances, or equal sample means.

FREQUENCY = percentage of all transects at the BLM site on which M. decactis occurred at least once.

TABLE B-9
CORAL POPULATION LEVEL PARAMETERS BY SITE, TAXON, AND TRANSECT
SITE - BLM SPECIES - Stephanocoenia michelini

TRANSECT	DOMINANCE (% COVER)	RELATIVE DOMINANCE (C)	RELATIVE DOMINANCE (C&CA)	RELATIVE DENSITY (C)	RELATIVE DENSITY (C&CA)
HPLT-A1	0.00	0.00	0.00	0.00	0.00
HPLT-A2	0.00	0.00	0.00	0.00	0.00
HPLT-A3	0.00	0.00	0.00	0.00	0.00
HPLT-B1	0.00	0.00	0.00	0.00	0.00
HPLT-B2	0.00	0.00	0.00	0.00	0.00
HPLT-B3	0.00	0.00	0.00	0.00	0.00
HPLT-C1	0.00	0.00	0.00	0.00	0.00
HPLT-C2	0.00	0.00	0.00	0.00	0.00
HPLT-C3	0.00	0.00	0.00	0.00	0.00
MEAN VALUES	0.00	0.00	0.00	0.00	0.00
C.V.					

FREQUENCY: 0%

STATISTICAL VALUES	DOMINANCE (% COVER)	RELATIVE DOMINANCE (C)	RELATIVE DOMINANCE (C&CA)	RELATIVE DENSITY (C)	RELATIVE DENSITY (C&CA)
S ²	0	0	0	0	0
S	0	0	0	0	0
F-test	∞; Rej H ₀	∞; Rej H ₀	∞; Rej H ₀	∞; Rej H ₀	∞; Rej H ₀
t-test	1.20; Acc H ₀	1.28; Acc H ₀	1.28; Acc H ₀	1.64; Acc H ₀	1.51; Acc H ₀
95% C.I.	—	—	—	—	—

C = corals only

CA = corals and coralline algae

S², S = variance and standard deviation, respectively.

C.I. = confidence interval around the sample mean.

C.V. = S^2 / \bar{X} (coefficient of variation).

F- and t-tests compare the variances and means, respectively, of S. michelini population parameters at the CSA and BLM sites. H₀ = equal sample variances, or equal sample means.

FREQUENCY = percentage of all transects at the BLM site on which S. michelini occurred at least once.

TABLE B-10
CORAL POPULATION LEVEL PARAMETERS BY SITE, TAXON, AND TRANSECT
SITE - BLM SPECIES - Siderastrea siderea

TRANSECT	DOMINANCE (% COVER)	RELATIVE DOMINANCE (C)	RELATIVE DOMINANCE (C&CA)	RELATIVE DENSITY (C)	RELATIVE DENSITY (C&CA)
HPLT-A1	0.00	0.00	0.00	0.00	0.00
HPLT-A2	0.00	0.00	0.00	0.00	0.00
HPLT-A3	0.00	0.00	0.00	0.00	0.00
HPLT-B1	0.00	0.00	0.00	0.00	0.00
HPLT-B2	0.00	0.00	0.00	0.00	0.00
HPLT-B3	0.00	0.00	0.00	0.00	0.00
HPLT-C1	0.00	0.00	0.00	0.00	0.00
HPLT-C2	0.00	0.00	0.00	0.00	0.00
HPLT-C3	0.00	0.00	0.00	0.00	0.00
MEAN VALUES	0.00	0.00	0.00	0.00	0.00
C.V.					

FREQUENCY: 0%

STATISTICAL VALUES	DOMINANCE (% COVER)	RELATIVE DOMINANCE (C)	RELATIVE DOMINANCE (C&CA)	RELATIVE DENSITY (C)	RELATIVE DENSITY (C&CA)
S ²	0	0	0	0	0
S	0	0	0	0	0
F-test	∞; Rej H ₀	∞; Rej H ₀	∞; Rej H ₀	∞; Rej H ₀	∞; Rej H ₀
t-test	1.03; Acc H ₀	1.02; Acc H ₀	1.02; Acc H ₀	1.00; Acc H ₀	1.00; Acc H ₀
95% C.I.	—	—	—	—	—

C = corals only

CA = corals and coralline algae

S², S = variance and standard deviation, respectively.

C.I. = confidence interval around the sample mean.

C.V. = S^2 / \bar{X} (coefficient of variation).

F- and t-tests compare the variances and means, respectively, of S. siderea population parameters at the CSA and BLM sites. H₀ = equal sample variances, or equal sample means.

FREQUENCY = percentage of all transects at the BLM site on which S. siderea occurred at least once.

TABLE B-11
CORAL POPULATION LEVEL PARAMETERS BY SITE, TAXON, AND TRANSECT
SITE - BLM SPECIES - Scolymia cubensis

TRANSECT	DOMINANCE (% COVER)	RELATIVE DOMINANCE (C)	RELATIVE DOMINANCE (C&CA)	RELATIVE DENSITY (C)	RELATIVE DENSITY (C&CA)
HPLT-A1	0.00	0.00	0.00	0.00	0.00
HPLT-A2	0.00	0.00	0.00	0.00	0.00
HPLT-A3	0.00	0.00	0.00	0.00	0.00
HPLT-B1	0.00	0.00	0.00	0.00	0.00
HPLT-B2	0.00	0.00	0.00	0.00	0.00
HPLT-B3	0.00	0.00	0.00	0.00	0.00
HPLT-C1	0.00	0.00	0.00	0.00	0.00
HPLT-C2	0.00	0.00	0.00	0.00	0.00
HPLT-C3	0.00	0.00	0.00	0.00	0.00
MEAN VALUES	0.00	0.00	0.00	0.00	0.00
C. V.					

FREQUENCY: 0%

STATISTICAL VALUES	DOMINANCE (% COVER)	RELATIVE DOMINANCE (C)	RELATIVE DOMINANCE (C&CA)	RELATIVE DENSITY (C)	RELATIVE DENSITY (C&CA)
s ²	0	0	0	0	0
S	0	0	0	0	0
F-test	∞; Rej H ₀	∞; Rej H ₀	∞; Rej H ₀	∞; Rej H ₀	∞; Rej H ₀
t-test	--	--	--	--	--
95% C.I.	--	--	--	--	--

C = corals only

CA = corals and coralline algae

s², S = variance and standard deviation, respectively.

C.I. = confidence interval around the sample mean.

C.V. = s^2 / \bar{X} (coefficient of variation).

F- and t-tests compare the variances and means, respectively, of S. cubensis population parameters at the CSA and BLM sites. H₀ = equal sample variances, or equal sample means.

FREQUENCY = percentage of all transects at the BLM site on which S. cubensis occurred at least once.

TABLE B-12
CORAL POPULATION LEVEL PARAMETERS BY SITE, TAXON, AND TRANSECT
SITE - BLM SPECIES - Mussa angulosa

TRANSECT	DOMINANCE (% COVER)	RELATIVE DOMINANCE (C)	RELATIVE DOMINANCE (C&CA)	RELATIVE DENSITY (C)	RELATIVE DENSITY (C&CA)
HPLT-A1	0.00	0.00	0.00	0.00	0.00
HPLT-A2	0.00	0.00	0.00	0.00	0.00
HPLT-A3	1.87	2.25	2.17	10.71	8.11
HPLT-B1	0.00	0.00	0.00	0.00	0.00
HPLT-B2	0.50	0.65	0.62	7.69	5.00
HPLT-B3	0.00	0.00	0.00	0.00	0.00
HPLT-C1	0.00	0.00	0.00	0.00	0.00
HPLT-C2	2.00	2.49	2.30	2.78	2.17
HPLT-C3	0.00	0.00	0.00	0.00	0.00
MEAN VALUES	0.49	0.60	0.57	2.35	1.70
C. V.	1.44	1.77		7.01	

FREQUENCY: 33.33%

STATISTICAL VALUES	DOMINANCE (% COVER)	RELATIVE DOMINANCE (C)	RELATIVE DOMINANCE (C&CA)	RELATIVE DENSITY (C)	RELATIVE DENSITY (C&CA)
s^2	0.71	1.06	0.94	16.48	8.70
S	0.84	1.03	0.97	4.06	2.95
F-test	∞ ; Rej H_0	∞ ; Rej H_0	∞ ; Rej H_0	∞ ; Rej H_0	∞ ; Rej H_0
t-test	1.75; Acc H_0	1.75; Acc H_0	1.76; Acc H_0	1.74; Acc H_0	1.73; Acc H_0
95% C.I.	0 - 1.14	0 - 1.39	0 - 1.32	0 - 5.47	0 - 3.97

C = corals only

CA = corals and coralline algae

s^2 , S = variance and standard deviation, respectively.

C.I. = confidence interval around the sample mean.

C.V. = s^2 / \bar{X} (coefficient of variation).

F- and t-tests compare the variances and means, respectively, of M. angulosa population parameters at the CSA and BLM sites. H_0 = equal sample variances, or equal sample means.

FREQUENCY = percentage of all transects at the BLM site on which M. angulosa occurred at least once.

TABLE B-13
 POPULATION LEVEL PARAMETERS: FILAMENTOUS ALGAE AND TOTAL LIVE CORAL
 SITE - BLM

TRANSECT	FILAMENTOUS ALGAE (PERCENT COVER)	TOTAL LIVE CORAL (PERCENT COVER)
HPLT - A1	21.50	74.62
HPLT - A2	16.75	75.85
HPLT - A3	11.87	83.23
HPLT - B1	8.12	83.99
HPLT - B2	9.87	76.62
HPLT - B3	30.00	58.62
HPLT - C1	23.62	66.98
HPLT - C2	8.12	80.23
HPLT - C3	28.25	56.24
MEAN VALUES	17.01	72.93
C.V.	5.07	1.42
FREQUENCY	100%	no value

STATISTICAL VALUES	FILAMENTOUS ALGAE (PERCENT COVER)	TOTAL LIVE CORAL (PERCENT COVER)
s^2	86.36	103.23
S	9.29	10.16
F-test	1.50; Acc H_0	1.55; Acc H_0
t-test	2.80; Rej H_0	4.89; Rej H_0
95% C.I.	9.87 - 24.15	53.02 - 92.84

s^2 , S = variance and standard deviation, respectively.

C.I. = confidence interval around the sample mean.

C.V. = s^2 / \bar{X} (coefficient of variation).

F- and t-tests compare the variances and means, respectively, of population level parameters for filamentous algae and live coral cover at the CSA and BLM sites. H_0 = equal sample variances, or equal sample means.

FREQUENCY = percentage of all transects at the BLM site on which the particular taxonomic group occurred at least once.

TABLE B-14
CORAL POPULATION LEVEL PARAMETERS BY SITE, TAXON, AND TRANSECT
SITE - CSA SPECIES - Montastrea annularis

TRANSECT	DOMI NANCE (% COVER)	RELATI VE DOMI NANCE (C)	RELATI VE DOMI NANCE (C&CA)	RELATI VE DENSITY (C)	RELATI VE DENSITY (C&CA)
HPLT-A1	15.87	23.69	22.48	26.92	21.21
HPLT-A2	24.00	34.35	32.99	27.78	20.00
HPLT-A3	12.87	20.93	19.14	23.53	16.00
HPLT-B1	18.87	45.21	39.43	24.00	15.38
HPLT-B2	20.25	50.78	37.85	47.83	28.95
HPLT-B3	22.12	52.52	45.85	34.62	26.47
HPLT-C1	20.12	35.62	32.53	15.38	11.43
HPLT-C2	30.87	48.62	40.96	45.00	30.00
HPLT-C3	22.37	51.73	42.22	20.00	11.76
MEAN VALUES	20.82	40.38	34.83	29.45	20.13
C.V.	1.24	3.69		4.10	

FREQUENCY: 100%

STATI STICAL VALUES	DOMI NANCE (% COVER)	RELATI VE DOMI NANCE (C)	RELATI VE DOMI NANCE (C&CA)	RELATI VE DENSITY (C)	RELATI VE DENSITY (C&CA)
S ²	25.91	148.84	81.36	120.96	50.27
S	5.09	12.20	9.02	10.99	7.09
F-test	3.84; Acc H ₀	1.72; Acc H ₀	2.28; Acc H ₀	1.01; Acc H ₀	1.05; Acc H ₀
t-test	6.99; Rej H ₀	3.75; Rej H ₀	4.68; Rej H ₀	3.07; Rej H ₀	3.63; Rej H ₀
95% C.I.	16.91-24.73	31.00-49.76	27.90-41.76	21.00-37.90	14.68-25.58

C = corals only

CA = corals and coralline algae

S², S = variance and standard deviation, respectively.

C.I. = confidence interval around the sample mean.

C.V. = s^2 / \bar{X} (coefficient of variation).

F- and t-tests compare the variances and means, respectively, of M. annularis population parameters at the CSA and BLM sites. H₀ = equal sample variances, or equal sample means.

FREQUENCY = percentage of all transects at the CSA site on which M. annularis occurred at least once.

TABLE B-15
CORAL POPULATION LEVEL PARAMETERS BY SITE, TAXON, AND TRANSECT
SITE - CSA SPECIES - Diploria strigosa

TRANSECT	DOMINANCE (% COVER)	RELATIVE DOMINANCE (C)	RELATIVE DOMINANCE (C&CA)	RELATIVE DENSITY (C)	RELATIVE DENSITY (C&CA)
HPLT-A1	24.62	36.75	34.87	7.69	6.06
HPLT-A2	21.50	30.77	29.55	11.11	8.00
HPLT-A3	38.37	62.40	57.06	47.06	32.00
HPLT-B1	3.87	9.28	8.09	12.00	7.69
HPLT-B2	0.37	0.94	0.70	4.35	2.63
HPLT-B3	4.87	11.57	10.10	11.54	8.82
HPLT-C1	1.87	3.32	3.03	7.69	5.71
HPLT-C2	25.87	40.75	34.33	25.00	16.67
HPLT-C3	6.25	14.45	11.79	10.00	5.88
MEAN VALUES	14.18	23.36	21.06	15.16	10.39
C.V.	13.06	18.10		11.62	

FREQUENCY: 100%

STATISTICAL VALUES	DOMINANCE (% COVER)	RELATIVE DOMINANCE (C)	RELATIVE DOMINANCE (C&CA)	RELATIVE DENSITY (C)	RELATIVE DENSITY (C&CA)
S^2	185.31	422.71	356.11	176.12	80.34
S	13.61	20.56	18.87	13.27	8.96
F-test	54.71; Rej H_0	76.54; Rej H_0	72.91; Rej H_0	3.92; Acc H_0	4.07; Acc H_0
t-test	2.28; Acc H_0	2.64; Rej H_0	2.57; Rej H_0	1.05; Acc H_0	1.05; Acc H_0
95% C.I.	3.72 - 24.64	7.56 - 39.16	6.55 - 35.57	4.96 - 25.36	3.50 - 17.28

C = corals only

CA = corals and coralline algae

S^2 , S = variance and standard deviation, respectively.

C.I. = confidence interval around the sample mean.

C.V. = S^2 / \bar{X} (coefficient of variation).

F- and t-tests compare the variances and means, respectively, of D. strigosa population parameters at the CSA and BLM sites. H_0 = equal sample variances, or equal sample means.

FREQUENCY = percentage of all transects at the CSA site on which D. strigosa occurred at least once.

TABLE B-16
CORAL POPULATION LEVEL PARAMETERS BY SITE, TAXON, AND TRANSECT
SITE - CSA SPECIES - Montastrea cavernosa

TRANSECT	DOMINANCE (% COVER)	RELATIVE DOMINANCE (C)	RELATIVE DOMINANCE (C&CA)	RELATIVE DENSITY (C)	RELATIVE DENSITY (C&CA)
HPLT-A1	0.87	1.31	1.24	3.85	3.03
HPLT-A2	16.87	24.15	23.20	33.33	24.00
HPLT-A3	0.00	0.00	0.00	0.00	0.00
HPLT-B1	8.87	21.26	18.54	24.00	15.38
HPLT-B2	0.00	0.00	0.00	0.00	0.00
HPLT-B3	5.25	12.46	10.88	7.69	5.88
HPLT-C1	7.00	12.39	11.31	7.69	5.71
HPLT-C2	0.00	0.00	0.00	0.00	0.00
HPLT-C3	9.50	21.97	17.92	10.00	5.88
MEAN VALUES	5.37	10.39	9.23	9.62	6.65
C. V.	6.31	10.31		14.13	

FREQUENCY: 66.67%

STATISTICAL VALUES	DOMINANCE (% COVER)	RELATIVE DOMINANCE (C)	RELATIVE DOMINANCE (C&CA)	RELATIVE DENSITY (C)	RELATIVE DENSITY (C&CA)
s^2	33.87	107.12	85.47	135.93	65.94
S	5.82	10.35	9.24	11.66	8.10
F-test	1.49; Acc H_0	2.71; Acc H_0	2.52; Acc H_0	4.06; Acc H_0	3.98; Acc H_0
t-test	0.77; Acc H_0	1.45; Acc H_0	1.38; Acc H_0	1.25; Acc H_0	1.24; Acc H_0
95% C.I.	0.90 - 9.84	2.43 - 18.34	2.12 - 16.34	0.66 - 18.58	0.42 - 12.88

C = corals only

CA = corals and coralline algae

s^2 , S = variance and standard deviation, respectively.

C.I. = confidence interval around the sample mean.

C.V. = s^2 / \bar{X} (coefficient of variation).

F- and t-tests compare the variances and means, respectively, of M. cavernosa population parameters at the CSA and BLM sites. H_0 = equal sample variances, or equal sample means.

FREQUENCY = percentage of all transects at the CSA site on which M. cavernosa occurred at least once.

TABLE B-17
CORAL POPULATION LEVEL PARAMETERS BY SITE, TAXON, AND TRANSECT
SITE - CSA SPECIES - Colpophyllia spp.

TRANSECT	DOMINANCE (% COVER)	RELATIVE DOMINANCE (C)	RELATIVE DOMINANCE (C&CA)	RELATIVE DENSITY (C)	RELATIVE DENSITY (C&CA)
HPLT-A1	8.75	13.06	12.39	3.85	3.03
HPLT-A2	4.00	5.72	5.50	5.56	4.00
HPLT-A3	0.00	0.00	0.00	0.00	0.00
HPLT-B1	5.50	13.17	11.49	12.00	7.69
HPLT-B2	14.50	36.36	27.10	8.70	5.26
HPLT-B3	4.00	9.50	8.29	3.85	2.94
HPLT-C1	9.00	15.93	14.55	11.54	8.57
HPLT-C2	0.00	0.00	0.00	0.00	0.00
HPLT-C3	0.00	0.00	0.00	0.00	0.00
MEAN VALUES	5.08	8.95	7.54	5.06	3.50
C.v.	4.86	16.04		4.53	

FREQUENCY: 66.67%

STATISTICAL VALUES	DOMINANCE (% COVER)	RELATIVE DOMINANCE (C)	RELATIVE DOMINANCE (C&CA)	RELATIVE DENSITY (C)	RELATIVE DENSITY (C&CA)
s^2	24.69	143.50	85.91	22.95	10.48
S	4.97	11.98	9.27	4.79	3.24
F-test	2.66; Acc H_0	1.35; Acc H_0	1.13; Acc H_0	3.19; Acc H_0	3.72; Acc H_0
t-test	0.69; Acc H_0	0.13; Acc H_0	0.34; Acc H_0	0.99; Acc H_0	1.15; Acc H_0
95% C.I.	1.26 - 8.90	0 - 18.16	0.42 - 14.66	1.38 - 8.74	1.01 - 5.99

C = corals only

CA = corals and coralline algae

s^2 , S = variance and standard deviation, respectively.

C.I. = confidence interval around the sample mean.

C.v. = s^2 / \bar{X} (coefficient of variation)

F- and t-tests compare the variances and means, respectively, of Colpophyllia spp. population parameters at the CSA and BLM sites. H_0 = equal sample variances, or equal sample means.

FREQUENCY = percentage of all transects at the CSA site on which Colpophyllia spp. occurred at least once.

TABLE B-18
CORAL POPULATION LEVEL PARAMETERS BY SITE, TAXON, AND TRANSECT
SITE - CSA SPECIES - Millepora spp.

TRANSECT	DOMINANCE (% COVER)	RELATIVE DOMINANCE (C)	RELATIVE DOMINANCE (C&CA)	RELATIVE DENSITY (C)	RELATIVE DENSITY (C&CA)
HPLT-A1	16.75	8.21	7.79	15.38	12.12
HPLT-A2	3.25	4.65	4.47	16.67	12.00
HPLT-A3	8.87	14.43	13.20	11.76	8.00
HPLT-B1	2.50	5.99	5.22	8.00	5.13
HPLT-B2	0.75	1.88	1.40	4.35	2.63
HPLT-B3	0.50	1.19	1.04	3.85	2.94
HPLT-C1	13.25	23.45	21.41	23.08	17.14
HPLT-C2	0.87	1.38	1.16	15.00	10.00
HPLT-C3	1.25	2.89	2.36	10.00	5.88
MEAN VALUES	5.33	7.12	6.45	12.01	8.43
C.V.	7.00	7.75		3.23	

FREQUENCY: 100%

STATISTICAL VALUES	DOMINANCE (% COVER)	RELATIVE DOMINANCE (C)	RELATIVE DOMINANCE (C&CA)	RELATIVE DENSITY (C)	RELATIVE DENSITY (C&CA)
s^2	37.36	55.26	47.01	38.75	23.23
S	6.11	7.43	6.86	6.23	4.82
F-test	3.10; Acc H_0	2.62; Acc H_0	2.48; Acc H_0	1.52; Acc H_0	1.23; Acc H_0
t-test	0.74; Acc H_0	0.82; Acc H_0	0.73; Acc H_0	1.74; Acc H_0	1.31; Acc H_0
95% C.I.	0.70 - 7.46	1.04 - 12.83	1.18 - 11.72	7.23 - 16.79	4.72 - 12.14

C = corals only

CA = corals and coralline algae

s^2 , S = variance and standard deviation, respectively.

C.I. = confidence interval around the sample mean.

C.V. = s^2 / \bar{X} (coefficient of variation).

F- and t-tests compare the variances and means, respectively, of Millepora spp. population parameters at the CSA and BLM sites. H_0 = equal sample variances, or equal sample means.

FREQUENCY = percentage of all transects at the CSA site on which Millepora spp. occurred at least once.

TABLE B-19
CORAL POPULATION LEVEL PARAMETERS BY SITE, TAXON, AND TRANSECT
SITE - CSA SPECIES - Porites astreoides

TRANSECT	DOMINANCE (% COVER)	RELATIVE DOMINANCE (C)	RELATIVE DOMINANCE (C&CA)	RELATIVE DENSITY (C)	RELATIVE DENSITY (C&CA)
HPLT-A1	2.50	3.73	3.54	15.38	12.12
HPLT-A2	0.25	0.36	0.34	5.56	4.00
HPLT-A3	0.25	0.41	0.37	5.88	4.00
HPLT-B1	0.00	0.00	0.00	0.00	0.00
HPLT-B2	2.50	6.27	4.67	17.39	10.53
HPLT-B3	3.37	8.01	6.99	23.08	17.65
HPLT-C1	0.87	1.55	1.41	3.85	2.86
HPLT-C2	1.87	2.95	2.49	10.00	6.67
HPLT-C3	2.62	6.07	4.95	25.00	14.71
MEAN VALUES	1.58	3.26	2.75	11.79	8.06
C. V.	1.00	3.69		6.63	

FREQUENCY: 88.89%

STATISTICAL VALUES	DOMINANCE (% COVER)	RELATIVE DOMINANCE (C)	RELATIVE DOMINANCE (C&CA)	RELATIVE DENSITY (C)	RELATIVE DENSITY (C&CA)
S ²	1.58	8.74	6.00	78.15	35.71
S	1.26	2.96	2.45	8.84	5.98
F-test	4.16; Acc H ₀	1.27; Acc H ₀	1.55; Acc H ₀	1.21; Acc H ₀	1.76; Acc H ₀
t-test	0.77; Acc H ₀	0.07; Acc H ₀	0.12; Acc H ₀	0.11; Acc H ₀	0.15; Acc H ₀
95% C.I.	0.62 - 2.54	0.99 - 5.53	0.87 - 4.63	4.99 - 18.59	3.47 - 12.65

C = corals only

CA = corals and coralline algae

S², S = variance and standard deviation, respectively.

C.I. = confidence interval around the sample mean.

C.V. = S^2 / \bar{X} (coefficient of variation).

F- and t-tests compare the variances and means, respectively, of P. astreoides population parameters at the CSA and BLM sites. H₀ = equal sample variances, or equal sample means.

FREQUENCY = percentage of all transects at the CSA site on which P. astreoides occurred at least once.

TABLE B-20
CORAL POPULATION LEVEL PARAMETERS BY SITE, TAXON, AND TRANSECT
SITE - CSA SPECIES - Agaricia spp.

TRANSECT	DOMINANCE (% COVER)	RELATIVE DOMINANCE (C)	RELATIVE DOMINANCE (C&CA)	RELATIVE DENSITY (C)	RELATIVE DENSITY (C&CA)
HPLT-A1	3.25	4.85	4.60	11.54	9.09
HPLT-A2	0.00	0.00	0.00	0.00	0.00
HPLT-A3	1.12	1.83	1.67	11.76	8.00
HPLT-B1	2.12	5.09	4.44	20.00	12.82
HPLT-B2	1.50	3.76	2.80	17.39	10.53
HPLT-B3	1.25	2.97	2.59	11.54	8.82
HPLT-C1	0.00	0.00	0.00	0.00	0.00
HPLT-C2	0.00	0.00	0.00	0.00	0.00
HPLT-C3	1.25	2.89	2.36	25.00	14.71
MEAN VALUES	1.17	2.38	2.05	10.80	7.11
C.V.	1.02	1.75		7.89	

FREQUENCY: 66.67%

STATISTICAL VALUES	DOMINANCE (% COVER)	RELATIVE DOMINANCE (C)	RELATIVE DOMINANCE (C&CA)	RELATIVE DENSITY (C)	RELATIVE DENSITY (C&CA)
s^2	1.18	4.16	3.24	85.21	32.67
S	1.09	2.04	1.80	9.23	5.72
F-test	1.04; Acc H_0	1.24; Acc H_0	1.23; Acc H_0	2.10; Acc H_0	1.66; Acc H_0
t-test	0.77; Acc H_0	1.28; Acc H_0	1.20; Acc H_0	1.39; Acc H_0	1.36; Acc H_0
95% C.I.	0.33 - 2.01	0.81 - 3.95	0.67 - 3.43	3.70 - 17.89	2.72 - 11.50

C = corals only

CA = corals and coralline algae

s^2 , S = variance and standard deviation, respectively.

C.I. = confidence interval around the sample mean.

C.V. = s^2 / \bar{X} (coefficient of variation).

F- and t-tests compare the variances and means, respectively, of Agaricia spp. population parameters at the CSA and BLM sites. H_0 = equal sample variances, or equal sample means.

FREQUENCY = percentage of all transects at the CSA site on which Agaricia spp. occurred at least once.

TABLE B-21
CORAL POPULATION LEVEL PARAMETERS BY SITE, TAXON, AND TRANSECT
SITE - CSA SPECIES - Madracis decactis

TRANSECT	DOMINANCE (% COVER)	RELATIVE DOMINANCE (C)	RELATIVE DOMINANCE (C&CA)	RELATIVE DENSITY (C)	RELATIVE DENSITY (C&CA)
HPLT-A1	5.62	8.40	7.96	15.38	12.12
HPLT-A2	0.00	0.00	0.00	0.00	0.00
HPLT-A3	0.00	0.00	0.00	0.00	0.00
HPLT-B1	0.00	0.00	0.00	0.00	0.00
HPLT-B2	0.00	0.00	0.00	0.00	0.00
HPLT-B3	0.00	0.00	0.00	0.00	0.00
HPLT-C1	3.50	6.19	5.66	23.08	17.14
HPLT-C2	0.00	0.00	0.00	0.00	0.00
HPLT-C3	0.00	0.00	0.00	0.00	0.00
MEAN VALUES	1.01	1.62	1.51	4.27	3.25
C. V.	4.28	6.56		17.73	

FREQUENCY: 22.22%

STATISTICAL VALUES	DOMINANCE (% COVER)	RELATIVE DOMINANCE (C)	RELATIVE DOMINANCE (C&CA)	RELATIVE DENSITY (C)	RELATIVE DENSITY (C&CA)
s^2	4.32	10.65	9.35	75.61	43.19
S	2.08	3.26	3.06	8.70	6.57
F-test	18.09; Rej H_0	10.47; Rej H_0	11.19; Rej H_0	1.17; Acc H_0	2.42; Acc H_0
t-test	1.13; Acc H_0	1.04; Acc H_0	1.05; Acc H_0	0.33; Acc H_0	0.37; Acc H_0
95% C.I.	0 - 2.61	0 - 4.13	0 - 3.86	0 - 10.92	0 - 8.30

C = corals only

CA = corals and coralline algae

S^2 , S = variance and standard deviation, respectively.

C.I. = confidence interval around the sample mean.

C.V. = s^2 / \bar{X} (coefficient of variation).

F- and t-tests compare the variances and means, respectively, of M. decactis population parameters at the CSA and BLM sites. H_0 = equal sample variances, or equal sample means.

FREQUENCY = percentage of all transects at the CSA site on which M. decactis occurred at least once.

TABLE B-22
CORAL POPULATION LEVEL PARAMETERS BY SITE, TAXON, AND TRANSECT
SITE - CSA SPECIES - Stephanocoenia michelini

TRANSECT	DOMINANCE (% COVER)	RELATIVE DOMINANCE (C)	RELATIVE DOMINANCE (C&CA)	RELATIVE DENSITY (C)	RELATIVE DENSITY (C&CA)
HPLT-A1	0.00	0.00	0.00	0.00	0.00
HPLT-A2	0.00	0.00	0.00	0.00	0.00
HPLT-A3	0.00	0.00	0.00	0.00	0.00
HPLT-B1	0.00	0.00	0.00	0.00	0.00
HPLT-B2	0.00	0.00	0.00	0.00	0.00
HPLT-B3	0.75	1.78	1.55	3.85	2.94
HPLT-C1	0.00	0.00	0.00	0.00	0.00
HPLT-C2	4.00	6.30	5.31	5.00	3.33
HPLT-C3	0.00	0.00	0.00	0.00	0.00
MEAN VALUES	0.53	0.90	0.76	0.98	0.70
C.V.	3.34	4.95		3.27	

FREQUENCY: 22.22%

STATISTICAL VALUES	DOMINANCE (% COVER)	RELATIVE DOMINANCE (C)	RELATIVE DOMINANCE (C&CA)	RELATIVE DENSITY (C)	RELATIVE DENSITY (C&CA)
s^2	1.76	4.45	3.17	3.89	1.92
S	1.33	2.11	1.78	1.79	1.39
F-test	∞ ; Rej H_0	∞ ; Rej H_0	∞ ; Rej H_0	∞ ; Rej H_0	∞ ; Rej H_0
t-test	1.20; Acc H_0	1.28; Acc H_0	1.28; Acc H_0	1.64; Acc H_0	1.51; Acc H_0
95% C.I.	0 - 1.55	0 - 2.52	0 - 2.13	0 - 2.50	0 - 1.76

C = corals only

CA = corals and coralline algae

s^2 , S = variance and standard deviation, respectively.

C.I. = confidence interval around the sample mean.

C.V. = s^2 / \bar{X} (coefficient of variation).

F- and t-tests compare the variances and means, respectively, of S. michelini population parameters at the CSA and BLM sites. H_0 = equal sample variances, or equal sample means.

FREQUENCY = percentage of all transects at the CSA site on which S. michelini occurred at least once.

TABLE B-23
CORAL POPULATION LEVEL PARAMETERS BY SITE, TAXON, AND TRANSECT
SITE - CSA SPECIES - Siderastrea siderea

TRANSECT	DOMINANCE (% COVER)	RELATIVE DOMINANCE (C)	RELATIVE DOMINANCE (C&CA)	RELATIVE DENSITY (C)	RELATIVE DENSITY (C&CA)
HPLT-A1	0.00	0.00	0.00	0.00	0.00
HPLT-A2	0.00	0.00	0.00	0.00	0.00
HPLT-A3	0.00	0.00	0.00	0.00	0.00
HPLT-B1	0.00	0.00	0.00	0.00	0.00
HPLT-B2	0.00	0.00	0.00	0.00	0.00
HPLT-B3	0.00	0.00	0.00	0.00	0.00
HPLT-C1	0.87	1.51	1.41	7.69	5.71
HPLT-C2	0.00	0.00	0.00	0.00	0.00
HPLT-C3	0.00	0.00	0.00	0.00	0.00
MEAN VALUES	0.10	0.17	0.16	0.85	0.63
C.V.	0.84	1.47		7.71	

FREQUENCY: 22.22%

STATISTICAL VALUES	DOMINANCE (% COVER)	RELATIVE DOMINANCE (C)	RELATIVE DOMINANCE (C&CA)	RELATIVE DENSITY (C)	RELATIVE DENSITY (C&CA)
S^2	0.084	0.25	0.22	6.57	3.62
S	0.29	0.50	0.47	2.56	1.90
F-test	∞ ; Rej H_0	∞ ; Rej H_0	∞ ; Rej H_0	∞ ; Rej H_0	∞ ; Rej H_0
t-test	1.03; Acc H_0	1.02; Acc H_0	1.02; Acc H_0	1.00; Acc H_0	1.00; Acc H_0
95% C.I.	0 - 0.32	0 - 0.56	0 - 0.52	0 - 2.82	0 - 2.09

C = corals only

CA = corals and coralline algae

S^2 , S = variance and standard deviation, respectively.

C.I. = confidence interval around the sample mean.

C.V. = S^2 / \bar{X} (coefficient of variation).

F- and t-tests compare the variances and means, respectively, of S. siderea population parameters at the CSA and BLM sites. H_0 = equal sample variances, or equal sample means.

FREQUENCY = percentage of all transects at the CSA site on which S. siderea occurred at least once.

TABLE B-24
CORAL POPULATION LEVEL PARAMETERS BY SITE, TAXON, AND TRANSECT
SITE - CSA SPECIES - Scolymia cubensis

TRANSECT	DOMINANCE (% COVER)	RELATIVE DOMINANCE (C)	RELATIVE DOMINANCE (C&CA)	RELATIVE DENSITY (C)	RELATIVE DENSITY (C&CA)
HPLT-A1	0.00	0.00	0.00	0.00	0.00
HPLT-A2	0.00	0.00	0.00	0.00	0.00
HPLT-A3	0.00	0.00	0.00	0.00	0.00
HPLT-B1	0.00	0.00	0.00	0.00	0.00
HPLT-B2	0.00	0.00	0.00	0.00	0.00
HPLT-B3	0.00	0.00	0.00	0.00	0.00
HPLT-C1	0.00	0.00	0.00	0.00	0.00
HPLT-C2	0.00	0.00	0.00	0.00	0.00
HPLT-C3	0.00	0.00	0.00	0.00	0.00
MEAN VALUES	0.00	0.00	0.00	0.00	0.00
C.V.	—	—	—	—	—

FREQUENCY: 0%

STATISTICAL VALUES	DOMINANCE (% COVER)	RELATIVE DOMINANCE (C)	RELATIVE DOMINANCE (C&CA)	RELATIVE DENSITY (C)	RELATIVE DENSITY (C&CA)
s ²	0	0	0	0	0
S	0	0	0	0	0
F-test	∞; Rej H ₀	∞; Rej H ₀	∞; Rej H ₀	∞; Rej H ₀	∞; Rej H ₀
t-test	—	—	—	—	—
95% C.I.	—	—	—	—	—

C = corals only

CA = corals and coralline algae

s², S = variance and standard deviation, respectively.

C.I. = confidence interval around the sample mean.

C.V. = s^2 / \bar{X} (coefficient of variation).

F- and t-tests compare the variances and means, respectively, of S. cubensis population parameters at the CSA and BLM sites. H₀ = equal sample variances, or equal sample means.

FREQUENCY = percentage of all transects at the CSA site on which S. cubensis occurred at least once.

TABLE B-25
CORAL POPULATION LEVEL PARAMETERS BY SITE, TAXON, AND TRANSECT
SITE - CSA SPECIES - Mussa angulosa

TRANSECT	DOMINANCE (% COVER)	RELATIVE DOMINANCE (C)	RELATIVE DOMINANCE (C&CA)	RELATIVE DENSITY (C)	RELATIVE DENSITY (C&CA)
HPLT-A1	0.00	0.00	0.00	0.00	0.00
HPLT-A2	0.00	0.00	0.00	0.00	0.00
HPLT-A3	0.00	0.00	0.00	0.00	0.00
HPLT-B1	0.00	0.00	0.00	0.00	0.00
HPLT-B2	0.00	0.00	0.00	0.00	0.00
HPLT-B3	0.00	0.00	0.00	0.00	0.00
HPLT-C1	0.00	0.00	0.00	0.00	0.00
HPLT-C2	0.00	0.00	0.00	0.00	0.00
HPLT-C3	0.00	0.00	0.00	0.00	0.00
MEAN VALUES	0.00	0.00	0.00	0.00	0.00
C.V.	--	--	--	--	--

FREQUENCY: 0%

STATISTICAL VALUES	DOMINANCE (% COVER)	RELATIVE DOMINANCE (C)	RELATIVE DOMINANCE (C&CA)	RELATIVE DENSITY (C)	RELATIVE DENSITY (C&CA)
s ²	0	0	0	0	0
S	0	0	0	0	0
F-test	∞; Rej H ₀	∞; Rej H ₀	∞; Rej H ₀	∞; Rej H ₀	∞; Rej H ₀
t-test	1.75; Acc H ₀	1.75; Acc H ₀	1.76; Acc H ₀	1.74; Acc H ₀	1.73; Acc H ₀
95% C.I.	--	--	--	--	--

C = corals only

CA = corals and coralline algae

s², S = variance and standard deviation, respectively.

C.I. = confidence interval around the sample mean.

C.V. = s^2 / \bar{X} (coefficient of variation).

F- and t-tests compare the variances and means, respectively, of M. angulosa population parameters at the CSA and BLM sites. H₀ = equal sample variances, or equal sample means.

FREQUENCY = percentage of all transects at the CSA site on which M. angulosa occurred at least once.

TABLE B-26
 POPULATION LEVEL PARAMETERS: FILAMENTOUS ALGAE AND TOTAL LIVE CORAL
 SITE - CSA

TRANSECT	FILAMENTOUS ALGAE (PERCENT COVER)	TOTAL LIVE CORAL (PERCENT COVER)
HPLT - A1	10.87	66.98
HPLT - A2	19.37	72.74
HPLT - A3	29.25	61.48
HPLT - B1	45.75	41.73
HPLT - B2	39.50	39.87
HPLT - B3	37.62	42.11
HPLT - C1	33.37	56.48
HPLT - C2	21.75	63.48
HPLT - C3	39.12	43.24
MEAN VALUES	30.73	54.23
C.V.	4.21	2.95
FREQUENCY	100%	

STATISTICAL VALUES	FILAMENTOUS ALGAE (PERCENT COVER)	TOTAL LIVE CORAL (PERCENT COVER)
s^2	129.21	159.77
S	11.37	12.64
F-test	1.50; Acc H_0	1.55; Acc H_0
t-test	2.80; Rej H_0	4.89; Rej H_0
95% C.I.	22.00 - 39.47	29.46 - 79.00

s^2 , S = variance and standard deviation, respectively.

C.I. = confidence interval around the sample mean.

C.V. = s^2 / \bar{X} (coefficient of variation).

F- and t-tests compare the variances and means, respectively, of population level parameters for filamentous algae and live coral cover at the CSA and BLM sites. H_0 = equal sample variances, or equal sample means.

FREQUENCY = percentage of all transects at the CSA site on which the particular taxonomic group occurred at least once.

TABLE B-27
CORAL POPULATION LEVEL PARAMETERS AT THE FLOWER GARDEN BANKS
SPECIES - Montastrea annularis

TRANSECT	DOMINANCE (% COVER)	RELATIVE DOMINANCE (C)	RELATIVE DOMINANCE (C&CA)	RELATIVE DENSITY (C)	RELATIVE DENSITY (C&CA)
BANK: EFG					
MEAN VALUES	33.86	52.94	47.57	37.38	26.27
C. V.	7.06	6.75		4.80	
STATISTICAL VALUES					
s ²	239.07	357.46	297.46	179.64	88.21
S	15.46	18.90	17.25	13.40	9.39
F-test	1.78; Acc H ₀	1.60; Acc H ₀	1.71; Acc H ₀	2.26; Acc H ₀	2.57; Acc H ₀
t-test	0.20; Acc H ₀	0.23; Acc H ₀	0.29; Acc H ₀	0.44; Acc H ₀	0.33; Acc H ₀
95% C.I.	26.17 - 41.55	43.54 - 62.34	38.99 - 56.15	30.71 - 44.04	21.60 - 30.94
FREQUENCY: 100%					
BANK: WFG					
HPLT-A1	6.12	17.95	14.20	30.00	13.04
HPLT-A2	22.75	44.83	32.85	37.04	21.28
HPLT-A3	28.75	65.90	44.92	33.33	16.13
HPLT-A4	29.37	57.46	50.43	41.18	22.58
HPLT-A5	68.75	91.36	83.46	68.42	48.15
HPLT-A6	60.37	79.05	67.74	73.68	50.00
HPLT-B1	7.25	28.86	23.02	38.89	24.14
HPLT-B2	52.75	77.01	71.16	52.17	33.33
HPLT-B3	14.87	30.26	20.65	50.00	33.33
HPLT-B4	11.62	22.52	19.62	20.00	12.50
HPLT-B5	32.87	69.39	56.80	61.54	43.24
HPLT-B6	6.50	15.29	12.41	21.43	9.09
HPLT-C1	25.37	41.51	34.18	15.38	7.41
HPLT-C2	52.75	73.78	64.53	69.47	50.00
HPLT-C3	57.37	82.41	71.72	25.81	17.02
HPLT-C4	55.62	71.09	66.62	11.11	6.82
HPLT-C5	37.12	61.36	55.10	54.17	29.55
HPLT-C6	17.12	52.29	32.46	14.81	10.00
MEAN VALUES	32.63	54.57	45.66	39.91	24.87
C. V.	13.07	10.47		10.17	
STATISTICAL VALUES					
s ²	426.34	571.17	509.37	405.92	226.94
S	20.65	23.90	22.57	20.15	15.06
F-test	1.78; Acc H ₀	1.60; Acc H ₀	1.71; Acc H ₀	2.26; Acc H ₀	2.57; Acc H ₀
t-test	0.20; Acc H ₀	0.23; Acc H ₀	0.29; Acc H ₀	0.44; Acc H ₀	0.33; Acc H ₀
95% C.I.	22.45 - 42.93	42.68 - 66.46	34.44 - 56.88	29.89 - 49.93	17.38 - 32.36
FREQUENCY: 100%					

The symbols and abbreviations used are the same as presented in previous tables.

TABLE B-28
CORAL POPULATION LEVEL PARAMETERS AT THE FLOWER GARDEN BANKS
SPECIES - Diploria strigosa

TRANSECT	DOMINANCE (% COVER)	RELATIVE DOMINANCE (C)	RELATIVE DOMINANCE (C&CA)	RELATIVE DENSITY (C)	RELATIVE DENSITY (C&CA)
BANK: EFG					
MEAN VALUES	8.95	14.25	12.91	12.56	8.64
C. V.	13.15	20.30		8.84	
STATISTICAL VALUES					
S ²	111.14	273.29	226.86	104.95	47.53
S	10.85	17.01	15.50	10.54	7.09
F-test	2.34; Acc H ₀	2.22; Acc H ₀	2.39; Acc H ₀	1.14; Acc H ₀	1.52; Acc H ₀
t-test	1.14; Acc H ₀	0.98; Acc H ₀	1.09; Acc H ₀	1.18; Acc H ₀	1.66; Acc H ₀
95% C.I.	3.56 - 14.35	5.79 - 22.71	5.20 - 20.62	7.32 - 17.80	5.11 - 12.17
FREQUENCY: 100%					
BANK: WFG					
HPLT-A1	0.00	0.00	0.00	0.00	0.00
HPLT-A2	4.25	8.37	6.14	11.11	6.38
HPLT-A3	0.00	0.00	0.00	0.00	0.00
HPLT-A4	13.37	26.16	22.96	17.65	9.68
HPLT-A5	0.00	0.00	0.00	0.00	0.00
HPLT-A6	6.75	8.84	7.57	5.26	3.57
HPLT-B1	3.50	13.93	11.11	23.08	11.11
HPLT-B2	4.25	6.20	5.73	4.35	3.13
HPLT-B3	0.00	0.00	0.00	0.00	0.00
HPLT-B4	0.00	0.00	0.00	0.00	0.00
HPLT-B5	6.00	12.66	10.37	25.00	13.64
HPLT-B6	3.62	8.53	6.92	7.41	5.00
HPLT-C1	18.37	30.06	24.75	13.89	8.62
HPLT-C2	0.00	0.00	0.00	0.00	0.00
HPLT-C3	0.00	0.00	0.00	0.00	0.00
HPLT-C4	18.25	23.32	21.86	26.67	16.67
HPLT-C5	20.00	33.06	29.68	19.23	13.51
HPLT-C6	0.00	0.00	0.00	0.00	0.00
MEAN VALUES	5.46	9.51	8.18	8.54	5.07
C. V.	9.21	13.70		11.41	
STATISTICAL VALUES					
S ²	50.28	130.10	100.64	97.46	33.12
S	7.09	11.41	10.03	9.87	5.76
F-test	2.34; Acc H ₀	2.22; Acc H ₀	2.39; Acc H ₀	1.14; Acc H ₀	1.52; Acc H ₀
t-test	1.14; Acc H ₀	0.98; Acc H ₀	1.09; Acc H ₀	1.18; Acc H ₀	1.66; Acc H ₀
95% C.I.	1.93 - 8.99	3.84 - 15.18	3.19 - 13.17	3.63 - 13.45	2.21 - 7.93
FREQUENCY: 55.56%					

The symbols and abbreviations used are the same as presented in previous tables.

TABLE B-29
CORAL POPULATION LEVEL PARAMETERS AT THE FLOWER GARDEN BANKS
SPECIES - Montastrea cavernosa

TRANSECT	DOMINANCE (% COVER)	RELATIVE DOMINANCE (C)	RELATIVE DOMINANCE (C&CA)	RELATIVE DENSITY (C)	RELATIVE DENSITY (C&CA)
BANK: EFG					
MEAN VALUES	4.41	7.46	6.71	6.90	4.78
C.V.	6.25	10.48		12.70	
STATISTICAL VALUES					
S ²	26.05	73.72	59.38	82.68	40.02
S	5.25	8.84	7.93	9.36	6.51
F-test	1.16; Acc H ₀	1.95; Acc H ₀	1.33; Acc H ₀	1.57; Acc H ₀	1.01; Acc H ₀
t-test	0.17; Acc H ₀	0.38; Acc H ₀	0.03; Acc H ₀	0.93; Acc H ₀	0.43; Acc H ₀
95% C.I.	1.80 - 7.02	3.07 - 11.85	2.77 - 10.65	2.25 - 11.55	1.54 - 8.02
FREQUENCY: 55.56%					
BANK: WFG					
HPLT-A1	3.87	11.36	8.99	30.00	13.04
HPLT-A2	8.12	16.01	11.73	22.22	12.77
HPLT-A3	3.75	8.60	5.86	8.33	3.23
HPLT-A4	4.87	9.54	8.37	5.88	3.23
HPLT-A5	0.00	0.00	0.00	0.00	0.00
HPLT-A6	0.00	0.00	0.00	0.00	0.00
HPLT-B1	0.00	0.00	0.00	0.00	0.00
HPLT-B2	4.87	7.12	6.58	8.70	6.25
HPLT-B3	18.87	35.70	24.35	19.35	12.77
HPLT-B4	0.00	0.00	0.00	0.00	0.00
HPLT-B5	0.00	0.00	0.00	0.00	0.00
HPLT-B6	16.62	39.12	31.74	25.93	17.50
HPLT-C1	0.00	0.00	0.00	0.00	0.00
HPLT-C2	0.00	0.00	0.00	0.00	0.00
HPLT-C3	0.00	0.00	0.00	0.00	0.00
HPLT-C4	2.87	3.67	3.44	26.67	16.67
HPLT-C5	2.25	3.72	3.34	7.69	5.41
HPLT-C6	7.75	23.66	14.69	28.57	12.12
MEAN VALUES	4.10	8.81	6.62	10.18	5.72
C.V.	7.18	17.34		13.52	
STATISTICAL VALUES					
S ²	32.07	152.79	83.38	137.62	42.77
S	5.66	12.36	9.13	11.73	6.54
F-test	1.16; Acc H ₀	1.95; Acc H ₀	1.33; Acc H ₀	1.57; Acc H ₀	1.01; Acc H ₀
t-test	0.17; Acc H ₀	0.38; Acc H ₀	0.03; Acc H ₀	0.93; Acc H ₀	0.43; Acc H ₀
95% C.I.	1.28 - 6.92	2.66 - 14.96	2.08 - 11.16	4.35 - 16.00	2.47 - 8.97
FREQUENCY: 55.56%					

The symbols and abbreviations used are the same as presented in previous tables.

TABLE B-30
CORAL POPULATION LEVEL PARAMETERS AT THE FLOWER GARDEN BANKS
SPECIES - Colpophyllia spp.

TRANSECT	DOMINANCE (% COVER)	RELATIVE DOMINANCE (C)	RELATIVE DOMINANCE (C&CA)	RELATIVE DENSITY (C)	RELATIVE DENSITY (C&CA)
BANK: EFG					
MEAN VALUES	6.18	9.31	8.31	6.63	4.85
C.V.	7.09	12.64		7.22	
STATISTICAL VALUES					
S ²	43.76	111.13	81.96	45.21	23.85
S	6.62	10.85	9.32	6.92	5.02
F-test	12.14; Rej H ₀	9.72; Rej H ₀	10.19; Rej H ₀	2.12; Acc H ₀	2.64; Acc H ₀
t-test	3.12; Rej H ₀	2.72; Rej H ₀	2.88; Rej H ₀	1.77; Acc H ₀	2.04; Rej H ₀
95% C.I.	2.89 - 9.45	3.92 - 14.70	3.68 - 12.94	3.19 - 10.07	2.35 - 7.35
FREQUENCY: 61.11%					
BANK: WFG					
HPLT-A1	0.00	0.00	0.00	0.00	0.00
HPLT-A2	0.00	0.00	0.00	0.00	0.00
HPLT-A3	0.00	0.00	0.00	0.00	0.00
HPLT-A4	0.00	0.00	0.00	0.00	0.00
HPLT-A5	0.50	0.66	0.61	5.26	3.70
HPLT-A6	5.50	7.20	6.17	15.79	10.71
HPLT-B1	0.00	0.00	0.00	0.00	0.00
HPLT-B2	0.00	0.00	0.00	0.00	0.00
HPLT-B3	0.00	0.00	0.00	0.00	0.00
HPLT-B4	4.62	8.96	7.81	11.11	6.82
HPLT-B5	4.62	9.76	7.99	8.33	4.55
HPLT-B6	2.87	6.76	5.49	7.41	5.00
HPLT-C1	0.00	0.00	0.00	0.00	0.00
HPLT-C2	1.37	1.92	1.68	4.35	2.78
HPLT-C3	0.00	0.00	0.00	0.00	0.00
HPLT-C4	0.00	0.00	0.00	0.00	0.00
HPLT-C5	0.50	0.83	0.74	3.85	2.70
HPLT-C6	0.00	0.00	0.00	0.00	0.00
MEAN VALUES	1.11	2.01	1.69	3.12	2.01
C.V.	3.25	6.03		7.23	
STATISTICAL VALUES					
S ²	3.61	12.09	8.54	22.56	9.57
S	1.90	3.48	2.92	4.75	3.09
F-test	12.14; Rej H ₀	9.72; Rej H ₀	10.19; Rej H ₀	2.12; Acc H ₀	2.64; Acc H ₀
t-test	3.12; Rej H ₀	2.72; Rej H ₀	2.88; Rej H ₀	1.77; Acc H ₀	2.04; Acc H ₀
95% C.I.	0.17 - 2.05	0.28 - 3.74	0.24 - 3.14	0.76 - 5.48	0.47 - 3.55
FREQUENCY: 38.89%					

The symbols and abbreviations used are the same as presented in previous tables.

TABLE B-31
CORAL POPULATION LEVEL PARAMETERS AT THE FLOWER GARDEN BANKS
SPECIES - Millepora spp.

TRANSECT	DOMINANCE (% COVER)	RELATIVE DOMINANCE (C)	RELATIVE DOMINANCE (C&CA)	RELATIVE DENSITY (C)	RELATIVE DENSITY (C&CA)
BANK: EFG					
MEAN VALUES	4.46	5.93	5.46	9.68	7.01
C.V.	5.38	6.32		3.72	
STATISTICAL VALUES					
S ²	24.04	37.41	32.09	36.02	21.93
S	4.90	6.12	5.67	6.00	4.68
F-test	1.40; Acc H ₀	1.78; Acc H ₀	1.46; Acc H ₀	1.43; Acc H ₀	1.22; Acc H ₀
t-test	0.28; Acc H ₀	0.95; Acc H ₀	0.54; Acc H ₀	0.47; Acc H ₀	1.42; Acc H ₀
95% C.I.	2.17 - 5.51	2.89 - 8.97	2.64 - 8.28	6.70 - 12.66	4.68 - 9.34
FREQUENCY: 88.89%					
BANK: WFG					
HPLT-A1	2.75	8.06	6.38	10.00	4.35
HPLT-A2	6.87	13.55	9.93	7.41	4.26
HPLT-A3	5.50	16.33	11.13	16.67	6.45
HPLT-A4	0.00	0.00	0.00	0.00	0.00
HPLT-A5	3.37	4.49	4.10	10.53	7.41
HPLT-A6	3.75	4.91	4.21	5.26	3.57
HPLT-B1	2.25	8.96	7.14	7.69	3.70
HPLT-B2	0.00	0.00	0.00	0.00	0.00
HPLT-B3	0.87	1.65	1.13	3.23	2.13
HPLT-B4	16.75	32.45	28.27	25.93	15.91
HPLT-B5	3.25	6.86	5.62	8.33	4.55
HPLT-B6	7.00	16.47	13.37	11.11	7.50
HPLT-C1	7.25	11.86	9.76	13.89	8.62
HPLT-C2	7.87	11.01	9.63	17.39	11.11
HPLT-C3	2.62	3.77	3.28	3.85	2.56
HPLT-C4	0.00	0.00	0.00	0.00	0.00
HPLT-C5	0.00	0.00	0.00	0.00	0.00
HPLT-C6	2.50	7.63	4.74	14.29	6.06
MEAN VALUES	4.03	8.22	6.59	8.64	4.90
C.V.	4.25	8.10		5.97	
STATISTICAL VALUES					
S ²	17.13	66.58	46.92	51.55	17.89
S	4.14	8.16	6.85	7.18	4.23
F-test	1.40; Acc H ₀	1.78; Acc H ₀	1.46; Acc H ₀	1.43; Acc H ₀	1.22; Acc H ₀
t-test	0.28; Acc H ₀	0.95; Acc H ₀	0.54; Acc H ₀	0.47; Acc H ₀	1.42; Acc H ₀
95% C.I.	2.04 - 6.20	4.16 - 12.28	3.18 - 10.00	5.07 - 12.21	2.89 - 7.00
FREQUENCY: 77.78%					

The symbols and abbreviations used are the same as presented in previous tables.

TABLE B-32
CORAL POPULATION LEVEL PARAMETERS AT THE FLOWER GARDEN BANKS
SPECIES - Porites astreoides

TRANSECT	DOMINANCE (% COVER)	RELATIVE DOMINANCE (C)	RELATIVE DOMINANCE (C&CA)	RELATIVE DENSITY (C)	RELATIVE DENSITY (C&CA)
BANK: EFG					
MEAN VALUES	1.94	3.21	2.83	11.55	8.31
C. V.	2.06	2.92		7.04	
STATISTICAL VALUES					
s ²	3.99	9.35	7.23	81.40	46.57
S	2.00	3.06	2.69	9.02	6.82
F-test	1.19; Acc H ₀	2.13; Acc H ₀	1.38; Acc H ₀	1.31; Acc H ₀	1.57; Acc H ₀
t-test	1.06; Acc H ₀	1.72; Acc H ₀	1.36; Acc H ₀	1.18; Acc H ₀	0.12; Acc H ₀
95% C.I.	0.95 - 2.93	1.69 - 4.73	1.49 - 4.17	7.06 - 16.04	4.92 - 11.70
FREQUENCY: 83.33%					
BANK: WFG					
HPLT-A1	2.37	6.96	5.51	20.00	8.70
HPLT-A2	2.37	4.68	3.43	11.11	6.38
HPLT-A3	4.00	9.17	6.25	33.33	12.90
HPLT-A4	2.12	4.16	3.65	11.76	6.45
HPLT-A5	1.00	1.33	1.21	5.26	3.70
HPLT-A6	0.00	0.00	0.00	0.00	0.00
HPLT-B1	0.87	3.48	2.78	23.08	11.11
HPLT-B2	0.00	0.00	0.00	0.00	0.00
HPLT-B3	6.75	12.77	8.71	29.03	19.15
HPLT-B4	4.87	9.44	8.23	22.22	13.64
HPLT-B5	0.00	0.00	0.00	0.00	0.00
HPLT-B6	2.37	5.59	4.53	11.11	7.50
HPLT-C1	5.12	8.38	6.90	19.44	12.07
HPLT-C2	5.37	7.52	6.57	17.39	11.11
HPLT-C3	4.75	6.82	5.94	23.08	15.38
HPLT-C4	0.87	1.12	1.05	13.33	8.33
HPLT-C5	0.62	1.03	0.93	7.69	5.41
HPLT-C6	4.87	14.89	9.24	28.57	12.12
MEAN VALUES	2.68	5.41	4.16	15.36	8.55
C. V.	1.77	3.69		6.95	
STATISTICAL VALUES					
s ²	4.77	20.00	9.96	106.75	29.71
S	2.18	4.47	3.16	10.33	5.45
F-test	1.19; Acc H ₀	2.13; Acc H ₀	1.38; Acc H ₀	1.31; Acc H ₀	1.57; Acc H ₀
t-test	1.06; Acc H ₀	1.72; Acc H ₀	1.36; Acc H ₀	1.18; Acc H ₀	0.12; Acc H ₀
95% C.I.	1.60 - 3.76	3.19 - 7.63	2.59 - 5.73	10.22 - 20.50	5.84 - 11.26
FREQUENCY: 83.33%					

The symbols and abbreviations used are the same as presented in previous tables.

TABLE B-33
CORAL POPULATION LEVEL PARAMETERS AT THE FLOWER GARDEN BANKS
SPECIES - Agaricia spp.

TRANSECT	DOMINANCE (% COVER)	RELATIVE DOMINANCE (C)	RELATIVE DOMINANCE (C&CA)	RELATIVE DENSITY (C)	RELATIVE DENSITY (C&CA)
BANK: EFG					
MEAN VALUES	0.97	1.80	1.57	8.20	5.47
C. V.	1.20	2.16		8.08	
STATISTICAL VALUES					
s ²	1.17	3.88	3.01	66.32	27.48
S	1.08	1.97	1.73	8.14	5.24
F-test	1.11; Acc H ₀	1.04; Acc H ₀	1.30; Acc H ₀	1.87; Acc H ₀	1.87; Acc H ₀
t-test	0.38; Acc H ₀	0.41; Acc H ₀	0.61; Acc H ₀	1.50; Acc H ₀	1.71; Acc H ₀
95% C.I.	0.43 - 1.51	0.82 - 2.78	0.71 - 2.43	4.15 - 12.25	2.86 - 8.08
FREQUENCY: 61.11%					
BANK: WFG					
HPLT-A1	0.00	0.00	0.00	0.00	0.00
HPLT-A2	0.00	0.00	0.00	0.00	0.00
HPLT-A3	0.00	0.00	0.00	0.00	0.00
HPLT-A4	1.12	2.20	1.93	17.65	9.68
HPLT-A5	1.50	1.99	1.82	5.26	3.70
HPLT-A6	0.00	0.00	0.00	0.00	0.00
HPLT-B1	0.50	1.99	1.59	7.69	3.70
HPLT-B2	0.87	1.28	1.18	8.70	6.25
HPLT-B3	3.87	7.33	5.00	3.23	2.13
HPLT-B4	1.00	1.94	1.69	7.41	4.55
HPLT-B5	0.62	1.32	1.08	4.17	2.27
HPLT-B6	1.62	3.82	3.10	7.41	5.00
HPLT-C1	0.62	1.02	0.84	2.78	1.72
HPLT-C2	0.00	0.00	0.00	0.00	0.00
HPLT-C3	3.25	4.67	4.06	19.23	12.82
HPLT-C4	0.00	0.00	0.00	0.00	0.00
HPLT-C5	0.00	0.00	0.00	0.00	0.00
HPLT-C6	0.00	0.00	0.00	0.00	0.00
MEAN VALUES	0.83	1.53	1.24	4.64	2.88
C. V.	1.57	2.64		7.63	
STATISTICAL VALUES					
s ²	1.29	4.05	2.30	35.39	13.74
S	1.14	2.01	1.52	5.95	3.71
F-test	1.11; Acc H ₀	1.04; Acc H ₀	1.30; Acc H ₀	1.87; Acc H ₀	1.87; Acc H ₀
t-test	0.38; Acc H ₀	0.41; Acc H ₀	0.61; Acc H ₀	1.50; Acc H ₀	1.71; Acc H ₀
95% C.I.	0.26 - 1.40	0.53 - 2.53	0.49 - 1.99	1.68 - 7.60	1.53 - 4.41
FREQUENCY: 55.56%					

The symbols and abbreviations used are the same as presented in previous tables.

TABLE B-34
CORAL POPULATION LEVEL PARAMETERS AT THE FLOWER GARDEN BANKS
SPECIES - Madracis decactis

TRANSECT	DOMINANCE (% COVER)	RELATIVE DOMINANCE (C)	RELATIVE DOMINANCE (C&CA)	RELATIVE DENSITY (C)	RELATIVE DENSITY (C&CA)
BANK: EFG					
MEAN VALUES	2.72	3.53	3.38	4.98	3.84
C.V.	15.39	17.37		15.62	
STATISTICAL VALUES					
S ²	39.54	57.94	54.12	73.42	42.72
S	6.47	7.83	7.57	8.82	6.73
F-test	3.87; Rej H ₀	1.24; Acc H ₀	1.66; Acc H ₀	1.59; Acc H ₀	2.54; Acc H ₀
t-test	0.54; Acc H ₀	0.12; Acc H ₀	0.12; Acc H ₀	0.00; Acc H ₀	0.43; Acc H ₀
95% C.I.	0 - 5.85	0 - 7.43	0 - 7.14	0.60 - 9.36	0.49 - 7.19
FREQUENCY: 33.33%					
BANK: WFG					
HPLT-A1	0.00	0.00	0.00	0.00	0.00
HPLT-A2	2.37	4.68	3.43	3.70	2.13
HPLT-A3	0.00	0.00	0.00	0.00	0.00
HPLT-A4	0.00	0.00	0.00	0.00	0.00
HPLT-A5	0.00	0.00	0.00	0.00	0.00
HPLT-A6	0.00	0.00	0.00	0.00	0.00
HPLT-B1	4.37	17.41	13.89	15.38	7.41
HPLT-B2	0.00	0.00	0.00	0.00	0.00
HPLT-B3	5.62	10.64	7.26	12.90	8.51
HPLT-B4	12.75	24.70	21.52	22.22	13.64
HPLT-B5	0.00	0.00	0.00	0.00	0.00
HPLT-B6	0.50	1.18	0.95	7.41	5.00
HPLT-C1	4.37	7.16	5.89	11.11	6.90
HPLT-C2	0.00	0.00	0.00	0.00	0.00
HPLT-C3	1.62	2.33	2.33	3.85	2.56
HPLT-C4	0.62	0.80	0.75	13.33	8.33
HPLT-C5	0.00	0.00	0.00	0.00	0.00
HPLT-C6	0.00	0.00	0.00	0.00	0.00
MEAN VALUES	1.79	3.83	3.11	4.99	3.03
C.V.	6.05	12.94		9.82	
STATISTICAL VALUES					
S ²	10.80	49.61	34.57	48.95	17.74
S	3.29	7.04	5.88	7.00	4.22
F-test	3.87; Rej H ₀	1.24; Acc H ₀	1.66; Acc H ₀	1.59; Acc H ₀	2.54; Acc H ₀
t-test	0.54; Acc H ₀	0.12; Acc H ₀	0.12; Acc H ₀	0.00; Acc H ₀	0.43; Acc H ₀
95% C.I.	0.15 - 3.43	0.33 - 7.33	0.19 - 6.03	1.51 - 8.47	0.93 - 5.13
FREQUENCY: 44.44%					

The symbols and abbreviations used are the same as presented in previous tables.

TABLE B-35
CORAL POPULATION LEVEL PARAMETERS AT THE FLOWER GARDEN BANKS
SPECIES - Stephanocoenia michelini

TRANSECT	DOMINANCE (% COVER)	RELATIVE DOMINANCE (C)	RELATIVE DOMINANCE (C&CA)	RELATIVE DENSITY (C)	RELATIVE DENSITY (C&CA)
BANK: EFG					
MEAN VALUES	0.26	0.45	0.38	0.49	0.35
C. V.	3.47	5.13		4.23	
STATISTICAL VALUES					
s ²	0.90	2.31	1.65	2.09	1.03
S	0.95	1.52	1.28	1.44	1.02
F-test	3.13; Rej H ₀	16.11; Rej H ₀	14.30; Rej H ₀	2.09; Acc H ₀	1.16; Acc H ₀
t-test	0.73; Acc H ₀	0.97; Acc H ₀	0.93; Acc H ₀	0.59; Acc H ₀	0.31; Acc H ₀
95% C.I.	0 - 0.73	0 - 1.21	0 - 1.02	0 - 1.21	0.30 - 0.40
FREQUENCY: 11.11%					
BANK: WFG					
HPLT-A1	0.00	0.00	0.00	0.00	0.00
HPLT-A2	3.62	7.14	5.23	3.70	2.13
HPLT-A3	0.00	0.00	0.00	0.00	0.00
HPLT-A4	0.00	0.00	0.00	0.00	0.00
HPLT-A5	0.00	0.00	0.00	0.00	0.00
HPLT-A6	0.00	0.00	0.00	0.00	0.00
HPLT-B1	6.37	25.37	20.24	7.69	3.70
HPLT-B2	0.00	0.00	0.00	0.00	0.00
HPLT-B3	0.00	0.00	0.00	0.00	0.00
HPLT-B4	0.00	0.00	0.00	0.00	0.00
HPLT-B5	0.00	0.00	0.00	0.00	0.00
HPLT-B6	0.62	1.47	1.19	3.70	2.50
HPLT-C1	0.00	0.00	0.00	0.00	0.00
HPLT-C2	0.00	0.00	0.00	0.00	0.00
HPLT-C3	0.00	0.00	0.00	0.00	0.00
HPLT-C4	0.00	0.00	0.00	0.00	0.00
HPLT-C5	0.00	0.00	0.00	0.00	0.00
HPLT-C6	0.00	0.00	0.00	0.00	0.00
MEAN VALUES	0.59	1.89	1.48	0.84	0.46
C. V.	4.78	19.68		5.15	
STATISTICAL VALUES					
s ²	2.81	37.21	23.47	4.35	1.21
S	1.68	6.10	4.84	2.08	1.10
F-test	3.13; Rej H ₀	16.11; Rej H ₀	14.30; Rej H ₀	2.09; Acc H ₀	1.16; Acc H ₀
t-test	0.73; Acc H ₀	0.97; Acc H ₀	0.93; Acc H ₀	0.59; Acc H ₀	0.31; Acc H ₀
95% C.I.	0 - 1.43	0 - 4.92	0 - 3.89	0 - 1.87	0 - 1.01
FREQUENCY: 16.67%					

The symbols and abbreviations used are the same as presented in previous tables.

TABLE B-36
CORAL POPULATION LEVEL PARAMETERS AT THE FLOWER GARDEN BANKS
SPECIES - Siderastrea siderea

TRANSECT	DOMINANCE (% COVER)	RELATIVE DOMINANCE (C)	RELATIVE DOMINANCE (C&CA)	RELATIVE DENSITY (C)	RELATIVE DENSITY (C&CA)
BANK: EFG					
MEAN VALUES	0.05	0.08	0.08	0.43	0.32
C.V.	0.80	1.62		7.62	
STATISTICAL VALUES					
S ²	0.04	0.13	0.11	3.29	1.81
S	0.20	0.36	0.33	1.81	1.35
F-test	106; Rej H ₀	1330; Rej H ₀	997; Rej H ₀	2.97; Rej H ₀	1.80; Acc H ₀
t-test	1.39; Acc H ₀	1.21; Acc H ₀	1.23; Acc H ₀	1.00; Acc H ₀	0.79; Acc H ₀
95% C.I.	0 - 0.15	0 - 0.26	0 - 0.25	0 - 1.33	0 - 0.99
FREQUENCY: 5.65%					
BANK: WFG					
HPLT-A1	19.00	55.68	44.06	10.00	4.35
HPLT-A2	0.00	0.00	0.00	0.00	0.00
HPLT-A3	0.00	0.00	0.00	0.00	0.00
HPLT-A4	0.00	0.00	0.00	0.00	0.00
HPLT-A5	0.00	0.00	0.00	0.00	0.00
HPLT-A6	0.00	0.00	0.00	0.00	0.00
HPLT-B1	0.00	0.00	0.00	0.00	0.00
HPLT-B2	5.75	8.39	7.76	8.70	6.25
HPLT-B3	0.00	0.00	0.00	0.00	0.00
HPLT-B4	0.00	0.00	0.00	0.00	0.00
HPLT-B5	0.00	0.00	0.00	0.00	0.00
HPLT-B6	0.00	0.00	0.00	0.00	0.00
HPLT-C1	0.00	0.00	0.00	0.00	0.00
HPLT-C2	3.37	4.72	4.13	4.35	2.78
HPLT-C3	0.00	0.00	0.00	0.00	0.00
HPLT-C4	0.00	0.00	0.00	0.00	0.00
HPLT-C5	0.00	0.00	0.00	0.00	0.00
HPLT-C6	0.00	0.00	0.00	0.00	0.00
MEAN VALUES	1.56	3.82	3.11	1.28	0.74
C.V.	13.62	45.13		7.61	
STATISTICAL VALUES					
S ²	21.26	172.34	108.51	9.71	3.28
S	4.61	13.13	10.42	3.12	1.81
F-test	106; Rej H ₀	1330; Rej H ₀	997; Rej H ₀	2.97; Rej H ₀	1.80; Acc H ₀
t-test	1.39; Acc H ₀	1.21; Acc H ₀	1.23; Acc H ₀	1.00; Acc H ₀	0.79; Acc H ₀
95% C.I.	0 - 3.85	0 - 10.35	0 - 8.29	0 - 2.38	0 - 1.64
FREQUENCY: 16.67%					

The symbols and abbreviations used are the same as presented in previous tables.

TABLE B-37
CORAL POPULATION LEVEL PARAMETERS AT THE FLOWER GARDEN BANKS
SPECIES - Scolymia cubensis

TRANSECT	DOMINANCE (% COVER)	RELATIVE DOMINANCE (C)	RELATIVE DOMINANCE (C&CA)	RELATIVE DENSITY (C)	RELATIVE DENSITY (C&CA)
BANK: EFG					
MEAN VALUES	0%	0%	0%	0%	0%
C. V.					
STATISTICAL VALUES					
s^2	0	0	0	0	0
S	0	0	0	0	0
F-test	∞ ; Rej H_0	∞ ; Rej H_0	∞ ; Rej H_0	∞ ; Rej H_0	∞ ; Rej H_0
t-test	1.27; Acc H_0	1.48; Acc H_0	1.33; Acc H_0	1.41; Acc H_0	1.43; Acc H_0
95% C.I.	0 - 0.15	0 - 0.15	0 - 0.15	0 - 1.15	0 - 0.15
FREQUENCY: 0%					
BANK: WFG					
HPLT-A1	0.00	0.00	0.00	0.00	0.00
HPLT-A2	0.37	0.74	0.54	3.70	2.13
HPLT-A3	0.00	0.00	0.00	0.00	0.00
HPLT-A4	0.25	0.49	0.43	5.88	3.23
HPLT-A5	0.00	0.00	0.00	0.00	0.00
HPLT-A6	0.00	0.00	0.00	0.00	0.00
HPLT-B1	0.00	0.00	0.00	0.00	0.00
HPLT-B2	0.00	0.00	0.00	0.00	0.00
HPLT-B3	0.00	0.00	0.00	0.00	0.00
HPLT-B4	0.00	0.00	0.00	0.00	0.00
HPLT-B5	0.00	0.00	0.00	0.00	0.00
HPLT-B6	0.00	0.00	0.00	0.00	0.00
HPLT-C1	0.00	0.00	0.00	0.00	0.00
HPLT-C2	0.00	0.00	0.00	0.00	0.00
HPLT-C3	0.00	0.00	0.00	0.00	0.00
HPLT-C4	0.00	0.00	0.00	0.00	0.00
HPLT-C5	0.00	0.00	0.00	0.00	0.00
HPLT-C6	0.00	0.00	0.00	0.00	0.00
MEAN VALUES	0.03	0.07	0.05	0.53	0.30
C. V.					
	0.33	0.57		4.77	
STATISTICAL VALUES					
s^2	0.01	0.04	0.02	2.54	0.79
S	0.10	0.20	0.16	1.59	0.89
F-test	∞ ; Rej H_0	∞ ; Rej H_0	∞ ; Rej H_0	∞ ; Rej H_0	∞ ; Rej H_0
t-test	1.27; Acc H_0	1.48; Acc H_0	1.33; Acc H_0	1.41; Acc H_0	1.43; Acc H_0
95% C.I.	0 - 0.08	0 - 0.17	0 - 0.13	0 - 1.32	0 - 0.74
FREQUENCY: 11.11%					

The symbols and abbreviations used are the same as presented in previous tables.

TABLE B-38
CORAL POPULATION LEVEL PARAMETERS AT THE FLOWER GARDEN BANKS
SPECIES - Mussa angulosa

TRANSECT	DOMINANCE (% COVER)	RELATIVE DOMINANCE (C)	RELATIVE DOMINANCE (C&CA)	RELATIVE DENSITY (C)	RELATIVE DENSITY (C&CA)
BANK: EFG					
MEAN VALUES	0.24	0.30	0.28	1.18	0.85
C. V.	1.65	1.98		7.83	
STATISTICAL VALUES					
S ²	0.39	0.59	0.53	9.22	4.85
S	0.63	0.77	0.72	3.04	2.20
F-test	4.13; Rej H ₀	1.40; Acc H ₀	2.25; Acc H ₀	1.40; Acc H ₀	2.04; Acc H ₀
t-test	0.42; Acc H ₀	0.17; Acc H ₀	0.15; Acc H ₀	0.33; Acc H ₀	0.08; Acc H ₀
95% C.I.	0 - 0.55	0 - 0.68	0 - 0.64	0 - 2.69	0 - 1.95
FREQUENCY: 16.67%					
BANK: WFG					
HPLT-A1	0.00	0.00	0.00	0.00	0.00
HPLT-A2	0.00	0.00	0.00	0.00	0.00
HPLT-A3	0.00	0.00	0.00	0.00	0.00
HPLT-A4	0.00	0.00	0.00	0.00	0.00
HPLT-A5	0.12	0.17	0.15	5.26	3.70
HPLT-A6	0.00	0.00	0.00	0.00	0.00
HPLT-B1	0.00	0.00	0.00	0.00	0.00
HPLT-B2	0.00	0.00	0.00	0.00	0.00
HPLT-B3	0.87	1.65	1.13	6.45	4.26
HPLT-B4	0.00	0.00	0.00	0.00	0.00
HPLT-B5	0.00	0.00	0.00	0.00	0.00
HPLT-B6	0.75	1.76	1.43	3.70	2.50
HPLT-C1	0.00	0.00	0.00	0.00	0.00
HPLT-C2	0.75	1.05	0.92	4.35	2.78
HPLT-C3	0.00	0.00	0.00	0.00	0.00
HPLT-C4	0.00	0.00	0.00	0.00	0.00
HPLT-C5	0.00	0.00	0.00	0.00	0.00
HPLT-C6	0.50	1.53	0.95	7.14	3.03
MEAN VALUES	0.17	0.34	0.25	1.49	0.90
C. V.	0.57	1.24		4.43	
STATISTICAL VALUES					
S ²	0.10	0.42	0.23	6.62	2.37
S	0.31	0.65	0.48	2.57	1.54
F-test	4.13; Rej H ₀	1.40; Acc H ₀	2.25; Acc H ₀	1.40; Acc H ₀	2.04; Acc H ₀
t-test	0.42; Acc H ₀	0.17; Acc H ₀	0.15; Acc H ₀	0.33; Acc H ₀	0.08; Acc H ₀
95% C.I.	0.01 - 0.33	0.02 - 0.66	0.01 - 0.49	0.21 - 2.77	0.13 - 1.67
FREQUENCY: 28.78%					

The symbols and abbreviations used are the same as presented in previous tables.

TABLE B-39
POPULATION LEVEL PARAMETERS AT THE FLOWER GARDEN BANKS:
FILAMENTOUS ALGAE AND TOTAL LIVE CORAL

TRANSECT	FILAMENTOUS ALGAE (PERCENT COVER)	TOTAL LIVE CORAL (PERCENT COVER)
BANK: EFG		
MEAN VALUES	24.15	63.58
C.V.	5.86	3.40
STATISTICAL VALUES		
s^2	141.50	216.29
S	11.90	14.71
F-test	1.59; Acc H_0	1.19; Acc H_0
t-test	0.49; Acc H_0	1.65; Acc H_0
95% C.I.	17.68 - 30.62	34.75 - 92.41
FREQUENCY	100%	
BANK: WFG		
HPLT-A1	53.87	34.11
HPLT-A2	22.87	50.72
HPLT-A3	34.25	43.62
HPLT-A4	31.00	51.10
HPLT-A5	16.12	75.24
HPLT-A6	8.87	76.37
HPLT-B1	62.62	25.11
HPLT-B2	19.12	68.49
HPLT-B3	13.00	52.85
HPLT-B4	31.62	51.61
HPLT-B5	30.25	47.36
HPLT-B6	30.50	42.47
HPLT-C1	13.50	61.10
HPLT-C2	16.50	71.48
HPLT-C3	13.12	69.61
HPLT-C4	9.25	78.23
HPLT-C5	26.75	60.49
HPLT-C6	41.62	32.74
MEAN VALUES	26.38	55.15
C.V.	8.55	4.65
STATISTICAL VALUES		
s^2	225.46	256.32
S	15.02	16.01
F-test	1.59; Acc H_0	1.19; Acc H_0
t-test	0.49; Acc H_0	1.65; Acc H_0
95% C.I.	18.22 - 34.53	23.77 - 86.53
FREQUENCY:	100%	

The symbols and abbreviations used are the same as presented in previous tables.

TABLE B-40
CORAL DIVERSITY, EVENNESS, RICHNESS
SITE - BLM

TRANSECT	SHANNON-WIENER DIVERSITY INDEX	EVENNESS	RICHNESS
HPLT-A1	1.354	0.528	4.328
HPLT-A2	1.427	0.556	5.461
HPLT-A3	1.667	0.650	3.601
HPLT-B1	1.606	0.626	3.882
HPLT-B2	1.304	0.508	4.678
HPLT-B3	1.518	0.592	3.403
HPLT-C1	1.153	0.450	3.942
HPLT-C2	1.724	0.672	3.349
HPLT-C3	1.388	0.541	3.728
MEAN VALUES	1.460	0.569	4.041
C.V.	0.023	0.009	0.115

STATISTICAL VALUES	SHANNON-WIENER DIVERSITY INDEX	EVENNESS	RICHNESS
S ²	0.034	0.052	0.465
S	0.185	0.072	0.682
F test	1.38; Acc H ₀	1.36; Acc H ₀	9.97; Rej H ₀
t test	1.96; Acc H ₀	1.98; Acc H ₀	0.64; Acc H ₀
95% C.I.	1.32 - 1.60	0.51 - 0.62	3.52 - 4.56

S², S = variance and standard deviation, respectively.

C.I. = confidence interval around the sample mean.

C.V. = S^2 / \bar{X} (coefficient of variation).

F- and t-tests compare the variances and means, respectively, of population level parameters at the CSA and BLM sites. H₀ = equal sample variances, or equal sample means.

TABLE B-41
CORAL DIVERSITY, EVENNESS, RICHNESS
SITE - CSA

TRANSECT	SHANNON-WIENER DIVERSITY INDEX	EVENNESS	RICHNESS
HPLT-A1	1.914	0.746	3.683
HPLT-A2	1.586	0.618	4.152
HPLT-A3	1.365	0.532	4.235
HPLT-B1	1.718	0.670	3.728
HPLT-B2	1.446	0.564	3.827
HPLT-B3	1.777	0.693	3.683
HPLT-C1	1.931	0.753	3.683
HPLT-C2	1.371	0.534	4.006
HPLT-C3	1.706	0.665	4.006
MEAN VALUES	1.646	0.642	3.889
C.V.	0.029	0.011	0.012

STATISTICAL VALUES	SHANNON-WIENER DIVERSITY INDEX	EVENNESS	RICHNESS
s^2	0.047	0.007	0.046
S	0.217	0.084	0.216
F-test	1.38; Acc H_0	1.36; Acc H_0	9.97; Rej H_0
t-test	1.96; Acc H_0	1.98; Acc H	0.64; Acc H_0
95% C.I.	1.48 - 1.81	0.577 - 0.707	3.72 - 4.06

s^2 , S = variance and standard deviation, respectively.

C.I. = confidence interval around the sample mean.

C.V. = s^2 / \bar{x} (coefficient of variation).

F- and t-tests compare the variances and means, respectively, of population level parameters at the CSA and BLM sites. H_0 = equal sample variances, or equal sample means.

TABLE B-42
CORAL DIVERSITY, EVENNESS, RICHNESS: EFG/WFG

TRANSECT	SHANNON-WIENER DIVERSITY INDEX	EVENNESS	RICHNESS
<u>BANK: EFG</u>			
MEAN VALUES	1.553	0.605	3.965
C. V.	0.031	0.012	0.062
STATISTICAL VALUES			
S ²	0.045	0.007	0.233
S	0.218	0.085	0.497
F-test	2.24; Acc H ₀	2.23; Acc H ₀	1.07; Acc H ₀
t-test	1.17; Acc H ₀	1.14; Acc H ₀	0.42; Acc H ₀
95% C.I.	1.445 - 1.661	0.563 - 0.647	3.718 - 4.212
<u>BANK: WFG</u>			
HPLT-A1	1.505	0.587	5.212
HPLT-A2	1.749	0.682	3.641
HPLT-A3	1.237	0.482	4.829
HPLT-A4	1.563	0.609	4.235
HPLT-A5	1.117	0.435	4.075
HPLT-A6	0.826	0.322	4.075
HPLT-B1	1.845	0.719	4.678
HPLT-B2	1.026	0.400	3.827
HPLT-B3	1.689	0.659	3.494
HPLT-B4	1.700	0.663	3.641
HPLT-B5	1.225	0.478	3.776
HPLT-B6	2.136	0.833	3.641
HPLT-C1	1.578	0.615	3.349
HPLT-C2	1.357	0.529	3.827
HPLT-C3	1.253	0.488	3.683
HPLT-C4	1.564	0.610	4.431
HPLT-C5	1.136	0.443	3.683
HPLT-C6	1.512	0.590	4.547
MEAN VALUES	1.445	0.564	4.036
C. V.	0.074	0.029	0.066
STATISTICAL VALUES			
S ²	0.100	0.015	0.251
S	0.326	0.127	0.515
F-test	2.24; Acc H ₀	2.23; Acc H ₀	1.07; Acc H ₀
t-test	1.17; Acc H ₀	1.14; Acc H ₀	0.42; Acc H ₀
95% C.I.	1.283 - 1.607	0.501 - 0.627	3.800 - 4.292

The symbols and abbreviations used are the same as presented in previous tables.

CHAPTER IV

WATER AND SEDIMENT DYNAMICS AT THE FLOWER GARDEN BANKS

D. McGrail, M. Carnes, D. Horne, T. Cecil, J. Hawkins, F. Halper

INTRODUCTION

There were several goals for the investigations carried out under the category of water and sediment dynamics. The large scale objective was to establish what the oceanographic climate of the East and West Flower Garden Banks actually is; i.e., to determine the nature of the prevailing currents, how they are modulated, and the salinities, temperatures, and sediment loads of the passing waters. The investigation was also to determine the circulation over the banks and, in particular, the possibility of sweeping sediment from the base of the banks up to the crests.

In order to fulfill the objectives of this study, a three-element program of research was designed and carried out. First, long-term current meter moorings were established in the vicinity of both banks. The instruments on the moorings all measured temperature and current velocity. During the course of the deployments, new transmissometers were added to the deepest instruments on each mooring to record the relative amount of suspended sediment in the water column as a function of time. The second element of the field work involved the use of instruments deployed from a surface ship to measure current velocity, transmissivity, conductivity, and temperature as a function of depth. An instrumented package was developed to substantially increase the number of stations that could be occupied per unit of ship time and to increase the quantity and quality of data acquired at each station. These profiles provide a measure of the spatial variation of the various parameters. The third element of the investigation was in situ dye emission experimentation in the bottom boundary layer. This study was designed to analyze the structure of the flow in the boundary layer and the magnitude of the shear stresses that were applied to the bottom under known flow conditions. The boundary layer work was tied to the other elements by locating some of the experiments near the moored current meters and by taking profiles during the dye experiments.

LONG-TERM CURRENT MEASUREMENTSMethodsEquipment and Deployment

For long-term current measurements, current meter moorings were deployed near the East and West Flower Garden Banks. Two types of current meters were used: sixteen HydroProducts SeaTrak meters with Savonius rotor for speed measurement and a vane for indicating direction; and one Marsh-McBirney 585 electromagnetic current meter. Tem-

perature, time, speed, and direction were stored on cassette tapes at twenty-minute increments. A HydroProducts temperature-conductivity probe with an accuracy of .1 mho was deployed along with the electromagnetic current meter. Sea Tech transmissometers equipped with a light-emitting diode (L.E.D.) were installed into the directional vanes on the bottom meters on each array and integrated into the recording circuitry of the meters. Four meters were attached to each array, with the Marsh-McBirney as the fifth meter on one of the arrays. On each array one meter was placed four metres from the bottom, and another meter forty-five to fifty metres from the bottom. The remaining two meters on each array were positioned on the array between six and eighty-one metres from the bottom, depending on the depth where critical observations were sought.

Before deployment of a current meter array, the hardware for the array was assembled and the meters checked out. Each length of quarter-inch cable was pre-cut and attached to the appropriate shackle, swivel, and pear ring assembly prior to beginning mobilization in Galveston, TX. At sea, the current meters, acoustic releases, and buoys were shackled into the array, and all shackles were seized immediately before deployment.

Each current meter was checked before deployment. The checkout procedure for the HydroProducts 550 current meter requires that batteries be replaced and voltage be at least 12.3 volts with the instrument off. The rotor sensor circuit was adjusted for proper symmetry. The analog-to-digital converter was adjusted and calibrated. Calibration of the temperature measurement circuit was checked. O-rings were cleaned and inspected; bad rings were replaced. New cassette tapes were installed. With the meter turned on, the tape advance was verified. At the beginning of the next sample period, the number of rotor revolutions during the sampling time was counted to verify that the instrument was making the correct speed measurement. To check compass headings, the instrument was rotated 90° through 360°, in 90° increments, over four sampling periods. After sample data points were recorded, the cassette tape was removed from the instrument and read to insure that proper speed and direction were actually recorded by the HydroProducts current meter.

After this checkout, board #1 was wired for the desired sample rate, the tape was mounted, and the instrument was turned on. The time that the instrument was turned on was recorded as the start time of the tape. Before sealing the unit, the pressure case was purged with argon gas, rotor bearings were cleaned, and the rotor was blocked to prevent rotation in the air.

Checkout for the Marsh-McBirney 585 electromagnetic current meter was similar to that for the HydroProducts 550, except that speed verification was not possible (except a speed of zero in still water). The 585 was connected to an RS232C terminal for checkout, thus allowing for a printout of data as the data were measured. Compass measurements (for orientation of the meter) were checked by rotating the instrument through 360°. Zero speed output was obtained by placing

the sensor in a container of ordinary tap water. Before deployment, 1) the batteries were charged and the voltage checked; 2) the internal time clock and sample rates were reset; 3) the O-rings were cleaned, fresh desiccant was placed in the pressure housing and sacrificial anodes were mounted on the case. The electromagnetic meter was also purged with inert gas immediately before the pressure housing was sealed.

When all instruments were checked out and the ship neared the site for deployment, the array was assembled and laid out on deck. Immediately before reaching the deployment site, the array was strung out behind the ship. At the exact position where the current meter array was to be deployed, the anchor was released over the side so that the array could free-fall to the bottom. Exact time and position were recorded. On the October 1980 cruise, position data were obtained by means of LORAC navigation; LORAN C was used for navigation on the March 1981 and July 1981 cruises.

Recovery of the current meter was accomplished by sending a frequency-encoded acoustic signal to the acoustic release located immediately above the anchor in the array. Upon receipt of this signal, the array separated from the bottom anchor and floated to the surface. Meters, releases, and buoys were brought on deck. The meters were immediately rinsed with fresh water and cleaned. Rotors and gimbals were checked for any wear or obstructions that might influence data collection. When possible, tapes were given a preliminary check to determine that the instruments had worked satisfactorily. Cycle time and clock accuracy were verified.

Synthesis

Data Correction

Following the recovery of the current meters and removal of the cassette tapes, a preliminary reading of all the tapes was performed to determine the length of the data record and whether any obvious malfunction had occurred. The tapes were read using an M-80 Memodyne cassette reader which sends a bit pattern through a serial port to an S-100 board micro-computer system, where the bit pattern is translated into meaningful data. Data in the form of time, east velocity, north velocity, current speed, direction, temperature, and transmissivity were then sent via a hardwired modem to the TAMU Amdahl, where final analysis of the data was performed.

For all meters, auto spectra, cross spectra, coherency, phase, and rotary spectra have been compiled for U and V velocity, V velocity versus transmissivity, and U velocity versus transmissivity. This computing program, developed by Oppenheimer (personal communication) at South Florida State, uses a Cooley-Tukey Fast Fourier Transform (FFT). In addition, mean speed, direction, temperature, and velocity have been calculated for all meters.

Digitization of tidal data from Calcasieu Pass is now in progress. Because cotidal lines run through both the Flower Gardens and Calcasieu Pass, it is possible to equate Calcasieu Pass tidal data with that for the Flower Gardens. In addition, wind data for the Flower Gardens area has been gathered for January-December 1979, and July-December 1980. These data are reported below.

In the process of evaluating the quality of the time series current meter data, it was found that the HydroProducts current meters sometimes stopped recording speed before the end of the deployment period due to instrument malfunction and/or marine biofouling (see Figures IV-2 through 4). In some cases, there are gaps in the recorded speeds but no gaps in the recorded directions.

It was important to salvage the information on direction, since direction alone is often an indicator of the types of events that are taking place. Analysis of this information relies on computer-generated stick plots of speed and direction. To run the program that produces these stick plots, however, some non-zero speeds must be entered. Therefore, speeds were synthesized for most of the speed gaps by combining the measured direction with synthesized direction-dependent speeds. These fabricated speeds (marked by an arrow on the stick plots) were determined using the part of the current record where both speed and direction were recorded. An average speed in each of 36 10° compass intervals was calculated from the useful velocity portion of the record. This synthesized speed, corresponding to a particular direction, was inserted into records where speed was absent and the direction was within the given 10° interval.

On several current meters the time span of useful velocity was so short that data fabrication from such a limited velocity record would be inappropriate. Therefore, a fixed speed of 20 cm/sec was inserted in these speed gaps in order to illustrate the useful current direction.

On one, mooring 1 meter 3 (July 1981), a significant event of high velocity occurred early in the record. Closer scrutiny of this section reveals that about one out of five speeds was erroneously high (between 40 and 200 cm/sec). The extremely high velocities (greater than 40 cm/sec) were replaced by interpolated values. This procedure resulted in a velocity time series which displays a high degree of correlation with the velocities recorded by the bottom current meter on the same mooring.

Currents

Time series of current velocity, temperature, transmissivity, and conductivity were recorded for extended periods between January 1979 and July 1981 at locations near the East and West Flower Garden Banks. Mooring positions are shown in Figure IV-1. There were six different deployments of the mooring arrays. Each deployment consisted of from two to four moorings with multiple instruments on each mooring.

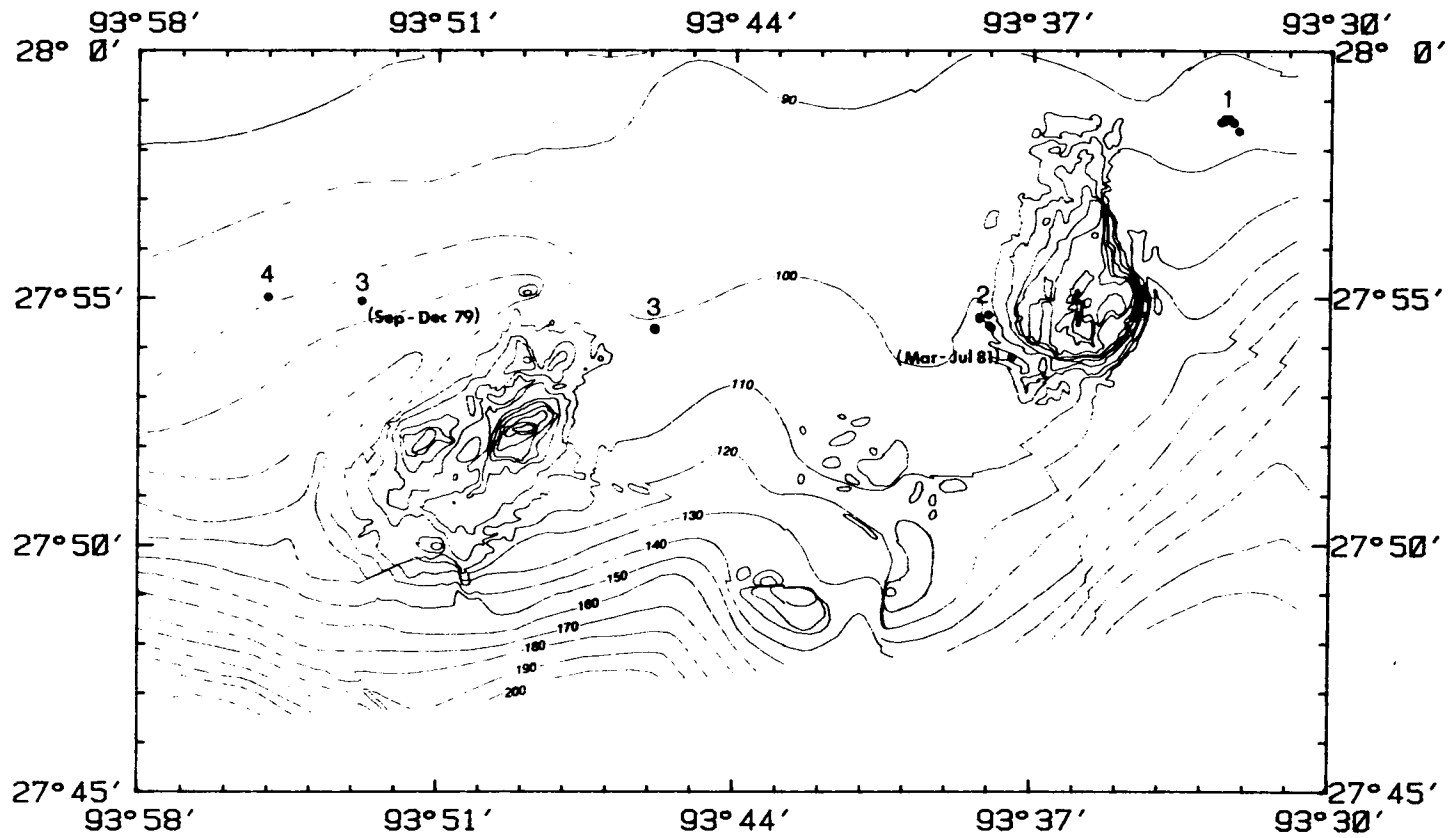


Figure IV-1. Mooring positions for all six current meter array deployments from January 1979 to July 1981. The two cases where a mooring position was significantly changed are indicated by the deployment dates in parentheses.

Besides these moorings, an electromagnetic current meter and a temperature and conductivity probe were initially deployed at the top of the East Flower Garden Bank at a depth of 30 m. The first three main deployments consisted of only HydroProducts Savonius rotor current meters, but on the last three deployments, the electromagnetic current meter was removed from the bank and placed near the top of mooring 2. Tables IV-1 through 4 give the inventory of all time series data collected from these arrays. The tables are divided into two sets, one pertaining to the HydroProducts current meters and their auxiliary sensors, and the other to the electromagnetic current meter and associated temperature and conductivity data. The location, depth, recording dates, and other pertinent data for each HydroProducts current meter are listed in Table IV-1. Table IV-2 gives an assessment of the quality of each data record listed in Table IV-1. The inventory and assessment of electromagnetic current meter data and the associated temperature and conductivity data are given in Tables IV-3 and 4.

The time series data records are also displayed graphically in bar-graph-time plots in Figures IV-2, 3, and 4. The seasonal coverage of the velocity data set is fairly complete in the depth interval from 32 m to 64 m. Velocity data sets for the near bottom (4 to 8 m from bottom) are rather sparse from September through February (all years combined), and there is little or no data for the middle layer data set (11 to 18 m from bottom) for the September through February period, 1979-1981. The temperature data sets are more complete, since all temperature records, except one, contain good quality data throughout all of the deployment periods. Transmissivity time series data were recorded only in the near-bottom region at depths where the bottom nepheloid layer is often found. Typically, the good portion of the transmissivity records ends well before the end of the deployment period. Usually, the transmissivity decreases toward the end of the record to well below reasonable levels of transmission. This decrease is caused by biofouling of the optical lenses of the transmissometers. In later deployments, this biofouling was alleviated by heavily coating the cases surrounding the lenses with a highly toxic anti-fouling paint.

One-Month Averaged Velocities

One-month vector averages of all current meter velocity data have been computed. For purposes of presentation, these data have been divided by depth into three groups: from 32 m to 64 m deep; from 11 m to 18 m from the bottom; and within 8 m of the bottom. The bottom depths range from 95 m to 107 m.

The speed and direction of the monthly averaged currents have been plotted versus time of year for each of the three depth groups (Figure IV-5). These values are plotted at the times corresponding to the middle of each monthly segment. Note that some vertical lines have been displaced slightly left or right to aid in presentation. The normal oceanographic convention for direction is used: 0° toward north and increasing clockwise in the direction of flow. To aid in visualizing the direction clustering, the monthly mean current vectors are

DATA INVENTORY FOR CURRENT METER ARRAYS: JANUARY 1979 THROUGH DECEMBER 1979

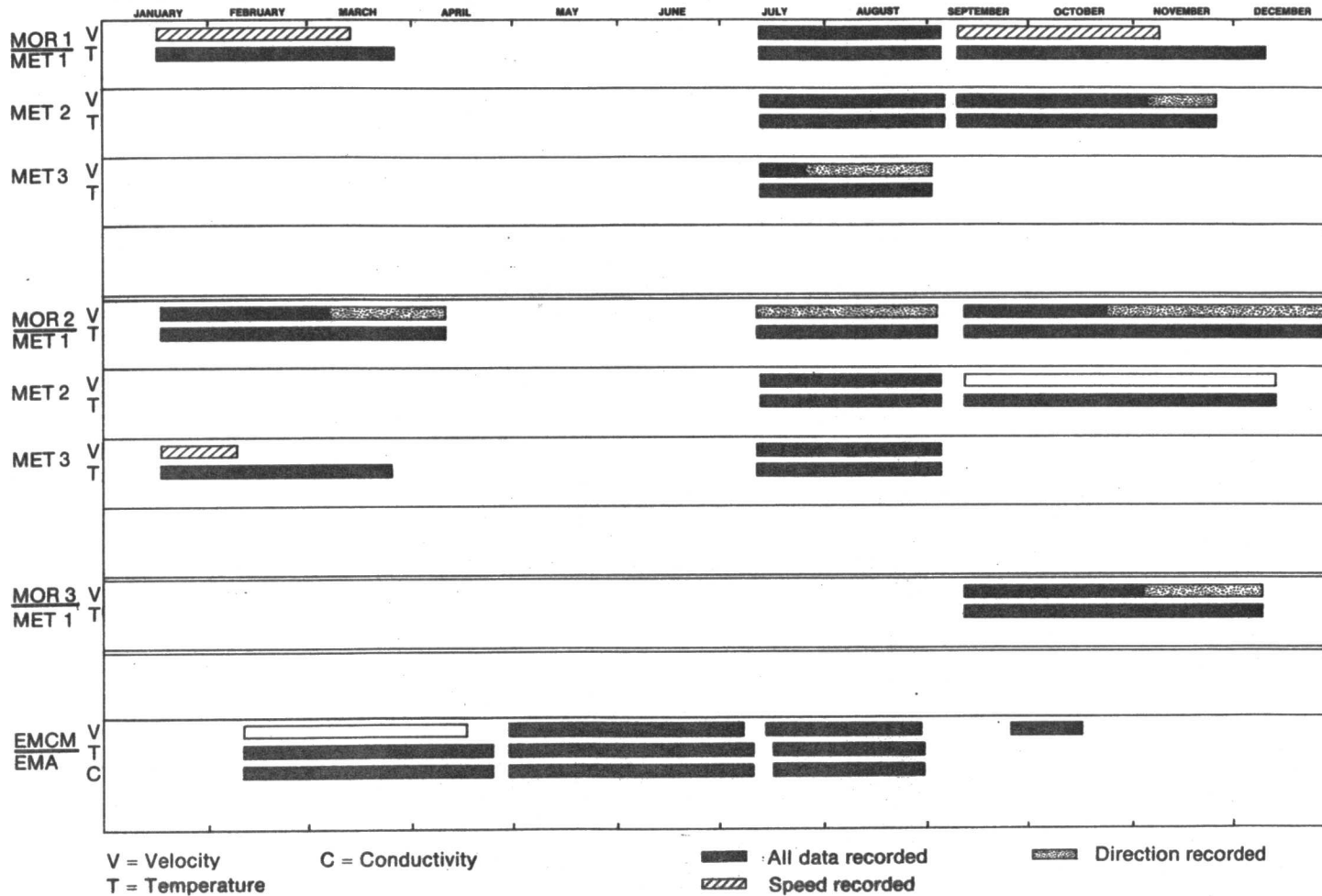


Figure IV-2. Data inventory for current meter arrays: January 1979 through December 1979.

DATA INVENTORY FOR CURRENT METER ARRAYS: APRIL 1980 THROUGH OCTOBER 1980

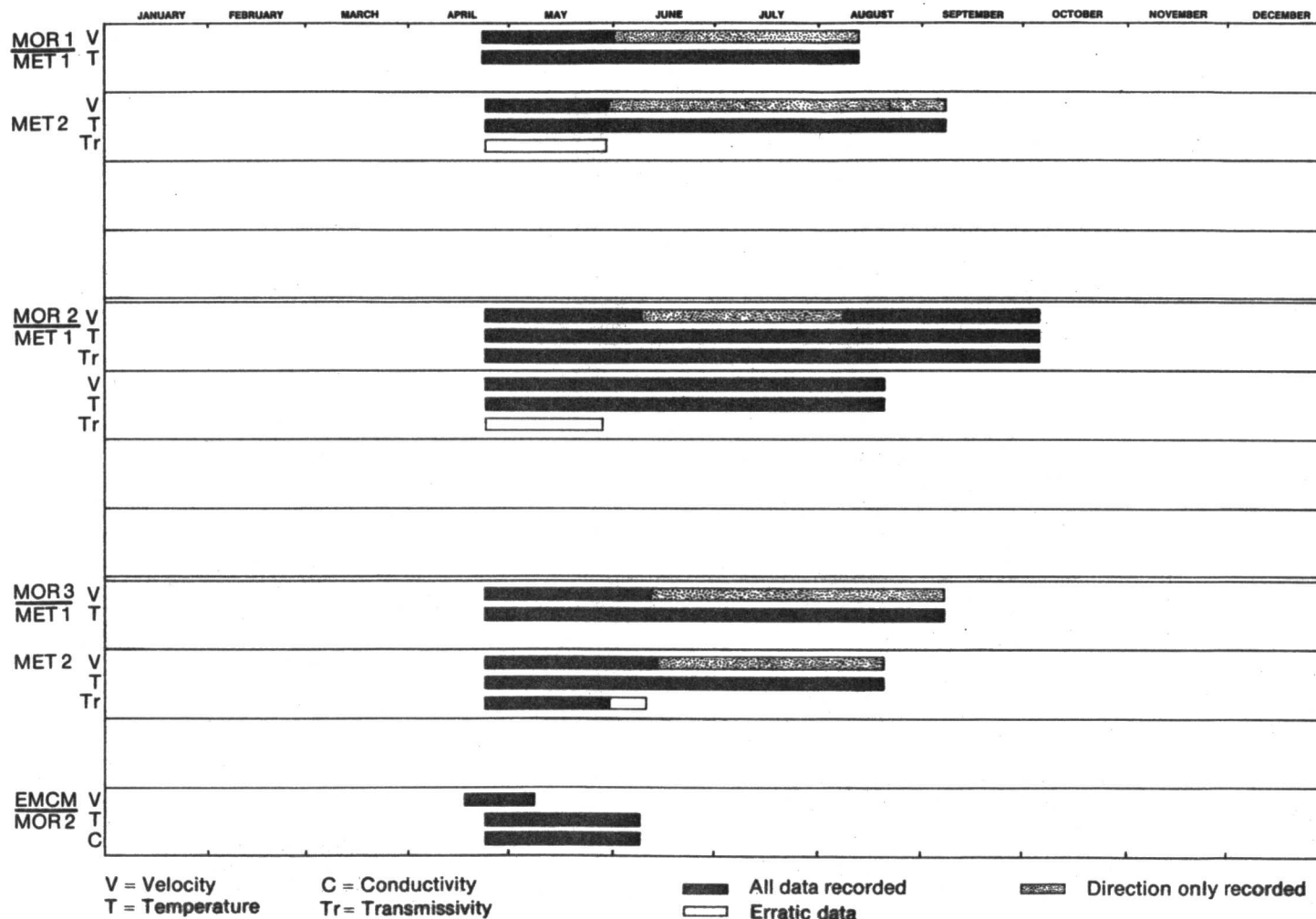


Figure IV-3. Data inventory for current meter arrays: April 1980 through October 1980.

DATA INVENTORY FOR CURRENT METER ARRAYS: OCTOBER 1980 THROUGH JULY 1981

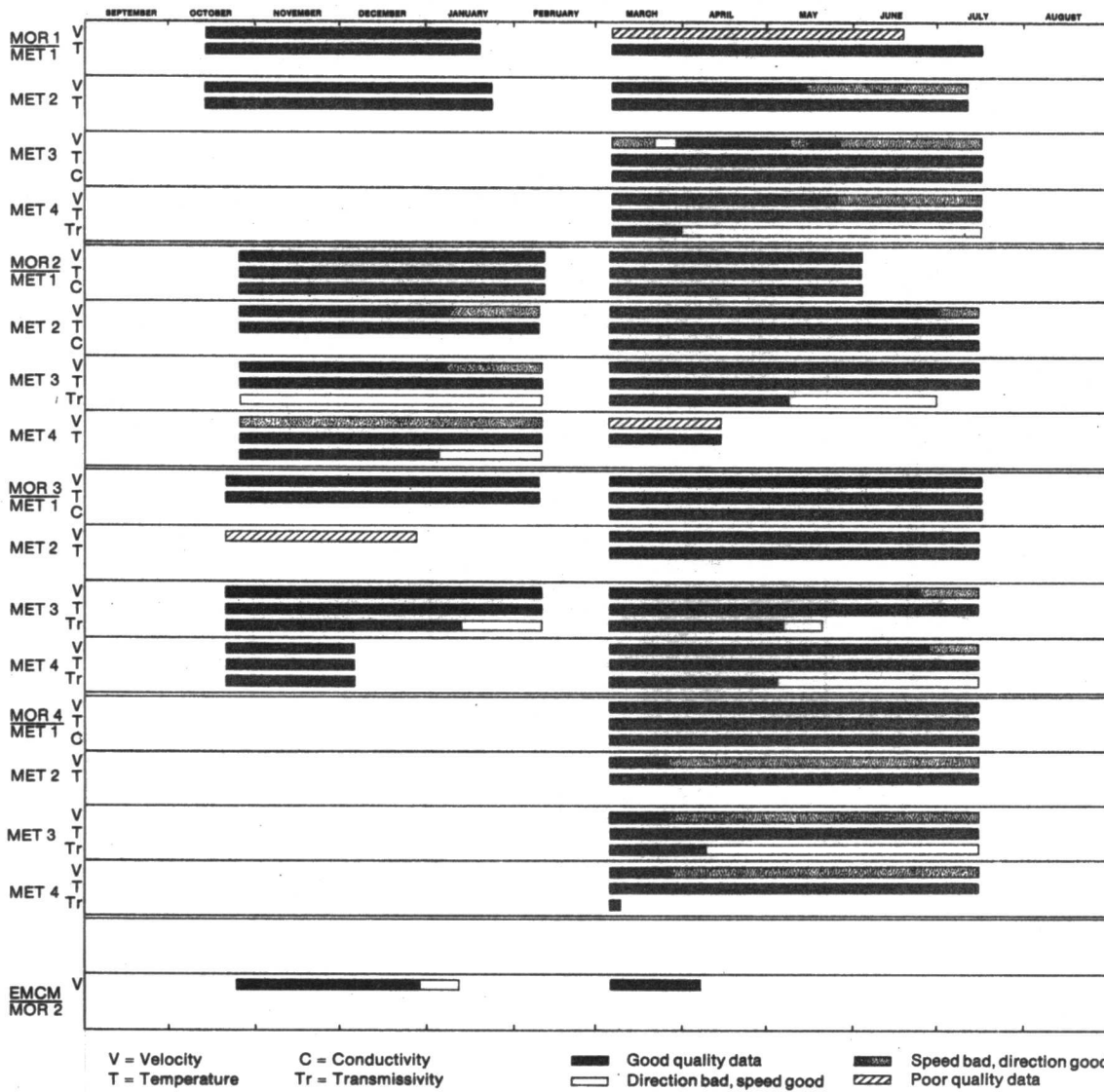


Figure IV-4. Data inventory for current meter arrays: October 1980 through July 1981.

TABLE IV-1
HYDROPRODUCTS CURRENT METER AND ASSOCIATED TIME SERIES DATA INVENTORY,
EAST AND WEST FLOWER GARDEN BANKS
(All Deployments from Jan 79 - Jul 81)

MOORING & METER	MONTH OF RECOVERY	INSTRUMENT SERIAL NUMBER	LOCATION	DEPTH (m) METER/BOTTOM	TIME OF FIRST GOOD RECORDING	FINAL TIME	RECORDING INTERVAL (minutes)	TOTAL RECORDS (including 6 header records)
Mor 1Met1	Apr 79	677754	27°58.63'N, 93°32.42'W	56/96	1/16/79 10:34	3/26/79 23:52	6	16700
Mor2Met1	Apr 79	677764	27°54.65'N, 93°38.02'W	60/100	1/17/79 21:16	4/10/79 19:22	6	19908
Mor2Met3	Apr 79	677755	27°54.65'N, 93°38.02'W	96/100	1/17/79 21:52	3/25/79 22:46	6	16096
Mor 1Met1	Sep 79	677764	27°58.38'N, 93°32.19'W	60/100	7/12/79 18:05	9/4/79 19:11	6	12978
Mor 1Met2	Sep 79	677755	27°58.38'N, 93°32.19'W	94/100	7/12/79 18:21	9/5/79 11:15	6	13136
Mor 1Met3	Sep 79	611219	27°58.38'N, 93°32.19'W	96/100	7/12/79 18:38	9/1/79 21:26	6	12276
Mor2Met1	Sep 79	677754	27°54.57'N, 93°38.23'W	60/100	7/11/79 22:05	9/3/79 14:41	6	12892
Mor2Met2	Sep 79	611201	27°54.57'N, 93°38.23'W	94/100	7/12/79 02:09	9/4/79 12:21	6	13068
Mor2Met3	Sep 79	677763	27°54.57'N, 93°38.23'W	96/100	7/11/79 21:41	9/4/79 07:47	6	13068
Mor 1Met1	Dec 79	677764	27°58.55'N, 93°32.32'W	53/99	9/9/79 15:01	12/10/79 04:19	6	21979
Mor 1Met2	Dec 79	611219	27°58.55'N, 93°32.32'W	95/99	9/9/79 15:10	11/25/79 07:10	6	18411
Mor2Met1	Dec 79	677754	27°54.60'N, 93°38.23'W	53/99	9/11/79 16:19	11/28/79 14:19	6	18707
Mor2Met2	Dec 79	677763	27°54.60'N, 93°38.32'W	95/99	9/11/79 16:20	12/13/79 05:44	6	22220
Mor3Met1	Dec 79	677755	27°54.93'N, 93°52.79'W	61/107	9/11/79 18:15	12/9/79 22:39	6	21410
Mor 1Met1	Sep 80	611219	27°58.56'N, 93°32.61'W	53/99	4/22/80 23:20	8/12/80 20:20	20	8061
Mor 1Met2	Sep 80	611227	27°58.56'N, 93°32.61'W	95/99	4/23/80 18:00	9/7/80 04:20	20	9745
Mor2Met1	Sep 80	677764	27°54.43'N, 93°38.00'W	49/95	4/23/80 20:00	10/5/80 17:20	20	11734
Mor2Met2	Sep 80	611225	27°54.43'N, 93°38.00'W	90/95	4/23/80 20:00	8/20/80 07:40	20	8529
Mor3Met1	Sep 80	677763	27°54.35'N, 93°45.90'W	58/104	4/23/80 16:00	9/7/80 04:20	20	9760
Mor3Met2	Sep 80	677754	27°54.35'N, 93°45.90'W	100/104	4/23/80 16:00	8/20/80 06:00	20	8545

TABLE IV-1 (Continued)

MOORING & METER	MONTH OF RECOVERY	INSTRUMENT SERIAL NUMBER	LOCATION	DEPTH (m) METER/BOTTOM	TIME OF FIRST GOOD RECORDING	FINAL TIME	RECORDING INTERVAL (minutes)	TOTAL RECORDS (Including 6 header records)
Mor1Met1	Jan 81	677764	27°58.63'N, 93°32.52'W	54/96	10/13/80 19:40	1/19/81 21:20	20	7063
Mor1Met2	Jan 81	611239	27°58.63'N, 93°32.52'W	80/96	10/13/80 17:40	1/23/81 18:00	20	7360
Mor2Met1	Feb 81	677748	27°54.39'N, 93°37.95'W	32/99	10/25/80 09:35	2/11/81 15:15	20	7872
Mor2Met2	Feb 81	677755	27°54.39'N, 93°37.95'W	57/99	10/25/80 08:15	2/9/81 16:35	20	7736
Mor2Met3	Feb 81	611236	27°54.39'N, 93°37.95'W	83/99	10/25/80 09:15	2/10/81 03:55	20	7767
Mor2Met4	Feb 81	611225	27°54.39'N, 93°37.95'W	95/99	10/25/80 09:55	2/10/81 11:35	20	7788
Mor3Met1	Feb 81	611219	27°54.34'N, 93°45.89'W	52/101	10/20/80 17:50	2/9/81 17:11	20	8086
Mor3Met2	Feb 81	667763	27°54.34'N, 93°45.89'W	63/101	10/20/80 21:10	2/11/81 20:10	20	8212
Mor3Met3	Feb 81	611240	27°54.34'N, 93°45.89'W	90/101	10/20/80 21:10	2/10/81 06:50	20	8100
Mor3Met4	Feb 81	667754	27°54.34'N, 93°45.89'W	97/101	10/20/80 21:30	12/5/80 05:50	20	3270
Mor1Met1	Jul 81	677763	27°58.58'N, 93°32.53'W	47/97	3/6/81 00:40	7/16/81 00:00	20	9491
Mor1Met2	Jul 81	611226	27°58.58'N, 93°32.53'W	58/97	3/6/81 00:00	7/11/81 10:00	20	9182
Mor1Met3	Jul 81	677713	27°58.58'N, 93°32.53'W	85/97	3/6/81 00:20	7/16/81 00:00	20	9497
Mor1Met4	Jul 81	611225	27°58.58'N, 93°32.53'W	91/97	3/6/81 00:20	7/16/81 00:00	20	9492
Mor2Met1	Jul 81	668218	27°53.79'N, 93°37.47'W	50/103	3/5/81 22:20	6/3/81 21:40	20	6485
Mor2Met2	Jul 81	677748	27°53.79'N, 93°37.47'W	71.5/103	3/5/81 22:20	7/15/81 16:00	20	9495
Mor2Met3	Jul 81	611236	27°53.79'N, 93°37.47'W	85/103	3/5/81 22:20	7/15/81 16:40	20	9492
Mor2Met4	Jul 81	677754	27°53.79'N, 93°37.47'W	97/103	3/5/81 22:20	4/14/81 03:20	20	2830
Mor3Met1	Jul 81	668224	27°54.38'N, 93°45.90'W	53/103	3/5/81 17:40	7/16/81 05:40	20	9545
Mor3Met2	Jul 81	611219	27°54.38'N, 93°45.90'W	64/103	3/5/81 17:20	7/15/81 16:20	20	9508
Mor3Met3	Jul 81	611244	27°54.38'N, 93°45.90'W	91/103	3/5/81 17:20	7/15/81 15:00	20	9504
Mor3Met4	Jul 81	611229	27°54.38'N, 93°45.90'W	97/103	3/5/81 17:20	7/15/81 15:00	20	9505
Mor4Met1	Jul 81	677725	27°55.01'N, 93°55.01'W	47/97	3/5/81 22:20	7/15/81 15:00	20	9488
Mor4Met2	Jul 81	677755	27°55.01'N, 93°55.01'W	58/97	3/5/81 16:20	7/15/81 22:40	20	9526
Mor4Met3	Jul 81	611239	27°55.01'N, 93°55.01'W	85/97	3/5/81 16:20	7/15/81 13:40	20	9498
Mor4Met4	Jul 81	611240	27°55.01'N, 93°55.01'W	91/97	3/5/81 16:00	7/15/81 13:20	20	9503

TABLE IV-2
 QUALITY ASSESSMENT OF HYDROPRODUCTS CURRENT METER AND ASSOCIATED TIME SERIES DATA,
 EAST AND WEST FLOWER GARDEN BANKS
 (All Deployments from Jan 79 - Jul 81)

MOORING & METER	DATE OF RECOVERY	INVENTORY AND QUALITY (x indicates good throughout record)					DEPTH SENSOR
		SPEED	DIRECTION	TEMPERATURE	TRANSMISSIVITY (serial #)	CONDUCTIVITY	
Mor1Met1	Apr 79	1/16/79 10:34 - 3/13/79 15:04 (Recs 7-13492) good speed; bad thereafter.	Bad (Constant)		x		
Mor2Met1	Apr 79	1/17/79 21:16 - 3/6/79 19:16 (Recs 7-11507) good speed; fabricated speed thereafter.	x	x			
Mor2Met3	Apr 79	1/17/79 21:52 - 2/8/79 18:22 (Recs 7-5252) good speed; bad thereafter.	Bad (Constant)		x		

Mor1Met1	Sep 79		x	x			
Mor1Met2	Sep 79		x	x			
Mor1Met3	Sep 79	7/12/79 18:38 - 7/25/79 11:38 (Recs 7-3057) good speed; speed set = 20.0 thereafter.	x	x			
Mor2Met1	Sep 79	no recording (speed set = 20.0 throughout record).	x	x			
Mor2Met2	Sep 79		x	x			
Mor2Met3	Sep 79		x	x			

Mor1Met1	Dec 79	9/9/79 15:01 - 11/8/79 22:07 (Recs 7-14477) good speed; fabricated constant speed thereafter.	Bad (Constant)		x		
Mor1Met2	Dec 79	9/9/79 15:10 - 11/4/79 13:10 (Recs 7-13432) good speed; fabricated speed thereafter.	x	x			
Mor2Met1	Dec 79	9/11/79 16:19 - 10/23/79 08:19 (Recs 7-10007) good speed; fabricated speed thereafter.	Poor	x			
Mor2Met2	Dec 79	9/11/79 16:20 - 10/23/79 04:20 (Recs 7-9967) intermittent speed; fabricated speed thereafter.	x	x			
Mor3Met1	Dec 79	9/11/79 18:15 - 11/3/79 00:15 (Recs 7-12547) good speed; fabricated speed thereafter.	x	x			

Mor1Met1	Sep 80	4/22/80 23:20 - 5/31/80 07:20 (Recs 7-2767) good speed; fabricated speed thereafter.	x	x			
Mor1Met2	Sep 80	4/23/80 18:00 - 5/29/80 14:20 (Recs 7-2577) good speed; fabricated speed thereafter.	x	x		4/23 - 5/29, erratic decrease to 0; no recording thereafter. (#14)	
Mor2Met1	Sep 80	4/23/80 20:00 - 6/8/80 21:40 (Recs 7-3324) good speed; 6/8/80 22:00 - 8/8/80 19:40 (Recs 3325-7710) speed set = 20.0; 8/8/80 20:00 - 9/29/80 17:40 (Recs 7711-11447) good speed; low values thereafter.	x	x			

TABLE IV-2 (Continued)

MOORING & METER	DATE OF RECOVERY	INVENTORY AND QUALITY (x indicates good throughout record)					DEPTH SENSOR
		SPEED	DIRECTION	TEMPERATURE	TRANSMISSIVITY (serial #)	CONDUCTIVITY	
Mor2Met2	Sep 80	x	x	x	4/23 - 5/28, erratic decrease to 0; no recording thereafter.		
Mor3Met1	Sep 80	4/23/80 16:00 - 6/11/80 08:00 (Recs 7-3507) good speed; fabricated speed thereafter.	x	x			
Mor3Met2	Sep 80	4/23/80 16:00 - 6/13/80 08:40 (Recs 7-3657) good speed; fabricated speed thereafter.	x	x	4/24 - 5/30, good data. 5/30 - 6/10, rapid decrease; values < 50% thereafter. (#15)		
Mor1Met1	Jan 81	x	x	x			
Mor1Met2	Jan 81	x	x	x			
Mor2Met1	Feb 81	x	x	x		x	
Mor2Met2	Feb 81	10/25/80 08:15 - 12/8/80 16:35 (Recs 7-3207) good speed; fabricated speed thereafter.	x	x			
Mor2Met3	Feb 81	10/25/80 09:15 - 2/7/81 03:15 (Recs 7507) good speed; fabricated speed thereafter.	x	x	10/25 - 12/11, good data. 12/11 - 12/16, rapid decrease to below 56%. 12/16 - 12/27, rise to 60-64%. 12/27 - 2/10, decrease to below 56%. (#15)		
Mor2Met4	Feb 81	All speeds bad and set = 20.0 throughout record	x	x	10/25 - 1/4, good data; rapid decrease below 55% thereafter. (#30)		
Mor3Met1	Feb 81	10/20/80 17:50 - 2/7/81 16:51 (Recs 7-7927) good speed; fabricated speed thereafter.	x	x			
Mor3Met2	Feb 81	10/20/80 21:10 - 12/27/80 02:30 (Recs 7-4847) good speed; fabricated speed thereafter.	Bad (Constant)	No Good			
Mor3Met3	Feb 81	x	x	x	10/20 - 1/12, good data; rapid decrease below 55% thereafter. (#14)		
Mor3Met4	Feb 81	x	x	x	x (#31)		
Mor1Met1	Jul 81	3/6/81 00:40 - 6/18/81 01:20 (Recs 7-7496) good speed; fabricated speed thereafter.	Bad (Constant)	x			
Mor1Met2	Jul 81	3/6/81 00:00 - 5/14/81 10:40 (Recs 7-5007) good speed; fabricated speed thereafter.	x	x			

TABLE IV-2 (Continued)

MOORING & METER	DATE OF RECOVERY	INVENTORY AND QUALITY (x indicates good throughout record)						
		SPEED	DIRECTION	TEMPERATURE	TRANSMISSIVITY (serial #)	CONDUCTIVITY	DEPTH SENSOR	
Mor1Met3	Jul 81	3/6/81 00:20 - 3/27/81 14:40 (Recs 7-1103) fabricated speed. 3/27/81 14:60 - 4/4/81 16:40 (Recs 1104-1685) interpolations for speeds >40.0; 4/14/81 16:60 - 6/7/81 11:60 (Recs 1686-4551) and 5/16/81 20:00 - 5/27/81 03:40 (Recs 5223-5966) good speed; 6/7/81 12:00 - 5/16/81 19:40 (Recs 4552-5222) and 5/27/81 04:00-Record end (Recs 5967-9497) fabricated data.		x	x		x	
Mor1Met4	Jul 81	3/6/81 00:20 - 5/25/81 13:40 (Recs 7-5807) good speed; fabricated speed thereafter.		x	x	3/6 - 3/31, good data. 3/31 - 6/14, rapid decrease to <40%; values <40% thereafter. (#31)		
Mor2Met1	Jul 81	x		x	x		x	x
Mor2Met2	Jul 81	3/5/81 22:20 - 6/30/81 14:20 (Recs 7-8407) good speed; fabricated speed thereafter.		x	x		x	
Mor2Met3	Jul 81	x		x	x	3/5 - 5/8, good data. 5/8 - 6/30 rapid decrease to 25%; no recording thereafter. (#15)		
Mor2Met4	Jul 81	x		Bad (Constant)		x	Bad throughout record (#61)	
Mor3Met1	Jul 81	x		x	x		x	x
Mor3Met2	Jul 81	x		x	x			
Mor3Met3	Jul 81	3/5/81 17:20 - 6/24/81 20:00 (Recs 7-8007) good speed; fabricated speed thereafter.		x	x	3/5 - 5/6, good data. 5/6 - 5/20, rapid decrease; No recording thereafter. (#62)		
Mor3Met4	Jul 81	3/5/81 17:20 - 6/27/81 14:40 (Recs 7-8207) good speed; fabricated speed thereafter.		x	x	3/5 - 5/4, good data. 5/4 - 6/14, slow decrease; low values (25-30%) thereafter. (#14)		
Mor4Met1	Jul 81	x		x	x		x	
Mor4Met2	Jul 81	3/5/81 16:20 - 3/26/81 12:20 (Recs 7-1507) good speed; speed set = 20.0 thereafter.		x	x			
Mor4Met3	Jul 81	3/5/81 16:20 - 3/26/81 12:20 (Recs 7-1507) good speed; speed set = 20.0 thereafter.		x	x	3/5 - 4/8, good data. 5/6 - 6/12, drops below 40%. 6/13 climbs to 65%; steady decrease thereafter. (#30)		
Mor4Met4	Jul 81	3/5/81 16:00 - 3/26/81 12:00 (Recs 7-1507) good speed; speed set = 20.0 thereafter.		x	x	3/5 - 3/9, good data; no recording thereafter. (#7)		

TABLE IV-3
MARSH-McBIRNEY ELECTROMAGNETIC CURRENT METER DATA INVENTORY

The first four deployments were made on top of the East Flower Garden Bank. The last three deployments were on mooring 11, near the southwest edge of the East Flower Garden Bank.
x: Means good velocity.

ELECTROMAGNETIC CURRENT METER DISC FILE	LOCATION	DEPTH (m) METER/BOTTOM	TIME OF FIRST GOOD READING	FINAL TIME	RECORDING INTERVAL (minutes)	TOTAL RECORDS	VELOCITY
EMCM,EMA,Apr79	27°54.65'N, 93°35.92'W	28/30	2/10/79 18:00	4/16/79 05:30	15	6197	Low values
EMCM,EMA,Jul79	27°54.65'N, 93°35.92'W	28/30	4/29/79 18:00	7/07/79 05:20	20	4937	x
EMCM,EMA,Sep79	27°54.65'N, 93°35.92'W	28/30	7/14/79 23:30	8/29/79 14:20	20	3358	x
EMCM,EMA,Dec79	27°54.65'N, 93°35.92'W	28/30	9/25/79 00:00	10/16/79 13:50	10	3114	x
MOR2,EMCM,Sep80	27°54.43'N, 93°38.00'W	15/95	4/17/80 15:40	5/08/80 00:40	20	1469	x
MOR2,EMCM,Feb81	27°54.39'N, 93°37.95'W	20/99	10/24/80 22:25	1/11/81 19:54	20	5038	*
MOR2,EMCM,Jul81	27°53.79'N, 93°37.47'W	38/103	3/05/81 16:53	4/06/81 13:13	20	2315	x

*10/24/80 22:25 - 12/28/80 16:45 (Recs 7-4668) Good Velocity

12/28/80 17:05 - 1/11/81 19:54 (Recs 4669-5038) Steady increase in speed from 50.0 - 110.0 cm/sec.

TABLE IV-4
 DATA INVENTORY FOR CONDUCTIVITY-TEMPERATURE PROBE DEPLOYED ON MOORING LINE
 ADJACENT TO THE MARSH-McBIRNEY ELECTROMAGNETIC CURRENT METER

The first three deployments were on top of the East Flower Garden Bank. The last deployment was on mooring 11, near the southwest edge of the East Flower Garden Bank.

x: Means good data.

DISC FILE	LOCATION	FIRST GOOD TIME	FINAL TIME	RECORDING INTERVAL (minutes)	DEPTH (m) METER/BOTTOM	TOTAL RECORDS	TEMPERATURE	COND.
CONTMP.EMA.APR2379	27°54.65'N 93°35.92'W	2/10/79 16:44	4/24/79 09:10	6	27/30	18448	x	x
CONTMP.EMA.JUL1279	27°54.65'N 93°35.92'W	4/29/79 13:40	7/10/79 18:46	6	27/30	17330	x	x
CONTMP.EMA.SEP79	27°54.65'N 93°35.92'W	7/16/79 14:10	8/30/79 23:22	6	27/30	10893	x	x
CONTMP.EMA.SEP80	27°54.43'N 93°38.00'W	4/23/80 20:00	6/8/80 04:00	20	14/95	2904	x	x

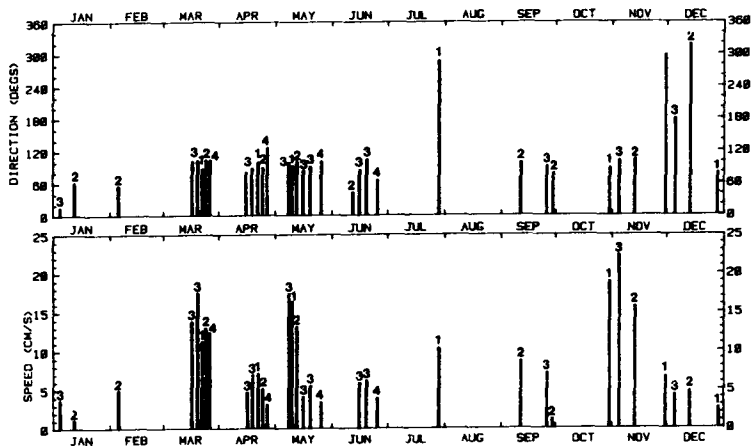


Figure IV-5a

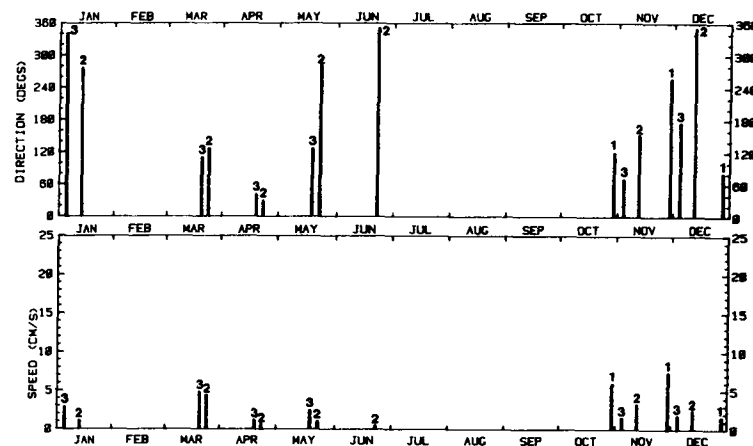


Figure IV-5b

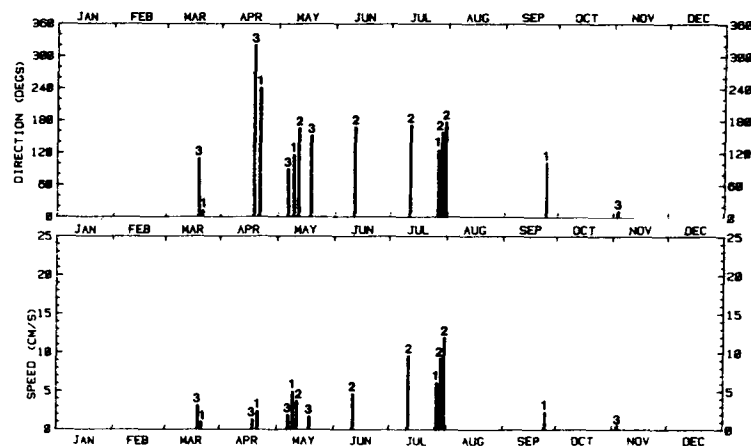


Figure IV-5c

Figure IV-5. One-month averages of speed and direction for current meters in the range: (a) from 32 m to 64 m depth; (b) from 11 m to 18 m from the bottom; and (c) from 4 m to 8 m from the bottom. The mooring number is printed above each average.

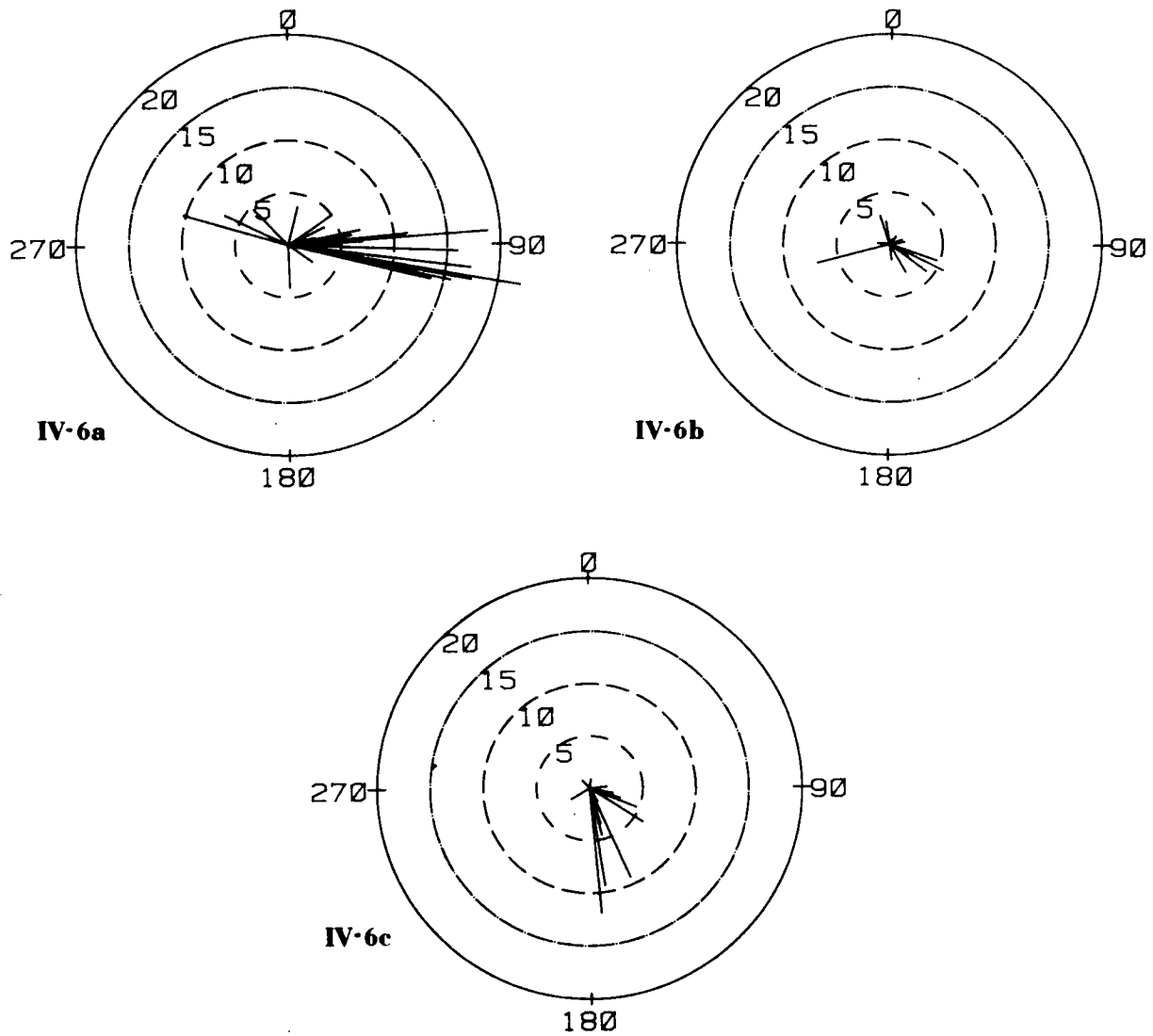


Figure IV-6. Monthly mean current vectors for all deployments and all moorings. Speed labels are in cm/sec. Data set divided into three depth ranges: (a) 32 m to 64 m depth (all measurements but one were taken in the depth interval from 47 m to 64 m; (b) 11 m to 18 m from bottom; (c) 4 m to 8 m from bottom.

also plotted on current-rose diagrams (Figure IV-6). In these diagrams, monthly averages from all deployments and all moorings are combined to produce separate composite plots for each of the three depth ranges.

The currents in the 32 m to 64 m layer are predominantly toward the east, with two exceptions. The first exception occurs from mid-July 1979 to mid-August 1979, when the upper layer one-month average direction was toward the northwest. During this period, the near-bottom layer velocity was toward the south. The probable reason for this period of anomalous currents was the passage of Tropical Storm Claudette. Claudette passed over the Flower Garden region travelling northward early on July 25, 1979, with windspeeds over 40 knots. Winds from this tropical storm also produced strong inertial currents from July 22 to July 30.

The second period with currents having a sustained westerly component was during December 1980. Currents in the upper layer were typically toward NNW or SSW, averaging NW. The cause of this abnormal current direction is not yet clear. Average winds in December were toward the southwest, whereas the normal average for the rest of the year is toward the northwest. During the last two-thirds of December, the winds went through cycles, caused by the passage of anticyclonic waves (or northers). During each of these cycles, winds were first toward the southwest with windspeeds of 30 to 45 knots, lasting about 24 hours; then a period lasting for two, three, or more days ensued with light and variable winds. Apparently, the usual condition of average-currents toward the east is associated with winds which are directed on the average toward the northwest.

The bottom currents are directed primarily toward east to south. Stronger bottom flows are directed more to the south. The monthly average speeds near the bottom are highly variable, normally between 1 to 5 cm/sec, but sometimes near 10 cm/sec. Currents in the depth range from 11 m to 18 m of the bottom have the most variable monthly direction averages with the overall vector mean toward the southeast. The speed is mainly from 1 to 5 cm/sec. There is apparently no seasonal trend in the monthly averages in any of the three depth ranges. This may be due to the lack of a large enough sample.

In the 32 m to 64 m depth range, the monthly means have little variation from mooring to mooring in either speed or direction. However, in the bottom depth range (within 8 m of the bottom) the monthly mean direction at mooring 2 (the mooring closest to any bank) appears to be steered along the local isobaths. The average direction for the five one-month velocity averages in the bottom layer on mooring 2 is 166.3° (standard deviation, 7.33°). The tangent to the isobaths at their location is about 150° . Also, the average speeds at the bottom of mooring 2 are greater than the current speeds at the bottom of the other moorings. After excluding these bathymetrically steered currents from the set of bottom current records so that what remains is more representative of the general circulation near the shelf break, we find that the vector average of the remaining monthly averages has a speed of 1.6 cm/sec and a direction of 112° (about ESE). The variance among

the individual estimates is large, but six out of the ten estimates had directions within 20° to 30° of the mean, and they also had the greatest speeds, the others having speeds less than 1 cm/sec, except in a single case. So the mean also appears to be the mode.

Away from the banks, the average speeds near the bottom are greatly attenuated and the bottom currents are directed only a few tens of degrees to the right of the surface currents. More important, the bottom currents have an offshore component of flow.

Velocity Variance

The measured currents, U , at a point may be conveniently represented as the sum of two components, the monthly mean, \bar{U} , plus the fluctuations from the mean, u :

$$U = \bar{U} + u.$$

The fluctuations are due to such factors as the fairly deterministic internal and barotropic tidal currents, inertial currents excited by local winds, various long waves such as shelf waves and Kelvin waves, high frequency internal waves, turbulence, and other shorter time scale fluctuations in the currents due to winds. Methods such as spectral analysis may be employed to examine the time series of current fluctuations in the frequency domain. A good deal of useful information may also be determined by manipulation of the velocity variance tensor; i.e., the tensor of the second moments of velocity. Examination of the variance tensor is particularly useful when topographic steering of the currents is occurring, although it gives unambiguous results only when the entire frequency range of motions is affected in the same way by the topography.

The velocity variance of horizontal currents is described by the variance tensor \bar{V} , which is composed of four terms,

$$\bar{V} = \begin{vmatrix} \overline{u^2} & \overline{uv} \\ \overline{vu} & \overline{v^2} \end{vmatrix}$$

where u and v are the horizontal velocity components in the two orthogonal coordinate directions, x and y , respectively. The overbar indicates a time average. In general, the variance tensor is not invariant under a coordinate rotation; i.e., the components of \bar{V} change as the orientation of the coordinate axes changes. \bar{V} is a symmetric tensor. Symon (1960) shows that by rotation of the coordinate axes through an angle θ , the tensor becomes diagonalized. The axes at this particular orientation are called the principal axes, and the diagonal terms are

the characteristic values. The off-diagonal terms (the cross covariances) are, of course, zero, and the diagonal terms (the autocovariances) are a maximum and minimum. The trace, or the sum of the diagonal terms, is invariant under rotation, and for the velocity variance tensor the trace is proportional to the kinetic energy. The characteristic values are the eigenvalues, λ , of the original (unrotated) tensor; i.e., the λ are found from the determinant,

$$\begin{vmatrix} \overline{u^2} - \lambda & \overline{uv} \\ \overline{vu} & \overline{v^2} - \lambda \end{vmatrix} = 0.$$

The orientation, θ , of the principal axis is

$$\theta = 1/2 \tan^{-1} \left(\frac{\overline{2uv}}{\overline{u^2} - \overline{v^2}} \right)$$

The autocovariances $\overline{u^2}$ and $\overline{v^2}$ and the cross-covariance \overline{uv} have been computed over one-month segments for all good current meter velocity data recorded during the six deployment periods. The following statistics were then computed in the manner discussed above:

- (1) θ , the orientation of the major principal axis; the variance $\overline{u^2}$ is a maximum in this direction; the convention for θ is 0° to north and increasing clockwise;
- (2) $\epsilon = \overline{u_0^2} / \overline{v_0^2}$, the ratio of the maximum, $\overline{u_0^2}$, to the minimum, $\overline{v_0^2}$, variances, along the principal axes;
- (3) $K = \overline{u_0^2} + \overline{v_0^2}$, the sum of the maximum and minimum variances, proportional to the total kinetic energy.

In a few cases, the velocity time series appeared to have attenuated speeds, perhaps due to a broken rotor bearing or to biofouling. Some of these records have been used for determining values of θ and ϵ , but not K .

Plots of major axis direction, θ , versus magnitude of ϵ and of K have been prepared. The major factor determining θ appears to be the position of the mooring relative to the banks. Therefore, results for each mooring appear on separate plots. Figure IV-7 shows plots of ϵ versus θ for all meters on mooring 2 for (a) the first five deployments, and for (b) deployment 6 (recovered July 1981). They are separated into two groups because mooring 2 was moved on deployment 6 to a position southward of the previous position group of the first five

deployments. On each plot of θ versus ϵ or of θ versus K , the local isobath direction is indicated. Also, the direction of the bank from the mooring position is drawn in. The bank direction is determined as the range of direction of the bank where bottom depth is 10 m or less than the depth of the mooring.

The major axis of variance closely aligns with the bottom isobaths at both sites of mooring 2 except in two cases. Both exceptions occur in the upper layer: meter 1 (at 49 m depth) on deployment 4, and meter 1 (50 m depth) on deployment 6. Table IV-5 lists the average direction $\bar{\theta}$ (computed by averaging the estimates of θ) for each deployment at mooring 2. The standard deviation of direction, θ , the local isobath direction (θ isobath), and the difference in direction between $\bar{\theta}$ and the local isobaths are also listed. The two cases mentioned above, where the monthly average directions did not align with the isobaths, were excluded from the total averages. The direction difference is always positive and ranges from 6° to 24° . Some of the difference in direction may be caused by uncertainties in the determination of isobath direction. However, the fact that the difference is always

TABLE IV-5
AVERAGE DIRECTION OF MAJOR AXIS OF VARIANCE COMPARED TO
LOCAL ISOBATH DIRECTION

DEPLOYMENT	AVERAGE DIRECTION ($\bar{\theta}$)	LOCAL ISOBATH DIRECTION (θ isobath)	STD. DEV. OF DIRECTION	Δ DIR. $\bar{\theta} - \theta_{\text{isobath}}$	NUMBER OF ESTIMATES
1	170.1	156.4	--	13.7°	1
2	166.4	149.4	7.14	17°	2
3	173.5	149.4	--	24°	1
4	157.0	152.0	3.7	5°	3
5	158.2	152.0	7.82	6°	6
6	136.9	122.8	6.9	14°	7

positive strongly suggests that the current variance is also aligned somewhat toward the major axis of the entire East Flower Garden Bank.

In all but one case, the variance ratio, ϵ , is between 1.1 and 2.5 for the top meters at mooring 2. For the deeper meters at this mooring, ϵ ranges from 2 to 15. The ratio at the upper meter is similar in magnitude to the value found at all depths at all of the other moorings. Apparently, in the depth range of the top meters (32 m to 60 m) the bathymetric effect on ϵ is negligible, but in many cases the major axis still aligns with isobaths.

The bathymetric steering effect is not so obvious at the other moorings. Figure IV-8 shows ϵ versus θ for all meters and deployments at mooring 1. The direction, θ , ranges mainly between 90° and 135° , whereas the local isobaths are roughly along 90° , and there appears to be no relationship to depth. The variance ratio (ϵ) ranges from about 1.2 to 3.6. The results for magnitude of ϵ are similar at mooring 3, shown in Figure IV-9, but the direction is more southerly, with θ

grouped around 135° to 180° (with a few exceptions). The direction change may be related to the channelling of flow between the two Flower Garden Banks.

Meters were placed at mooring 4 only during the last deployment. During deployment 2 and only then, mooring 3 was also placed on the northwest side of the West Flower Garden Bank. Only the top meter of mooring 3 returned good velocity data on that deployment. A plot of ϵ versus θ for mooring 4 is shown in Figure IV-10. On both moorings, the direction of the major axis of variance is within about 30° of the direction of the local isobaths, except in one case. In that case, a line extending along the major axis direction through the mooring position passes just south of the West Flower Garden Bank. In fact, the major variance direction is directed in such a manner as to pass north or south of the bank. A very significant fact is that this is also a general result: at all depths at all moorings, the major axis direction is such as to miss the banks. A few exceptions are found in the surface region of mooring 2, and one each at moorings 1 and 3.

Figure IV-11 is a bathymetric map of the Flower Garden region. Centered at each mooring position is a circle with pie-shaped sections indicating the range of directions of the major axis of velocity variance. Most, but not all, of the one-month estimates were used in constructing these ranges. Note that the major axis of variance is directed principally in directions other than toward a nearby bank.

It must be remembered that, except at the lower meters of mooring 2, the ratio, ϵ , is not too far from unity (the variance ellipse is often nearly circular) so that variance has the same order of magnitude in all directions. In other words, current fluctuations are often directed toward the bank, and the bank's influence only slightly decreases the average fluctuation speed in the direction toward the bank.

The sum of the variances, K , along the major and minor axis directions (proportional to total kinetic energy density) has been plotted versus direction, θ , for all four moorings (Figures IV-12 through 16). K generally ranges between 50 and 200 cm/sec. The exceptionally high energy cases all occur at the upper meters (depth less than 64 m). K decreases with depth in nearly every case where coincident velocity records at different depths are available. The magnitude of K has no apparent preferred direction within the scatter of directions found at each mooring.

Severe Weather Episodes and Periods of Anomaly

Some of the most violent meteorological conditions occur at the Flower Garden region when a hurricane passes by. The velocity and temperature data obtained during one of these periods are briefly discussed below. Three hurricanes and two other periods when anomalous currents and temperature fluctuations were observed are discussed.

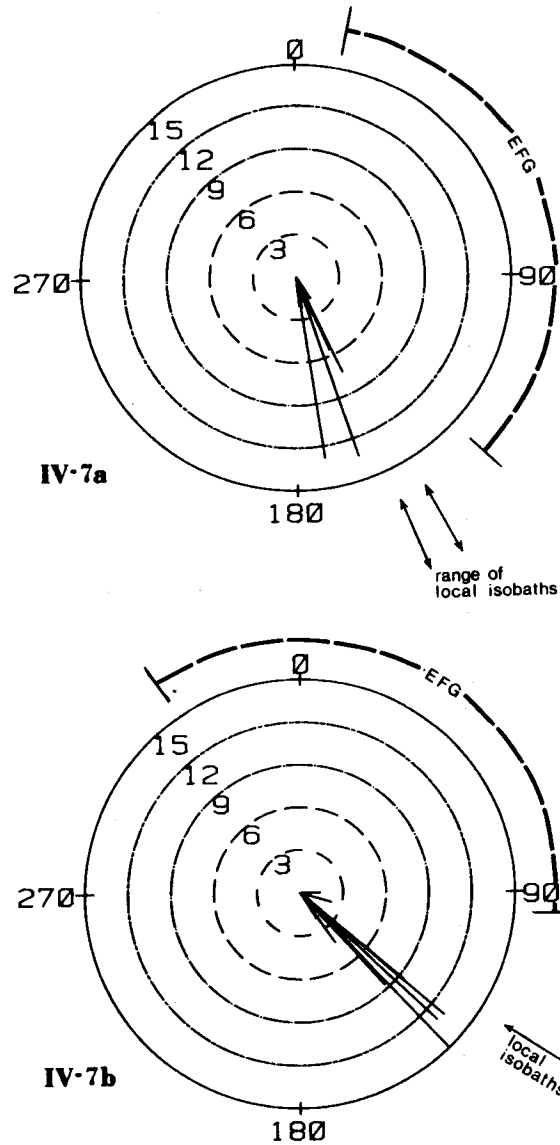


Figure IV-7. Ratio, ϵ , of the variance along the major axis to the variance along the minor axis, plotted in the direction, θ , of the major axis for (a) all meters on mooring 2 deployed before March 1981, and (b) all meters on mooring 2 for the March to July 1981 deployment.

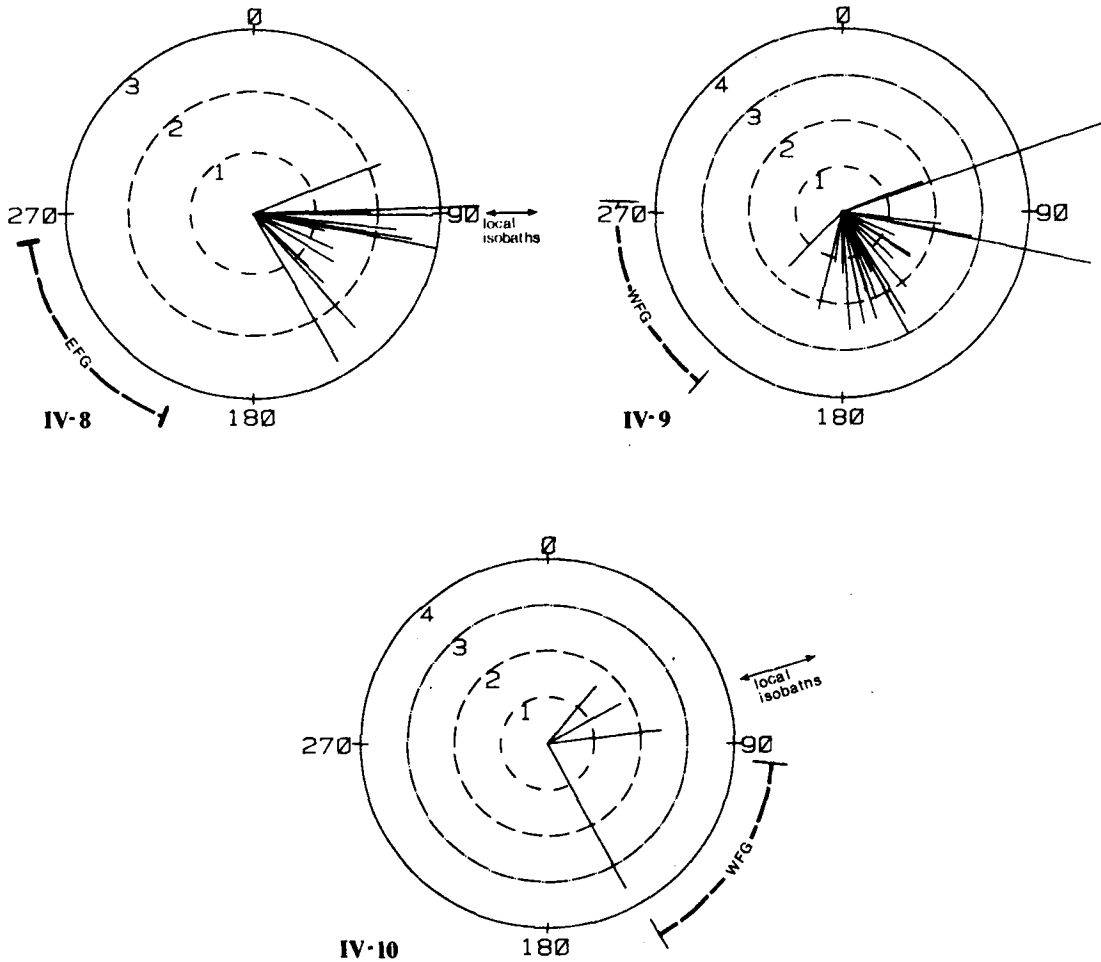


Figure IV-8. Ratio, ϵ , of the variance along the major axis to the variance along the minor axis, plotted in the direction, θ , of the major axis for all meters on mooring 1.

Figure IV-9. Ratio, ϵ , of the variance along the major axis to the variance along the minor axis, plotted in the direction, θ , of the major axis for all meters on mooring 3.

Figure IV-10. Ratio, ϵ , of the variance along the major axis to the variance along the minor axis, plotted in the direction, θ , of the major axis for all meters on mooring 4.

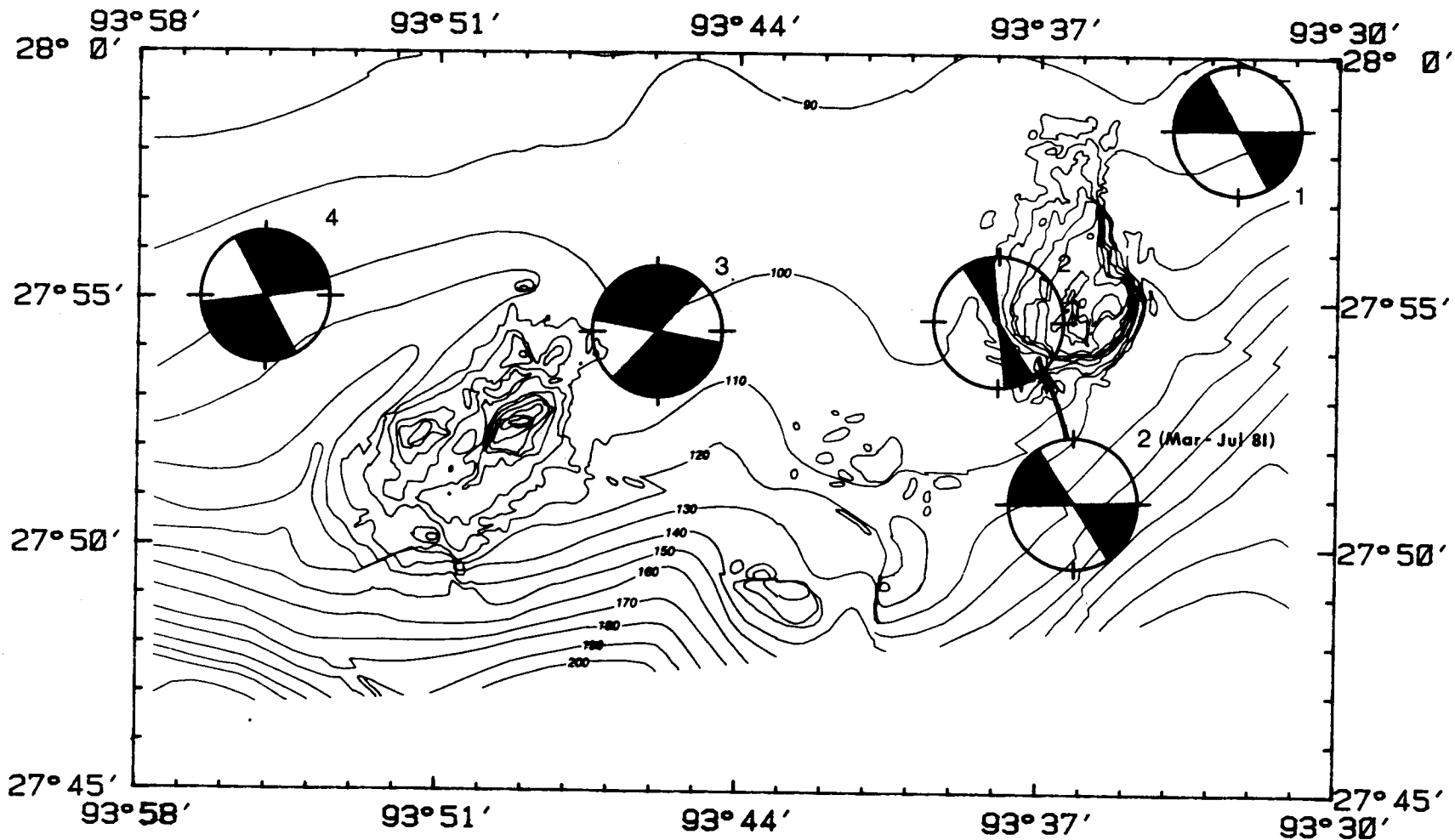


Figure IV-11. Shaded region in each circle shows the range of directions of the major axis of velocity variances for most one-month velocity segments at each mooring (see text for exceptions). Each circle is centered at the mooring position, except for the Mar-Jul 81 deployment of mooring II. The arrow tip indicates the position of mooring II during Mar-Jul 81.

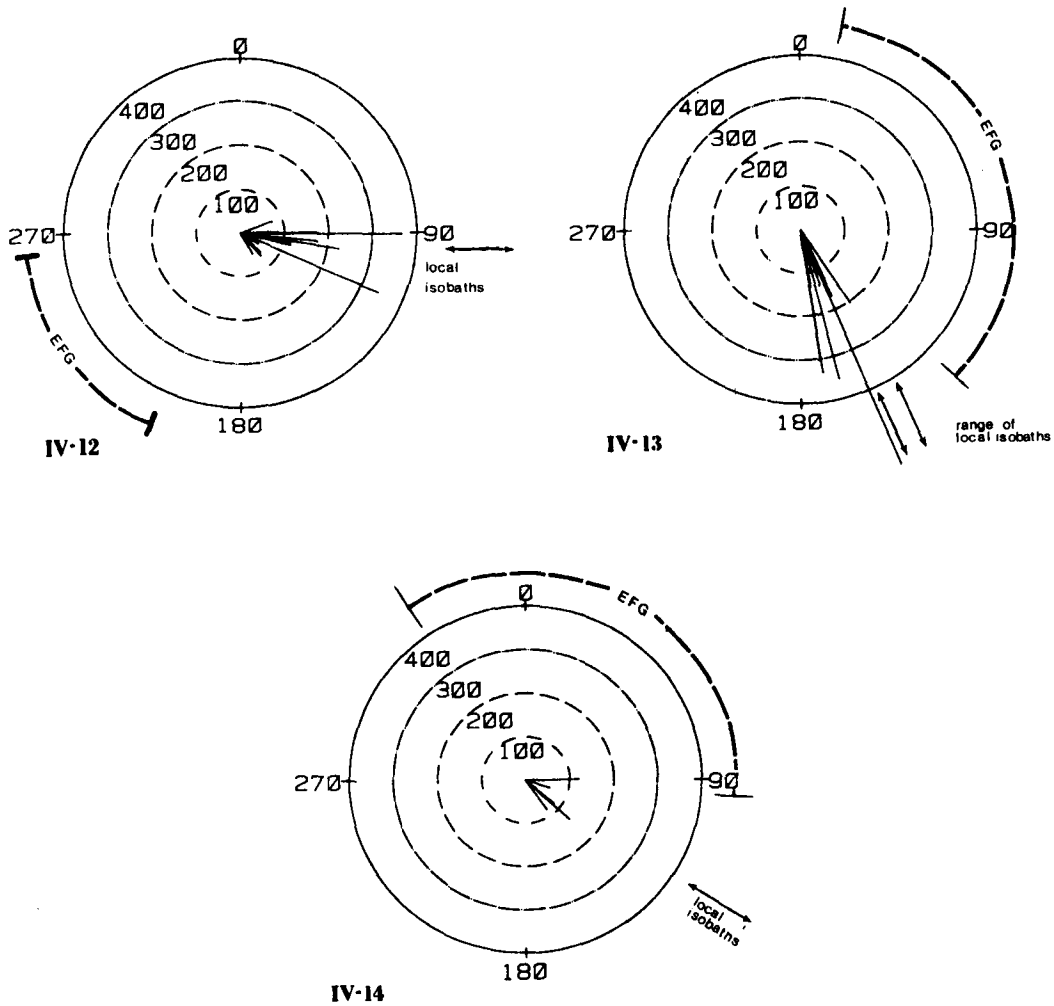


Figure IV-12. Sum, K , of the variances along the major and minor axis directions, plotted in the direction, \ominus , of the major axis for all meters on mooring 1.

Figure IV-13. Sum, K , of the variances along the major and minor axis directions, plotted in the direction, \ominus , of the major axis for all meters on mooring 2 deployed before March 1981.

Figure IV-14. Sum, K , of the variances along the major and minor axis directions, plotted in the direction, \ominus , of the major axis for all meters on mooring 2 for the March to July 1981 deployment.

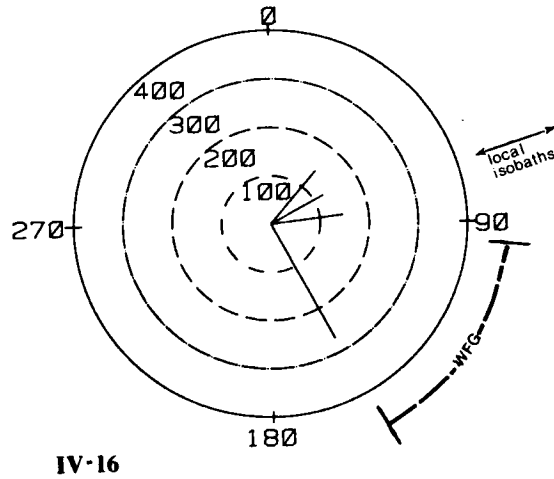
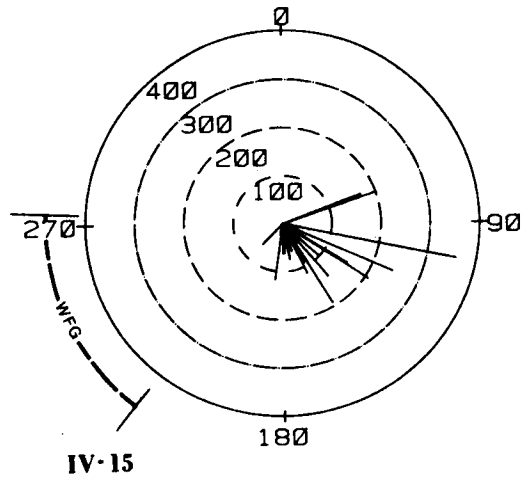


Figure IV-15. Sum, K , of the variances along the major and minor axis directions, plotted in the direction, Θ , of the major axis for all meters on mooring 3.

Figure IV-16. Sum, K , of the variances along the major and minor axis directions, plotted in the direction, Θ , of the major axis for all meters on mooring 4.

The summer of 1979 was a period of exceptionally severe weather for the northwest Gulf of Mexico. Four tropical cyclones passed over or near the Flower Garden region between 11 July and 13 September 1979. These events all occurred during the previous contract period and will not be discussed here, but intensive research into these episodes is planned.

Hurricane Henri

Two more periods of severe weather occurred later in 1979 during periods when current meter and temperature time series data are available. The first of these was Hurricane Henri, which both developed and died in the Gulf without making landfall. It was only a minor disturbance in the Flower Garden region. Winds up to 25 m/sec were recorded as coming from the northeast for two and a half days and then from the southeast for another two and a half days during the period from 15 to 20 September 1979, the period of its greatest intensity in the Flower Garden region. No appreciable long-term currents or temperature changes occurred, but substantial inertial currents with speeds near 25 cm/sec were generated and lasted throughout the 5-day period. Only the upper meters at moorings 2 and 3, at depths of 53 m and 61 m, respectively, were operational at this time, so that only temperature data are available at greater depths.

3-15 October 1979

The next event occurred between 3 October and 15 October, 1979, during a period of fairly calm weather. Winds were predominantly out of the southwest at 5 to 10 m/sec. Current meter and temperature data from this period are shown in Figure IV-17. These time series have been filtered to eliminate oscillations with periods less than 28 hours. Thus, the diurnal and semidiurnal tidal currents and the inertial currents have been eliminated. At the beginning of this period, temperatures at the upper meters rose by more than 4°C over about two to three days. These meters were situated within the very strong thermocline just below the surface mixed layer. Therefore, the rise in temperature can be accounted for by as little as an 8 m increase in the thermocline depth, judging by the XBT profiles taken during the ROSS SEAL cruise in October 1979. The thermocline dropped enough so that for part of the time the upper current meters were in the upper mixed layer. This is revealed by the flat-topped appearance of the temperature oscillations once the layer of constant temperature is entered. A strong current toward the east, with speeds from 30 to 40 cm/sec, developed during this period. Superimposed on this current was a strong north-south oscillation with a period of about two days and north-south velocity amplitudes of 10 cm/sec. Temperature fluctuations of the same period and with amplitudes about the mean of approximately 2°C, closely correspond to the velocity fluctuations; temperature is at its minimum (thermocline closest to the surface) when velocity is most northerly (toward the north). Apparently, the temperature drop is not related to pure advection, since in that case the two oscillations would be 90° out of phase. The bottom meter at mooring 2, which was situated 5 m from the bottom, has the same two-day period temperature

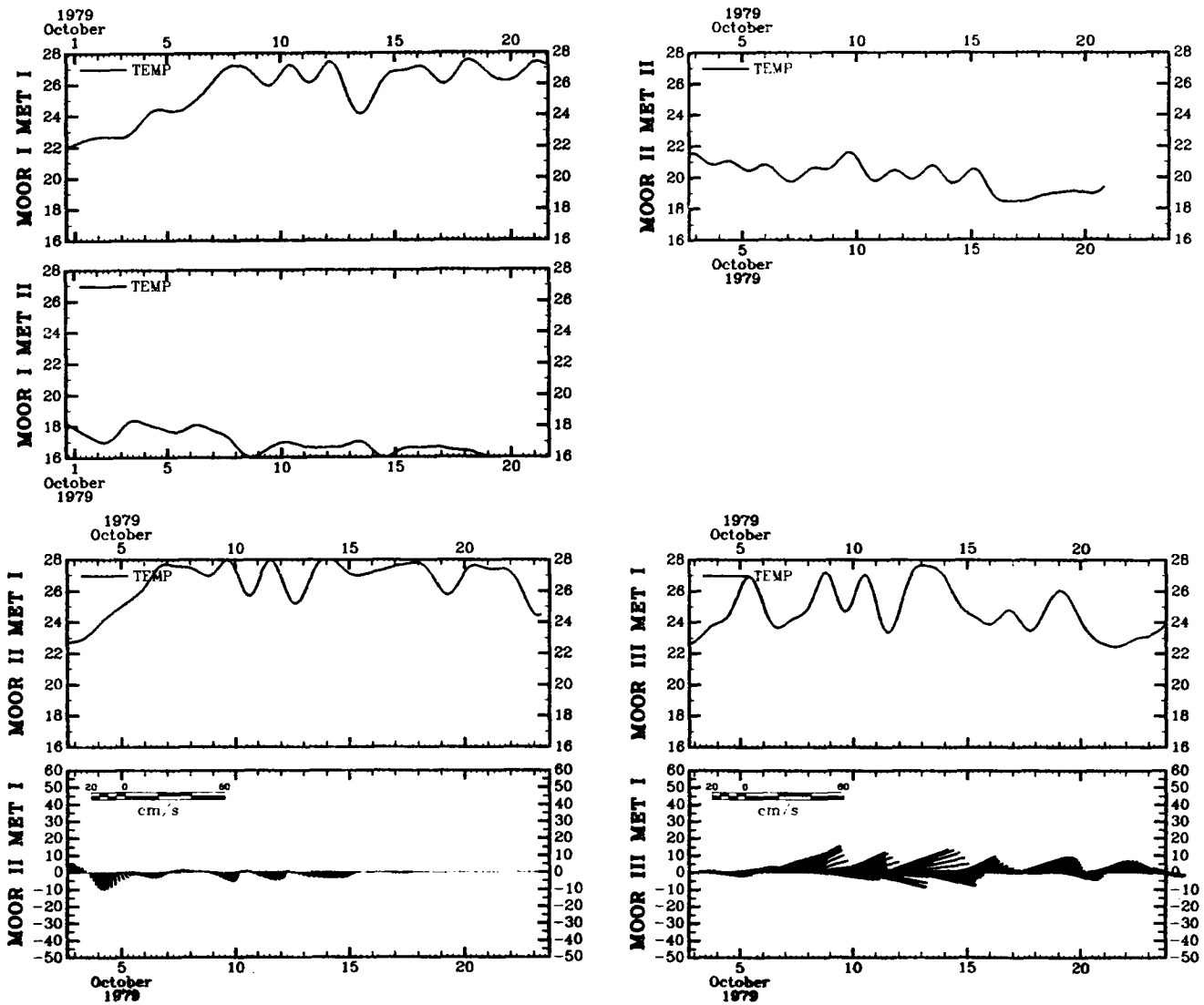


Figure IV-17. Low-pass filtered time series of temperature and horizontal velocity at the moorings and meters indicated.

fluctuations, but with amplitudes less than 1°C . However, the temperature oscillations at the lower meters are not phase locked to the temperatures of the upper meter.

Hurricane Allen

Hurricane Allen passed through the Yucatan Channel into the Gulf of Mexico on August 7, 1980. It then travelled WNW through the Gulf, finally hitting land just north of Brownsville, Texas at 0600 GMT 10 August. Sustained winds in the Gulf were in the neighborhood of 100 knots. The eye of Allen passed about 170 n.m. south of the Flower Garden Banks. Unfortunately, out of the entire current meter array, only the bottom current meter on mooring 2 was recording currents at this time. This meter is situated 5 m from the bottom at the southwest edge of the East Flower Garden Bank. Figure IV-18 shows the raw temperature series and the velocity stick plot time series during the period when Hurricane Allen passed by. The principal effect of the storm at this meter was to cause inertial currents with maximum velocities of 30 cm/sec and strong temperature oscillations with peak to peak amplitudes of about 2°C . The strongest inertial currents occurred just after the hurricane hit land.

It is very curious that these temperature oscillations have a period which is one-half that of the inertial currents. They are apparently not due to the semidiurnal tides, although their periods are nearly the same. At the moorings which are not too close to the banks, the inertial currents are nearly circular; i.e., the velocity vector remains nearly constant in magnitude as it rotates 360° during each inertial period. But at mooring 2, due to the nearness of the bank, the inertial current direction remains tangent to the local isobaths, and reverses direction every half inertial period. In Figure IV-18, vertical lines are drawn through each point in time when the current velocity goes to zero as the current reverses direction. These lines are extended down through the temperature curve to demonstrate that the temperature minima line up well with these velocity reversal times, and that they do so even when the time period between reversals is somewhat erratic. For this reason, the temperature oscillations are thought to be related to the inertial currents rather than to the semidiurnal tides.

The temperature oscillations may be indicative of large vertical excursions of the isotherms up and down the sides of the bank. A typical temperature gradient near the bottom at this time of year is probably from $2^{\circ}\text{C}/15\text{ m}$ to $2^{\circ}\text{C}/10\text{ m}$. Therefore, the isotherms may undergo vertical migrations of 10 m to 15 m every six hours, if we assume that the temperature change is due to sloping of the isotherms near the bank and not to horizontal advection. Horizontal advection may be discounted because if it were to occur, the temperature and velocity oscillations would have the same period.

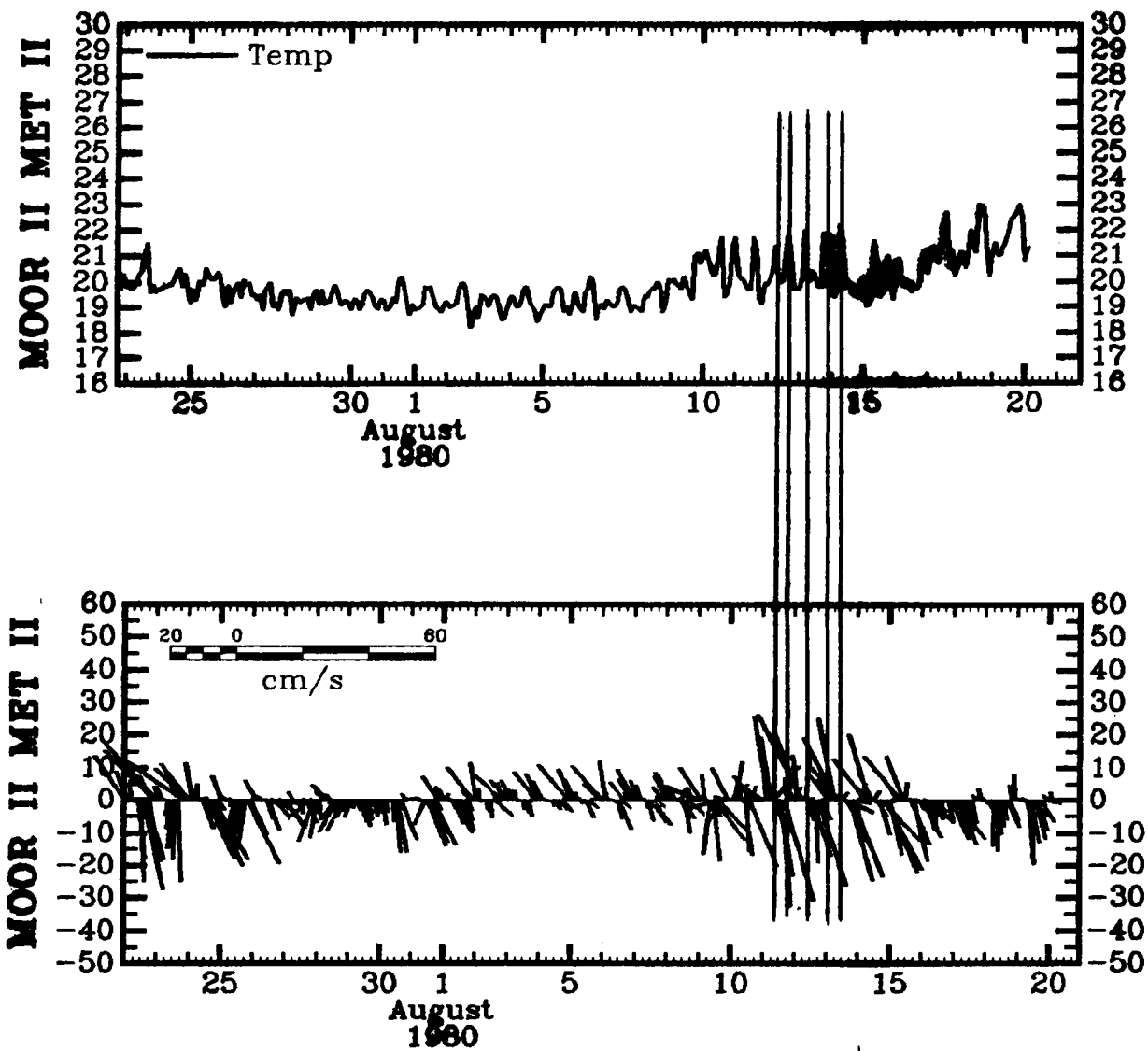


Figure IV-18. Time series of temperature and horizontal velocity from meter 2 of mooring 2, which is situated near the southwest edge of the East Flower Garden Bank at 5 m from the bottom. Hurricane Allen travelled through the Gulf of Mexico 7-10 August 1980.

15-19 May 1980

Inertial oscillations with speeds similar to those caused by Hurricane Allen were also recorded at the bottom meter of mooring 2 (same deployment), from about 15 to 19 May 1980. Plots of the velocity and temperature time series during this period are shown in Figures IV-19 and 20 for the upper and lower meters of all three moorings. Inertial currents with similar magnitudes were also recorded during this period at the upper meter (49 m depth) on this mooring and also on the upper meters of moorings 1 and 3. However, the bottom meters at moorings 1 and 3 did not show the strong inertial oscillations. Therefore it is speculated that the close proximity of mooring 2 to the edge of the bank may be the critical factor in finding inertial currents near the bottom. If this is so, then these strong inertial currents might also occur along the entire perimeter of the bank and probably along the slopes of the bank. A review of all current meter data collected during this project reveals that, in general, inertial waves are greatly attenuated with depth at all moorings, except mooring 2, which is the only mooring immediately adjacent to a bank.

The temperature oscillations near the bottom on mooring 2 during the period from 15 to 19 May are unlike those observed during Hurricane Allen since they have a predominantly inertial period. In fact, inertial period oscillations of the isotherms are the norm during periods of strong inertial currents. In these normal cases, the temperature at mooring 2 reaches an upper limit just as the velocity reaches its strongest southerly flow, and the temperature reaches its minimum when the velocity is most northerly. Once again, this cannot be due to simple advection by the inertial currents of a water mass which has a horizontal, north-south temperature gradient. Nor do these observations match the simple model of isotherm displacement by the current component normal to the bank, as discussed before.

Hurricane Jeanne

Hurricane Jeanne stayed within about 100 n.m. of the Flower Garden region from 13 to 15 November 1980. During this stage, it was only a tropical storm (from 27 to 66 knots, by definition) and was weakening to a tropical depression (less than 27 knots) by the 15th. Meteorological measurements were not taken at the High Island Platform during the most violent part of the storm. However, wind speeds of 40 knots were measured early on November 13, one day before its closest approach. The only effect on the currents was the development of inertial currents with maximum velocities of 30 to 40 cm/sec at meter 1 on mooring 2, which was located at a depth of only 32 m. At the depth of the upper meters on the other moorings (52 to 57 deep), the inertial oscillations were very small. Once again, though, inertial currents were fairly strong (about 20 cm/sec maximum) at the near-bottom (83 m deep) meter of mooring 2.

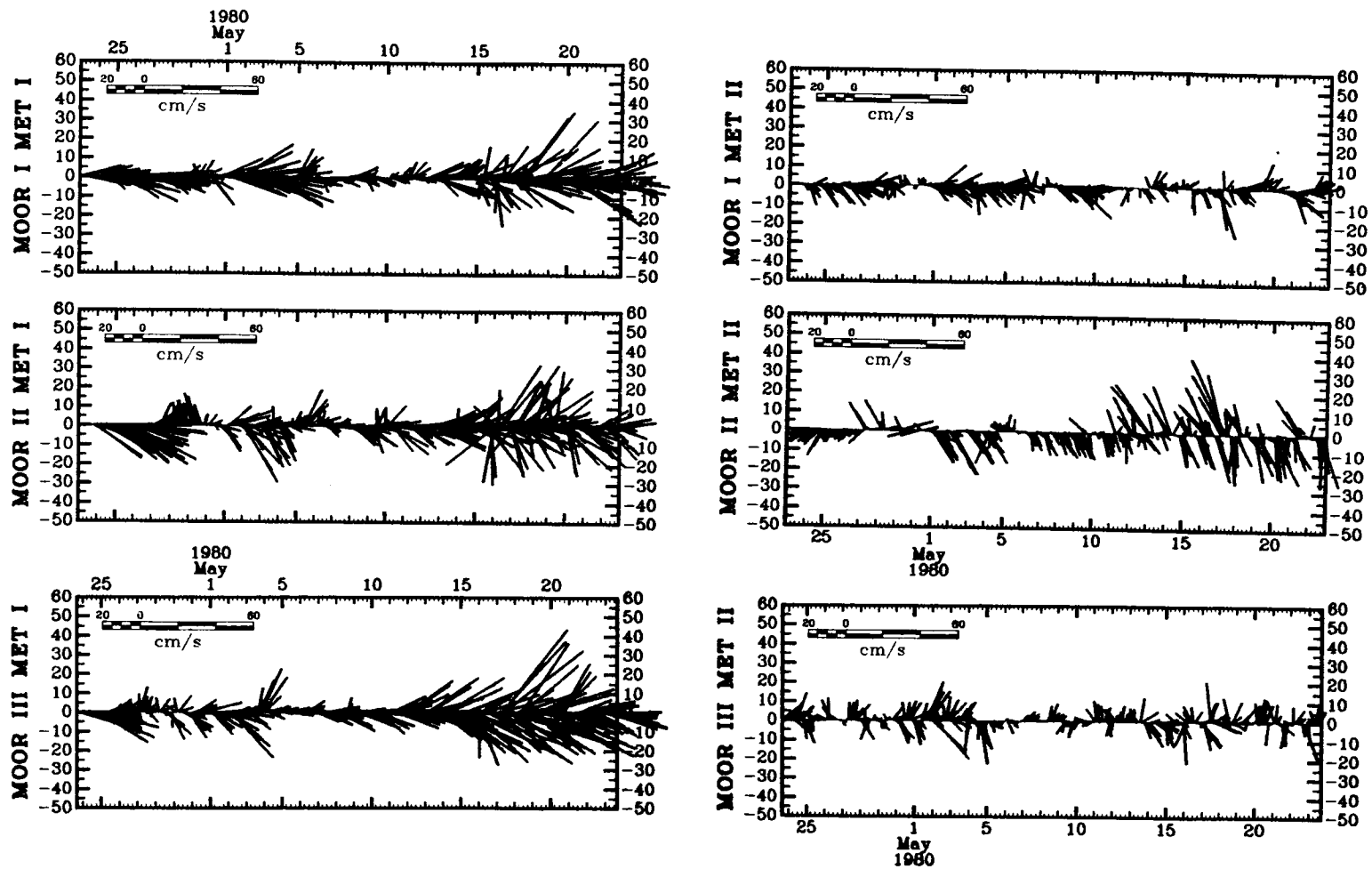


Figure IV-19. Time series of horizontal currents at the upper and lower meters of moorings 1, 2, and 3. Strong inertial currents are observed 15-19 May 1980.

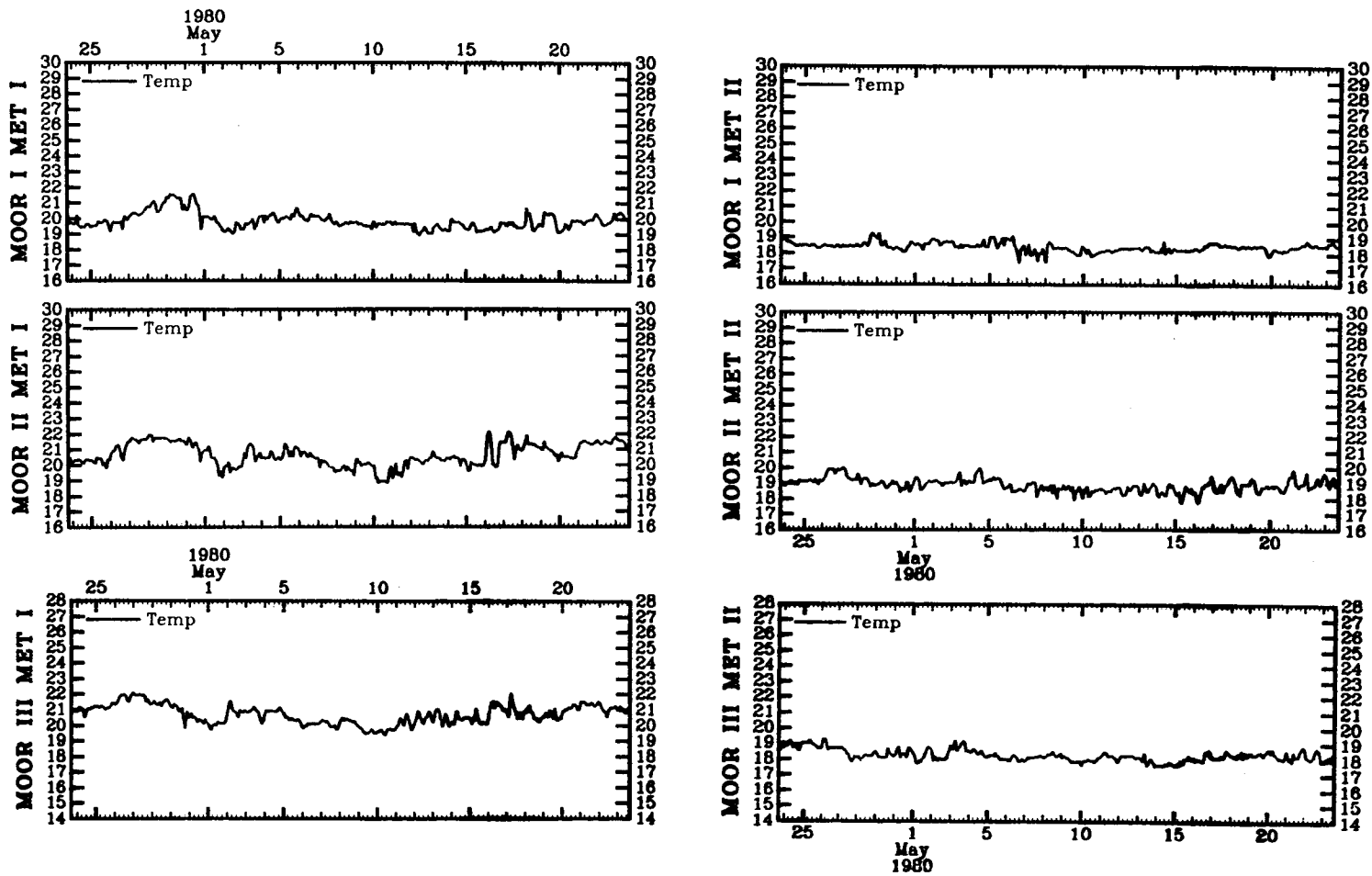


Figure IV-20. Time series of temperature at the upper and lower meters of moorings 1, 2, and 3. Strong inertial currents are observed 15-19 May 1980.

Spectral Analysis

Methods

A principal technique in the analysis of time series is spectral analysis. The theory and methods of spectral analysis are the subject of many books (e.g., Bendat and Piersol, 1971; Jenkins and Watts, 1968). This section is intended to present an elementary introduction to the theory and techniques of spectral analysis and to provide some relationships which may be useful for the interpretation of spectra.

The finite range Fourier transform $X(f,T)$ of the finite length time series $x(t)$ is obtained by

$$X(f,T) = \int_0^T x(t) e^{-i2\pi ft} dt \quad (1)$$

where

$$i = \sqrt{-1}$$

T = the length of the series x

and

$2\pi f$ = the radian frequency.

The raw spectral density estimate is

$$S_x(f) = \frac{1}{T} XX^* \quad (2)$$

where

X^* is the complex conjugate of X .

S (the two-sided spectral density estimate) is defined over the frequency range $(-\infty, \infty)$, but it is common to define the one-sided estimate $G_x(f) = 2S_x(f)$ where f varies only over $(0, \infty)$. G is normally used rather than S since S is symmetric about $f = 0$ when x is real, and the computation of S for negative f is redundant. An important property of $G_x(f)$ is that

$$K_x(T) = \frac{1}{T} \int_0^T x_k^2(t) dt = \int_0^\infty G_x(f) df \quad (3)$$

where K_x is the variance or second moment of the series x over the interval $(0,T)$. Hence the area under the curve on a plot of the spectral density is proportional to the variance (but only on a linear-linear plot).

The fundamental bandwidth for a time series of length T is $1/T$. The time series is completely determined by values of the Fourier transform spaced $\Delta f_T = 1/T$ apart in frequency. Therefore, independent spectral density estimates are also spaced $1/T$ apart. The part of the total variance within a frequency bandwidth Δf_T centered on the frequency f_0 is given by $G_x(f_0) \Delta f_T = G_x(f_0)/T$, and therefore the area under each segment of the spectrum (on a linear-linear plot) is proportional to the variance in that band of frequency. Comparisons of spectral density magnitudes at sharp peaks in the spectrum computed for different time series cannot be made directly unless the two series have the same length. For instance, tidal energy is contained within a number of very narrow bands of frequency. Suppose that for a very long series the tidal energy for a particular constituent is contained within a frequency band which is narrower than $1/T$ (the bandwidth determined by the series length). As the length of the series is shortened, the bandwidth and $1/T$ increases, but since the variance stays constant, the magnitude of $G_x(f)$ must decrease. $G_x(f) \Delta f_T$ must stay essentially constant as long as Δf_T is larger than the bandwidth of the true physical process. A finite length time series of a very narrow band process can be represented by a sinusoid with frequency f_0 and amplitude

$$A_{f_0} = \left(\frac{2}{T} G_x(f_0) \right)^{1/2} \quad (4)$$

However, over regions of the spectrum where $G_x(f)$ is relatively flat or has a constant slope, direct comparisons between different spectra are possible since changes in T have a relatively small effect on the magnitude of G in these regions.

This report considers mainly the spectra of velocity and temperature. The velocity records are a special case since they are vector series. Spectral analysis of vector time series is discussed in Gonella (1972) and in Mooers (1973). They developed the theory for separating the spectral density into clockwise and anticlockwise components. The sum of the clockwise and anticlockwise spectra equal the sum of the spectra of the two orthogonal velocity components of the vector series.

The relationship between two scalar series may be investigated by calculation and analysis of coherence, response, and phase spectra between the two series. Consider two time series $x(t)$ and $y(t)$ of length T with Fourier transforms $X(T,f)$ and $Y(T,f)$. The two raw auto spectra, G_x and G_y , and the cross spectrum, G_{xy} , can then be computed. The cross spectrum, which is complex in general, is defined by

$$G_{xy}(f) = \frac{2}{T} X(f)Y^*(f). \quad (5)$$

The raw functions may be smoothed by either ensemble averaging (usually from separate segments of the same series) or by averaging over con-

secutive frequency bands. The following functions can be computed from the averaged spectra: the frequency response function,

$$H(f) = \frac{G_{xy}(f)}{G_x} \quad (6)$$

which is complex in general,

and the coherency (squared) function,

$$\gamma^2 = \frac{|G_{xy}|^2}{G_x G_y} \quad (7)$$

The coherency has the range $0 \leq \gamma^2 \leq 1$. The vertical bars designate the modulus. It is convenient to express H in polar notation as

$$H = |H(f)| e^{-i\theta(f)} \quad (8)$$

where $|H(f)|$ is called the gain factor (called frequency response on plots in this report), and $\theta(f)$ is the phase factor.

The interpretation of the response and coherence functions is made very clear by study of the linear relationship between time series in the form of a least squares error problem as discussed in Bendat and Piersol (1971). The results of this line of development are summarized as follows. Let $\hat{y}(t)$ be the time series computed by a linear transformation on $x(t)$ which best approximates $y(t)$ in the least squares sense; i.e., the mean square error

$$\epsilon^2 = \int_0^{\infty} (y - \hat{y})^2 dt \quad (9)$$

is a minimum. Further, if $\Delta y(t) = y(t) - \hat{y}(t)$, let the one-sided "smoothed" spectra of x , y , \hat{y} , and Δy be G_x , G_y , $G_{\hat{y}}$, and $G_{\Delta y}$, respectively, and the cross spectrum between x and y be G_{xy} . Then, the following relationships hold,

$$G_{\hat{y}} = \gamma^2 G_y \quad (10)$$

$$G_{\Delta y} = G_y [1 - \gamma^2] \quad (11)$$

where γ^2 is defined as in (7). Therefore, γ^2 is the fractional part of the variance at each frequency of $y(t)$ which can be predicted

by linear transformation of $x(t)$. The linear transformation occurs by convolution of $x(t)$ with the impulse response function, $h(t)$ as,

$$\hat{y}(t) = \int_0^{\infty} h(\tau) x(t-\tau) d\tau. \quad (12)$$

The frequency response function, $H(f)$, is the Fourier transform of $h(t)$

$$H(f) = \int_0^{\infty} h(t) e^{-I2\pi ft} dt. \quad (13)$$

The relationships between G_x , $G_y^{\hat{}}$, and G_y in terms of H are given by

$$G_y^{\hat{}}(f) = |H(f)|^2 G_x(f) \quad (14)$$

$$G_y(f) = \frac{G_y^{\hat{}}(f)}{\gamma^2(f)} = \frac{|H(f)|^2}{\gamma^2(f)} G_x(f) \quad (15)$$

We may wish to compare the average sinusoidal amplitudes of two series, $x(t)$ and $y(t)$, at a particular frequency where a sharp peak in the spectrum occurs. For instance, $x(t)$ may be the north-south velocity component and $y(t)$ may be the temperature. The ratio of the amplitudes is

$$\frac{A_y(f)}{A_x(f)} = \left(\frac{G_y(f)}{G_x(f)} \right)^{1/2} = \frac{|H(f)|}{(\gamma^2)^{1/2}}. \quad (16)$$

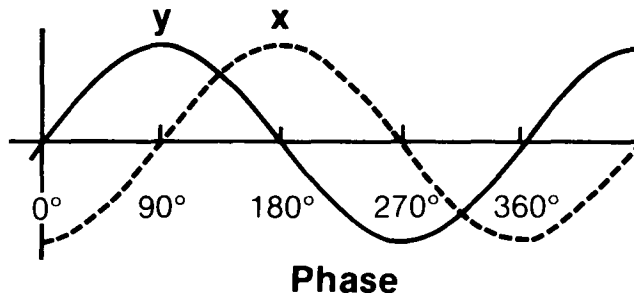
But the ratio of that part of $y(t)$ which is coherent with x , with the amplitude of $x(t)$ at a particular frequency is

$$\frac{A_y^{\hat{}}(f)}{A_x(f)} = \left(\frac{G_y^{\hat{}}(f)}{G_x(f)} \right)^{1/2} = |H(f)|. \quad (17)$$

The phase difference between the x and y series is $\theta(f)$, the phase function, given by

$$\theta(f) = \text{ATAN} [-\text{IMAG}(H(f)) / \text{REAL}(H(f))]. \quad (18)$$

For example, at a particular frequency f , the value $\theta = 90^\circ$, means that series y lags series x at that frequency by 90° :



Spectra of Velocity and Temperature

Preliminary spectral analyses of the velocity and temperature time series from the four moorings have been performed. The autospectra show many similarities, but there are significant differences among them related to the proximity to the banks, to the depth within the water column, and to season. A complete analysis will not be presented here. Rather, some particular examples will be discussed to assess a few of the most important features. A complete analysis is planned for the future, including studies of the tides, inertial currents, and shelf waves.

Velocity Spectra

The current and temperature records from mooring 3 (east side of West Flower Garden Bank) recorded during the last deployment (6 Mar to 16 Jul 81) comprise the most complete vertical array of current meter data taken during this project. This is due to both the quality and length of the series and to the fact that four current meters and their associated sensors were used on this mooring. The autospectra of both the u-component (east-west) and v-component (north-south) of velocity; the response function, coherency, and phase between u and v; and the clockwise and anticlockwise rotary spectra of each of four meters on mooring 3 are shown in Figures IV-21 through 40. The four current meters, numbered 1-4, were positioned at the depths 53 m, 64 m, 91 m, and 97 m, respectively, and the water depth was 103 m.

The u and v autospectra are composed of two primary parts. One, due to random fluctuations of the currents, appears as a constant slope of the power density, $G(f)$, versus frequency, f , on the log-log plots. The functional relationship is therefore,

$$G(f) = Af^{-a} \quad (19)$$

where $a > 0$. In many cases, two lines of different slope (different value of "a") are joined at some intermediate frequency (usually near a period of 10 hours). The slope parameter, a , is nearly constant throughout the frequency range of the u-autospectra for the upper two meters of mooring 3. However, the value of "a" decreases at periods greater than 12 to 24 hours for the v-components of the upper two

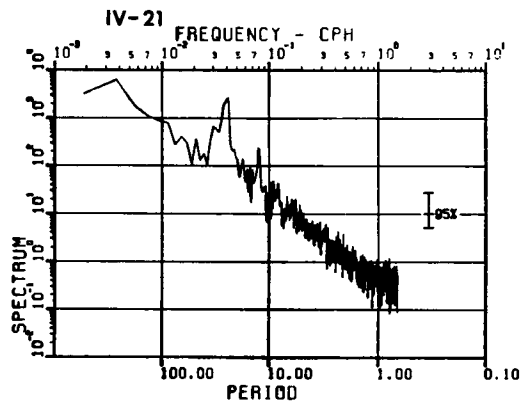


Figure IV-21. Autospectrum of u-component (east-west) of the velocity for meter 1 of mooring 3, recovered July 1981. The units of spectral density are $(\text{cm}^2/\text{sec}^2)/\text{cph}$.

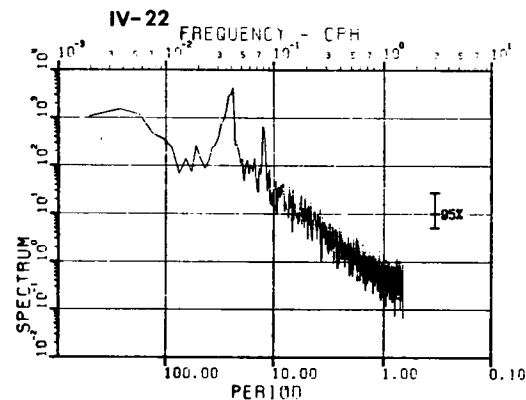
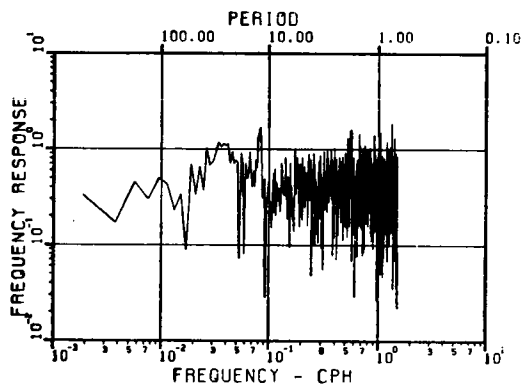


Figure IV-22. Autospectrum of v-component (north-south) of the velocity for meter 1 of mooring 3, recovered July 1981. The units of spectral density are $(\text{cm}^2/\text{sec}^2)/\text{cph}$.



IV-23

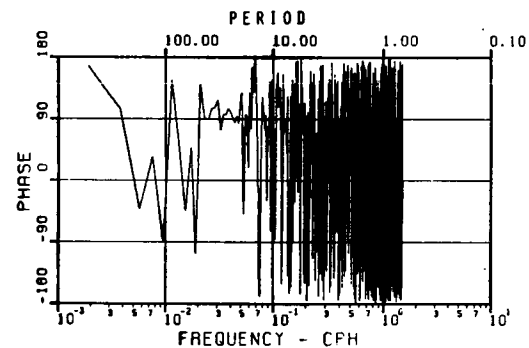


Figure IV-23. Frequency response and phase between the u and v components of velocity for meter 1 of mooring 3, recovered July 1981.

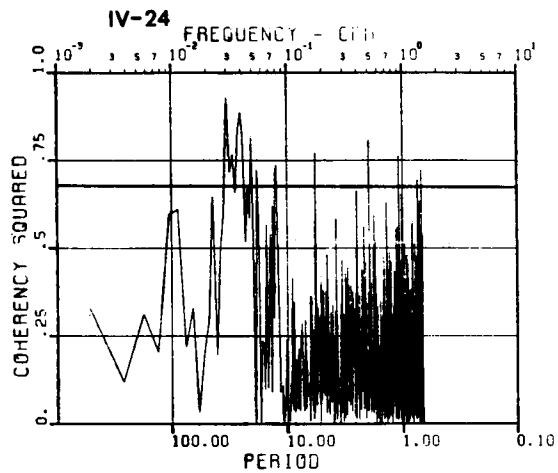
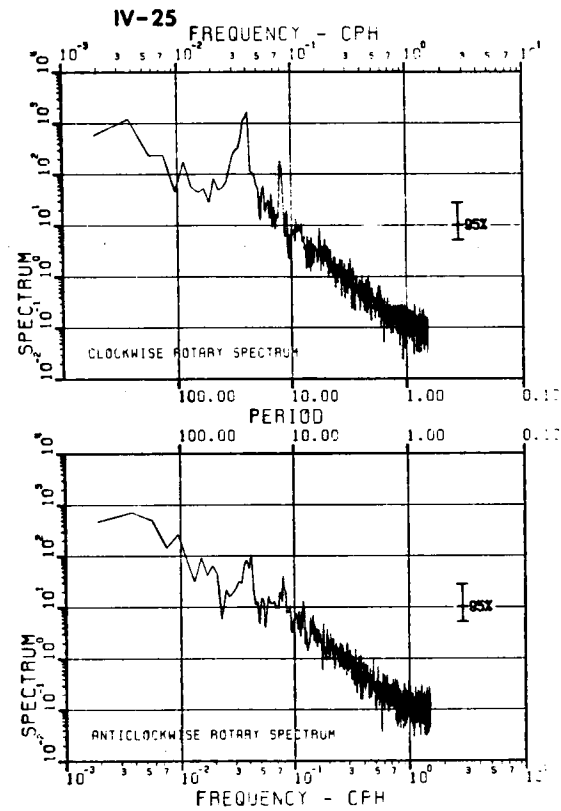


Figure IV-24. Coherence squared between the u and v components of velocity for meter 1 of mooring 3, recovered July 1981.

Figure IV-25. Rotary spectrum of the u-v velocity vector for meter 1 of mooring 3, recovered July 1981. The units of spectral density are $(\text{cm}^2/\text{sec}^2)/\text{cph}$.



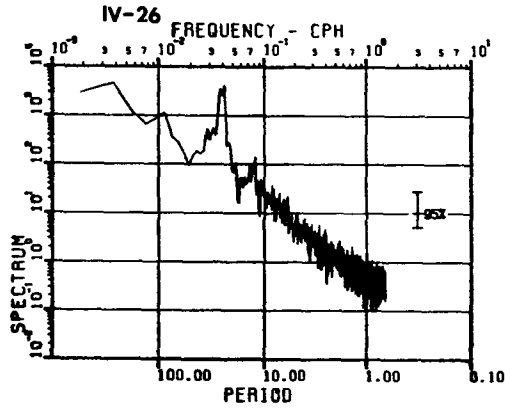


Figure IV-26. Autospectrum of u-component (east-west) of velocity for meter 2 of mooring 3, recovered July 1981. The units of spectral density are $(\text{cm}^2/\text{sec}^2)/\text{cph}$.

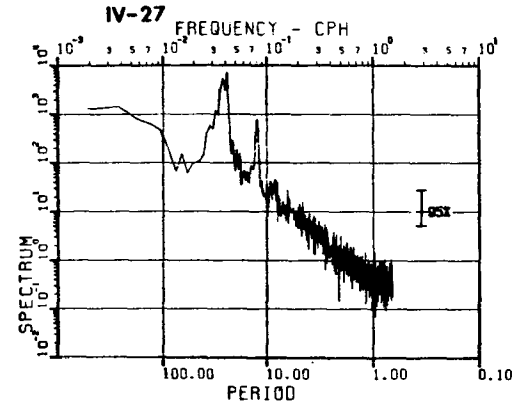
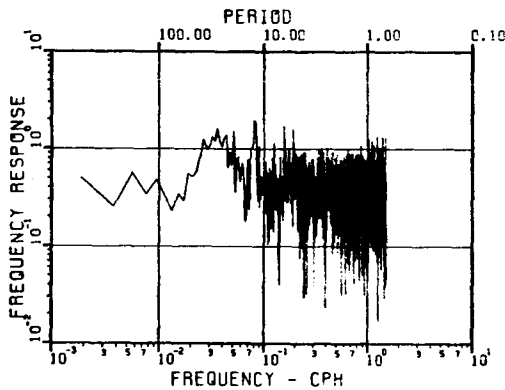


Figure IV-27. Autospectrum of v-component (north-south) of velocity for meter 2 of mooring 3, recovered July 1981. The units of spectral density are $(\text{cm}^2/\text{sec}^2)/\text{cph}$.



IV-28

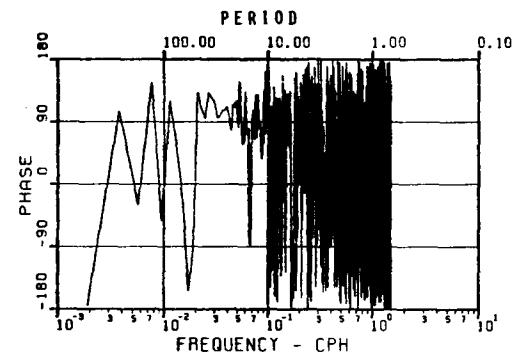


Figure IV-28. Frequency response and phase between the u and v components of velocity for meter 2 of mooring 3, recovered July 1981.

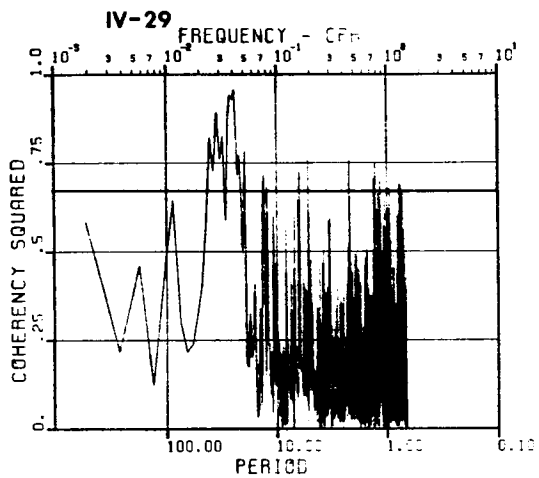
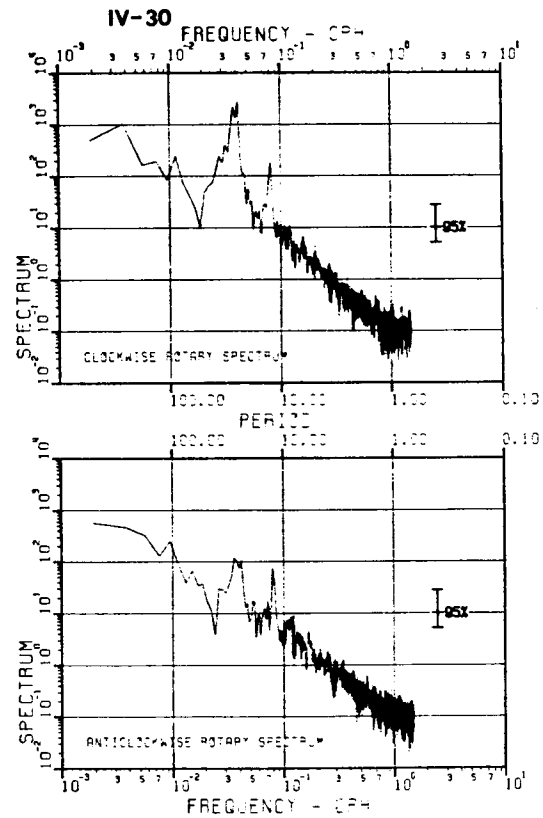


Figure IV-29. Coherence squared between the u and v components of velocity for meter 2 of mooring 3, recovered July 1981.

Figure IV-30. Rotary spectra of the u-v velocity vector for meter 2 of mooring 3, recovered July 1981. The units of spectral density are $(\text{cm}^2/\text{sec}^2)/\text{cph}$.



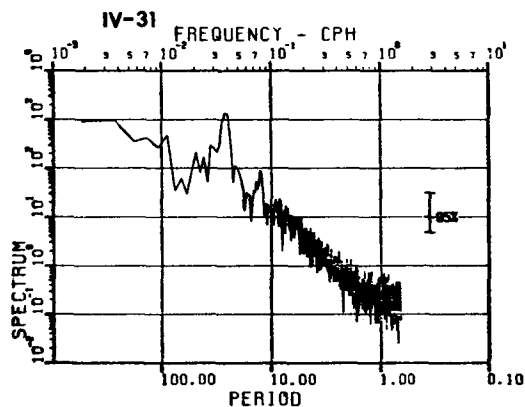


Figure IV-31. Autospectrum of u-component (east-west) of velocity for meter 3 of mooring 3, recovered July 1981. The units of spectral density are $(\text{cm}^2/\text{sec}^2)/\text{cph}$.

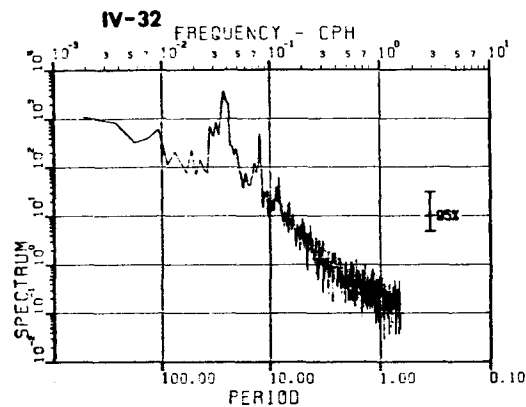
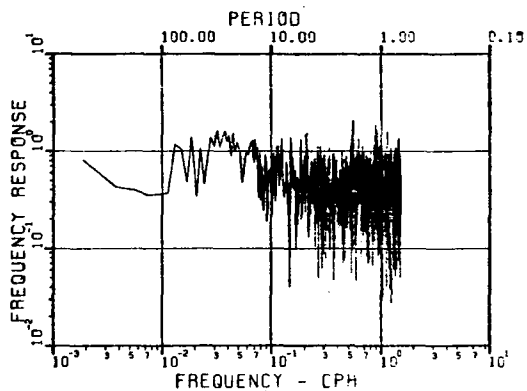


Figure IV-32. Autospectrum of v-component (north-south) of velocity for meter 3 of mooring 3, recovered July 1981. The units of spectral density are $(\text{cm}^2/\text{sec}^2)/\text{cph}$.



IV-33

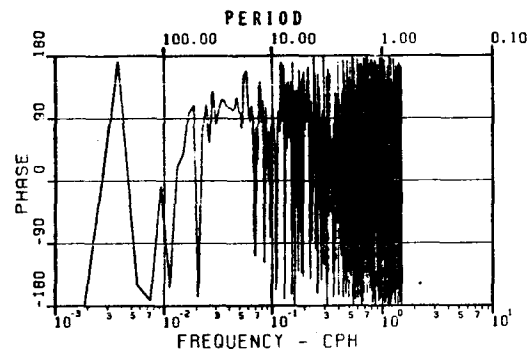


Figure IV-33. Frequency response and phase between the u and v components of velocity for meter 3 of mooring 3, recovered July 1981.

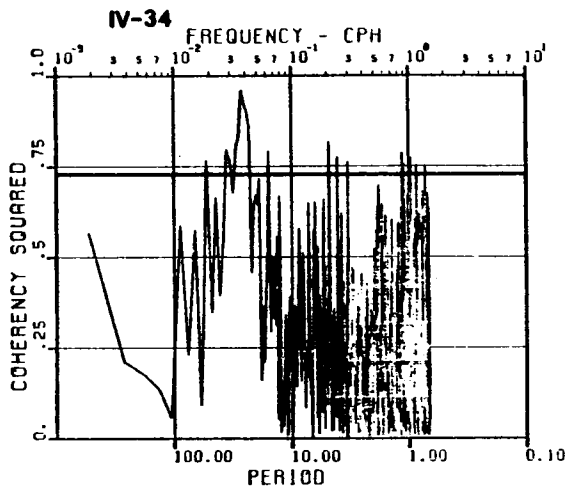
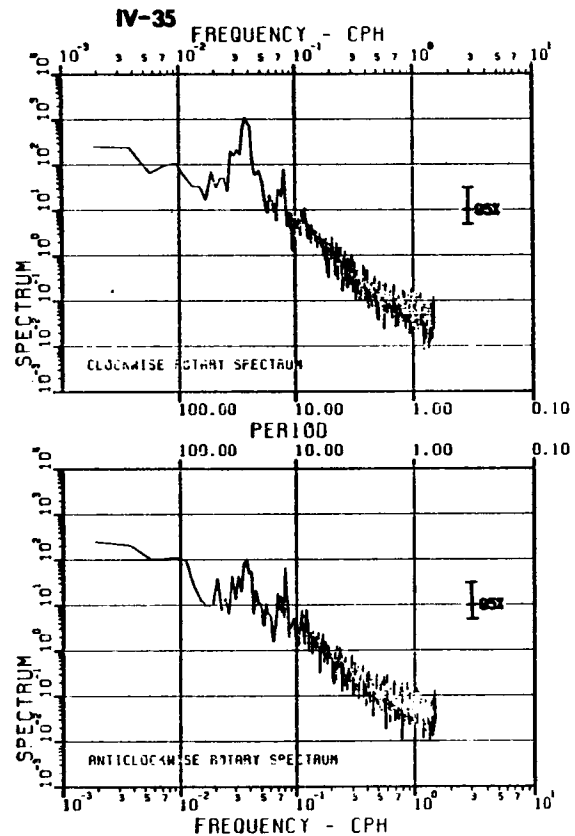


Figure IV-34. Coherence squared between the u and v components of velocity for meter 3 of mooring 3, recovered July 1981.

Figure IV-35. Rotary spectra of the u-v velocity vector for meter 3 of mooring 3, recovered July 1981. The units of spectral density are $(\text{cm}^2/\text{sec}^2)/\text{cph}$.



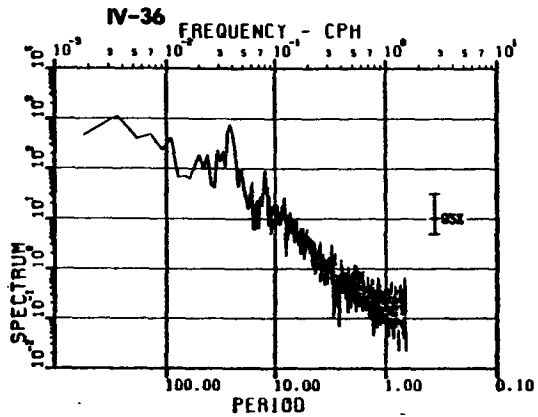


Figure IV-36. Autospectrum of u-component (east-west) of velocity for meter 4 of mooring 3, recovered July 1981. The units of spectral density are $(\text{cm}^2/\text{sec}^2)/\text{cph}$.

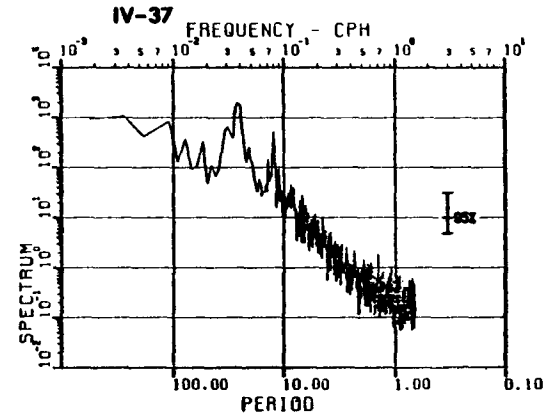
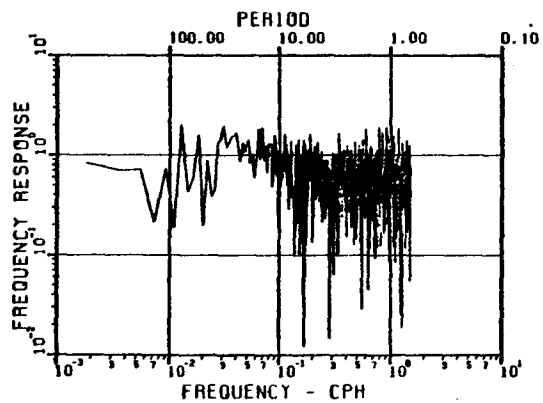


Figure IV-37. Autospectrum of v-component (north-south) of velocity for meter 4 of mooring 3, recovered July 1981. The units of spectral density are $(\text{cm}^2/\text{sec}^2)/\text{cph}$.



IV-38

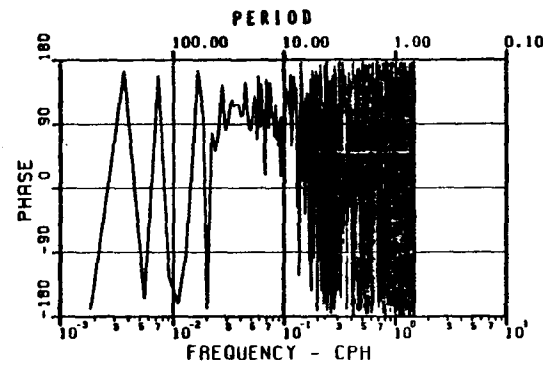


Figure IV-38. Frequency response and phase between the u and v components of velocity for meter 4 of mooring 3, recovered July 1981.

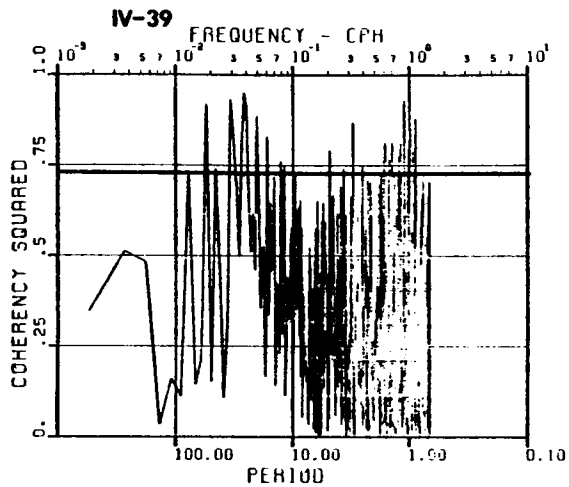
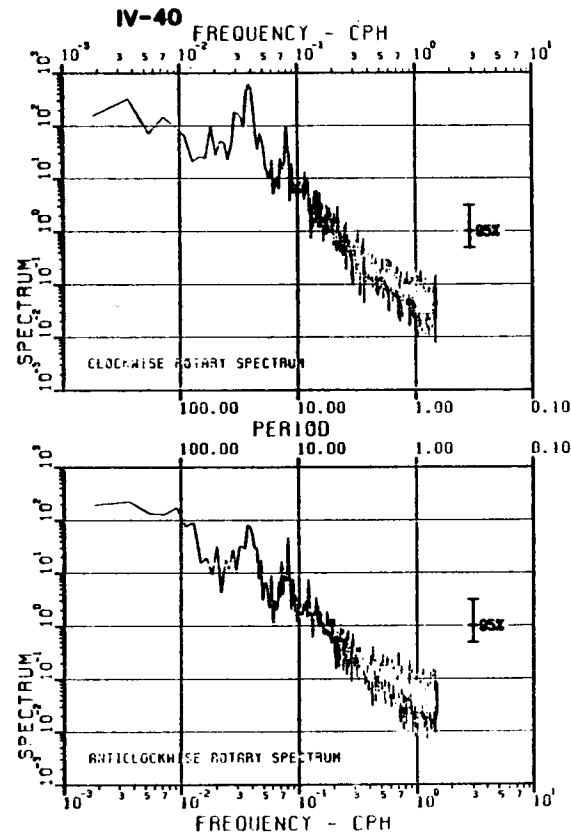


Figure IV-39. Coherence squared between the u and v components of velocity for meter 4 of mooring 3, recovered July 1981.

Figure IV-40. Rotary spectra of the u-v velocity vector for meter 4 of mooring 3, recovered July 1981. The units of spectral density are $(\text{cm}^2/\text{sec}^2)/\text{cph}$.



meters and for both velocity components of the two near-bottom meters. These facts indicate a general suppression of low frequency variance in the cross isobath direction near the surface, and an increased suppression at lower frequencies in all directions near the bottom. The value of A in equation (19) decreases with depth. However, the slope parameter, a , remains essentially unchanged at periods shorter than 12 or 24 hours. The decrease in A is expected as a result of dissipation by bottom friction and because the primary energy input at most frequencies is through the surface interface.

Superimposed on the background noise are a number of spectral peaks due to tidal and inertial currents and possibly to shelf waves. The theoretical frequency and period of the major tidal constituents and of the inertial currents are listed for reference in Table IV-6.

TABLE IV-6
THEORETICAL FREQUENCY AND PERIOD OF MAJOR TIDAL
CONSTITUENTS AND OF INERTIAL CURRENTS

DARWIN NAME OF TIDAL HARMONIC	PERIOD (hrs)	1/PERIOD (hrs ⁻¹)
S ₂	12.00	.0833
M ₂	12.42	.0805
K ₁	23.93	.04178
O ₁	25.82	.03872
<hr/>		
INERTIAL CURRENTS AT 27°55'N LATITUDE	25.56	.03912

Tidal Currents. The tides at many places in the Gulf of Mexico are either diurnal or mixed diurnal (Marmor, 1954). At Galveston Bay, Texas the tides are classified as mixed diurnal (two high and two low tides each lunar day of 24.84 hours, but with a large inequality between either the two highs or the two lows). The amplitudes of the three major constituents (K₁, O₁, M₂) range only from 9 cm to 12 cm (.31 to .39 ft).

Tidal currents may be in phase with the sea level, as with progressive tidal waves, or out of phase as with standing waves, or somewhere in between. Tidal currents are typically rotary in nature, being more circular but weaker in the open sea, and often becoming stronger and more elliptical near shore. The barotropic tide (related to sea surface elevation) is often augmented by internal tides. The internal tides may be particularly strong near the continental shelf break, where they are generated (Rattray, 1960). The strong vertical stratification throughout much of the year and the close proximity of the East and West Flower Garden Banks to the continental shelf break suggest that the internal tides may have significant amplitudes there. From only the autospectra it is not possible to determine what part of

the tidal current is barotropic and which is baroclinic (internal tides). The barotropic tidal current is depth independent except near the bottom, where bottom friction causes a reduction in speed. The baroclinic tide is in general composed of a number of modes, each depending upon the vertical density structure and each having a different vertical velocity structure. A complete analysis of the tidal currents to determine the amplitudes and phases of the major constituents by both the harmonic methods and a modified response method will be the subject of a future study. However, preliminary estimates of the total tidal current at each major harmonic have been determined from the autospectra using equation (4). The amplitude estimates for the u- and v-components of the M_2 and K_1 tides are listed for each current meter of mooring 3 in Table IV-7.

TABLE IV-7
TIDAL CURRENT AMPLITUDES IN CM/SEC AT MOORING 3
FOR 6 MAR TO 16 JUL 81

METER #	DEPTH (m)	TIDAL CONSTITUENT			
		K_1		M_2	
		u	v	u	v
1	53	3.2	4.0	1.3	2.1
2	64	3.9	5.2	0.9	2.4
3	91	1.8	2.7	0.8	1.5
4	97	1.4	2.5	0.8	1.6

Due to the technique employed (spectral analysis via fast fourier transforms [FFT]), these amplitudes may be somewhat inaccurate. One reason is that the method of computing spectra by FFT allows spectral density estimates to be computed only at particular frequencies which are determined by the length of the time series. When the frequency of the tidal harmonic and the frequency determined by use of the FFT do not coincide, the variance from even a sharp peak can be separated into two adjacent frequency bands. This presents a problem only when two otherwise resolvable spectral peaks are combined into the same frequency band. For example, the M_2 and S_2 variances might be lumped together by this process. Another reason is that band averaging or segment averaging of the raw estimates has been employed in order to decrease the size of the confidence intervals. Although this procedure is necessary for certain applications, it increases the frequency bandwidth, perhaps again resulting in combining two adjacent spectral peaks. Thus, for some calculations the M_2 and S_2 harmonics may be combined, but even more seriously, the K_1 , O_1 , and inertial bands may overlap. In fact, no matter how long the series of data and how small the bandwidth, the O_1 and inertial bands will probably still overlap because of the broad inertial peak.

Table IV-7 shows that both the K_1 and M_2 amplitudes at the bottom two meters are less than at the upper two meters. This difference may be due to bottom friction or, more likely, it is a con-

sequence of the baroclinicity of the tides. Another indication of the baroclinicity is the increased amplitude at meter 2 relative to meter 1. However, this is only speculative, and the proper interpretation requires a complete tidal analysis where phases are also determined.

The rotary spectra show the partition of spectral density between the clockwise and anticlockwise rotation of the velocity vectors at each frequency band. Both the diurnal and semidiurnal tides and the inertial currents rotate in a clockwise manner.

Inertial Currents. Inertial current vectors rotate in a clockwise direction (in the Northern Hemisphere) with a radian frequency, ω , near the local inertial frequency,

$$\omega_0 = 2\Omega \sin(\text{latitude}),$$

where Ω is the angular velocity of the earth,

$$\Omega = 2\pi / (1 \text{ sidereal day}).$$

These currents reach speeds of 20 to 30 cm/sec and are usually strongest near the surface. Kundu (1976) notes from his own measurements off the coast of Oregon and from other studies that the observed frequency is normally 3% to 20% above ω_0 . In the Flower Garden region, a 6.8% increase in frequency above ω_0 is equal to the K_1 tidal frequency. But most of the spectra from the present data set show two separate spectral peaks, so that the observed inertial frequency increase over ω_0 is certainly less than 6.8%. However, due to the wide bandwidths caused by smoothing of the spectra, the true frequency has not yet been determined accurately. This will be determined in future studies using high resolution spectra.

Kundu (1976) also finds that inertial currents are highly intermittent and last only a few oscillations (perhaps five days, judging by his data). Perkins (1970) analyzed current meter data from the Mediterranean and found inertial oscillations persisting for as long as two weeks. The present data are more similar in many respects to the Oregon coast data than to the Mediterranean data. The inertial oscillations often last for as long as 8-10 days. These bursts of inertial oscillation of the currents are related to the passage of storms. A few examples of the relationship between storms and inertial currents are discussed above (Severe Weather Episodes and Periods of Anomaly).

The vertical structure of both the tides and the inertial currents will be the subject of future studies, but for the present some of the general features of the vertical phase structure of the inertial currents can be determined by visual inspection of the velocity time series plots. Three distinct types of vertical phase structure are found. The phase difference between inertial currents at 50 m and those near the bottom is either 0° , 90° , or 180° . For example, the phase change is 0° between 53 m and 97 m at mooring 3 near 16 July 81; the phase change is about 90° between 54 m and 80 m at mooring 1 near 24 Nov 80; and at mooring 3 near 10 Dec 80 the phase is 180° between

52 m and 90 m. These phase change differences may depend upon the type of wind field which generates the inertial oscillations.

The amplitudes of the inertial oscillations decrease rapidly with depth at moorings 1, 3, and 4. However, the decrease with depth is not as great at mooring 2, which is the only mooring immediately adjacent to a bank. Therefore, it is possible that inertial oscillations are an important source of energy along the side of the bank.

Shelf Waves. The velocity autospectra usually show peaks near periods of 33 hours, two days, and four days. They are all likely due to shelf waves. The best examples of the 33-hour velocity oscillation occurred during the last deployment (Feb-Jul 81). At this frequency, the u and v-components of velocity are often highly coherent, sometimes even more so than the tides. The velocity vector rotates clockwise, as do the tides and inertial current vectors. The phase difference and the response function between u and v imply that the current ellipse is nearly circular and with the major axis aligned along the north-south direction. The possibility of intermittency of the 33-hour oscillation, its vertical structure, and its relationship to surface wind stress will be the subject of future studies.

The two-day period oscillations are intermittent, and appear to be related to the passage of storms. The single best example is from the period 6-22 Oct 79 at the upper meter (61 m depth) on mooring 3, shown in Figure IV-17 (above). At this meter, which is located just below the surface mixed layer within the strongest part of the thermocline, two-day oscillations with amplitudes up to 15 cm/sec are observed. Normally, however, the amplitudes are only about 4 cm/sec.

The four-day oscillations may be the result of direct forcing by wind stress caused by the eastward passage of anticyclonic waves of approximately the same period. It is more likely, though, that they are shelf waves excited by the passage of the anticyclones.

Temperature Spectra

Knowledge of both the spatial and temporal variation of temperature is important, for a number of reasons. For biotic communities at the Flower Gardens, seasonal temperature changes are of great, while the short-term fluctuation of only one or two degrees centigrade may be relatively insignificant. From the point of view of hydrodynamics, time series of temperature are important indicators of the relationship of temperature to density. Below a thin surface layer, the salinity is often nearly constant in the first 100 m or more, so that the water density is determined mainly by temperature.

Short-term fluctuations of temperature with periods on the order of one or two days can be considered to be caused by either vertical displacement of the isotherms or horizontal, advection of the horizontal gradient of temperature. The largest horizontal gradients of temperature seen in the Flower Gardens region are about 0.2°C/km in the north-south direction. In fact, horizontal gradients of temperature

near the shelf-slope break are much larger than elsewhere either over the shelf or over the continental slope. The temperature drop at a fixed location caused by horizontal advection due to inertial currents in one half-cycle (assuming the inertial current to be horizontally uniform or coherent over at least 5-10 km) is near 1°C when the velocity amplitude is 20 cm/sec.

The vertical gradients of temperature change significantly with season, ranging in the strongest part of the thermocline from greater than $0.17^{\circ}/\text{m}$ in the summer to less than $0.04^{\circ}/\text{m}$ in the winter. The vertical displacements required to produce a 1°C change is 5.9 m in summer and 25 m in winter. The phase relationship between horizontal velocity and the temperature changes induced by vertical displacement is rather complex. It depends upon whether the waves are progressive, standing, or somewhere in between, and upon the phase difference between u and v .

One set of temperature spectra has been chosen for discussion. This is the set of four temperature records on mooring 3 taken during the 6 Mar to 16 Jul 81 deployment (the same mooring was discussed in the previous section on velocity spectra). The temperature autospectra and the frequency response, coherence, and phase between the temperature (T) and the north-south component of velocity (v) are shown for each meter on mooring 3 in Figures IV-41 through 52. The temperature spectra are noisier than the velocity spectra and the significant peaks are not as clearly defined.

The amplitude of the temperature fluctuations at the K_1 tidal frequency is largest at the upper meter and decreases with depth. The average amplitude is $.15^{\circ}\text{C}$ for the upper meter on mooring 3 for March to July 1981. This value varies seasonally as the vertical gradient of temperature changes. For example, during the October to February 1981 deployment, when the vertical gradients of temperature were lower on the average, the amplitude at the K_1 frequency was only about 0.1°C .

The horizontal line on the coherence plots is the 95% confidence level. It shows the level that would be exceeded by 5% of the coherence values computed from randomly related records. The coherence between T and v at the K_1 frequency fails this test at all meters on mooring 3, but only by a small amount. These somewhat low coherences are probably due to the change in the thermal structure from winter to summer during the four months of the deployment. The lower coherences over such a period of temperature change may be another indication that a significant part of the K_1 tide is baroclinic.

The frequency response between T and v at the K_1 frequency is about 20 at the upper meter, meaning that on the average over the entire record a velocity amplitude of 5 cm/sec corresponds to a temperature amplitude of 0.25°C . At this meter the velocity phase leads the temperature by 75° . This phase difference could be caused by horizontal advection. Such would be the case with a north-south gradient of temperature where temperature increases northward. Much of the tem-

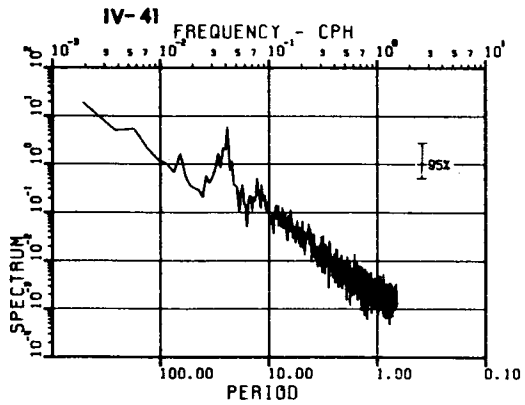


Figure IV-41. Autospectrum of temperature for meter 1 of mooring 3, recovered July 1981. The units of spectral density are $^{\circ}\text{C}^2/\text{cph}$.

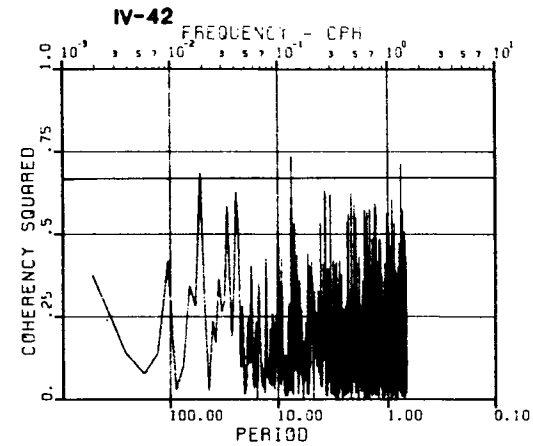
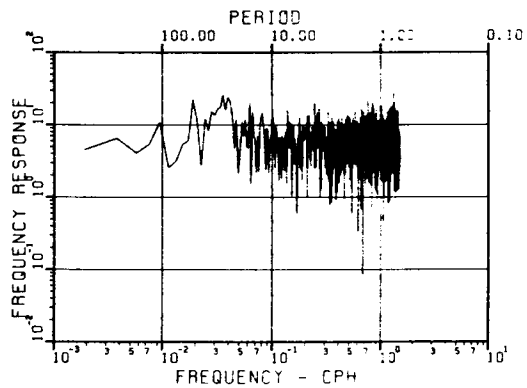


Figure IV-42. Coherence squared between temperature and the v (north-south) component of velocity for meter 1 of mooring 3, recovered July 1981.



IV-43

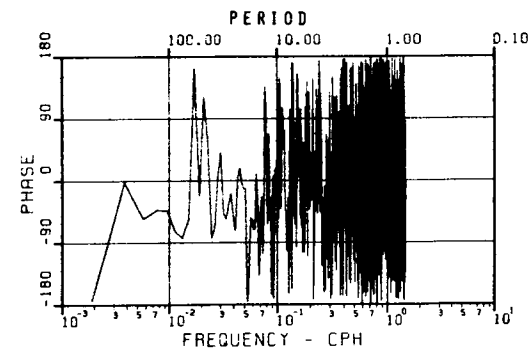


Figure IV-43. Frequency response $[(\text{cm}/\text{sec})/^{\circ}\text{C}]$ and phase between temperature and the v (north-south) component of velocity for meter 1 of mooring 3, recovered July 1981.

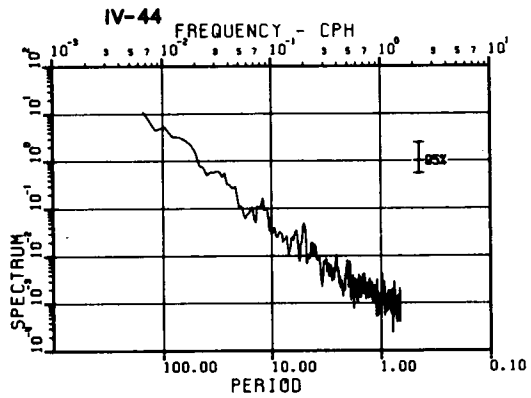


Figure IV-44. Autospectrum of temperature for meter 2 of mooring 3, recovered July 1981. The units of spectral density are $^{\circ}\text{C}^2/\text{cph}$.

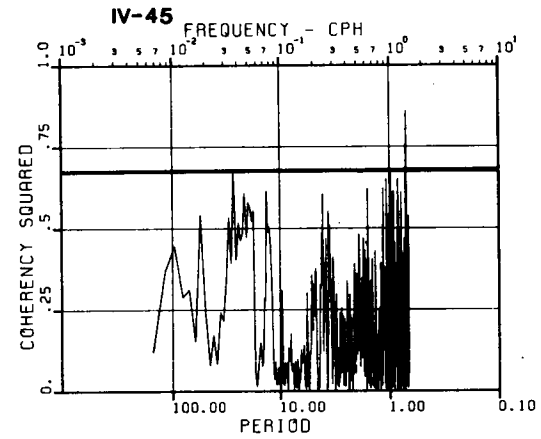
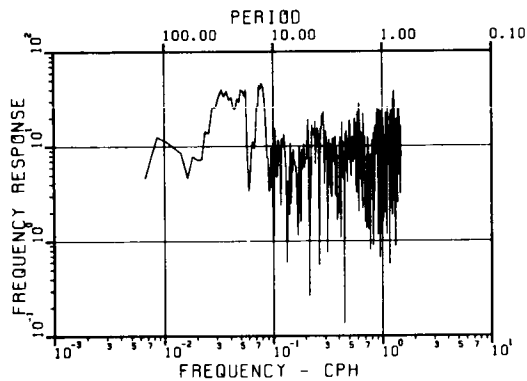


Figure IV-45. Coherence squared between temperature and the v (north-south) component of velocity for meter 2 of mooring 3, recovered July 1981.



IV-46

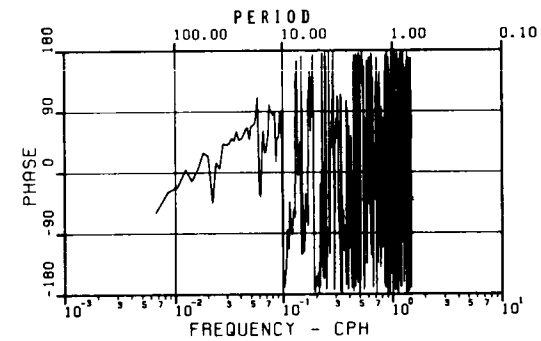


Figure IV-46. Frequency response [(cm/sec)/ $^{\circ}\text{C}$] and phase between temperature and the v (north-south) component of velocity for meter 2 of mooring 3, recovered July 1981.

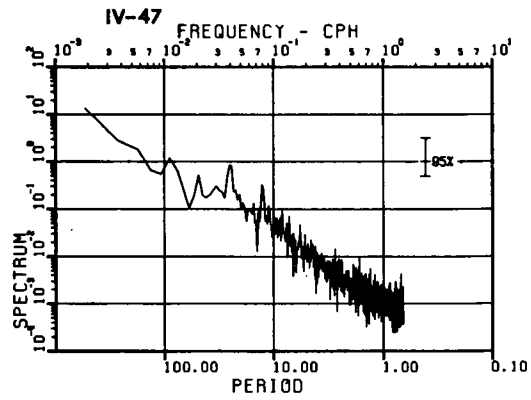


Figure IV-47. Autospectrum of temperature for meter 3 of mooring 3, recovered July 1981. The units of spectral density are $^{\circ}\text{C}^2/\text{cph}$.

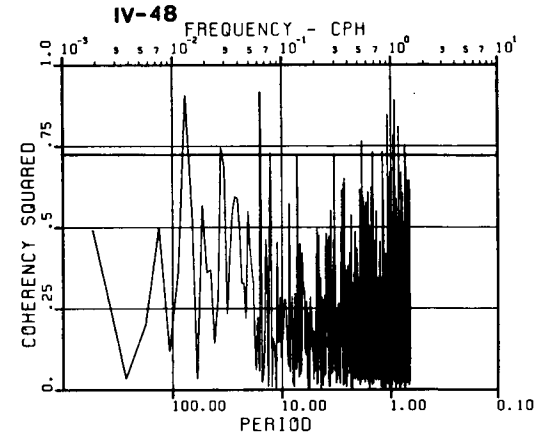
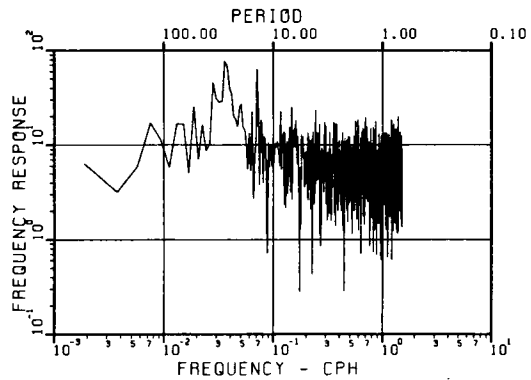


Figure IV-48. Coherence squared between temperature and the v (north-south) component of velocity for meter 3 of mooring 3, recovered July 1981.



IV-49

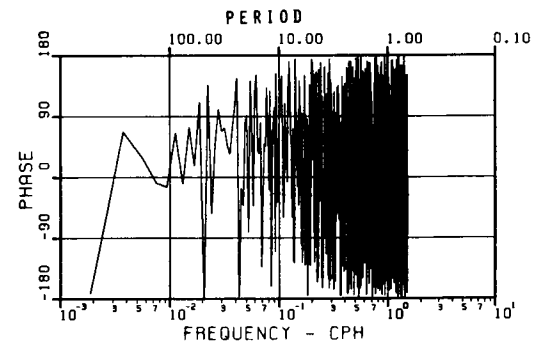


Figure IV-49. Frequency response $[(\text{cm}/\text{sec})/^{\circ}\text{C}]$ and phase between temperature and the v (north-south) component of velocity for meter 3 of mooring 3, recovered July 1981.

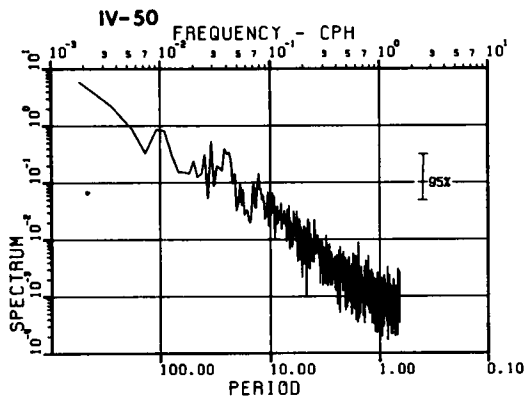


Figure IV-50. Autospectrum of temperature for meter 4 of mooring 3, recovered July 1981. The units of spectral density are $^{\circ}\text{C}^2/\text{cph}$.

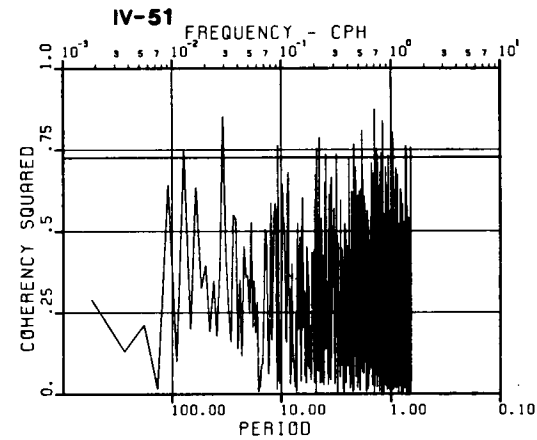
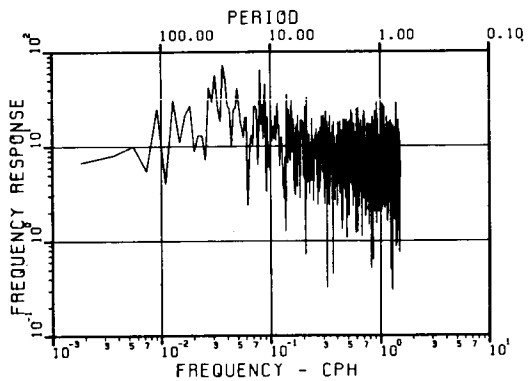


Figure IV-51. Coherence squared between temperature and the v (north-south) component of velocity for meter 4 of mooring 3, recovered July 1981.



IV-52

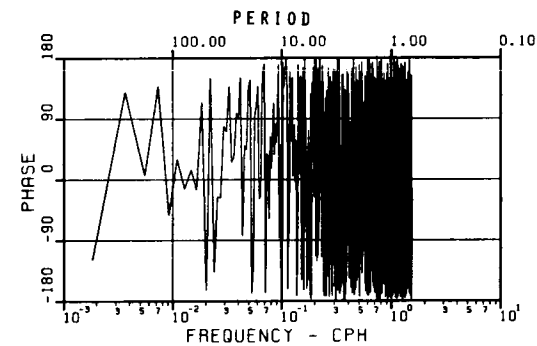


Figure IV-52. Frequency response [(cm/sec)/ $^{\circ}\text{C}$] and phase between temperature and the v (north-south) component of velocity for meter 4 of mooring 3, recovered July 1981.

perature variance, however, is likely due to the vertical migrations of the isotherms caused by the internal K_1 tides.

The coherence between T and v is significant near a period of 33 hours at the bottom two meters. The phase is near 90° (T leads v by 90°), and the response is near 30.

Coherence between T and v is not significant at the M_2 frequency at all depths. Coherence is lowest at the upper meter, probably because a slight valley rather than a peak is found in the autospectrum of temperature.

A complete analysis of the temperature, its variation with season and relationship to velocity is forthcoming. Little can be said yet with only the preliminary analyses completed so far.

TRANSMISSIVITY TIME SERIES DATA

Near-bottom transmissivity (XMS) was measured from late April 1980 through the last deployment, July 1981. The records of transmissivity are generally shorter than the velocity records from the same depth because biofouling fogged the lenses, even though very strong antifouling paint was used. During all deployments when transmissivity was measured, each mooring had one instrument at 4 m above the bottom. On the later deployments another transmissometer was added to each mooring at approximately 12 m above the bottom (see Table IV-1 above).

Conventional wisdom says that (a) because high velocity flows exert high shear stresses on the bottom and (b) because high shear stresses on the bottom are known to cause sediment resuspension, then (c) high speeds should be well correlated with low XMS. So much for conventional wisdom. Transmissivity records show the speed of the flow and the amount of suspended sediment 4 m to 12 m above the bottom to be poorly correlated. In fact, the highest velocity flow recorded at mooring 1 meter 2 (see above, Figure IV-1 for locations and Table IV-1 for depths) is attended by a sharp rise in XMS, or reduction in suspended sediment load. Even though every current meter speed record shows a major spectral peak at the diurnal period, the XMS spectra reveal only a very modest energy density at that period.

As if this lack of correlation were not perplexing enough, the lowest XMS values recorded between late April 1980 and mid June 1980 at both mooring 1 and mooring 3 occurred during low speed, onshore flow. Note, for example, mooring 3 on April 28 and May 9, 1980 (Figure IV-53b).

In order to study these unexpected results thoroughly, the records of mooring 1 meter 2 and mooring 3 meter 2 were plotted several ways. First, of course, the XMS and velocity were plotted in raw form (Figure IV-53). Next, the records were lowpass filtered to remove high frequency signals (> 1 cycle per day) and replotted (Figure IV-54).

Finally, the records were bandpass filtered (to retain only variations with periods of 3 to 28 hours) and plotted again (Figures IV-55 and 56). In addition, spectral analyses were run. These analyses included autospectra and cross spectra of XMS with v (north-south) and u (east-west) velocity components.

The XMS and velocity components appear to be well correlated only at periods greater than 30 hours, and even where they are correlated the phase relationships are quite complex. That is, high speeds do not correspond in time (phase) with low XMS values, even though they have the same periods. This lack of correlation suggests that at 4 to 12 m above the bottom, sediment concentrations are modulated more strongly by advective processes than by local turbulent resuspension. The lack of statistical correlation does not mean that the currents are not effective in resuspending sediment. It means that variations in concentration are not linearly related to variations in velocity.

An examination of Figure IV-55 reveals just how chaotic the relationship between velocity and XMS is. Looking at the third panel on Figure IV-55, which shows XMS and v , one can see that at times an increase in v is attended by an increase in XMS, while a few days later the XMS decreases with increasing v . From 26 April to 6 May, and from 8 May to 16 May, however, the temperature and XMS are very well correlated. As the temperature drops, so does the XMS. This correlation suggests that vertical motions are causing the high frequency oscillations in XMS. Because there is usually a strong vertical gradient of suspended sediment near the seafloor, a doming of the bottom boundary layer would lead to just such a relationship. The lapses in correlation of temperature and XMS appear to occur during longer term onshore flow (6 to 8 May) and during unusually strong flow events like those on 16 through 17 May. These interruptions may be due to alterations of the vertical gradients of suspended sediment during unusual flow conditions.

Our working hypothesis is that near-bottom shear stresses exceed the threshold required to resuspend silt and clay most of the time and that the periods during which the shear stresses fall below this threshold are too short for the sediment to settle out. After all, it takes nearly a day for medium silt-sized material to settle 10 m in still water, and the near-bottom water is never still. At 4 m above the bottom, suspended sediment concentrations vary primarily because of convergence and vertical motion rather than direct resuspension. From our shelf/slope transects (to be detailed at a later date) it appears that the mean circulation on the shelf segment upon which the Flower Garden Banks are situated is dominated by offshore, downslope flow (downwelling) in the bottom boundary layer (BBL). Flow on the outer shelf and upper slope exhibits frequent upwelling of the bottom waters. Where these opposing flows meet, there is convergence and a doming of the BBL and nepheloid layer. The location of the convergence undoubtedly migrates as the relative intensities of the shelf and slope currents change. When the convergence zone is near the XMS records, one would expect low velocity horizontal flow and low XMS values.

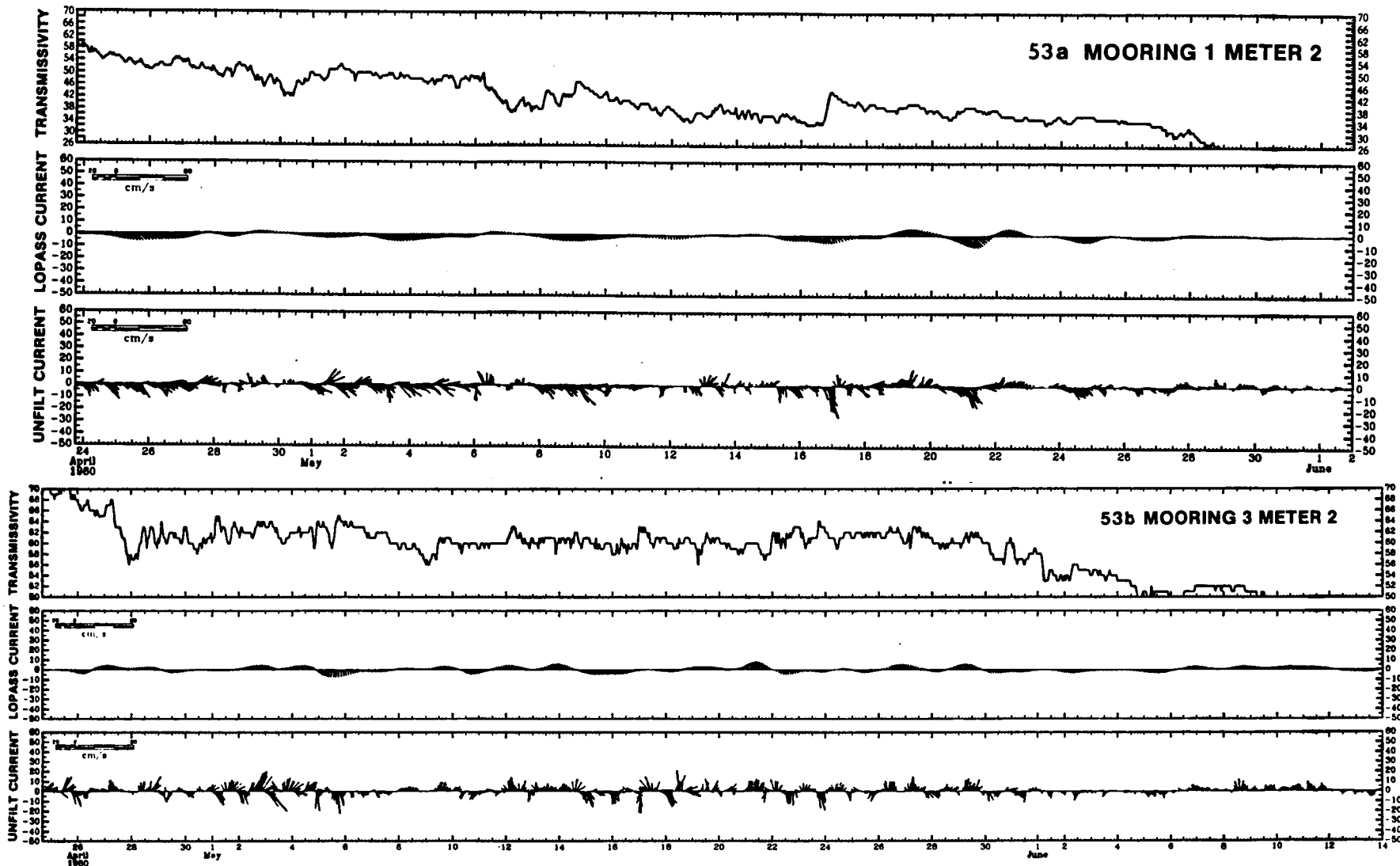


Figure IV-53. Raw velocity and transmissivity (XMS) time series records for April-June 1980 from (a) mooring 1 meter 2, and (b) mooring 3 meter 2. See Figure IV-1 for mooring locations.

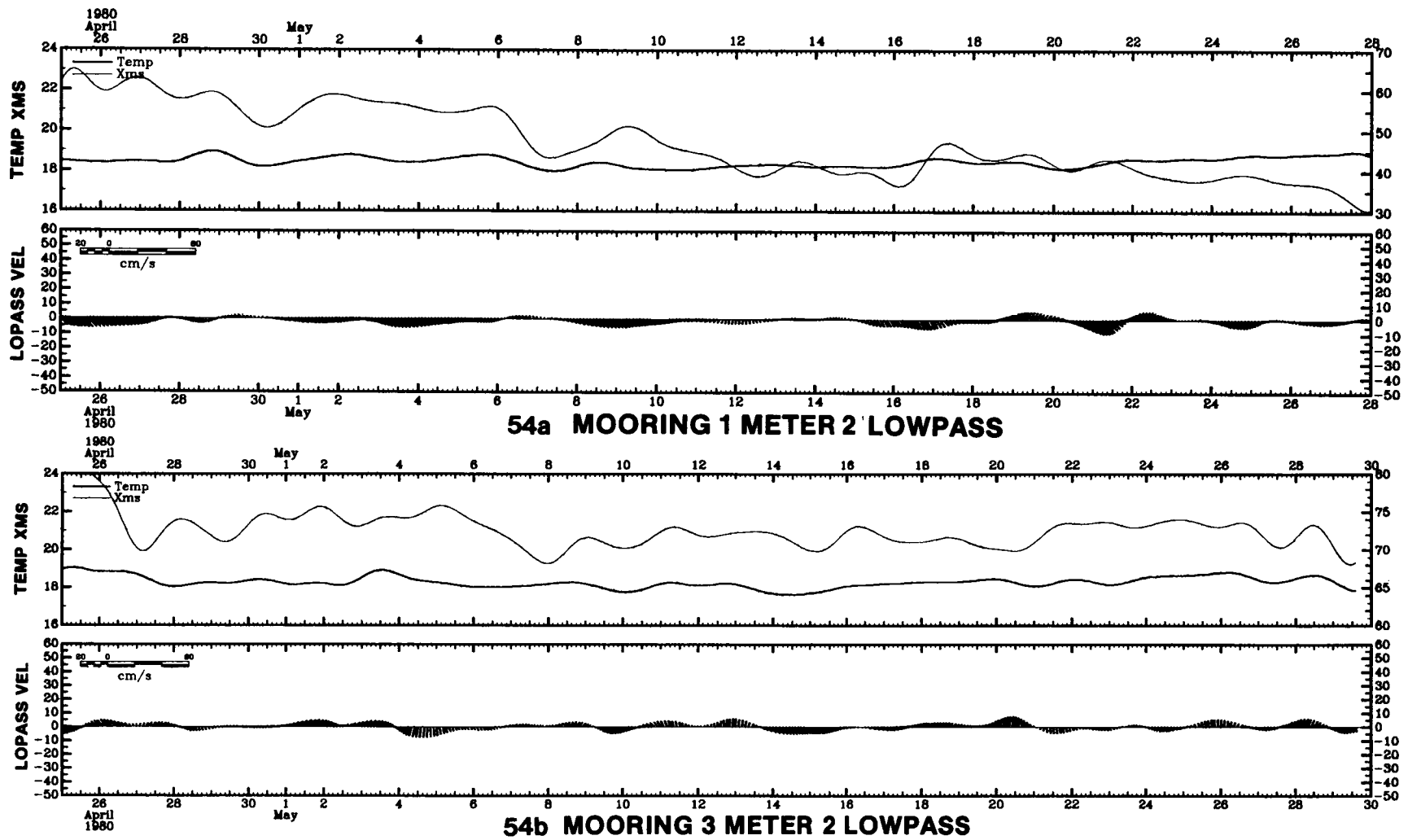
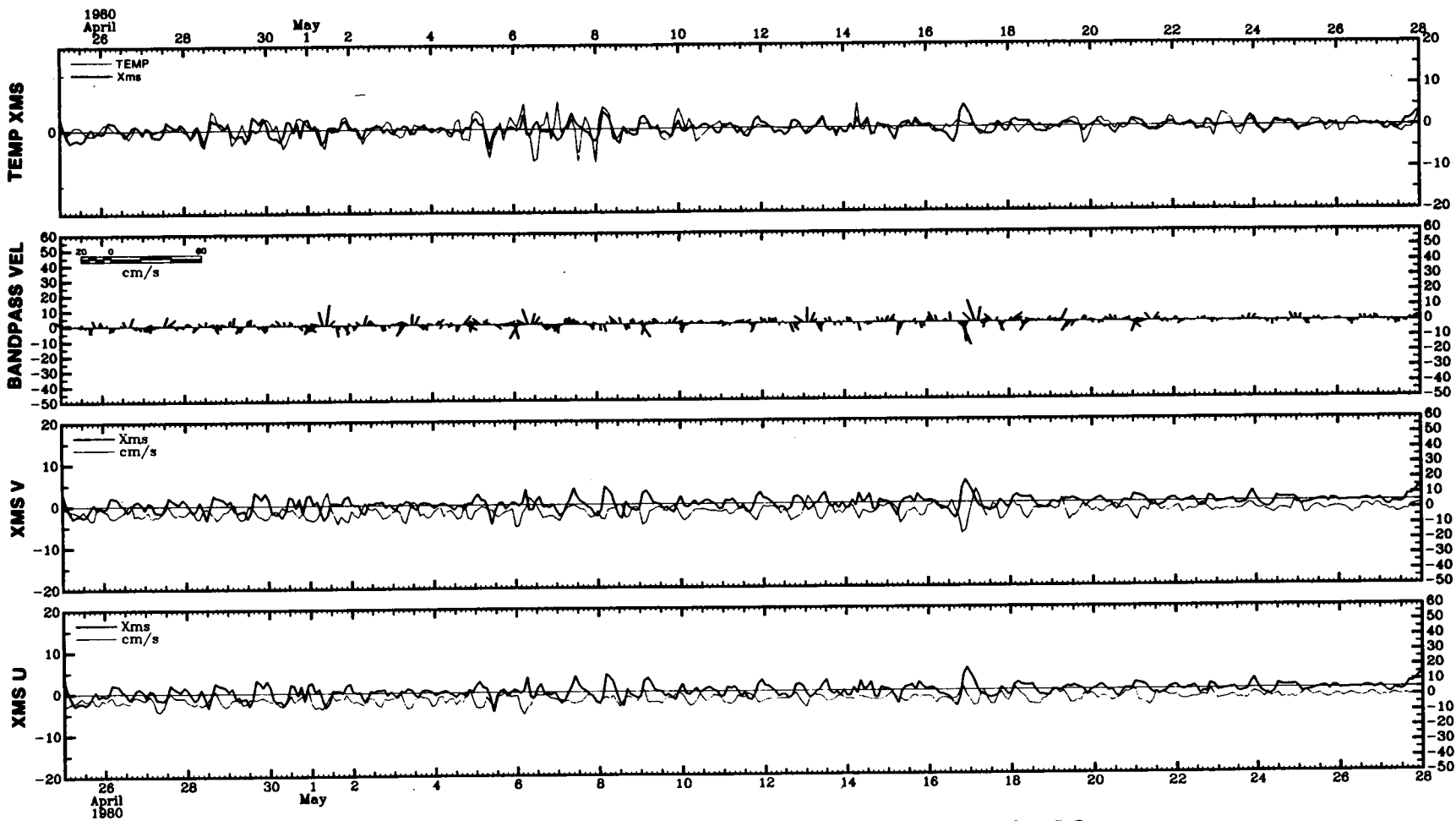


Figure IV-54. Lowpass filtered records of velocity and transmissivity (XMS) time series records for April-June 1980 from (a) mooring 1 meter 2, and (b) mooring 3 meter 2. See Figure IV-1 for mooring locations.



MOORING 1 METER 2 BANDPASS, 3 TO 28 HOURS

Figure IV-55. Bandpass velocity and transmissivity (XMS) time series records for April-June 1980 from Mooring 1 meter 2. See Figure IV-1 for mooring locations.

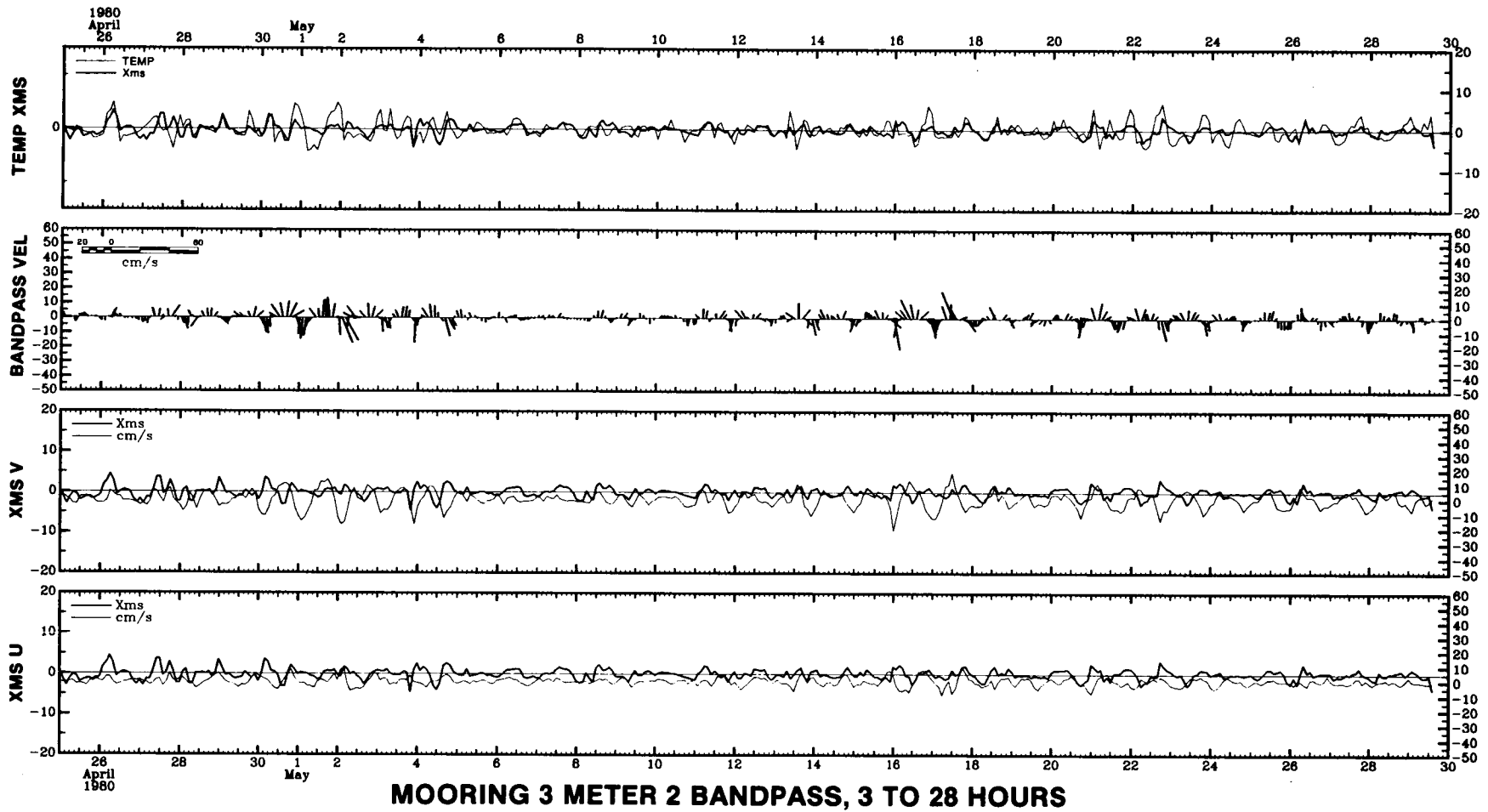


Figure IV-56. Bandpass velocity and transmissivity (XMS) time series records for April-June 1980 from mooring 3 meter 2. See Figure IV-1 for mooring location.

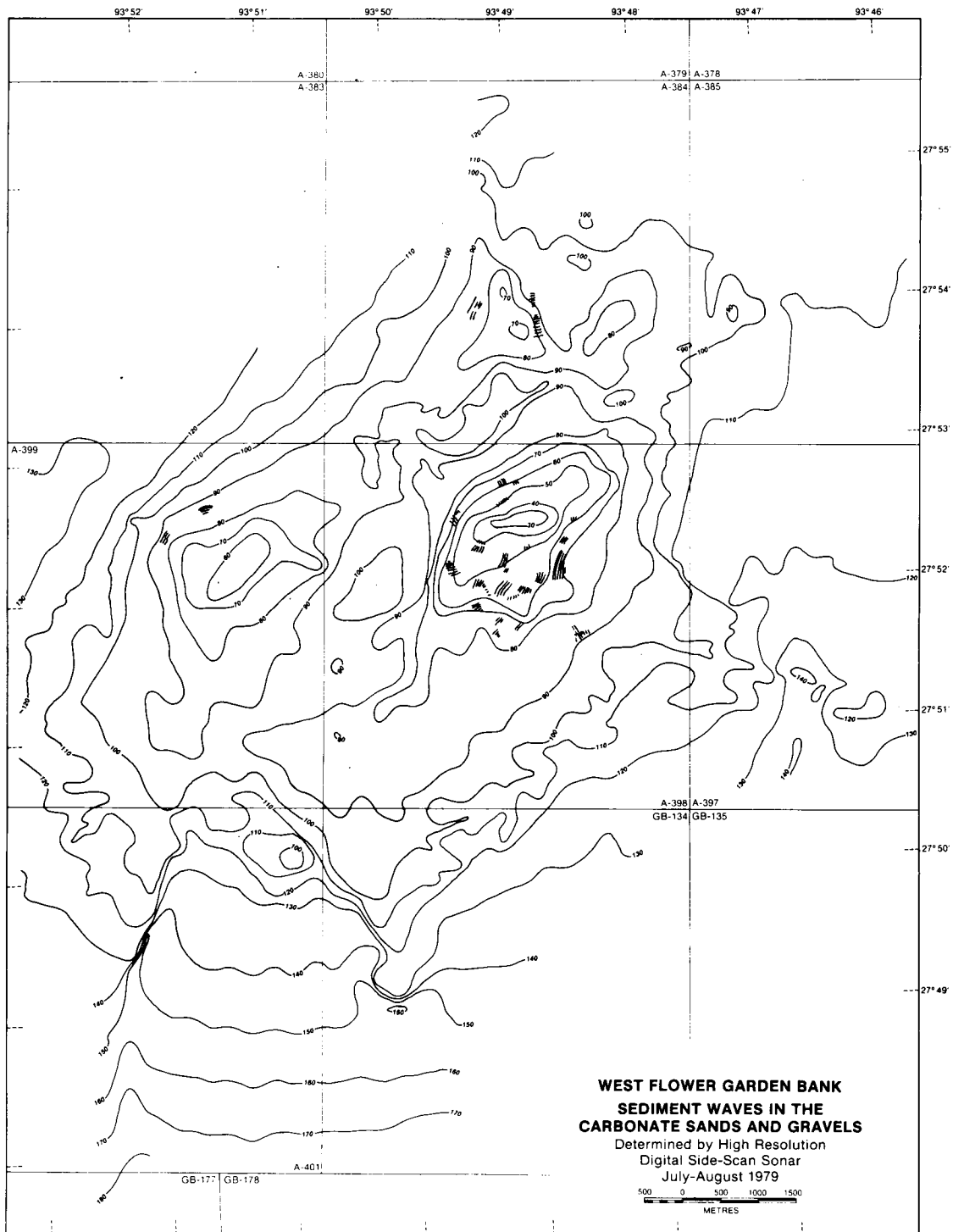


Figure IV-57. Large scale bedforms on the West Flower Garden Bank as determined from a digital side-scan sonar mosaic. Wave lengths and crest lengths are plotted to scale.

Another factor is that during northers, cold water (approximately 17°C) forms near shore, sinks because of its density, and moves offshore along the bottom. This process leads to a stacking of boundary layers at the shelf edge and may account for the approximately 20 m thick BBL's that could not be formed by local turbulence.

Since the above processes are so different, it is not surprising that flow from the north (at the bottom) could sometimes lead to low XMS values and sometimes to high values. This circumstance is reflected in the poor statistical correlation between velocity and XMS.

Spectral analysis of mooring 3, meters 3 and 4, for the period October-December 1980 reveals that the XMS readings for the meters (12 and 4 m above the bottom, respectively) were incoherent at the 95% confidence level. This incoherence reinforces the suspicion that the processes governing the dynamics of sediment distribution in the water column at those two levels are fundamentally different and therefore possess different natural time scales.

LARGE SCALE BEDFORMS

The digital side-scan sonar mosaic of the West Flower Garden Bank (Plate 1, pocket) reveals large, long wavelength sedimentary bedforms in the Algal Nodule Zone. These have been plotted to scale on a topographic base map (Figure IV-57, above). Similar bedforms in even greater profusion were found in the old side-scan records of the East Flower Garden Bank (Figure IV-58, above).

These bedforms are waves about 1 m high with wavelengths of from 10 m to 30 m. They are formed primarily of gravel sized algal nodules. Formation of bedforms of this size and coarseness of sediment would require very high velocity flow. The gravel waves are most prevalent on the west side of both banks. This distribution, together with the orientation of the crests and asymmetry of their form, indicates that the flow forming them comes from the west. With few exceptions, the crests of the bedforms are nearly perpendicular to the local isobaths. Those exceptions occur on the upstream side of the East Flower Garden Bank, where the flow bifurcates. South of this region the beds indicate southerly, isobath-parallel flow, and north of it they indicate northerly isobath-parallel flow. On the West Flower Garden Bank, crests of the bedforms are isobath-parallel on the downstream side of the bank, suggesting a separation point.

The significance of these features is that their formation requires exceptionally high velocities and their orientation is such that even during this extraordinary flow, it must remain essentially parallel to the isobaths. These features provide additional confirmation of the hypothesis that, even under extreme conditions, the currents flow around, not up and over, the banks.

CLIMATOLOGICAL WIND TIME SERIES MEASUREMENTSClimatic Summary of the Texas-Louisiana Shelf Region

Background information on Gulf of Mexico climatology was obtained from Franceschini (1953) and from Orton (1964). The climate of the Texas-Louisiana shelf region could best be described as humid subtropical, i.e., controlled by both tropical and polar air masses. The seasons are predominantly summer (May to October) and winter (December to March) with spring and fall being short transitional periods, possessing characteristics of either summer or winter. The mean circulation during the summer is controlled by maritime tropical air masses originating from the western side of the oceanic high-pressure cell near Bermuda. During winter, outbreaks of continental and maritime polar air occur about once per 5-6 days. Occasionally arctic air mass intrusions bring severe cold weather to the region.

From March to October the general pattern of winds for the Texas-Louisiana shelf region is of an easterly origin. Predominantly, the winds are veering southeasterly to southerly as the summer months progress. By November the intrusion of polar air becomes more regular and from November to March the predominant wind direction is northerly.

On the whole, the summer weather for this region has little day-to-day variation. At this time of year the air is hot and the winds are generally calm. The temperature rises up to and through August and then slowly decreases through September. In the latter part of summer the amplitude of the easterly waves traversing the Gulf becomes increasingly large. The tropical storms associated with the easterly wave activity and the increased thunderstorm activity due to the higher sea-surface temperatures of late summer cause this to be the rainiest time of year.

About once per two years a tropical cyclone (hurricane), the most severe of the tropical storms, hits the Texas-Louisiana Gulf Coast. These storms can produce wind speeds, generally easterly, of up to 75 knots, and rainfall amounts in the tens of inches can occur. These storms follow either of two routes: through the Straits of Florida, or through the Yucatan Channel. Hurricane winds are of sufficient duration and force to cause high waves and to deviate currents, but since they occur only occasionally, their influence on the climate of the Gulf is not as significant as the influence of the nearly omnipresent summer thunderstorms.

A Texas norther is probably the single most influential winter-time weather phenomenon experienced in the Gulf. A norther is a strong burst of cold air coming from the northeast-northwest, dropping the air temperature by as much as 25°F in one hour. Thirty-knot winds can occur with this cold air mass outbreak that is associated with the southward progression of a ridge (anticyclone) of polar air. Generally, warm, cloudy or rainy weather with southerly winds precedes the arrival of a norther.

High Island 323 Winds

The wind velocity near the Flower Garden Banks has been measured at High Island Platform 323 at a height of 187' (57 m) above sea level. Wind records for the years 1979 and the latter half of 1980 are summarized below. Monthly mean wind vectors for 1979 and for July-December 1980 are shown in Figure IV-59.

From the beginning of spring to early summer of 1979 the winds were out of the southeast and ranged from a monthly mean maximum of 6.5 m/sec in April to a minimum of 4.3 m/sec in March and May. The calmest month of the year, as usual, occurred in summer: July had a mean monthly speed of 2.2 m/sec from the south. Hurricane Bob passed to the south of the wind recording station (9 July - 11 July); no winds stronger than 30 knots (15 m/sec) were measured. One and a half weeks later Tropical Storm Claudette advanced northward along the Texas-Louisiana border, passing over High Island. Because no wind records were available for that time (22 July - 29 July), the monthly averages are most likely low. The winds began backing in August, shifting south-southeasterly, and becoming southeasterly in September. Wind magnitudes were 5.4 m/sec in August and 5.9 m/sec in September. This is generally the situation during late summer, when the amplitude of the easterly waves increases, encouraging cyclonic activity and thunderstorms.

By October, the mean circulation pattern backed into a northeasterly flow, as the polar jet stream advanced southward. Northers intensified during November, producing a monthly mean magnitude of 7.0 m/sec, the highest all year, out of the northeast.

In December, the winds were more easterly than in November, suggesting the possibility of a strong Bermuda anticyclone, forcing air easterly into the region. A tug-of-war may have resulted, as the mean monthly wind speed was just 3.7 m/sec, from the east-northeast. The winds continued to veer, directed from the east-southeast at 4.0 m/sec. Several strong northers induced strong northerly winds into the region, but a strong and steady southeasterly wind precluded the northerly influence.

During February, the winds backed to nearly easterly and had a mean speed of 4.1 m/sec. This was likely due to a slight weakening of the huge Bermuda high pressure cell which controlled the circulation in January. The flow became nearly zonal during February with the passage of two or three weak northers.

The month of July 1980 was nearly calm with a monthly mean wind speed of 1.6 m/sec from the south-southeast. This is the typical mid-summer time situation for most of the Gulf of Mexico. In August, the direction was essentially the same as in July, but the monthly mean wind speed was over three times as great, 5.1 m/sec. This wind speed intensity was about the same for September, when the winds were more southeasterly. A wind speed of this magnitude coming from the

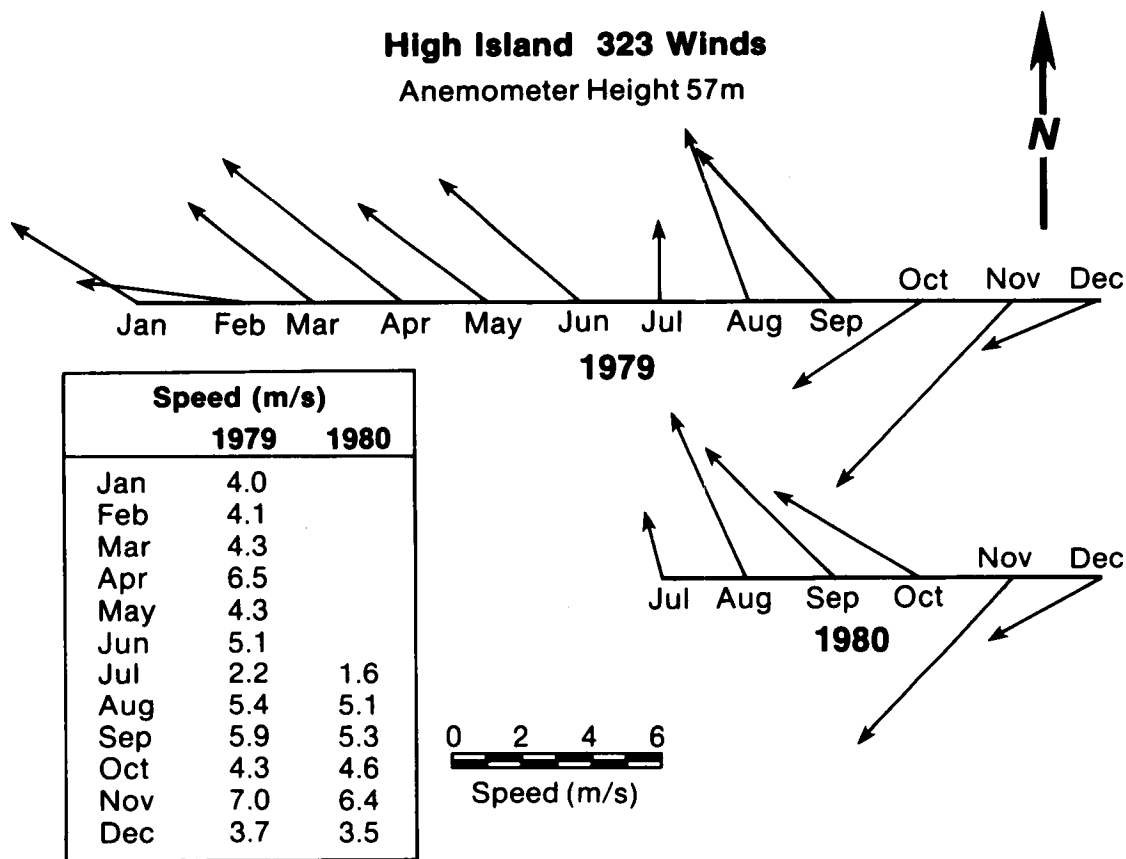


Figure IV-59. Monthly averaged wind vectors at the High Island weather station near the East and West Flower Garden Banks for 1979 and the last half of 1980.

southeast indicates the presence of the summer tropical storms associated with the easterly circulation.

The easterly circulation predominated through October, which had a monthly mean wind speed of 4.6 m/sec from the southeast. The polar influx in November, however, produced a northeasterly wind vector mean of 6.4 m/sec. Its magnitude and direction are both due to the northers prevalent at this time of year. In December, northeasterly circulation was sustained as the monthly mean wind speed was 3.5 m/sec. However, during December the wind direction was slightly more easterly than northerly, possibly indicating that an easterly zonal flow was established for a short while.

PHISH DATA

Methods

The Profiling Hardwired Instrumented Sensor for Hydrography (PHISH) was developed by Texas A&M researchers under BLM contracts. The PHISH system provides concurrent measurements of temperature, conductivity, transmissivity, current velocity, and depth, as vertical profiles while being lowered on 7-conductor well logging cable.

System Operation

The PHISH system consists of the instrument package, a winch with cable, an A-frame, and the "PHISH PHACTORY," a small portable van containing the deck unit, computers used in logging and analyzing the data, and the Loran receivers used for navigation. With a lowering rate of 20 m/min, three sets of data can be obtained per metre since the sample rate is 1/sec. Data are also logged on the ascent, which was at the rate of 20 m/min before July 1981, and 40 m/min thereafter. The present instrument consists of commercially available sensors which are integrated into one package. Raw power is supplied from the surface, to a DC to DC converter in the underwater unit. Data from the individual sensors are converted to frequencies before being sent up the wire to the deck unit. The deck unit is hardwired to a microcomputer which manipulates the data and stores the result on magnetic diskettes.

PHISH Instrument Package, Sensors, and Calibration

Each sensor in the PHISH package is calibrated in the laboratory before data are collected with it at sea. Standard procedure, however, dictates that calibration procedures be carried out at sea to verify any drift or malfunction which may occur during a cruise. Fortunately, post-cruise assessment of calibration data taken at sea has shown no need to adjust PHISH data for at-sea sensor drift. Two "derived quantities," salinity and suspended particulate concentration, however, require calibration data to be taken at sea, irrespective of any sensor drift. The reasons will be explained below. The following is a

description of each sensor, its accuracy, calibration procedures, and in some cases the quantities derived from them.

Current Velocity

Current speed and direction are measured with a Marsh-McBirney 585 electromagnetic current meter (EMCM) which has been modified for use with the PHISH. Deviations from true currents may occur due to drift of the ship while the speed is being measured, or because of tilt of the current meter axis from the vertical. The actual ship drift is calculated by determining changes in the ship's position during each PHISH profile. The ship's position is determined once each minute and logged on magnetic diskette (with other data) via a hardwired connection between a Micrologic LORAN-C set and the microprocessor. The recorded ship drift is smoothed slightly to account for the finite accuracy of the LORAN-C derived positions. Thus ship drift errors can be removed from the current record.

The tilt of the PHISH package from the vertical is determined to within $.1^\circ$ from two orthogonal inclinometers, and is recorded once each second along with the other sensor data. Tilt-related errors in recorded velocity from the EMCM are then corrected.

As a check on the EMCM readings, PHISH profiles are taken near current meter moorings, providing comparisons between moored meters and the EMCM.

Transmissivity

A 25 cm Sea Tech beam transmissometer is used to measure the transmissivity of the water column. The instrument measures the transmission of light with a wavelength of 600 nm over a 25 cm pathlength. The transmissivity is related to the concentration of suspended sediment in the path of the light beam.

The transmissometer is calibrated by the manufacturer. In our laboratory, a filtered water calibration is used to check this sensor. After cleaning the lenses, air readings are recorded. At sea, air readings are taken before and after each cast to ensure that the sensor output has not changed since the laboratory calibrations.

Transmissivity is a function of suspended particulate matter (SPM) concentration. Transmissivity also depends upon the particular type or make-up of the suspended particulates and on the existence of dissolved light-absorbing substances such as yellow substance. The SPM concentration is defined in practice as the dry weight of SPM in a given volume of water, which has been separated by filtering through 0.4 micron filters.

In order to relate the measurements of transmissivity to the concentration of SPM, the relationship between the two must be determined empirically for the particular SPM found in the study region. This is done in two ways. First, water samples are taken from bottom-tripped Niskin bottles mounted on the PHISH case. SPM concentration

determined from these water samples is compared to the transmissivity readings which were taken concurrently with the water samples. Second, transmissivity readings are taken in a temperature-controlled salt water bath equipped with stirrers to which various concentrations of SPM are added. The SPM concentrations are prepared by diluting bottom sediment samples obtained from the study area.

Temperature

Temperature is measured with a Seabird temperature probe, accurate to $.01^{\circ}\text{C}$. The temperature sensor received an initial National Bureau of Standards (NBS) calibration. It is also tested in our laboratory against an NBS certified platinum thermistor. At sea, it is checked against NBS certified reversing thermometers on each cast.

Depth

Pressure is measured with National Semiconductor pressure sensors which are accurate to 1% of full scale. To provide maximum resolution, pressure sensors are interchanged, depending on the depth of the profile. The sensors are calibrated using a dead-weight pressure tester. The pressure sensor is depressed by a hydraulic piston which can be adjusted to provide a wide range of accurately known pressures, by means of a set of weights.

Conductivity-Salinity

Salinity is computed from conductivity, temperature, and pressure. The conductivity sensor received an initial NBS calibration. Because of the slow flushing rate of the conductivity cell, the time response of the conductivity sensor does not match that of the temperature sensor. This mismatch results in sharp spiking of the salinity data in regions of strong vertical gradients of either temperature or salinity. To overcome this problem, the time response of the two sensors is matched digitally by lagging the temperature data by a given depth increment (since the conductivity cell response time depends upon the vertical descent velocity of the probe). Through this procedure, some of the spiking can be removed. The amount of lagging to apply is determined empirically by comparing the PHISH-derived salinities with those obtained from Niskin bottle water samples. Salinity samples are obtained from two Niskin bottles mounted on the PHISH case. These trip automatically at one metre from the bottom. Additional salinity samples are taken at the surface and at some intermediate point within the water column. The salinity of the water samples is determined with an inductive salinometer, calibrated against standard seawater before and after each run.

To eliminate the spiking problem, a pump was installed on the conductivity sensor in June 1981 to provide faster flushing action. As a result, the accuracy of salinities determined from the PHISH are within .02 ppt of those determined from the water samples. This accuracy is obtained when the PHISH is descending at the rate of 20 m/min.

When the PHISH is held at a constant depth, the accuracy is about .01 ppt.

Future modifications will allow calibration data to be obtained from a six-bottle (five-litre) rosette sampler which will sample sequentially at the command of the computer operator.

PHISH Profiles

The temperature and salinity structure near the East and West Flower Garden Banks was determined on five separate cruises during the period September 1979 to July 1981. Although the first two cruises were conducted during a previous study (Rezak and Bright, 1981a), the hydrographic data reporting requirement was designated for the present study. The cruise dates and the ships used were: M/V BLACK SEAL, 5-18 Sep 79; M/V ROSS SEAL, 12-21 Oct 79; M/V BALTIC SEAL, 12-27 Oct 80; R/V GYRE, 3-8 Mar 81; and the M/V NORTH SEAL, 13-17 Jul 81. The complete set of vertical profiles of temperature, salinity, transmissivity, and velocity taken during these cruises is reported in the Hydrographic Data Report issued in January 1982 (McGrail et al., 1982a).

Cross Shelf Transects

Future analyses of these data will encompass a number of different themes. Transects across the shelf and out over the slope where XBT's or PHISH profiles were taken will contribute to a study of the general shelf circulation. For this study, transects will be combined with the current meter and meteorological data of the present project, and with historical data and the results of mathematical models of shelf circulation. Preliminary analysis of these transects reveals the plunging of isotherms near and south of the Flower Garden Banks over the continental slope. The sloping isotherms are indicative of strong geostrophic currents heading eastward, in agreement with currents derived from 1) profiling current meter data taken with the PHISH on these same transects and 2) records of the moored instruments.

Another prominent feature on the cross-shelf transect taken on the March 1981 cruise is a reversal of currents toward the west, northward of the shelf break. There is some speculation that this is a semi-permanent feature which moves northward and southward or perhaps even disappears seasonally.

Seasonal Temperature Variations

The vertical density structure is of ultimate dynamical importance to the characteristics of internal tides, shelf waves, and inertial currents. A critical problem in the study of these processes in the Flower Garden region is the seasonal variability of temperature. Vertical profiles of temperature and salinity are not available for the long periods between cruises. Historical data will be helpful in filling this gap since seasonal variability should not change significantly from year to year. The temperature time series measured at fixed depths on the current meter moorings provide a means of

constructing a seasonal picture of temperature, particularly when combined with vertical profiles from historical data.

Composite plots of vertical temperature and salinity profiles have been prepared for each of the last three cruises. Composite plots of temperature and salinity profiles taken on the October 1980, March 1981, and July 1981 cruises are shown in Figure IV-60. Only those stations where the bottom depth was less than 150 m were used. All stations come from the immediate vicinity of the banks, between about 27°49'N to 28°N latitude and 93°30'W to 93°58'W longitude. These represent, in chronological order, conditions in the fall, late winter or early spring, and summer. Seasonal changes in salinity are small compared to changes in temperature, relative to their effect on density. Much of the variance in salinity on the October 1980 and March 1981 profiles is attributable to the time response mismatch between the conductivity and temperature sensors on the PHISH conductivity, temperature, and depth probe (CTD). The addition of a pump to speed the flow through the conductivity cell resulted in greatly improved salinity measurements on the July 1981 cruise. The only appreciable changes in salinity occur in the upper 30 m or so. By contrast, however, profiles taken in 1979 in the Flower Garden region show salinities near the surface as low as 31 ppt.

The late winter temperature profiles taken when stratification was at a minimum show a greater degree of spatial variability than in the other seasons. The temperature profiles shown in Figure IV-60a,c,e correspond well to the annual progression of the isotherms in the outer Texas-Louisiana continental shelf reported by Nowlin and Parker (1974) and by Angelovic (1976), although Angelovic's data seem to provide the better correspondence to the present data set. The annual cycle derived from Angelovic indicates that the lowest vertical gradients of temperature occur in late February, ranging from 19°C to 20°C at the surface to 17°C to 18°C at a depth of 125 m. At this time, a partially mixed surface layer extends from the surface down to 30 to 50 m depth. Rapid warming near the surface begins in April, raising surface temperatures to about 28°C by the middle of June. During this period, the surface mixed layer becomes very thin or essentially nonexistent. The surface temperature peaks in the range of 29°C to 30°C in August, but remains relatively constant from June through September.

A strong thermocline is established in June. From June to October, its depth increases as the surface mixed layer thickness increases. In October, cooling of the mixed layer begins, which leads to a gradual further deepening of the surface mixed layer and the erosion of the thermocline. The temperature near 100 m varies from a low of about 17°C in March to a high of 20°C to 21°C in January (Angelovic, 1976).

Temperature and Velocity Structure

Two different methodologies were considered for the design of the hydrographic sampling schemes over and near the Flower Garden Banks. The first method takes stations in as direct a fashion as possible to answer specific questions identified as project goals. These questions

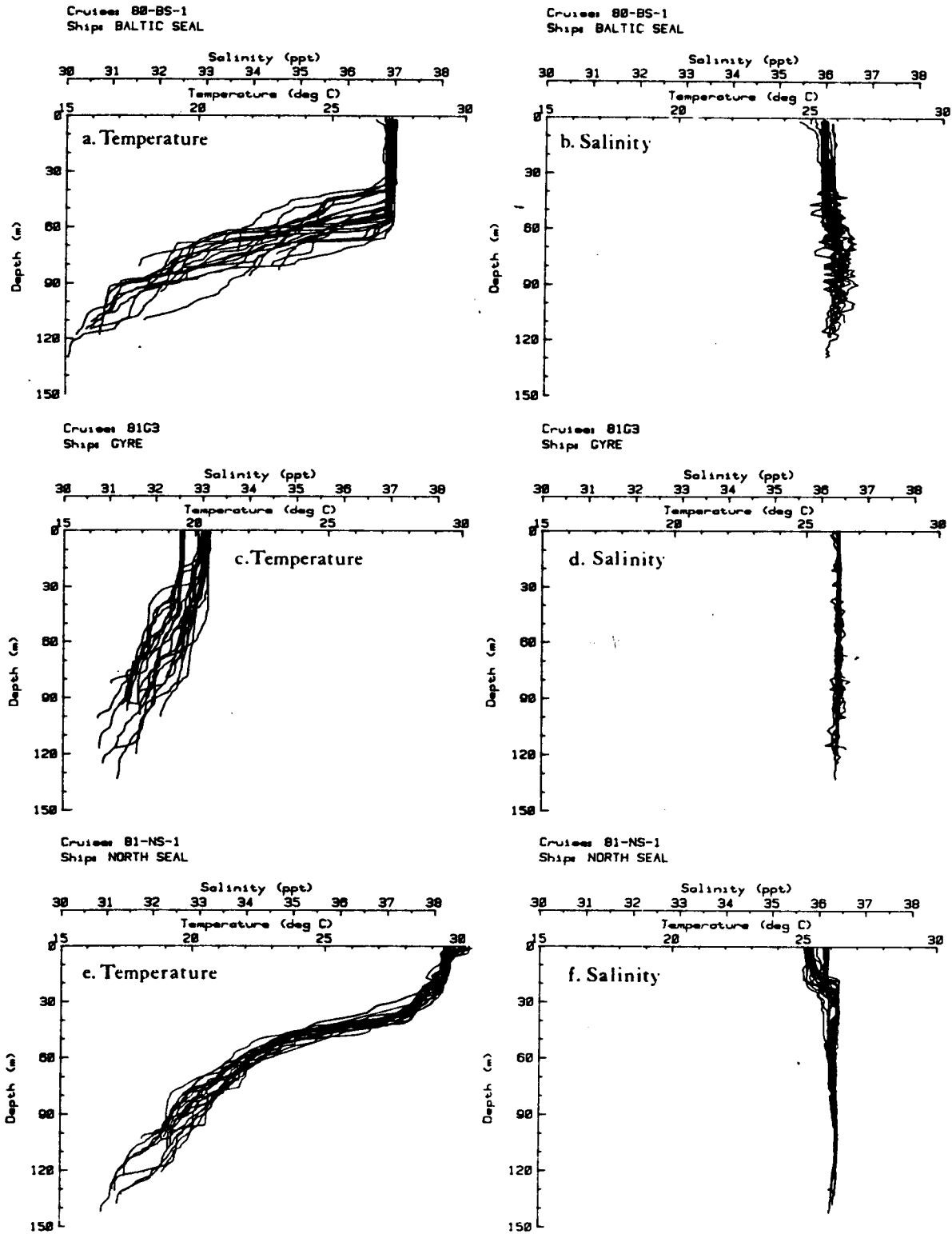


Figure IV-60. Composite plots of temperature and salinity profiles taken near the East and West Flower Garden Banks on three cruises: (a and b) October 1980; (c and d) March 1981; (e and f) July 1981.

are: (a) in what manner do the currents traverse the banks; i.e., do they go around the banks or do they go up and over the banks? and (b) what is the upper depth limit of the nepheloid layer? Much of the data collected was meant to answer these questions directly, but they can only be answered for those particular periods when observations were made, and only at those particular places sampled. The advantage of this method is that it probably gives a sufficient amount of information with a minimal amount of ship time.

A potentially more powerful method, but more expensive to implement, is to sample in such a way as to determine specific critical parameters needed to develop and verify theoretical models of flow around banks. Such models provide predictive capability to examine situations not encountered during the cruises, and at any point around the banks. No adequate theoretical model exists for the particular scales found at the Flower Garden Banks, and therefore the sampling program could not be designed a priori to test such a model. However, some useful general guidelines for sampling are found in the literature, though their results cannot be applied directly to the present situation. The last cruise (NORTH SEAL, July 1981) was designed with this latter philosophy in mind. However, due to the failure of the profiling current meter on this cruise, the goals of the sampling scheme were not completely attained. Nevertheless, data from this cruise and from previous cruises may still prove adequate for developing and evaluating a dynamic model.

Since water parcels remain at the same isotherm if mixing or diffusion is negligible, the isotherms provide a means of determining vertical excursions of the water parcels as they traverse the banks. For example, a NW to SE vertical section of temperature over the East Flower Garden Bank taken on the October 1980 cruise is shown in Figure IV-61. Figure IV-62 shows the station positions and names on a bathymetric map of the East and West Flower Garden Banks; the transect is indicated by the heavy line connecting stations.

During the period when these stations were taken, the current speeds were from 30 to 50 cm/sec at mid depth, directed toward the east. The isotherms in the vertical sections indicate a thickening of the mixed layer in the downcurrent side of the bank. As the thermocline is depressed (about 15 m), it also intensifies. Over the period when the stations were taken, temporal changes in temperature were also occurring. To interpret these data, one must determine whether the temperature changes from one location to the next are due to the relative position of the bank to the station, and not to the time at which the station was taken. The separation of temporal from spatial temperature change can be accomplished to some degree by referencing the profiles to the temperature time series data taken at fixed depths on nearby moorings. The temperature at 54 m depth from mooring 1 is plotted versus time in Figure IV-63. The temperature at 54 m for each station is also plotted on this figure versus station time. The temperature on mooring 1 drops by 4°C from 1800 GMT 24 Oct to 0300 GMT 25 Oct, but remains relatively constant immediately afterward during the period when stations were being taken around the East Flower Garden

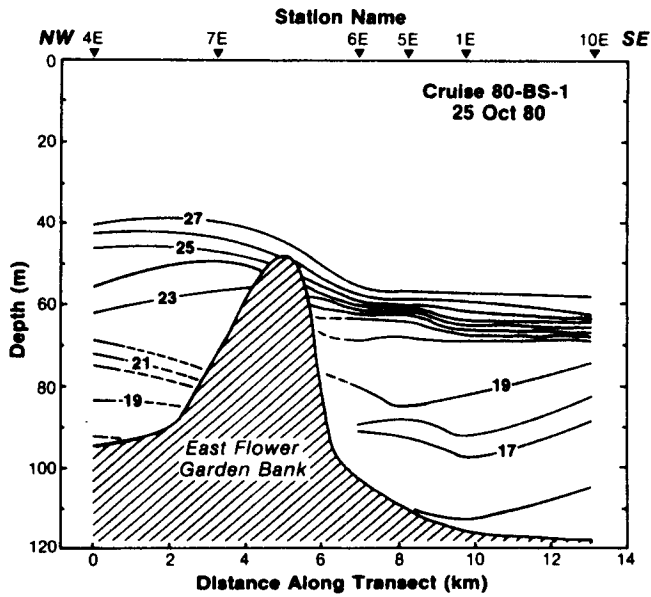


Figure IV-61. Vertical section of temperature from northwest to southeast across the East Flower Garden Bank. Stations were taken on 25 October 1980.

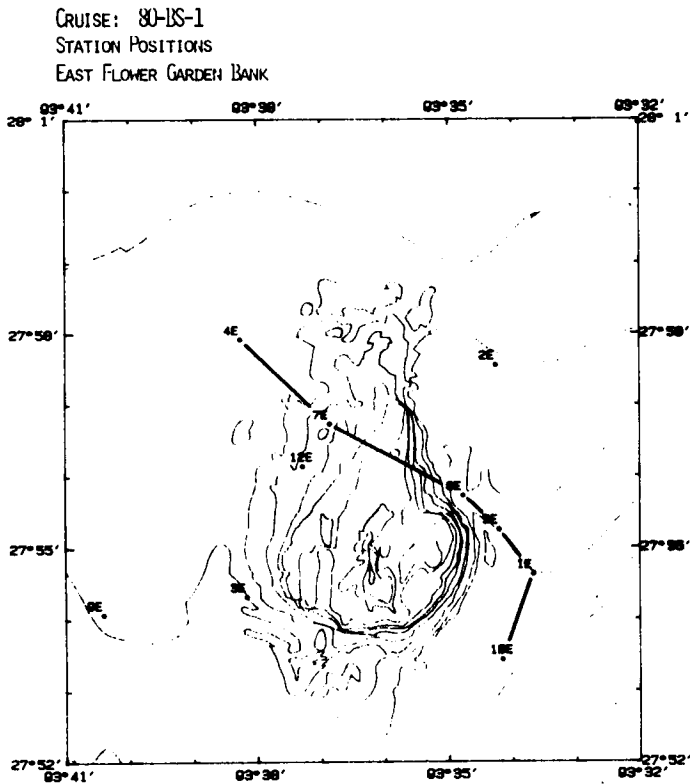


Figure IV-62 Map of the East Flower Garden Bank showing locations of stations taken on the BALTIC SEAL cruise of October 1980. The heavy line connects the stations used in the vertical section of Figure IV-61.

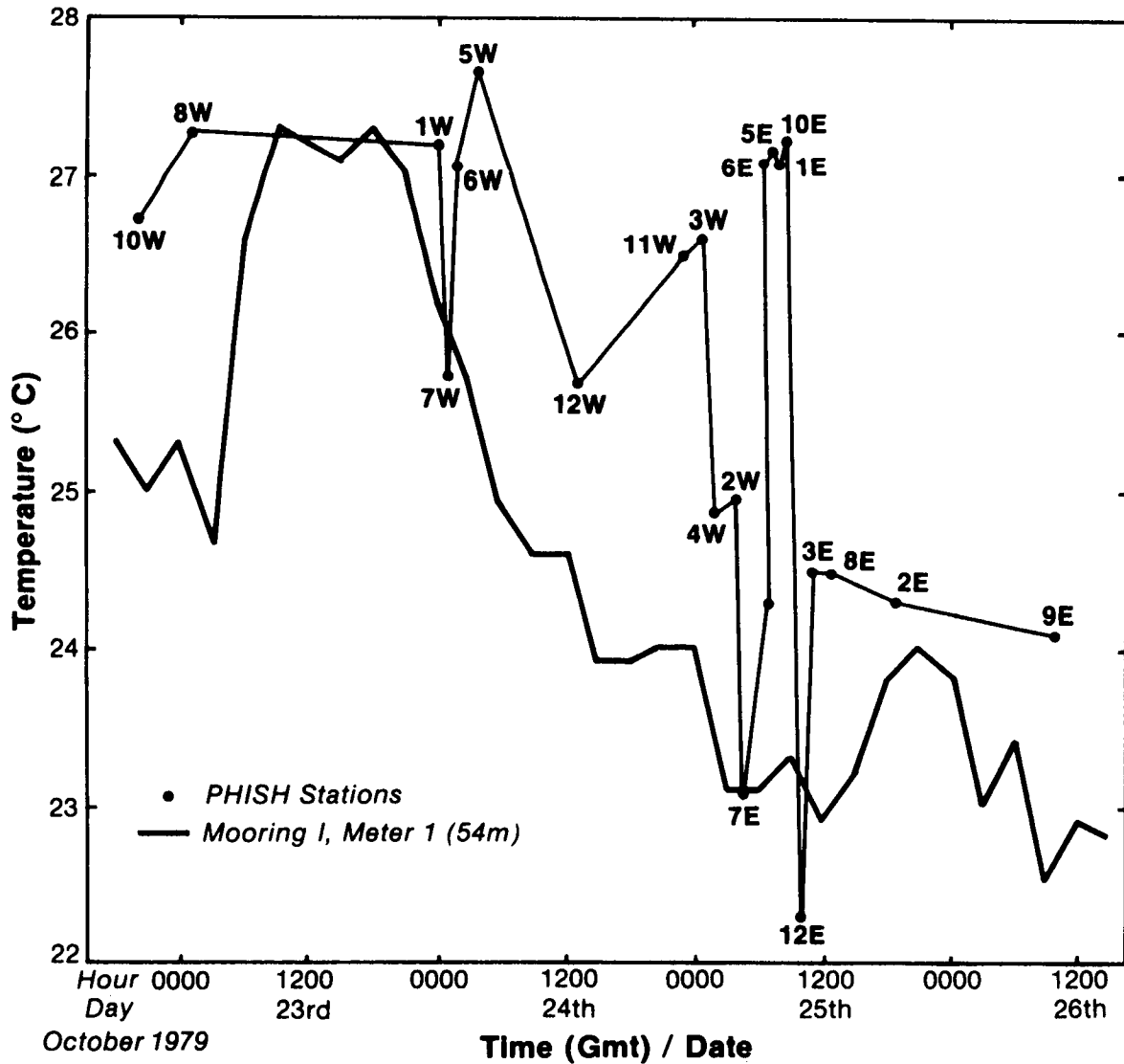


Figure IV-63. Temperature at meter 1 of mooring 1 (54 m depth) during the period when PHISH stations were taken around the East and West Flower Garden Banks on the October 1980 BAL TIC SEAL cruise. Temperature at 54 m depth is plotted for each PHISH station at the station time.

Bank. Therefore it appears that the higher temperatures (greater isotherm depths) at Stations 1E, 5E, 6E, and 10E are due to their proximity to the eastern edge of the bank. Note that Stations 2E and 8E, which are also on the eastern side of the bank, have temperatures similar to those from stations on the west side (or up-current side) of the bank. This similarity is apparently due to their greater distance from the main part of the bank.

The velocity vectors at 70 m depth are plotted at all stations on a bathymetric map (Figure IV-64). The current direction is toward the east-southeast around the East Flower Garden at all stations except 5E and 6E. Vertical profiles of salinity, temperature, transmissivity, sigma-t, and horizontal currents at these two stations are shown in Figures IV-65 and 66. Velocities at Stations 5E and 6E are greatly attenuated, and both show a direction reversal at and below the mixed layer.

The thermal structure may not be a useful indicator of flow around the banks in the winter, when vertical stratification is small. During the March 1981 cruise, the temperature difference between the surface and 100 m depth was only 2°C to 2.5°C. Figure IV-67 lists the depth of the 19.6°C isotherm above the position on a bathymetric map of each station taken near the Flower Garden Banks during this cruise. This isotherm was chosen because of its large depth changes. Over the West Flower Garden Bank, all temperatures are greater than 19.6°C, but on the west side of the East Flower Garden Bank the 19.6°C isotherm is nearly 80 m deep, reaching almost as deep as the bottom nepheloid layer. The entire region is dominated by a strong north-south gradient of temperature, with isotherms plunging down the continental shelf break into deeper water. The complete disappearance of water warmer than 19.6°C over the West Flower Garden implies either meandering of the current or the existence of small isolated blobs of water of differing temperatures.

The velocity vectors one metre from the bottom of each profile at each station near the Flower Garden Banks taken on the March 1981 cruise are shown on the bathymetric map in Figure IV-68. In almost every case, they are nearly parallel to the local bathymetry. The current, coming from the west, flows around the bank following the bank contours on the eastern side. The current finally breaks away near the north-south center of the eastern side of the bank.

Only a brief preliminary survey of some of the PHISH data has been presented here. A complete analysis is in progress relating temporal changes recorded on the current meter moorings to measurements made with the PHISH.

Transmissivity

Turbidity, or the relative concentration of suspensates in the water column, has been measured in this study in order to observe, understand, and explain sedimentary processes and water movements on the continental shelf in the Flower Gardens region. The ease and

Cruise: 80-B5-1
Velocity Vectors at 70 m Depth
East and West Flower Garden Banks

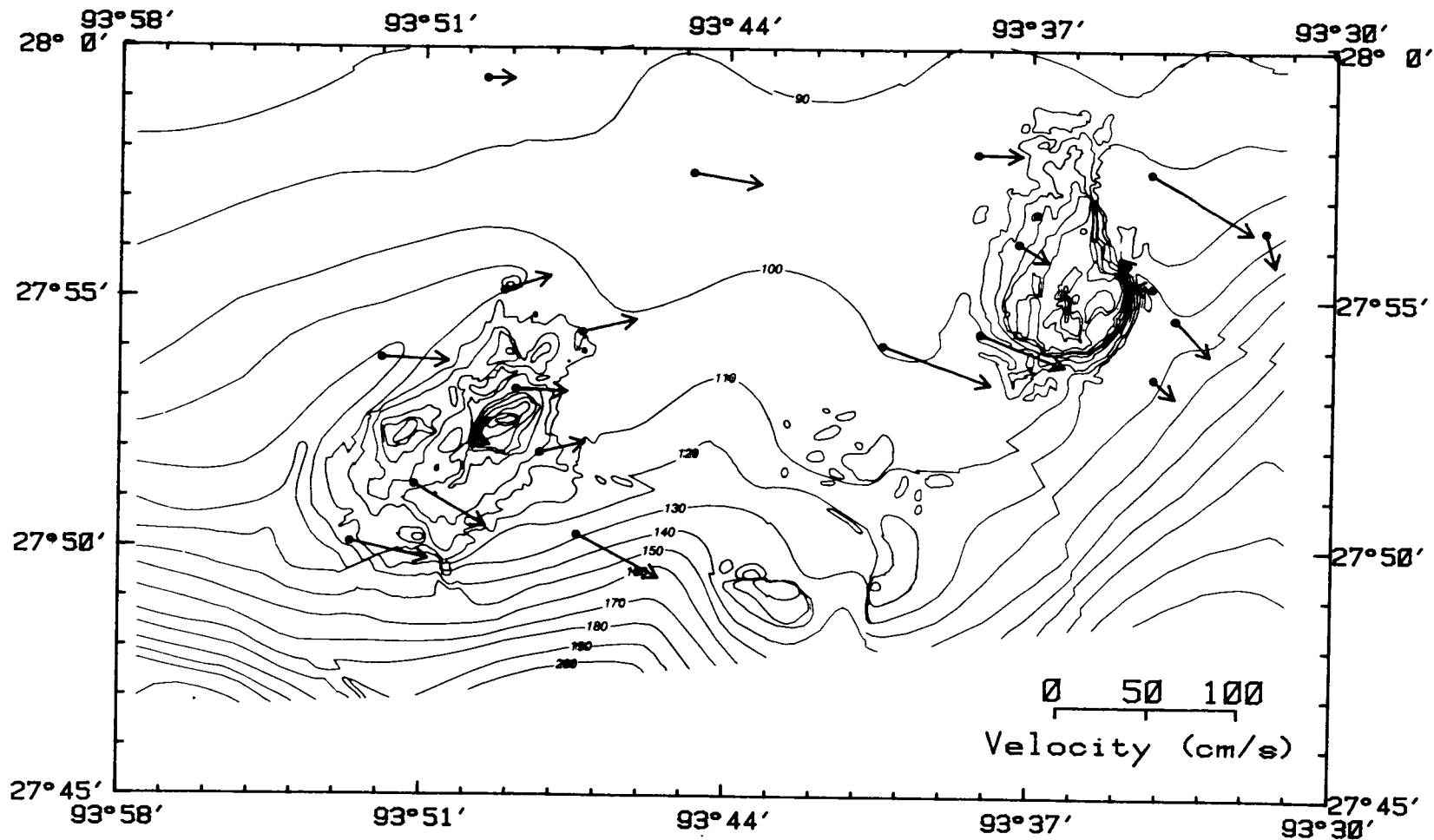


Figure IV-64. Horizontal velocity vectors at a depth of 70 m determined from PHISH stations taken on the October 1980 BALTIC SEAL cruise.

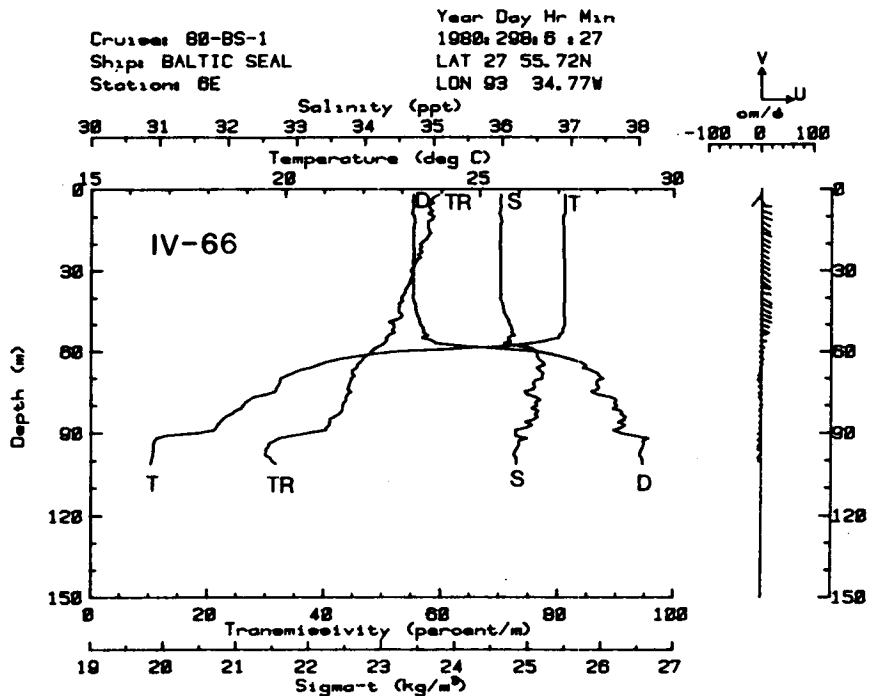
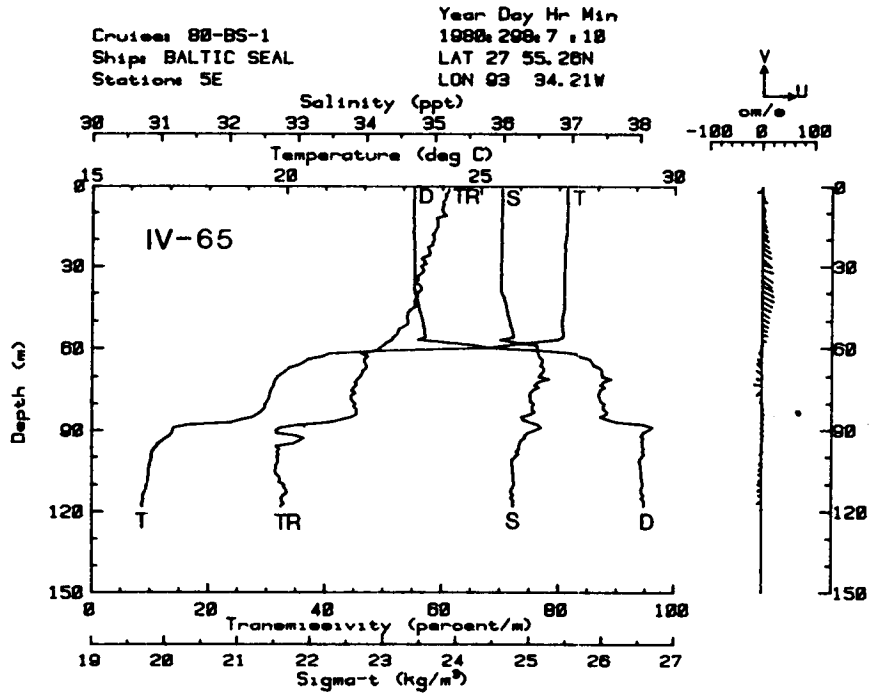


Figure IV-65. Plot of temperature (T), salinity (S), transmissivity (TR), and sigma-t (D) at EFG station 5E, October 1980. Note the extensive block type BNL associated with a well mixed bottom zone.

Figure IV-66. Plot of temperature (T), salinity (S), transmissivity (TR), and sigma-t (D) at EFG station 6E, October 1980. Another example of a block type BNL associated with a well mixed bottom zone.

Cruise: 81G3

Depth (m) Where Temperature (deg C) = 19.6

East and West Flower Garden Banks

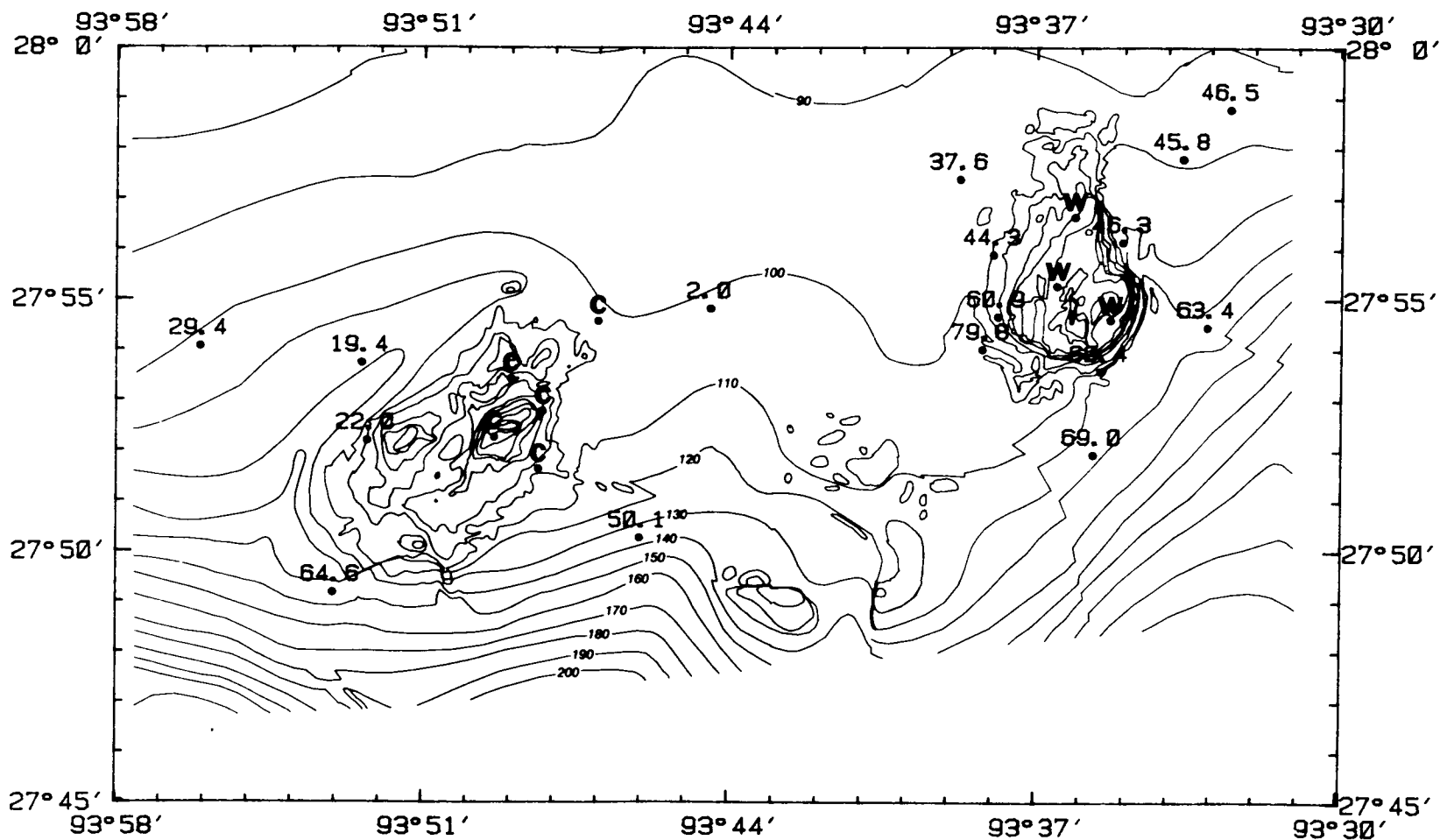


Figure IV-67. Depth in metres of the 19.6°C isotherm at stations taken around the East and West Flower Garden Banks in March 1981 on the GYRE cruise. The "C" indicates stations where temperatures are all lower (colder) than 19.6°C, and "W" indicates stations where temperatures are all higher (warmer) than 19.6°C.

Cruise: 81-G-3
Velocity Vectors at 1 m From Bottom
East and West Flower Garden Banks

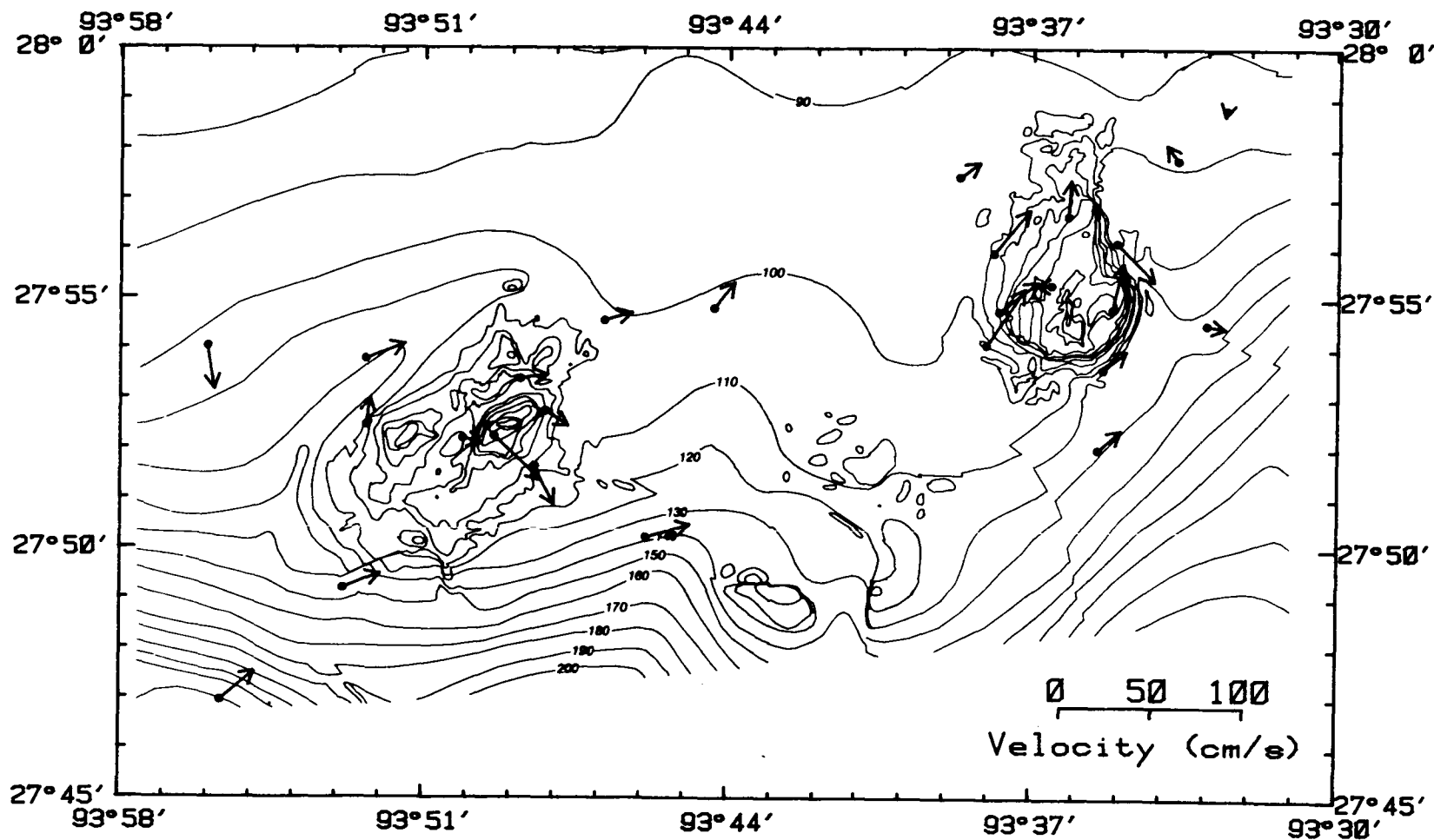


Figure IV-68. Horizontal velocity vectors at 1 m from bottom determined from PHISH stations taken on the March 1981 GYRE cruise.

potential accuracy of in situ light measurements make them particularly advantageous for the study of suspended sediment patterns near the Flower Garden Banks since numerous measurements are necessary for wide spatial and temporal coverage.

Instrumentation

The basic configuration of an in situ underwater light beam instrument (transmissometer) consists of a beam of light emitted from a source which travels through a water path and then projects onto an optical receiver. The percent of light transmitted through this travel path is recorded. Transmissometer designs may vary according to a) the path length between light source and optical receiver, and b) light source wavelength.

The underwater reduction of light beam transmittance (attenuation) is affected by two basic processes: absorption and scattering. Absorption involves a change of energy form, and scattering entails a change in direction of light travel. The three factors controlling the amount of light transmitted are the water, suspended particulate matter, and dissolved substances--particularly organic dyes. The loss of light beam transmittance over a given travel path through the water column is an indirect measurement of the amount of suspended particulate matter (SPM). An increased concentration of SPM in the water column results in a decreased percentage of light transmitted over a given distance. Therefore, in situ light beam transmittance recordings are useful for several areas of oceanographic study: biological productivity and migration, water pollutant study, and suspension of inorganic matter.

Continuous vertical profiles of transmissivity were recorded with the Sea Tech transmissometer mounted on the PHISH*. Increased amounts of suspended matter, particularly near the bottom or on strong density interfaces, form turbid or nepheloid layers which are easily identified on a transmissivity profile. A PHISH profile gives the investigator an immediate picture of the water column via continuous and simultaneous recordings of transmissivity, temperature, conductivity, water density (σ_t), and current velocity.

The Sea Tech model transmissometer used on the PHISH is most appropriate in a nearshore study since this instrument has a light source with a wavelength (λ) of 660 nm and a beam path length of 25 cm. Since the absorption of light by yellow matter decreases exponentially with increasing λ , the attenuation of light at 660 nm by dissolved substances is negligible. Thus dissolved substances will not seriously

*Transmissivity has also been measured at fixed depths near the bottom over long periods of time with Sea Tech transmissometers mounted on current meter moorings. These time series data will later be used to determine relationships between the transmissivity fluctuations and tides, storm-induced currents, and other events capable of sediment suspension and transport.

affect transmissivity and will not be erroneously interpreted as particulate matter. Transmissivity is a function of path length. A 25 cm path length minimizes the signal-to-noise ratio and maximizes sensitivity in the range of particle concentration between 100 g to 140 mg/l.

Relationship Between XMS and SPM

Transmissivity (XMS) in the bottom nepheloid layer is principally an indirect measure of the concentration of suspended particulate matter (SPM). The relationship between XMS and SPM depends upon the variable properties of particle types between different samples; XMS varies with particle size, concentration, composition, shape, and index of refraction. This relationship must therefore be determined empirically.

The conversion of transmissivity to suspended particulate matter concentration has been calculated for the Sea Tech transmissometer by comparing the concentration of particulate matter ($\mu\text{g/l}$) filtered from water samples taken at the identical location and time that a transmissometer reading was recorded. Simultaneous sampling is made possible by the PHISH which is equipped with both a Niskin sampler and a transmissometer. The field data for the conversion were gathered on three seasonal sampling cruises to the Flower Garden Banks (October 1980, March 1981, and July 1981). The data from the October 1980 cruise were not used in the conversion process due to contamination of the water samples.

The log of the XMS is linearly proportional to the particle volume (Sea Tech, Inc., 1980). Sediment weight may be substituted for volume since weight and volume are directly proportional for a given density. The log of XMS has been plotted versus SPM for the data from the March 1981 and July 1981 cruises in (see Figure IV-69). The linear regression of log XMS on SPM was performed for the individual cruise data set as well as for the combined data, thus determining three best-fit linear curves. The equation for the combined data set is

$$\text{SPM } (\mu\text{g/l}) = 3898 - 924 \ln [\text{XMS } (\%/m)]. \quad (20)$$

Due to wide variations of particle properties, this conversion is a rough estimate of the relationship between suspended particulate matter and transmissivity.

The March data indicate a higher transmissivity for a given weight of suspended matter than in July. Therefore a larger particle size (e.g., silt vs. clay) is suspected to form the bottom nepheloid layers in March than in July, because for a given particle mass, large particles will transmit a greater amount of light than an equal weight of small particles. The small particles have a greater surface/mass ratio capable of increased light attenuation.

For a future report, an additional conversion of XMS to SPM and the intercalibration of the Sea Tech and Martek model transmissometers

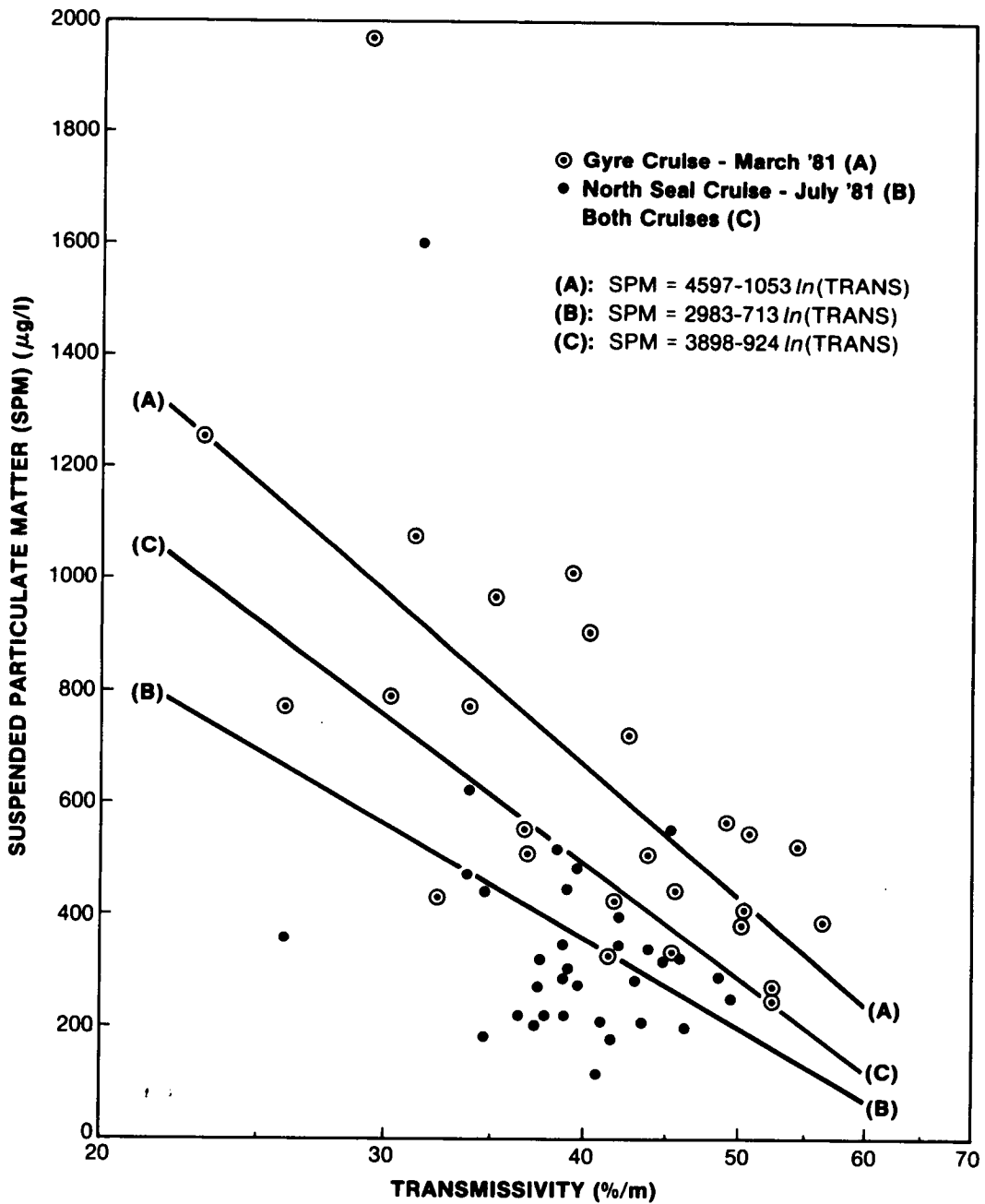


Figure IV-69. Transmissivity versus SPM concentration determined from samples taken at the bottom of PHISH cast from stations near the East and West Flower Garden Banks. Linear regression used to determine curves (A) and (B) for the GYRE and NORTH SEAL cruise data, respectively. Combined data sets used to determine curve (C).

will be experimentally determined in a controlled ocean water tank. Transmissivity readings will be recorded as predetermined amounts of suspended matter are added. The possibility that XMS measurements are influenced by water temperature will also be investigated.

XMS Profiles

The transmissivity profiles collected at the Flower Garden region during the three seasonal cruises (BALTIC SEAL, October 1980; GYRE, March 1981; NORTH SEAL, July 1981) indicate both spatial and temporal variability of the water column turbidity. Locations of PHISH stations during the three cruises are shown in Figures IV-70 through 73. Although the bottom nepheloid layer (BNL) is the principal concern in the analysis of these profiles because of the relationship of BNL's to bottom sediment resuspension and movement, an initial description of surface and intermediate transmissivity values is also given because of their importance relative to available light for organisms on the bank.

Surface Values

Surface transmissivity from all three data sets generally ranges between 50% and 60%. Two distinct transmissivity groupings of the BALTIC SEAL (October 1980) profiles are identified: (1) the majority of the West Flower Garden profiles (2W, 3W, 4W, 8W, 10W, 11W, 12W) and one East Flower Garden profile (2E) have low XMS values in the range of 44.5-56.3%; (2) four West Flower Garden profiles (1W, 5W, 6W, 7W) and eleven East Flower Garden profiles (1E, 3E through 10E, and 12E) have much clearer surface water, with XMS readings of 59.4-61.5%. Surface XMS values recorded for the March and July 1981 cruises do not vary significantly during the course of each cruise; values range from 55-60% throughout the Flower Garden region on all profiles. It must be remembered when comparing these data to those in previous reports that the new Sea Tech transmissometers have different attenuation coefficients and thus different XMS values (lower) than those produced by the previously used Martek unit.

Intermediate Values

In general, transmissivity gradually decreases as depth increases in the upper portion of the water column. During the October 1980 cruise, a gentle gradient of roughly 0.22%/m extends through the surface mixed layer. During the March 1981 cruise, suspended particulate matter concentrations in the surface mixed layer were also nearly uniform or increased slightly with depth. In addition, particulates accumulate on intermediate depth density interfaces to form XMS spikes at Stations 13S and 17S (Figure IV-74). Since high biological activity is restricted to the surface waters, a mid-depth decrease of suspended matter occurs in a number of profiles. Good examples of this relationship are profiles 2W and 4E (Figure IV-75). During the July 1981 cruise, a second XMS gradient, stronger than the gentle slope which is common to all cruise profiles in the surface mixed layer, occurs below a 40 m surface mixed zone.

Cruise: 80-BS-1
Station Names
East and West Flower Garden Banks

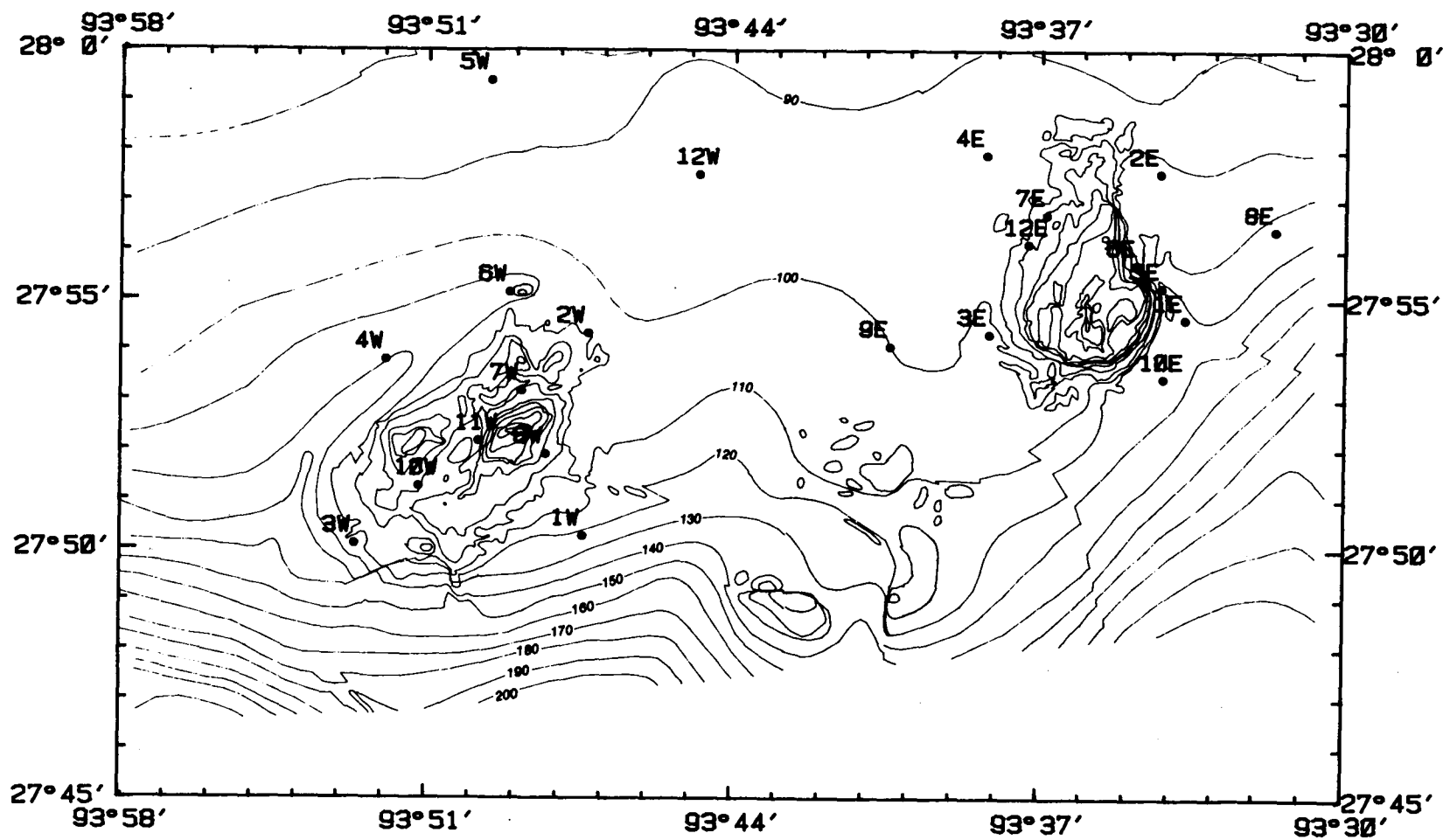


Figure IV-70. Hydrographic station location map for the BALTIC SEAL cruise, October 10-20, 1980.

Cruise: 81-G-3
Station Names
East and West Flower Garden Banks

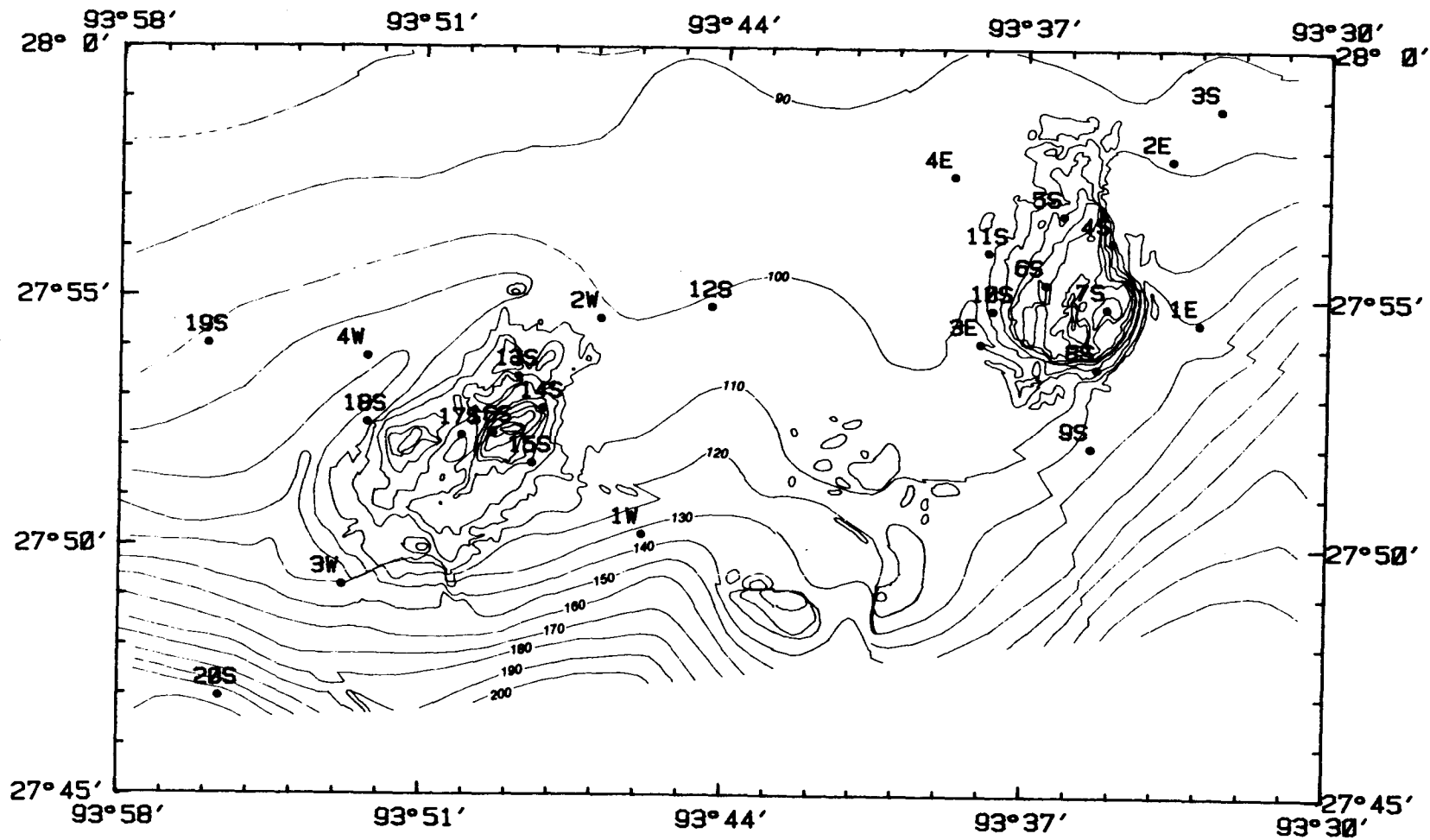


Figure IV-71. Hydrographic station location map for the GYRE cruise,
March 3-8, 1981.

Cruise: 81-NS-1
Station Names
East and West Flower Garden Banks

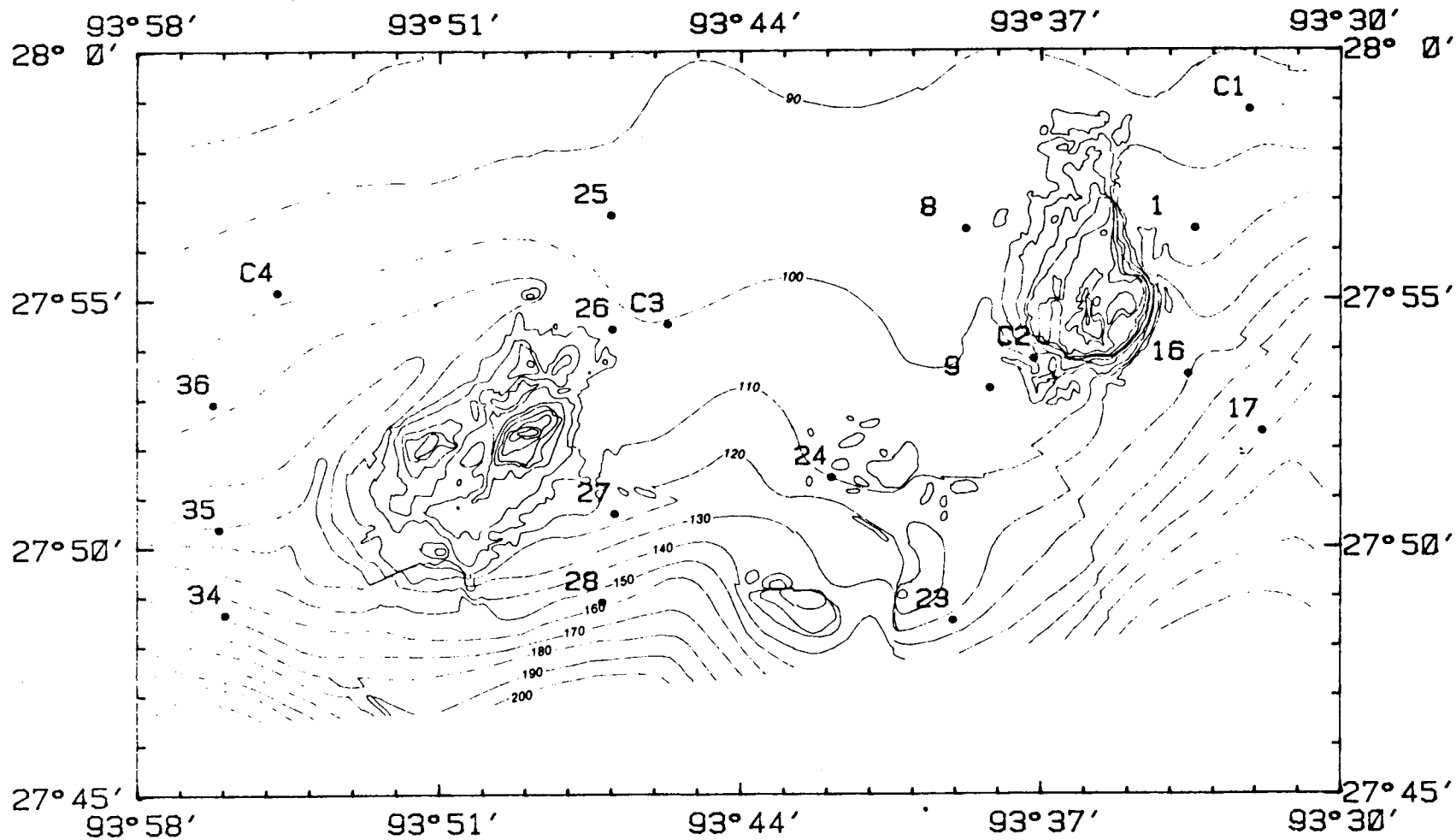


Figure IV-72. Hydrographic station location map for the NORTH SEAL cruise, July 13-17, 1981. (For complete East Flower Garden stations, see Figure IV-73.)

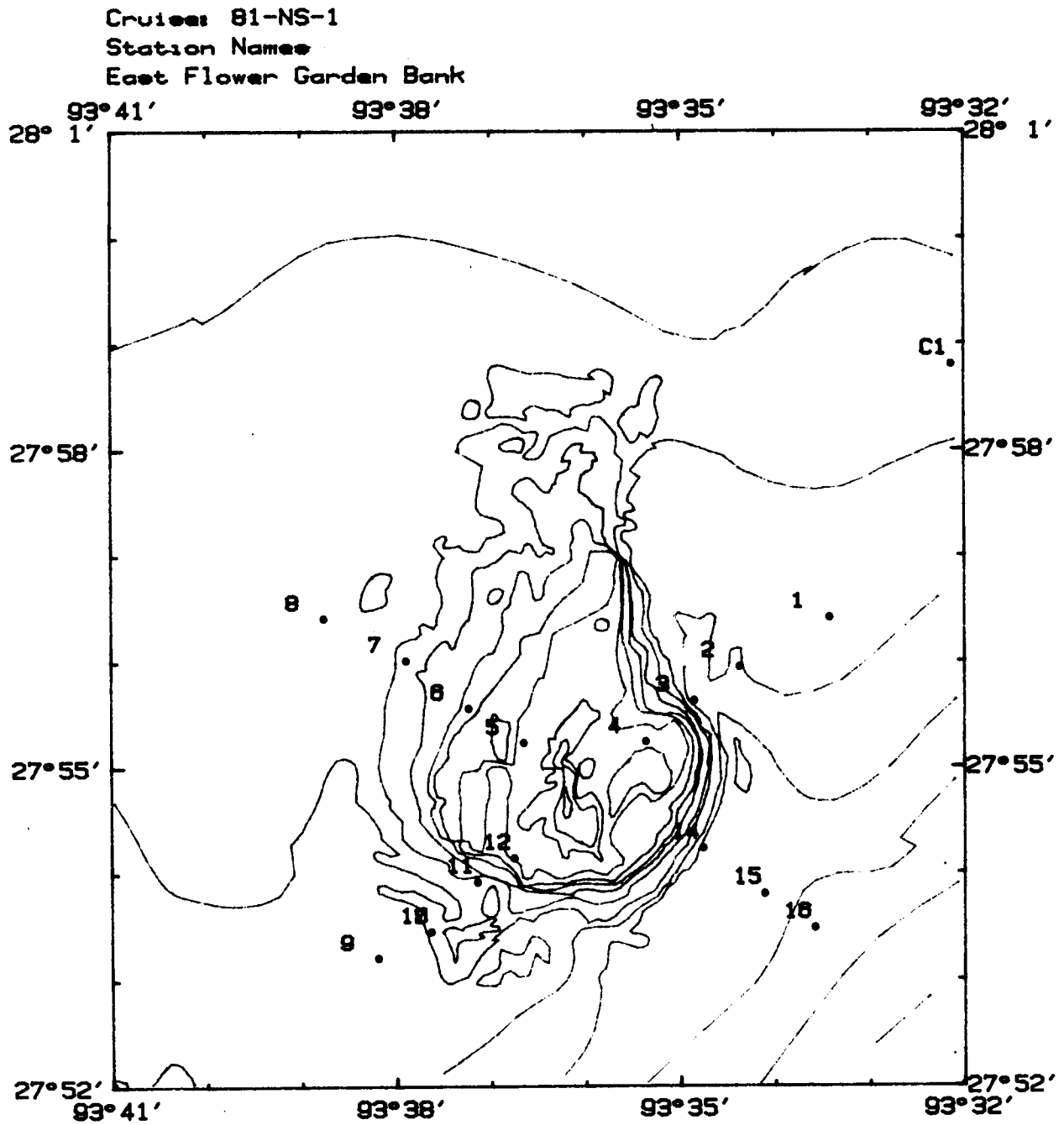


Figure IV-73. Hydrographic stations at the East Flower Garden Banks for the NORTH SEAL cruise, July 13-17, 1981.

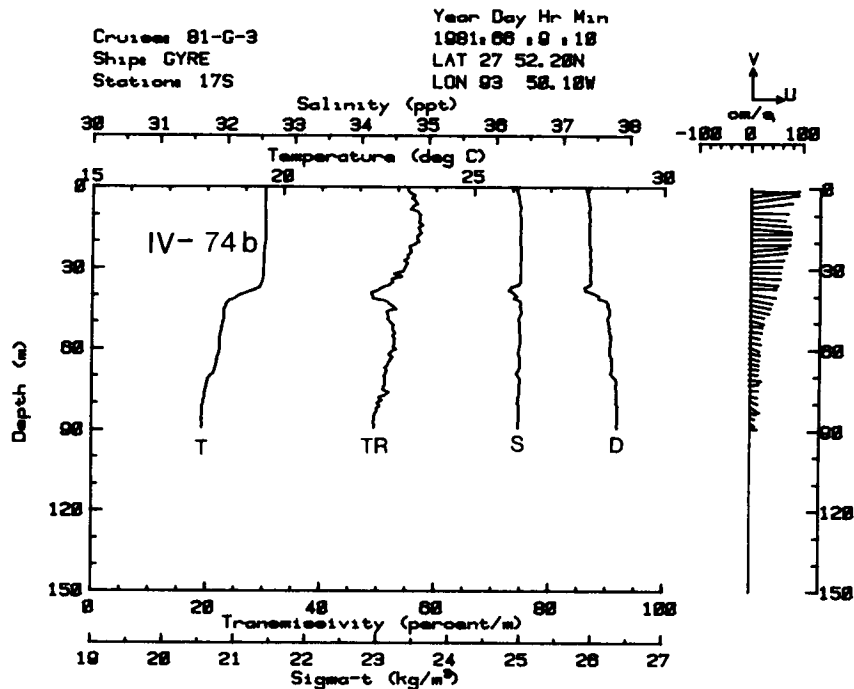
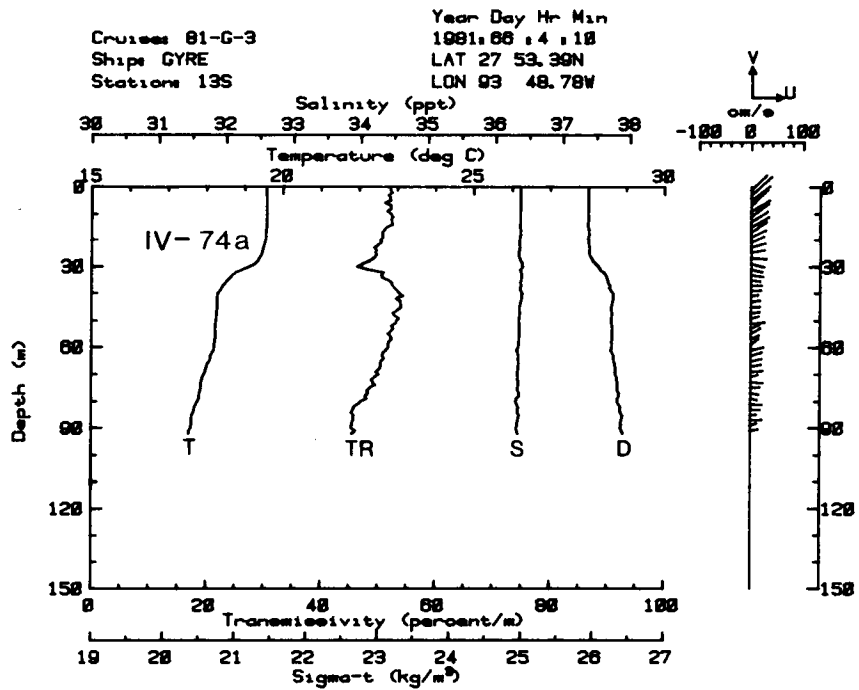


Figure IV-74. Plots of temperature (T), salinity (S), transmissivity (TR), and sigma-t (D) from WFG stations 13S and 17S, March 1981. Station 13S illustrates a transmissivity spike due to the accumulation of particulates on the intermediate depth density interface. At station 17S (IV-74b) note the bottom mixed layer and absence of BNL.

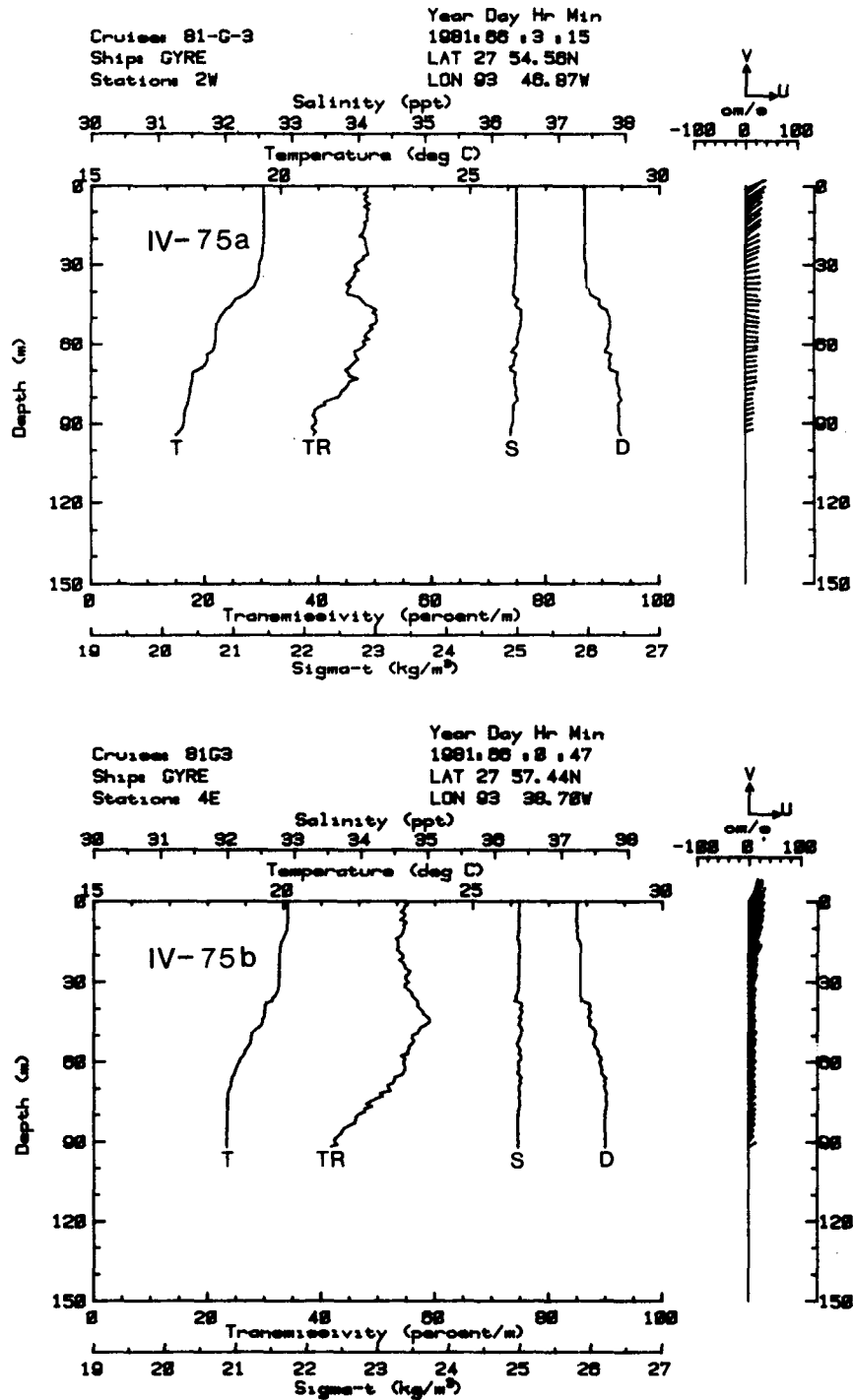


Figure IV-75. Plots of temperature (T), salinity (S), transmissivity (TR), and sigma-t (D) from WFG station 2W and EFG station 4E, March 1981, illustrating a mid-depth decrease of suspended matter (XMS increase) caused by high biological activity restricted to surface waters.

Except for the two distinct surface transmissivity groupings of the October 1980 cruise, the XMS profiles extending through surface and mid-depth waters generally showed little variation between the two Flower Garden Banks during the same cruise.

Bottom Turbid Waters (Bottom Nepheloid Layer)

The form and strength of the bottom nepheloid layer appears to vary both seasonally and spatially near the Flower Garden Banks. The vertical extent of the BNL during the three cruises is illustrated in Figures IV-76 through 79; the minimum transmissivity of the BNL for the same periods is shown in Figures IV-80 through 83. Amounts of suspended particulate matter are typically greater near the East Flower Garden than the West Flower Garden. BNL's are also more common and extensive near the East Flower Garden than near the West Flower Garden.

Definition of BNL

The BNL is an obvious feature in some transmissivity profiles. For example, BNL's on the October 1980 cruise are characterized by a distinct and abrupt XMS drop. In contrast, a distinct bottom turbid layer is generally absent in the July 1981 data. The determination of what is or is not a BNL is rather arbitrary. Certain criteria have therefore been established to aid in determining whether or not a BNL exists for a particular profile. The entire set of transmissivity profiles taken during this study was examined in order to develop these criteria. The top of the BNL is defined to be the point along the vertical profile where the transmissivity suddenly drops by at least 1.5% over 1 m or by 3.0% over a 3 m range. Mid-depth irregularities in XMS which appear to be unrelated to the bottom zone are discounted. Also, a nepheloid layer is not considered a BNL unless at least part of it is found in the lower third of the water column.

Comparison of EFG/WFG BNL's

The difference between the BNL's found near the East and West Flower Garden is most apparent in the October 1980 cruise data. BNL's are found in eleven out of twelve East Flower Garden stations and five out of nine West Flower Garden stations. The five sites without a bottom turbid layer during October were located either on top of a bank or at a relatively shallow site along the side of a bank. The vertical extent of the BNL during October varied from 7 m (Station 3W) to 42 m (Station 1W) (Figure IV-84). The bottom waters near the East Flower Garden are more turbid than the West Flower Garden bottom waters. The minimum XMS at several stations is below 30% near the East Flower Garden Bank, whereas at stations near the West Flower Garden Bank, the lowest value found is 31.8% (at Station 4W).

The same general trends--the exclusion of a BNL atop the banks and greater turbidity at the East Flower Garden than at the West Flower Garden--are consistent in the two other seasonal cruises. However, Stations 14S and 16S of the March 1981 cruise, located atop the West

Cruise: 80-BS-1
VERTICAL EXTENT OF BOTTOM NEPHELOID LAYER FROM BOTTOM
East and West Flower Garden Banks

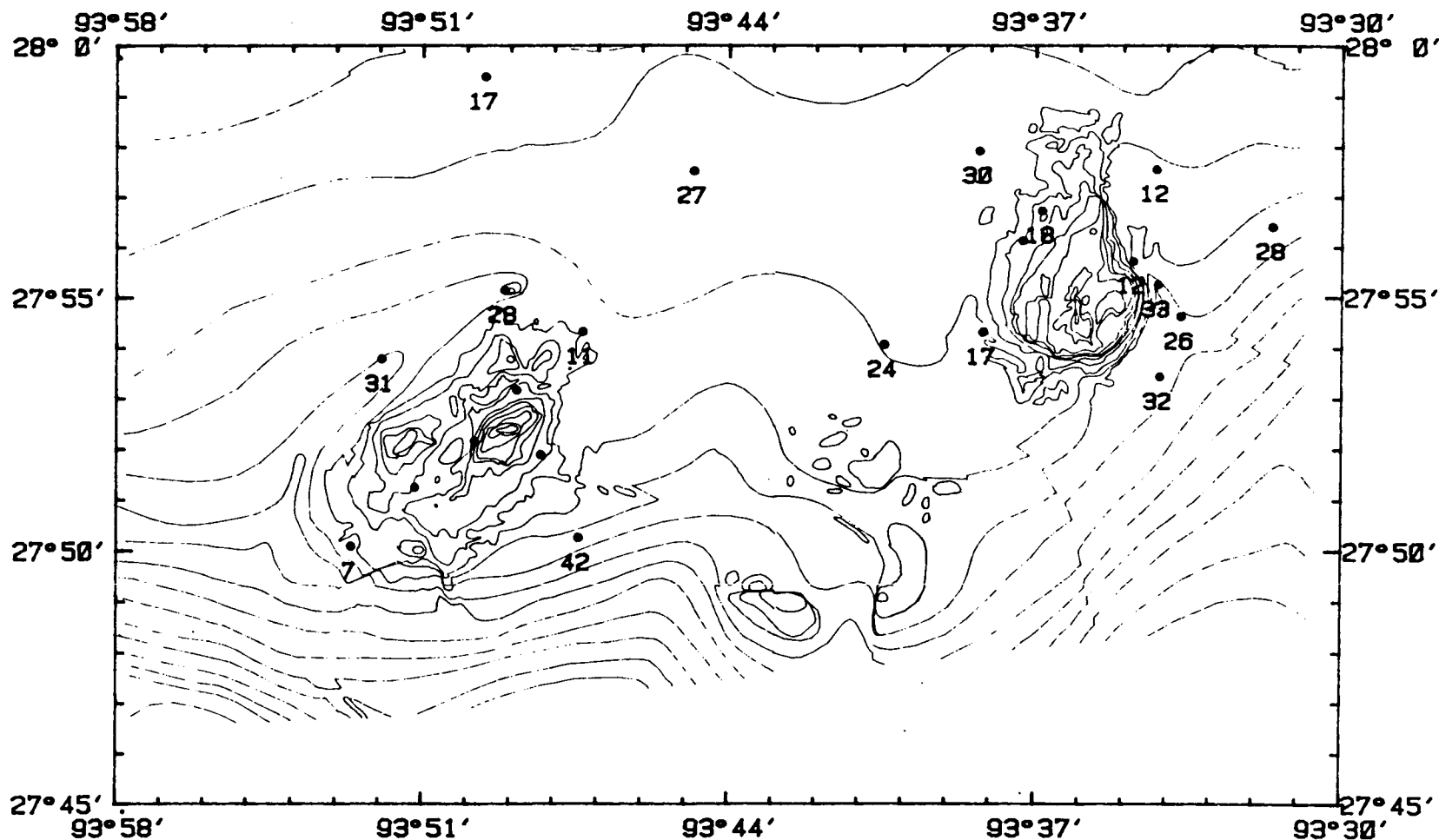


Figure IV-76. Vertical extent (metres) of BNL from bottom during BALTIC SEAL cruise, October 1980. Points not labeled indicate no BNL at that station.

Cruise: 81-G-3

VERTICAL EXTENT OF BOTTOM NEPHELOID LAYER FROM BOTTOM
East and West Flower Garden Banks

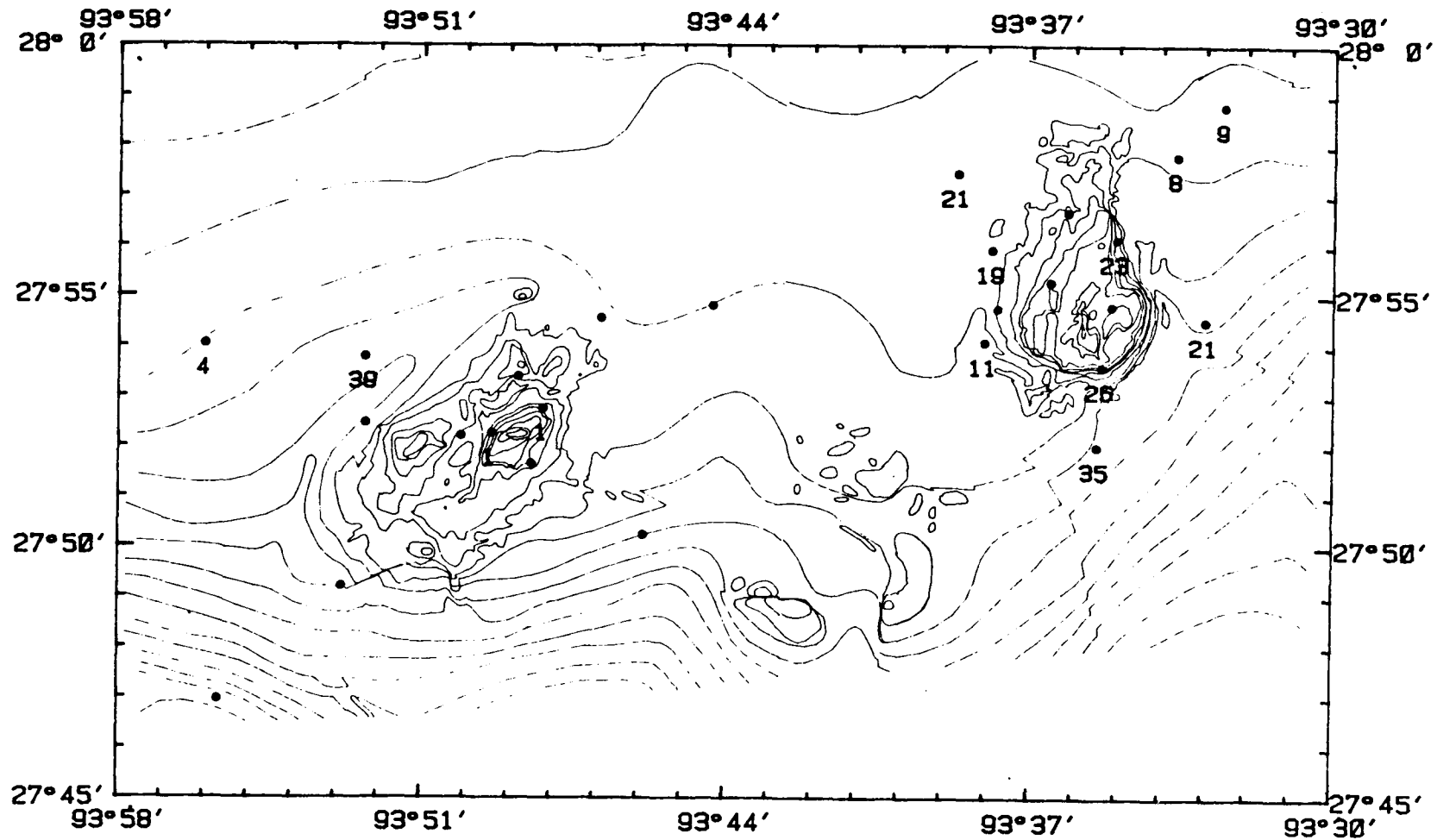


Figure IV-77. Vertical extent (metres) of BNL from bottom during GYRE cruise, March 1981. Points not labeled indicate no BNL at that station.

Cruise: 81-NS-1
VERTICAL EXTENT OF BOTTOM NEPHELOID LAYER FROM BOTTOM
East and West Flower Garden Banks

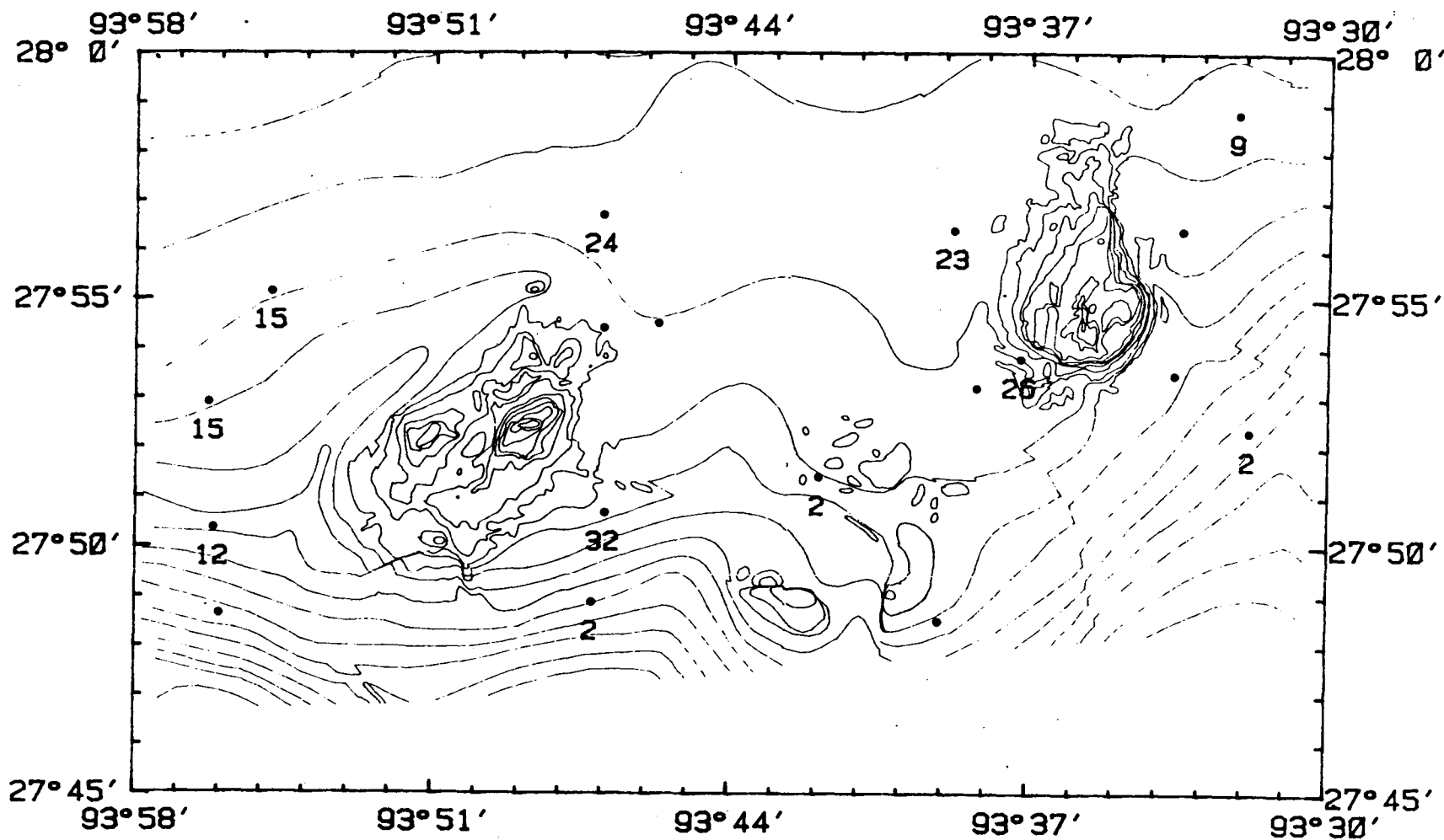


Figure IV-78. Vertical extent (metres) of BNL from bottom during NORTH SEAL cruise, July 1981. Points not labeled indicate no BNL at that station.

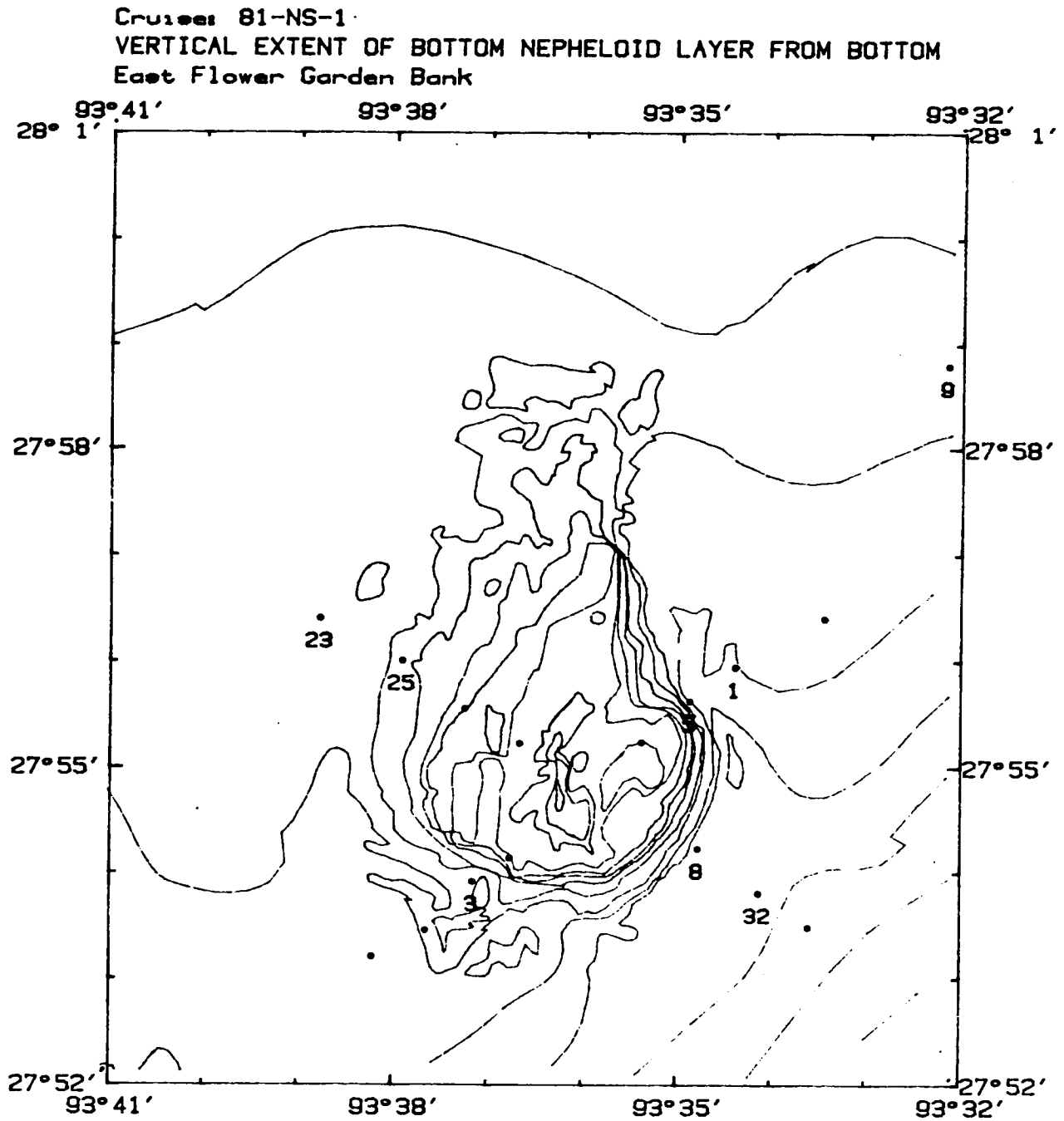


Figure IV-79. Vertical extent (metres) of BNL from bottom of EFG during NORTH SEAL cruise, July 1981. Points not labeled indicate no BNL at that station.

Cruise: 80-BS-1
 MINIMUM TRANSMISSIVITY OF BOTTOM NEPHELOID LAYER
 East and West Flower Garden Banks

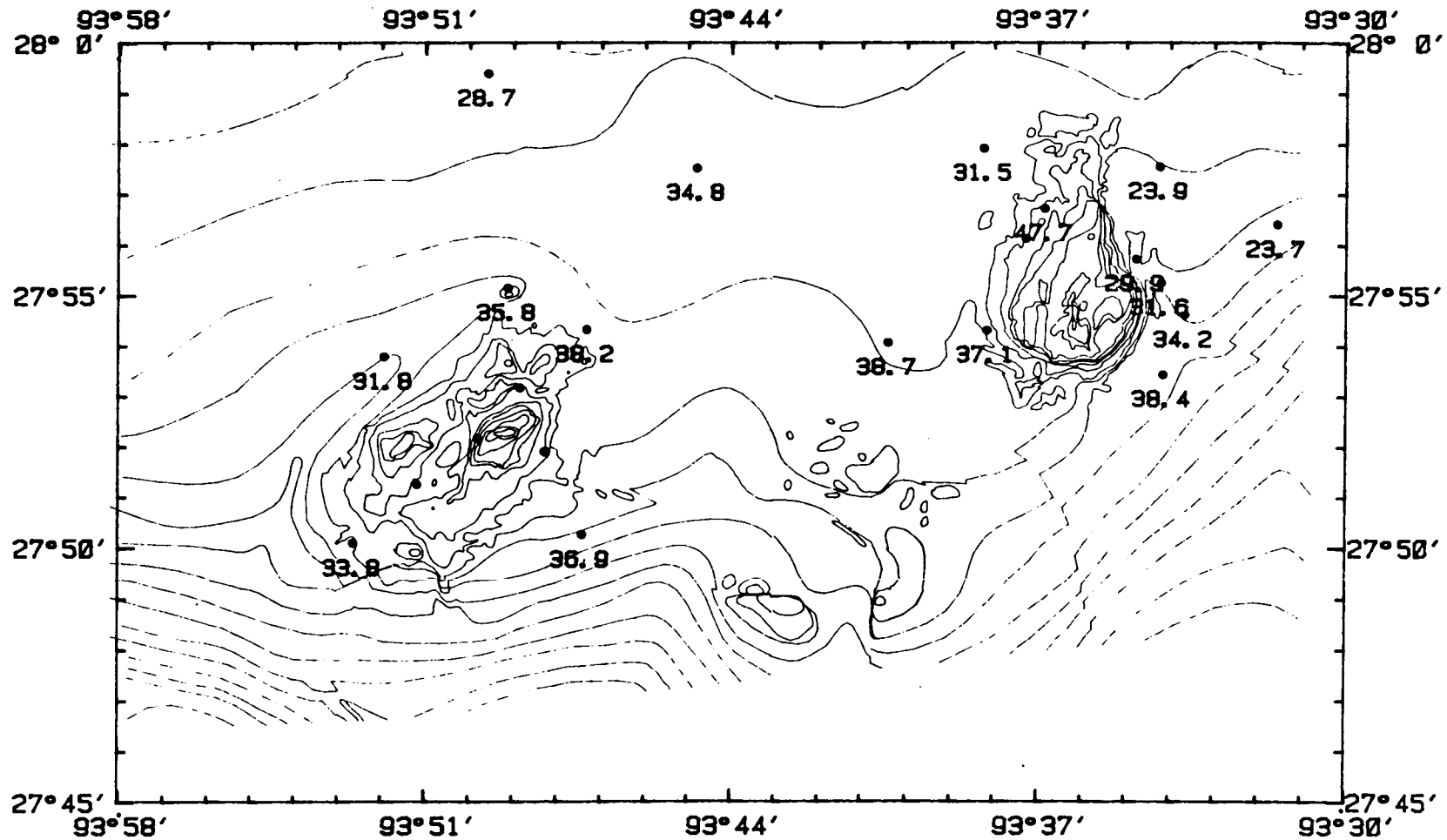


Figure IV-80. Minimum XMS (%/25 cm) of BNL during the BALTIC SEAL cruise, October 1980. Points not labeled indicate no BNL at that station.

Cruise: 81-G-3
 MINIMUM TRANSMISSIVITY OF BOTTOM NEPHELOID LAYER
 East and West Flower Garden Banks

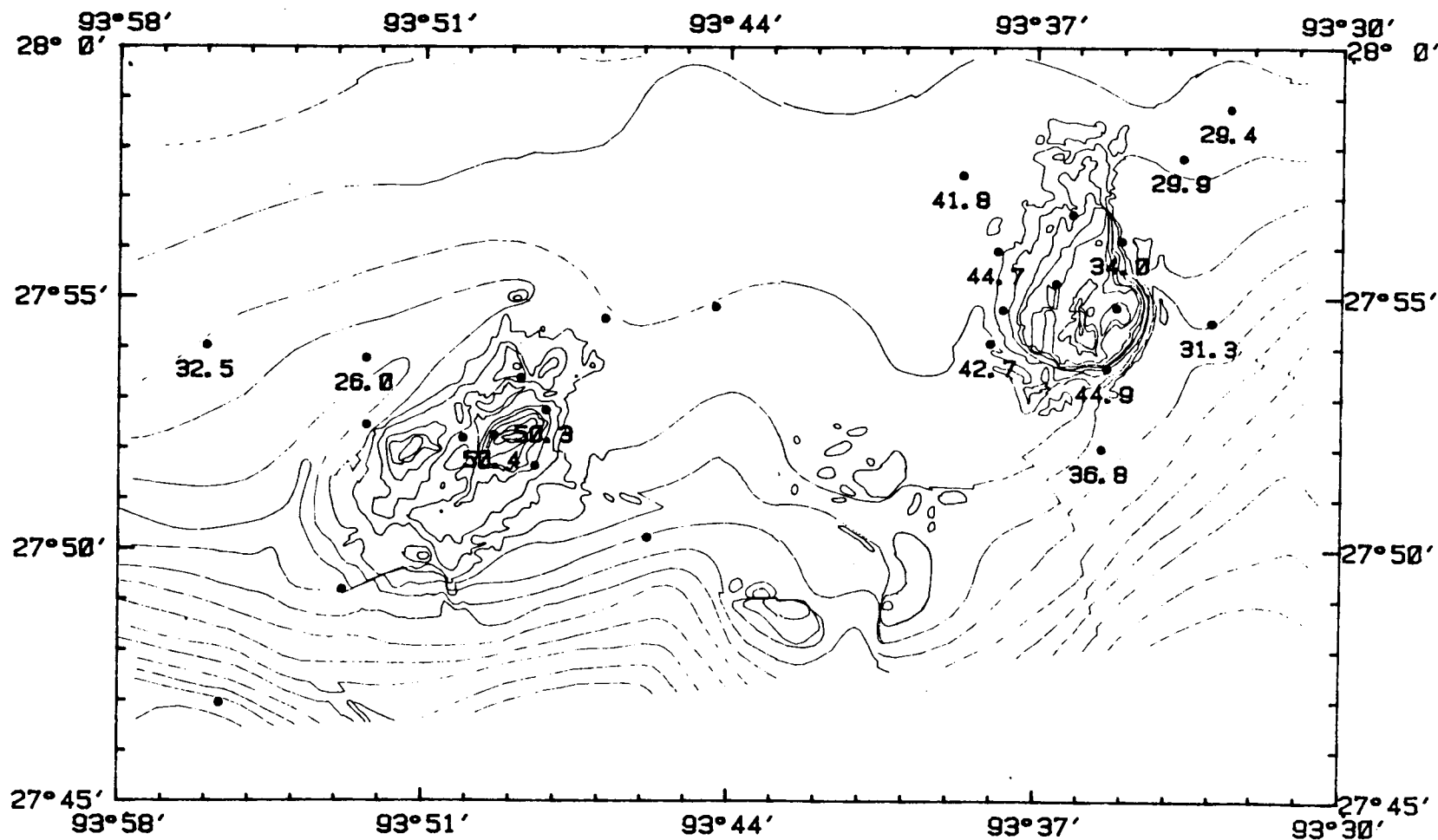


Figure IV-81. Minimum XMS (%/25 cm) of BNL during the GYRE cruise, March 1981. Points not labeled indicate no BNL at that station.

Cruise: 81-NS-1

MINIMUM TRANSMISSIVITY OF BOTTOM NEPHELOID LAYER

East and West Flower Garden Banks

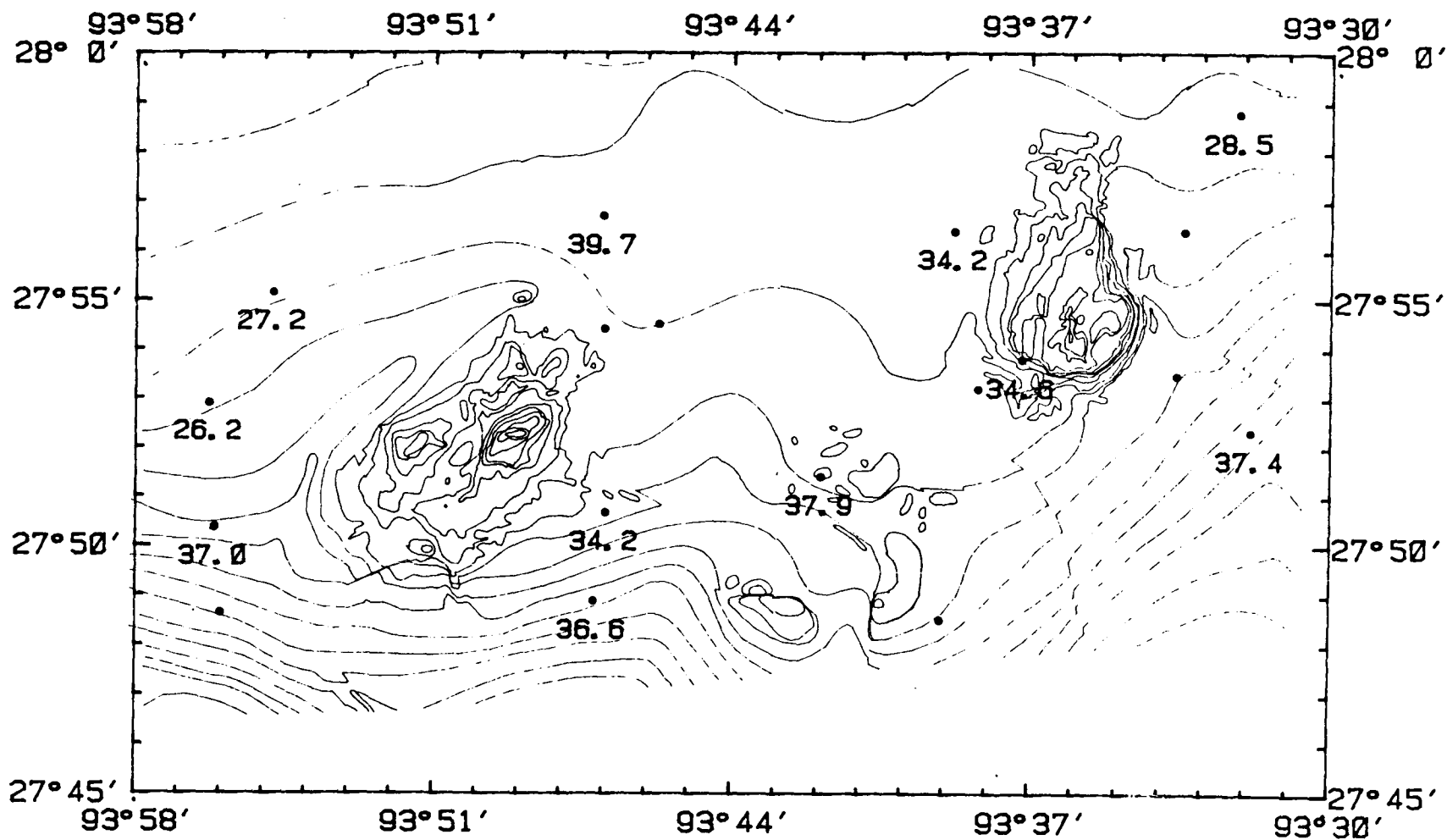


Figure IV-82. Minimum XMS (%/25 cm) of BNL during the NORTH SEAL cruise, July 1981. Points not labeled indicate no BNL at that station.

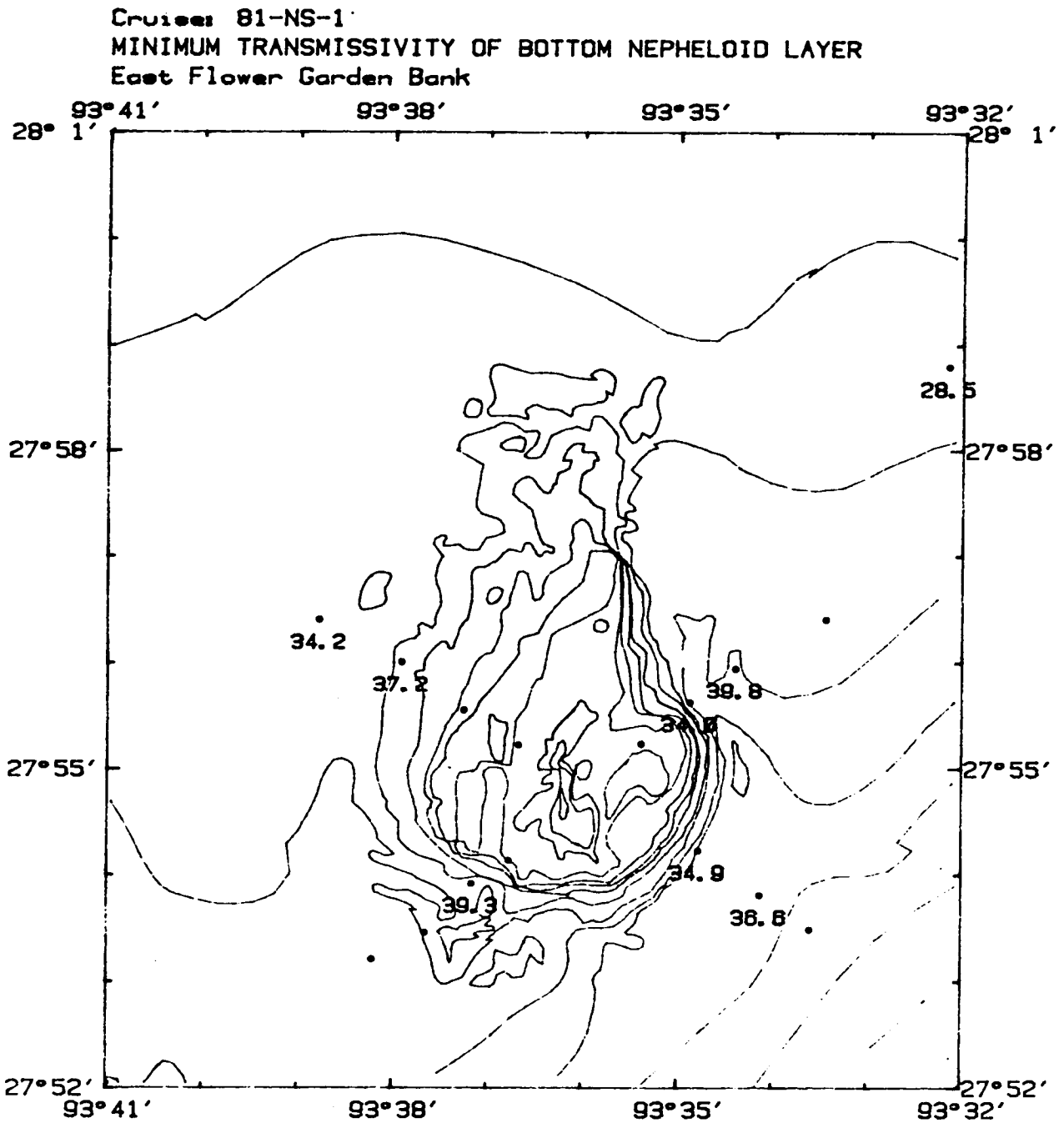


Figure IV-83. Minimum XMS (%/25 cm) of BNL at EFG during the NORTH SEAL cruise, July 1981. Points not labeled indicate no BNL at that station.

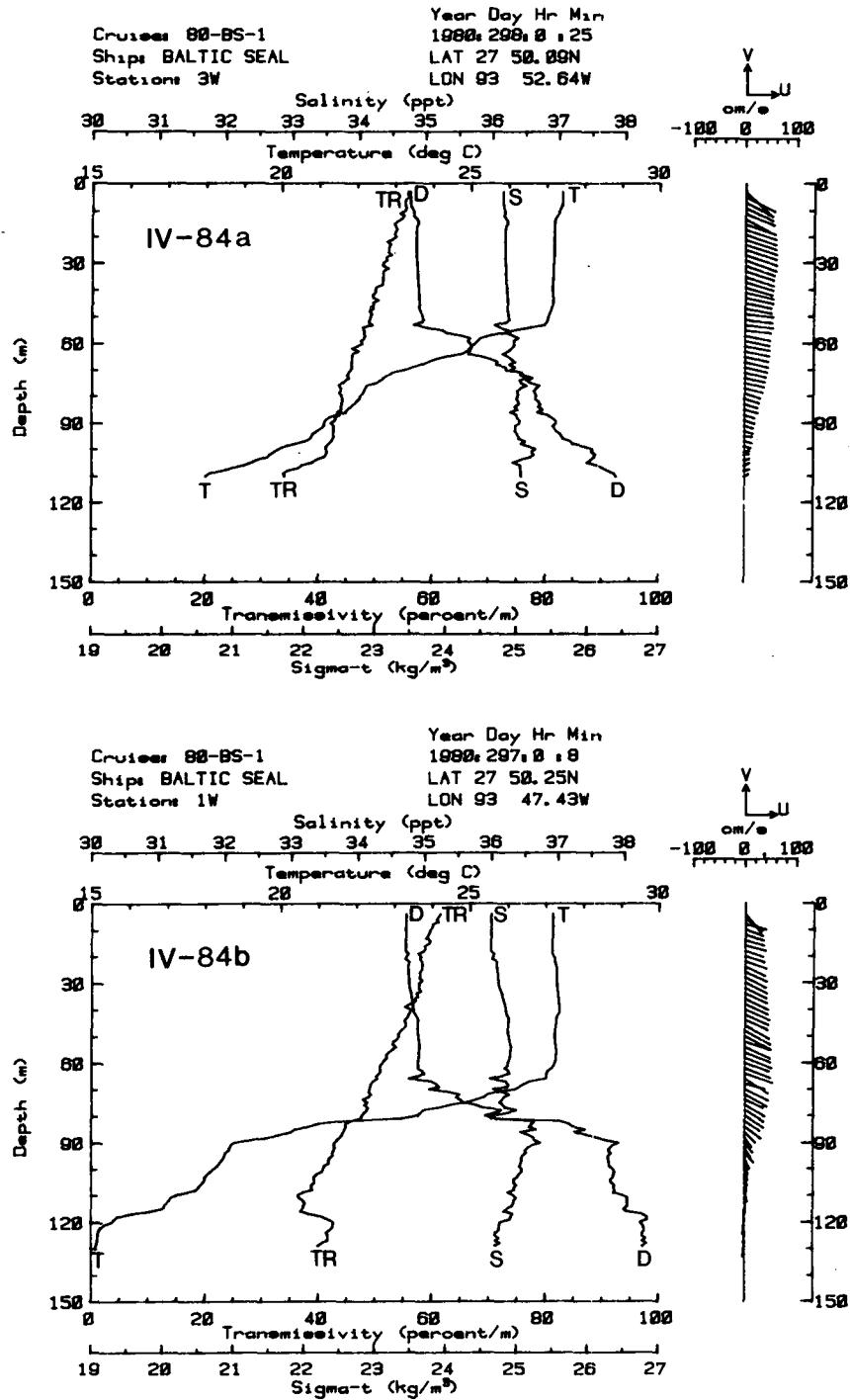


Figure IV-84. Plots of temperature (T), salinity (S), transmissivity (TR), and sigma-t (D) at WFG stations 1W and 3W, October 1980, showing minimum (IV-84a) and maximum (IV-84b) vertical extent of BNL in October. Note also the linear XMS decrease in a thin bottom layer (IV-84a).

Flower Garden Bank, do contain a very thin (1 m) and weak turbid layer. Although these thin turbid layers meet the criteria established for a BNL in terms of gradient, the minimum transmissivities observed are above 50.0% (the least turbid of all nepheloid layers of all cruises). Other than these two bank-top turbid layers, only two of the remaining ten stations near the West Flower Garden Bank have BNLs. By contrast, BNL's are found in the majority of East Flower Garden stations (9 of 13), with the 4 shallowest stations devoid of turbid water.

The general lack of BNL's atop the banks is due to the lack of fine sediment (silt and clay) there and because an advected near-bottom turbid layer cannot be transported up the bank against the pressure gradient (McGrail and Horne, 1981). The greater turbidity at the East Flower Garden Bank relative to that at the West Flower Garden Bank is a result of differences in the sedimentary facies surrounding the two banks: the East Flower Garden has a greater zone of fine terrigenous material or carbonate hash which can be more readily resuspended. The east side of the East Flower Garden is a prime area for fine particle resuspension; the majority of all very low XMS values (< 30%) are recorded in this area.

Types of BNL's

The shapes of the observed BNL have a variety of forms or combination of forms which provide clues to their origin and growth. The local formation of a BNL by bottom forces may produce a very thin turbid layer in which transmissivity rapidly decreases in a linear manner, as indicated by BALTIC SEAL Station 3W (Figure IV-84a), or a more extensive thick nepheloid layer like BALTIC SEAL Station 5E (Figure IV-65, above, p. 183) if the near-bottom turbulence has sufficient duration and intensity.

BNL's in areas where sand and coarser sediment form the substrate have probably been advected in from elsewhere and are often detached from the bottom by clearer water. Two examples of advected turbid layers are BALTIC SEAL Station 10E and NORTH SEAL Station 25 (Figure IV-85). The advected BNL at GYRE Station 1E (Figure IV-86) overlays a thin bottom zone of cold, relatively clean water with a sharp temperature gradient that inhibits bottom turbulent mixing.

A distinct block style of turbid water formation is usually related to a thick, well-mixed bottom zone of uniform temperature, salinity, and density, which is abruptly terminated at its upper surface by strong stratification in the water column. The steep thermocline at the upper limit of the block type nepheloid layer inhibits further upward mixing. The strength of the turbulent vortices in those cases is insufficient to overcome the buoyant forces in the thermocline, and upward mixing is terminated. This block-type of nepheloid layer occurs most often below the strongly stratified water column found in October. Stations 3E through 6E have block-type bottom layers and well mixed bottom zones. These are best seen at Stations 5E and 6E (Figure IV-65 and 66, above).

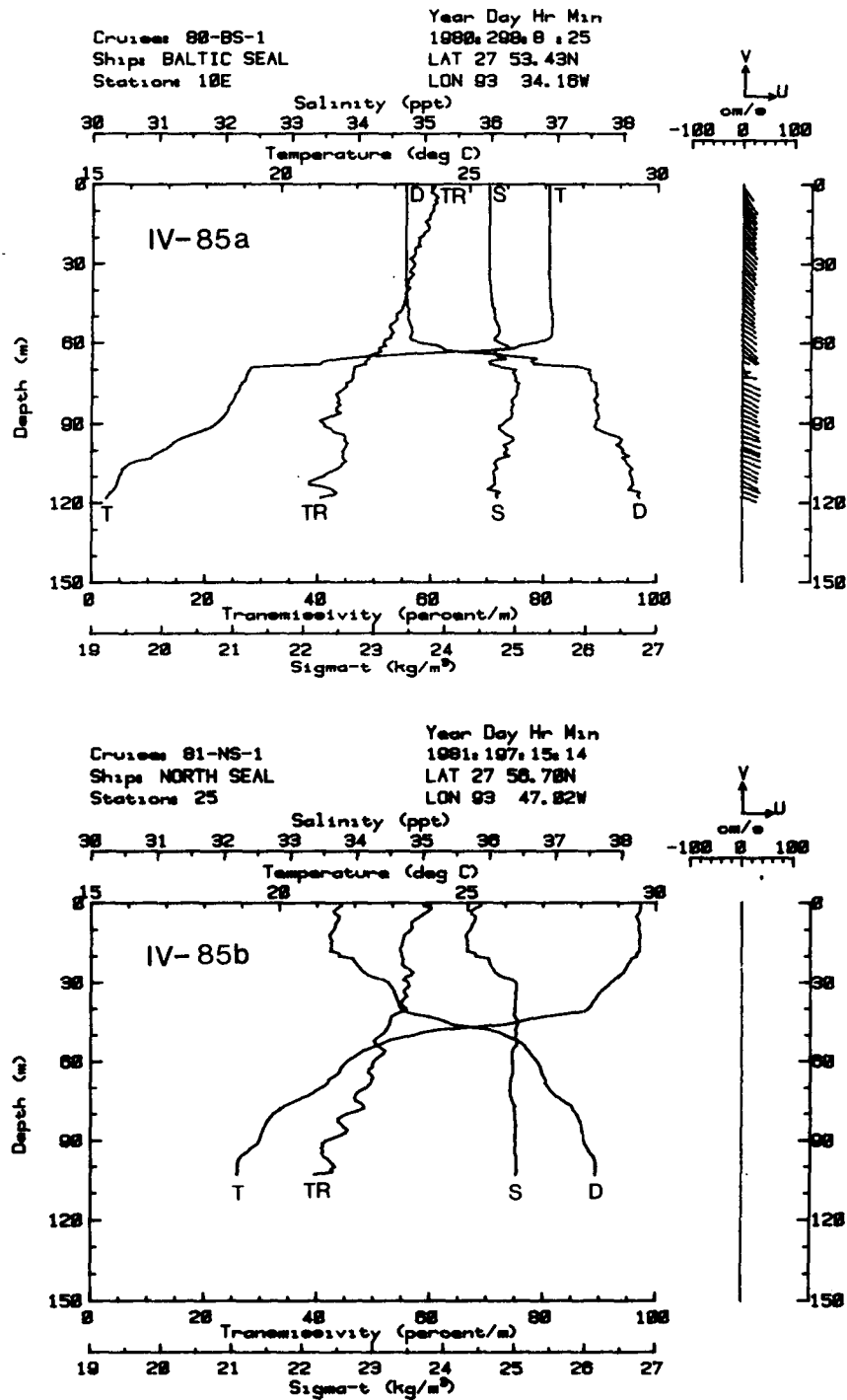


Figure IV-85. Plots of temperature (T), salinity (S), transmissivity (TR), and sigma-t (D) from EFG station 10E (October 1980) and WFG station 25 (July 1981) illustrating an advected turbid layer.

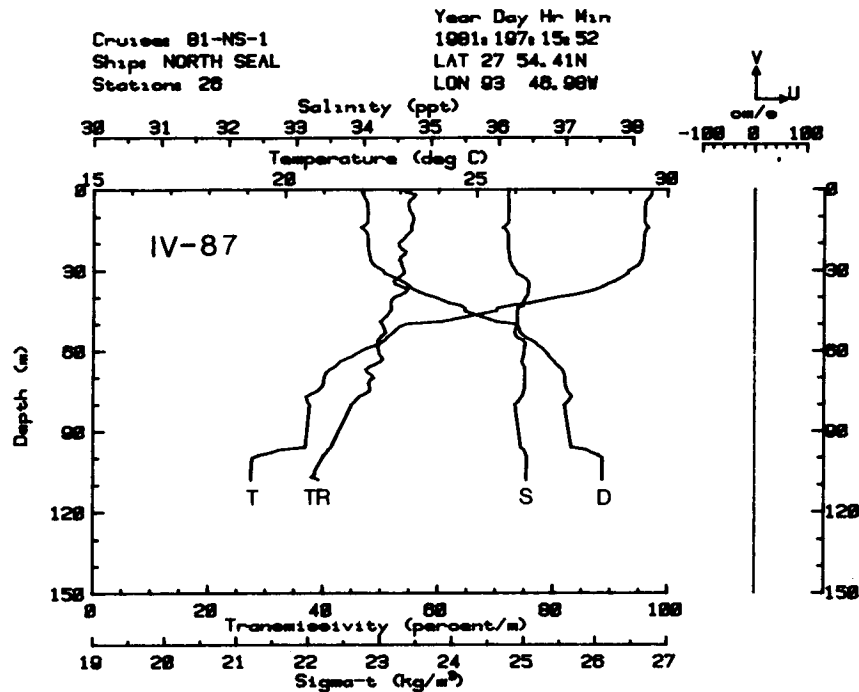
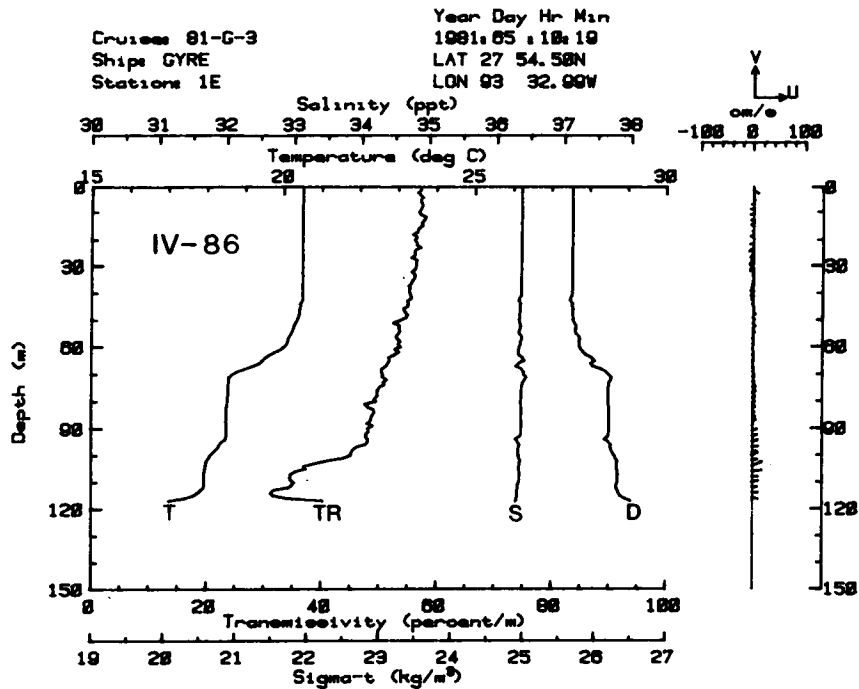


Figure IV-86. Plot of temperature (T), salinity (S), transmissivity (TR), and sigma-t (D) from EFG station 1E (March 1981) showing an advected BNL overlaying a thin bottom layer of cold clean water containing a sharp temperature decrease which inhibits bottom mixing.

Figure IV-87. Plot of temperature (T), salinity (S), transmissivity (TR), and sigma-t (D) from WFG station 26 (July 1981) showing a bottom mixed layer formation with no associated BNL.

BNL's and bottom mixed layers are not always directly related. The bottom mixed layers found at GYRE Station 17S (Figure IV-74b, above) and NORTH SEAL Station 26 (Figure IV-87) have no BNL associated with them, probably because the rather coarse material underlying these stations could not be suspended.

BOUNDARY LAYER DYNAMICS

Introduction

The purpose of bottom boundary layer (BBL) studies is to investigate the resuspension of bottom sediments and subsequent sediment movement both horizontally and vertically up into the water column. Hydrographic stations determine the density structure of the water column, and current meters determine flow within a coarse time scale. These factors influence the occurrence of suspended matter, but they do not really explain the dynamics of the suspension and diffusion of sediment. To this end, dye emission experiments were carried out on two submersible cruises to the East and West Flower Garden Banks, in October 1979 and October 1980.

Dye experiments were conducted at six locations during 1979 and at five locations during 1980. Some interesting insights into the bottom boundary layer can be obtained simply from watching the videotapes of these experiments and performing a few rough calculations of flow rates at different depths. Non-quantitative evaluation of factors such as flow variability, vertical and angular current shear, and intensity of diffusion is easily accomplished. This report includes comments on these values and discussion of additional techniques (which are currently underway) for analyzing these data.

The quantification of dye pulses released at different depths in the bottom boundary layer can provide information about the diffusion, current shear, and bottom stresses. By observing the expansion of the dye pulse in time, one can determine both vertical and horizontal diffusivity. Mean velocities, velocity fluctuation, shear, and spectra can be determined from the speed at which the pulse moves. From these parameters bottom stresses and variability of this stress can be determined.

The exact relationship of these parameters to each other depends on such factors as the density structure of the water column, the amount of suspended material in the column, and the bottom composition and roughness. Digitization of the video tapes and a substantial amount of computerized data manipulation are necessary for calculation of most of the parameters. These are planned for a future report. However, an initial examination of the data can provide some insight into what is happening in the BBL around the East and West Flower Garden Banks.

Factors Affecting Boundary Layer Dynamics

Currents moving across the bottom transfer momentum to the bottom as tangential stress. The intensity of this stress depends on the mean flow as well as factors like the history of the flow, superposition of waves on the mean flow, bottom composition, structure of the water column, and amount of suspended sediment. Resuspension of sediment requires that the stress exerted by the water flowing over the bottom overcome the shear strength of the bottom sediment. Once stress is adequate to resuspend sediment in the lower portion of the water column, other factors determine the movement of the sediment within the water column. Suspended sediment may be advected or diffused horizontally and vertically.

The height to which sediment is moved in the water column and the length of time it remains in suspension depend on four factors: 1) the characteristics of the sediment (weight, shape, and tendency to flocculate); 2) the intensity of the turbulence; 3) the vertical component of current; and 4) the stratification of the water column. Normally, lighter water overlies denser bottom water containing suspended sediment. The density gradient between these two water types is often very sharp. Turbulence randomly forces parcels of bottom water from the lower layer into the upper layer. Because this bottom water parcel is then surrounded by lighter water, it tends to sink back down. In this way, sediment-laden bottom waters are prevented from entering the lighter, clearer water above, except momentarily. If the turbulence is strong, the bottom water is mixed with the lower portion of the less dense water above, thus creating a thicker (though less dense) mixed layer beneath the density gradient. The nepheloid layer (the bottom layer of turbid water) is usually not thicker than the mixed layer below a strong density gradient.

The parameters governing sediment movement into and within the water column may be classified in three ways:

- 1) characteristics of the sediment: how easily is the sediment resuspended and how much energy is required to keep it in suspension?
- 2) characteristics of forces in the water column: how much stress can the water exert on the bottom, and how fast can the water move the suspended material into another area?
- 3) interactions between the water column and suspended sediment: how does sediment in the water column alter the stability of the column and the turbulence? how does the shape of the bottom affect turbulence and flow?

Parameters of the second type have been determined by using data from dye experiments and the accompanying water column work. However, these measurements are influenced by bottom interactions which can not be separated out. For example, diffusion computed from the expansion of a dye pulse reflects turbulence caused by flow over a particular bottom with a certain amount and kind of sediment entrained in the water. Because the Flower Garden area has a variety of bottom sediments and current regimes (including tidal fluctuations and inertial

oscillations) and because of the seasonal variations in the structure of the water column, experiments at several locations and times would be required to completely describe the BBL in this area. Enough experiments have been performed to show some of the variations in the BBL that can occur around the bank.

Known Relationships Within the BBL

Some simple relationships pertinent to these experiments have long been known to hold within the BBL. In general, the bottom boundary layer of the ocean is subject to viscous forces, Reynolds stresses, and the Coriolis force. Viscous forces are almost always unimportant and dominate only in a very thin (a few millimetres) near-bottom layer when the bottom is smooth and the currents slow. Often the viscous sublayer does not exist in the ocean, since turbulence effects dominate even very near the bottom. The boundary layer is usually considered bounded by the height at which the velocity reaches 98% of the free stream velocity.

When the upper portion of the BBL is dominated by the Coriolis force, flow responds in the classical Ekman sense. In the near-bottom layer (below the Ekman layer) where viscous forces are dominated by Reynolds stresses, the stress in the water column is nearly constant. This is the inertial sublayer where the mean velocity profile fits the logarithmic equation

$$U/u_* = 1/K [\ln(z/z_0)] \quad (21)$$

where

U = measured velocity at depth z

$u_* = \sqrt{\tau/\rho}$ is frictional velocity (τ is bottom stress and ρ is density)

K = the von Karman coefficient

z_0 = the characteristic length scale associated with boundary roughness, considered to be the distance from bottom at which velocity goes to 0.

This logarithmic profile appears to extend above the constant stress layer into the Ekman layer.

One would expect flow in the logarithmic layer to be unidirectional with angular veering occurring in the region of a strong density gradient above the log layer in the turbulent Ekman layer. The log layer would be expected to extend upward to include all of the emitters in the experiments, except possibly the fourth emitter (at 3 m height). A calculated thickness of the log layer can be expected to be approximately $.1 (u_*/f)$, where f is the Coriolis force (Tochko, 1978). On a typical area of the shelf, the log layer might be 10 m thick. Angular shear would be expected to be greatest above the log layer (Deardorff, 1970).

In theory, therefore, one wouldn't expect much angular shear to appear in the dye experiments under steady, homogeneous conditions.

However, other experiments using current meters have discovered angular shear near the bottom (Weatherly, 1971). In cases where strong angular shear is seen, the log law equations probably should not be used to determine the bottom stresses or the eddy diffusivity (both of which determine the diffusion of the suspended sediment in the water column).

Techniques for Determining Bottom Stress and Diffusivity

If the conditions of steady flow are met, bottom stress can be determined by using data from dye experiments. Bottom stress can be computed from dye data in three ways. The first method is to use log law equations to compute u_* from a mean current at two depths. A second technique uses Reynolds stresses obtained from the dye fluctuations in the constant stress layer. The third method begins by using measurements of the dispersion of dye pulses at one or more depths to compute eddy diffusivity (K_e). In a log layer, the relationship between the eddy viscosity (ν) and stress (stress is constant in a log layer) is $\nu = u_*z$. Therefore, u_* may be computed from the eddy diffusivity determined at a depth z from the previous equation, if it is assumed that $K_e = \nu$. This latter assumption is thought to be valid under neutrally stable conditions. If von Karman's constant is known (it should be .4 in clear water, but is less in turbid water), then the eddy diffusivity determined by this technique would be expected to be the same as that determined by the expansion of the dye pulses.

It has been empirically determined (Wimbush and Munk, 1968) that

$$z_0 = \frac{d}{30} \quad \text{if } d > \frac{3\nu}{u_*} \quad (22)$$

where d = length of scale for the roughness (e.g., size of algal nodules in the Algal Nodule Zone)

and z_0 = the distance from the bottom where velocity goes to zero.

So in a constant stress layer one can either (a) use z_0 from empirical measurements and apply the log law equations at one depth, or (b) use velocity at different heights so that z_0 , u_* , and stress can be calculated without recourse to the length scale, d . However, the log law calculation would not be appropriate if von Karman's coefficient varies, or if several length scales are involved, or if the motion is unsteady.

Fluctuations in velocity at a particular depth determine the Reynolds stress at that depth. Reynolds stress at each depth can be calculated by

$$\tau = \rho u' w' \quad (23)$$

where

u' is the velocity fluctuation in the direction of flow

and

w' is vertical direction.

If conditions for a constant stress layer hold, then this value should be the same at each emitter. Otherwise a stress profile can be established. Reynolds stresses often show a great deal of variability (Heathershaw and Simpson, 1978). This variability of stress means that conditions may be erratically conducive to resuspension.

The quadratic law

$$\tau = C_D \rho U_D^2 = \rho U_*^2 \quad (24)$$

where

C_D is the frictional drag coefficient at depth D

and

U_D is the velocity at that depth,

is an attempt to determine bottom stress strictly on the basis of the mean current at some depth from the bottom. Thus the intermittently larger stresses which might cause resuspension can not be calculated from this technique. The friction coefficient can be calculated from the log layer equations at a particular depth by

$$C_D = (u_*/U_D)^2. \quad (25)$$

C_D (calculated from dye studies as a constant or calculated as a function of mean velocity) can be used with mean speeds from current meters at that same place to provide some indication of stresses over a long period. This same technique can be used at times of dye emitter malfunction to obtain stress from one emitter. C_D varies with bottom roughness, mean speed, history of the flow density structure, and velocity shear, so errors occur in the stress calculated using a constant C_D . C_D calculated from the log layer equations can be quite variable. This implies a variability in bottom stresses which is lost when using the quadratic law with a constant C_D to determine stress. However, for a first approximation, the frictional drag coefficient calculated from the dye experiment may be used in conjunction with mean currents obtained from current meters to determine a bottom stress during times when dye studies were not made.

Under certain conditions, frictional velocity (and hence stress) can also be estimated from velocity spectra in the log layer. This method uses the frictional velocity equation

$$u_* = \left[\frac{2\pi Kz}{v} \right]^{1/3} \left[\frac{S(n)n}{k} \right]^{5/3} \quad (26)$$

where

k is a universal constant

K is the von Karman constant

$S(n)$ is the wave number spectrum

and

n is the wave number

(Wimbush and Munk, 1970). This equation may be used if (1) effects of stratification are negligible, and (2) Taylor's frozen wave hypothesis is assumed valid, and (3) the frequency of n is in the inertial subrange

$$1/z \ll (2\pi/v)n \ll (U_*^3/kzv)^{1/4}. \quad (27)$$

Dye Emitter Apparatus

The dye emitter apparatus used in the bottom boundary layer experiments was redesigned for the October 1979 submersible cruise and then modified again for the October 1980 submersible cruise. The original emitter used in a previous study (Bright and Rezak, 1978b) released a continuous stream of dye and was mounted on a heavy and unwieldy tripod which required a crane for deployment. The most recent version emitted discrete pulses of dye at a predetermined rate at four heights above the bottom and was easily deployed by hand from the side of the ship.

The major advance in the experiment is the changed design of the emitter itself. The dye emitter contains a timing circuit which can be preset to trigger the pulsing mechanism at a particular timing interval. This interval was set between 4 seconds and 10 seconds. When all emitters are set for the same interval and turned on simultaneously, pulses will be emitted from each emitter at the same time. This allows the observer to readily determine the current speed at the depths of each emitter by observing the speed at which each pulse moves. Most commonly, the higher pulses move faster than the lower pulses, indicating vertical shear in the current, although flow which is constant with depth is also observed. Even though the size of the pulses varies from emitter to emitter (making it difficult to visualize which pulses are most rapidly diffused), these data can be extracted from video tapes as the data are quantitized.

The pulsing mechanism consists of an electromagnet (which is turned on and off by the timing circuit), a diaphragm, and a battery pack (see Figure IV-88). The diaphragm is a piece of rubber stretched tightly over one end of the emitter. A metal disk is attached to the outside of the diaphragm directly over the electromagnet. When the electromagnet is activated, the metal disk is pulled toward the electromagnet, bringing the diaphragm with it and forcing a small volume of the fluorescent dye through the aperture at the bottom of the emitter

DYE EMITTER

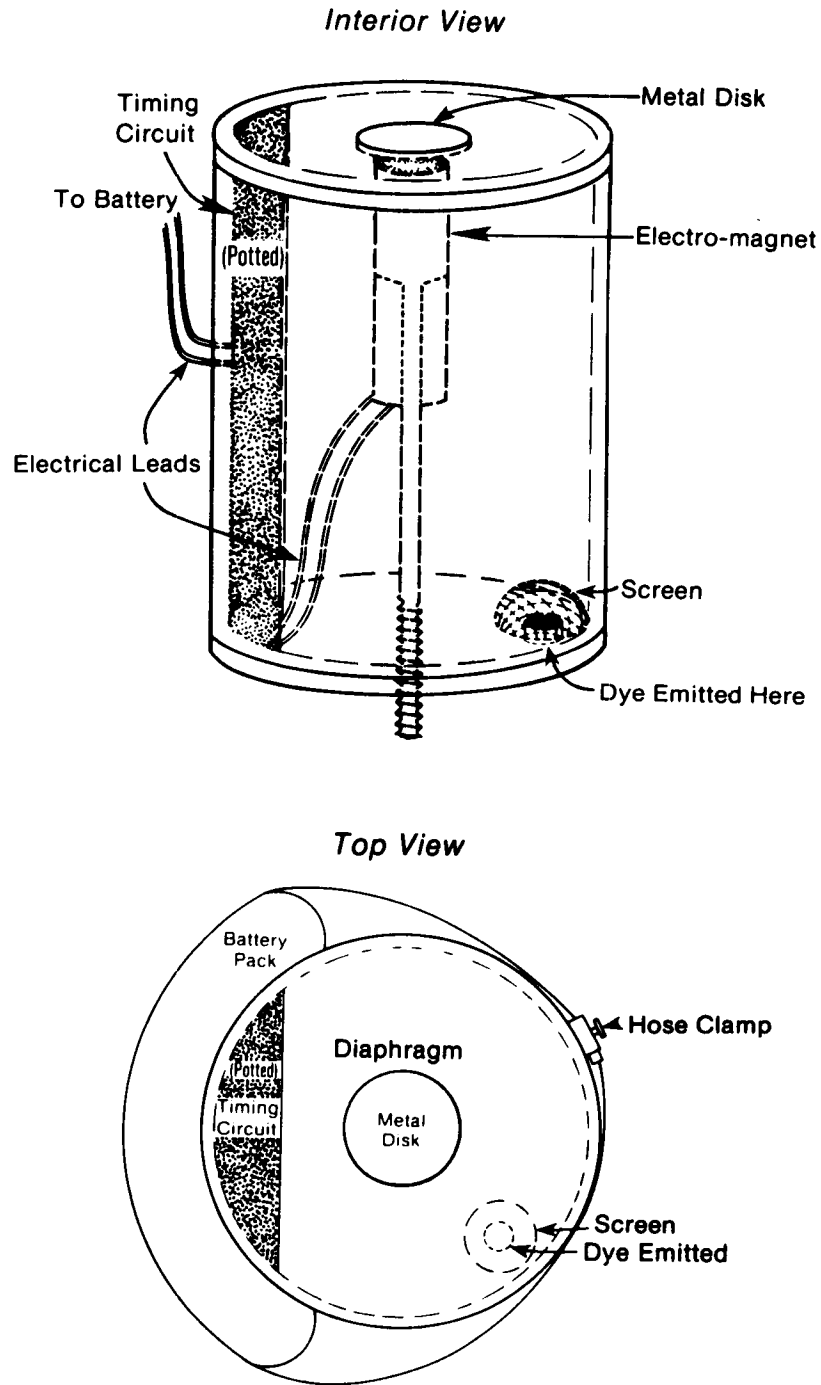


Figure IV-88. Diagrammatic representation of dye emitter apparatus used in October 1980 boundary layer experiments at the Flower Garden Banks.

DYE EXPERIMENT MOORING

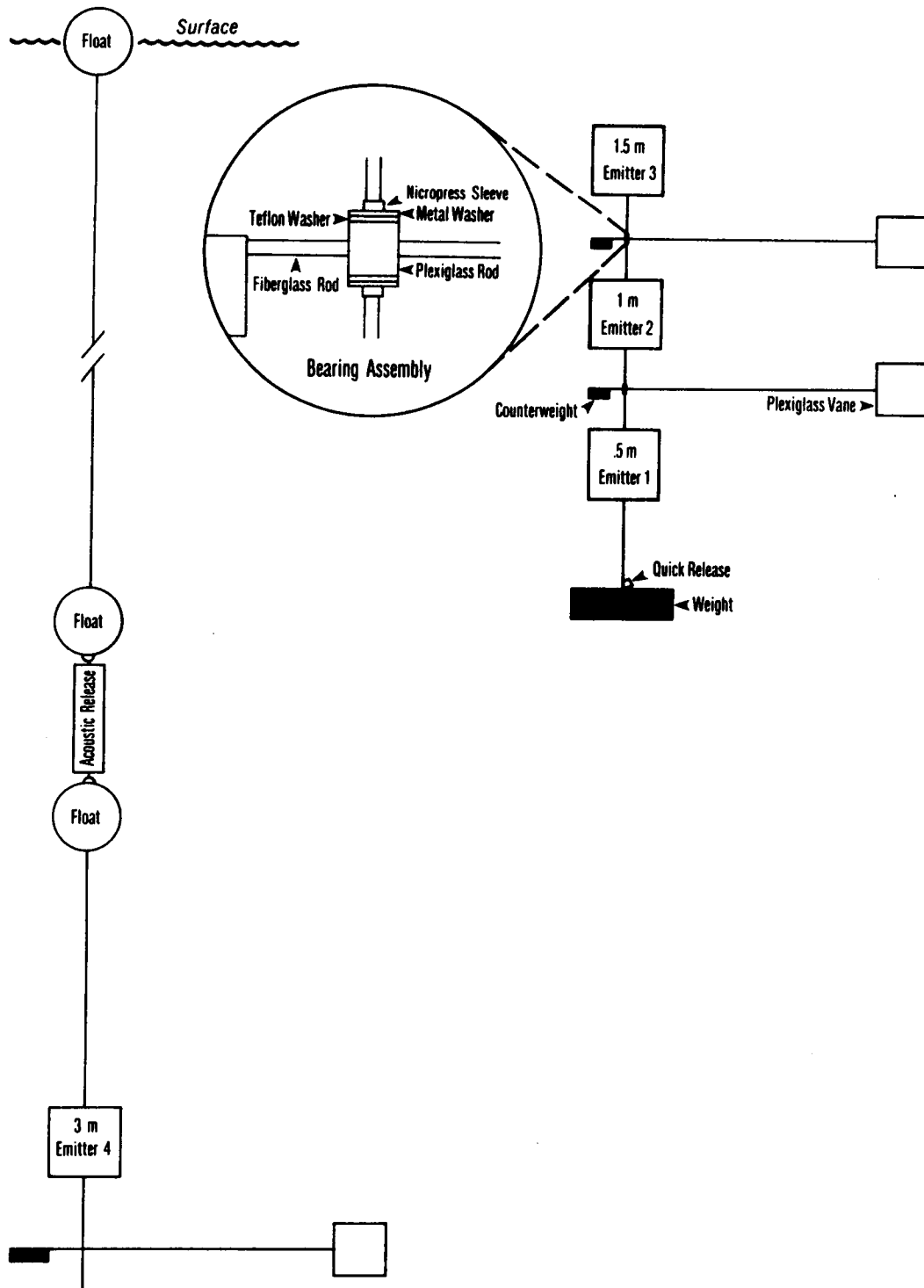


Figure IV-89. Diagrammatic representation of tautline mooring on which vanes and dye emitters were assembled for 1979 and 1980 boundary layer experiments at the Flower Garden Banks.

and into the water column. This pulse flows along a vane oriented with the flow and marked in 10 cm increments for scaling. The vane consists of a 1.2 m rod (a fishing rod blank) with a plexiglass fin at the end. The vane is balanced to stream horizontally in seawater and pivots on a teflon bearing to assure rapid response to changes in current direction.

The vanes and emitters are assembled in a taut line mooring with three emitters in the lower 1.5 m and one emitter at 3 m from the bottom (Figure IV-89). The emitters are kept tautly upright by a buoy above the upper emitter. All of the experimental apparatus are recoverable except for the bottom weight used to keep the buoy and emitters on the bottom. The weight is attached below the lower emitter by a device which allows quick release by the submersible crew at the completion of the experiment. This allows the buoy to float all of the emitters and vanes to the surface where they are recovered.

The initial deployment of the dye emission apparatus requires two additional buoys (for a total of three) and an acoustic release. One buoy is required as a surface marker for the site and is attached to the emitters by a line. The submersible follows this line down to the experiment for filming and observation of the dye pulses. This surface buoy is moved (sometimes violently) by surface waves and currents. If left attached to the experimental apparatus, the buoy would cause jerking of the emitters, which would force the dye emission at other than the pulsing times. The action of the surface buoy has even been observed to drag the emitter apparatus along the bottom, so the surface buoy must be disengaged from the dye emitters to avoid contamination of the experiments by surface motion. An acoustic release (with a support buoy) is attached above the lowest buoy (which maintains tension in the taut line moorings). When the submersible is in position for observation, the acoustic release is activated and the support buoy carries it to the surface, thereby severing the link between surface and experiment.

Deployment of the apparatus is accomplished from the side of the ship. A line 10 m longer than the bottom depth is attached to the surface buoy at one end and to the acoustic release support buoy at the other. The surface buoy is carried away from the ship by the Dunlap inflatable boat until the line is fully played out (to prevent tangling on deployment). When the ship is over the proposed dive site, the experimental apparatus is attached to the mooring below the acoustic release and allowed to free-fall to the bottom. The submersible is then launched near the surface buoy and descends to the experiment site.

Since the support ship cannot remain directly over the submersible (because of the danger to the submersible in case of an uncontrolled emergency ascent), the profiles taken in support of the dye experiments are always at some short distance from the experimental site. Because of the rapid changes in depth near the banks, this usually means these profiles are at a different depth. Often the dye pulses exhibited meandering in the vertical, undulating upwards and downwards. This meandering probably indicates a variability of the bottom stress as

higher momentum fluid from further up from the bottom moves downwards, imparting an increased stress on the bottom. However, the significance of this meandering on bottom stress can only be determined by a careful quantitative analysis of the video tapes.

Analysis of Video Tapes

1979 Dives

During the October 1979 submersible cruise, BBL experiments were conducted during six dives around the East and West Flower Garden banks (Figure IV-90) at depths of from 90-101 m. At these depths, visibility is often poor because of the suspended matter in the water, i.e., the nepheloid layer. Since the nepheloid layer was itself the phenomenon under investigation in these experiments, some experimental encumbrances were encountered on several 1979 dives. (Note: Shallower sites were selected for 1980 dye experiments.)

Water column data were taken in support of the experiment by separate lowerings of the Plessy 9006 STD, transmissometer, and profiling current meter. The Martek transmissometer (XMS) used during 1979 measured transmissivity per metre based on the attenuation of white light (resolution = 1%). To allow hand lowering, the transmissometer and cable were lightweight. This presented problems when the ship was drifting quickly since the transmissometer would string out horizontally rather than sinking to the bottom. To overcome this, the transmissometer sometimes was lowered at a faster rate than that required for close vertical spacing of data points. Spacing of data points varied from 3 to 10 m. Because of this coarse spacing near the bottom, the nepheloid layer often does not show in the transmissivity profile. If the transmissivity profile shows a great difference between the bottom data point and the point immediately above it, and if the temperature profile exhibits a bottom mixed layer, then it is very likely that a nepheloid layer exists but is masked by the coarse sample spacing.

A HydroProducts profiling current meter with Savonius Rotor and vane was used for the profiles. Measurements were made at 5 m intervals by visually averaging the speed and direction over a 30-second period. Direction and intensity of currents (as measured by the dye studies) varied substantially within a single experiment as well as between experiments.

At three experiment sites the results were reasonably easy to quantify.

Divesite 1979-9

Divesite 1979-9 was located on the west side of the East Flower Garden Bank in 90 m of water near current meter site 2. The bottom here consists of a thin covering of mud over a solid bottom. This mud was easily resuspended in the water column, as was apparent from the large cloud of material suspended when the submersible settled on the

1979 Dye Emitter Stations

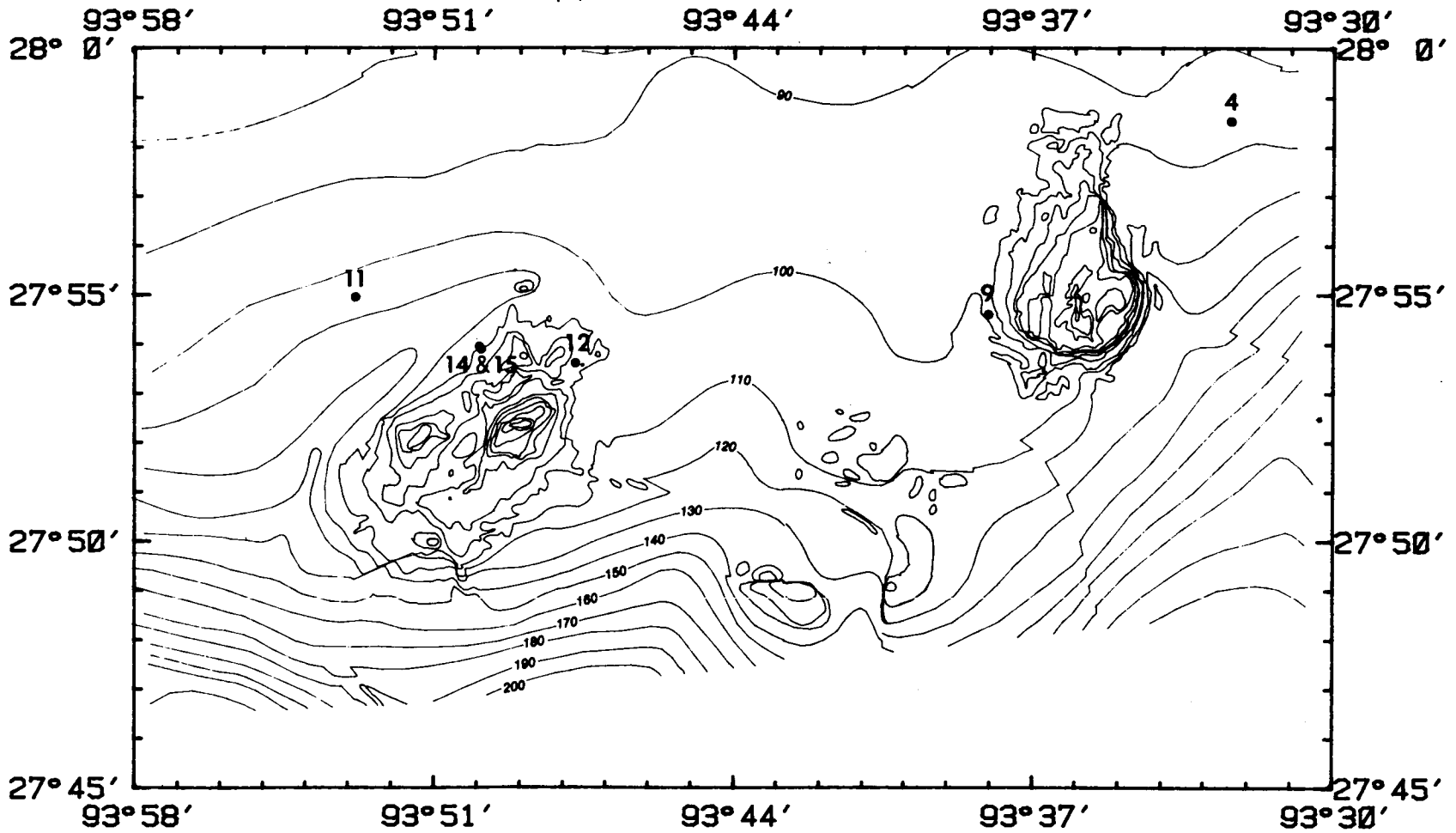


Figure IV-90. Location of October 1979 submersible dive stations where dye emission experiments were made.

bottom at the beginning of the experiment. At the completion of this dive a twelve-hour time series of XBT, transmissivity, and current meter profiles was taken near the experiment site at a depth of 105 m. The thermocline occurred between 60-70 m, with a bottom mixed layer at 100-105 m. Transmissivity profiles, however, did not indicate a bottom mixed layer with respect to suspended sediment, although transmissivity decreased sharply from 90 m to the bottom. Current profiles generally show flow becoming more southerly near the bottom. The dye emission studies were difficult to observe because of poor visibility (bottom transmissivity of 52%/m). Dye generally flowed at about 170°.

Divesite 1979-12

Divesite 1979-12 was on the northeast corner of the West Flower Garden Bank in 98 m of water. This dive occurred at a time of almost stagnant flow; velocities from the dye measurements were on the order of 1 cm/sec and less. At these velocities direction of flow varied greatly with depth (75° over 1 m).

Initially, flow was slow in the direction of 285° at the third vane, becoming more to the left (to 210°) at the bottom. While maintaining a counterclockwise shearing from top to bottom, all flow gradually shifted more to the south so that an hour later the flow ranged from 200° at 1.5 m height above the bottom to 170° at .30 m height above the bottom. During this very low velocity period, diffusion contributed greatly to dispersion of dye since pulses between two adjacent emitters merged during the time it took a pulse to travel 10 cm.

A profile in this area shows a 10 m isothermal BBL, but although transmissivity decreased in the bottom 15-20 m, no well-mixed nepheloid layer can be detected on the transmissivity plots. The secondary thermocline at 80 m is quite sharp with a gradient of approximately 1°C/m for about 2.5 m. This sharp gradient should provide an upward limit of diffusion under the observed low energy condition.

Divesite 1979-14

Divesite 1979-14 was located on the northwest portion of the West Flower Garden Bank at 98 m depth. The transmissivity profile again failed to show the bottom mixed layer, although a decrease in transmissivity occurs near the bottom. Visibility at site 14 was fairly good (7 m visibility downslope and 15 m upslope), with submersible-recorded transmissivity of 66%/m of white light.

The dye pulses indicate an average current of between 10 cm/sec and 12 cm/sec. The current at 70 cm was generally 1 to 3 cm/sec faster than the current at 15 cm from the bottom. Angular shearing was apparent, with the direction of flow at the bottom emitter 5° to 10° to the left of the third emitter (1.5 m from bottom).

Vertical diffusion initially seemed to be slight, but by the end of the dive vertical diffusion had increased and the pulses from the middle and the third emitter merged within 3 m of leaving the emitters.

Vertical meandering became more pronounced later in the dive. Initially, flow was at about 50° , but gradually rotated clockwise to about 80° . The directional difference between the flow at different depths decreased as flow became more easterly.

1980 Dives

Profiles taken during the 1980 submersible cruise were made using the PHISH system. In general, the PHISH profiles stop at 2 m from the bottom. Since data were acquired several times in each metre, the transmissivity profiles of the 1980 submersible cruise are more accurate than the 1979 profiles, providing a better indication of small-scale changes and the actual transmissivity. The electromagnetic current meter also provided more accurate current measurements than the older Savonius Rotor meter. Another improvement was that dive sites were selected at shallower depths in 1980 to insure greater visibility than in 1979. A problematical change is that two different transmissometers were used in 1980. The PHISH transmissometer is a Sea Tech 25 cm pathlength 600 nm wavelength system, and the transmissometer on the submersible was a Martek XMS white light instrument (like the one used for the 1979 profiles), so direct comparison between the two is not possible. Locations of the five 1980 divesites are shown in Figure IV-91.

Divesite 1980-14

The first experiment in 1980 (divesite 1980-14) was located near the site of current meter mooring 2 on the southwest flank of the East Flower Garden at 79 m depth. PHISH profiles were not made on this dive due to malfunction on this first use of the PHISH system. Temperature profiles from XBT's indicated that the thermocline began near 50 m and extended to a well mixed layer 5-10 m above the bottom. The temperature gradient above the BBL varied between $.25^\circ\text{C}/\text{m}$ to $1.5^\circ\text{C}/\text{m}$ at different locations and times around the dive site. This gradient provides a cap for vertical movement through the water column. The XBT's were all taken in water shallower than the dye experiment site. From the temperature profiles, one would expect a well mixed BBL (i.e., stably stratified) with likelihood of a logarithmic profile of the current.

Flow during dive 1980-14 was initially logarithmic, decreasing from 17 cm/sec at 172 cm to 14.5 cm/sec at 32 cm from the bottom. Flow showed no angular shear. Later, current speed decreased to 5 cm/sec and angular shear began to develop. The flow at the bottom meter was shifted 5° - 10° to the west of the southward flow at the third meter (1.72 m from bottom). Currents slowed as the direction shifted from south to west-southwest (240°). Stagnation of the flow was most noticeable at the lowest emitter (30 cm). The fourth emitter (3 m from bottom) reversed direction and became a slow northerly flow. Eventually all flow became nearly stagnant, with just enough movement to differentiate the angular shear between emitters. Flow at the fourth emitter was to the north, then formed an arc and circled back around the submersible, descending toward the bottom as it moved

1980 Dye Emitter Stations

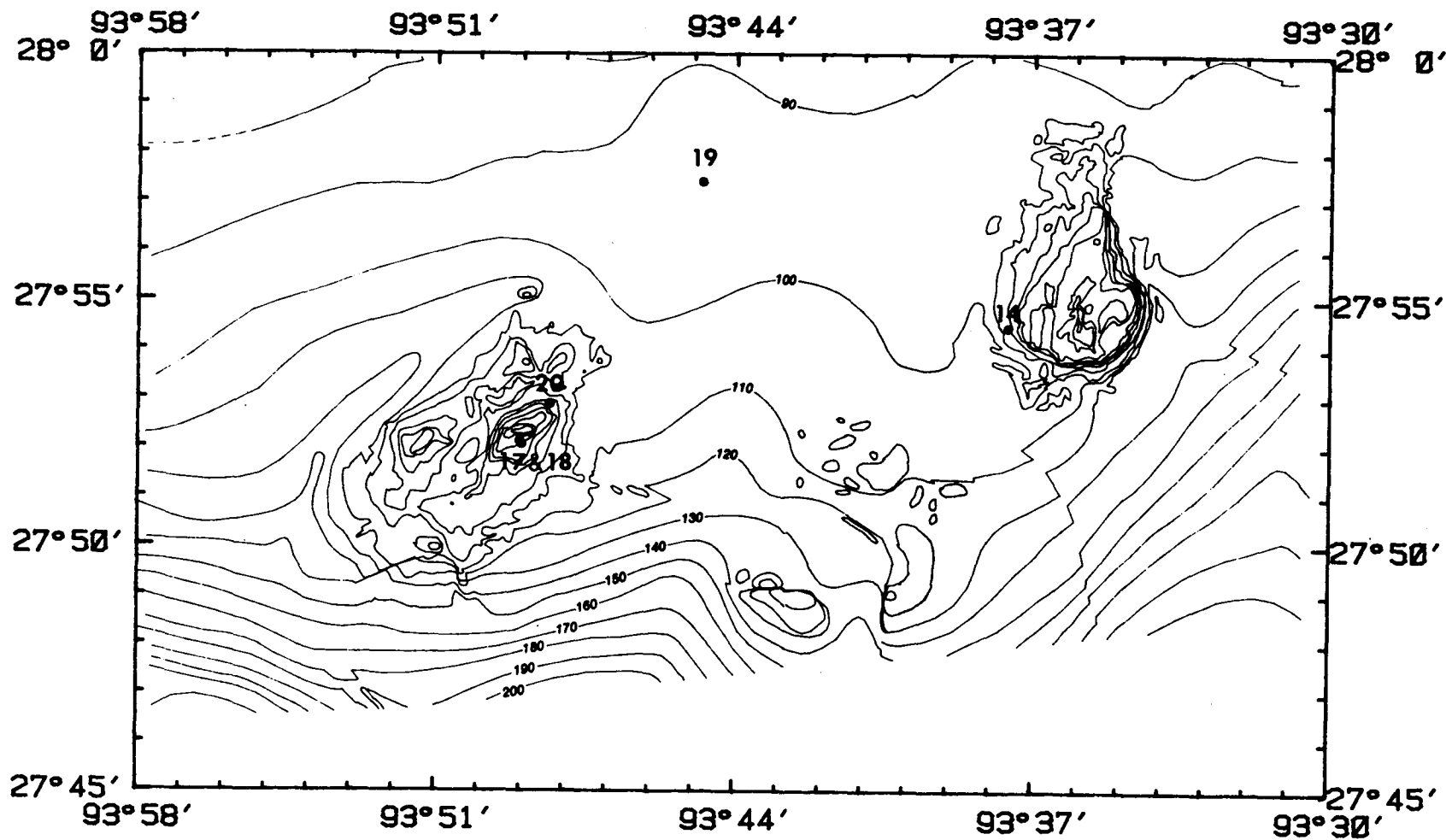


Figure IV-91. Location of October 1980 submersible dive stations where dye emission experiments were made.

downslope. Currents at other emitters remained slow (under 5 cm/sec), while the bottom flow was downslope to the southwest. The pulses maintained individual identities for considerable distance past the vanes, thus indicating small amounts of turbulence.

The bottom at site 14 consisted of small algal nodules and coarse carbonate sand. Temperature as measured in the submersible showed an increase of $.3^{\circ}\text{C}$ during the time the current underwent a change from southerly flow to almost stagnant mixed flow. Transmissivity remained high at 82%/m of white light as there was no nepheloid layer and water remained clear throughout the column.

Divesites 1980-17 and 18

Experiments on dives 1980-17 and 18 were made at the top of the West Flower Garden Bank. The dye emitter was at a depth of 49 m, which appeared to be within the upper mixed layer. Four PHISH profiles were made during dive 17, with only one showing the thermocline to be at a depth less than the dive site. Temperature in the mixed layer at the PHISH stations was 27.1°C , whereas the temperature recorded in the submersible during dive 17 was 26.4°C , a temperature which is not reached until 60 m in any of the profiles. If this lower reading is correct, then there must be a strong temperature gradient immediately above the bottom and hence the BBL would be a stably stratified layer. Transmissivity records do not indicate a nepheloid layer at this location. Currents from PHISH averaged 32 cm/sec at 120° .

During dive 17, the dye flow was to 120° and averaged 13 cm/sec in the bottom 1.5 m. No angular shear was noted in the bottom 3 m, although since all four emitters cannot be seen at the same time it is possible that the highest meter might be as much as 10° different in direction without being observed.

As would be expected, the highest emitter (3 m from bottom) consistently proved to be where the greatest speed occurs. The profiling current meter indicates consistent, practically barotropic flow and slight change with depth. Currents calculated from the dye emitters show profile variation in the bottom 1.5 m, varying from linear, to logarithmic, to flow with a maximum at .72 m (i.e., the current increases from the third emitter to the second emitter, then decreases from the second emitter to the bottom). Currents here vary from 10-18 cm/sec with constant direction. Frictional effects are important here since the change in velocity between 3 m and 1.5 m is quite large. The dye pulses often exhibit vertical meandering. The significance of this meandering on variability of bottom stress can only be determined by a careful quantitative analysis of the video tapes.

Dive 18 immediately followed dive 17. The dye emitters were replenished with dye and returned to almost the same location in 50 m of water. Current speed increased substantially near the bottom between the dives, becoming 21 cm/sec and increasing with height from the bottom. Often the flow was logarithmic with depth. Stress computed based on this logarithmic profile shows a bottom stress of near 2 dynes/cm^2 . The log layer ends between the fourth emitter (at 3 m)

and the third emitter (at 1.5 m). The velocity profile varies in shape, being logarithmic sometimes and linear at other times. The observed changes in velocity and velocity shear would cause variability in the bottom stress. No angular shear is observed.

Divesite 1980-19

Divesite 1980-19 was located between the East and West Flower Garden Banks at 97 m depth, the deepest site for 1980 dye experiments. As in the deep site experiments in 1979, poor visibility hampered the dye experiment. Visibility at 97 m was only 2 m. At this distance from the dye emitters, the camera used in the submersible could film only one emitter at a time. For this reason, no velocity profiles could be computed. Velocity decreased with depth, although no angular shear was apparent. Transmissivity was only 38-40%/m in the nepheloid layer, which was 25 m thick.

Divesite 1980-20

Divesite 20 was at 61 m depth on the Algal Nodule-Coral Debris Zone in the northeast corner of the West Flower Garden Bank. PHISH profiles in the area indicate eastward flow, with velocity decreasing gradually from 60 m to the bottom, although flow is 20 cm/sec at the bottom. The current direction varies about 15° from the surface to the bottom of the PHISH profile, flowing from 105° at 15 m to 90° at the bottom.

The PHISH station was northwest of the dive site, at 89 m depth. Transmissivity decreases linearly with depth from 61%/m at the surface to 48%/m at the bottom. Transmissivity at 61 m is 52%/m of the 600 nm light used in the PHISH, as compared to 80%/m of the white light Martek transmissometer used on the submersible.

At the PHISH site, the main thermocline extended between 52-67 m, so mixing in the BBL at the dive site would be immediately below the cap of the thermocline. Observations of the dye flow show more vertical meandering (moving slightly up, then slightly down) than in other dives.

There was little angular shear between any of the four emitters during most of the dive, with the current consistently flowing at 80°. The direction of flow gradually shifted to south of east as the dive neared completion; an angular shear of 15° developed between the third emitter and the bottom emitter. The vertical shear was consistently the same (speed decreasing with depth), although the profile does not fit into a logarithmic scheme in the bottom 1.5 m.

SUMMARY AND CONCLUSIONS

The most important observations from this study are connected with the discovery that the flow on the outer shelf and upper slope in the vicinity of the East and West Flower Garden Banks is persistently toward the east. This eastward flow occasionally attains speeds

approaching 100 cm/sec in the upper portions of the water column. Analyses of the records from mooring 2, located immediately adjacent to the East Flower Garden Bank, show that even during major storm events the vertical excursions of water particles do not exceed 10 to 15 m. The large scale sediment waves on both banks show that even under extreme flow conditions the water tends to parallel the isobaths. This tendency is also borne out by the orientation and magnitude of the variance tensors (tangent to the isobaths) computed from the records of meters on mooring 2. There is, therefore, excellent confirmation of the hypothesis that bottom waters in the vicinity of the Flower Garden Banks are never swept up and over them.

The effects of winter storms or northers appear to be: a deepening of the isothermal surface layer to a depth of about 60 to 80 m; establishment of strong, four-day cross-shelf oscillations; and generation of strong inertial oscillations which last for three to five days. Hurricanes produce similar phenomena, but they probably induce somewhat less deepening of the surface mixed layer. Northers induce greater deepening because they carry cold dry air over the Gulf. This cold dry air significantly reduces the surface water temperatures through evaporation and convection, thus making the surface water dense and creating instabilities that aid in vertical mixing. Tropical storms, on the other hand, are formed of warm moist tropical air and therefore do not produce such strong density-driven mixing.

Tides at the shelf edge appear to produce very small amplitude currents most of the year. During periods of strong stratification, the amplitudes seem to vary, and phase relations between surface and bottom oscillations wander. This wandering is caused by the complex interaction of the baroclinic (internal) tide and the shelf edge topography.

The boundary layer studies combined with time series transmissivity (XMS) records and PHISH profiles, reveal that the nepheloid layer is much more complex than was originally assumed. (The processes of erosion and local resuspension appear to be limited to the lowermost 2 or 3 m.) It is only within this thin layer that one would perceive a direct correlation between current speed and the amount of sediment in the water column. Above this layer is a zone of turbulent mixing that has longer time and length scales. This larger scale turbulence smooths out the short-term changes in sediment concentrations caused by differences in bottom shear stresses. At the level of the lowest current meters with transmissometers (4 m), this decoupling is evidenced by poor coherence between velocity and XMS variance. The variance between XMS values at 4 m and 12 m above the bottom at the same location is poorly correlated, except at long periods (> 2 days). The mean XMS gradient between 4 and 12 m off the bottom is on the order of 1%/m transmissivity per metre.

All of this implies that (local resuspension due to strong flow events contributes to significant changes in the sediment concentration only within the lowest 3 m of the bottom. Above that level, advective processes dominate the variances in sediment loading. These advective

processes include (a) stacking of boundary layers during periods of flow off the shelf and (b) creation of convergence zones produced by the intersection of downwelling shelf waters and upwelling slope waters in the bottom boundary layer.

The management implications are that the likelihood of drilling muds discharged in the bottom boundary layer near the Flower Garden Banks being resuspended to the level of the living reefs is remote beyond calculation. Sediment in the nepheloid layer above 4 m appears to undergo long distance transport (at least tens of kilometres) and, by inference, homogenization by large-scale mixing.

The mean direction of flow in the bottom boundary layer is to the east-southeast, but there are periods of rather strong onshore and off-shore flow when inertial oscillations penetrate to the bottom.

CHAPTER V
CHEMICAL ANALYSES

HIGH MOLECULAR WEIGHT HYDROCARBONS IN SPONDYLUS AMERICANUS

C. Giam, L. Ray, H. Murray, D. Allen

Introduction

This project was undertaken to analyze Spondylus americanus sampled from various sites in the northwestern Gulf of Mexico for high molecular weight hydrocarbons (HMWH). For these studies, S. americanus were collected from the East Flower Garden (EFG) and the West Flower Garden (WFG) during October 1980 by a team of oceanographers. These samples were analyzed using the contractually required techniques. Interpretation of the data was based on previous studies (Giam et al., 1978a,b, 1979, 1981) and on the report of Clark (1974).

Analytical Procedures

The analytical methods were essentially those reported in the previous studies and yielded adequate sensitivity and accuracy (Giam et al., 1978a,b). Procedure blanks were performed routinely and were < 0.01 ppm total hydrocarbons. The limit of detection for individual aliphatic hydrocarbons was 0.001 ppm; for aromatic hydrocarbons it was 0.005 ppm. The recovery of aliphatic hydrocarbons ($C_{14}-C_{32}$) subjected to all steps of the procedure averaged 80%, while that for aromatic hydrocarbons averaged 75%. Gas chromatography-mass spectrometry was used to confirm the identity of the major hydrocarbon peaks in 10% of the samples.

Carbon Preference Indices, CPI_{14-20} and CPI_{20-32} (Clark, 1974), were used for the determination of odd/even preference in hydrocarbon distribution. Because of the predominance of odd-carbon length chains in biological organisms, these ratios generally yield low, consistent values for petroleum, and high, variable values for biological hydrocarbons. The indices are calculated as follows:

$$CPI_{14-20} = \frac{1}{2} \left[\frac{\begin{array}{l} n = 19 \\ \Sigma \quad \text{HC odd} \\ n = 15 \end{array}}{\begin{array}{l} n = 20 \\ \Sigma \quad \text{HC even} \\ n = 16 \end{array}} + \frac{\begin{array}{l} n = 19 \\ \Sigma \quad \text{HC odd} \\ n = 15 \end{array}}{\begin{array}{l} n = 18 \\ \Sigma \quad \text{HC even} \\ n = 14 \end{array}} \right]$$

$$\text{CPI}_{20-32} = 1/2 \left[\begin{array}{l} n = 31 \\ \Sigma \quad \text{HC odd} \\ n = 21 \\ \hline n = 32 \\ \Sigma \quad \text{HC even} \\ n = 22 \end{array} + \begin{array}{l} n = 31 \\ \Sigma \quad \text{HC odd} \\ n = 21 \\ \hline n = 30 \\ \Sigma \quad \text{HC even} \\ n = 20 \end{array} \right]$$

The CPI_{20-32} is generally of the same magnitude for petroleum (mean 1.2) and for biological organisms (mean 1.0-1.5), but the CPI_{14-20} more accurately reflects the odd-carbon dominance of biological samples that is absent in petroleum. The CPI_{14-20} is almost always > 2 for organisms and averages < 1.0 for petroleum (Clark, 1974).

Results

Table V-1 lists the site of collection, sample weight, and total alkane content for each of the samples received. Analytical results for 20 *Spondylus* samples (sample SP16 consisted of a sand-filled shell and was not utilized) are given in Table V-2 as: percent distribution of *n*-paraffins; concentrations of *n*-paraffins, pristane, phytane, and total alkanes; the ratios of pristane/phytane, pristane/heptadecane (C_{17}), phytane/octadecane (C_{18}); and the Carbon Preference Indices, CPI_{14-20} and CPI_{20-32} .

Total *n*-paraffin concentrations varied from 0.038 to 0.65 ppm, with a mean of 0.18 ± 0.16 ppm (East Flower Garden mean = 0.16 ± 0.13 ; West Flower Garden mean = 0.20 ± 0.18). Pristane was present in eleven of the samples; it ranged from 0.004 to 0.036 ppm, with an average of 0.011 ± 0.010 ppm. Phytane was found in eighteen samples; it ranged from 0.001 to 0.008 ppm, with an average of 0.003 ± 0.002 ppm. Thus, the total and mean of *n*-alkanes had values similar to those for total paraffins (range: 0.038-0.66 ppm; mean: 0.19 ± 0.16 ppm).

The pristane/phytane ratio (11 samples) ranged from 0.80 to 20.03, with an average of 4.48 ± 5.47 , while the pristane/ C_{17} ratio (11 samples) ranged from 0.07 to 1.60, with an average of 0.31 ± 0.44 . The phytane/ C_{18} ratio ranged from 0.67 to 2.35, with an average of 1.18 ± 0.44 . The CPI_{14-20} varied from 4.41 to 21.19, with an average of 10.58 ± 4.01 . The CPI_{20-32} ranged from 0.05 to 2.28, with an average of 0.99 ± 0.55 . Squalene was the only compound identified in the aromatic fraction.

Discussion

The concentrations of hydrocarbons (*n*-paraffins and total alkanes) of the *S. americanus* samples collected during October 1980 (Table V-3) were generally within the ranges established and reported from

analyses of 1976 and 1977 samples (Giam et al., 1978a,b). Samples from the East Flower Garden had a relatively broad distribution of carbon chain lengths, as was also observed in 1977 and 1979; however, their CPI₁₄₋₂₀ values were high, consistent with a biological origin of the hydrocarbons. A CPI₁₄₋₂₀ value near one is suggestive of petroleum, whereas for biological organisms it is usually greater than two (Clark, 1974). Samples from the West Flower Garden showed an increased hydrocarbon content when compared to samples from the same region obtained in 1979, but were similar to other sampling locations. The distribution of hydrocarbons in the West Flower Garden samples was similar to that of samples from the East Flower Garden.

Phytane was present in low concentrations in all but two of the present samples (Table V-2). In contrast, it was previously detected only in two samples collected from the East Flower Garden in 1979. Phytane is generally considered to be of petroleum rather than biological origin; thus, its presence suggests contamination or pollution by petroleum (Farrington et al., 1972). Since the total concentrations of alkanes in these samples were similar to those of previous years (Table V-3) and since aromatic hydrocarbons could not be identified in any samples, petroleum contamination, if present, is at very low levels.

Conclusion and Management Implications

The majority of the samples obtained during 1980 were similar to samples from 1976-1979 in hydrocarbon concentrations and distributions. Based on the presence of phytane and a relatively broad range of carbon chain lengths, the current results are suggestive of slight petroleum contamination. However, this was not borne out by the high CPI₁₄₋₂₀ values or by the presence of aromatic hydrocarbons, which is a characteristic marker of petroleum. Thus, petroleum contamination, if present at all, is at very low levels.

Evidence suggesting possible low-level petroleum contamination in samples of S. americanus from the East and West Flower Garden Banks was first reported by Giam et al. (1981). However, further monitoring of the area would be necessary to determine if the observed distribution and concentration of petroleum is merely the normal, ambient value for the animals in this area.

TABLE V-1
 CONCENTRATION OF ALKANES* IN SPONDYLUS AMERICANUS (OCTOBER 1980)

STATION	SAMPLE CODE	SAMPLE WET WT.** (g)	CONC. IN PPM ($\mu\text{g/g}$ dry wt.)
WFG	SP1	63.4	0.038
EFG	SP2	50.5	0.043
EFG	SP3	56.3	0.22
EFG	SP4	66.8	0.068
EFG	SP5	41.8	0.13
EFG	SP6	36.3	0.10
WFG	SP7	56.2	0.094
WFG	SP8	55.3	0.082
EFG	SP9	81.6	0.046
WFG	SP10	34.1	0.18
EFG	SP11	14.0	0.47
WFG	SP12	6.3	0.66
WFG	SP13	18.7	0.26
EFG	SP14	14.3	0.33
WFG	SP15	11.6	0.32
WFG	SP16	0	--
WFG	SP17	32.2	0.12
WFG	SP18	40.8	0.25
WFG	SP19	40.5	0.092
EFG	SP20	64.4	0.076
EFG	SP21	39.1	0.21

*Total alkanes include paraffins, phytane, and pristane.

**Soft tissue only (no shell) was analyzed.

TABLE V-2
 PERCENT DISTRIBUTION OF n-PARAFFINS; CONCENTRATIONS OF n-PARAFFINS, PRISTANE, PHYTANE,
 AND TOTAL ALKANES; AND CALCULATED RATIOS FOUND IN SPONDYLUS (OCTOBER 1980)

STATION SAMPLE CODE	WFG SP1	EFG SP2	EFG SP3	EFG SP4	EFG SP5	EFG SP6	WFG SP7	WFG SP8	EFG SP9	WFG SP10
CARBON NO.										
14	2.2	2.0	0.4	2.8	0.9	2.2	2.0	3.3	2.5	0.5
15	3.7	8.1	2.8	9.1	4.8	9.2	7.0	9.1	10.2	3.3
16	3.0	2.0	0.4	2.7	1.8	2.2	3.4	3.6	4.2	1.8
17	66.2	48.6	18.6	60.5	47.5	42.2	72.2	55.1	53.8	23.6
18	2.2	0	0.4	1.4	1.2	1.3	1.7	3.3	1.3	1.0
19	2.2	0	0.4	1.4	1.2	1.8	1.7	2.9	1.3	1.4
20	2.2	0	0.4	1.1	1.2	1.3	1.3	2.2	1.3	1.0
21	0	0	1.6	0	0	0	2.0	2.2	2.1	0.7
22	4.4	2.0	4.4	3.2	3.0	4.4	3.4	5.8	9.7	1.2
23	3.7	2.0	6.7	2.1	2.7	4.8	2.7	3.3	2.1	2.3
24	3.7	2.0	9.1	3.2	3.6	5.3	2.7	3.3	2.1	0.7
25	3.7	0	9.9	4.3	5.4	8.6	0	4.0	2.1	6.0
26	3.0	9.1	7.7	3.6	3.9	4.8	0	2.2	1.3	1.2
27	0	0	21.0	0	9.0	11.9	0	0	0	7.6
28	0	0	5.5	0	2.7	0	0	0	1.3	14.3
29	0	0	4.8	0	3.6	0	0	0	0	5.7
30	0	24.3	4.0	1.4	3.6	0	0	0	2.5	7.8
31	0	0	0	0	0	0	0	0	0	0
32	0	0	2.0	3.2	3.9	0	0	0	2.1	20.0
Total paraffin, ppm	0.038	0.043	0.22	0.066	0.13	0.10	0.093	0.080	0.045	0.17
Pristane, ppm	*	*	*	*	*	*	*	*	*	0.004
Phytane, ppm	*	*	0.001	0.002	0.001	0.002	0.001	0.002	0.001	0.002
Total alkanes, ppm	0.038	0.043	0.22	0.068	0.13	0.10	0.094	0.082	0.046	0.18
Pr/Py	0	0	0	0	0	0	0	0	0	1.95
Pr/C ₁₇	0	0	0	0	0	0	0	0	0	0.11
Py/C ₁₈	0	0	1.00	1.76	0.75	1.34	0.79	0.67	1.00	1.43
CPI ₁₄₋₂₀	9.79	21.19	18.33	12.04	13.22	10.19	12.07	7.01	8.88	8.15
CPI ₂₀₋₃₂	0.61	0.05	1.38	0.48	1.07	1.67	0.71	0.77	0.34	0.67

*less than 0.001 ppm

TABLE V-2 (Continued)

STATION SAMPLE CODE CARBON NO.	EFG SP11	WFG SP12	WFG SP13	EFG SP14	WFG SP15	WFG SP17	WFG SP18	WFG SP19	EFG SP20	EFG SP21
14	0	0	0.8	0	0.5	1.2	0.6	1.2	0	0.3
15	0	0	4.0	0	2.3	7.3	5.8	8.7	4.9	3.0
16	0.8	0	1.4	1.0	1.4	2.3	2.2	2.3	2.5	1.1
17	19.1	12.2	10.0	14.5	30.0	36.4	47.9	31.3	24.5	16.0
18	0.8	1.0	1.2	0.8	1.6	2.1	1.6	1.6	1.3	0.6
19	1.1	16.3	1.8	1.4	1.8	2.1	2.6	1.6	1.7	0.8
20	0.9	14.2	1.2	1.0	1.2	1.5	1.0	1.4	1.3	0.6
21	9.6	1.8	1.2	5.5	1.2	2.1	2.8	1.6	0	0.5
22	1.2	1.8	16.1	1.0	1.2	1.7	1.0	1.6	2.1	0.9
23	1.5	0.4	16.1	1.0	1.4	3.5	1.8	2.1	3.4	1.2
24	1.5	2.4	16.1	0.8	1.2	2.4	1.6	1.9	3.7	1.3
25	7.6	8.1	7.4	6.6	21.7	9.1	3.7	6.8	26.2	4.1
26	1.2	1.8	1.8	0.8	1.8	2.8	0.9	2.8	1.5	2.2
27	4.9	11.2	7.6	5.4	0	0	2.6	0.9	6.0	8.5
28	20.4	5.3	9.6	30.7	15.9	7.5	9.0	13.3	0	16.4
29	18.6	18.3	0	20.1	12.3	8.7	4.4	5.1	5.9	25.3
30	5.2	5.1	3.6	5.8	4.6	9.5	5.4	5.9	7.0	5.3
31	0	0	0	0	0	0	0	0	0	0
32	5.6	0	0	3.9	0	0	5.2	9.8	7.9	12.0
Total paraffin, ppm	0.45	0.65	0.22	0.32	0.30	0.11	0.23	0.085	0.067	0.20
Pristane, ppm	0.012	0.005	0.036	0.005	0.019	0.006	0.013	0.006	0.008	0.005
Phytane, ppm	0.004	0.007	0.002	0.002	0.007	0.004	0.008	0.001	0.001	0.001
Total alkanes, ppm	0.47	0.66	0.26	0.33	0.32	0.12	0.25	0.092	0.076	0.21
Pr/Py	3.25	0.80	20.03	2.00	2.70	1.41	1.51	4.57	7.22	3.84
Pr/C ₁₇	0.13	0.07	1.60	0.11	0.21	0.14	0.12	0.24	0.50	0.15
Py/C ₁₈	1.00	1.00	0.67	1.00	1.43	1.70	2.35	1.00	1.28	1.00
CPI ₁₄₋₂₀	10.26	14.95	4.41	7.49	9.05	8.04	12.36	7.92	7.18	9.03
CPI ₂₀₋₃₂	1.29	1.86	0.68	0.93	1.45	0.95	0.73	0.54	2.28	1.27

*less than 0.001 ppm

TABLE V-3
COMPARISON OF SELECTED PARAMETERS FOR SPONDYLUS AMERICANUS FROM THE EAST FLOWER GARDEN AND OTHER SITES FOR 1976-1980

PARAMETERS	YEAR AND BANK SAMPLED									
	1976		1977		1978		1979		1980	
	EFG	Other Banks*	EFG	18 Fathom Bank	EFG	Sidner Bank	EFG	WFG	EFG	WFG
Number of samples	3	12	1	4	13	2	2	4	10	10
Total <u>n</u> -paraffins** (ppm)	0.007+ 0.004	0.016+ 0.038	0.28	0.01+ 0.01	0.10+ 0.13	0.25+ 0.28	0.30+ 0.02	0.014+ 0.013	0.16+ 0.13	0.20+ 0.18
Total alkanes** (ppm)	0.007+ 0.004	0.016+ 0.038	0.30	0.01+ 0.01	0.11+ 0.14	0.26+ 0.27	0.36+ 0.06	0.014+ 0.013	0.17+ 0.14	0.21+ 0.18
CPI *** 14-20	----	----	3.7	----	2.1-7.2 (6)	3.2 (1)	1.4-1.6	1.5 (1)	7.2-21.2	4.4-15.0
CPI *** 20-32	----	----	2.3	----	0.5-0.6 (2)	1.1 (1)	0.9-1.3	----	0.05-2.3	0.54-1.86

*28 Fathom, Stetson and Southern Banks, Hospital Rock.

**mean + standard deviation.

***Range; the number of samples for which CPI could be calculated is given in parentheses if less than the total number of samples.

HIGH MOLECULAR WEIGHT HYDROCARBONS, TOTAL ORGANIC CARBON,
AND DELTA C-13 IN SEDIMENTS

P. Parker, R. Scalan, R. Anderson

Introduction

Sediment analysis to deduce the degree of present day ecological damage from petroleum-derived organic compounds in the marine environment involves isolating the hydrocarbon fraction from samples and identifying molecules which are the common components of petroleum. The present report deals with hydrocarbons in the molecular weight range of C-12 to C-32, consisting of saturated, unsaturated, and aromatic compounds, isolated from the samples. In addition, measurements of total organic carbon (TOC) and Delta C-13 content were made as a further measure of petroleum-derived carbon in sediment.

Chemical studies of the Texas Outer Continental Shelf have shown that low concentrations of petroleum-like hydrocarbons are present in the water column, sediments, and biota. Baseline data obtained from the four-year BLM/STOCS program (1975-1979) are summarized in a three-volume report to BLM (Parker et al., 1979). In general, the total high molecular weight hydrocarbon (HMWH) concentration is in the range of a few parts per million, with individual components at the parts per billion level. These data serve as a baseline to evaluate future levels of HMWH which may be elevated by IXTOC-like events.

In addition to areas covered by the BLM/STOCS program, surveys in 1979/80 were made of the topographic high (Topo High) features of the Texas shelf (Rezak and Bright, 1981). These areas support fragile coral reef ecosystems which are unique in the Gulf because of their extreme northern occurrence and their great depth. As in the STOCS survey, low levels of HMWH compounds were found in the sediments of the Topo High region. The presence of these compounds again indicates that a low baseline concentration of HMWH is available as a reference point to judge future levels.

The full impact of catastrophic events such as the IXTOC I blowout and chronic additions from the shipping and handling of petroleum is technically difficult to assess in detail because of the size and complexity of the system. The implications of studies to date are quite clear, however. They suggest that because of toxicity, every precaution should be taken to prevent IXTOC-type events and to minimize additions by production, shipping, and handling operations.

Methods

Procedures for the Analysis of HMWH in Sediment

Samples were obtained in 1979/80 by subsampling Gray-O'Hara grab samples. Approximately 300 g of sediment taken from the top 5 cm of

the grab were transferred to precleaned Teflon jars. The jars were labeled, immediately frozen, then stored and transported for subsequent analyses.

Approximately 300 g of freshly thawed sediment were filtered on a Buchner funnel. The filtrate was transferred to a separatory funnel and extracted three times with 20 ml aliquots of chloroform. The sediment was covered with 200 ml of purified methanol and refluxed slowly over steam for six hours.

The sediment was again filtered and the reflux was repeated with fresh methanol for a total of three reflux periods. The dried sediments were then covered with 200 ml of distilled benzene and refluxed/filtered a further three times.

All filtrates were combined, concentrated under vacuum, and transferred to a separatory funnel with an approximately equal volume of 1 N HCL to remove salts. The solution was extracted twice with 30 ml of hexane and twice with 30 ml of benzene. These extracts were combined, concentrated under vacuum to near dryness, and saponified for six hours with 50 ml of 1 N KOH in 85% methanol. This was concentrated under vacuum to approximately 20 ml and transferred to a separatory funnel with an equal volume of water.

The saponification mixture was extracted with hexane (3 x 20 ml) and benzene (2 x 20 ml). The extracts were concentrated to near dryness and chromatographed on a hexane slurry packed silica gel column (300 x 11 mm).

Elution was accomplished by two column volumes (50 ml) each of hexane, benzene, and methanol. The hexane and benzene eluates, which contained the aliphatic and aromatic fractions, respectively, were collected and saved.

Gas chromatographic analyses were performed on a 0.25 mm (I.D.) x 27 m OV-101 glass capillary column installed in a Perkin-Elmer Model 910 Gas Chromatograph equipped with flame ionization detector. Operating conditions are shown in Table V-4.

Electronic integration of peak areas was performed by a Hewlett-Packard, 3352B Data System. The concentration of individual components was determined by coinjection of hydrocarbon standards. The identification of individual components was made by comparison with retention times of authentic standards and, for two samples, by combined gas chromatography-mass spectrometry.

Analysis by combined gas chromatography-mass spectrometry was performed on a Finnigan Model 4023 Mass Spectrometer with an INCOS Data System. The gas chromatography interfaced with the system was a Finnigan Model 9601 fitted with a 0.25 mm x 27 m SP-2100 fused silica capillary column. Operating conditions are shown in Table V-4.

TABLE V-4
GC-MS STANDARD OPERATING CONDITIONS

OPERATING CONDITIONS	*GAS CHROMATOGRAPH	
	Perkin-Elmer Model 910	Finnigan Model 9601
Carrier Gas	He	He
Carrier Flow	2 ml/min	2 ml/min
Initial Time	4 min	4 min
Initial Temperature	100°C	100°C
Programmed Rate	5°C/min	5°C/min
Final Temperature	275°C	265°C
Final Time	20 min	30 min
	*MASS SPECTROMETER	
	Finnigan Model 4023	
Source Temperature	250°C	
Electron Accelerating Potential	70 volts	
Ion Accelerating Potential	1400 volts	
Mass Range Scanned	50-300 amu	
Scan Speed	3 sec/decade	

*The Finnigan Model 9601 gas chromatograph was interfaced with the Finnigan Model 4023 Mass Spectrometer for combined GC-MS analysis.

Identification was accomplished by this GC/MS/DS analysis using specific mass chromatograms and mass spectra of individual components.

Procedures for the Analysis of Total Organic Carbon (TOC) in Sediment

Approximately 400 mg of freshly thawed sediment was acidified with excess 6 N HCL and set aside overnight until all carbonate material had been destroyed. The residue was filtered, rinsed with water until neutral, and dried overnight at 60°C. About 200 mg of the sample were sealed in a Pyrex tube with excess CuO, heated at 590°C in a box furnace for one hour, and allowed to cool slowly to room temperature. The evolved carbon dioxide was measured manometrically, and total organic carbon was calculated from this.

Procedures for the Analysis of Delta C-13 in Sediment

The carbon dioxide from the total organic carbon measurement was transferred quantitatively to a sample collection bulb, vented into a VG Micromass Model 602D Isotope Ratio Mass Spectrometer, and its $^{13}\text{C}/^{12}\text{C}$ isotope ratio was determined. The ratio is expressed as Delta C-13 relative to the PDB carbonate standard. The Delta C-13 values are valid to ± 0.2 ‰.

Results and Discussion

This section describes the results of the three types of analyses performed on eight sediment samples. Four of these samples were from the East Flower Garden Bank and four from the West Flower Garden Bank.

High Molecular Weight Hydrocarbons in Sediment

The results of HMWH analyses are given in Tables V-5 through 20. Examples of gas chromatograms are shown in Figures V-1 and 2, followed by sample mass spectra of selected peaks, shown in Figures V-3 through 6 (see also Table V-22). The levels of total HMWH concentrations range from 1.88 to 20.00 ppm ($\mu\text{g/g}$ dry weight). Comparison with data from previous years (Parker *et al.*, 1978, 1981) indicates that this approaches natural background levels. Although somewhat higher than previous years' ranges (0.1 to 0.5 ppm in 1977 and 0.3 to 11.2 ppm in 1978), the increase is probably not large enough to be considered significant.

The ratios of odd to even normal hydrocarbons (expressed by the average OEP index) range from 1.86 to 2.47. This is within the range reported for 1978 samples (range = 0.44-3.32; Parker *et al.*, 1981). The average pristane/phytane ratios, 0.95, are also quite similar to the average from the 1978 samples (1.11). Results of all parameters tested for 1979/80 samples, compared to results from previous years, show an apparent increase in the total amount of hydrocarbons in the 1979/80 samples. However, the levels are still close to background and probably are not significant.

Total Organic Carbon and Delta C-13

The total organic carbon (TOC) and Delta C-13 values are given in Table V-21. The TOC levels are similar to those of 1978 samples (Parker *et al.*, 1981): 0.59-1.36% this year, compared to 0.68-1.49% for 1978 samples. The C-13 values are slightly more positive than those from 1978 samples, which does not indicate petroleum contamination. The shift in three of the directly comparable samples is small and may reflect particle size or selective sampling of biota.

Conclusions and Management Implications

The distribution of HMWH, TOC, and Delta C-13 in the sediment samples does not display patterns consistent with major petroleum contamination. Comparison with previous data (Parker *et al.*, 1978, 1981) indicates that although levels of petroleum-like hydrocarbons may be slowly increasing in the Topo High region, they remain near baseline concentrations as compared to other Texas shelf sediments.

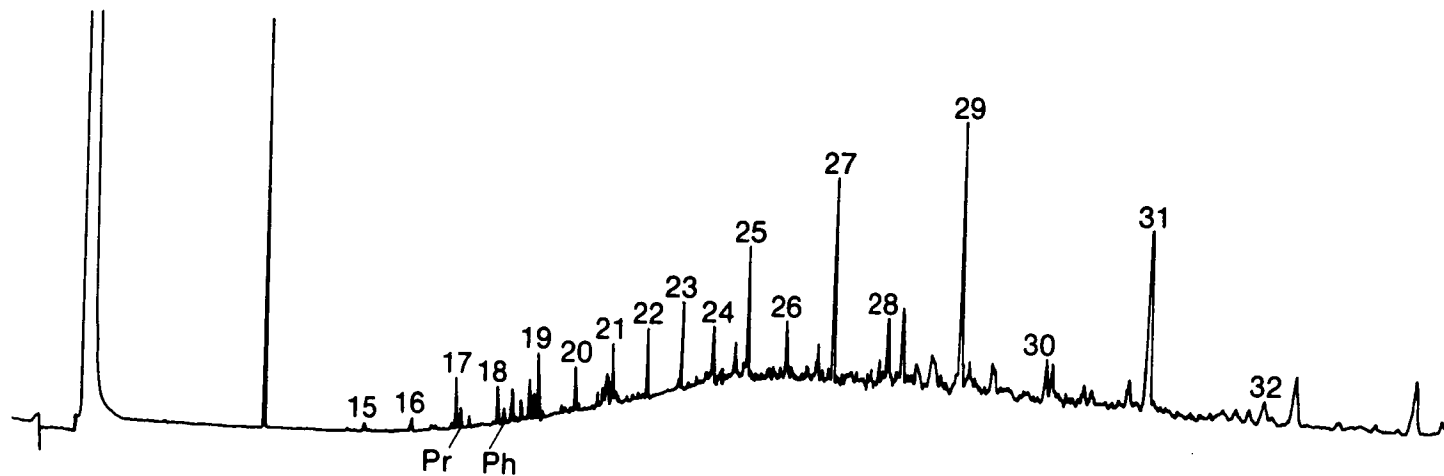


Figure V-1. Gas chromatogram of EFG-2G hexane eluate. Numbers indicate carbon numbers of normal alkanes; Pr = pristane; Ph = phytane.

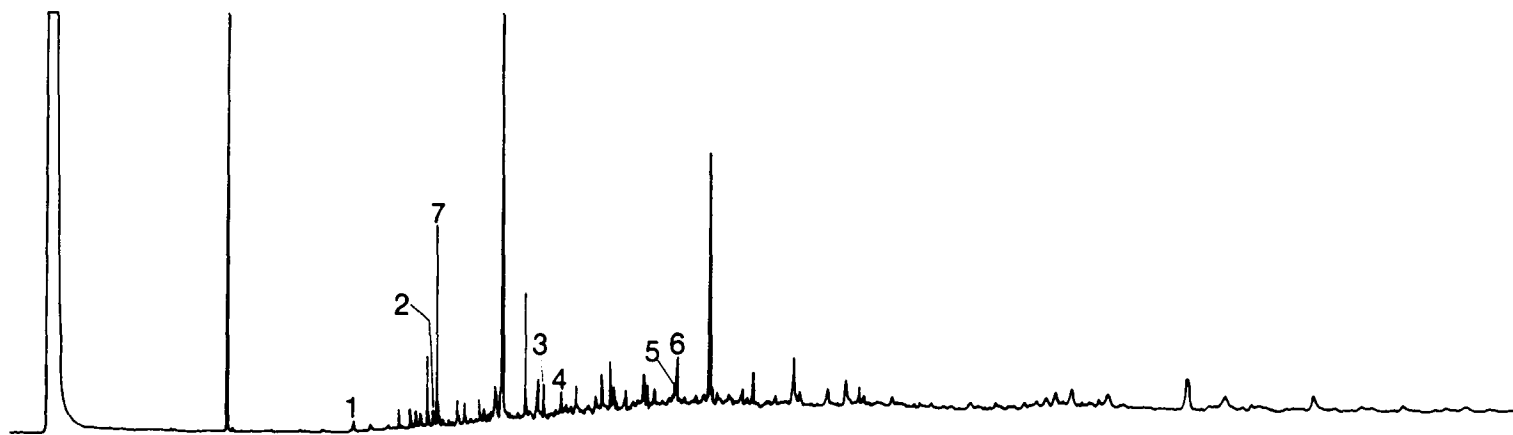


Figure V-2. Gas chromatogram of EFG-2G benzene eluate. See Table V-22 for peak identifications.

MASS SPECTRUM
06/29/81 11:54:00 + 27:18
SAMPLE: EFG-2G
ENHANCED (S 15B 2N 0T)

DATA: BA1 #1638
CALI: FC43N #12

BASE M/E: 202
R/C: 88704.

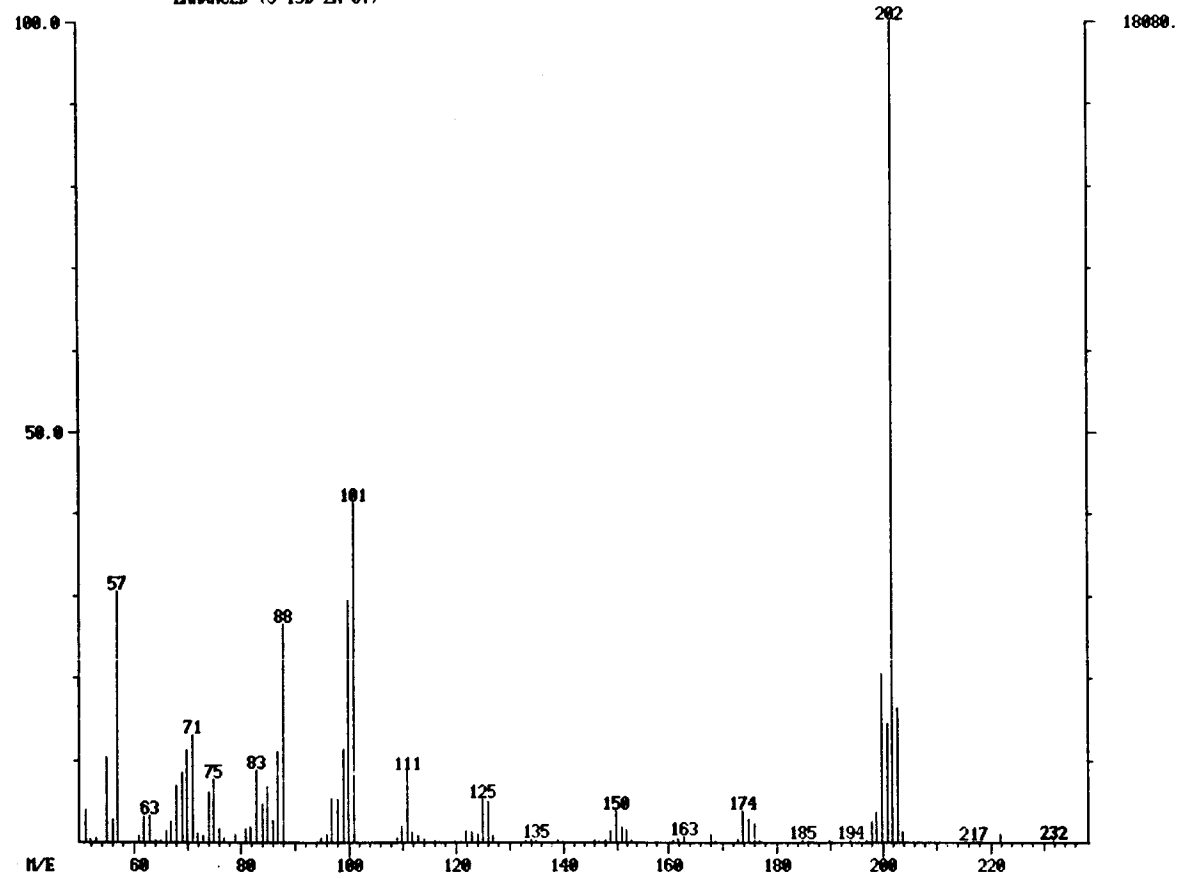


Figure V-3. Mass spectrum of fluoranthene (M/E = 202) from sample EFG-2G.

MASS SPECTRUM
06/29/81 11:54:00 + 28:17
SAMPLE: EFG-2G
ENHANCED (S 15B 2N 0T)

DATA: BA1 #1697
CALI: FC43N #12

BASE M/E: 202
RIC: 52032.

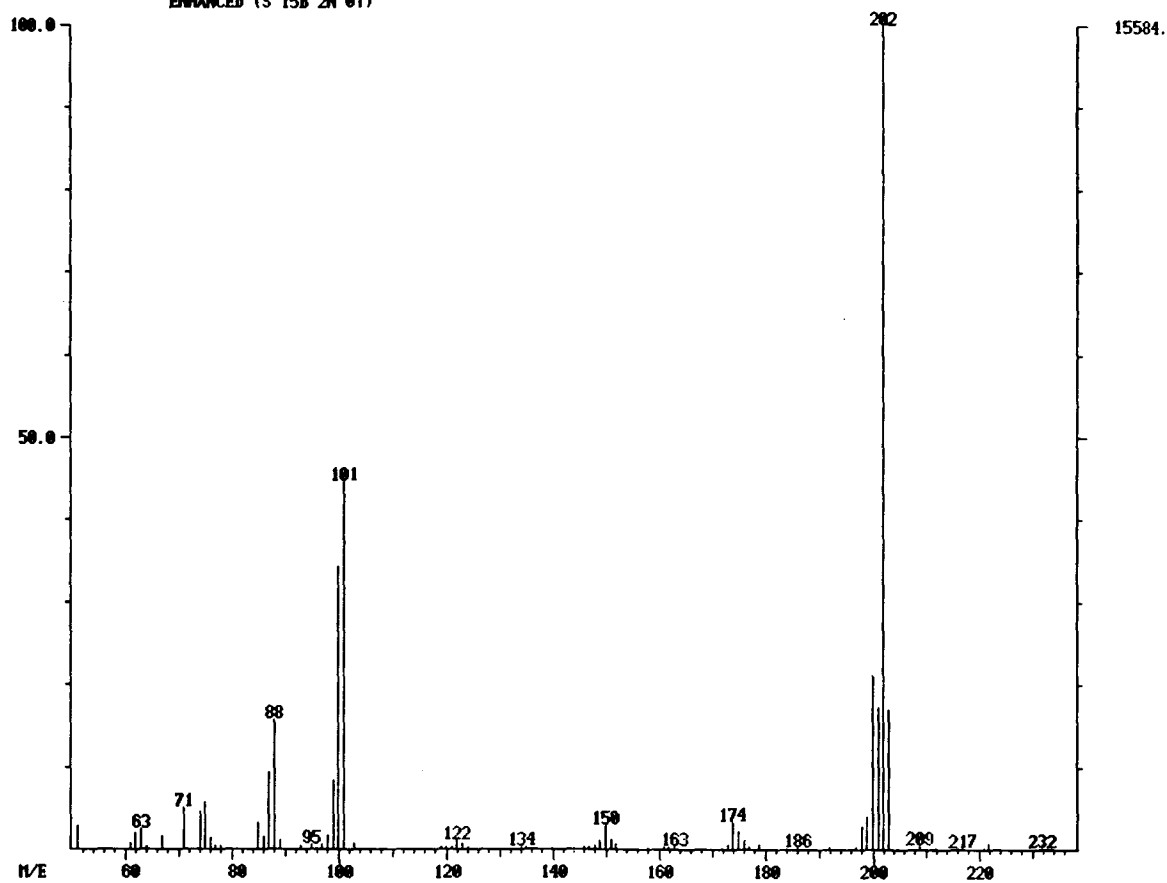


Figure V-4. Mass spectrum of pyrene (M/E = 202) from sample EFG-2G.

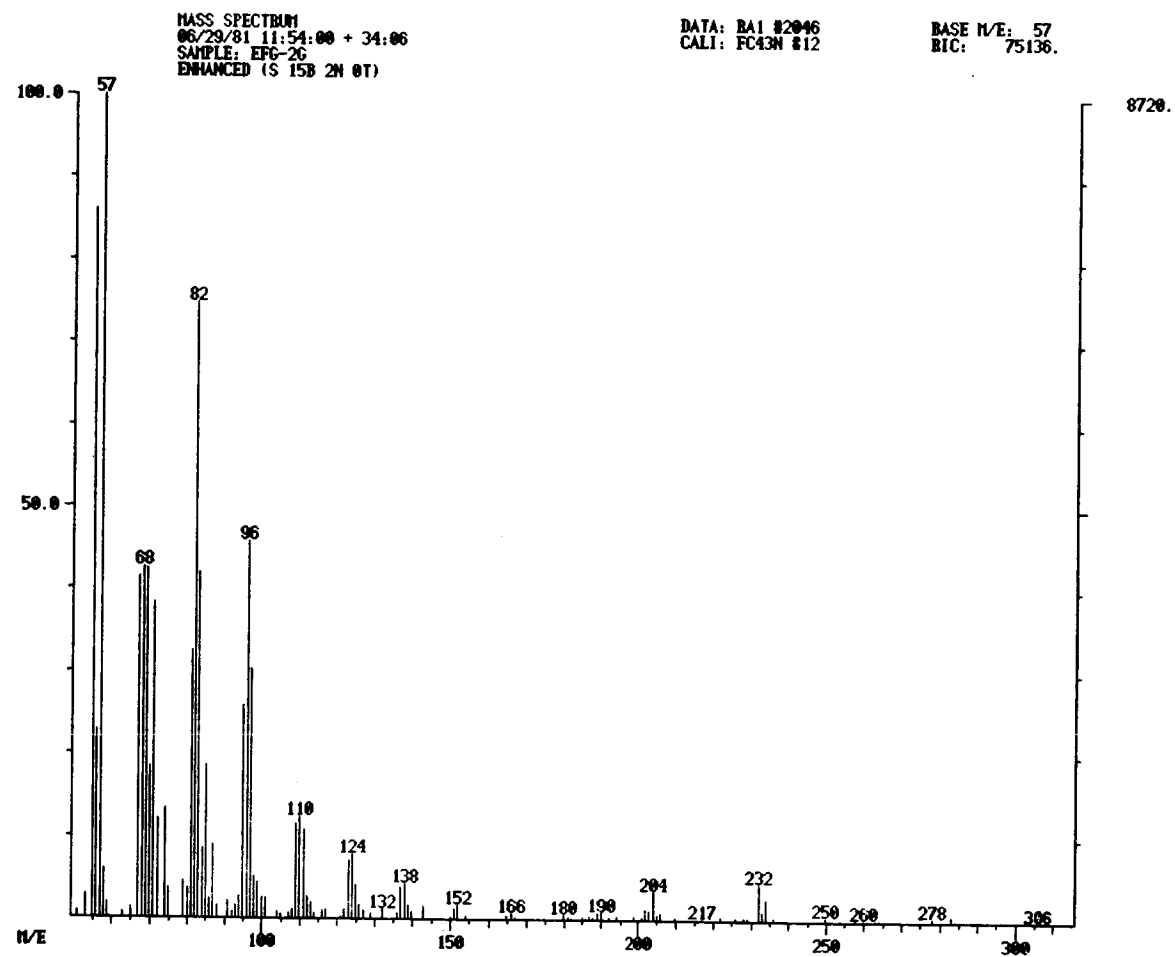


Figure V-5. Mass spectrum of chrysene (M/E = 228) from sample EFG-2G.

MASS SPECTRUM
06/29/81 11:54:00 + 34:39
SAMPLE: EFG-2G
ENHANCED (S 15B 2N 0T)

DATA: BA1 #2079
CALI: FC43N #12

BASE M/E: 228
EIC: 7392.

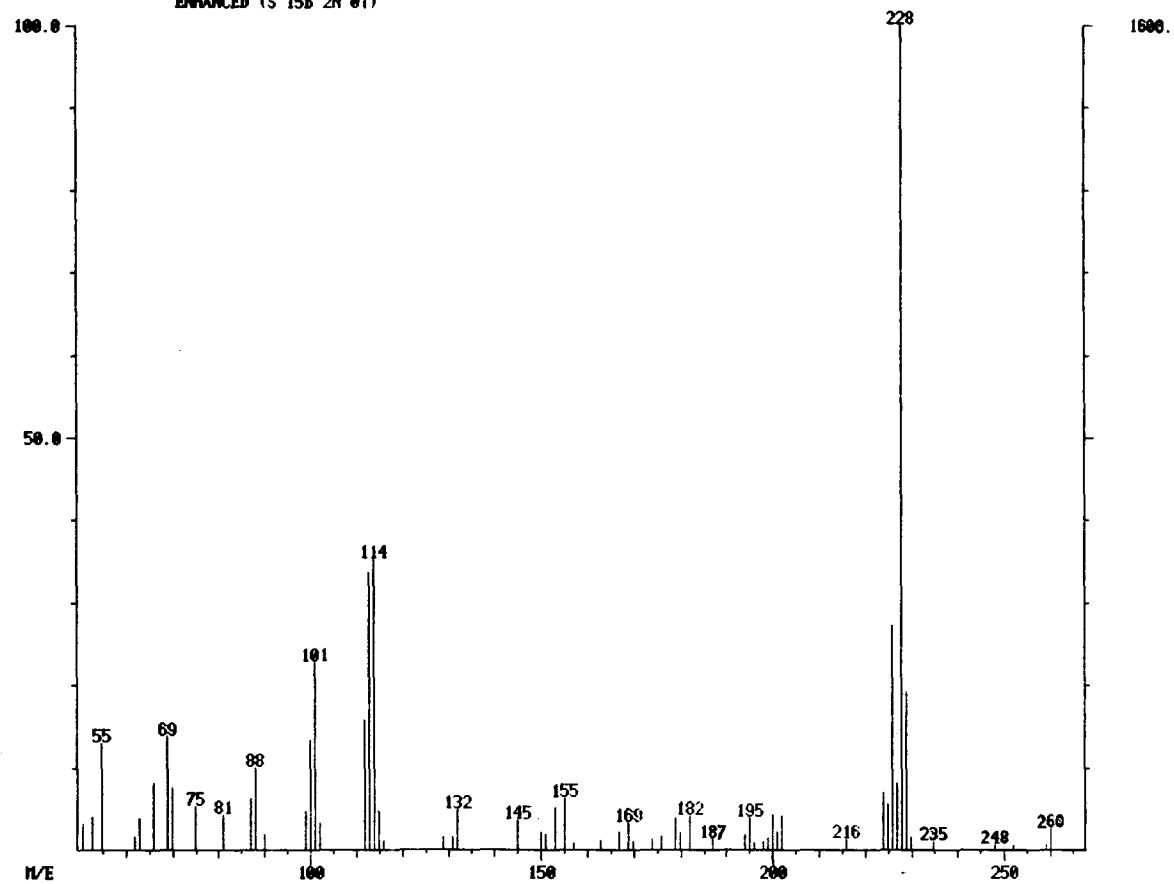


Figure V-6. Mass spectrum of benz[a]anthracene (M/E = 228) from sample EFG-2G.

TABLE V-5
NORMAL HYDROCARBON CONCENTRATIONS

SAMPLE: EFG-1Ga		SITE: EFG		
Carbon Number	Retention Time (Minutes)	Area	%	Concentration (µg/g)
14	13.20	276	.073	.010
15	16.01	140	.037	.005
16	18.69	167	.044	.006
17	21.24	496	.131	.017
18	23.64	593	.157	.021
19	25.93	1303	.345	.045
20	28.11	1297	.343	.045
21	30.19	2484	.657	.086
22	32.17	2483	.657	.086
23	34.09	4275	1.131	.148
24	35.93	3096	.819	.107
25	37.84	8161	2.160	.283
26	40.05	5805	1.536	.201
27	42.72	18826	4.982	.652
28	45.93	12401	3.281	.430
29	50.05	37445	9.908	1.297
30	54.92	4312	1.140	.149
31	60.79	41068	10.867	1.423
32	67.38	6124	1.620	.212
Total Saturate				
Fraction	12.7 µg/g			
Pristane	21.49	215	.057	.007
Phytane	23.97	319	.084	.011
Pr/Ph	0.67			
Pr/17	0.43			
Ph/18	0.54			
OEP (12-20)	0.83			
OEP (21-32)	3.28			

TABLE V-6
NORMAL HYDROCARBON CONCENTRATIONS

SAMPLE: EFG-2G		SITE: EFG		
Carbon Number	Retention Time (Minutes)	Area	%	Concentration (µg/g)
15	15.99	276	.103	.015
16	18.67	343	.128	.021
17	21.22	1416	.528	.087
18	23.63	1031	.384	.064
19	25.92	2265	.844	.140
20	28.09	1455	.543	.090
21	30.18	2525	.941	.156
22	32.16	1977	.737	.122
23	34.07	2831	1.056	.175
24	35.90	2230	.831	.138
25	37.82	5103	1.903	.315
26	40.01	2928	1.092	.181
27	42.68	10192	3.800	.629
28	45.86	6058	2.259	.374
29	49.93	21168	7.893	1.307
30	54.85	4913	1.832	.303
31	60.60	22208	8.281	1.371
32	67.19	3437	1.282	.212
Total Saturate				
Fraction	15.86 µg/g			
Pristane	21.48	860	.321	.053
Phytane	23.96	771	.288	.048
Pr/Ph	1.114			
Pr/17	0.608			
Ph/18	0.75			
OEP (12-20)	1.40			
OEP (21-32)	2.97			

TABLE V-7
NORMAL HYDROCARBON CONCENTRATIONS

SAMPLE: EFG-3Ga		SITE: EFG		
Carbon Number	Retention Time (Minutes)	Area	%	Concentration (µg/g)
17	21.38	260	.060	.002
18	23.78	378	.087	.002
19	26.05	1353	.312	.008
20	28.24	1455	.336	.009
21	30.32	2904	.670	.018
22	32.31	2967	.685	.018
23	34.23	5599	1.293	.034
24	36.07	3780	.873	.023
25	38.00	9383	2.167	.058
26	40.24	5177	1.195	.032
27	42.93	18753	4.330	.115
28	46.19	9140	2.111	.056
29	50.36	37858	8.742	.233
30	55.31	9718	2.244	.060
31	61.13	41733	9.637	.256
32	67.70	4652	1.074	.029
Total Saturate Fraction 2.63 µg/g				
Pristane	21.64	134	.031	.001
Phytane	24.11	606	.140	.004
Pr/Ph	0.22			
Pr/17	0.52			
Ph/18	1.60			
OEP (12-20)	0.88			
OEP (21-32)	3.28			

TABLE V-8
NORMAL HYDROCARBON CONCENTRATIONS

SAMPLE: EFG-4Ga		SITE: EFG		
Carbon Number	Retention Time (Minutes)	Area	%	Concentration (µg/g)
17	21.27	395	.685	.008
18	23.66	370	.641	.007
19	25.95	752	1.302	.015
20	28.13	656	1.136	.013
21	30.22	1025	1.776	.020
22	32.21	961	1.665	.019
23	34.11	1443	2.501	.028
24	35.95	1228	2.127	.024
25	37.90	4319	7.485	.084
26	40.09	1368	2.370	.027
27	42.74	4444	7.702	.086
28	45.48	1568	2.717	.030
29	49.96	-9456	-16.39	.183
30	54.90	2221	3.8	.043
31	60.64	10300	17.8	.200
32	67.35	2233	1.195	.043
Total Saturate Fraction 0.852 µg/g				
Pristane	21.53	236	.408	.005
Phytane	23.99	260	.451	.005
Pr/Ph	0.91			
Pr/17	0.60			
Ph/18	0.70			
OEP (12-20)	1.12			
OEP (21-32)	3.23			

TABLE V-9
NORMAL HYDROCARBON CONCENTRATIONS

SAMPLE: WFG-1Ga		SITE: WFG		
Carbon Number	Retention Time (Minutes)	Area	%	Concentration ($\mu\text{g/g}$)
16	18.80	196	.089	.010
17	21.09	212	.097	.011
18	23.74	274	.125	.014
19	26.03	559	.255	.028
20	28.21	669	.305	.033
21	30.29	1137	.519	.056
22	32.28	1213	.554	.060
23	34.19	2024	.923	.100
24	36.02	1661	.758	.082
25	37.96	3804	1.736	.189
26	40.19	3044	1.389	.151
27	42.87	8181	3.733	.406
28	46.15	5957	2.718	.295
29	50.26	17396	7.938	.862
30	55.23	3932	1.794	.195
31	60.97	17979	8.204	.891
32	67.61	3248	1.482	.161
Total Saturate				
Fraction	10.21 $\mu\text{g/g}$			
Pristane	21.34	210	.096	.010
Phytane	24.07	214	.098	.011
Pr/Ph	0.98			
Pr/17	0.99			
Ph/18	0.781			
OEP (12-20)	1.68			
OEP (21-32)	2.65			

TABLE V-10
NORMAL HYDROCARBON CONCENTRATIONS

SAMPLE: WFG-2Ga		SITE: WFG		
Carbon Number	Retention Time (Minutes)	Area	%	Concentration ($\mu\text{g/g}$)
15	16.11	130	.047	.044
16	18.78	274	.099	.009
17	21.33	688	.249	.023
18	23.74	515	.186	.017
19	26.02	1143	.413	.038
20	28.20	1063	.385	.035
21	30.28	1730	.626	.057
22	32.27	2721	.984	.090
23	34.18	2319	.839	.077
24	36.01	1571	.568	.052
25	37.95	4343	1.571	.144
26	40.19	2874	1.039	.095
27	42.86	8938	3.232	.296
28	46.10	7229	2.615	.240
29	50.24	20610	7.454	.683
30	55.15	4065	1.470	.135
31	60.89	19153	6.926	.635
32	67.62	3098	1.120	.103
Total Saturate				
Fraction	8.75 $\mu\text{g/g}$			
Pristane	21.59	394	.143	.013
Phytane	24.06	422	.153	.014
Pr/Ph	0.93			
Pr/17	0.57			
Ph/18	0.82			
OEP (12-20)	1.06			
OEP (21-32)	2.65			

TABLE V-11
NORMAL HYDROCARBON CONCENTRATIONS

SAMPLE: WFG-3Ga		SITE: WFG		
Carbon Number	Retention Time (Minutes)	Area	%	Concentration (µg/g)
12	7.38	291	.092	.011
13	—	—	—	—
14	13.17	161	.051	.006
15	—	—	—	—
16	18.66	351	.111	.013
17	21.20	1076	.340	.040
18	23.61	857	.271	.032
19	25.90	1492	.471	.056
20	28.07	1023	.323	.038
21	30.15	1650	.521	.062
22	32.14	2097	.662	.078
23	34.04	2742	.865	.102
24	35.88	2176	.687	.081
25	37.80	4683	1.478	.175
26	39.99	3171	1.001	.118
27	42.63	10640	3.358	.397
28	45.84	7547	2.382	.282
29	49.90	24959	7.878	.931
30	54.78	4629	1.461	.173
31	60.51	24699	7.796	.921
32	67.03	4130	1.304	.154
Total Saturate				
Fraction	11.33	µg/g		
Pristane	21.46	579	.183	.022
Phytane	23.93	412	.130	.015
Pr/Ph	1.41			
Pr/17	0.54			
Ph/18	0.48			
OEP (12-20)	0.96			
OEP (21-32)	2.92			

TABLE V-12
NORMAL HYDROCARBON CONCENTRATIONS

SAMPLE: WFG-4Ga		SITE: WFG		
Carbon Number	Retention Time (Minutes)	Area	%	Concentration (µg/g)
14	13.86	140	.048	.0045
15	16.03	573	.197	.018
16	18.71	704	.242	.023
17	21.26	2551	.863	.082
18	23.66	1740	.598	.056
19	25.95	3364	1.157	.108
20	28.12	1450	.499	.047
21	30.21	2228	.766	.072
22	32.20	2589	.890	.083
23	34.60	3075	1.057	.099
24	35.93	1895	.652	.061
25	37.86	5316	1.828	.171
26	40.06	3221	1.108	.104
27	42.72	11122	3.825	.357
28	45.94	5856	2.014	.188
29	50.00	19261	6.624	.619
30	54.91	3572	1.228	.115
31	60.61	17997	6.189	.578
32	66.	**	~	.175 .016
Total Saturate				
Fraction	8.83	µg/g		
Pristane	21.51	2787	.958	.090
Phytane	23.98	1986	.683	.064
Pr/Ph	1.40			
Pr/17	1.09			
Ph/18	1.14			
OEP (12-20)	1.59			
OEP (21-32)	3.34			

**Not Integrated. Area was measured by hand when program ended prematurely.

TABLE V-13
CONCENTRATION AND RETENTION TIME OF
AROMATIC HYDROCARBONS IN SEDIMENTS

SAMPLE: EFG-1Ga Benzene SITE: EFG

Retention Time (Minutes)	Area %	Concentration ($\mu\text{g/g}$)	Name
14.69	.123	0.005	Acenapthene
25.63	2.445	--	--
27.39	1.420	--	--
28.42	.563	0.024	Fluoranthene
29.50	1.114	0.048	Pyrene
33.84	2.645	--	--
35.96	1.876	0.081	BenzalAnthracene
37.97	9.850	--	--
39.75	1.163	--	--
40.09	1.834	--	--
42.73	4.199	--	--
45.97	1.797	0.078	Perylene
49.97	1.424	--	--
54.99	1.098	--	--
57.69	1.571	--	--
60.62	2.987	--	--
65.21	2.051	--	--
67.38	1.616	--	--
72.55	1.158	--	--

Total Benzene Eluate 3.301 $\mu\text{g/g}$

TABLE V-15
CONCENTRATION AND RETENTION TIME OF
AROMATIC HYDROCARBONS IN SEDIMENTS

SAMPLE: EFG-3Ga Benzene SITE: EFG

Retention Time (Minutes)	Area %	Concentration ($\mu\text{g/g}$)	Name
25.55	3.604	--	--
27.31	1.690	--	--
28.35	.745	.006	Fluoranthene
29.39	.767	.006	Pyrene
33.05	2.817	--	--
34.42	1.358	--	--
35.97	.446	.003	BenzalAnthracene
36.19	.430	.003	Chrysene
37.80	5.190	--	--
39.86	1.074	--	--
42.50	2.707	--	--
57.30	1.809	--	--
58.14	1.660	--	--
64.74	4.290	--	--
66.88	1.802	--	--
71.96	2.176	--	--

Total Benzene Eluate 0.703 $\mu\text{g/g}$

TABLE V-14
CONCENTRATION AND RETENTION TIME OF
AROMATIC HYDROCARBONS IN SEDIMENTS

SAMPLE: EFG-2G Benzene SITE: EFG

Retention Time (Minutes)	Area %	Concentration ($\mu\text{g/g}$)	Name
17.46	.275	0.011	Fluorene
21.83	1.644	--	--
22.17	.403	0.017	Phenanthrene
25.68	1.738	--	--
26.10	11.758	--	--
27.38	2.607	--	--
28.43	1.119	0.047	Fluoranthene
29.47	.938	0.039	Pyrene
30.25	1.031	--	--
31.85	1.377	--	--
32.28	1.081	--	--
35.87	.237	0.010	BenzalAnthracene
36.09	1.400	0.058	Chrysene
37.95	6.472	--	--
40.38	1.087	--	--
42.71	2.559	--	--
45.72	1.809	--	--
57.68	1.400	--	--
58.53	1.852	--	--
60.66	1.415	--	--

Total Benzene Eluate 4.132 $\mu\text{g/g}$

TABLE V-16
CONCENTRATION AND RETENTION TIME OF
AROMATIC HYDROCARBONS IN SEDIMENTS

SAMPLE: EFG-4Ga Benzene SITE: EFG

Retention Time (Minutes)	Area %	Concentration ($\mu\text{g/g}$)	Name
25.04	1.788	--	--
25.61	7.097	--	--
26.07	1.870	--	--
27.37	3.723	--	--
28.40	.984	--	--
29.48	3.424	0.036	Pyrene
31.55	.922	--	--
33.54	2.132	--	--
36.02	.878	0.009	Chrysene
37.36	1.546	--	--
37.95	12.429	--	--
42.17	1.634	--	--
47.74	1.949	--	--
51.80	1.635	--	--
52.09	9.273	--	--
53.14	1.066	--	--

Total Benzene Eluate 1.024 $\mu\text{g/g}$

TABLE V-17
CONCENTRATION AND RETENTION TIME OF
AROMATIC HYDROCARBONS IN SEDIMENTS

SAMPLE: WFG-1Ga Benzene SITE: WFG

Retention Time (Minutes)	Area %	Concentration (µg/g)	Name
25.62	3.286	--	--
26.08	1.015	--	--
27.38	2.130	--	--
28.43	.907	0.025	Fluoranthene
29.50	1.707	0.046	Pyrene
33.59	1.585	--	--
36.06	1.247	0.034	Chrysene
37.99	4.233	--	--
39.84	1.485	--	--
41.75	.977	--	--
42.82	3.492	--	--
43.16	1.371	--	--
44.80	1.636	--	--
46.01	1.785	--	--
50.11	1.998	--	--
50.68	1.244	--	--
57.90	.965	--	--
58.34	2.731	--	--
60.88	3.193	--	--
61.70	1.322	--	--
65.53	2.808	--	--
66.44	3.746	--	--
67.76	1.566	--	--
73.07	1.587	--	--
76.38	1.165	--	--
80.70	1.149	--	--
81.34	1.414	--	--

Total Benzene Eluate 2.68 µg/g

TABLE V-18
CONCENTRATION AND RETENTION TIME OF
AROMATIC HYDROCARBONS IN SEDIMENTS

SAMPLE: WFG-2Ga Benzene SITE: WFG

Retention Time (Minutes)	Area %	Concentration (µg/g)	Name
6.47	.101	.002	Napthalene
11.82	1.288	--	--
14.73	.121	.002	Acenaphthene
22.21	.307	.005	Phenanthrene
23.52	1.031	--	--
26.16	11.750	--	--
27.45	2.793	--	--
28.49	.917	.014	Fluoranthene
29.53	1.061	.016	Pyrene
31.94	1.622	--	--
34.48	1.007	--	--
35.98	.274	.004	Benz a]Anthracene
36.11	1.115	.017	Chrysene
37.23	1.068	--	--
38.04	3.732	--	--
39.92	1.195	--	--
42.85	2.869	--	--
45.93	2.676	.040	Perylene
57.39	1.840	--	--
58.70	1.356	--	--
60.86	1.545	--	--
65.43	4.578	--	--
72.92	1.859	--	--

Total Benzene Eluate 1.47 µg/g

TABLE V-19
CONCENTRATION AND RETENTION TIME OF
AROMATIC HYDROCARBONS IN SEDIMENTS

SAMPLE: WFG-3Ga Benzene SITE: WFG

Retention Time (Minutes)	Area %	Concentration (µg/g)	Name
21.89	1.231	--	--
22.23	.274	.0070	Phenanthrene
22.40	1.444	.0367	Anthracene
23.53	1.096	--	--
26.15	8.188	--	--
27.44	2.218	--	--
28.48	1.041	.0265	Fluoranthene
29.52	1.110	.0282	Pyrene
31.90	1.009	--	--
32.34	.965	--	--
35.94	.343	.0087	Benz a]Anthracene
36.09	1.349	.0343	Chrysene
37.68	.995	--	--
38.01	6.414	--	--
38.50	1.093	--	--
39.87	1.510	--	--
40.46	1.247	--	--
42.82	3.196	--	--
44.80	1.029	--	--
45.85	2.772	--	--
46.84	1.327	--	--
48.01	1.226	--	--
56.79	.923	--	--
57.32	1.481	--	--
57.80	2.003	--	--
58.67	1.090	--	--
58.75	1.247	--	--
60.83	1.739	--	--
65.43	6.242	--	--
67.60	1.940	--	--

Total Benzene Eluate 2.50 µg/g

TABLE V-20
CONCENTRATION AND RETENTION TIME OF
AROMATIC HYDROCARBONS IN SEDIMENTS

SAMPLE: WFG-4Ga Benzene SITE: WFG

Retention Time (Minutes)	Area %	Concentration (µg/g)	Name
17.41	0.12	.003	Fluorene
21.78	2.43	--	--
23.41	1.01	--	--
25.63	1.50	--	--
26.02	3.99	--	--
27.34	2.91	--	--
28.38	1.04	.027	Fluoranthene
35.98	0.44	.011	Benz a]Anthracene
36.06	0.75	.019	Chrysene
37.61	1.02	--	--
37.91	6.85	--	--
40.35	1.24	--	--
42.66	2.31	--	--
45.20	0.22	.006	Benzpyrene
45.70	3.47	.089	Perylene
46.45	1.31	--	--
57.62	1.40	--	--
58.54	1.38	--	--
65.21	4.39	--	--
67.38	2.74	--	--
72.69	1.60	--	--

Total Benzene Eluate 2.58 µg/g

TABLE V-21
TOC AND DELTA C-13 VALUES IN SEDIMENTS

SAMPLE	TOC*	DELTA C-13**
EFG-1Ga	1.24%	-20.19
EFG-2G	--	--
EFG-3Ga	1.35	-18.68
EFG-4Ga	0.59	-19.85
WFG-1Ga	1.26	-20.23
WFG-2Ga	1.14	-20.94
WFG-3Ga	1.36	-20.90
WFG-4Ga	1.08	-20.56

*Total Organic Carbon is measured on a carbonate free basis.

**Delta C-13 values reported relative to PDB carbonate standard.

TABLE V-22
PEAK IDENTIFICATIONS IN BENZENE ELUATES

PEAK NO.	COMPOUNDS	M.W.
1	Fluorene	166
2	Phenanthrene	178
3	Fluoranthene	202
4	Pyrene	202
5	Benz[a]anthracenes	228
6	Chrysene	228
7	Anthracene - d ₁₀ (C ₁₄ D ₁₀)	

CHAPTER VI

GEOLOGY OF SELECTED BANKS

R. Rezak

INTRODUCTION

Six of the banks described in this chapter were surveyed in previous studies (Bright and Rezak, 1978a,b). MacNeil Bank is the only one that was mapped for the present study. Table VI-1 summarizes the data for these surveys, including the number of sediment stations on each bank. Previous studies had no requirements for sub-bottom profiling. However, the profiling equipment was aboard the vessel and the data were acquired at no additional cost to the sponsor.

A major problem in the interpretation of structure on a few of the banks was that the length of survey lines was limited by bathymetry rather than geologic structure. An additional 1000 m of record on each end of each line would have yielded considerable additional information on the geologic history of the structures.

TABLE VI-1
SUMMARY OF SURVEY DATA ON SELECTED BANKS

BANK	DATE MAPPED	SURVEY LINES (km)	SEDIMENT STATIONS	SIDE- SCAN (no. of lines)	SEISMIC RECORDS		
					7 kHz	3.5 kHz	Boomer
Ewing	May/Jun 77	239.1	0	53	53	0	53
Parker	May/Jun 77	223.2	4	36	36	0	13
Bouma	May 77	131.9	0	24	24	0	0
18 Fathom	May 77	131.1	0	32	32	0	2
Bright	May/Jun 77	161.1	4	35	35	0	0
Stetson	Jul 76	18.9	33	16	0	16	1
MacNeil	Aug/Sep 80	233.3	0	44	0	44	36

EWING BANKGeneral Description

Ewing Bank is located at 28°05'43.87"N latitude and 90°59'41.37"W longitude (Figure VI-1). It lies in Lease Blocks 337, 349, 350, and 351 of the Ship Shoal Area, South Addition (Figure VI-2) and covers an area of approximately 25 km².

The bank is roughly triangular in shape and is enclosed by the 80 m isobath, with gentle slopes beyond that depth into deeper water (Figures VI-2 and 3). Two prominent peaks are situated at the southern corners, and one low prominence occurs at the northern corner of the

triangle. The northern prominence is very broad and rises to a depth of 74 m. The western peak rises to a depth of 56 m with a broad area enclosed by the 60 m isobath. The eastern peak is slightly smaller, but shallower, with a minimum depth of 55 m. A saddle at a depth of 67 m lies between the two major peaks.

Structure and Physiography

Ewing Bank is a mature salt dome with a well developed crestal graben (Figures VI-4a, 4b, and 5). Figure VI-5 is a classic example of a crestal graben. Boomer profiles (Figures VI-4a and 4b) show different topographic expression. Figure VI-4a depicts a profile over the main part of the bank. It shows well developed drag of the sediments in the northernmost lease block along a major fault. The relief here is positive owing to renewed uplift of the diapir without any relative motion between the lease blocks in the crestal graben. Figure VI-4b, a profile on the eastern side of the bank, displays negative relief on the crestal graben as this area has not been affected by the renewed uplift. The structure-isopach map (Figure VI-6) shows the thickness of sediments below the seafloor to the reflector shown on Figures VI-4a and 4b.

The seafloor roughness map (Figure VI-7) shows individual features from less than one metre up to five metres in height, with a spatial frequency ranging from 5 features to greater than 10 features per hectare. The side-scan sonar record on Figure VI-5 illustrates some of those features which appear to be growing on rock outcrops on the upthrown sides of normal faults.

Sedimentology

No sediment samples were collected at Ewing Bank.

PARKER BANK

General Description

Parker Bank is located at 27°56'49.10"N latitude and 92°00'40.08"W longitude (Figure VI-1). The bank lies in Lease Blocks 194, 195, 202, and 203 of the South Marsh Island Area (Figure VI-8). The bank is nearly rectangular in shape and covers an area of 38.5 km². A deep valley trending in an east-west direction lies in the north-central part of the bank giving the bank the appearance of an asymmetrical horseshoe (Figures VI-8 and 9). The valley bifurcates at the east side of the bank, one branch going towards the northeast and the other towards the southeast.

The shallowest depth is 57 m in the east central part of the bank. Water depths surrounding the bank vary from 100 to 140 m, and the central valley reaches depths of 120 m.

Structure and Physiography

The surface expression of the bank is fault controlled. The major faults are those trending towards the east on either side of the axial graben and the radial faults that bound the northeast and southeast arms of the valley (Figures VI-8 and 9). Parker is a mature salt dome. The faulting that created the axial graben occurred during or shortly after the Pleistocene epoch. The tilted surface of the fault block between shot points 1903 and 1909 on Figure VI-10 has been buried completely by Holocene sediments. The arrow on the north side of the record points to the horizon used as the base of the isopach interval on Figure VI-9. It was not possible to identify this horizon in other areas surrounding the bank because of the limited coverage of the survey lines.

Large areas on the bank are covered by drowned reefs (Figures VI-11 and 12). The side-scan records show these reefs to be aligned as though they were growing on the upper edges of steeply dipping beds. The relief on these reefs ranges up to 5 m with a spatial frequency varying to over 10 features per hectare (Figure VI-13).

Sedimentology

During June 1977, four sediment samples were taken at Parker Bank for sedimentological analysis. Station locations are shown on Figure VI-8. The results of these analyses are presented in Tables C-1 and 2 of Appendix C. All of the stations at this bank are at greater depths than many of the grain constituents would indicate. Sample 1-4 contains 33.5% coral fragments and 7% coralline algae. The depth at this station is 105 m, well below the depth limit for the growth of corals. The mud fraction in this sample is only 4.66%, which is also unusual at this depth.

Two hypotheses may be used to explain this anomalous occurrence. The present depth of the crest above Station 1-4 (65 m) is too great for healthy coral growth. The corals may have grown on the crest when sea level was 30 m lower and washed down the slope to the area of station 1-4. Alternatively, relatively recent subsidence of the crest may have resulted in mass mortality of coral at the crest. In either case, the transport of coral debris must have been by gravity movement, and the strong circumbank currents have prevented the deposition of muds which normally would be expected at this depth.

Conclusions and Recommendations

Based upon sedimentological and sub-bottom data, Parker Bank appears to be a structurally active diapir. Detailed hazard surveys should be conducted prior to emplacement of seafloor structures, particularly on the east side of the bank, where radial faults extend out into the surrounding soft bottom.

BOUMA BANK

General Description

Bouma Bank is located at 28°03'35.73"N latitude and 92°27'51.47"W longitude (Figure VI-1). It lies in Lease Blocks 370, 371, 384, and 385 of the Vermilion Area (Figures VI-14 and 15).

The eastern half of this bank is clearly defined by an almost semicircular 100 m isobath. On the west side of the bank, the slope from the 80 m isobath to deeper water is much more gradual. The major portions of the bank are enclosed by the 80 m isobath. However, even within this area, a number of major features are observed. The southernmost prominence rises from 100 m to a depth of 62 m. Immediately north of this peak lies a deep basin with a depth of 88 m (Figures VI-14 and 15). To the northwest of this area is a broad rise enclosed by the 72 m isobath. On the northwest side of this rise, a peak rises to a depth of 59 m. The gradient steepens between the 65 to 80 m isobaths towards the northwest of this peak. Additional peaks at 72, 82, and 84 m are located on the north side of the bank.

Structure and Physiography

Bouma Bank is a mature salt dome that shows evidence of crestal collapse. An outcrop of siltstone was encountered at a depth of 77 m on the northern flank of the south peak during Submersible Dive No. 9 on September 29, 1977. The occurrence of siltstone without encrustations of coralline algae at that depth indicates very recent exposure due to faulting. The structure map (Figure VI-16) does not indicate faulting in this area owing to the non-reflective nature of the sub-bottom strata. The non-reflectivity in this area is most likely due to excessively steeply dipping strata. Other outcrops of bedrock are indicated on the seafloor roughness map (Figure VI-17) prepared from the side-scan sonar data.

Faulting on Bouma Bank is both radial and annular. Figure VI-16 depicts only those faults that are discernible on the sub-bottom profiles. The annular fault on the northwest side of the non-reflective area is most probably continuous around the non-reflective area.

Outcrops of stratified rocks are shown on the seafloor roughness map (Figure VI-17) along the north side of the bank in water depths of from 60 m to 82 m. Another outcrop is shown at a depth of 76 m to 77 m on the northeast side of the deep basin. Local features vary in size from less than one metre to greater than five metres in height and from one to five features per hectare to more than ten features per hectare.

Sedimentology

No sediment samples were taken at Bouma Bank.

Conclusions and Recommendations

Bouma Bank is a mature salt dome that displays evidence for continuing active collapse at its crest. Detailed hazard surveys should be conducted prior to emplacement of structures on the seafloor.

18 FATHOM BANK

General Description

Eighteen Fathom Bank is located at 27°57'48.47"N latitude and 92°35'45.04"W longitude (Figure VI-1) in Lease Blocks 362 and 379 of the East Cameron Area, South Addition, and Lease Blocks 389, 410, and 409 of the Vermilion Area, South Addition. The feature is a pair of northwest-southeast trending ridges separated by a valley. It covers an area of approximately 28 km². The bank lies close to the shelf break and has the shallowest crest (46 m) of the shelf-edge banks west of the Mississippi delta except for the Flower Garden Banks. The crest of the bank lies at 46 m depth, with a depth of 130 m approximately one kilometre south of the crest (Figure VI-19). The maximum relief is approximately 85 m.

Structure and Physiography

The bank appears to be underlain by a northwest-southeast oriented ridge of salt. Dissolution of salt at the crest of the ridge has created an axial graben (Figures VI-19, 20, and 21). The faults on Figure VI-22 outline the graben.

The seafloor roughness map (Figure VI-23) shows large areas containing features ranging in size from less than one metre to over five metres in height and a spatial frequency of from 5 to 10 features per hectare.

Sedimentology

No sediments were collected at 18 Fathom Bank.

BRIGHT BANK

General Description

Bright Bank is located at 27°53'N latitude and 93°18'W longitude (Figure VI-1) in Blocks 650, 656, and 657 of the West Cameron Area, South Addition. It lies near the shelf edge and is about 10 n.m. east of 28 Fathom Bank. The bank is rhomboid in shape and covers an area of approximately 36.5 km² (Figures VI-24 and 25). The surrounding water depths range from 100 m to the west to 120 m to the southeast. Depths increase generally towards the south. The crest of the bank lies at 50 to 55 m depth. The total relief on the bank ranges from 50 to 65 m.

Structure and Physiography

Although 35 7 kHz sub-bottom profiles were taken at Bright Bank, the very poor reflectivity of the sub-bottom sediments prevented the preparation of a structure map for this bank. Natural gas seeps were observed during the submersible transect, and the poor quality of the sub-bottom profiles may be due to the presence of gas charged sediments. Figure VI-26 illustrates the poorly reflective nature of the sub-bottom and also depicts linear outcrops covered by reef growth on the side-scan sonar record between shot points 4 and 16. The dark areas on the record between shot points 21 and 26 are probably hard bottom without reef development.

Because of the limited sub-bottom data, the structure of the bank must be interpreted from the bathymetry. The steep slopes surrounding the bank are most probably the expression of a peripheral fault (Figure VI-24). The lineations on the west, north, and east sides of the bank are the results of radial faulting. The trough that lies to the south-east of the reentrant in the northwest corner of Lease Block 657 is probably the northwestern part of a central graben (Figure VI-24).

The crest of the bank at between 50 and 55 m is a broad surface of very low relief. Observations from the submersible reveal scattered outcrops of Pleistocene reef rock over this surface. Relief on the reef rock is estimated to be between 45 and 60 cm. The rock is jointed and the joints have been enlarged by solution. Large areas of coarse sand, coral, and algal nodules lie between the joint blocks.

The seafloor roughness map (Figure IV-27) shows individual features ranging in height from one to five metres and with spatial frequency ranging up to over 10 features per hectare. The outcrop trends indicated on this figure support the presumption of radial faulting on this bank.

Sedimentology

Analyses of the four samples show a variety of sediment types as follows:

Station	Sediment Type	Depth (m)
1	Sandy mud	122
2	Slightly gravelly sand	82
3	Sandy gravel	85
4	Algal nodules	66

Station 1 may be interpreted as the transition between the Amphistegina Sand Facies and the Quartz-Planktonic Foraminifers Facies. Stations 2 and 3 represent the lower portion of the Algal-Nodule Facies, and Station 4 is in the Algal Nodule Facies.

Recommendations

Because of the limited sub-bottom data, it is difficult to delineate hazardous features on this bank. It is quite probable that the lineations shown on Figure VI-26 represent faults that intersect the seafloor. These areas should be avoided as sites for permanent structures such as production platforms.

STETSON BANK

General Description

Stetson Bank is located at 28°09'55"N latitude and 94°17'40"W longitude (Figure VI-1) in Lease Block A-502 of the High Island Area, South Addition. It is a small bank covering only about 3 km². The bank is oval shaped and oriented in a northeast-southwest direction (Figures VI-28 and 30). The crest of the bank lies at a depth of 32 m; however, a pinnacle near the west side of the crest rises to a depth of 20 m (Figure VI-35). Surrounding depths are 64 m to the north and 62 m to the south. Total relief on the bank is approximately 40 m. Because of its small size, Stetson was mapped at a scale of 1:3000.

Structure and Physiography

The structure of Stetson Bank is almost impossible to determine from the 3.5 kHz records due to the poor reflectivity of the strata (Figure VI-34). Submersible observations of the bank reveal the cause of the poor reflectivity to be the nearly vertical orientation of the bedding. Figure VI-31 shows the poor reflectivity of the sub-bottom and two steeply dipping strata on the southeast side of the bank. The asymmetric profile of the bank is also illustrated in Figure VI-32 with the steep slope to the northwest.

Stetson appears to be a simple, small fault block that may be related to a much larger structure in the subsurface. Better quality seismic lines are necessary to determine its structural relationships to the surrounding area. Figures VI-31 and 32 show a relatively flat, eastward sloping surface at the crest of the bank. The average depth of this surface is about 22 m. Submersible observations show the surface of this terrace to consist of steeply dipping claystones and siltstones. The obvious interpretation is that this is an erosional terrace that has been tilted due to continued movement on the western boundary fault since sea level stood at approximately 17 m (approximately 6000 years ago).

Side-scan sonar records and direct observations of the bottom during 1974 using the DRV DIAPHUS reveal the bank to consist of steeply dipping claystones and siltstones. The strike of the beds varies from N22°E to N50°E, and the dips vary from 78° towards the southeast to nearly vertical. The claystones are extensively bored by molluscs and sponges but appear to be more resistant to submarine erosion than the

siltstones. The claystones form ridges, with valleys underlain by siltstones between them. The ridges are nearly parallel to the long dimensions of the bank and stand 3 to 4 m above the adjacent siltstones.

Sedimentology

Three sets of sediment samples have been collected at Stetson Bank over the years. The first set of 18 samples was collected by Conrad Neumann in 1957 (Table C-3) and used in a technical report (Neumann, 1958). The second set of 11 samples was collected in June 1974 by the present author for a baseline survey of Stetson Bank for Signal Oil and Gas Company (Tables C-3 and C-5). The third set of 28 samples taken from four stations was collected in 1976 for BLM (now MMS) (Bright and Rezak, 1978a). The locations of these samples are given in Figure VI-29. Appendix C, Table C-4, lists the available textural parameters and particle type identification for these samples.

Figure VI-33 shows the distribution of sediment types at Stetson Bank. The sediments range from gravelly sands to sandy muds; the amount of gravel generally increases towards the bank. The gravel fraction consists primarily of molluscs and rock fragments. The sand fraction is primarily quartz sand and mollusc fragments. Table C-5 in Appendix C gives the counts of particle types from the Signal Oil and Gas Co. samples. Table C-6 lists the particle type data for the samples taken in 1976.

Mineralogically, the sediments on and around Stetson Bank are similar to those on other banks where large areas of bare Tertiary bedrock are exposed. In the coarse fraction, quartz is the most abundant mineral. It is most probably derived from erosion of the siltstones that are so abundant on the bank. In the <.002 mm fraction, smectite is the most abundant clay mineral at stations surrounding the bank, but in the size range from .005 to .002 mm, illite may be the predominant clay mineral. Again, this is probably due to erosion of the claystones on the bank.

MACNEIL BANK

Introduction

MacNeil Bank was mapped during August 1980. Oceanonics, Inc. conducted the survey using the M/V JUNE BOLLINGER, a leased 39.6 m vessel. The survey was conducted using LORAC service chain "DE." The LORAC receivers were interfaced with a Decca Autocarta System. LORAC calibration was performed at known platform locations within the survey area. Survey equipment included a Raytheon DE 719B echosounder, an ORE Model 310 sub-bottom profiler operated at 3.5 kHz, an EG&G Model 231-232 Uniboom operated at 500 joules, and an EG&G SMS 960 side-scan sonar.

A benchmark made of a 55-gallon oil drum filled with concrete was emplaced at the crest of the shallowest peak.

General Description

MacNeil Bank is located at 28°00'25"N latitude and 93°31'W longitude (Figure VI-1), in Lease Blocks A-351 and A-368 of the High Island Area, Southeast Addition (Figures VI-36 and 37). It is situated approximately 10 km northeast of the East Flower Garden Bank.

The bank is ovoid in shape and is constricted on its southwestern extremity. Completely enclosed by the 80 m isobath, the bank lies on the edge of a four to six metre high, south-facing escarpment. The area mapped is considerably larger than the bank owing to uncertainty about its position prior to the survey. It is a small bank with an area of approximately 4 km². The western and southeastern slopes are the steepest, with more gentle slopes towards the northeast and north.

Structure and Physiography

The structure and physiography of MacNeil Bank are interpreted on the basis of the boomer seismic profiles and the side-scan sonar mosaic. The main structure of the bank is a tilted fault block, with the major fault trending northeast-southwest. The western boundary of the bank is along this fault (Figures VI-38 and 39b). Numerous discontinuous faults, subparallel to the major fault, lie on either side of it. One of these minor faults forms the eastern boundary of the bank (Figure VI-39b). Several east-west trending faults lie along the southern boundary of Lease Blocks A-350, A-351, and A-352 and coincide with the low, south-facing escarpment.

The entire survey area appears to have a thin veneer of sediments covering well lithified sedimentary formations similar to those seen at Coffee Lump, Stetson, and Claypile Banks. These sedimentary units are generally flat-lying, except where they have been deformed by faulting. The very sharp and regular lineations on the upthrown side of the major fault are bedrock outcrops that have little or no cover of reef rock. The very shallow occurrence of lithified sedimentary rocks accounts for the ringing in the upper 10 to 20 m of the seismic records (Figures VI-39a and 39b). This ringing masks any reflectors that may exist in that interval.

A large field of sand waves with steep sides towards the northeast lies in Lease Block A-352 and in the northeast quarter of Lease Block A-353 (Plate 2, side-scan mosaic). The intensity of the reflections is lower than that in the gravel waves at the West Flower Garden Bank, where the waves are composed of algal nodules. The MacNeil waves are most probably sand size sediment.

To the east of the main fault in Lease Block A-351 and the western half of Lease Block A-350, numerous irregular mottles are displayed on the side-scan sonar mosaic. The mottles vary from less than 5 m to over 200 m in diameter. These are most probably outcrops of bedrock that have been encrusted by thick deposits of coralline limestone. Numerous anchor scars are present in the area to the east of the main

fault. A major pipeline crosses the map area near the northeast corner of Lease Block A-350.

The structure at MacNeil bank supports the hypothesis that structures inherited from the Jurassic basement are important in the formation of salt diapirs. The diapir at MacNeil Bank occurs at the intersection of two fault systems, which creates a zone of weakness along which the salt has risen.

Hazards

The numerous faults that displace the seafloor at MacNeil Bank indicate that this area has a potential for tectonic activity. Sporadic movement along these faults should be expected.

Gas seeps were observed on the 3.5 kHz and the Uniboom records; these seeps are generally associated with the two major faults. Figure VI-39a and 39b show large areas of hazy and chaotic reflections that may be due to the presence of gas in the sediments.

Conclusions and Recommendations

Nothing is known of the nature of the seafloor at MacNeil Bank as no submersible work was conducted there. BLM Visual Graphic No. 3 shows the sediment in Lease Blocks A-350 and A-351 to be silty clays.

Because of the numerous faults that displace the seafloor, no structures should be emplaced until a detailed minisparker survey is conducted over the proposed site. Permanent structures should be located at least 152 m (500 ft) away from any surface or subsurface fault.

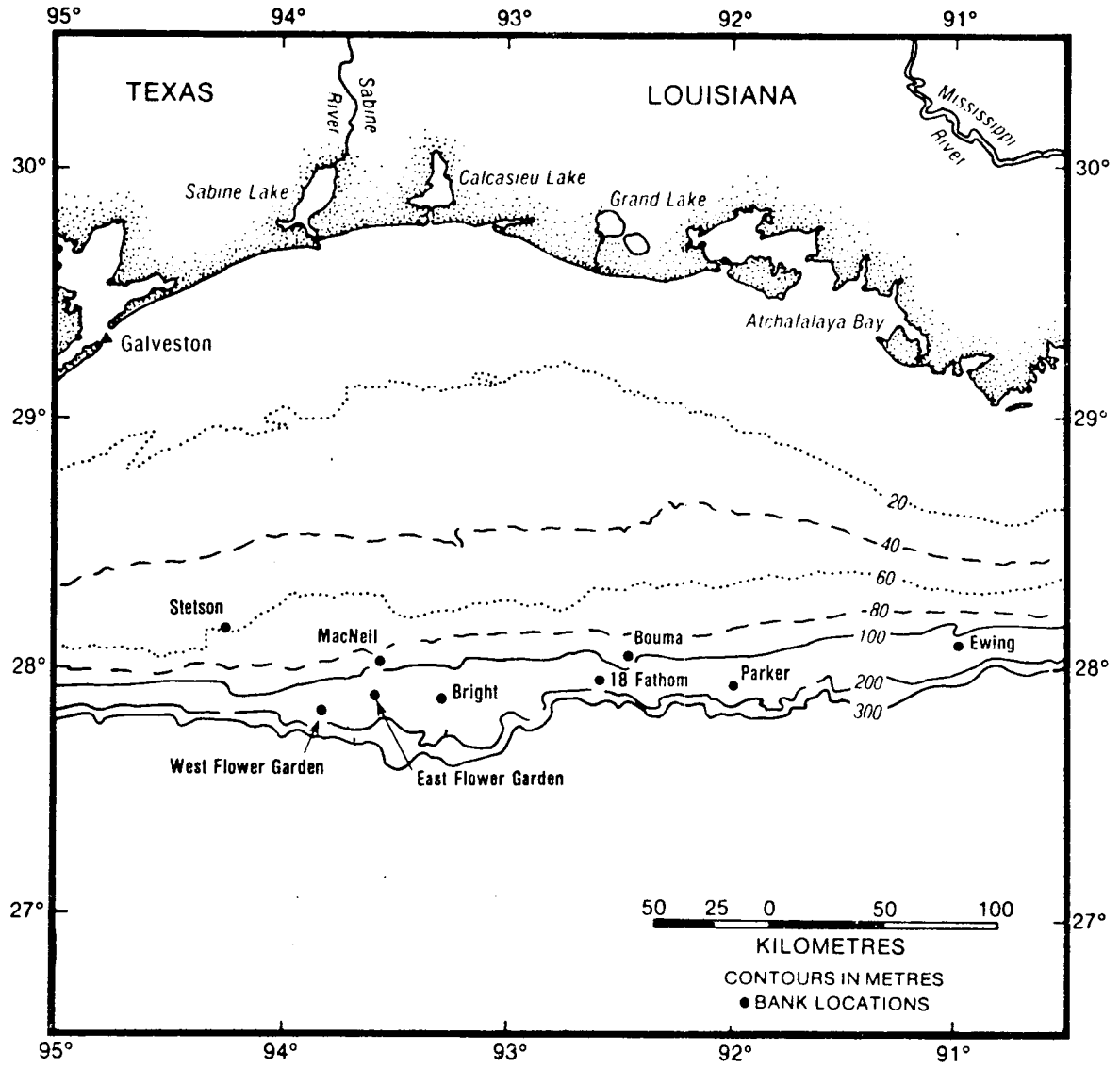


Figure VI-1. Location map for selected banks.

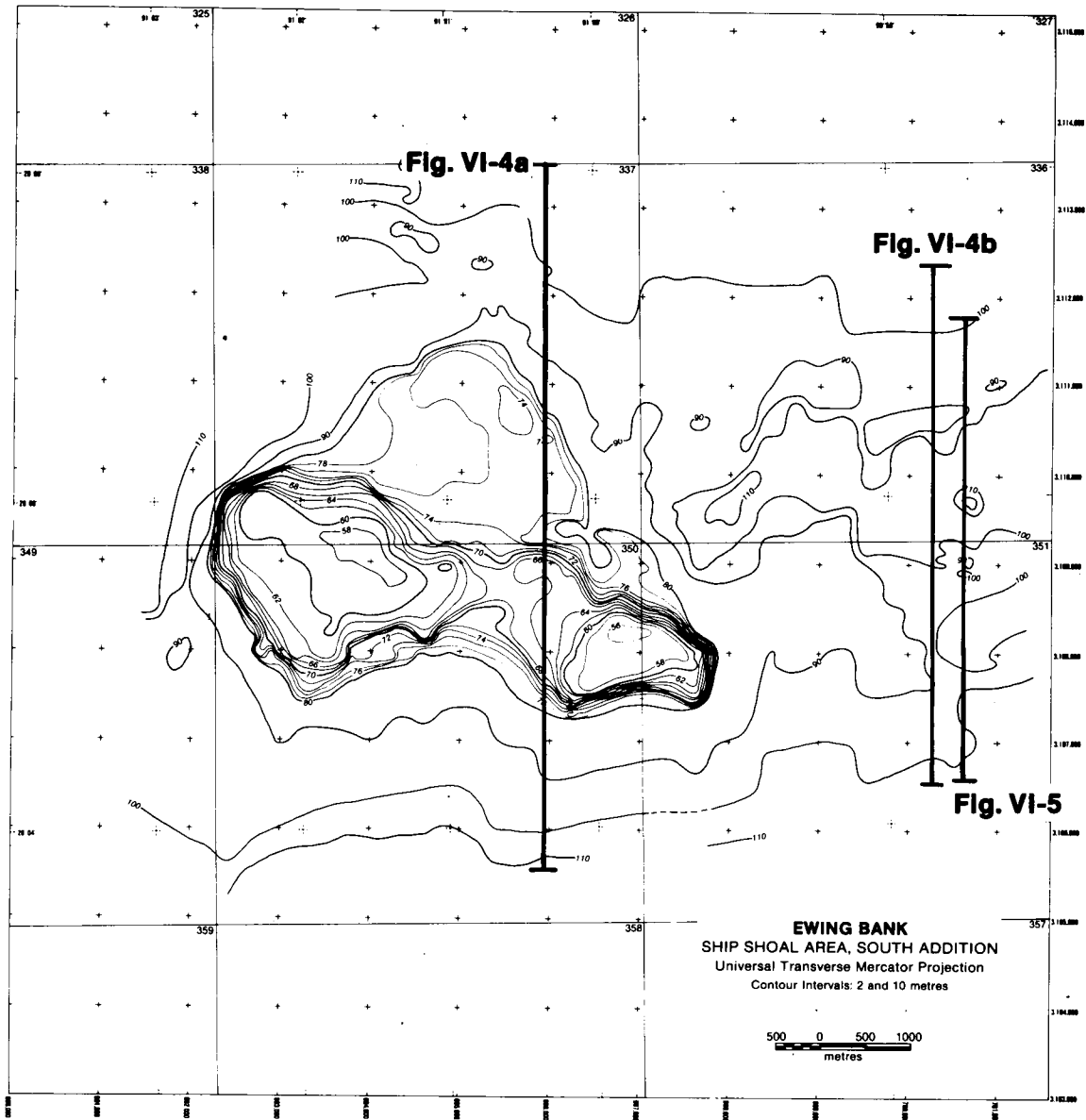
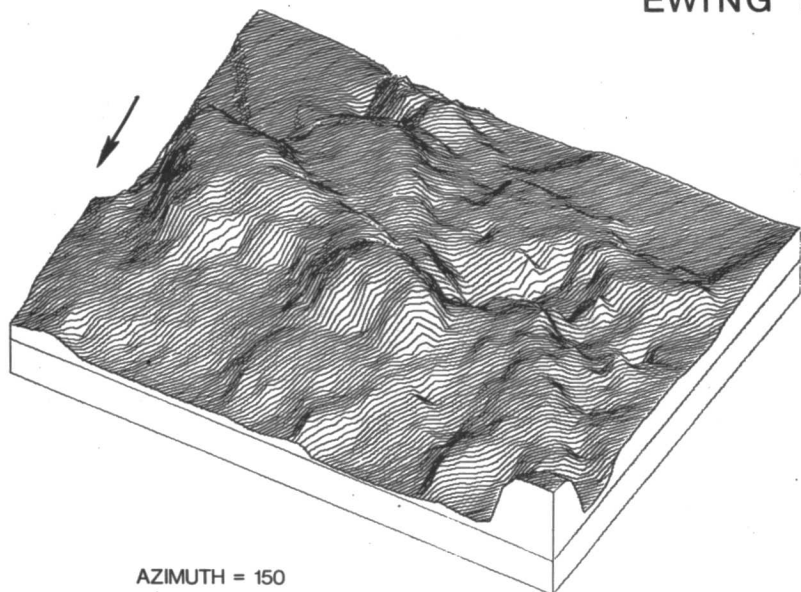


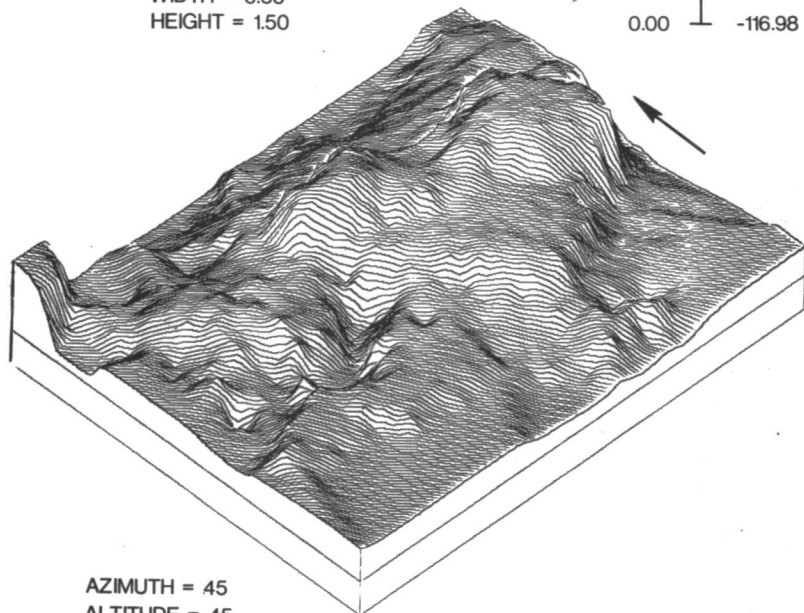
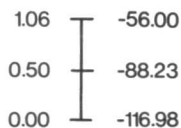
Figure VI-2. Bathymetric map of Ewing Bank showing locations of seismic lines illustrated in Figures VI-4 and 5.

EWING BANK



AZIMUTH = 150
 ALTITUDE = 45

BEFORE FORESHORTENING
 WIDTH = 6.50
 HEIGHT = 1.50



AZIMUTH = 45
 ALTITUDE = 45

BEFORE FORESHORTENING
 WIDTH = 6.50
 HEIGHT = 1.50

Prepared by
 Department of Oceanography
 Texas A&M University

Figure VI-3. Perspective views of Ewing Bank. Arrows point toward north. Graphic vertical scale relates the total range of water depths (right) to the arbitrary computer units after foreshortening (left).

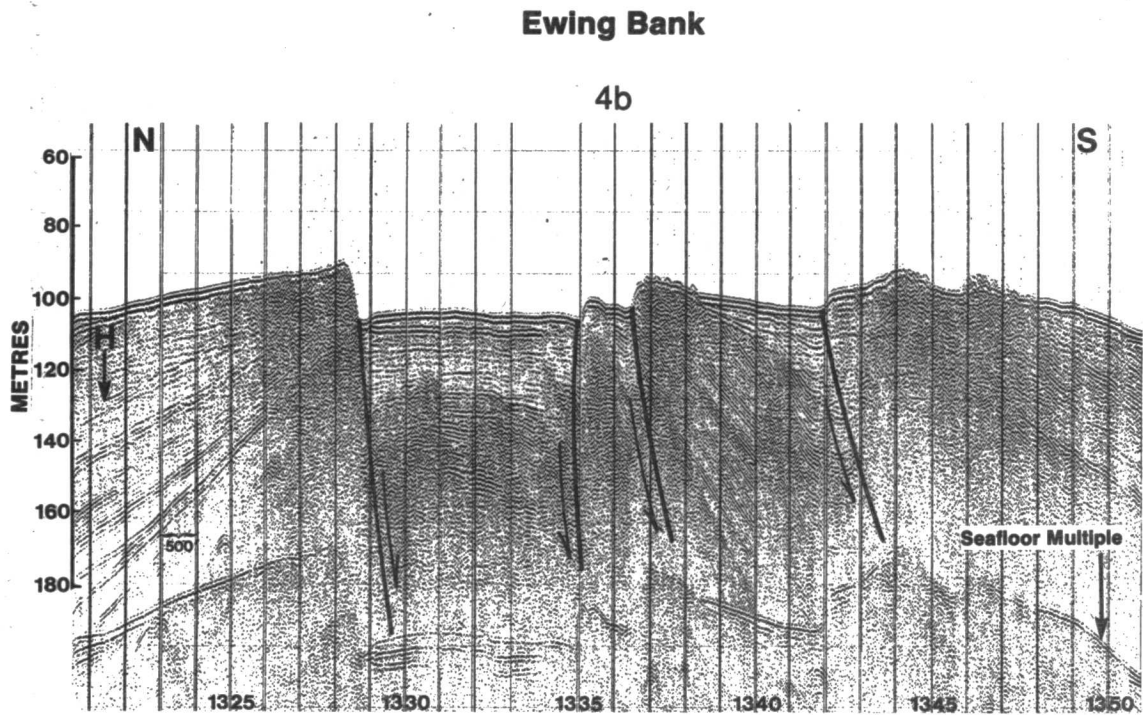
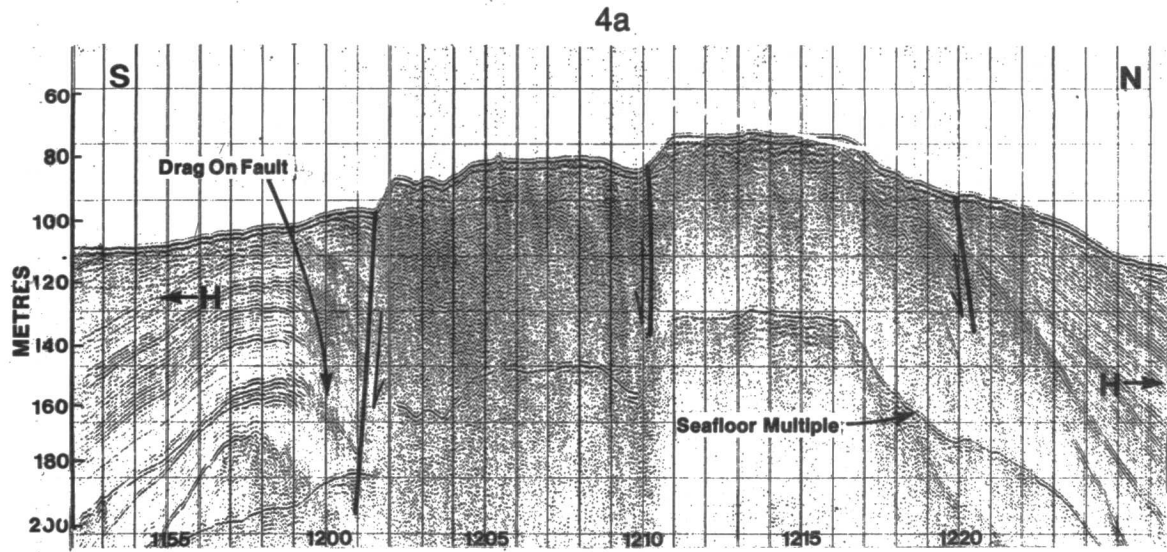


Figure VI-4. Boomer profiles on Ewing Bank. H = horizon.

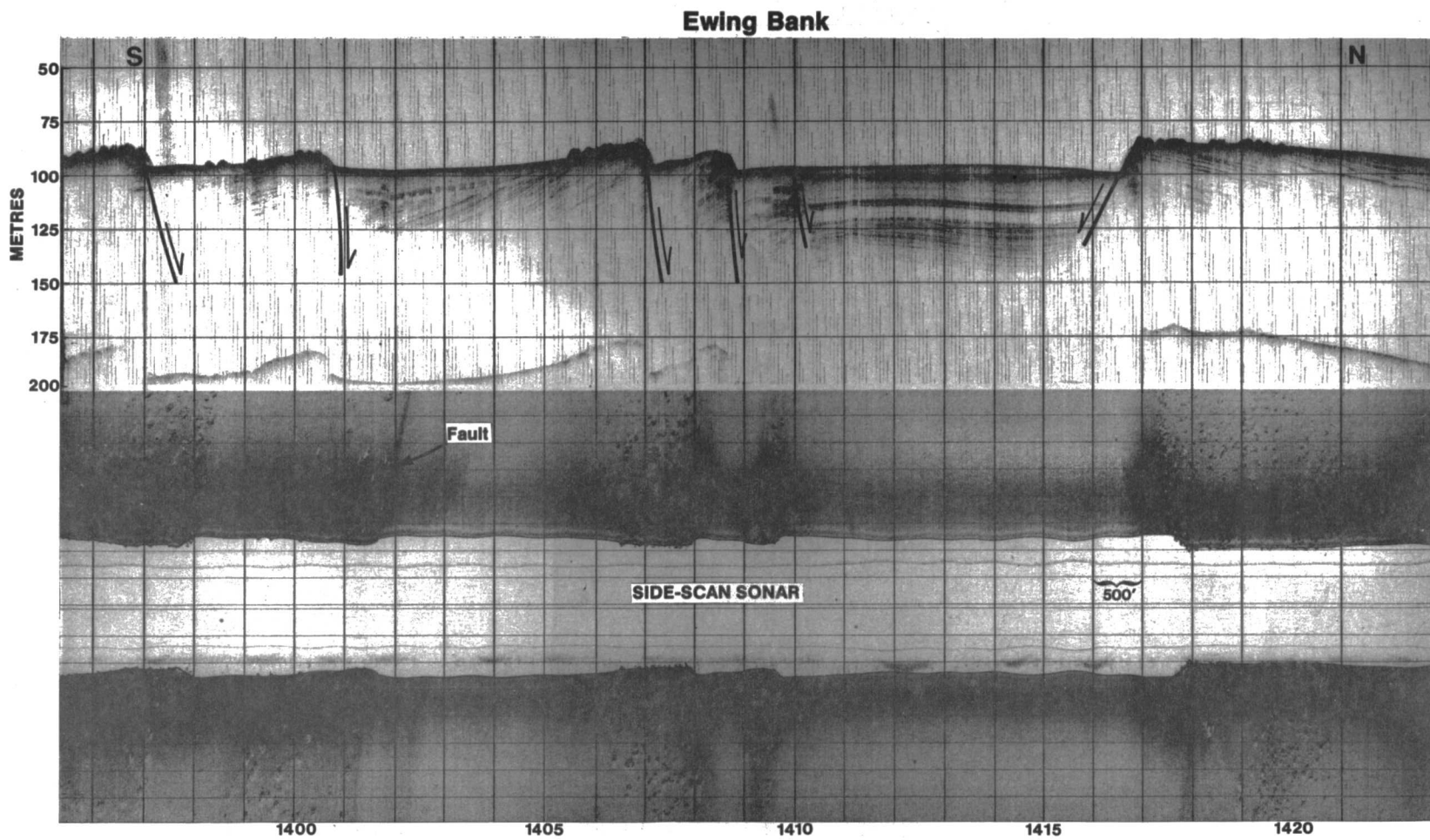


Figure VI-5. A 7 kHz high resolution sub-bottom profile and side-scan sonar record on Ewing Bank.

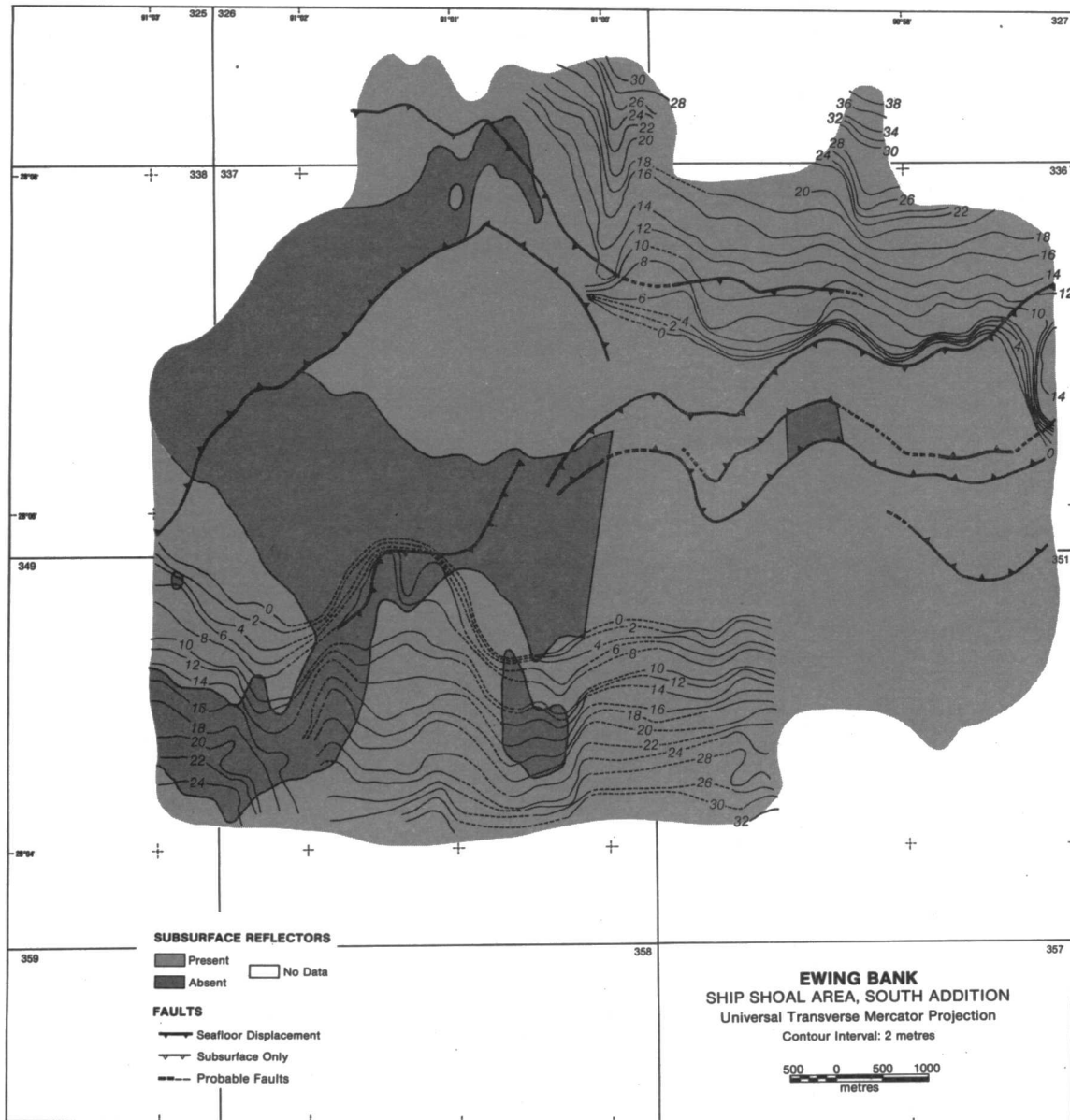


Figure VI-6. Structure-Isopach map of Ewing Bank. Contours are isopachs (sediment thickness) from the seafloor to reflector H on Figure VI-4.

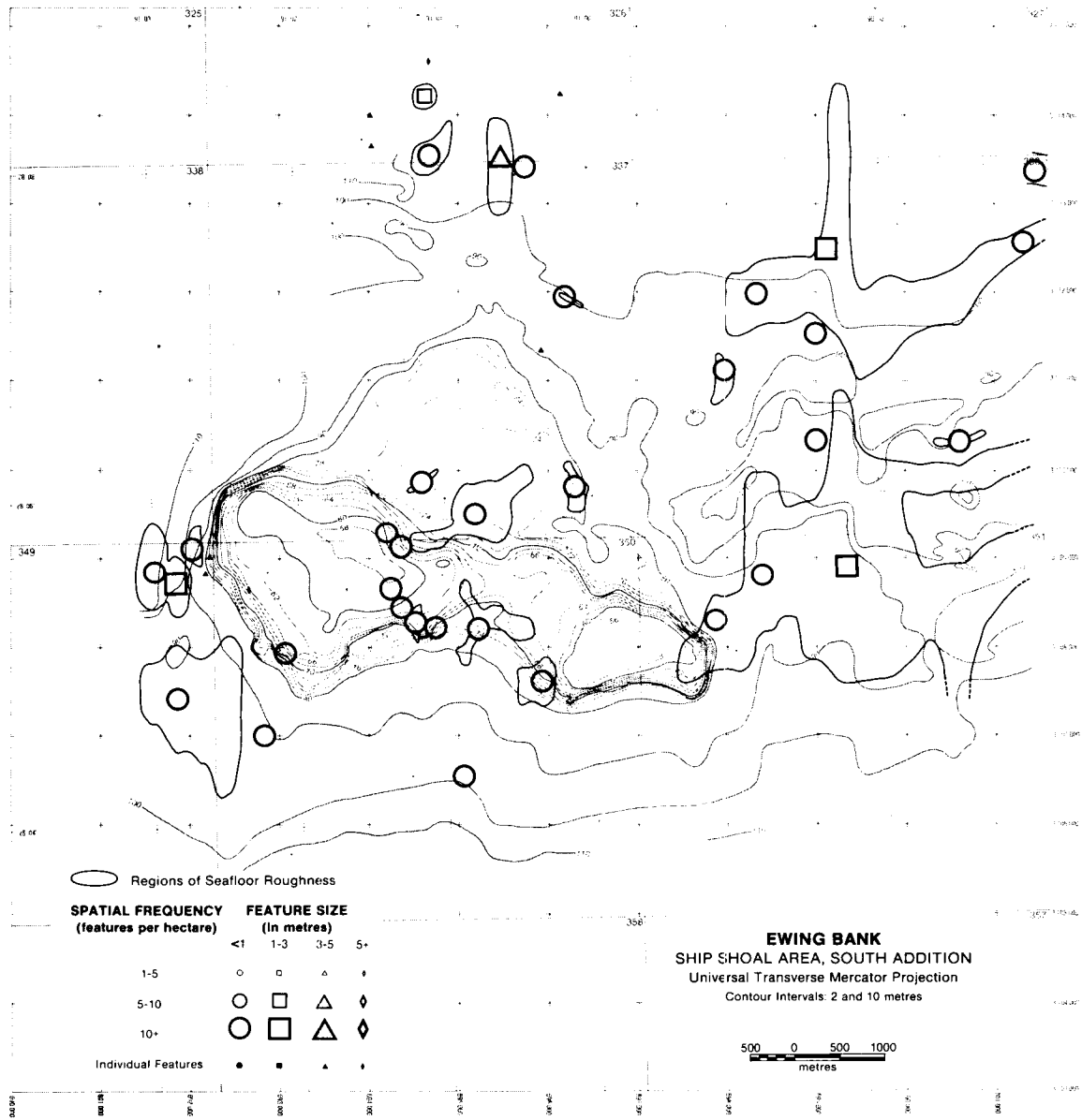


Figure VI-7. Seafloor roughness map of Ewing Bank.

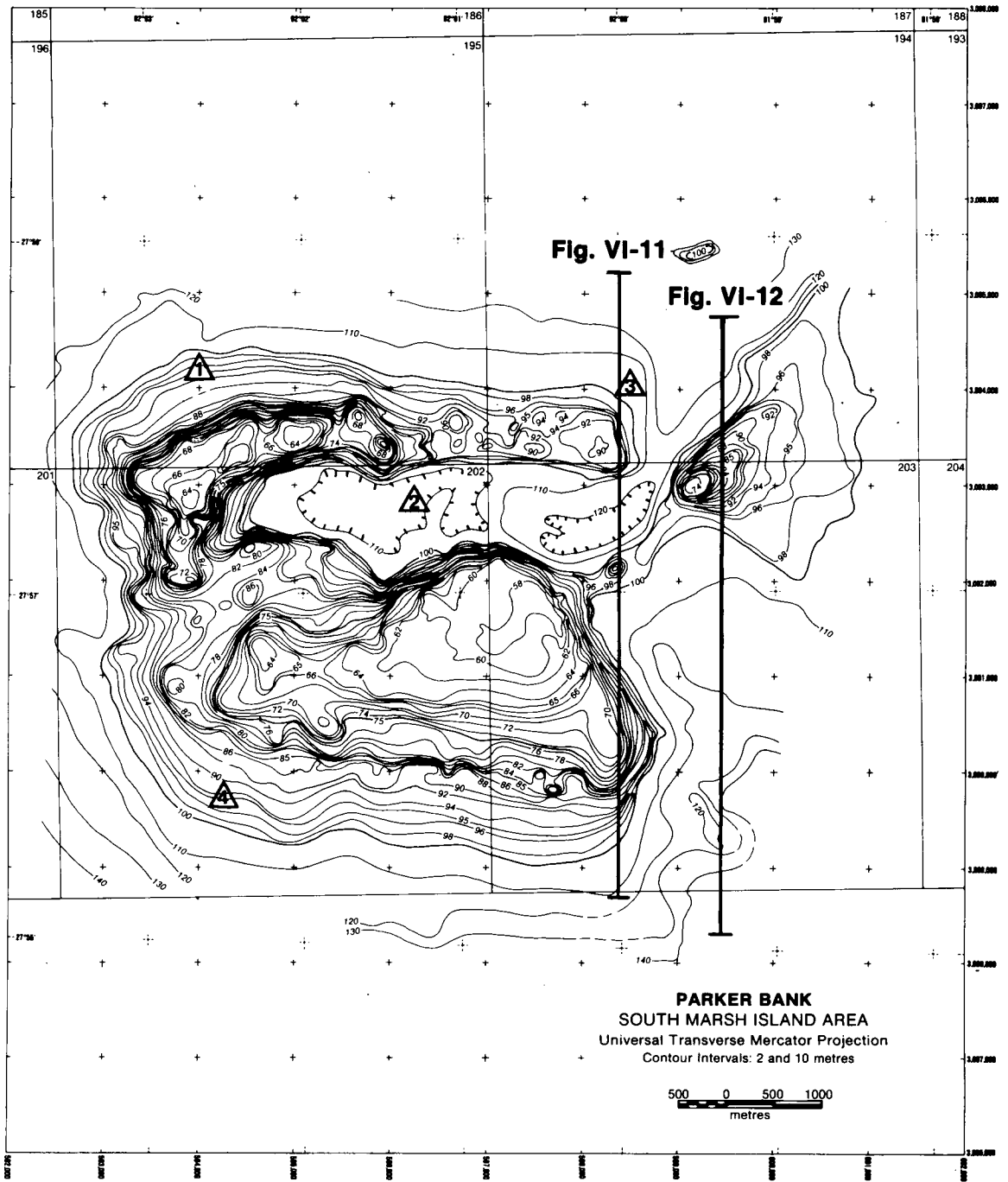


Figure VI-8. Bathymetric map of Parker Bank showing sediment sample locations and seismic lines illustrated in Figures VI-11 and 12.

PARKER BANK

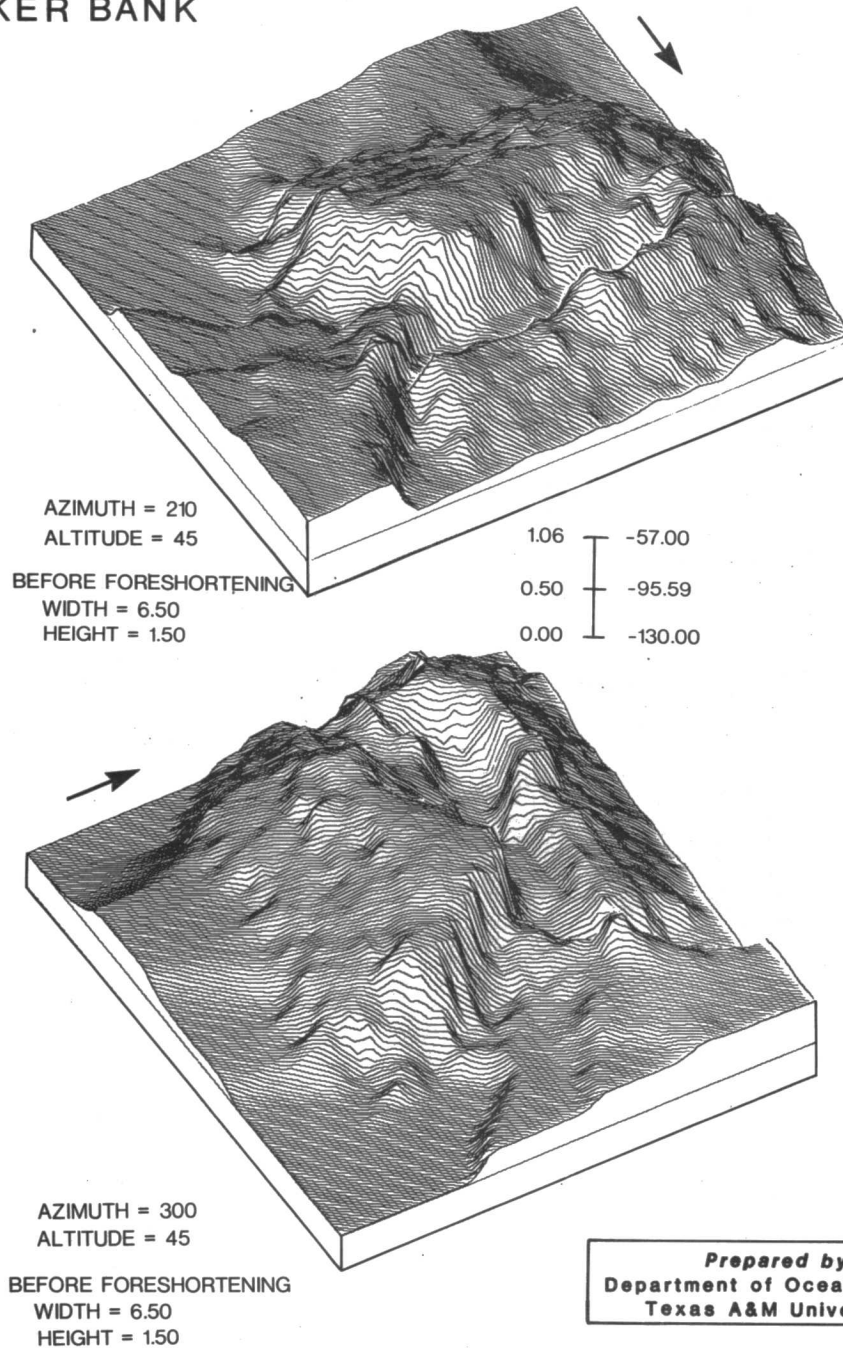


Figure VI-9. Perspective views of Parker Bank. Arrows point toward north. Graphic vertical scale relates the total range of water depths (right) to the arbitrary computer units after foreshortening (left).

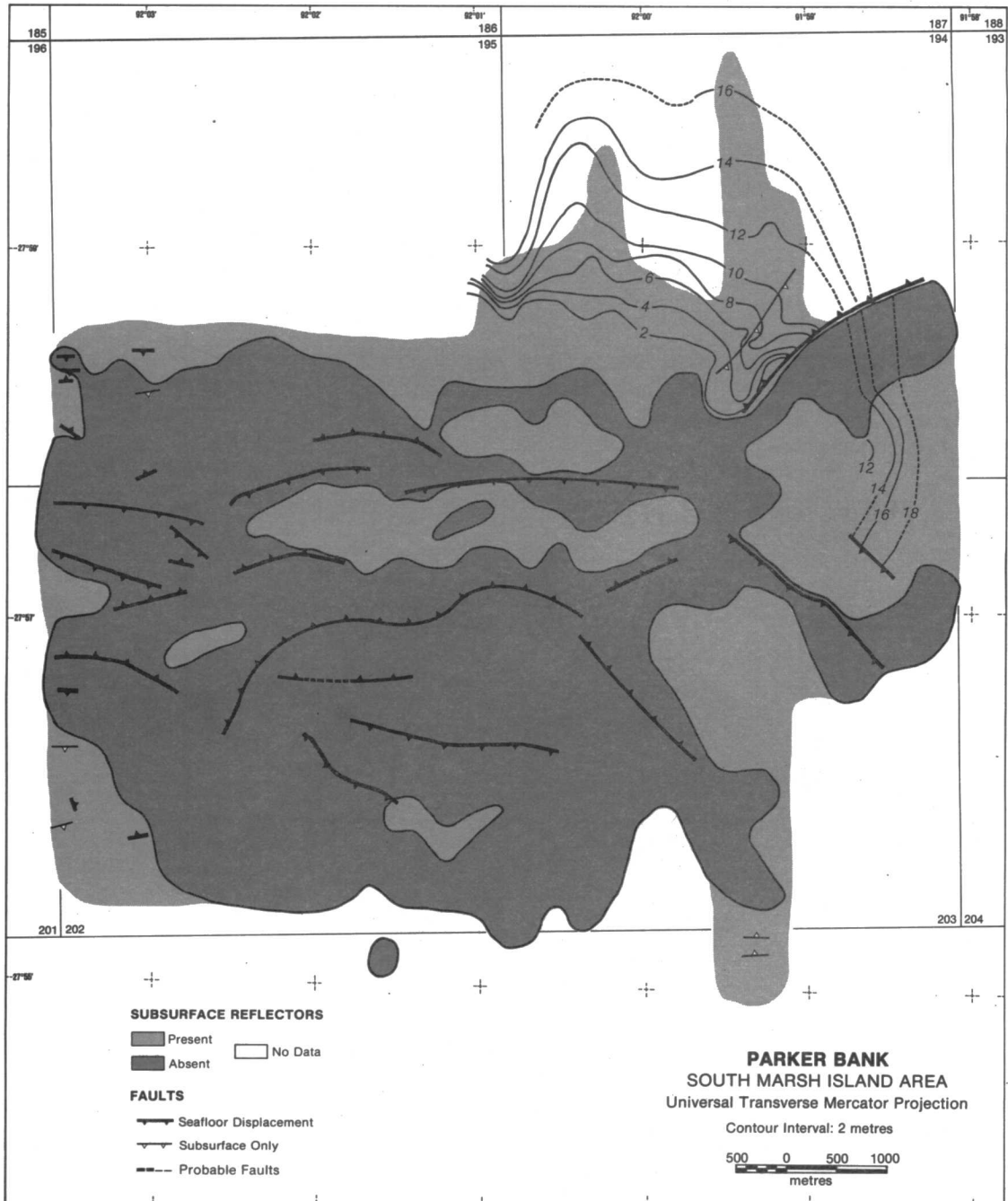


Figure VI-10. Structure-Isopach map of Parker Bank. Contours are isopachs (sediment thickness) from the seafloor to reflector H on Figures VI-11 and 20.

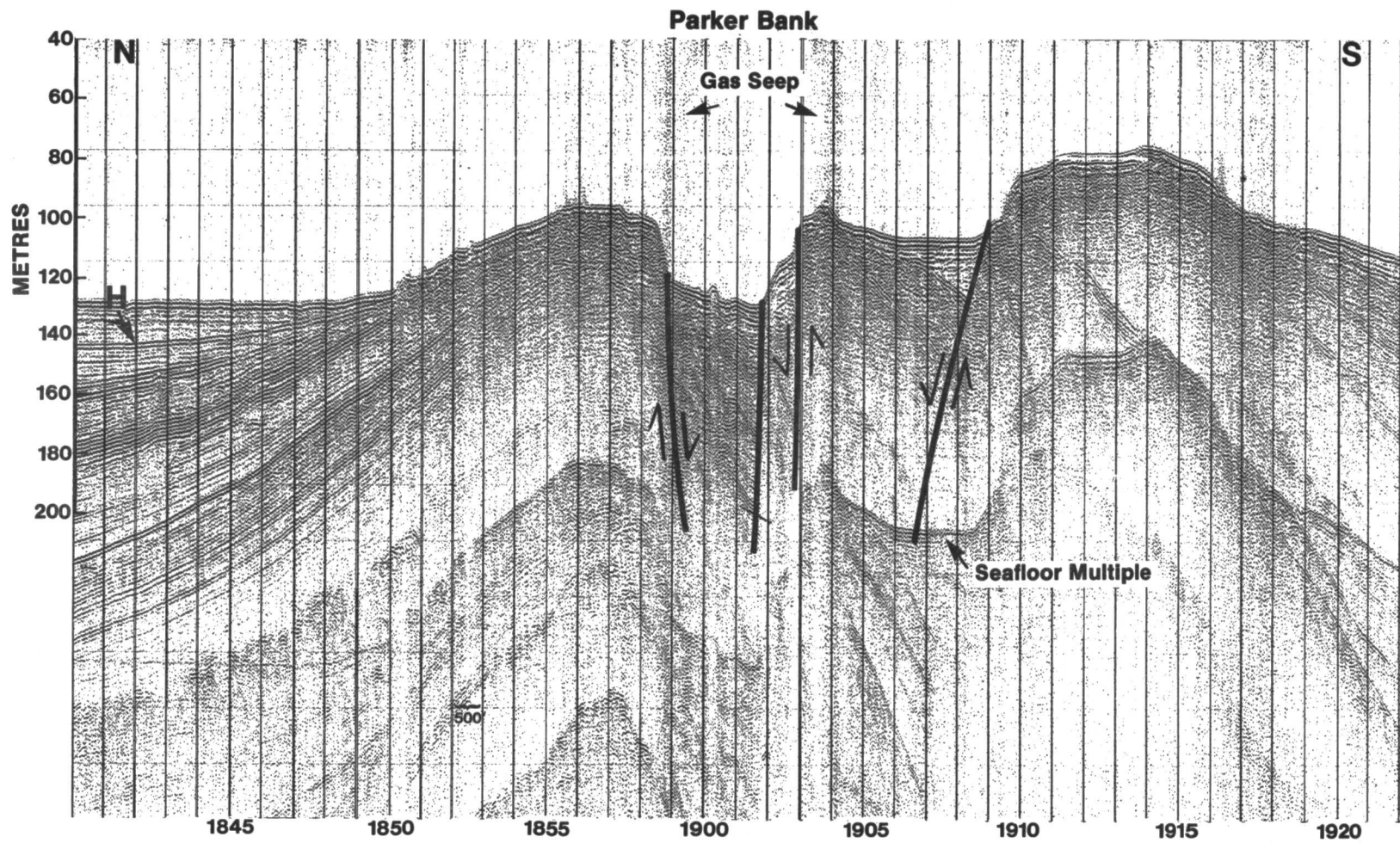


Figure VI-11. Boomer profile across Parker Bank. H = horizon.

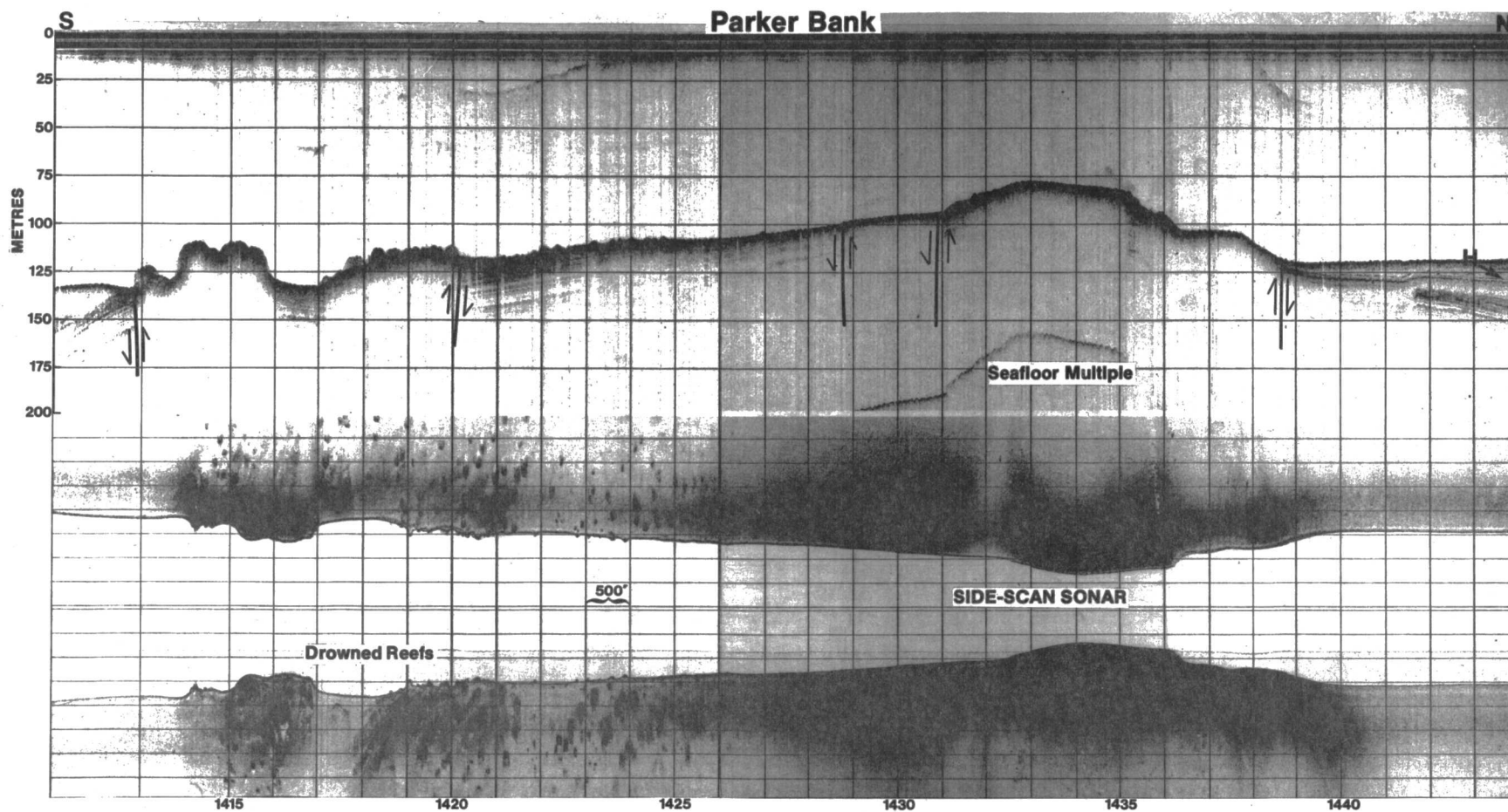


Figure VI-12. A 7 kHz high resolution sub-bottom profile across Parker Bank. H = horizon.

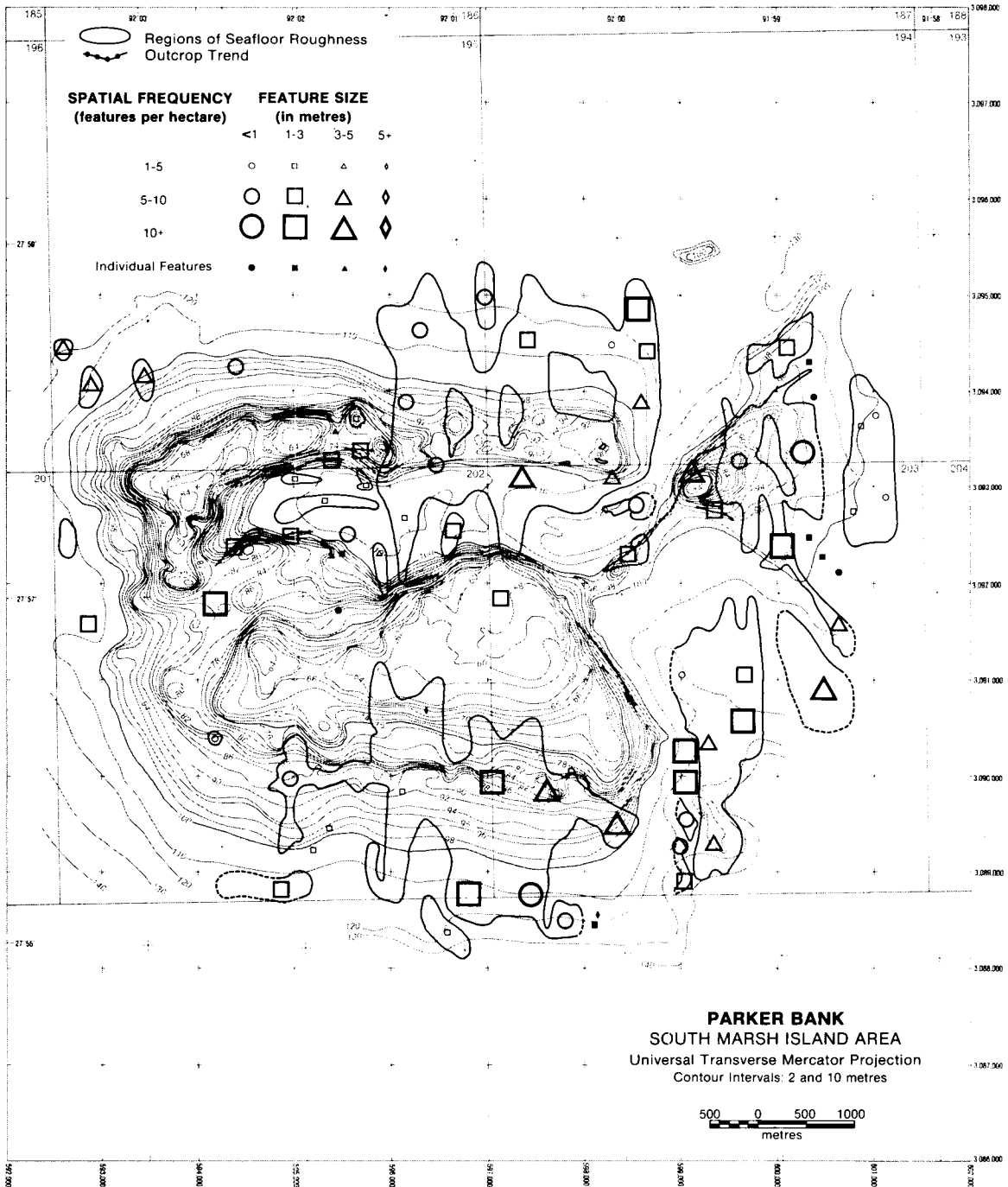


Figure VI-13. Seafloor roughness map of Parker Bank.

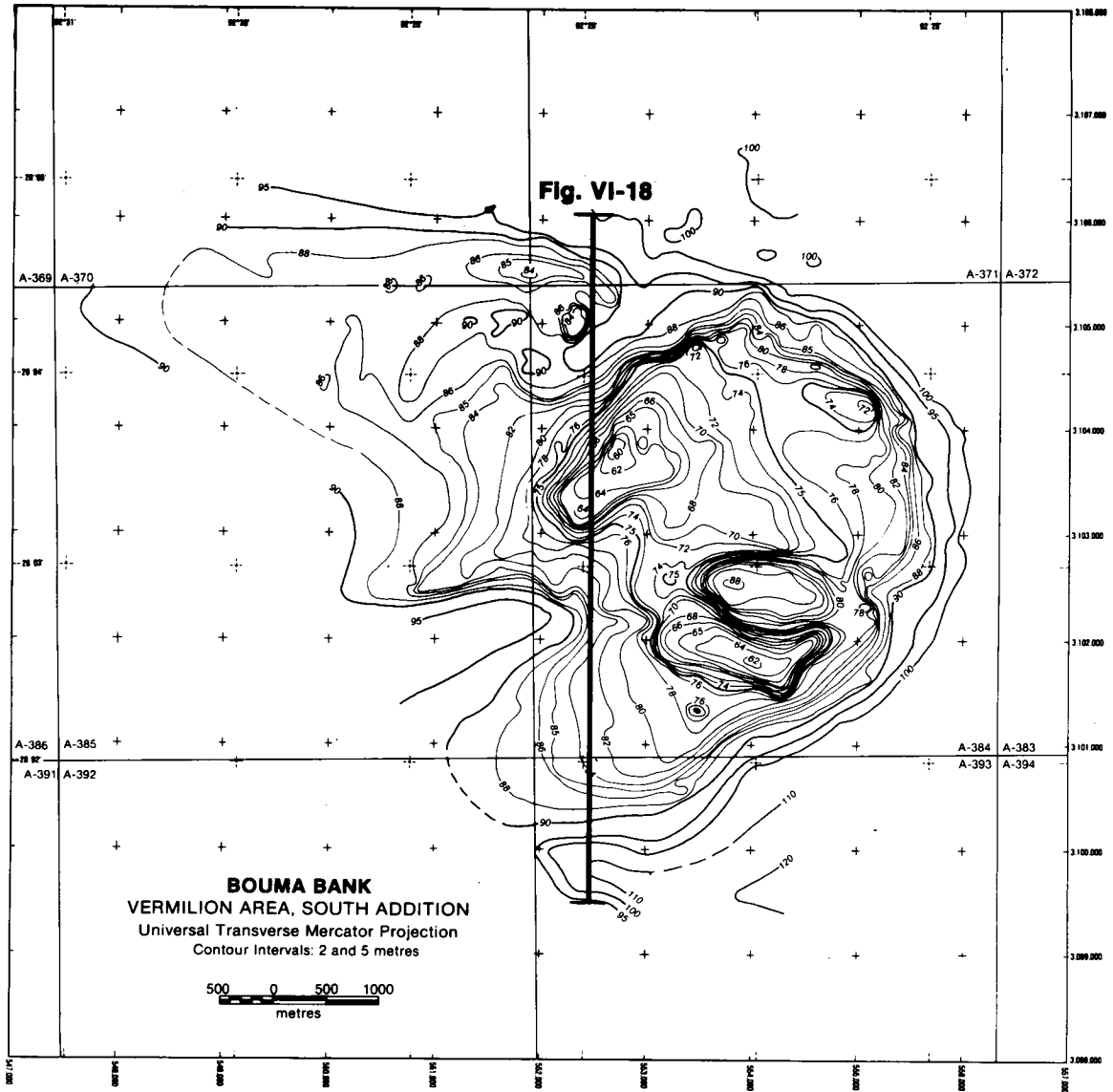


Figure VI-14. Bathymetric map of Bouma Bank showing location of seismic line and side-scan sonar record illustrated in Figure VI-18.

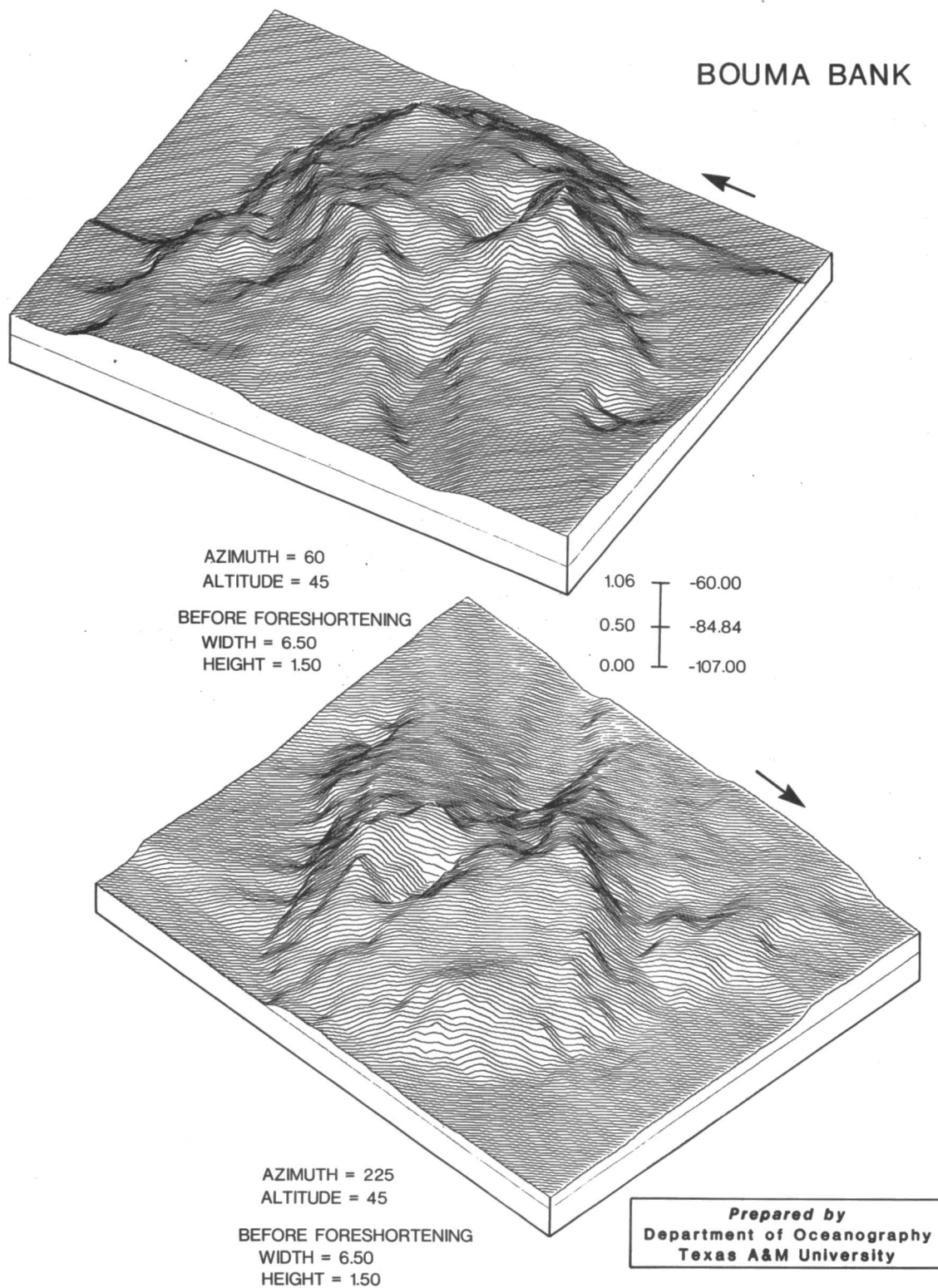


Figure VI-15. Perspective views of Bouma Bank. Arrows point toward north. Graphic vertical scale relates the total range of water depths (right) to the arbitrary computer units after foreshortening (left).

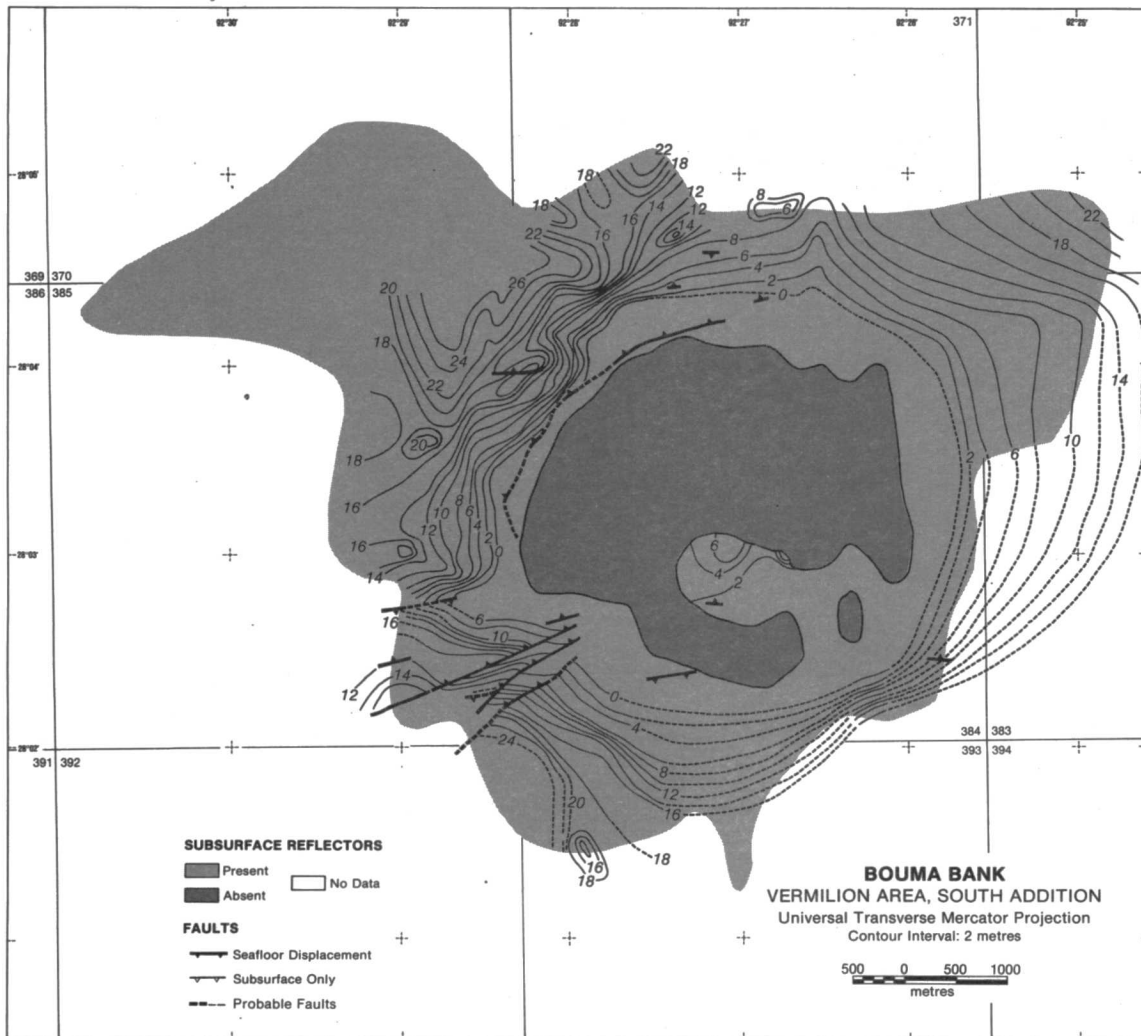


Figure VI-16. Structure-Isopach map of Bouma Bank. Contours are isopachs (sediment thickness) from the seafloor to reflector H on Figure VI-18.

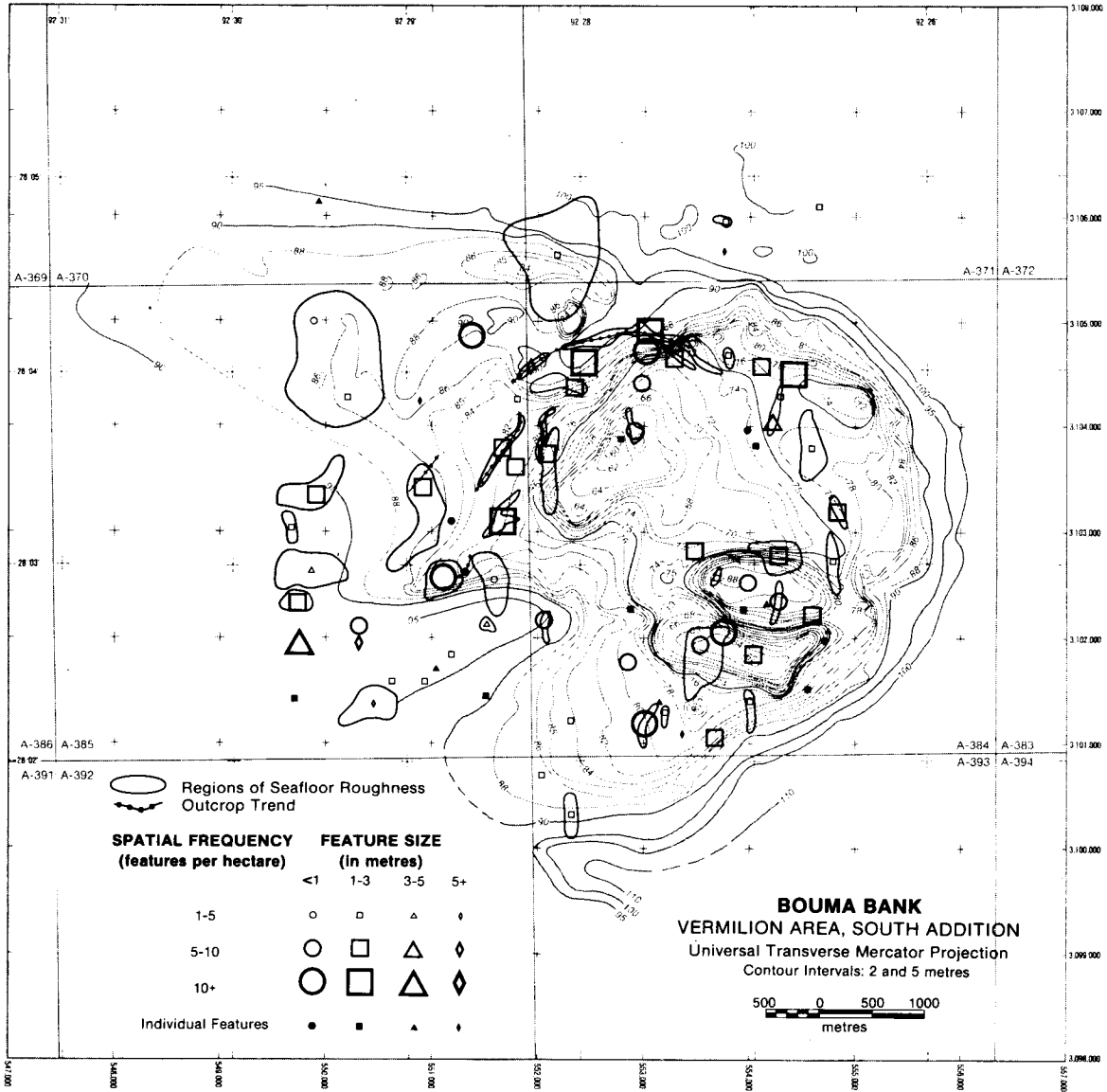


Figure VI-17. Seafloor roughness map of Bouma Bank.

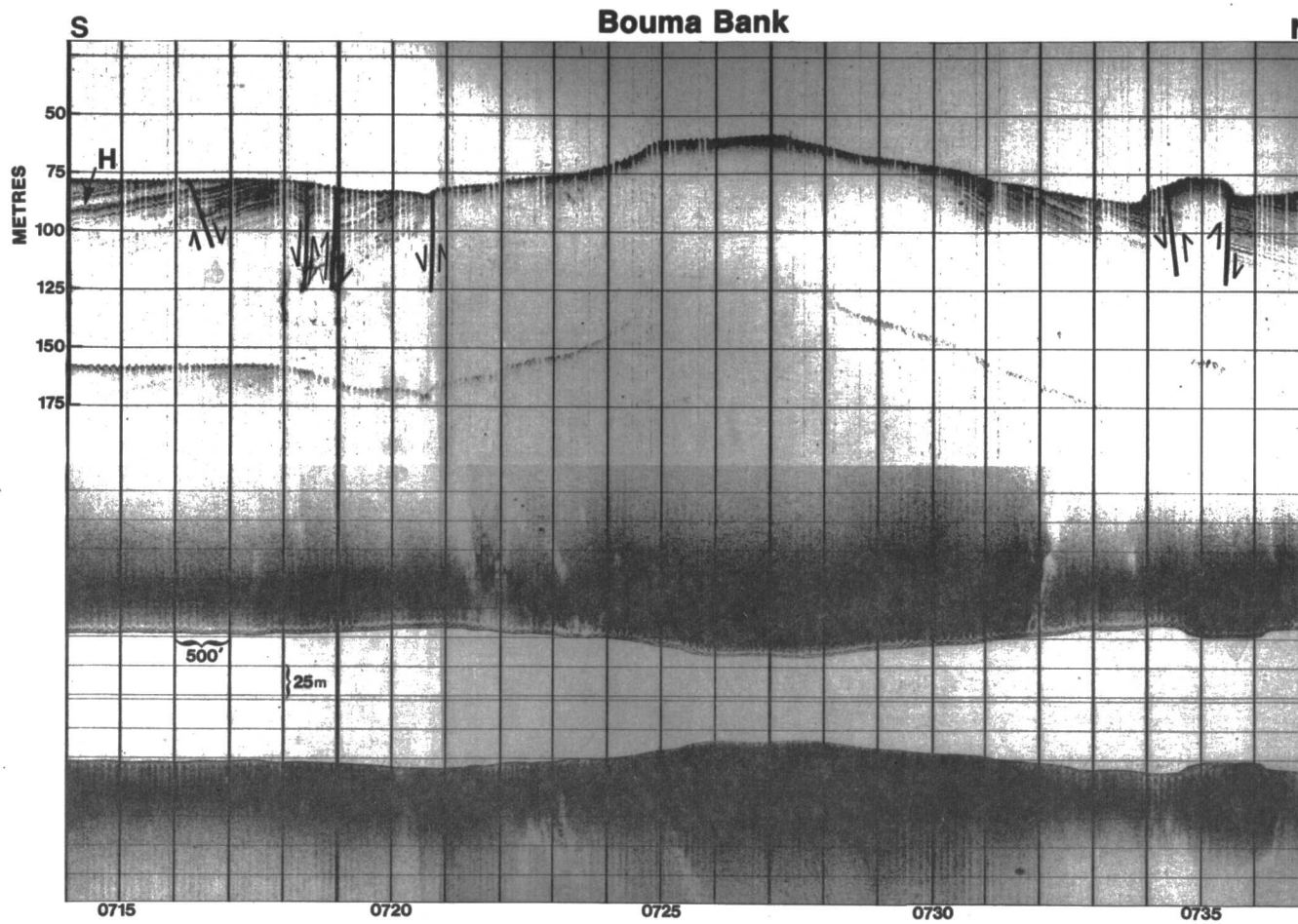


Figure VI-18. A 7 kHz high resolution sub-bottom profile and side-scan sonar record across Bouma Bank. .H = horizon.

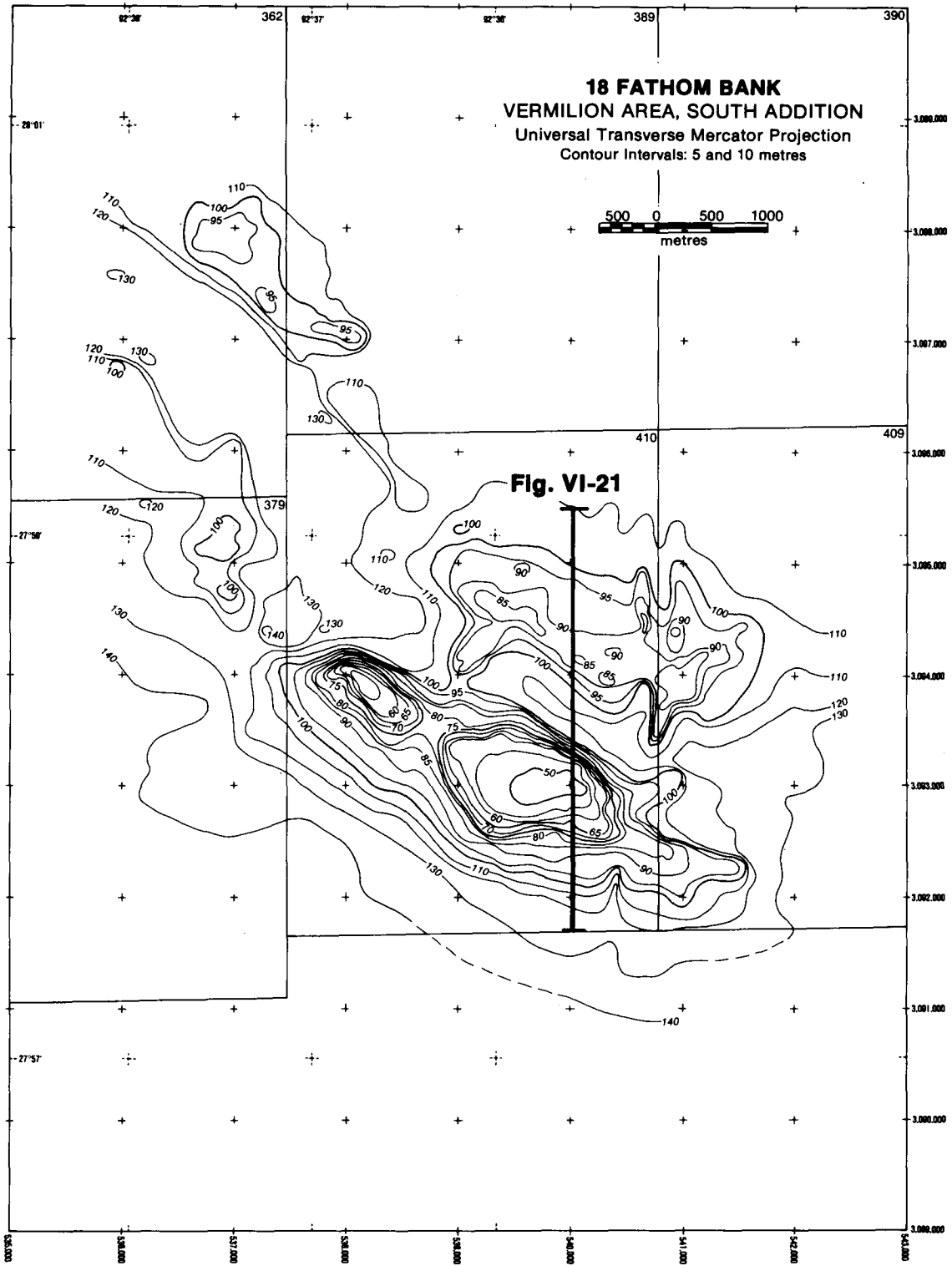


Figure VI-19. Bathymetric map of 18 Fathom Bank showing location of the seismic line illustrated in Figure VI-21.

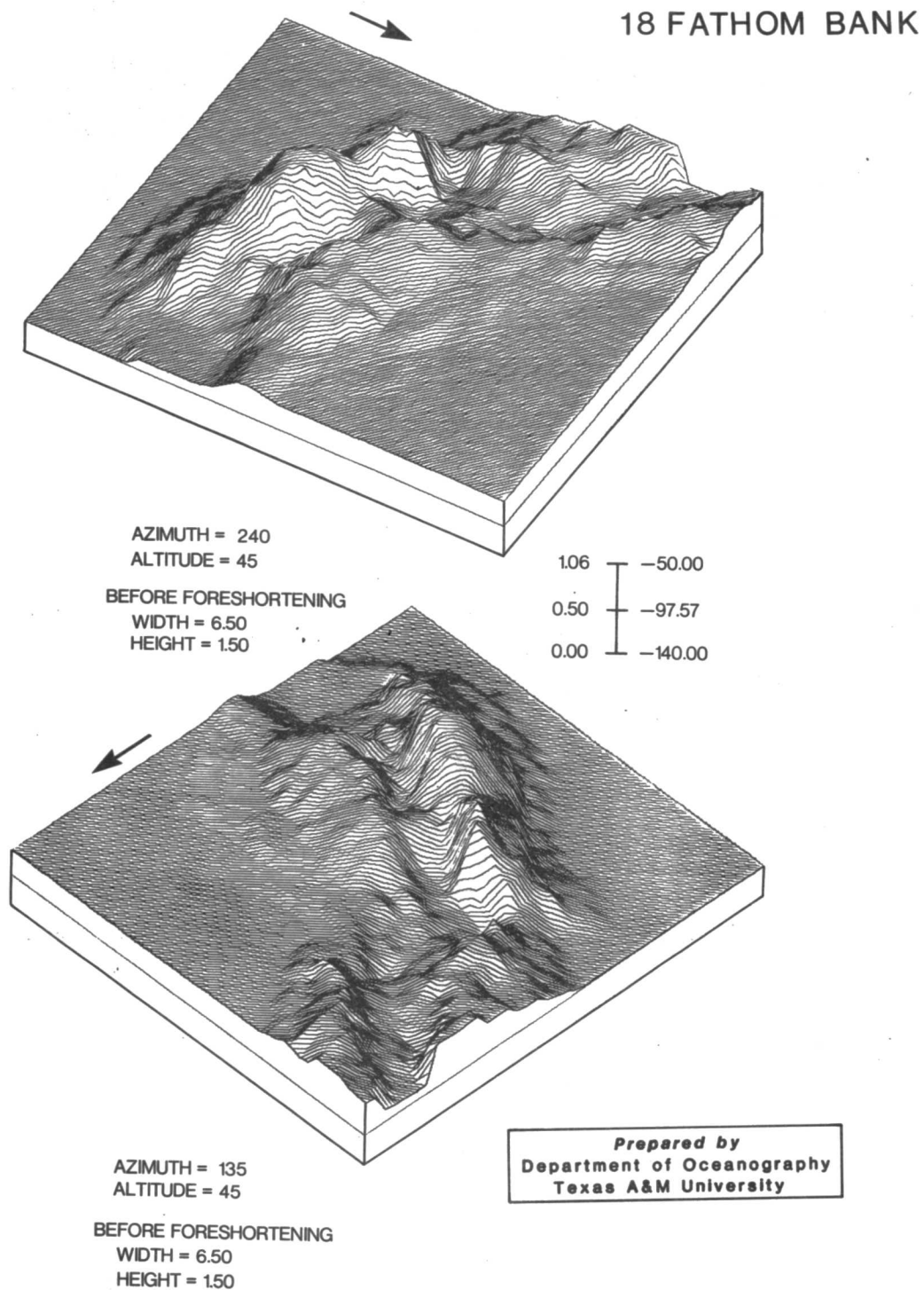


Figure VI-20. Perspective views of 18 Fathom Bank. Arrows point toward north. Graphic vertical scale relates the total range of water depths (right) to the arbitrary computer units after foreshortening (left).

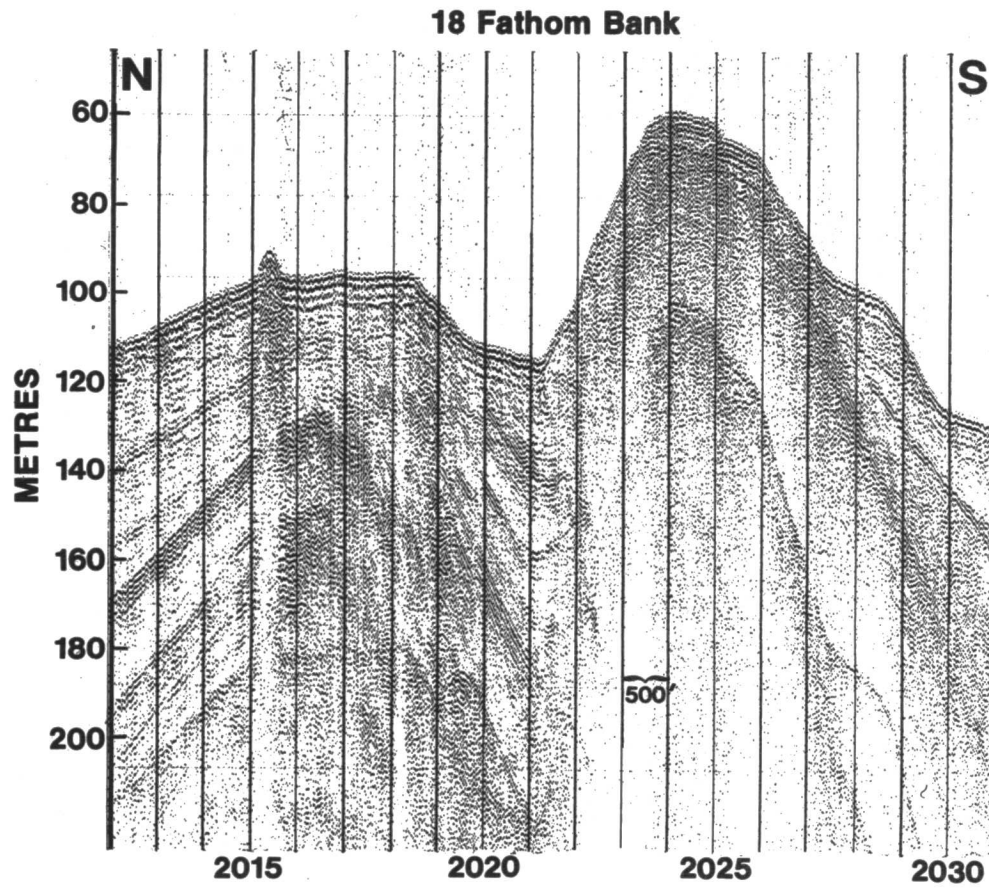


Figure VI-21. Boomer profile across 18 Fathom Bank.

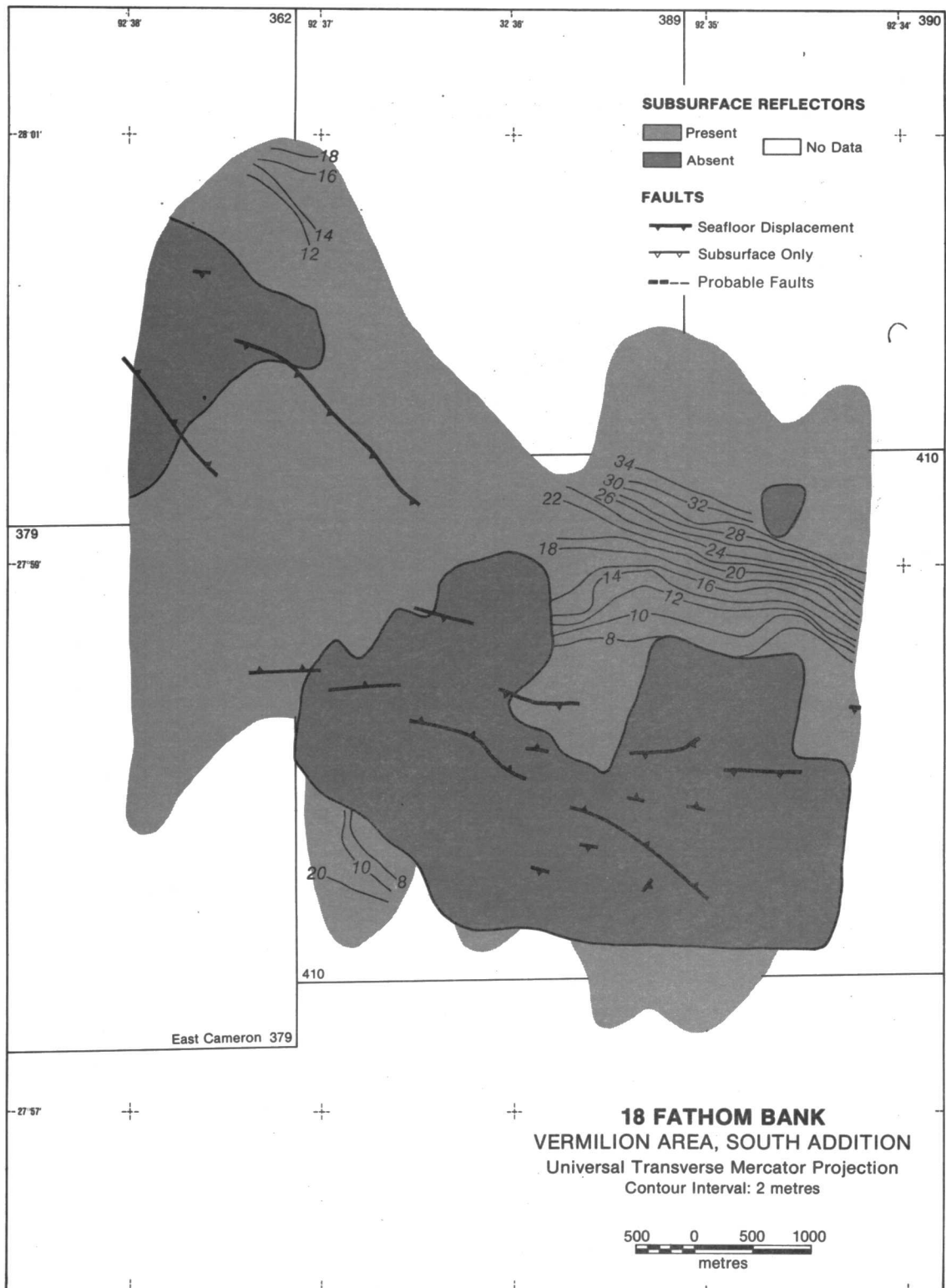


Figure VI-22. Structure-Isopach map of 18 Fathom Bank. Contours are isopachs (sediment thickness) from the seafloor to reflector H on Figure VI-21.

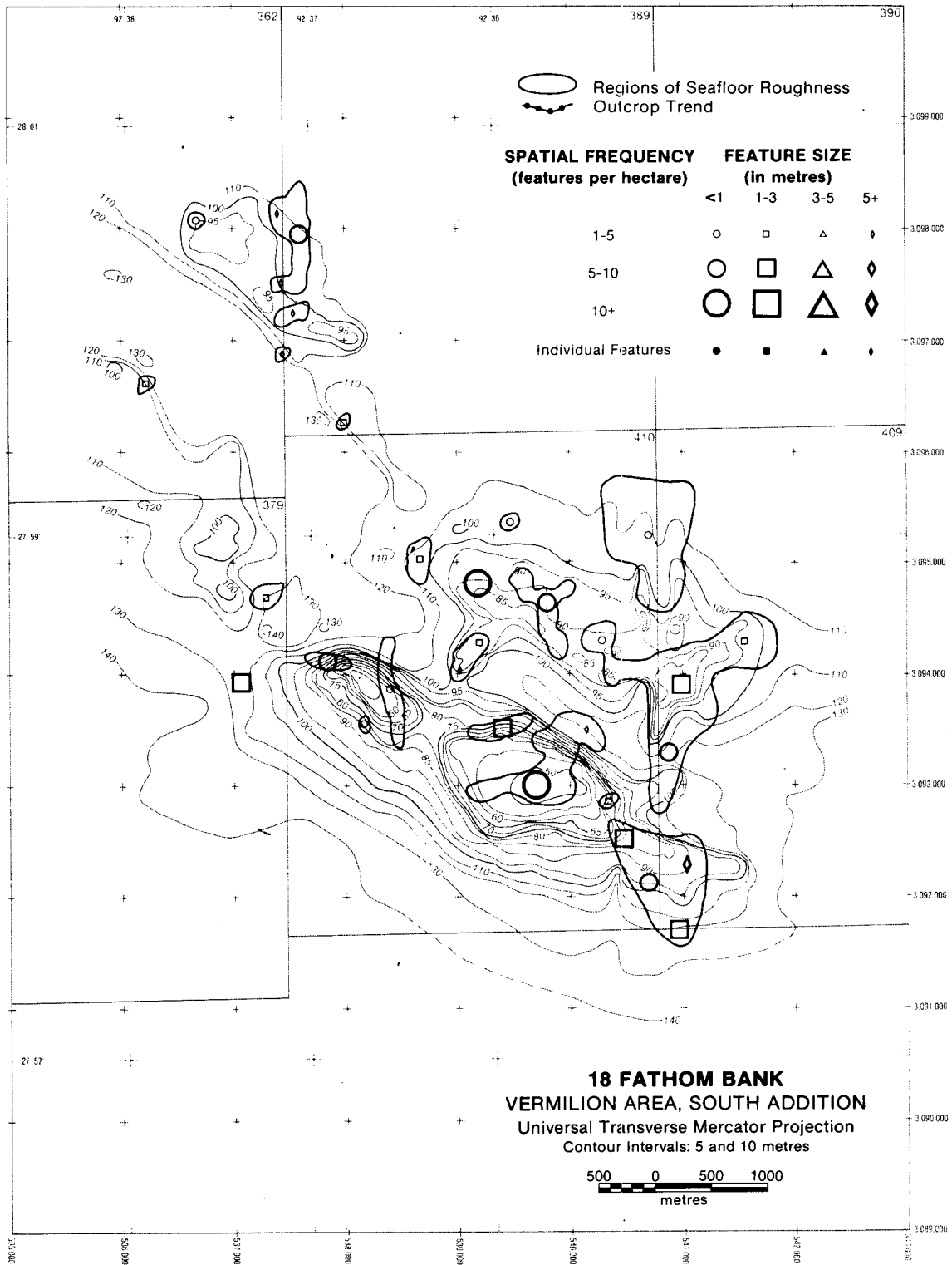


Figure VI-23. Seafloor roughness map of 18 Fathom Bank.

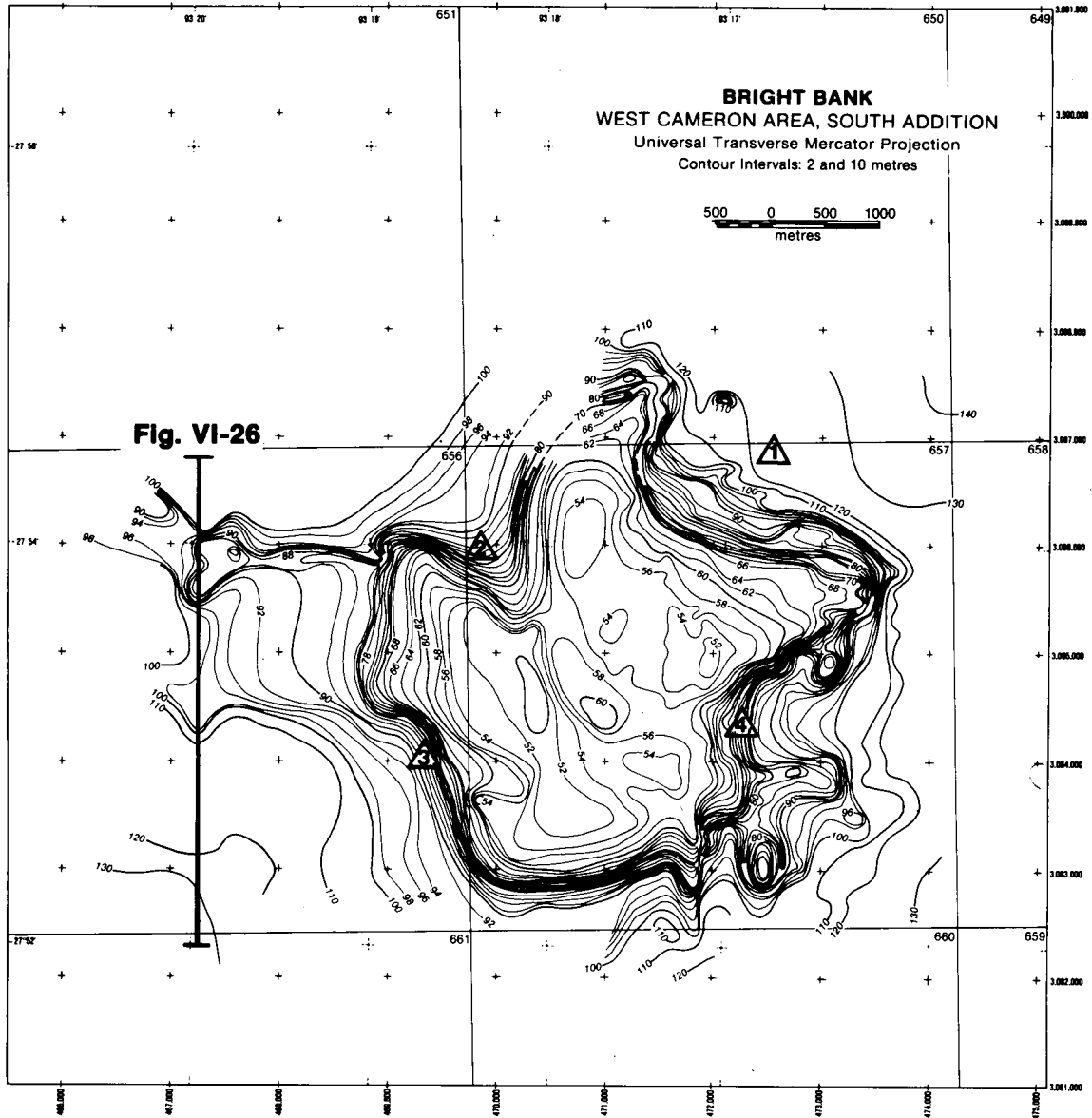
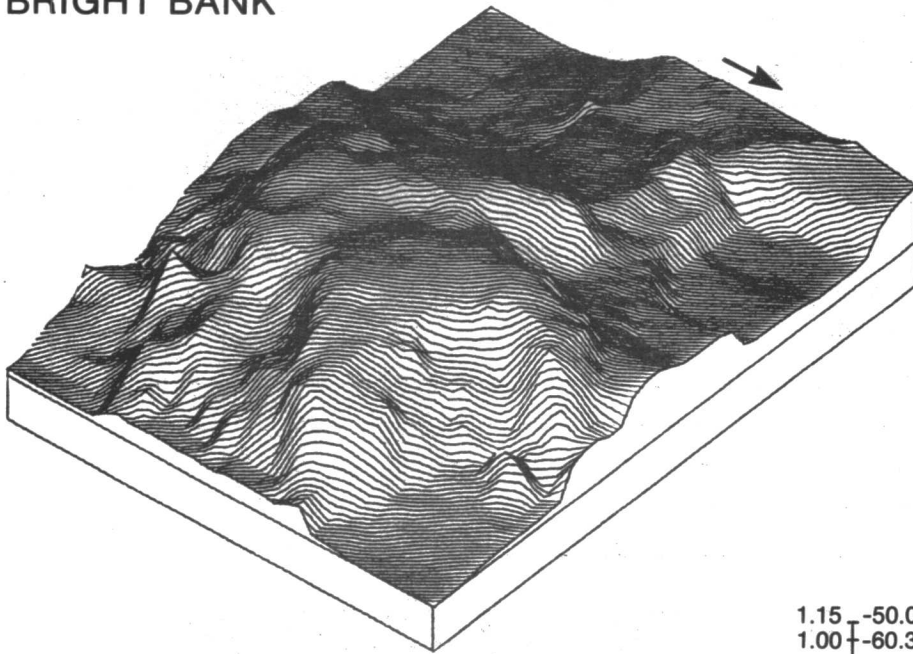


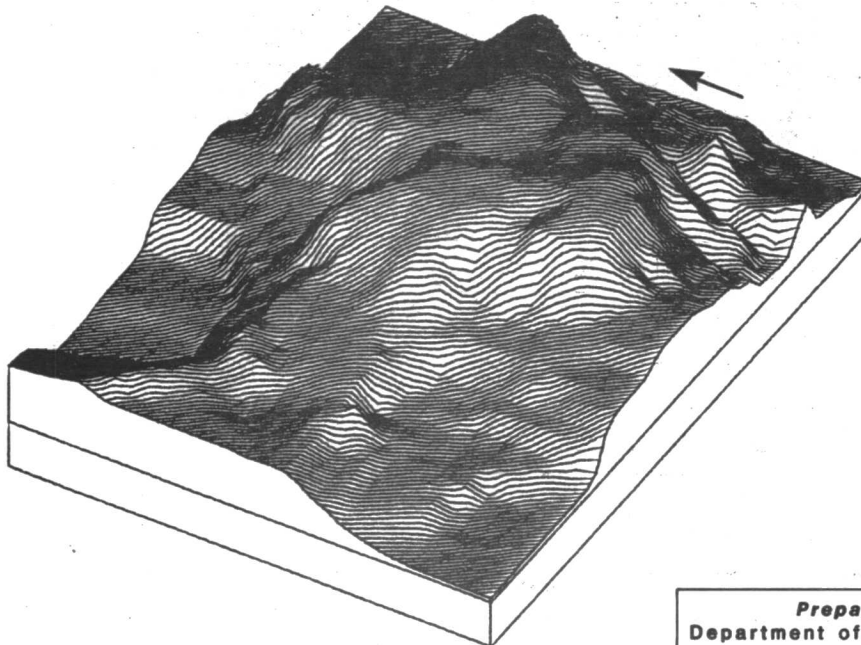
Figure VI-24. Bathymetric map of Bright Bank showing the location of the seismic line and side-scan sonar record illustrated in Figure VI-26 and locations of sediment sample stations.

BRIGHT BANK



AZIMUTH = 230 ALTITUDE = 40
 *WIDTH = 6.50 *HEIGHT = 1.50
 * BEFORE FORESHORTENING

1.15 -50.00
 1.00 -60.30
 0.50 -97.45
 0.00 -130.00



AZIMUTH = 60 ALTITUDE = 40
 *WIDTH = 6.50 *HEIGHT = 1.50
 * BEFORE FORESHORTENING

Prepared by
 Department of Oceanography
 Texas A&M University

Figure VI-25. Perspective views of Bright Bank. Arrows point toward north. Graphic vertical scale relates the total range of water depths (right) to the arbitrary computer units after foreshortening (left).

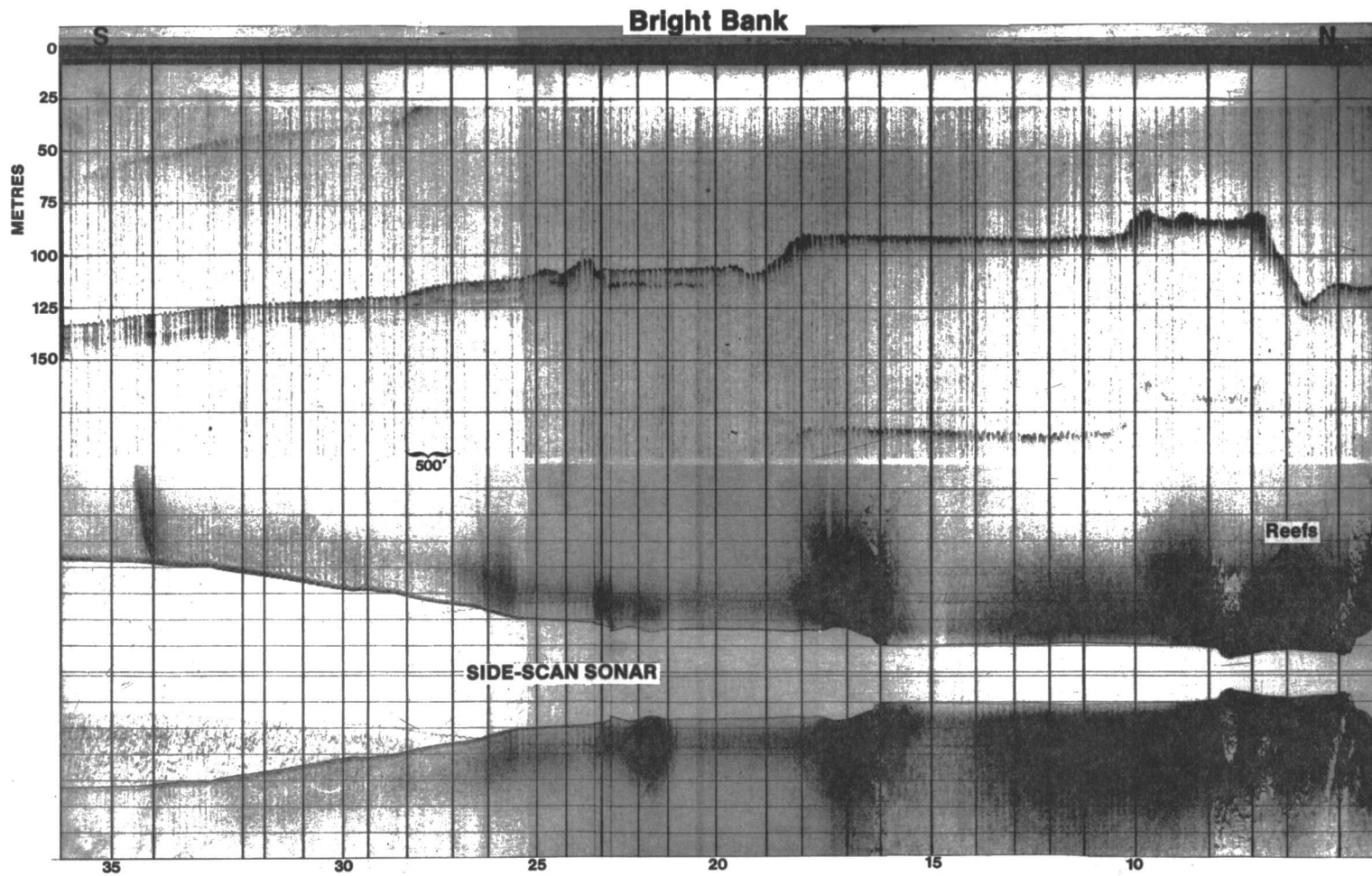


Figure VI-26. A 7 kHz high resolution sub-bottom profile and side-scan sonar record across Bright Bank.

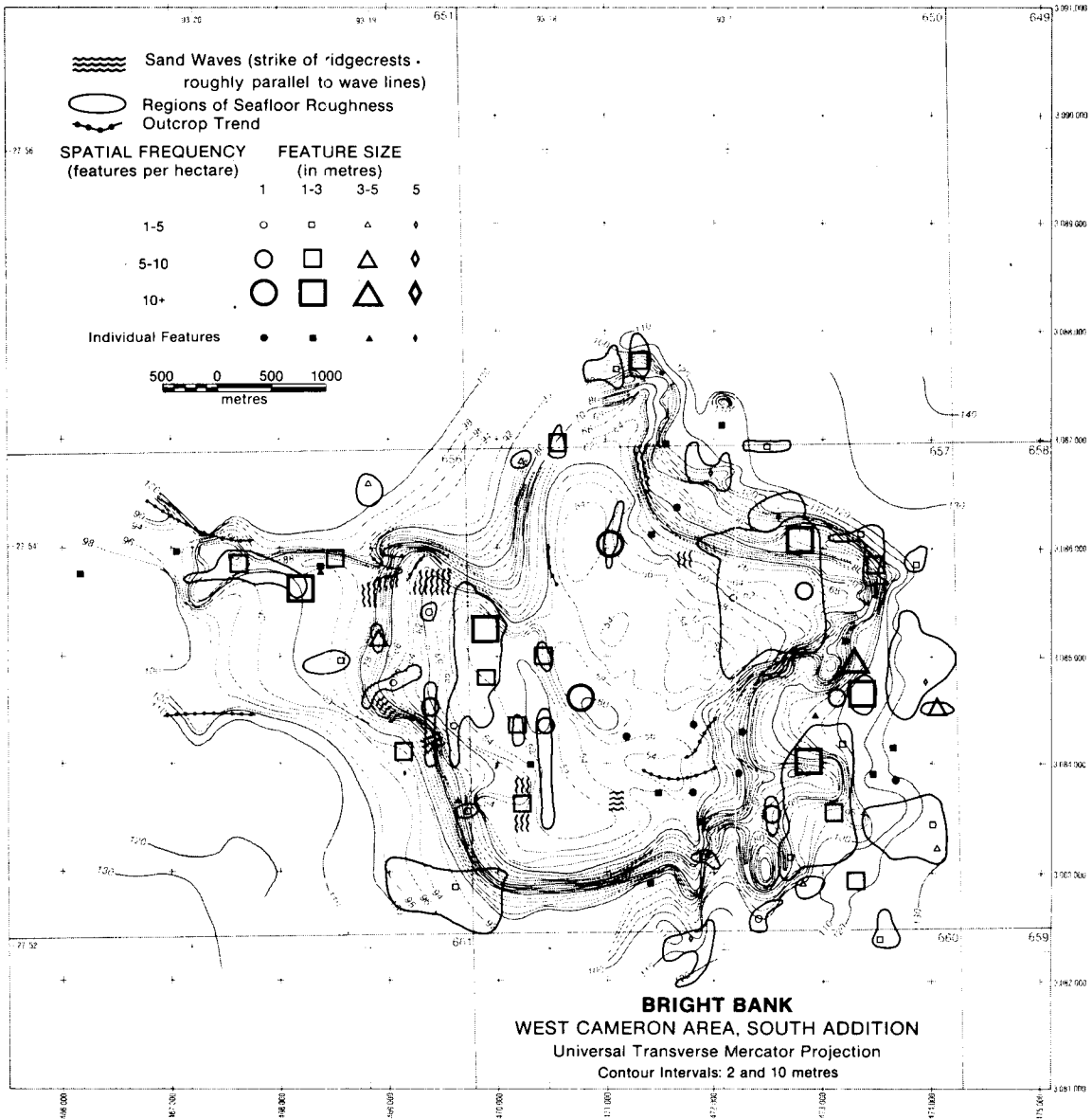


Figure VI-27. Seafloor roughness map of Bright Bank.

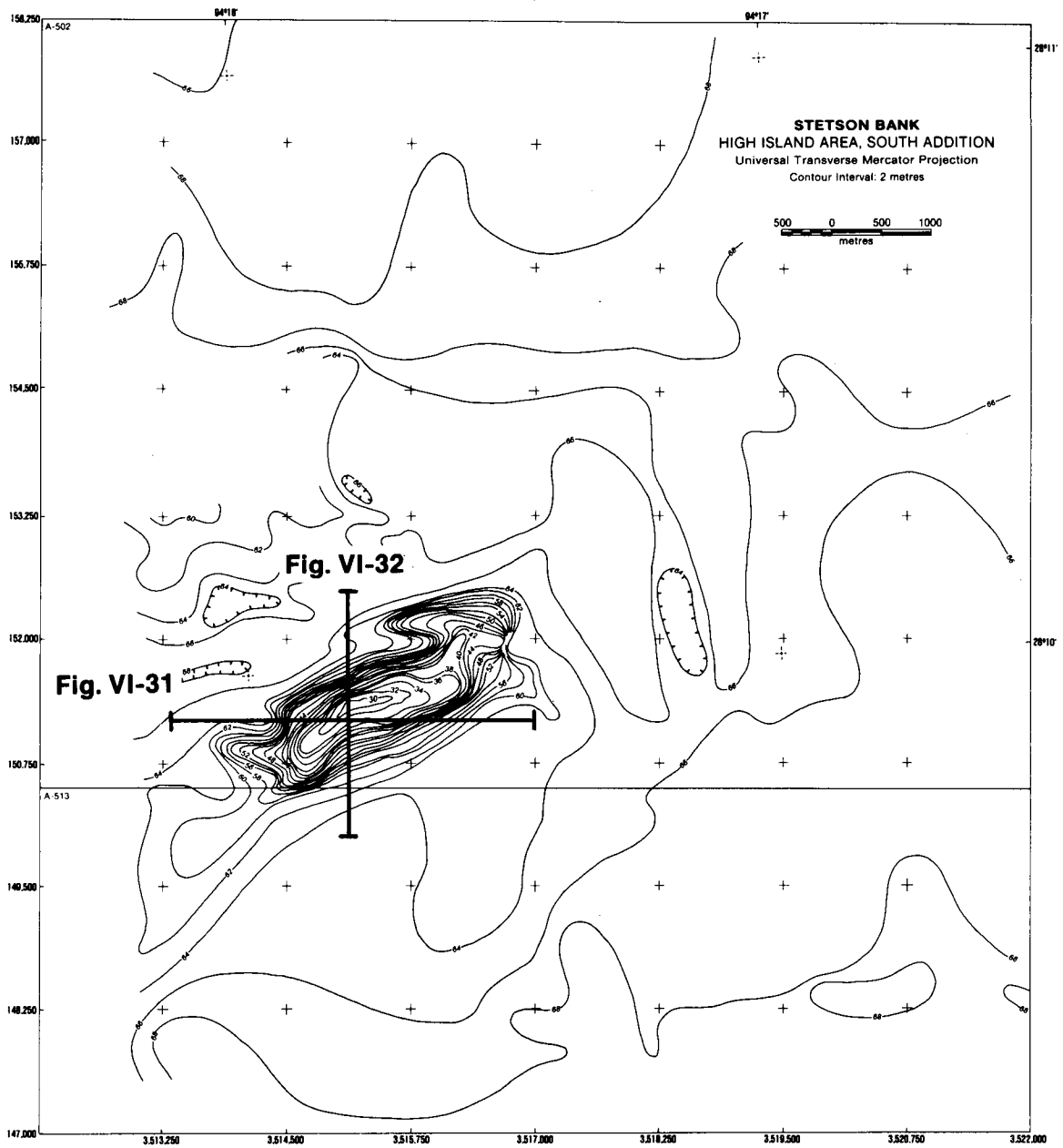


Figure VI-28. Bathymetric map of Stetson Bank, showing locations of bathymetric and sub-bottom profiles illustrated in Figures VI-31 and 32.

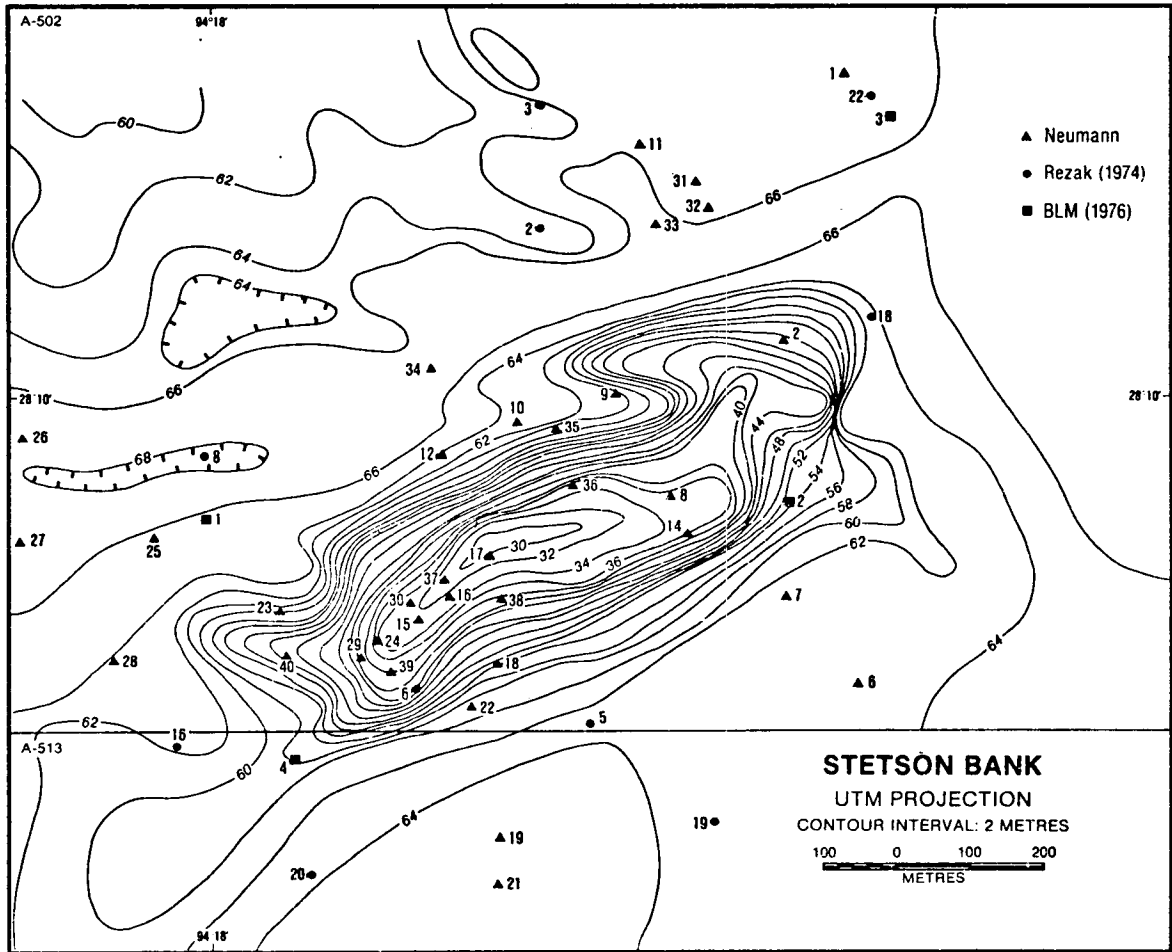
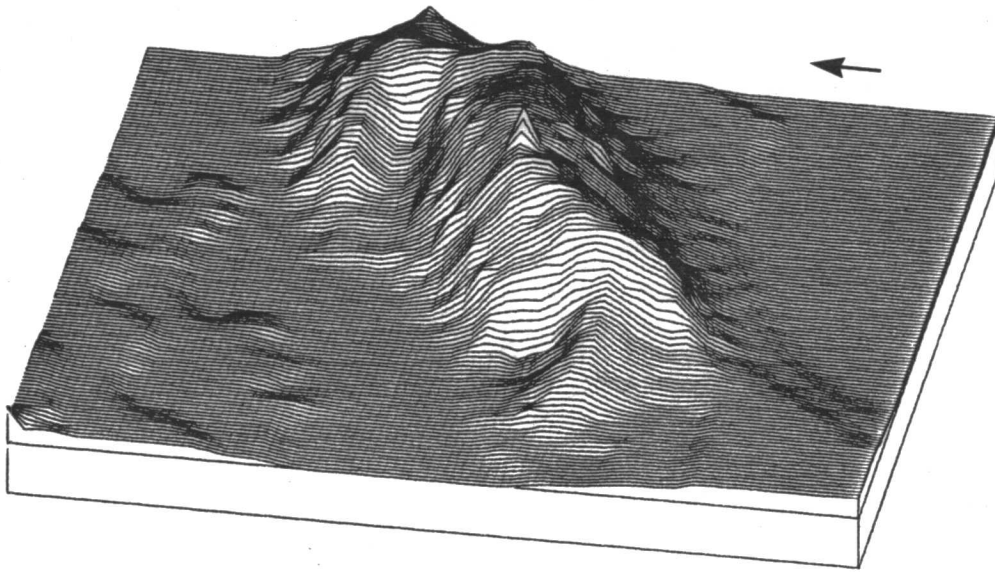


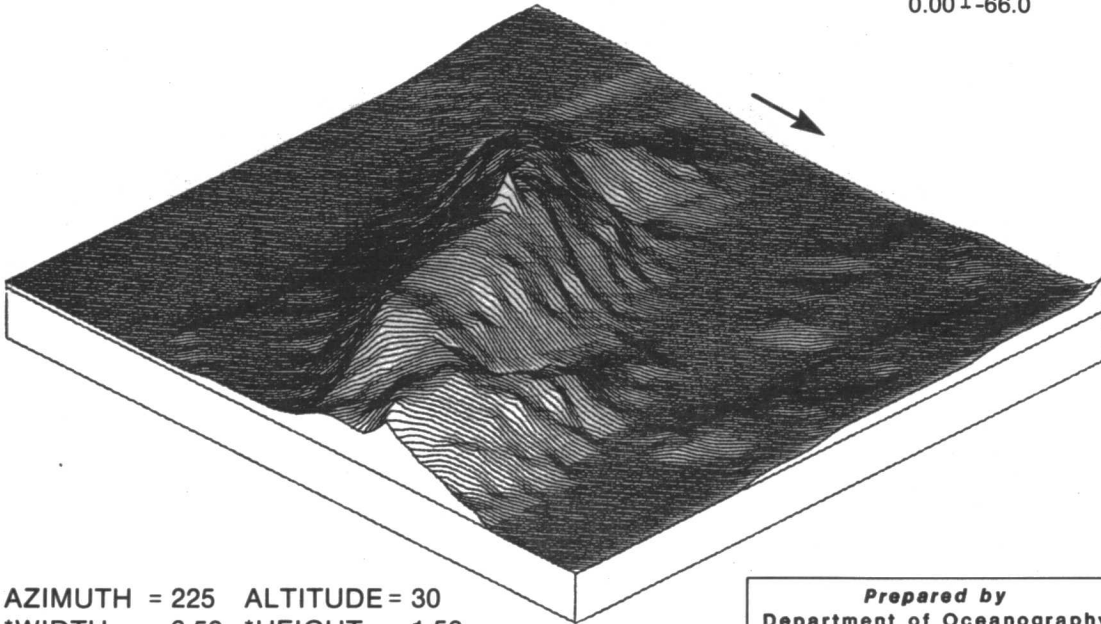
Figure VI-29. Sediment station locations at Stetson Bank.

STETSON BANK



AZIMUTH = 80 ALTITUDE = 30
 *WIDTH = 7.00 *HEIGHT = 1.50
 * BEFORE FORESHORTENING

1.30 -20.00
 1.00 -30.58
 0.50 -48.29
 0.00 -66.0



AZIMUTH = 225 ALTITUDE = 30
 *WIDTH = 6.50 *HEIGHT = 1.50
 * BEFORE FORESHORTENING

Prepared by
 Department of Oceanography
 Texas A&M University

Figure VI-30. Perspective views of Stetson Bank. Arrows point toward north. Graphic vertical scale relates the total range of water depths (right) to the arbitrary computer units after foreshortening (left).

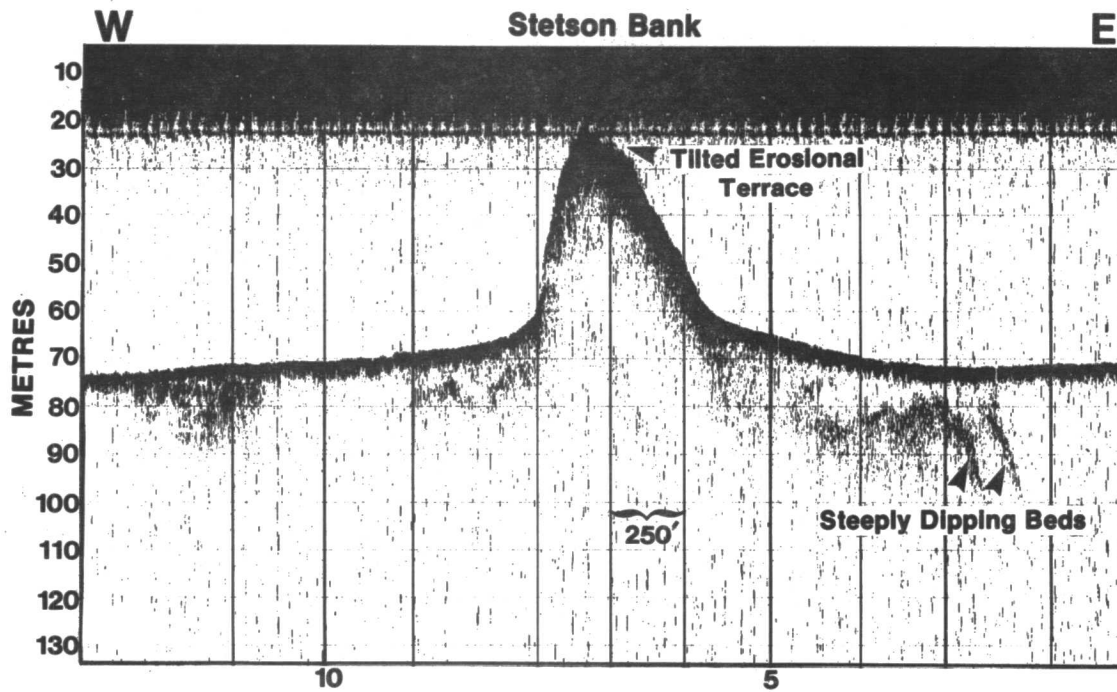


Figure VI-31. A 3.5 kHz high resolution sub-bottom profile across Stetson Bank. See Figure VI-28 for location of profile.

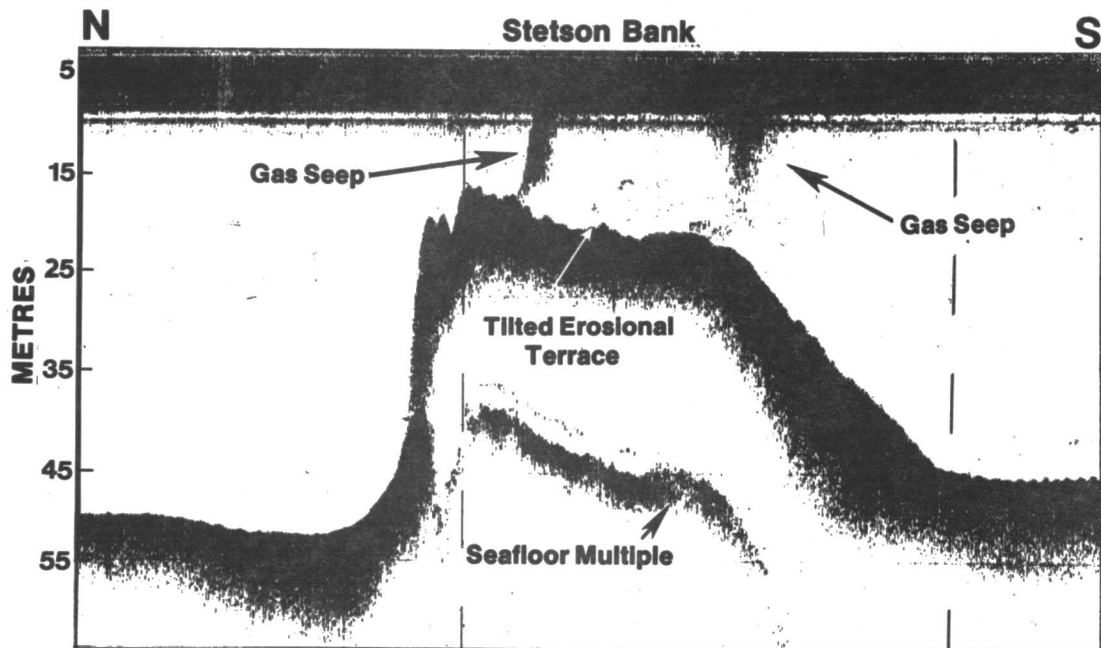


Figure VI-32. A 12 kHz bathymetric profile across Stetson Bank. See Figure VI-28 for location.

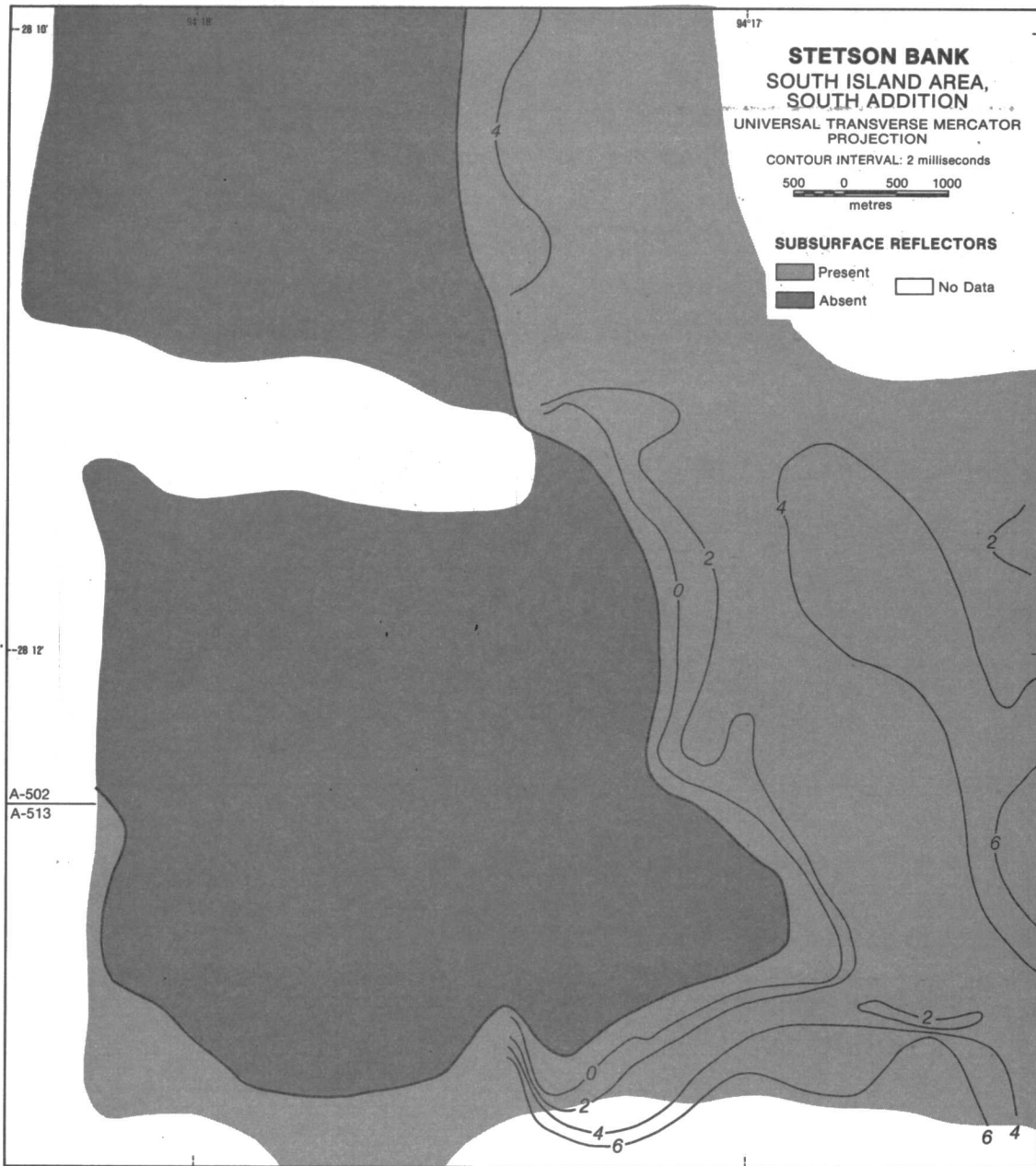


Figure VI-34. Structure-Isopach map of Stetson Bank. Contours are isopachs (sediment thickness) from the seafloor to reflector H on Figure VI-29.

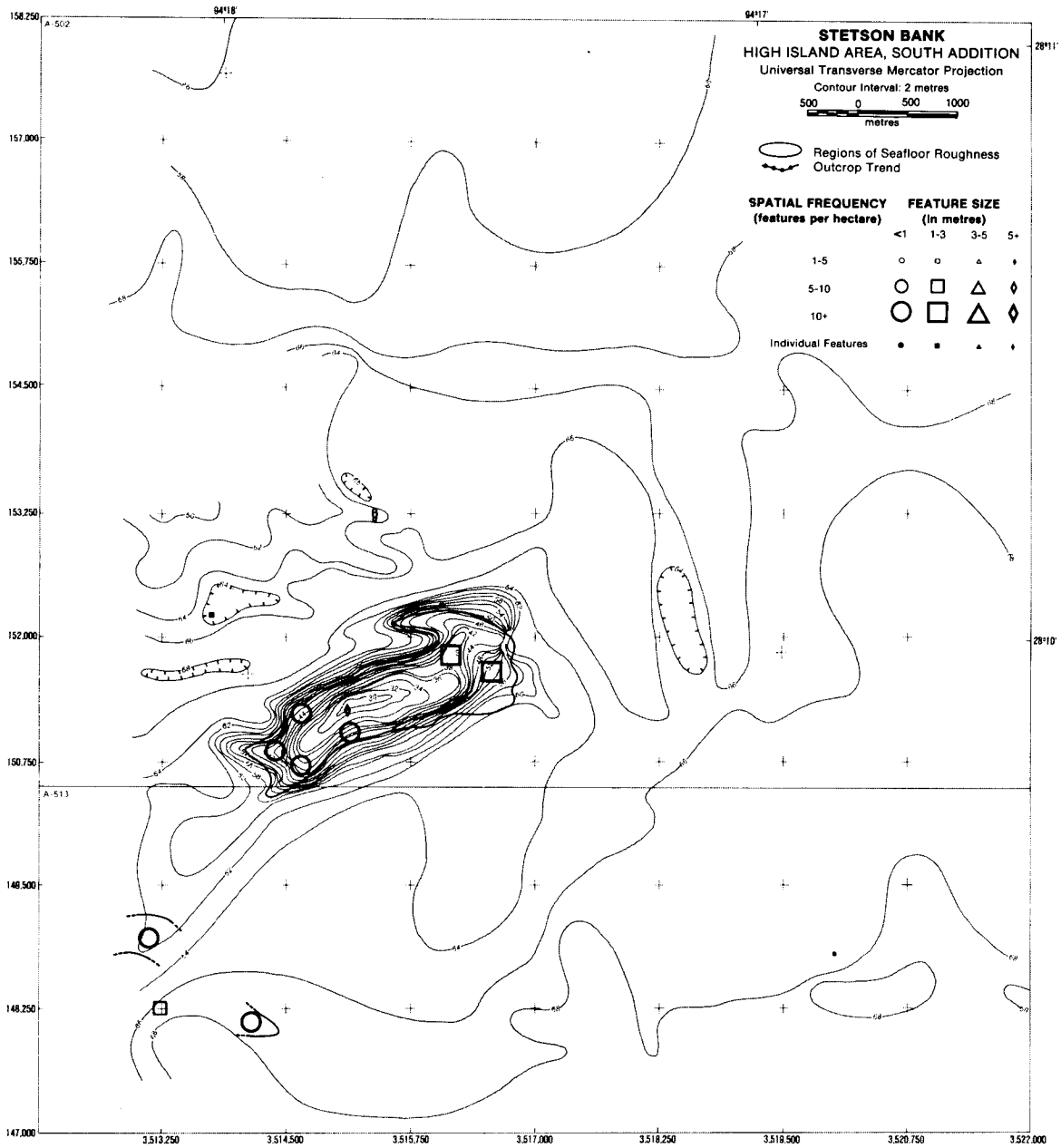
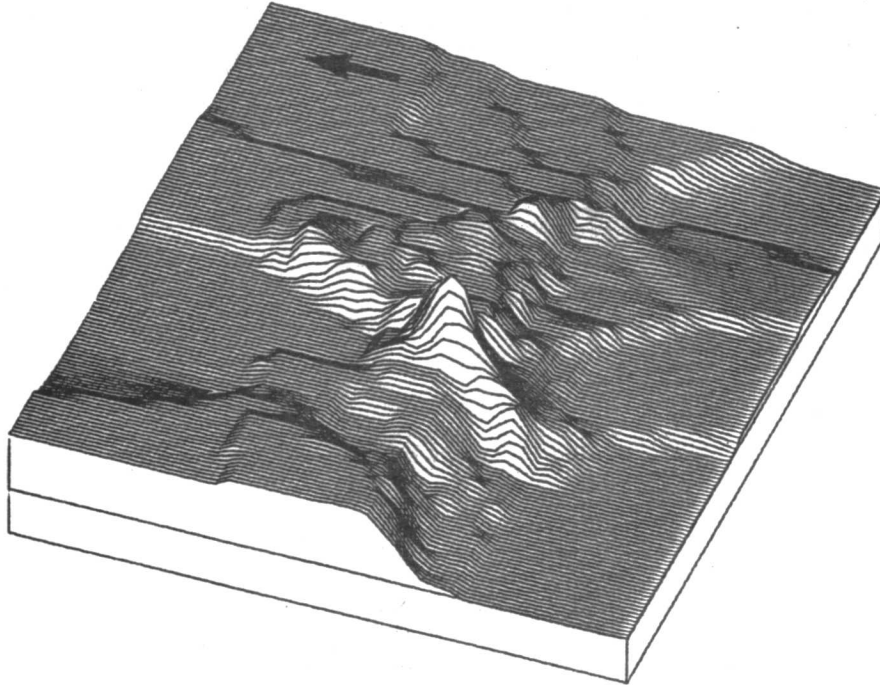


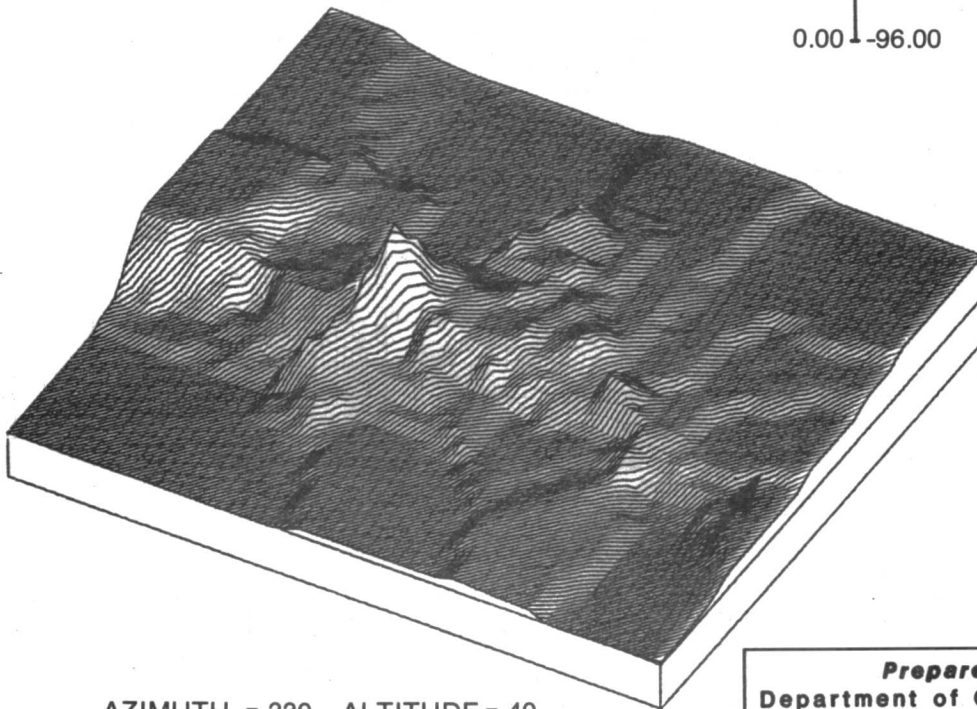
Figure VI-35. Seafloor roughness map of Stetson Bank.

MACNEIL BANK



AZIMUTH = 70 ALTITUDE = 40
 *WIDTH = 6.50 *HEIGHT = 1.50
 *BEFORE FORESHORTENING

1.15 -62.96
 1.00 -67.25
 0.50 -81.62
 0.00 -96.00



AZIMUTH = 330 ALTITUDE = 40
 *WIDTH = 6.50 *HEIGHT = 1.50
 *BEFORE FORESHORTENING

Prepared by
 Department of Oceanography
 Texas A&M University

Figure VI-37. Perspective views of MacNeil Bank. Arrows point toward north. Graphic vertical scale relates the total range of water depths (right) to the arbitrary computer units after foreshortening (left).

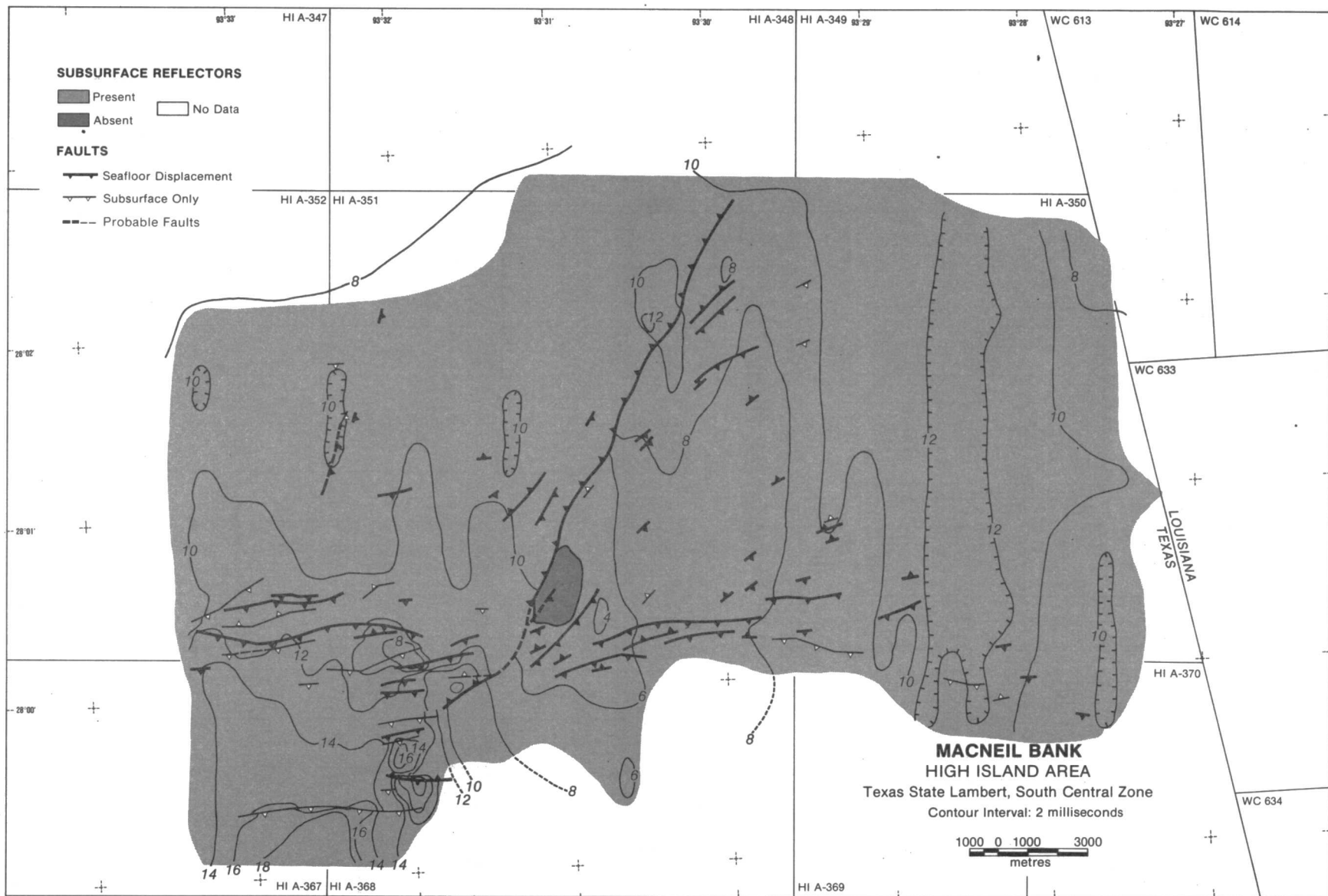
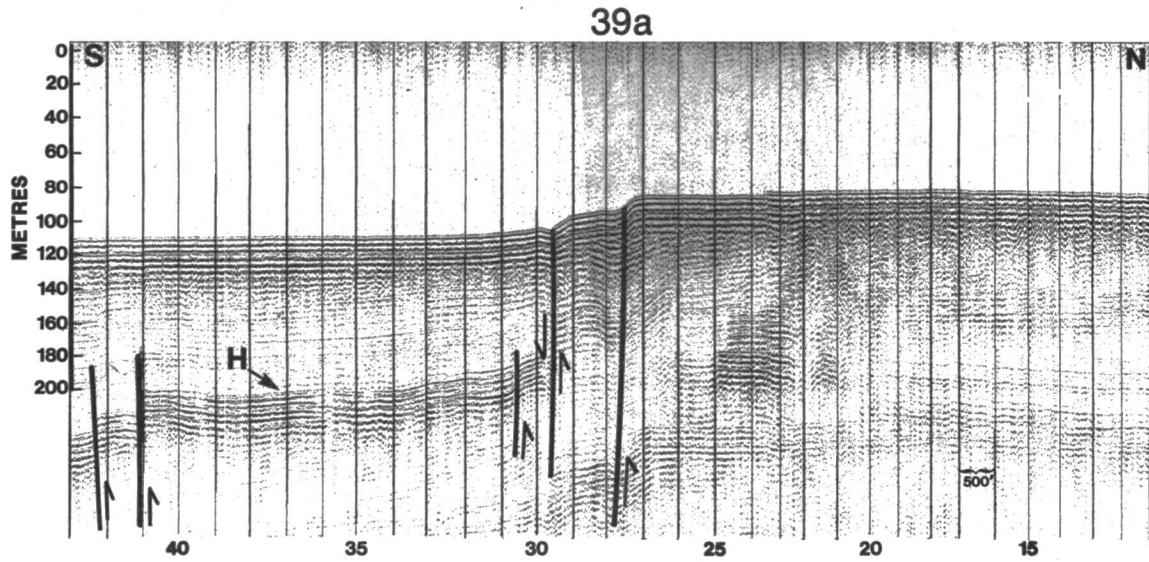


Figure VI-38. Structure-Isopach map of MacNeil Bank. Contours are isopachs (sediment thickness) from the seafloor to reflector H on Figure VI-39.



MacNeil Bank

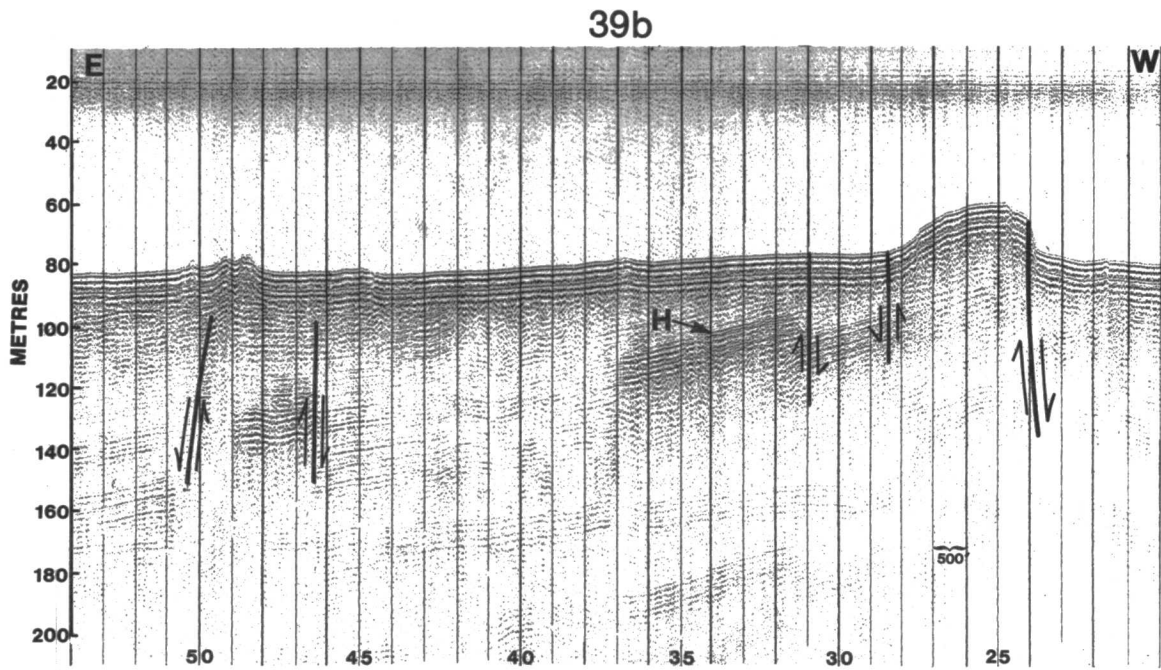


Figure VI-39. Boomer profiles on MacNeil Bank. H = horizon.

**APPENDIX C:
SEDIMENT ANALYSES:
PARKER AND STETSON BANKS**

TABLE C-1
PARKER BANK SEDIMENT TEXTURE DATA (1977)

STATION-GRAB	GRAVEL	SAND	SILT	CLAY	MEAN	MEDIAN	STD DEV	SKEWNESS	KURTOSIS
1-1	39.11	56.23	2.16	2.50	0.35	0.19	2.23	1.91	4.93
1-2	7.65	87.39	2.10	2.86	1.32	1.01	1.95	2.18	6.69
1-3	21.43	75.01	1.29	2.27	0.63	0.60	1.94	2.20	7.73
1-4	10.12	86.62	1.13	2.13	0.98	0.84	1.73	2.50	10.02
2-1	0.36	47.84	17.85	33.96	5.75	4.60	2.91	0.08	-1.49
2-2	0.44	49.73	22.28	27.55	5.36	3.99	2.89	0.22	-1.33
2-3	0.69	40.37	29.94	29.00	5.66	6.22	2.94	-0.15	-1.23
2-4	0.75	39.78	26.90	32.58	5.88	6.44	2.88	-0.14	-1.23
3-1	5.39	70.58	10.29	13.74	3.08	1.92	3.15	0.86	-0.33
3-2	6.49	69.24	9.64	14.62	2.93	1.74	3.23	0.96	-0.26
3-3	3.96	66.14	14.64	15.26	3.50	2.25	3.19	0.69	-0.74
3-4	4.83	76.27	10.41	8.50	2.52	1.71	2.82	1.17	0.53
4-1	10.87	79.17	4.19	5.77	1.52	1.02	2.54	1.77	2.97
4-2	17.79	71.62	4.26	6.32	1.28	0.72	2.73	1.74	2.63
4-3	4.31	76.24	8.95	10.50	2.88	2.00	2.90	0.96	0.15
4-4	1.43	64.26	15.61	18.69	4.15	3.59	3.02	0.55	-0.61

TABLE C-2
PARKER BANK GRAIN TYPE DATA (1977)
(All Values in Percent)

STATION-GRAB	SKELETAL					
	Foraminifers		Echinoderm	Mollusc	Coral	Algae
	Planktonic	Benthonic				
1-4	9.0	20.0	5.5	15.0	33.5	7.0
2-4	21.0	19.5	5.5	9.0	3.5	29.5
3-4	20.5	27.5	8.5	16.5	6.5	9.5
4-4	13.0	17.5	7.0	9.5	5.0	30.5

STATION-GRAB	NON-SKELETAL					TOTAL CARBONATE	
	Quartz	Pellets	Lithoclasts	Miscellanea	Schelbler Method	Weight % Method	
1-4	0.5	---	6.0	3.5	100	91.8	
2-4	4.0	---	---	8.0	58.23	44.4	
3-4	---	1.5	1.0	8.5	100	72.8	
4-4	6.0	1.0	---	10.5	100	91.2	

STATION-GRAB	COMMENTS ON MISCELLANEA
1-4	Bryozoans, Worm Tube, Pteropods
2-4	---
3-4	Spines, Alcyonarian Spicules, Pteropods, Bryozoans
4-4	Sponge, Pteropod, Ostracod, Diatom

TABLE C-3
STETSON BANK SEDIMENT TEXTURE DATA (1958 and 1974)

SAMPLE NUMBER	SAMPLE TYPE	WEIGHT PERCENT				MEDIAN (Ø)	DIAMETER (mm)
		Gravel	Sand	Silt	Clay		
1 N	grab	7.17	38.26	34.24	20.25	4.9	0.034
2 N	grab	18.80	42.28	20.60	18.34	3.4	0.095
3 N	grab	1.78	48.15	24.91	25.12	4.0	0.063
4 N	grab	3.10	56.40	20.83	19.65	3.4	0.095
5 N	grab	4.99	53.35	21.41	20.11	3.9	0.067
6 N	grab	6.05	74.48	9.25	9.93	3.1	0.117
9 N	grab	8.08	19.22	34.54	37.16	6.9	0.008
10 N	grab	32.19	40.31	16.40	11.12	0.8	0.574
11 N	grab	10.71	53.23	17.75	18.38	3.0	0.125
12 N	grab	32.69	34.60	15.61	17.40	1.7	0.038
19 N	core	0.13	68.61	13.98	17.24	3.5	0.088
21 N	core	1.87	65.49	15.40	16.74	3.3	0.102
22 N	grab	25.61	36.30	18.98	19.11	2.0	0.250
23 N	grab	13.65	58.79	14.81	12.56	2.3	0.203
25 N	grab	38.32	32.59	14.19	14.90	-0.1	1.072
26 N	core	1.24	85.70	10.24	1.80	3.0	0.125
27 N	core	9.28	20.08	32.24	38.39	5.9	0.017
28 N	grab	7.46	60.01	14.92	18.11	2.6	0.165
2 A	grab	6.26	63.20	11.38	19.16	2.8	0.150
3 A	grab	21.43	45.85	13.52	19.21	2.7	0.166
5 A	grab	0.70	62.73	14.46	22.11	2.9	0.140
6 A	grab	0.59	81.74	6.90	10.77	2.7	0.163
8 A	grab	2.66	47.80	18.95	30.59	3.9	0.070
16 A	grab	7.58	61.50	11.84	19.07	2.9	0.145
18 A	grab	6.50	42.61	21.10	29.80	4.2	0.065
19 A	grab	1.73	65.53	12.65	20.09	2.9	0.140
20 A	grab	0.57	53.65	22.36	23.42	3.9	0.073
21 A	grab	20.41	59.27	18.98	11.33	2.6	0.181
22 A	grab	2.16	53.25	16.34	28.25	3.7	0.085

N = Samples reported by A.C. Neumann (1958).
A = Samples collected by R. Rezak in 1974.

TABLE C-4
 STETSON BANK SEDIMENT TEXTURE DATA (1976)
 (Cruise 76SH2)

SAMPLE STATION/GRAB	WEIGHT PERCENT				MEAN	MEDIAN	STD DEV	SKEWNESS	KURTOSIS
	Gravel	Sand	Silt	Clay					
1/A	36.59	37.33	11.69	14.39	2.04	0.75	3.87	0.82	-0.68
1/B	41.63	28.91	13.41	16.05	2.10	0.47	4.13	0.73	-1.02
1/C	65.43	23.33	4.95	6.29	0.13	—	3.12	1.93	2.70
1/D	43.93	15.07	21.56	19.44	2.67	1.28	4.41	0.40	-1.45
1/E	21.03	51.34	15.82	11.82	2.85	2.19	3.44	0.50	-0.78
1/F	29.56	48.38	10.51	11.55	2.27	1.94	3.44	0.74	-0.30
1/J	31.69	50.81	7.26	10.24	1.73	1.17	3.39	1.08	0.26
2/A	8.45	84.53	3.77	3.25	2.22	2.11	1.93	1.21	4.55
2/B	23.21	58.87	8.27	9.65	2.39	1.97	3.15	0.74	-0.04
2/D	19.74	64.37	8.61	7.28	2.14	1.91	2.89	0.92	0.77
2/E	22.18	56.21	12.82	8.79	2.47	2.13	3.12	0.69	0.07
2/F	47.61	35.51	7.34	9.53	1.35	0.09	3.59	1.08	0.02
2/J	26.65	54.28	10.40	8.68	2.10	1.95	3.19	0.80	0.02
3/A	3.04	58.47	15.94	22.55	4.59	3.39	3.06	0.43	-0.93
3/B	2.40	60.76	21.73	15.11	4.26	3.45	2.65	0.65	-0.20
3/C	2.94	53.60	20.49	22.97	4.78	3.73	2.95	0.41	-0.74
3/D	3.04	60.62	15.35	20.98	4.50	3.26	2.94	0.51	-0.75
3/E	1.92	57.38	25.68	15.02	4.40	3.59	2.63	0.66	-0.22
3/F	6.78	64.15	20.37	8.69	3.38	2.92	2.67	0.61	0.60
3/J	5.79	65.41	11.73	17.07	3.81	2.61	3.05	0.71	-0.30
4/A	55.19	31.15	11.08	2.58	0.46	—	2.87	1.35	1.01
4/B	49.99	34.30	13.15	2.56	0.59	-1.00	2.84	1.28	0.88
4/C	43.74	41.68	6.07	8.50	1.14	0.29	3.33	1.31	0.81
4/D	45.78	41.37	7.86	5.00	0.69	-0.36	3.06	1.50	1.38
4/E	52.19	34.75	7.18	5.88	0.60	—	3.13	1.53	1.39
4/F	49.62	35.03	11.31	4.03	0.68	-0.92	3.00	1.35	1.07
4/J	24.36	54.24	17.29	4.12	1.95	1.37	2.94	0.68	-0.18

TABLE C-5
STETSON BANK GRAIN TYPE DATA (1974)

GRAIN TYPES Phi Size Class	STATION															
	2A					3A					5A					
	0	1	2	3	4	0	1	2	3	4	0	1	2	3	4	
Quartz	0	0	61	87	85	1	2	27	75	67	0	0	56	88	78	
Mollusc Fragments	85	81	23	2	3	84	79	46	15	12	81	81	30	4	3	
Heavy Minerals	0	0	1	1	5	0	0	3	3	5	0	3	6	3	5	
Benthonic Forams	0	3	1	0	0	2	0	5	1	0	1	3	2	0	2	
Planktonic Forams	0	0	0	0	0	0	0	1	0	0	0	0	0	1	3	
Rock Fragments	11	10	7	0	0	5	8	3	0	0	11	5	1	0	0	
Echinoid Fragments	1	0	4	6	2	3	5	3	1	5	1	5	5	2	6	
Bryozoan Fragments	2	3	0	0	0	2	0	0	0	0	0	0	0	0	0	
"Other" Particles	1	3	3	4	5	3	6	12	5	11	6	3	0	2	3	
	6A					8A					16A					
Quartz	0	1	77	92	87	0	3	79	87	81	0	2	81	92	83	
Mollusc Fragments	96	82	10	4	3	89	68	9	4	6	94	87	7	2	4	
Heavy Minerals	0	5	4	0	5	0	0	3	2	1	0	1	4	2	5	
Benthonic Forams	0	0	3	1	1	0	2	1	1	0	0	1	0	0	1	
Planktonic Forams	0	0	0	0	0	0	0	0	1	2	0	0	0	0	0	
Rock Fragments	1	2	2	0	1	4	5	0	0	0	4	3	0	0	0	
Echinoid Fragments	0	4	1	1	0	0	6	4	3	5	2	4	5	3	5	
Bryozoan Fragments	2	0	0	0	0	0	2	0	0	0	0	0	0	0	0	
"Other" Particles	1	6	3	2	3	7	14	4	2	5	0	2	3	1	2	
	18A					19A					20A					
Quartz	0	0	13	84	69	0	0	62	93	87	0	0	59	90	87	
Mollusc Fragments	56	61	49	7	13	91	83	20	3	3	91	76	19	3	0	
Heavy Minerals	0	0	7	2	6	0	7	6	1	4	0	4	7	1	5	
Benthonic Forams	1	3	3	0	0	0	0	3	0	0	0	0	3	0	0	
Planktonic Forams	0	0	0	0	1	0	0	0	0	0	0	0	0	0	0	
Rock Fragments	38	28	20	0	2	7	2	1	0	0	6	5	2	0	1	
Echinoid Fragments	1	3	5	2	4	2	4	5	0	4	0	7	7	3	5	
Bryozoan Fragments	4	4	0	0	0	0	3	0	0	0	0	0	0	0	0	
"Other" Particles	0	1	3	5	5	0	1	3	3	2	3	8	3	3	2	
	21A					22A										
Quartz	1	2	56	91	86	0	1	47	86	85						
Mollusc Fragments	78	78	18	2	1	88	84	23	7	4						
Heavy Minerals	0	1	7	0	3	0	1	13	1	6						
Benthonic Forams	0	1	3	1	0	0	0	2	1	0						
Planktonic Forams	0	0	2	0	0	0	0	0	0	0						
Rock Fragments	13	6	3	0	0	4	4	0	0	0						
Echinoid Fragments	6	7	8	2	5	1	5	10	3	1						
Bryozoan Fragments	1	0	0	0	0	3	0	0	0	0						
"Other" Particles	1	5	3	4	5	4	5	5	2	4						

TABLE C-6
 STETSON BANK GRAIN TYPE DATA (1976)
 (All Values In Percent)

STATION	SKELETAL					
	Foraminifers		Echinoderm	Mollusc	Coral	Algae
	Planktonic	Benthonic				
1	8.0	1.0	8.5	22.5	4.0	2.5
2	3.0	0.0	1.5	33.0	3.0	0.5
3	4.0	1.5	2.5	45.0	2.5	0.0
4	4.5	0.5	2.5	28.5	1.0	1.5

STATION	NON-SKELETAL			TOTAL CARBONATE
	Quartz	Lithoclasts	Miscellaneous	
1	7.5	36.5	9.5	19.1
2	18.5	33.5	7.0	24.6
3	19.0	22.5	4.0	10.6
4	16.5	42.5	3.5	43.8

SELECTED BIBLIOGRAPHY

SELECTED BIBLIOGRAPHY

- Abbott, R.E., 1975. The Faunal Composition of the Algal-Sponge Zone of the Flower Garden Banks, Northwest Gulf of Mexico. M.S. thesis. Department of Oceanography, Texas A&M University, College Station, TX, 205 pp.
- _____, 1979. Ecological Processes Affecting the Reef Coral Population at the East Flower Garden Bank, Northwest Gulf of Mexico. Ph.D. thesis. Department of Oceanography, Texas A&M University, College Station, TX, 154 pp.
- _____ and T.J. Bright, 1975. Benthic Communities Associated with Natural Gas Seeps on Carbonate Banks in the Northwestern Gulf of Mexico. Report for Study of Naturally Occurring Hydrocarbons in the Gulf of Mexico, 191 pp.
- Angelovic, J.W., 1976. Environmental studies of the South Texas Outer Continental Shelf, 1975. Phys. Oceanography, Vol. 2, NMFS, Gulf Fisheries Center, Galveston, TX, 290 pp.
- Antoine, J.W., 1972. Structure of the Gulf of Mexico. In Rezak, R. and V.J. Henry, eds., Contributions on the Geological and Geophysical Oceanography of the Gulf of Mexico, Texas A&M University Oceanographic Studies, Volume 3, Gulf Publishing Co., Houston, pp. 1-34.
- _____ and J.L. Hardin, 1965. Structure beneath continental shelf, northeastern Gulf of Mexico. AAPG Bull., 49, 157-171.
- _____, R.G. Martin, Jr., T.G. Pyle, and W.R. Bryant, 1974. Continental Margins of the Gulf of Mexico. In Burk, C.A. and C.L. Drake, eds., The Geology of Continental Margins, Springer-Verlag, New York, pp. 683-693.
- Armstrong, F.A.V., C.R. Stearns, and J.D.H. Strickland, 1967. The measurement of upwelling and subsequent biological processes by means of the Technicon Autoanalyzer and associated equipment. Deep Sea Re., 14, 381-389.
- Armstrong, R., 1978. Seasonal Circulation Patterns. In Jackson, W.B., ed., Environmental Assessment of an Active Oil Field in the Northwestern Gulf of Mexico 1977-1978, NOAA/NMFS/SEFC Galveston Laboratory.
- Atoda, K., 1947. The larva and postlarval development of some reef-building corals. II. Stylophora pistillata (Esper). Sci. Rep. Tohoku Univ., 4th Ser. (Biology), 18(1), 48-65.
- _____, 1951. The larva and postlarval development of the reef-building corals III. Acropora bruggemanni. J. Morph., 89, 1-15.

- Bak, R.P.M. and M.S. Engel, 1979. Distribution, abundance, and survival of juvenile hermatypic corals (Scleractinia) and the importance of life history strategies in the parent coral community. *Mar. Biol.*, 54, 341-352.
- _____ and Y. Steward-Van Es, 1980. Regeneration of superficial damage in the scleractinian corals Agaricia agaricites f. purpurea and Porites astreoides. *Bull. Mar. Sci.*, 30(4), 883-887.
- Bendat, J.S. and A.G. Piersol, 1971. *Random Data: Analysis and Measurement Procedures*. John Wiley and Sons, New York, 407 pp.
- Bergantino, R.H., 1971. Submarine regional geomorphology of the Gulf of Mexico. *Geol. Soc. Am. Bull.*, 82, 741-752.
- Bernard, B.B., J.M. Brooks, and W.M. Sackett, 1976. Natural gas seepage in the Gulf of Mexico. *Earth Plan. Sci. Lett.*, 31, 48-54.
- Bienfang, P. and K. Gundersen, 1977. Light effects on nutrient-limited, oceanic primary production. *Mar. Biol.*, 43, 187-199.
- Birkland, C., 1977. The importance of rate of biomass accumulation in early successional stages of benthic communities to the survival of coral recruits. In *Proc. 3rd Intl. Coral Reef Symp.*, Univ. of Miami, Miami, FL [May 1977)], 15-21.
- _____ and D. Rowley, 1981. Coral recruitment patterns at Guam. In *Abstract of Papers, Fourth International Coral Reef Symposium, Manila, Philippines, 18-21 May 1981*, Marine Sciences Center, Univ. Philippines, 6.
- Bright, T.J., 1977. Coral reefs, nepheloid layers, gas seeps and brine flows on hard-banks in the northwestern Gulf of Mexico. *Proc. Third Int. Coral Reef Symp.*, Univ. Miami, Rosenstiel School of Marine and Atmospheric Science, 1, 39-46.
- _____, P.A. LaRock, R.D. Lauer, and J.M. Brooks, 1980. A brine seep at the East Flower Garden Bank, northwestern Gulf of Mexico. *Int. Rev. gesamten Hydrobiol.*, 65, 321-335.
- _____ and L.H. Pequegnat, eds., 1974. *Biota of the West Flower Garden Bank*. Gulf Publishing Co., Houston, 435 pp.
- _____, E. Powell, and R. Rezak, 1980. Environmental effects of a natural brine seep at the East Flower Garden Bank, northwestern Gulf of Mexico. In Geyer, R.A., ed., *Marine Environmental Pollution*, Elsevier Oceanography Series, 27A, Elsevier, New York, 291-316.
- _____ and R. Rezak, 1976. *A Biological and Geological Reconnaissance of Selected Topographical Features on the Texas Continental Shelf*. Final Report to U.S. Dept. of Interior, Bureau of Land Management, Contract #08550-CT5-4, 377 pp.

- _____ and R. Rezak, 1977. Reconnaissance of reefs and fishing bank of the Texas Continental Shelf. In Geyer, R.A., ed., *Submersibles and Their Use in Oceanography*, Elsevier, New York, 113-150.
- _____ and R. Rezak, 1978a. South Texas Topographic Features Study. Final Report to U.S. Dept. of Interior, Bureau of Land Management, Contract #AA550-CT6-18. Texas A&M Univ., Dept. of Oceanography, Technical Report #78-13-T, 772 pp.
- _____ and R. Rezak, 1978b. Northwestern Gulf of Mexico Topographic Features Study. Final Report to U.S. Dept. of Interior, Bureau of Land Management, Contract #AA550-CT7-15. Texas A&M Univ., Dept. of Oceanography, Technical Report #78-14-T, 629 pp.
- _____, J.W. Tunnell, L.H. Pequegnat, T.E. Burke, C.W. Cashman, D.A. Cropper, J.P. Ray, R.C. Tresslar, J. Teerling, and J.B. Wills, 1974. Biotic zonation on the West Flower Garden Bank. In, *Biota of the West Flower Garden Bank*, Bright, T. and L. Pequegnat, eds., Gulf Publishing Co., 4-54.
- _____, S. Viada, C. Combs, G. Dennis, E. Powell, and G. Denoux, 1981. East Flower Garden monitoring study. In Rezak, R. and T. Bright, eds., *Northern Gulf of Mexico Topographic Features Study*, Final Report to U.S. Bureau of Land Management, Contract #AA551-CT8-35. Texas A&M Univ., Dept. of Oceanography, Technical Report #81-2-T, Vol. 3, Part C.
- Brooks, J.M., T.J. Bright, B. Bernard, and C. Schwab, 1979. Chemical aspects of a brine seep at the East Flower Garden Bank, northwestern Gulf of Mexico. *Limnol. Oceanogr.*, 24(4), 735-745.
- Canfield, R.H., 1941. Application of the line intercept method in sampling range vegetation, *J. Forest.*, 39, 388-394.
- Chamberlain, C.K., 1966. Some Octocorallia of Isla de Lobos, Veracruz, Mexico. *Brigham Young Univ. Geol. Studies*, 13, 47-54.
- Clark, R.C., Jr., 1974. Methods for establishing levels of petroleum contamination in organisms and sediment as related to marine pollution monitoring. In NBS Spec. Publ. 409, *Marine Pollution Monitoring (Petroleum)*, Proceedings of a Symposium and Workshop held at NSB, Gaithersburg, MD, pp. 189-194.
- Continental Shelf Associates, 1975. East Flower Garden Bank Environmental Survey. Report No. 1, Vol. I, and Report No. 2, Vol. I, prepared for Mobil Oil Corp.
- _____, 1978a. Monitoring Program for Wells #3 and #4, Lease OCS-G 2759, Block A-389, High Island Area, East Addition, South Extension, Near East Flower Garden Bank. Technical Report for Mobil Oil Corp, Sept. 14 - Dec. 15, 1977, Vol. I, 163 pp.

- _____, 1978b. Monitoring Program for Well #1, Lease OCS-G 3487, Block A-367, High Island Area, East Addition, South Extension, Near East Flower Garden Bank. 2 vols. Report to American Natural Gas Production Co.
- Curry, J.R., 1960. Sediments and history of Holocene transgressions, continental shelf, Northwest Gulf of Mexico. In Shepard, F.P., et al., eds., Recent Sediments, Northwest Gulf of Mexico, AAPG, Tulsa, OK, 221-266.
- _____, 1965. Late Quaternary history, continental shelves of the United States. In Wright, H.E., Jr. and D.G. Frey, eds., the Quaternary of the United States, Princeton Univ. Press, Princeton, NJ, pp. 728-736.
- Deardorff, J.W., 1970. A three-dimensional numerical investigation of the idealized planetary boundary layer. Geophysical Fluid Dynamics, 1, 377-410.
- Edwards, G.S., 1971. Geology of the West Flower Garden Bank. Texas A&M Sea Grant Pub. TAMU-SG-71-215, 199 pp.
- Ewing, M. and E.M. Thorndike, 1965. Suspended matter in deep ocean water. Science, 147, 1291-1294.
- Farrington, J.W., C.S. Giam, G.R. Harvey, P. Parker and J. Teal, 1972. Analytical techniques for selected organic compounds. Marine Pollution Monitoring: Strategies for a National Program Workshop sponsored by NOAA at Santa Catalina Marine Biological Laboratory, Oct. 25-28, pp. 152-176.
- Feely, H.W. and J.L. Kulp, 1957. Origin of Gulf Coast salt-dome sulphur deposits. AAPG Bull., 41, 1802-1853.
- Folk, R.L., 1974. Petrology of Sedimentary Rocks. Hemphill Publication Company, Austin, TX, 182 pp.
- Franceschini, G.A., 1953. The distribution of the mean monthly wind stress over the Gulf of Mexico. Texas A&M Univ., Dept. of Oceanography, Sci. Rept. #1, 18 pp.
- Fredericks, A.D. and W.M. Sackett, 1970. Organic carbon in the Gulf of Mexico. J. Geophys. Res., 75, 2199-2206.
- Freeland, H.J., P.B. Rhines, and T. Rossby, 1975. Statistical observations of the trajectories of neutrally buoyant floats in the North Atlantic. J. Mar. Res., 33, 383-404.
- Geyer, R.A., ed., 1980. Marine Environmental Pollution, 1: Hydrocarbons. Elsevier Oceanography Series, 27A, Elsevier, New York, 591 pp.

- Giam, C.S., H.S. Chan, G.S. Neff, and Y. Hrung, 1979. High molecular weight hydrocarbons in benthic macroepifauna and macronekton. In Flint, R.W. and N.N. Rabalais, eds., Environmental Studies, South Texas Outer Continental Shelf, 1975-1977. Submitted to BLM by the University of Texas. Vol. II, Chapter 5.
- _____, 1978a. High molecular weight hydrocarbons in macronekton and Spondylus samples. In Bright, T. and R. Rezak, eds., South Texas Topographic Features Study, Final Report to U.S. Dept. of Interior, Bureau of Land Management, Contract #AA550-CT6-18. Texas A&M Univ., Dept. of Oceanography, Technical Report #78-13-T, Chapter V.
- _____, 1978b. High molecular weight hydrocarbons in macronekton and Spondylus samples. In Bright, T. and R. Rezak, eds., Northwestern Gulf of Mexico Topographic Features Study, Final Report to U.S. Dept. of Interior, Bureau of Land Management, Contract #AA550-CT7-15. Texas A&M Univ., Dept. of Oceanography, Technical Report #78-14-T, Chapter VIII.
- _____, G. Neff, and Y. Hrung, 1981. High molecular weight hydrocarbons in Spondylus and macronekton. In Rezak, R. and T. Bright, eds., Northern Gulf of Mexico Topographic Features Study, Final Report to Dept. of Interior, Bureau of Land Management, Contract #AA551-CT8-35, Texas A&M Univ., Dept. of Oceanography, Technical Report No. 81-2-T, Vol. 2, Chapter IXB.
- Gibbons, J.D. and J.W. Pratt, 1975. P-values: Interpretation and methodology. Am. Stat., 29(1), 20-25.
- Goldberg, W.M., 1970. Some Aspects of the Ecology of the Reefs off Palm Beach County, Florida, with Emphasis on the Gorgonacea and Their Bathymetric Distribution. M.S. thesis. Florida Atlantic University, Boca Raton, Florida, 108 pp.
- Gonella, J., 1972. A rotary component method for analyzing meteorological and oceanographic vector time series, Deep Sea Re., 19, 833-846.
- Goreau, N.I., T.J. Goreau, and R.L. Hayes, 1981. Settling, survivorship, and spatial aggregation in planulae and juveniles of the coral Porites porites (Pallas). Bull. Mar. Sci., 31(2), 424-435.
- Greiner, G.O.G. 1970. Distribution of major benthonic foraminiferal groups in the Gulf of Mexico continental shelf. Micropalaeontol., 16, 83-101.
- Griffin, G.M., 1962. Regional clay minerals facies: Products of weathering intensity and current distribution in the northeastern Gulf of Mexico. Geol. Soc. Am. Bull., 73, 737-768.

- _____, 1971. Interpretation of x-ray diffraction data. In Carver, R.E., ed., *Procedures in Sedimentary Petrology*. Wiley Interscience, New York, pp. 541-569.
- Grim, R.E., 1968. *Clay Mineralogy*. McGraw Hill, New York, 596 pp.
- _____, R.H. Bray, and W.F. Bradley, 1937. The mica in argillaceous sediments. *Am. Mineralogist*, 7, 813-829.
- Grimm, D.E. and T.S. Hopkins, 1977. Preliminary characterization of the octocorallian and scleractinian diversity at the Florida Middle Ground. *Proc. Third Int. Coral Reef Symp.*, Univ. Miami, Rosenstiel School of Marine and Atmospheric Science, 1, 135-141.
- Heathershaw, A.D. and J.H. Simpson, 1978. The sampling variability of the Reynolds stress and its relation to boundary shear stress and drag coefficient measurements. *Est. Coas. M.*, 6, 263-274.
- Heilprin, A., 1890. The corals and coral reefs of the western waters of the Gulf of Mexico. *Proc. Acad. Nat. Sci. Phil.*, 42, 301-316.
- Hudson, J.H. and D.M. Robbin, 1980. Effects of drilling mud on the growth rate of the reef-building coral, *Montastrea annularis*. In Geyer, R.A. ed., *Marine Environmental Pollution*, Elsevier Oceanography Series, 27A, Elsevier, New York, 455-470.
- Huff, D.W. and D.W. McGrail, 1978. Large scale turbulence and resuspension of sediment on the Texas continental shelf. (Abs.) *Trans. Amer. Geophys. Union*, 59, 1110.
- Humphris, C.C., Jr., 1978. Salt movement on continental slope, northern Gulf of Mexico. In Bouma, A.H., G.T. Moore, and J.M. Coleman, eds., *Framework, Facies, and Oil Trapping Characteristics of the Upper Continental Margin*, AAPG Studies in Geology, 7, 69-85.
- Huntsman, G.R. and I.G. MacIntyre, 1971. Tropical coral patches in Onslow Bay. *Underwater Nat. Bull. Am. Littoral Soc.*, 7(2), 32-34.
- Jenkins, G.M. and D.G. Watts, 1968. *Spectral Analysis and Its Applications*. Holden-Day, San Francisco, 541 pp.
- Johannes, R.E., 1975. Pollution and degradation of coral reef communities. In Wood, E.J.F. and R.E. Johannes, eds., *Tropical Marine Pollution*, Elsevier Scientific Publishing Co., New York, pp. 13-51.
- Johns, W.D. and R.E. Grim, 1958. Clay mineral composition of recent sediment from the Mississippi River delta. *J. Sediment. Petrol.*, 28, 186-199.
- _____, R.E. Grim, and W.F. Bradley, 1954. Quantitative estimation of clay minerals by diffraction methods. *J. Sediment. Petrol.*, 24, 242-251.

- Jordan, G.F., 1952. Reef formation in the Gulf of Mexico off Appalachicola Bay, Florida. *Geol. Soc. Am. Bull.*, 63, 741-744.
- Jorgensen, B.B., 1977. Bacterial sulfate reduction within reduced microniches of oxidized marine sediments. *Mar. Biol.* 41: 7-17.
- Joyce, E.A., Jr., and J. Williams. 1969. *Memoirs of the Hourglass Cruises: Rationale and pertinent data.* Florida Dept. Nat. Res. Mar. Res. Lab. St. Petersburg, Florida. Vol. i(1). 50 pp.
- Kasahara, A., 1980. Influence of orography on the atmospheric general circulation. In *Orographic Effects in Planetary Flows*, GARP Publications Series No. 23, WMO-ICSU Joint Scientific Committee, pp. 4-52.
- Kornicker, L.S., F. Bonet, R. Cann, and C.M. Hooker, 1959. Alacran Reef, Campeche Bank, Mexico. *Bull. Inst. Mar. Sci., Univ. Texas*, 6, 1-22.
- Kundu, P.K., 1976. An analysis of inertial oscillations observed near Oregon coast. *J. Phys. Ocea.*, 6, 879-893.
- Lewis, J.B., 1974a. The importance of light and food upon the early growth of the reef coral Favia fragum (Esper). *J. Exp. Mar. Biol. Ecol.*, 15, 299-304.
- _____, 1974b. The settlement behaviour of planulae larvae of the hermatypic coral Favia fragum (Esper). *J. Exp. Mar. Biol. Ecol.*, 15, 165-172.
- Logan, B.W., 1969. Carbonate Sediments and Reefs, Yucatan Shelf, Mexico: Part 2, Coral Reefs and Banks, Yucatan Shelf, Mexico (Yucatan Reef Unit). *AAPG Mem.* 11:129-198.
- _____, J.L. Harding, W.M. Ahr, J.D. Williams, and R.G. Snead, 1969. Late Quaternary carbonate sediments of Yucatan Shelf, Mexico. In Logan, B.W., et al., Carbonate Sediments and Reefs, Yucatan Shelf, Mexico, *AAPG Mem.*, 11, 5-128.
- Loya, Y., 1972. Community structure and species diversity of hermatypic corals at Eilat, Red Sea. *Mar. Biol.*, 13, 100-123.
- Mackin, J., 1971. A Study of the Effect of Oil Field Brine Effluents on Biotic Communities in Texas Estuaries. Texas A&M Research Foundation Reports, Project 735, 73 pp.
- _____, 1973. A Review of Significant Papers on Effects of Oil Spills and Oil Field Brine Discharges on Marine Biotic Communities. Texas A&M Research Foundation Reports, Project 737, 87 pp.
- Marine Technical Consulting Service, 1976. Ecological Assessment of Drilling Activities, Well No. 1, Block 584, High Island. Technical Report for Union Oil Co. of California.

- Marmar, H.A., 1954. Tides and sea level in the Gulf of Mexico. Fishery Bulletin of the United States Fish and Wildlife Service, 55, 101-118.
- Martin, R.G., 1978. Northern and eastern Gulf of Mexico continental margin: Stratigraphic and structural framework. In Bouma, A.H., G.T. Moore, and J.M. Coleman, eds., Framework, Facies, and Oil Trapping Characteristics of the Upper Continental Margin, AAPG Studies in Geology, 7, 21-42.
- Maul, G.A., 1974. The Gulf Loop Current. In Smith, R.E., ed., Proceeding of Marine Environment, Implications of Offshore Drilling in the Eastern Gulf of Mexico, State Univ. Syst., Fla. Inst. of Oceanography, St. Petersburg, FL, pp. 87-96.
- McGrail, D.W., 1977. Shelf edge currents and sediment transport in the northwestern Gulf of Mexico. (Abs.) Trans. Amer. Geophys. Union, 58, 1160.
- _____, 1978. Boundary layer processes, mixed bottom layers, and turbid layers on continental shelves. (Abs.) Trans. Amer. Geophys. Union, 59, 1110.
- _____, 1979. The role of air-sea interaction in sediment dynamics. (Abs.) Abstracts of Papers at the 145th National Meeting, American Assoc. for the Advancement of Science, p. 45.
- _____, M. Carnes, D. Horne, and J. Hawkins, 1982a. Hydrographic Data Report. Northern Gulf of Mexico Topographic Features Study. U.S. Dept. of Interior, Bureau of Land Management, Contract #AA851-CT0-25. Texas A&M Univ., Dept. of Oceanography, Technical Report #82-4-T, 516 pp.
- _____, F. Halper, D. Horne, T. Cecil, M. Carnes, 1982b. Time Series Data Report. Northern Gulf of Mexico Topographic Features Study. U.S. Dept. of Interior, Bureau of Land Management, Contract #AA851-CT0-25. Texas A&M Univ., Dept. of Oceanography, Technical Report #82-5-T, 155 pp.
- _____ and D. Horne, 1981. Water and sediment dynamics [Flower Garden Banks]. In Rezak, R. and T. Bright, eds., Northern Gulf of Mexico Topographic Features Study, Final Report to U.S. Dept. of Interior, Bureau of Land Management, Contract #AA551-CT8-35. Texas A&M Univ., Dept. of Oceanography, Technical Report #81-2-T, Vol. 3, Part B.
- _____ and D. Horne, 1979. Currents, thermal structure and suspended sediment distribution induced by internal tides on the Texas Continental Shelf. Paper presented at the spring meeting of the American Geophysical Union SANDS Symposium.

- _____ and D.W. Huff, 1978. Shelf sediment and local flow phenomena: in situ observations. (Abs.) Program, AAPG-SEPM Annual Convention, p. 93.
- _____, D.W. Huff, and S. Jenkins, 1978. Current measurements and dye diffusion studies. In Bright, T. and R. Rezak, eds., Northwestern Gulf of Mexico Topographic Features Study, Final Report to U.S. Dept. of Interior, Bureau of Land Management, Contract #AA550-CT7-15. Texas A&M Univ., Dept. of Oceanography, Technical Report #78-14-T, pp. III-3 - III-72.
- _____ and R. Rezak, 1977. Internal waves and the nepheloid layer on continental shelf in the Gulf of Mexico. Trans. Gulf Coast Assoc. Geological Soc., 27, 123-124.
- Mooers, C.N.K., 1973. A technique for the cross spectrum analysis of pairs of complex-valued time series, with emphasis on properties of polarized components and rotational invariants. Deep Sea Re., 20, 1129-1141.
- Moore, D.R., 1958. Notes on Blanquilla Reef, the most northerly coral formation in the western Gulf of Mexico. Publ. Inst. Mar. Sci. Univ. Tex., 5, 151-155.
- National Oceanic and Atmospheric Administration (U.S. Department of Commerce), 1979. Draft Environmental Impact Statement on the Proposed East and West Flower Garden Marine Sanctuary. Office of Coastal Zone Management, Washington, D.C., 330 pp.
- Nettleton, L.L., 1934. Fluid mechanics of salt domes. AAPG Bull., 18, 1175-1204.
- _____, 1957. Gravity survey over a Gulf Coast continental mound. Geophys., 22, 630-642.
- Neumann, A.C., 1958. The configuration and sediments of Stetson Bank, northwest Gulf of Mexico. Texas A&M Univ., Dept. of Oceanography, Tech. Rept. #58-ST, 125 pp.
- Nichols, J., 1976. The effect of stable dissolved-oxygen stress on marine benthic invertebrate community diversity. Int. Rev. gesamten Hydrobiol., 61, 747-760.
- Orton, R.B., 1964. The Climate of Texas and the Adjacent Gulf Waters. U.S. Dept. of Commerce. Weather Bureau No. 161.
- Parker, P.L., 1954. Distribution of the foraminifera in the north-eastern Gulf of Mexico. Harvard Univ. Mus. Comp. Zoology Bull., 111(10), 453-588.

- _____, 1978. High molecular weight hydrocarbons in sediments. In Bright, T. and R. Rezak, eds., Northwest Gulf of Mexico Topographic Features Study, Final Report to U.S. Dept. of Interior, Bureau of Land Management. Texas A&M Univ., Dept. of Oceanography, Technical Report #78-14-T, Chapter IX.
- _____, E.W. Behrens, J.A. Calder, and D. Schultz, 1972. Stable carbon isotope ratio variation in the organic carbon from Gulf of Mexico sediments. *Contrib. Mar. Sci.*, 16, 139-147.
- _____, et al., 1976. Environmental Studies, South Texas Outer Continental Shelf, 1975, Biology and Chemistry. Final Report to U.S. Dept. of Interior, Bureau of Land Management, Contract #08550-CT5-17, 598 pp.
- _____, R.S. Scalan, and J.K. Winters, 1979. Biology and chemistry. In Flint, R.W. and N. Rabalais, eds., Environmental Studies, South Texas Outer Continental Shelf, Biology and Chemistry, Final Report to Bureau of Land Management, Washington, D.C., Contract #AA550-CT7-11.
- _____, R. Scalan, K. Winters, and D. Boatwright, 1981. High molecular weight hydrocarbons, Delta C-13, and total organic carbon in sediment. In Rezak, R. and T. Bright, eds., Northern Gulf of Mexico Topographic Features Study, Final Report to Dept. of Interior, Bureau of Land Management, Contract AA551-CT8-35. Texas A&M Univ., Dept. of Oceanography, Technical Report #82-2-T, Vol. 2, Chapter IXC.
- _____, ed., 1979. Ixtoc I: Chemical Characteristic and Acute Biological Effects. Final Report submitted to the Department of Transportation, United States Coast Guard. Contract DOT-CG08-8174.
- Parker, R.H. and J.R. Curray, 1956. Fauna and bathymetry of banks on continental shelf, northwest Gulf of Mexico. *AAPG Bull.*, 40, 2428-2439.
- Pearson, R.G., 1981. Recovery and recolonization of coral reefs. *Mar. Ecol. Prog. Ser.*, 4, 105-122.
- Perkins, H.T., 1970. Inertial Oscillations in the Mediterranean. Ph.D. thesis. M.I.T./W.H.O.I., 155 pp.
- Potts, D.C., 1977. Suppression of coral populations by filamentous algae within damselfish territories. *J. Exp. Mar. Biol. Ecol.*, 28, 207-216.
- Powell, E.N. and T.J. Bright, 1981. A thionibios does exist--Gnathostomulid domination of the canyon community at the East Flower Garden brine seep. *Int. Rev. gesamtten Hydrobiol.*, 66(5), 675-683.

- _____, T.J. Bright, A. Woods, S. Gittings, and J. Johansen, 1982. The East Flower Garden Brine Seep: Implications for Benthic Community Structure. Final Report, U.S. Dept. of Commerce, NOAA, Contract #NA80-AA-H-CZ118, Texas A&M Dept. of Oceanography Technical Report #81-6-T, 101 pp.
- Pulley, T.E., 1963. Texas to the tropics. Houston Geol. Soc. Bull. 6, 13-19.
- Rattray, M., Jr., 1960. On the coastal generation of internal tides. Tellus, 12, 54-62.
- Rezak, R., 1977. West Flower Garden Bank, Gulf of Mexico Stud. Geol., 4, 27-35.
- _____, 1981. Proceedings: Second Annual Gulf of Mexico Information Transfer Meeting. Held April 30-May 1, 1981, New Orleans, LA. Texas A&M Univ., Dept. of Oceanography, Technical Report #81-5-T, 115 pp.
- _____ and T.J. Bright, 1981a. Northern Gulf of Mexico Topographic Features Study. Final Report to U.S. Dept. of Interior, Bureau of Land Management, Contract AA551-CT8-35. Texas A&M Univ., Dept. of Oceanography, Technical Report #81-2-T, 5 vols, 995 pp.
- _____ and T.J. Bright, 1981b. Seafloor instability at East Flower Garden Bank, northwest Gulf of Mexico. Geo-Marine Letters, 1(2), 97-103.
- _____ and W.R. Bryant, 1973. West Flower Garden Bank. Trans. Gulf Coast Assoc. of Geol. Soc. 23rd Annual Conv. (Oct. 24-26), pp. 377-382.
- _____ and G.S. Edwards, 1972. Carbonate sediments of the Gulf of Mexico. Tex. AM Univ. Oceanogr. Stud., 3, 263-280.
- Rhoads, D., 1974. Organism sediment relations on the muddy sea floor. Ocean. Mar. Biol. Ann. Rev., 12, 263-300.
- Rigby, J.K. and W.G. McIntire, 1966. The Isla de Lobos and associated reefs, Veracruz, Mexico. Brigham Young Univ. Geol. Studies. 13: 1-46.
- Robinson, M.K., 1973. Atlas of Monthly Mean Sea Surface and Sub-Surface Temperature and Depth of the Top of the Thermocline Gulf of Mexico and Caribbean Sea. Scripps Institute of Oceanography. Ref. 73-8, 105 pp.
- Sackett, W.M., 1975. Evaluation of the effects of man-derived wastes on the viability of the Gulf of Mexico. Texas A&M University, Oceanography Dept. Technical Report, Ref. 75-8-T, National Science Foundation I.D.O.E. grant GX-37344, 27 pp.

- Sammarco, P.W., 1978. The Effects of Grazing by Diadema antillarum Philippi on a Shallow-water Coral Reef Community. Ph.D. thesis. State University of New York at Stony Brook, 371 pp.
- _____, 1980. Diadema and its relationship to coral spat mortality: Grazing, competition, and biological disturbance. J. Exp. Mar. Biol. Ecol., 45, 245-272.
- Shaw, J.K. and T.S. Hopkins, 1977. The distribution of the family Hapalocarcinidae (Decapoda, Brachyura) on the Florida Middle Ground with a description of Pseudocryptochirus hypostegus new species. Proc. Third Int. Coral Reef Symp., Univ. Miami, Rosenstiel School of Marine and Atmospheric Science, 1, 177-183.
- Shepard, F.P., 1937. Salt domes related to Mississippi submarine trough. Geol. Soc. Am. Bull., 40, 2428-2489.
- Shideler, G.L., 1976. Textural distribution of sea floor sediments, South Texas outer continental shelf. J. Res. U.S. Geol. Surv., 4(6), 703-713.
- Shokes, R.F., P. Trabant, B. Presley, and D. Ried, 1977. Anoxic, hypersaline basin in the northern Gulf of Mexico. Science, 196, 1443-1446.
- Smith, F.G.W., 1971. Atlantic Reef Corals: A Handbook of the Common Reef and Shallow-water Corals of Bermuda, Florida, the West Indies, and Brazil. Univ. Miami Press, Coral Gables, FL, 164 pp.
- Smith, G.B., 1976. Ecology and distribution of eastern Gulf of Mexico reef fishes. Fla. Mar. Res. Florida Marine Research Laboratory. Publ. 19. 78 pp.
- Smith, N.P., 1980. On the hydrography of shelf waters off Central Texas Gulf Coast. J. Phys. Ocea., 10 (5), 806-813.
- Steel, R.G.D. and J.H. Torrie, 1960. Principles and Procedures of Statistics. McGraw-Hill, New York, 481 pp.
- Stetson, H.C., 1953. The sediments of the western Gulf of Mexico, part I--The continental terraces of the western Gulf of Mexico: Its surface sediments, origin, and development. Papers in Physical Oceanography and Meteorology, M.I.T./W.H.O.I., 12(4), 1-45.
- Stoddart, D.R., 1969. Ecology and morphology of recent coral reefs. Biol. Rev. Camb. Philos. Soc., 44, 433-498.
- _____, 1972. Field methods in the study of coral reefs. Proc. Symp. Corals and Coral Reefs, Mar. Biol. Assoc. India, 71-80.
- Symon, K.R., 1960. Mechanics. Addison-Wesley, Reading, MA, 557 pp.

- Tatum, T.E., Jr., 1979. Shallow Geological Features of the Upper Continental Slope, Northwestern Gulf of Mexico. Technical Report 79-2-T, Department of Oceanography, Texas A&M University, 60 pp.
- Thierstein, H. and W. Berger, 1978. Injection events in ocean history. *Nature*, 276, 461-466.
- Thompson, J.H. and T.J. Bright, 1977. Effects of drill mud on sediment clearing rates of certain hermatypic corals. Proc. of Oil Spill Conference (Prevention, Behavior, Control, Cleanup) New Orleans, LA, March 8-10, American Petroleum Institute Publ. No. 4284, American Petroleum Institute, Washington, D.C., 495-498.
- _____, E.A. Shinn, and T.J. Bright, 1980. Effects of drilling mud on seven species of reef-building corals as measured in the field and laboratory. In Geyer, R.A., ed., *Marine Environmental Pollution*, Elsevier Oceanography Series, 27A, Elsevier, New York, 433-453.
- Tochko, J.S., 1978. A Study of the Velocity Structure in a Marine Boundary Layer--Instrumentations and Observations. WHOI-78-90, Woods Hole Oceanographic Institution, 187 pp.
- Trefry, J.H. and B.J. Presley, 1976. Heavy metals in sediments from San Antonio Bay and the northwest Gulf of Mexico. *Envir. Geol*, 1, 283-294.
- Tresslar, R.C., 1974. Corals. In Bright, T.J. and L.H. Pequegnat, eds., *Biota of the West Flower Garden Bank*, Gulf Publishing Co., Houston, TX, pp. 116-139.
- Viada, S.T., 1980. Species Composition and Population Levels of Scleractinean Corals Within the Diploria-Montastrea-Porites Zone of the East Flower Garden Bank, Northwest Gulf of Mexico. M.A. thesis, Texas A&M University, College Station, Tx., 96 pp.
- Villalobos, A. 1971. Estudios Ecologicos en un Arrecife Coraline en Vera Cruz, Mexico. Symposium on Investigations and Resources of the Caribbean Sea and Adjacent Regions: 531-545.
- Weatherly, G.L., 1971. A study of the bottom boundary layer of the Florida current. *J. Phys. Ocea.*, 2, 54-72.
- Wilson, D., 1972. Diel migration of sound scatterers into and out of the Cariaco Trench anoxic water. *J. Mar. Res.*, 30, 168-176.
- Wimbush, R. and W. Munk, 1970. The benthic boundary layer. In Maxwell, A., ed. *The Sea*, Vol. 4, Part 1, Wiley, New York, 731-758.
- Wormuth, J.H., 1979. Neuston Project. In Flint, R.W. and C.W. Griffin, eds., *Environmental Studies, South Texas Outer Continental Shelf, Biology and Chemistry, Final Report to the U.S. Bureau of Land Management, Contract #AA550-CT7-11, Chapter 15, 15-1 to 15-66.*



The Department of the Interior Mission

As the Nation's principal conservation agency, the Department of the Interior has responsibility for most of our nationally owned public lands and natural resources. This includes fostering sound use of our land and water resources; protecting our fish, wildlife, and biological diversity; preserving the environmental and cultural values of our national parks and historical places; and providing for the enjoyment of life through outdoor recreation. The Department assesses our energy and mineral resources and works to ensure that their development is in the best interests of all our people by encouraging stewardship and citizen participation in their care. The Department also has a major responsibility for American Indian reservation communities and for people who live in island territories under U.S. administration.



The Minerals Management Service Mission

As a bureau of the Department of the Interior, the Minerals Management Service's (MMS) primary responsibilities are to manage the mineral resources located on the Nation's Outer Continental Shelf (OCS), collect revenue from the Federal OCS and onshore Federal and Indian lands, and distribute those revenues.

Moreover, in working to meet its responsibilities, the **Offshore Minerals Management Program** administers the OCS competitive leasing program and oversees the safe and environmentally sound exploration and production of our Nation's offshore natural gas, oil and other mineral resources. The MMS **Minerals Revenue Management** meets its responsibilities by ensuring the efficient, timely and accurate collection and disbursement of revenue from mineral leasing and production due to Indian tribes and allottees, States and the U.S. Treasury.

The MMS strives to fulfill its responsibilities through the general guiding principles of: (1) being responsive to the public's concerns and interests by maintaining a dialogue with all potentially affected parties and (2) carrying out its programs with an emphasis on working to enhance the quality of life for all Americans by lending MMS assistance and expertise to economic development and environmental protection.